



Chloroplast RNA-Binding Proteins (cpRNPs): Novel
Candidates for the Environmental Control of
Photosynthesis.

By

Jonathan Griffin

Supervisor: Dr. Gabriela Toledo-Ortiz

Co-supervisor: Dr. Elizabete Carmo-Silva

This thesis is submitted to the Lancaster Environment
Centre in partial fulfilment of the requirements for a
PhD in Environmental Science.

Lancaster University

March 2021

Declaration.

Except where reference is made to other sources, I declare that the contents of this thesis are my own work and have not previously been submitted for the award of a higher degree elsewhere.

Jonathan Griffin

Lancaster University

March 2021

Summary

Phytochromes (phy) are key regulators of photosynthesis that act in the nucleus to orchestrate signalling pathways involved in co-ordinating plant growth and development in response to environmental cues, including light and temperature. Using publicly available transcriptomic datasets, this thesis identifies phys as master modulators for the control of nuclear genes involved in plastome gene expression mechanisms in response to red light, regulating genes involved in both the transcriptional and post-transcriptional signalling pathways. This thesis also identifies that the bZIP transcription factor HY5 may be a key transducer for phys in regulating these pathways.

Among the RNA-binding proteins families that conduct the post-transcriptional regulation of the plastome are the chloroplast RNA-binding proteins (cpRNPs). Published research has shown that the cpRNPs are global modulators of plastome genes, and this thesis further identifies them as a part of an R-phyB-HY5-cpRNP signalling cascade. This thesis also shows that cpRNPs are essential to R-light mediated greening responses in *Arabidopsis thaliana* and are involved in delivering light signals to the required chloroplast-encoded genes during de-etiolation. Through phyB and HY5, this thesis also shows that in addition to light quality signals, cpRNPs also integrate a diverse range of light intensity and temperature environmental signals to maintain photosynthesis.

The cpRNP family has previously been characterised as regulators of the plastome but this thesis shows that they are also involved in the nucleus. Reverse genetics studies identify reductions in photosynthesis-associated nuclear-encoded gene (PhANG) transcripts in *cpnp* mutants, making cpRNPs a part of the co-ordination of nuclear- and plastid-encoded genes pathways for tuning photosynthesis to environmental changes. The evidence gathered here also reveals that through the phyB-modulation of alternative transcriptional start sites (TSS), cpRNP isoforms are generated with alternative nuclear subcellular localisations. Furthermore, this thesis shows that *cpRNP* expression is linked to retrograde signals from the chloroplast through chemical retrograde signal activator treatments affecting both cpRNP subcellular localisation and transcript accumulation.

Finally, this thesis shows that the conservation of cpRNPs across higher plants makes them notable for the global efforts to generate new toolkits to maintain photosynthetic rates in crops under changing environments. This thesis describes a novel role for cpRNPs in plastid transition processes, using *Solanum lycopersicum* as a model crop to study chloroplast-to-chromoplast transitions.

Professional Acknowledgements.

I would like to thank very much my primary supervisor and mentor Dr. Gabriela Toledo-Ortiz for her unwavering and patient support, guidance, and tutelage over the course of the degree, especially for her help in guiding my scientific writing style and her behind-the-scenes effort to put together all of the collaborations that made this project so comprehensive. My gratitude also extends to my co-supervisor Dr. Elizabete Carmo-Silva, who helped me keep perspective and stay grounded in our monthly meetings.

I am also very grateful to Dr. Karine Prado, Dr. Daniel Seaton, Professor Karen Halliday, and all of the Halliday lab members for their help; especially so to Dr. Karine Prado, whose assistance and pointers for the bioinformatics analysis made all the difference.

I'd also like to extend my thanks to collaborators in Kyoto, Japan, and in Barcelona, Spain. Thanks to Ms. Sera Akune and Professor Tomonao Matsushita from Kyoto University for their invaluable contributions; and to Dr. Lucio D'Andrea, Dr. Miguel Simon, and Dr. Manuel Rodriguez-Concepcion and all the members of the Rodriguez-Concepcion Lab in the Centre of Research for Agricultural Genomics who were so welcoming, friendly, and helpful during my time studying there.

Finally, I'd like to thank my colleagues, laboratory members, and technical support staff of the Molecular Plant Biology laboratories at Lancaster University for their ongoing support, including Dr. Geoff Holroyd, and Dr. Elizabeth Shaw.

Table of Contents.

List of Abbreviations	9
List of Figures and Tables.....	11
Chapter 1: Literature review of the Chloroplast RNA-binding Proteins (cpRNPs) as novel sensors for the environmental control of photosynthesis.	15
1.1. Environmental control of Photosynthesis.	15
1.1.1. Climate Change is predicted to impact crop yields.....	15
1.1.2 Photosynthesis is a vital process performed in the chloroplast.	15
1.1.3. Photosynthesis is a stress-sensitive process in a changing world.	18
1.2. Photoreceptors in the Regulation of Photosynthesis.	21
1.2.1. Phytochrome is a key regulator of Photosynthesis.	21
1.3. Chloroplast RNA Binding Proteins (cpRNPs): a new role for phytochrome in Post-Transcriptional Regulation?	25
1.3.1. Regulation of the chloroplast genome expression.	25
1.3.2. The cpRNPs are key Post-Transcriptional Regulators of Photosynthesis.	27
1.3.3. cpRNPs are Global Post-Transcriptional regulators of Plastid Gene Expression	29
1.3.4. cpRNPs are integrators of multiple environmental signals.	31
1.3.5 cpRNPs may be involved in plastid-to-nuclear communication.	33
1.4. Hypotheses and aims.	34
Chapter 2: Characterising the cpRNPs as Novel Candidates for the Environmental Regulation of Photosynthesis.....	35
2.1 Introduction.	35
2.2 Materials and Methods.....	37
2.3 Results: Characterization of cpRNPs in red-light responses.	43
2.3.1. phyB regulates post-transcriptional mechanisms of plastome gene expression.	43
2.3.2. cpRNPs are downstream signalling components of phytochrome B.....	46
2.3.3. cpRNPs integrate red light signalling to promote greening during de-etiolation.....	46
2.3.4. Investigating the cpRNPs' role in delivering phytochrome-red light signals to plastid encoded genes.	49
2.3.5. Photoreceptors in the modulation of plastid gene expression.	52
2.3.6. cpRNPs are global regulators of plastid gene expression.	54
2.3.7. Identifying plastome target genes sensitive to R-light and dependent on cpRNP action during de-etiolation.	54
2.3.8. HY5 links phy activation to cpRNPs modulation in response to red light.....	59
2.4. Results: Are cpRNPs involved in the photosynthetic stress responses induced by high light and fluctuating light intensities?.....	66

2.4.1. Photosynthetic apparatus in chloroplasts are vulnerable to fluctuations in light intensity and high light stress.	66
2.4.2. Investigating the phenotypic response of <i>cprnp</i> mutants to high light stress (HL).	68
2.5. Results: Investigating the cpRNPs sensitivity to photoperiodicity.....	71
2.5.1. phyB is a key integrator of photoperiodicity.	71
2.5.2 Bioinformatic examination of cpRNPs' response to different photoperiods.	72
2.5.3 Phenotypic characterisation of cpRNPs' response to different photoperiods.	75
2.6. Results: Beyond light: the cpRNPs and photoreceptor-dependent temperature sensing.	78
2.6.1. Ambient Temperature responses.	78
2.6.2. phyB and HY5 are a key integrators of ambient temperature responses, linking temperature sensitivity to cpRNPs' regulation.	78
2.6.3. <i>cpRNP</i> transcript accumulation is ambient temperature-dependent.	79
2.6.4 Biomass and chlorophyll accumulation in <i>cprnp</i> mutants are sensitive to warm and cold temperatures.	80
2.6.5. The plastome response to ambient temperature changes is mediated by cpRNPs.....	84
2.7. Discussion.....	88
2.7.1. cpRNPs integrate Red-Light phyB- and HY5- signals to regulate greening in Arabidopsis.	88
2.7.2. Examining cpRNPs functions beyond light quality inputs.....	93
2.7.3. Beyond Light: cpRNPs in the delivery of temperature signals to regulate the plastome... ..	95
Chapter 3: Beyond the chloroplast: plastid-nuclear communication to acclimate photosynthesis to environmental change	99
3.1. Introduction.	99
3.2. Material and Methods.	101
3.3. Results: Investigating a potential dual subcellular localization (chloroplastic-nuclear) for cpRNPs.	106
3.3.1. cpRNP structure, function, and published literature imply a role for cpRNPs in nuclear-encoded gene expression.	106
3.3.2. Bioinformatics predict cpRNPs localise to the nucleus.....	106
3.3.3. Phytochrome-mediated alternative promoter selection for cpRNPs induces non-plastid localisations.....	108
3.3.4. <i>In planta</i> examination of Alternatively Transcribed cpRNP Isoforms reveals nuclear localisation in Arabidopsis.	113
3.4. Results: Investigating a potential role for cpRNPs in modulating nuclear-encoded transcript abundance.	123
3.4.1. Identification of R-phys regulated nuclear-encoded transcript targets.	123
3.4.2. Nuclear-encoded transcript accumulation for selected photosynthesis related genes is lower in <i>cprnp</i> mutants.....	126

3.5 Results: Investigating the effect of temperature on the modulation of cpRNP subcellular localisation and function.....	130
3.5.2. Cell Biological studies of Native-Promoter driven GFP fusion of <i>cp31A</i> and <i>cpSEBF</i> using confocal microscopy.	130
3.5.2. cpRNPs integrate light and temperature signals to modulate nuclear gene expression .	139
3.6. Results: Investigating whether a retrograde signalling pathway regulates cpRNP transcript accumulation and localisation.	144
3.6.1. Analysis of published Retrograde Signalling datasets and experimental validation.	145
3.6.2. Retrograde Signal Activator treatments alter the subcellular localisation of <i>cp31A</i> , but not <i>cpSEBF</i>	150
3.7. Discussion.....	156
3.7.1. cpRNPs localise to the nucleus and are critical to photosynthesis-associated nuclear gene transcript accumulation.	156
3.7.2. Temperature is a significant regulator of cpRNP subcellular distribution and nuclear functioning.....	158
3.7.3. cpRNPs are regulated by the retrograde signalling pathway.	161
Chapter 4: Beyond Arabidopsis: Investigation into the functional conservation of cpRNPs between Arabidopsis and tomato.....	166
4.1. Introduction.	166
4.2. Materials and Methods.....	168
4.3. Results: Investigating cpRNPs conservation across plant species.	173
4.3.1. cpRNPs are conserved across green plants.	173
4.3.2. Investigating sequence differences between paralogous cpRNPs.	176
4.4. Results: Investigating cpRNP functionality in plastid development in <i>Solanum lycopersicum</i>	178
4.4.1. Tomato as a model to crop to investigate cpRNP role in plastid developmental transitions.	178
4.4.2 Increasing cpRNP transcript abundance indicates they remain active in chloroplast-chromoplast transitions.	180
4.5. Results: Carotenogenesis as an indicator pathway of plastid transition in <i>Solanum lycopersicum</i>	184
4.5.2 Using Virus Induced Gene Silencing (VIGS) to silence cpRNPs during plastid transitions in tomato fruits.	185
4.5.3. Investigating the effects of silencing <i>Slcp31</i> on the Carotenoid Biosynthesis Pathway...	188
4.6. Results: CRISPR/Cas9-mediated knockout of <i>Slcp29A</i>	191
4.7. Discussion.....	193
4.7.1. Members of the Arabidopsis cpRNPs family are conserved across multiple dicot and monocot crop species.	193
4.7.2. cpRNPs are active in different plastids.	196
Chapter 5. General Discussion of Results.	199

5.1. Novel mechanisms behind the photoreceptors' modulation of greening and photosynthetic responses	199
5.2. cpRNPs are key regulators of transcripts encoded in the plastome and in the nucleus and could synchronise photosynthesis to the environment.	201
5.3. cpRNPs are conserved across plant species and may have further roles in plastid functions.	203
5.4. Conclusions.	205
Chapter 6: References used in this thesis.....	207
Statement for Submission with a Thesis Impacted by the COVID-19 Pandemic for PGR Students....	230
Chapter 7: Appendix	231
Chapter 8: Publication.	249

List of Abbreviations

ABI4: ABA-insensitive 4	GGPP: geranylgeranyl diphosphate
accD: acetyl-CoA carboxylase subunit	GGPS: GGPP synthase
ACS2: 1-aminocyclopropane-1-carboxylate synthase 2	GLK: golden2-like
ACT4: Actin 4	GO: gene ontology
ANOVA: analysis of variance	GUN1: Genome uncoupled 1
ATP: adenosine triphosphate	HL: high light
BAR: Bio-analytic resource for plant biology	HMR: HEMERA
bHLH: basic helix loop helix	HMWC: High molecular weight complex
bZIP: basic leucine zipper protein	hnRNP: Heterogenous nuclear ribonucleoproteins
CCA1: circadian clock associated 1	HY5: elongated hypocotyl 5
cDNA: complementary DNAs	IG: Immature green
Chl: chlorophyll	IPP: isopentenyl diphosphate
CO ₂ : carbon dioxide	LD: long days
COP1: Constitutive photomorphogenic 1	LHCI/LHCII/LHCA/LHCB: light harvesting complex
cp: chloroplast	LHY: late elongated hypocotyl
cpRNPs: chloroplast RNA-binding proteins	Linc: lincomycin
CRTISO: Carotenoid Isomerase	LL: low light
Crys: cryptochromes	LYC-B: lycopene β -cyclase
D: dark	LYC-E: lycopene ϵ -cyclase
DAPI: 4',6-diamidino-2-phenylindole	MEP: methylerythritol phosphate
DEG: degradation of periplasmic proteins	MG: Mature green
Del: Delila	MS: Murashige and Skoog media
DMAPP: dimethylallyl diphosphate	mTERF: mitochondrial transcription termination factor
EDTA: Ethylenediaminetetraacetic acid	NADPH: Nicotinamide adenine dinucleotide phosphate
ELF4: early flowering 4	ndh: NADH dehydrogenase subunit
FDR: false discovery rate	NEP: nuclear-encoded polymerase
FW: fresh weight	Nor: norflurazon
gDNA: genomic DNA	
GFP: green fluorescent protein	

NPQ: non-photochemical quenching

O: Orange

OEC: oxygen evolving complex

PABP: Poly-A binding protein

PDS: phytoene desaturase

PEP: plastid-encoded polymerase

Pet: Cytochrome b_6f

PG2A: Polygalacturonase 2

PhANG: photosynthesis associated nuclear genes (s)

Phots: phototropin (s)

phyB: phytochrome B

Phys: phytochrome (s)

PIF: phytochrome-interacting factor

PMT: photomultiplier tube

PP2A: Serine/threonine protein phosphatase 2A

PPR: pentatricopeptide repeat

PQL: Photosynthetic ndh subcomplex L 2

PRIN2: Plastid redox insensitive 2

psa: photosystem I subunit

psb: photosystem II subunit

PSI/II: photosystem I/photosystem II

PSRPs: plastid specific ribosomal proteins

PSY: phytoene synthase

pTAC: plastid transcriptionally active chromosome

PTM: Phd type transcription factor with transmembrane domains

R-80: red continuous light at an intensity of $80 \mu\text{mol m}^{-2} \text{s}^{-1}$

rbcl: rubisco large subunit

RBP: RNA-binding protein

RIN: Ripening inhibitor

ROS: reactive oxygen species

Ros1: Rosea1

Rpl: large ribosomal protein subunit

Rpo: RNA polymerase subunit

Rps: small ribosomal protein subunit

RR: Red ripe

RRM: RNA recognition motif

RTA: relative transcript abundance

RUBISCO: Ribulose-1,5-bisphosphate carboxylase-oxygenase

SD: short days

SDS: Sodium dodecyl sulfate

sgRNA: single guide RNA

SIG: sigma factor

STN7: STT7 HOMOLOG STN7

T-DNA: Transfer DNA

TOC1: timing of cab1

TPRs: tetratricopeptide domain-containing family

tracrRNA: transactivating crRNA

tRNA: transfer RNA

TSS: alternative transcriptional start site

UTR: untranslated region

UVR-8: UVB Resistance 9

VIGS: Virus induced gene silencing

WT: wild-type

ZDS: ζ -carotene desaturase

ZISO: ζ -carotene Isomerase

ZT: Zeitgeber

List of Figures and Tables

Chapter 1

Figure 1.1. Simplified schematic showing some of the key apparatus of the light reactions of photosynthesis.

Figure 1.2. Protein sequences and features of the *Arabidopsis thaliana* cpRNP family.

Figure 1.3. De-etiolating *cpRNP* mutants *cp29b* and *cp31a* express greening deficient phenotypes.

Figure 1.4. Bioinformatic data shows that *cp31A* is expressed highly in leaf tissue during early development.

Chapter 2.

Table 2.1. Genotyping primers used in Chapter 2.

Table 2.2. qPCR primers used in Chapter 2.

Figure 2.1. Phytochromes modulate red-light induction of genes with functions in multiple aspects of plastome gene expression.

Figure 2.2. Transcript levels for *cpRNPs* in red light is phyB-dependent.

Table 2.3. Mutant allele information for *cpRNP* mutants used in thesis.

Figure 2.3. *cpsebf* and *cp31a* mutants accumulate less chlorophyll than WT plants.

Table 2.4. List of protein-encoding genes in the plastome by gene name and product in the chloroplast.

Figure 2.4. phyB has a broad impact on chloroplast genome expression in short days (SD).

Figure 2.5. *cpRNP* mutation reduces transcript accumulation of key ATP synthase, photosystem I, and photosystem II plastome-encoded subunits.

Figure 2.6. HY5 modulates the light induction of genes with potential functions in multiple aspects of plastome gene expression.

Figure 2.7. Upstream promoter sequences of *cp31A*, *cp29B*, and *cpSEBF* contain multiple HY5 binding motifs.

Figure 2.8. Transcript abundances of *cp29B*, *cpSEBF*, and *cp31A* are HY5-dependent in red light.

Figure 2.9. Transcript abundance of key ATP synthase, photosystem I, and photosystem II plastome-encoded subunits is HY5-dependent in red light.

Figure 2.10. Working model for a red-light mediated phytochrome and HY5 involvement in the regulation of the plastome via the cpRNP family.

Figure 2.11. Short-term fluctuating light stress reduced Fresh Weight accumulation in *cpRNP* mutants.

Figure 2.12. *cp29B*, *cpSEBF*, and *cp31A* expression cycles in Long Day photoperiods.

Figure 2.13. *cp29B*, *cpSEBF*, and *cp31A* expression cycles in Short Day photoperiods.

Figure 2.14. *cp29b* and *cp31a* mutants do not express a Long Day-sensitive phenotype.

Figure 2.15. *cprnp* mutants did not express a Short Day-sensitive phenotype.

Figure 2.16. Transcript abundance of *cp29B*, *cpSEBF*, and *cp31A* is temperature-dependent.

Figure 2.17. *cprnp* mutants express cold- and warm- temperature-sensitive phenotypes.

Figure 2.18. *cprnp* mutation affects temperature-dependent regulation of key plastome-encoded subunits.

Figure 2.19. Working model for a phyB-HY5-cpRNP pathway that integrates a range of environmental signals.

Chapter 3.

Table 3.1. Transgenic lines used for cell biological analysis using confocal microscopy.

Table 3.2. qPCR primers used in this Chapter 3.

Figure 3.1. Bioinformatic tools predict that *cp29A*, *cp29B*, *cp31A*, *cp33B*, *cp33C* may localise to the nucleus.

Figure 3.2. phyB-mediated alternative transcription of cpRNPs produces different length isoforms, some of which do not contain the chloroplast transit peptide.

Table 3.3. Alternative-transcriptional start site (TSS) transcribed cpRNPs are differentially expressed in R-light compared to full length counterparts.

Figure 3.3. Confocal microscopy shows longer cpRNP forms localise to the plastid and shorter cpRNP forms localise to the nucleus when transiently expressed in onion cells.

Figure 3.4. Confocal microscopy shows *cp31A* (TSS_A) localises to the chloroplast.

Figure 3.5. Confocal microscopy shows *cp31A* (TSS_B) localises to the nucleus.

Figure 3.6. Confocal microscopy shows WT control.

Figure 3.7. Confocal microscopy shows 3-D representations of *cp31A* (TSS_A) and *cp31A* (TSS_B).

Figure 3.8. Confocal microscopy shows *cpSEBF* (TSS_A) localises to the chloroplast.

Figure 3.9. Confocal microscopy shows *cpSEBF* (TSS_B) localises to the nucleus.

Figure 3.10. Confocal microscopy shows 3-D representations of *cpSEBF* (TSS_A) and *cpSEBF* (TSS_B).

Table 3.4. List of experimental genes delineated for examination in *cprnp* mutants.

Figure 3.11. *cprnp* mutation affects the transcript abundance of key nuclear-encoded photosynthesis-associated genes.

Figure 3.12. Confocal microscopy shows GFP fluorescence intensity in Native Promoter (NP)-expressed *cp31A* tagged with GFP appears highest in cold temperatures *in planta*.

Figure 3.13. Confocal microscopy shows Native Promoter-expressed cp31A tagged with GFP localises to chloroplast and nucleus in 17°C and 22°C.

Figure 3.14. Confocal microscopy shows GFP fluorescence intensity in Native Promoter (NP)-expressed cpSEBF tagged with GFP appears highest in cold temperatures *in planta*.

Figure 3.15. Confocal microscopy shows Native Promoter-expressed cpSEBF tagged with GFP localises to chloroplast in all temperature conditions.

Figure 3.16. *cpnnp* mutation affects temperature-dependent regulation of key nuclear-encoded photosynthesis-associated genes.

Figure 3.17. *cpRNP* expression in WT plants is repressed by Lincomycin treatment.

Figure 3.18. *cpRNP* expression in WT plants is repressed by Norflurazon treatment.

Figure 3.19. All *cpRNPs* and marker gene expression is repressed in Lincomycin-treated WT; *cp29B* expression is repressed in Norflurazon-treated WT.

Figure 3.20. Confocal microscopy shows Native Promoter (NP)-expressed cp31A tagged with GFP localises to chloroplast *in planta* in control conditions.

Figure 3.21. Confocal microscopy shows Native Promoter (NP)-expressed cp31A tagged with GFP localises to the nucleus *in planta* when treated with Lincomycin.

Figure 3.22. Confocal microscopy shows Native Promoter (NP)-expressed cpSEBF tagged with GFP localises to chloroplast *in planta* in control conditions.

Figure 3.23. Confocal microscopy shows Native Promoter (NP)-expressed cpSEBF tagged with GFP does not localise to the nucleus *in planta* when treated with Lincomycin.

Figure 3.24. Working model showing that red light, temperature, and retrograde signals modulate *cpRNP* expression and subcellular localisation.

Chapter 4.

Table 4.1. qPCR primers used in Chapter 4.

Table 4.2. Primers used to sequence and screen for *Slcp29A* in Money maker tomato plants.

Figure 4.1. Phylogenetic analysis of cpRNP proteins from Arabidopsis and a range of other species.

Figure 4.2. Comparison of sequences for cp31A and cp31B, and cpSEBF and cp29A show that they are likely duplications of each other.

Figure 4.3. *SlcpRNP* transcripts are differentially accumulated in different fruit ripening stages.

Figure 4.4. *SlcpRNP* accumulation changes with fruit ripening progression in *Solanum lycopersicum* cultivar Micro-Tom fruits.

Figure 4.5. Silencing *Slcp31* in transgenic *Delila-Rosea1* fruits delayed fruit ripening progression.

Figure 4.6. Representation of the Carotenoid Biosynthesis pathway and the effect of silencing *Slcp31* on genes associated with plastid transitions.

Figure 4.7. CRISPR/Cas-9 construct guides and targets for *Slcp29A*.

Figure 4.8. Working model showing *Solanum lycopersicum* cpRNPs are up- and down- regulated during different plastid transition stages.

Chapter 7.

Supplementary Figure 1.1. *cpRNPs cp28A, cp29A, cp29B, cpSEBF, cp31B, cp33A, and cp33B* accumulate strongly in aerial leaf tissues in *Arabidopsis thaliana*.

Supplementary Figure 1.2. Sequences and T-DNA inserts for *cpRNP* single mutants *cp29b_2*, *cpsebf_1*, and *cp31a_2*.

Supplementary Figure 2.2. *cp29b* expresses a Long Day-sensitive phenotype.

Supplementary Figure 3.1. *cp28A, cpSEBF, cp29C, cp31B, cp33A, and cp33B* are not predicted to localise to the nucleus.

Supplementary Figure 3.2. Confocal microscopy shows Native Promoter (NP)-expressed *cp31A* tagged with GFP localises to the chloroplast and not the nucleus at 27°C.

Supplementary Figure 3.3. Confocal microscopy shows 3-D representations of Native Promoter (NP)-expressed *cp31A* tagged with GFP co-localises with the nucleus and chloroplast at 17°C and 22°C.

Supplementary Figure 3.4. Confocal microscopy shows 3-D representations of Native Promoter (NP)-expressed *cpSEBF* tagged with GFP co-localises with chloroplast and not the nucleus at 27°C.

Supplementary Figure 3.5. Confocal microscopy shows 3-D representations of Native Promoter (NP)-expressed *cpSEBF* tagged with GFP co-localises with chloroplast at 17°C, 22°C, and 27°C.

Supplementary Figure 3.6. Confocal microscopy shows 3-D representations of Native Promoter (NP)-expressed *cp31A* tagged with GFP co-localises with the nucleus and chloroplast in control conditions, but principally to the nucleus when treated with Lincomycin.

Supplementary Figure 3.7. Confocal microscopy shows 3-D representations of Native Promoter (NP)-expressed *cpSEBF* tagged with GFP co-localises with chloroplast and the nucleus in control conditions, but principally to the chloroplasts when treated with Lincomycin.

Supplementary Table 4.1. List of accession numbers used to generate the phylogenetic tree presented in Figure 4.1.

Supplementary Figure 4.1. Pairwise alignment of *cp31A, cp31B, and cp31A* acidic domain Ser-phosphorylation sites.

Supplementary Figure 4.2. Transcript accumulation of fruit ripening marker genes *E8, PG2A, and ACS2* were used to confirm fruit ripening stages in *Solanum lycopersicum* cultiv. MicroTom fruits.

Supplementary Figure 5.1. *cp31A* (TSS_A) contains a C-box HY5 binding site upstream of the *cp31A* (TSS_B) transcription initiation site.

Chapter 1: Literature review of the Chloroplast RNA-binding Proteins (cpRNPs) as novel sensors for the environmental control of photosynthesis.

1.1. Environmental control of Photosynthesis.

1.1.1. Climate Change is predicted to impact crop yields.

Climate change is ongoing crisis, projected to reduce crop growth rates, yields, and lower overall agricultural productivity (Lobell and Gourdj, 2012). Furthermore, climate change is also likely to reduce water availability, and induce an accompanying increase the frequency of droughts (Varela-Ortega et al., 2016) that will be exacerbated by an increasing average global temperature and sharply decreasing winter temperatures (Wallace, 2014). Forecasts predict a high risk of yield loss for areas in the Northern Hemisphere, and there is still much uncertainty regarding how quickly farms can adapt (Moore and Lobell, 2014). Specifically for crop plants, current weather change trends predict reduced yields for maize, wheat, and rice (Bassu et al., 2014; Challinor et al., 2014; Asseng et al., 2013); one of the primary ways productivity in these important food crops will be affected is through a reduction in photosynthetic activity (Galmes et al., 2013).

1.1.2. Photosynthesis is a vital process performed in the chloroplast.

Photosynthesis is the primary factor behind biomass accumulation and crop yield. This process captures light and converts it to biomass through a complex series of biochemical reactions (Long et al., 2006). This process occurs in the chloroplast and can be divided into the light reactions, in which electrons pass through protein complexes in the chloroplast thylakoid membranes, and the Calvin-Benson cycles involving of carbon fixation in the stroma (Renger and Kuhn, 2007).

The light reactions of photosynthesis involve Photosystem II (PSII), the electron transport chain and cytochrome *b6f* complex, and Photosystem I (PSI), all leading to the production of ATP and NADPH to drive carbon fixation (Rochaix, 2011; Foyer et al., 2012). Photons are captured in the light-harvesting antenna complexes of PSII by chlorophyll *a*, providing an electron separated by the Oxygen-Evolving Complex (OEC) with an excited energy level. This electron is transferred through the electron transport chain to generate series of redox reactions, and then enters PSI, where it receives further energy from the Light Harvesting Complexes (LHC), finally moving through a system of electron acceptors to drive the movement of hydrogen ions from the thylakoid lumen to the stroma, driving the ATP synthase reaction. The key photosynthetic apparatus used for light reactions of photosynthesis are summarised in Figure 1.1.

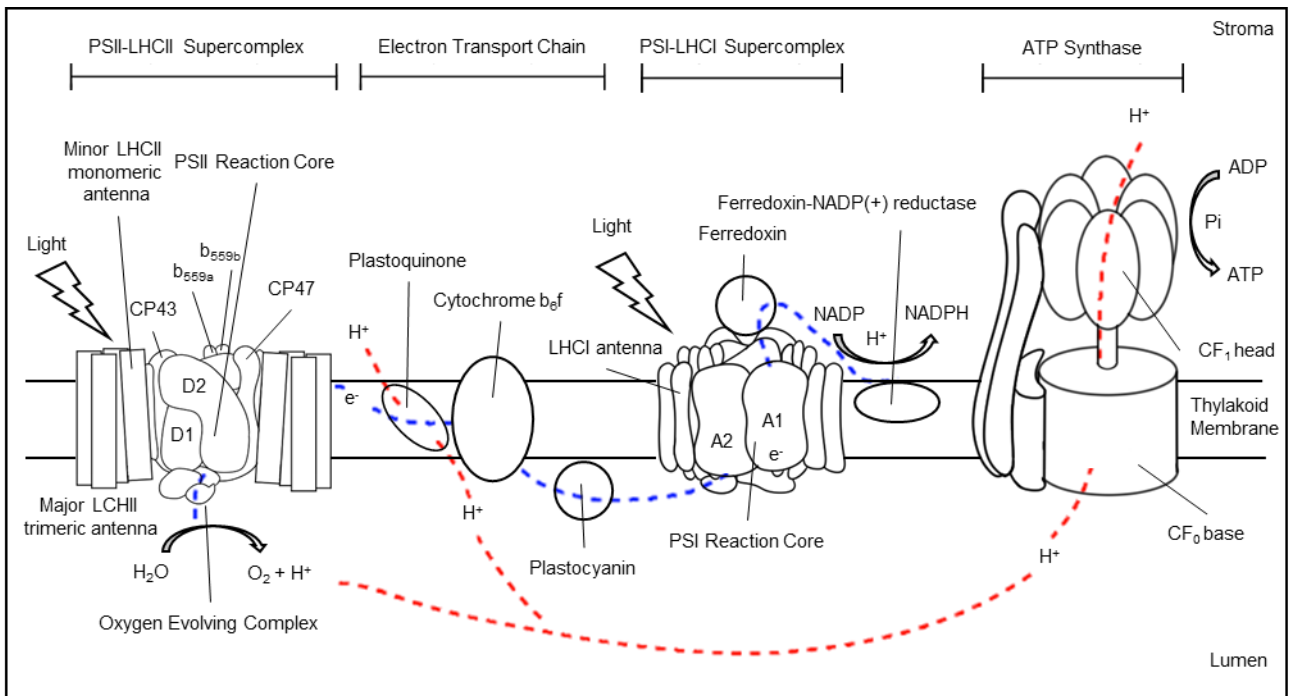


Figure 1.1. Simplified schematic showing some of the key apparatus of the light reactions of photosynthesis. In this figure, the path of a high-energy electron split from water by the Oxygen Evolving Complex (OEC) is indicated with a blue dotted line, and the path of H^+ is indicated with a red dotted line. Figure is adapted from figures presented in Minagawa and Takahashi (2004), Malnoë (2011, and Bashir et al. (2015).

Photosystem II. The core apparatus of Photosystem II is a large, multi-subunit chlorophyll-protein complex located in thylakoid membranes and drives the oxidation of water, oxygen evolution, and plastoquinone reduction (Shi and Schroder, 2004; Minagawa and Takahashi, 2004). The complex is composed of over 30 protein subunits comprising the core reaction centre proteins, the low molecular mass proteins, the extrinsic Oxygen-Evolving Complex proteins (OEC), and additional light-harvesting complex proteins, all encoded by genes from both the chloroplast and the nucleus (Kouril et al., 2012).

The core complex is formed from reaction centre proteins D1 and D2 (encoded by chloroplast genome-genes *psbA* and *psbD*), the core chlorophyll *a*-binding antenna proteins CP43 and CP47 (encoded by plastid genes *psbC* and *psbB*), and the two (alpha and beta) cytochrome *b*₅₅₉ subunits (encoded by plastid genes *psbE* and *psbF*); all of which are essential components for PSII assembly (Pakrasi et al., 1991; Swiatek et al., 2003; Minagawa and Takahashi, 2004).

The low molecular mass proteins PSBH, PSBI, PSBJ, PSBK, PSBL, PSBM, PSBN, PSBT, and PSBZ are encoded in the chloroplast, and both PSBX and PSBY are encoded in the nucleus (Nickelsen and Rengstl, 2013). Their specific functions are reviewed in Shi and Shroder (2004), but each broadly

contributes to photoautotrophic growth, protection from photoinhibition, and electron transport. In *Arabidopsis*, the OEC contains nuclear-encoded PSBO, PSBP, and PSBQ subunits (Thornton et al., 2004; Bricker et al., 2012): PSBO assists in stabilising the catalytic Mn cluster, and PSBP and PSBQ are involved in optimizing the availability of Ca²⁺ and Cl⁻ cofactors to maintain the active Mn-Ca²⁺-Cl⁻ cluster of PSII (Yabuta et al., 2010). The Light-Harvesting antenna Complex of PSII (LHCII) is composed of three major antenna trimeric proteins LCHB1, LHCB2, LHCB3, and three minor monomeric proteins CP29, CP26, and CP24 are formed from LHCB4, LHCB5, and LHCB6, all encoded in the nucleus (Liu et al., 2004). Furthermore, there is a wide range of auxiliary proteins, enzymes, and trafficking systems that both directly and indirectly assist in PSII biosynthesis and maintenance (Lu, 2016).

Photosystem I. Photosystem I (PSI) is also located in the thylakoid membrane, and mediates electron transport from water to NADPH (Bashir et al., 2015). It contains at circa 19 protein subunits, 175 chlorophylls, 2 phylloquinones, and 3 ferredoxin proteins (Ben-Shem et al., 2003). There are 15 core subunits of PSI, encoded by *psaA*, *psaB*, *psaC*, *psal*, and *psaj* in the chloroplast genome, and by *PSAD*, *PSAE*, *PSAF*, *PSAG*, *PSAH*, *PSAK*, *PSAL*, *PSAN*, *PSAO*, and *PSAP* in the nucleus; of these *PSAD*, *PSAE*, and *PSAH* have two known forms (Scheller et al., 2001). Of these proteins, only *psaA*, *psaB*, and *psaC* encode proteins that bind electron transport cofactors; *psaA* and *psaB* encode the P700 (primary electron donor of PSI) apoproteins A1 and A2; other the remaining subunits have complementary functions that include: interactions with the luminal electron donor plastocyanin (*PSAF*, *PSAN*, *PsaJ*) (Farah et al., 1995; Haldrup et al., 1999; Fischer et al., 1999; Hansson et al., 2007; Jensen et al., 2007); docking sites for soluble stromal ferredoxin (*PSAD* and *PSAE*) (Varotto et al., 2000; Ilnatowicz et al., 2004); and acting as binding proteins for the antenna complex (*PSAF*) (Haldrup et al., 2000). Subunits such as *PsaI*, *PsaJ*, *PSAK*, and *PSAL* contribute to stabilisation of the core antenna, itself composed of 100 chlorophyll A and 22 β -carotene molecules (Fromme et al., 2001). *PSAG* and *PSAK* bind *PsaB* and *PsaA*, and are respectively also predicted to be involved in the binding of the LHCA complex with *PSAG* contributing towards stability of the PSI complex (Ben-Shem et al., 2003; Varotto et al., 2002). It has also been described that *PSAH*, *PSAL*, *PSAO*, and *PSAP* act together to form an interaction domain to link PSI to LHCII to balance excitation energy between PSI and PSII (Jensen et al., 2004; Zhang and Scheller, 2004; Khrouchtchova et al., 2005).

The Light Harvesting Complex I (LHCI) is another key part of PSI that acts as a peripheral antenna to balance light energy distribution through state transitions, organised to maintain optimum photosynthetic output and avoid photoinhibition (Huang et al., 2021). LHCI is comprised

of the nuclear-encoded subunits LHCA1, LHCA2, LHCA3, LHCA4, LHCA5, and LHCA6, which form heterodimers LHCA1/4 and LHCA2/3 (Mullet and Arntzen, 1980; Ihalainen et al., 2000; Croce et al., 2002).

The correct expression and maintenance of the Photosynthetic apparatus over both photosystems and co-ordination between plastid- and nuclear-encoded subunit-encoding genes is vital for a plant to maintain biomass accumulation, and by extension for crop production.

1.1.3. Photosynthesis is a stress-sensitive process in a changing world.

As sessile organisms' plants must tolerate and cope with abiotic stress rather than avoid it or seek a better location. Many abiotic stresses such as drought and increased and decreased temperatures- or even just suboptimal environmental factors- can reduce photosynthetic efficiency. This can occur through photoinhibition, oxidative stress, RUBISCO activity, or stomatal conductance, often affecting Photosystems I and II, electron transport, and chlorophyll biosynthesis and significantly reducing crop yield, as was reviewed in Sharma et al (2020). Robust photosynthesis therefore requires a complex and tightly controlled regulatory signalling network to sustain it in a changing environment. To best navigate the inevitable problems posed by climate change, the mechanisms involved to maintaining homeostasis must be properly understood.

Temperature is a major regulator of photosynthesis. Temperature has a profound effect on photosynthetic efficiency (Hikosaka et al., 2006; Sharma et al., 2020). At both low and high extremes of temperature, internal cellular homeostasis is disrupted; for example, the light-saturation rates of photosynthesis are much lower than their optimum at an intermediate temperature, and can induce marked phenotypic changes (Hikosaka et al., 2006; Mathur and Jajoo, 2014). Another key factor affected by alterations in temperature is the fluidity of cell membranes. Low temperature, for example, changes the chloroplast membrane bilayer from a fluid-crystalline state to a solid-gel state; this affects the properties of protein transporters, kinases, and G-protein-associated receptors, and has a downstream effect on chloroplast and can trigger Reactive Oxygen Species (ROS) generation when regulatory mechanisms (eg NADPH) cannot function (Niu and Xiang, 2018). The mechanisms plants employ to cope with non-optimal changes to temperature can include changes in expression of photosynthetic components or CO₂ concentration at carboxylation sites (Berry and Bjorkman, 1980; Hikosaka et al., 1999). Some of the temperature-specific effects on photosynthesis are summarised below.

Low temperature-specific effects on photosynthesis. Low temperatures can impact photosynthesis at many levels, impairing photosynthetic activity through stomatal closure, internal CO₂ concentration, ROS accumulation, RUBISCO activity, and impairing thylakoid electron transport (Allen and Ort, 2001; Hou et al., 2016a). The coping strategies are varied and dependent upon the specific temperature range and developmental stage: for example, in *Nerium oleander* (Oleander), lower temperature acclimation for desert-grown plants was regulated by increasing quantities of photosynthetic proteins (Badger et al., 1982). Similar mechanisms involving higher photosynthetic proteins in low-temperature conditions have been observed in many crop and model organisms: in *Arabidopsis*, a cold-temperature (5°C) acclimation response resulted in new leaves grown in cold conditions performing photosynthesis at an equal rate to those at ambient temperature (Strand et al., 1999). This feat was accomplished through adjustments in the partitioning in carbon from starch to sucrose, and increases in activity in Calvin-cycle enzymes and sucrose biosynthesis enzymes, with a greater cytoplasmic volume (Strand et al., 1999). The chilling response involves the repression of photosynthetic gene expression in *Arabidopsis* (Krapp and Stitt, 1995; Strand et al., 1999), as well as interrupting circadian-regulated expression of nuclear-encoded photosynthetic genes in *Arabidopsis* and tomato mutants (Martino-Catt and Ort; Kreps and Simon, 1997). Furthermore, leaves that originate in cold conditions (5°C) rather than undergoing an acclimation response exhibit an altered phenotype and have a greater rate of photosynthesis, and do not undergo a compensatory suppression of photosynthetic gene expression (Strand et al., 1997). In cold temperatures photo-damage is also often observed (Hou et al., 2016b) and in conjuncture with high light can induce oxidative damage to the D1-D2 heterodimer, affecting the D1 repair cycle through expression of *psbA* (Barber, 1995) and necessitating effective LHCII- and PSII/PSI-reaction centre quenching strategies to dissipate excess energy (Velitchkova et al., 2020). Much research documenting the effect of cold on photosynthesis is conducted in chilling conditions, but even a drop of a few degrees can impact greening and plant morphology (Samach and Wigge, 2005).

High temperature-specific effects on photosynthesis. In heat stress conditions, photosynthetic apparatus is prone to damage and inhibition (Berry and Bjorkman, 1980; Mathur and Jajoo, 2014). In some plants such as spinach, data indicates that leaves grown at a higher temperature have a higher ratio of cytochrome *b6f* to Rubisco (Yamori et al., 2005b; Yamori et al., 2005a), indicating one of the pathways for altered environmental temperature in the differential regulation of the photosynthetic apparatus. In addition, the increased fluidity of the thylakoid membrane in PSII in high temperature results in dislodging of the light harvesting complex and disruption of the water-oxidizing complex and reaction centres through dissociation of chloride, magnesium, and calcium ions from pigment-protein complexes (Havaux and Gruszecki, 1993; Wise

et al., 2004; Lipova et al., 2010). Specific proteins such as D1 are also cleaved in high temperatures in spinach thylakoids (Yoshioka et al., 2006). This highlights a complex regulatory network integrating environmental signals to affect photosynthesis, affecting numerous processes and photosynthetic apparatus subunits.

High light stress and photosynthesis. With a crucial role in plant development, light is nevertheless a key stress factor when present at levels in excess of what the photosynthetic apparatus can process (Sharma et al., 2020). A high light stress can overload the electron transport chain and ATP synthesis systems, as light harvesting and energy transfer to reaction centres by antennae occur at faster rates than the electron transport chain can contend with (Ruban et al., 2012). This leads to over-accumulation of energy in the thylakoid membrane and a closure of the PSII reaction centres and results in photoinhibition (Aro et al., 1993). A classical by-product of oxygenic photosynthesis is triplet oxygen $^3\text{O}_2$ generated during oxidation of water- the excess of energy provided during photoinhibition of PSII results can convert triplet oxygen to singlet oxygen ($^1\text{O}_2$), a Reactive Oxygen Species (ROS) (Dmitrieva et al., 2020). Singlet oxygen can destroy membranes, proteins, and DNA, inhibiting protein synthesis in the chloroplast, requiring a high turnover of D1 and D2 proteins (Malnoe et al., 2014; Dmitrieva et al., 2020). ROSs can be dissipated through the antioxidants produced in the chloroplast, detoxifying enzymes, and other repair mechanisms (Falk and Munne-Bosch, 2010) or managed through carotenoids, tocopherols, plastoquinone, and secondary metabolites like anthocyanins (Gould, 2004; Ksas et al., 2015; Falk and Munne-Bosch, 2010; Mène-Saffrané and DellaPenna, 2010).

1.2. Photoreceptors in the Regulation of Photosynthesis.

1.2.1. Phytochrome is a key regulator of Photosynthesis.

Although integrating many varied environmental cues, photosynthesis is foremost a light-dependent process, using photon excitation energy to drive the electron transport chain. However, light plays an additional role in photosynthesis as a key signal stimulus: plants use light to best coordinate growth, development, and photosynthetic functioning with a changing environment. Light provides information on location, circadian and seasonal status, and plants integrate light signals to modulate multiple responses including the breaking of seed dormancy, growth, flowering, stomatal activity, metabolic responses (Matthews et al., 2005). Plants sense light cues through families of photoreceptors, including the red/far red light sensing phytochromes (phys); blue light sensing cryptochromes (crys), Phototropins (phots) and UV-B sensing UVR-8 (Quail, 2002).

The phys, crys, and phots light signalling networks orchestrate complex and large-scale changes in gene expression, to control photomorphogenesis, photoperiodic responses and shade-avoidance (Jiao et al., 2007). Phototropins are involved in optimising photosynthetic efficiency through stomatal opening and chloroplast movements (Christie et al., 2007). However, whilst crys also play a role in the control of photosynthetic and plastid gene expression (Ohgishi et al., 2004), this thesis will focus on the contribution of phytochrome and red-light signalling to photosynthesis.

Phytochromes are soluble, dimeric chromoproteins that can undergo light-induced reversible conformational changes between active and inactive forms depending on the far-red/red light wavelengths they are exposed to (Quail, 2002). The biologically active forms are the far-red light-absorbing forms, or 'Pfr', and phytochromes are inactive when in the red light-absorbing form, Pr (Quail, 2002). In *Arabidopsis* there are five known phytochromes, named respectively PhyA through PhyE. When activated they act as a trigger for plant growth and photomorphogenic development, including the transcription of the genes involved in assembling the photosynthetic machinery (Quail, 2002). This is an evolutionary response for plants to detect when appropriate light conditions have been met in the external environment to allow photosynthesis to occur. Reverse-genetics approaches have elucidated many different phytochrome-controlled responses, including some of the molecular mechanisms to promote photomorphogenic gene expression.

phyA and phyB are the best characterised phytochromes and are the most abundant proteins of the family (Shen et al., 2007; Tepperman et al., 2006; Quail, 2002). Labile phyA is accumulated highest in dark-grown seedlings and is closely associated with early-light modulation of changes in gene expression in response to red and far-red light (Quail, 2002); phyB is the most active

and abundant phytochrome in de-etiolated seedlings in the light, promoting de-etiolation and red-light induced molecular and physiological responses (Clough et al., 1995; Sharrock and Clack, 2002). Key features of phyA and phyB activity relevant to the thesis are described below.

phyB regulates greening. One of the main de-etiolation responses induced by phyA is greening. De-etiolation is the process through which plants first transition from a dark-grown to a light-grown state and induces the development of chloroplasts from etioplasts (Lifschitz et al., 1990). Greening principally involves chlorophyll biosynthesis and the expression of photosynthetic apparatus encoded from both the nucleus and plastome (Lifschitz et al., 1990). A mutant lacking fully functioning phyB showed not only elongated hypocotyls and reduced cotyledon expansion, but reduced chlorophyll synthesis and greening (Reed et al., 1993).

phyA and the modulation of gene expression. phyA coordinate multiple signalling cascades to regulate plant growth and development in response to red/far red light (Quail, 2002). When converted to its biologically active form, phyA translocates to the nucleus (Sakamoto and Nagatani, 1996) where it physically interacts with families of transcription factors to regulate a network of around 3000 genes (Quail, 2002; Tepperman et al., 2006; Lee et al., 2007). Among the phyA targets of these cascades are key nuclear genes coding for proteins required for photosynthesis, referred to as 'Photosynthesis-Associated Nuclear Genes' (PhANGs), which are then localised to the chloroplast via a transit peptide (Berry et al., 2013). As described in section 1.1.2, these nuclear-encoded proteins are vital for the functioning of all the photosynthetic complexes, including the Photosystems I and II, the cytochrome b6f, and the ATP synthase complexes (Nelson and Ben-Shem, 2004; Eberhard et al., 2008). phyA also impacts upon chloroplast gene expression mechanisms, contributing to the expression of over 60% of plastid-encoded genes in Short Day (SD)-cycling conditions (Michael et al., 2008; Griffin et al., 2020).

phyB is also a temperature sensor. In addition to being key light-sensors, phyA have also been linked to temperature sensing (Legris et al., 2016). phyB can sense temperatures up to 30°C through temperature-dependent reversion from active Pfr to inactive Pr state (Legris et al., 2016). In this capacity, increased rates of thermal reversion in warm environments reduces the abundance of biologically active Pfr-Pr phyB pool, in turn reducing phyB's downstream effects. Evidence also shows that phyB directly associates with key temperature-sensitive genes in a temperature-dependent manner, in a range between 17°C and 27°C (Jung et al., 2016). Current evidence also supports a role for phyB as an important light and temperature sensor for integrating a wide range of variability in regular daily cycles for *Arabidopsis* (Halliday and Davis; Casal and Questa, 2018). Although these studies identified roles for phyB as a temperature sensor predominantly at night,

phyB also plays a critical role in the day through the PHYTOCHROME-INTERACTING FACTOR 4 (PIF4)/HEMERA (HMR) pathway in red light (Qiu et al., 2019).

phyB modulates transcription factor activity. phyB co-ordinates multiple signalling cascades required for greening in part by controlling the activity of multiple transcription factor families, including the PHYTOCHROME INTERACTING FACTORS (PIFs), a subfamily of bHLH transcription factors involved in repressing photomorphogenesis in the dark (Lee et al., 2007); as well as GARP nuclear transcription factors GOLDEN2-LIKE (GLK), and the bZIP-LONG HYPOCOTYL 5 (HY5) transcription factors, that activate greening (Lee et al., 2007; Waters et al., 2009; Toledo-Ortiz et al., 2014). The bZIP transcription factor HY5 controls many different light-modulated processes including hormone accumulation, light-developmental responses, anthocyanin and photopigment biosynthesis, and reactive oxygen stress responses in high-light (Kobayashi et al., 2012; Toledo-Ortiz et al., 2014; Gangappa and Botto, 2016).

HY5 is affected by phytochrome abundance (Lee et al., 2007); phyB suppresses the activity of COP1, an E3 ubiquitin ligase that suppresses photomorphogenesis-promoting transcription factors like HY5 through proteasome-mediated degradation (Li et al., 2011b). Without COP1 accumulation in the nucleus, HY5 accumulates. Genome wide chromatin immunoprecipitation (chip) experiments established that HY5 binds to the promoters of approximately 20% of all light-inducible genes, inducing both up- and down-regulation (Lee et al., 2007). HY5 recognition sites in the promoters of light modulated genes include multiple motifs, such as G-box, T/G-box, E-box, ACE-box, Z-box, GATA-box, and hybrids therein (Gangappa and Botto, 2016).

In addition to transducing red-light signals through phyB, HY5 also integrates blue light signalling inputs from the cryptochromes (Wang et al., 2017). Like phytochromes, cryptochromes also target COP1 and allow accumulation of HY5 in the nucleus. This allows HY5 to promote photomorphogenesis in both light conditions (Osterlund et al., 2000), including the regulation of plastid and nuclear gene expression mechanisms (Griffin et al., 2020) .

HY5 has also been connected to other inputs, including the circadian clock and temperature. Like phyB, HY5 is also temperature-sensitive, especially at cooler temperatures where it contributes to modulation of greening (Toledo-Ortiz et al., 2014; Jung et al., 2016; Legris et al., 2016). Toledo-Ortiz et al (2014) demonstrated that carotenoid and chlorophyll levels vary at different temperatures, accumulating at higher levels at higher temperatures and lower levels in cooler conditions, finding this was HY5-dependent. HY5 is also involved in circadian responses and can bind to four clock oscillator components: dusk regulators TIMING OF CAB1 (TOC1) and EARLY FLOWERING 4 (ELF4), and dawn regulators CIRCADIAN CLOCK ASSOCIATED 1 (CCA1) AND LATE ELONGATED

HYPOCOTYL (LHY) (Lee et al., 2007; Andronis et al., 2008; Li et al., 2011a; Gangappa and Botto, 2016).

By integrating multiple light wavelengths and circadian responses, HY5 is therefore a master regulator of light responses. While many of the described functions of HY5 relate to the setup of nuclear signalling cascades, recent research points at the relevance of HY5 in controlling genes that act in the chloroplast such as the sigma factors and plastid Transcriptionally Active Chromosome (pTAC) family (Pfalz et al., 2006; Chen et al., 2010; Mellenthin et al., 2014) involved in the transcription of the plastome. Bioinformatic studies suggest that HY5 could be an important component for the light dependent regulatory mechanisms linking the activity of the photoreceptors to the expression of the chloroplast genome (Ruwe et al., 2011; Griffin et al., 2020), and therefore a key regulator of photosynthesis.

1.3. Chloroplast RNA Binding Proteins (cpRNPs): a new role for phytochrome in Post-Transcriptional Regulation?

1.3.1. Regulation of the chloroplast genome expression.

The chloroplast genome, also known as the plastome, is evolutionally separate to that of a plant nucleus. Originally free-living cyanobacteria, chloroplasts became integrated into plant cells and entered into an endosymbiotic relationship, after which the chloroplast genome subsequently shrunk to around 200 genes (Martin and Kowallik, 1999). Comparisons of typical cyanobacterial genomes containing around 5,000 nuclear-encoded gene products, against contemporary plastid genomes that encode between 60-200 proteins (Raven and Allen, 2003) show that over time, genes from the plastid genome migrated to the nuclear genome.

As described in section 1.1.2, many of the components of the photosynthetic apparatus are encoded across both the chloroplast and the nuclear genomes. For example, genes *psaA*, *psaB*, *psbA*, and *psbB* for Photosystem II remain in the chloroplast, but genes *PSBO*, *PSBP*, *PSBQ*, and the LHCII genes are encoded in the nucleus (Sugiura, 1992; Jarvi et al., 2015). This gene migration likely allowed greater regulatory control over the chloroplast by the plant nucleus in synchronising gene expression to environmental conditions, increasing resource use efficiency and improving the whole organism fitness (Mullet, 1988a). Accordingly, the gene expression mechanisms must also be tightly co-ordinated.

Transcriptional regulation of the plastome. Chloroplast gene expression is mediated by two RNA polymerases: the plastid-encoded plastid RNA polymerase (PEP) and the nuclear-encoded plastid polymerase (NEP) (Börner et al., 2015). The PEP transcribes proteins for photosynthetic machinery, and the NEP transcribes components for plastid transcription and translation regulation (Börner et al., 2015). This divides expression into three classes: class I expression is exclusively by PEP, and involves photosynthesis-related genes; class II expression involves housekeeping genes by both PEP and NEP; and class III genes that involve polymerase transcription are transcribed by NEP (Allison et al., 1996; Hajdukiewicz et al., 1997). The specificity of transcriptional regulation of the plastome is regulated by the sigma factors, a family of six genes in Arabidopsis (Lerbs-Mache, 2011). Knockout mutants and recombinant protein studies have been used to deduce that SIG1 binds the Large Rubisco subunit (*rbcL*) and *psbA*, a gene encoding the D1 reaction centre precursor (Privat et al., 2003); SIG2 binds PSII subunits that complement the chlorophyll-deficient phenotype (Nagashima et al., 2004b); and SIG3 and SIG4 may influence the expression of the *psbB* operon and *ndhF* but *sig3*

and *sig4* mutants do not show notable phenotypes (Favory et al., 2005; Zghidi-Abouzid et al., 2011). SIG5 is responsive to blue light and regulates the *psbD-psbC* operon encoding the D2 reaction centre protein and chlorophyll-binding antenna CP43 of PSII (Nagashima et al., 2004c; Nagashima et al., 2004a). The *sig6* mutant shows major chlorophyll deficiencies in the cotyledons, affecting *psb*, *ndh*, and *psb* transcripts (Ishizaki et al., 2005; Loschelder et al., 2006). The sigma factors were the first link made between the nuclear photoreceptors and light signalling components, like HY5, and the transcriptional control of the plastome (Oh and Montgomery, 2014; Griffin et al., 2020). However, chloroplast gene expression involves the co-transcription of often large, polycistronic precursor RNAs that require a large degree of RNA processing (Sugita and Sugiura, 1996) to generate mature and translatable mRNAs. Therefore, post-transcriptional regulation is a highly significant in the modulation of plastid gene expression.

Post-transcriptional modulation of the plastome. Research by Deng et al (1989) first indicated that a primary mechanism for regulation of chloroplast gene expression occurs through post-transcriptional processes. In different light conditions, the differential accumulation of plastid transcripts could not be explained by transcriptional mechanisms. Similar levels of transcriptional activity were observed occurring in contrasting light conditions, despite differences in active transcript accumulation, and it was deduced that an additional level of post-transcriptional regulation was therefore a major contributor (Deng et al., 1989). Post-transcriptional editing can involve site-specific editing of RNA sequences, nucleolytic enzymes, and translational events. In all post-transcriptional modulatory events, RNA-binding proteins (RBPs) play essential roles and are required for normal plant growth and development (Gutteridge et al., 2018).

However, there are multiple families of RBPs and their functions are still under investigation. Among the chloroplastic RBPs, the pentatricopeptide repeat proteins (PPRs) are a major family: containing approximately 100 members in both rice and *Arabidopsis*, PPRs recognise their RNA ligands with a high specificity (Lurin et al., 2004; Schmitz-Linneweber et al., 2005; Sugita et al., 2016). PPRs perform roles in RNA metabolism in chloroplasts and are also involved in RNA editing, splicing, and cleavage (Hashimoto et al., 2003; Schmitz-Linneweber et al., 2005; Okuda et al., 2007). A second large family of chloroplast RBPs is the RRM family, containing 23 members (Ruwe et al., 2011). Among the RRMs, the largest subgroup is the Chloroplast RNA-Binding Proteins (cpRNPs) family (Li and Sugiura, 1990). Members of this family have been documented as environmental sensors for cold (Kupsch et al., 2012) and are linked to light-induced activation (Li and Sugiura, 1990; Schuster and Gruissem, 1991; Churin et al., 1999; Wang et al., 2006). In addition, 4 members of the family were identified as phyB-induced genes during de-etiolation (Tepperman et al., 2006).

1.3.2. The cpRNPs are key Post-Transcriptional Regulators of Photosynthesis.

The cpRNPs were first identified as a family of 5 proteins in tobacco, and more were identified in maize, spinach and later 10 cpRNPs were described in Arabidopsis (Li and Sugiura, 1990; Schuster and Gruissem, 1991; Ohta et al., 1995). All cpRNPs nuclear-encoded and imported into the chloroplast post-translationally, accumulating in the stroma and plastid nucleoid (Nakamura et al., 2001; Melonek et al., 2016). Studies on the spinach 28RNP determined that cpRNPs could bind specifically to RNA transcripts- notably regulate the 3' UTR processing required for RNA stabilisation (Lisitsky and Schuster, 1995). Since then, cpRNPs have been characterised by their global RNA-binding capacity to the plastid-encoded genome and their contribution to photosynthesis-associated transcript accumulation (Ruwe et al., 2011; Kupsch et al., 2012; Teubner et al., 2017).

Members of the cpRNP family are 250 to 370 amino acids (aa) long and consist of an N-terminal transit peptide, an acidic region, and two RNA-Recognition Motifs (RRM) separated by a 10-20 aa long spacer (Ohta et al., 1995; Sugita et al., 2016) (Figure 1.2). The RRM are canonical consensus sequences, called RNP1 and RNP2, and bind RNA via hydrophobic and stacking interactions between conserved aromatic sidechains- the presence of two RRM in a single protein allows long RNA sequences to be bound, and with higher affinity (Maris et al., 2005; Cléry et al., 2008).

cpRNPs are conserved across dicot plants. Previous phylogenetic analysis using the amino acid sequences of first RRM for each cpRNP showed that the family is conserved in dicot higher plants (Ohta et al., 1995). This phylogenetic analysis further grouped cp29A, cp31A and cp33A into distinct subgroups by sequence similarity; some cpRNP members were later identified as paralogues of each other and it was hypothesised that there may be gene duplication and functional redundancy between family members (Churin et al., 1999; Tillich et al., 2009). Phylogenetic analysis of a wider range of RNPs revealed a long-term conservation of binding domains for RNPs between PABP, the cpRNPs, hnRNPs, and nucleolin (Maruyama et al., 1999). This suggested a potentially similar role for cpRNPs to the hnRNPs, which target RNA transcripts in the nucleocytoplasm for RNA processing (Ruwe et al., 2011).

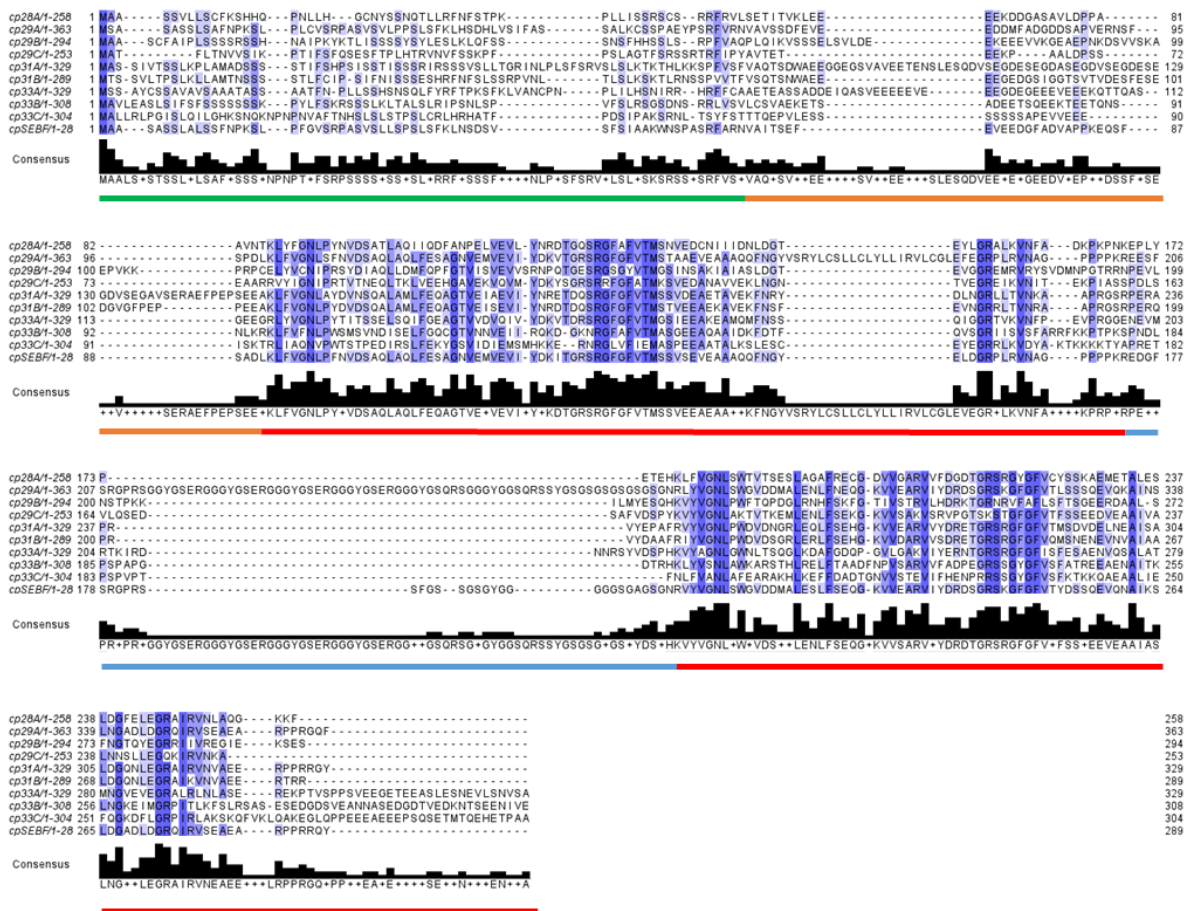


Figure 1.2. The *Arabidopsis thaliana* cpRNP family contain a chloroplast transit peptide (green), acidic domain (orange), two RNA Recognition Motifs (RRM) (red), and a linker domain (blue) indicated in a coloured bar at the bottom. Protein sequences were aligned in MEGA X using a pairwise alignment (Kumar et al., 2018). Conserved regions are indicated by strength of conservation in the 'Consensus' bar beneath the alignments. Accession numbers are listed in Supplementary Table 1.1.

1.3.3. cpRNPs are Global Post-Transcriptional regulators of Plastid Gene Expression

cpRNPs were identified to be co-expressed with many photosynthetic mRNAs and were suggested play a role in their expression (Mentzen and Wurtele, 2008; Cho et al., 2009). Current studies indicate that cpRNPs regulate mRNA transcripts associated to photosynthesis through a variety of RNA processing mechanisms, including 3' ends processing, mRNAs splicing, message stabilization, and protection from nuclease activity (Zoschke and Bock, 2018). Following the identification that cpRNPs can bind ribosome-free RNA, (Nakamura et al., 2001), functional characterization of individual members revealed a role for cp31A in *Nicotiana benthamiana* in the editing of *psbL* mRNA (Hirose and Sugiura, 2001), and later for cpRNPs in 3' UTR processing and protection (Loza-Tavera et al., 2006; Tillich et al., 2009). In *Arabidopsis*, transcripts of *psaA*, *psbD*, *psbF*, *psbB*, *petB*, and *rbcl* were also found to have defects in their processing and editing in *cp31a* and *cp29a* mutants, correlating with disruption of the electron transport chain and impaired photosynthesis (Kupsch et al., 2012). In *cp33a* mutants, accumulation of *ndhB*, *psbA*, *rbcl*, and *psbF* transcripts was reduced, and a lower accumulation of chlorophyll biogenesis proteins from PSI and PSII was reported in sucrose-supplemented, Long Day (LD)-grown plants (Teubner et al., 2017).

cpRNPs' RNA processing occurs through the binding of RNA transcripts via two RNA Recognition Motifs (RRMs) (Ruwe et al., 2011). Each cpRNP has two RRM: RNP1 and RNP2 (Lorković and Barta, 2002); structurally, RRM are four-stranded beta pleated sheets packed against two alpha helices and can bind between two and eight nucleotides, and affinity for RNA increases with the number of RRM bound to a sequence (Ruwe et al., 2011). The binding specificity of cpRNPs is site-specific (Schuster et al., 1999; Hirose and Sugiura, 2001), and is predicted to be modulated by phosphorylation sites in the acidic domain (Lisitsky and Schuster, 1995; Okuzaki et al., 2019).

Current in-vivo RIP-chip evidence indicates that cpRNPs are capable of binding all the major groups of chloroplast RNAs, including RNA polymerases, ATPases, both photosystems, and the NDH complex (Kupsch et al., 2012; Teubner et al., 2017). This global binding capacity across the plastome encoded mRNAs indicates that they may be general modulators of post-transcription in contrast to the far more specific TPR and PPR families (Sugita et al., 2016).

However, cpRNPs themselves may not perform all the specific RNA modifications themselves and instead function as scaffold proteins for associating to multiple RNA processing high molecular weight complexes (HMWCs). For example, Hayes et al (1996) reported the association of the spinach 28RNP to an HMWC involved in RNA processing that contained an exoribonuclease polynucleotide phosphorylase (PNPase)-like activity. When the 28RNP did not associate to the 3' end of *petD*, this

mRNA could not be processed and transcript abundance was low. Processing and accumulation of the *petD* was reconstituted with the presence of the 28RNP (Hayes et al., 1996).

Yet, acting directly or indirectly, current experimental evidence supports an important role of cpRNPs in plastid mRNAs post-transcriptional control, and their removal reduces accumulation of multiple plastome transcripts. Preliminary experiments by Toledo-Ortiz et al (personal communication) for *Arabidopsis cp29b-1* and *cp31a-1* knockout mutants during de-etiolation show a greening phenotype (Figure 1.3), and defects in photopigment accumulation at 17°C compared to Wild-Type (WT) plants.

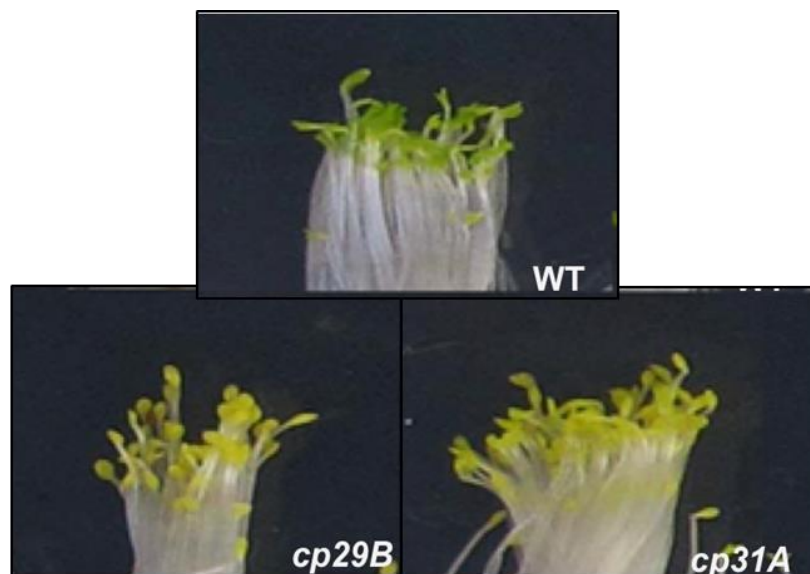


Figure 1.3. De-etiolating *cprnp* mutants *cp29b* and *cp31a* express greening deficient phenotypes compared to WT. Plants were grown for 3 days in darkness and treated with 24hrs of red light ($80 \mu\text{mol m}^{-2}\text{s}^{-1}$) at 17°C. Images were generated and provided by Dr. Gabriela Toledo-Ortiz (personal communication).

1.3.4. cpRNPs are integrators of multiple environmental signals.

cpRNPs are expressed abundantly throughout green tissues, and genomic studies revealed their transcript modulation by light, temperature, and potentially photoperiodicity (Zimmerman et al., 2004). Repression of cpRNP gene expression has also been documented following pathogen attack and hypoxia in a similar fashion to the PPR family (Zimmermann et al., 2005).

cpRNP expression is light-inducible and expressed in aerial tissues. In *Arabidopsis*, microarray data shows that light-grown plants accumulate higher cpRNP transcripts than dark grown plants, especially during the dark-light transition in de-etiolating plants (Dohmann et al., 2008). Light-inducible expression was also detected for cpRNPs across a range of plant species beyond *Arabidopsis* including tobacco, spinach and barley (Li and Sugiura, 1990; Schuster and Gruijssem, 1991; Churin et al., 1999; Wang et al., 2006). Expression of cpRNPs is notably found to be higher in aerial shoot and leaf tissues compared to a lower expression in the roots, further indicating an association with tissues exposed to light (Li and Sugiura, 1990; Churin et al., 1999). In this respect, data from the ePlant database, from the Bio-Analytic Resource for Plant Biology (BAR) (Waese et al., 2017) (Figure 1.4), shows *cp31A* transcript accumulation in different vegetative states. Similar expression profiles were observed for other members of the family (Supplementary Figure 1.1) with transcript accumulation in vegetative rosettes, and especially in the youngest leaves, but remains high in leaves over the course of the plant life cycle. These patterns indicate that cpRNPs accumulation is tied to photosynthetic tissues.

cpRNPs promoter sequence elements may be involved in their light-inducible expression patterns. A sequence analysis of *cpRNPs* promoters reveals that several family members include light regulatory elements in their promoters. These elements include but are not limited to the G-box, Light Responsive Elements (LRE), A-box, C/G-box, and ACGT-containing element (ACE) (Toledo-Ortiz, unpublished). The G-box motif is a promoter motif typically bound by bZIP and bHLH proteins (Ishige et al., 1999; Leivar et al., 2012). The presence of these elements suggest a close relationship of light to the transcriptional modulation of this genes, and a potential role for of photoreceptor signalling components such as phyB and HY5 in their modulation (Gangappa and Botto, 2016). In addition to classical light regulatory elements, *cp29A*, *cp29B*, *cp31A*, and *cp33C* all contain a promoter motif for CCA1, which hints at a potential for these cpRNPs to integrate light and circadian signalling (Seaton et al., 2014).

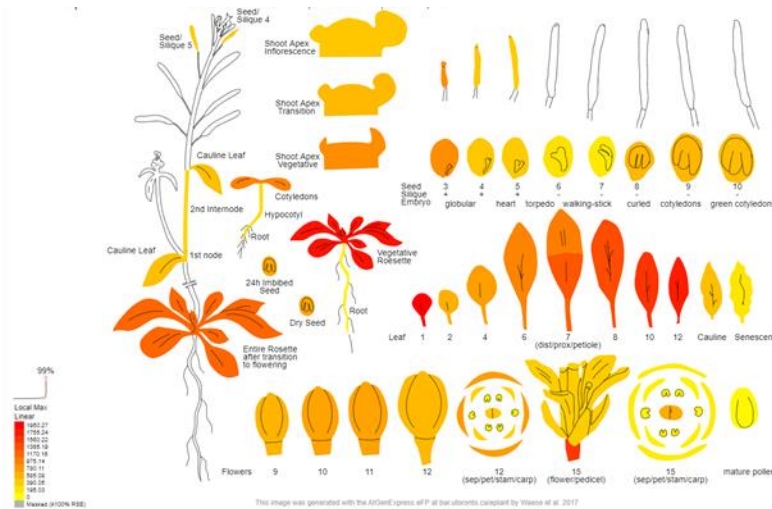


Figure 1.4. Bioinformatic data shows that *cp31A* is expressed highly in leaf tissue, especially both early in development and just before senescing leaf. Data was obtained and reproduced from ePlant database (Schmid et al., 2005, Nakabayashi et al., 2005, Waese et al., 2017). Scale bar indicates a linear expression intensity of protein to the subcellular compartment on a scale of lowest (yellow) to highest (red) probability.

cpRNP activity is modulated by light-dependent phosphorylation. Lisitsky and Schuster (1995) first identified that cpRNPs can be phosphorylated in a light-dependent manner. Although the role of phosphorylation on cpRNPs remains unclear, phosphorylation of the cpRNPs occurs within the acidic domain (Reiland et al., 2009; Okuzaki et al., 2019). For *Spinacia oleracea* CP28, light-induced phosphorylation was shown to impair its RNA-binding ability *in-vitro*, however phosphorylation for CP24 increased RNA binding, resulting in more stable RNA/RNP complexes and protection from endolytic cleavages (Lisitsky and Schuster, 1995; Loza-Tavera et al., 2006; Vargas-Suárez et al., 2013). Phosphorylation has further been reported for cp29 in *Oryza sativa* (rice) (Kleffmann et al., 2006), and for Arabidopsis cp31A, linked to the cold acclimation response (Schönberg and Baginsky, 2012; Okuzaki et al., 2019).

cpRNP expression and activity is also linked to a cold-temperature response. Cold temperature treatments can affect cpRNP protein abundance of cp29, cp31, and cp33 in the chloroplast stroma in *Triticum aestivum* (wheat) (Sarhadi et al., 2010). A similar increase in protein abundance in the stroma was observed for cp29B and cpSEBF after cold-shock and cold acclimation treatments of Arabidopsis (Amme et al., 2006; Goulas et al., 2006). Further experimental evidence of a role for cpRNPs in the cold was provided for *cp29a* and *cp31a* mutants, for which cold stress induced a bleaching phenotype in newly emerged tissues; this cold-induced phenotype was rescued when the plants were returned to physiological conditions (Kupsch et al., 2012). A screen of 11,000 T-DNA

mutants for a sensitivity to chilling also identified *cp29A* and *cp31a* mutants that exhibited a bleaching phenotype and lowered biomass accumulation at 4°C (Wang et al., 2016).

Based on their described sensitivity to light and temperature, cpRNPs may therefore be molecular integrators of signals that are delivered to the chloroplast, and a link to the signalling pathways of the photoreceptors.

1.3.5 cpRNPs may be involved in plastid-to-nuclear communication.

Chloroplast biogenesis, operation, and development is influenced by the flow of information between nucleus and the organelle (Chan et al., 2016). There are two signalling pathways regulating this: an anterograde pathway from the nucleus to the chloroplast to direct protein expression, and a retrograde pathway in the opposite direction to allow the chloroplast to communicate stressors to the nucleus following the original endosymbiosis event (Krause et al., 2012; Berry et al., 2013). As reviewed by Berry et al (2013), these signalling networks are dynamic, and can respond to many different stimuli to adjust gene expression to the environment.

In the anterograde signalling pathways, chloroplast gene expression is regulated through transcriptional, post-transcriptional, and translational processes by nuclear-encoded trans-acting factors, including RNA-binding proteins like the cpRNPs (Stern et al., 2010; Barkan and Goldschmidt-Clermont, 2000). The retrograde signalling pathway relays information about the status of chloroplast to the nucleus, and involves multiple signalling molecules, including a combination of carotenoid derivatives, isoprenoids, phosphoadenosines, tetrapyrroles, heme, and reactive oxygen species (Chan et al., 2016).

In addition to participating in anterograde signalling pathways, some preliminary indications that cpRNPs point at a potential nuclear localization for some members of the family. A truncated form of Arabidopsis cp31A was identified to have nuclear DNA-binding capacity in regulating telomere length (Kwon and Chung, 2004) and Potato PR-10a- a homolog of Arabidopsis cpSEBF- is reported as a transcriptional repressor of the nuclear genes with a dual nuclear/chloroplast localisation (Boyle and Brisson, 2001).

1.4. Hypotheses and aims.

This thesis will explore the primary hypotheses that:

1. Phytochrome B (phyB) acts in the nucleus to orchestrate post-transcriptional signalling pathways involved in coordinating photosynthesis, plant growth, and development in response to environmental cues including light and temperature.
2. The chloroplast RNA-Binding proteins (cpRNPs) function as integrators of light and temperature environmental signals to maintain photosynthesis.
3. cpRNPs are involved in nuclear gene regulation, and their regulation may be linked to retrograde signalling pathway.

The specific aims of this thesis are to:

1. Identify the contribution of cpRNP activity to the phytochrome R-light signalling cascades controlling greening, biomass production and photosynthesis. (Chapter 2)
2. Address if the cpRNPs are part of the mechanisms involved in adjusting chloroplasts, not only to light quality, but to changing light environments including high-intensity light and photoperiods. (Chapter 2)
3. Address if the cpRNPs' environmental sensing capacity extends to the co-ordination of light and temperature responses. (Chapter 2, Chapter 3)
4. Investigate the molecular mechanisms behind cpRNP function as phy signalling components, including their chloroplastic targets. (Chapter 3)
5. Address whether the cpRNPs act beyond the chloroplast and can be involved in retrograde signalling communication channels. (Chapter 3)
6. Investigate a role for cpRNPs in plastid-to-plastid transitions using tomato as a model plant. (Chapter 4)

Chapter 2: Characterising the cpRNPs as Novel Candidates for the Environmental Regulation of Photosynthesis

2.1 Introduction.

Recent advances in research have provided evidence that the phytochrome (phy) photoreceptor family are significant modulators of the regulatory mechanisms for chloroplast genome, or plastome, gene expression (Griffin et al., 2020). The first links to the modulation of the plastome came from studies addressing transcriptional mechanisms and the role of light signals in the modulation of sigma factors, the Plastid-Encoded Polymerase (PEP), and HEMERA (HMR) complexes (Chen et al., 2010; Oh and Montgomery, 2013; Yoo et al., 2019). Yet, the role of the phytochromes in modulating other levels of plastome expression, such as for post-transcriptional regulatory mechanisms, has not been explored in-depth. Genome-wide bioinformatics studies (Griffin et al., 2020) identified that, in particular, red light signals and phyB controlled the expression of a number of RNA-binding proteins with a predicted function in the chloroplast. Among the RNA-binding proteins identified were members of the Chloroplast-RNA Binding protein family (cpRNPs).

Four members of the cpRNP family were among genes early identified to be modulated by red light in a phy-dependent manner (Tepperman et al., 2006). This transcriptional control by light may indicate that cpRNPs may be components linking phyB to the light signalling cascades that deliver light environmental signals to the plastome. cpRNPs act as post-transcriptional regulators of the chloroplast genome (Lisitsky and Schuster, 1995), and they are co-expressed with and involved in the modulation of transcript abundance of photosynthetic mRNAs (Nakamura et al., 2001; Mentzen and Wurtele, 2008; Kupsch et al., 2012).

cpRNPs represent interesting candidates to characterise for their significant role in regulation of the plastome through RNA processing (Loza-Tavera et al., 2006; Tillich et al., 2009). In comparison to other chloroplast RNA binding protein families, such as the Pentatricopeptide-domain containing (PPR) family, cpRNPs have a global binding capacity for the plastome (Kupsch et al., 2012; Teubner et al., 2017) and can therefore regulate multiple transcripts' accumulation for the whole photosynthetic apparatus, including the electron transport chain, Photosystems I and II, NADH Dehydrogenase, and carbon fixing processes (Kupsch et al., 2012).

Additionally, cpRNPs are expressed abundantly throughout green tissues, with genomic studies revealing that cpRNPs' transcript abundance is regulated by light and temperature (Zimmermann et al., 2005). cpRNPs are therefore potential integrators of a wide range of environmental signals to globally regulate the plastome. Their characterisation could lead to a better

understanding of how the plastome perceives and adapts to environmental cues and could have a future impact on the development of new strategies to modulate photosynthesis in crops.

This chapter examines the role of cpRNPs, post-transcriptional regulators of plastid-encoded RNAs, as new components in the environmental regulation of photosynthesis coordinated by the phytochrome photoreceptors. Using a reverse genetics approach and a variety of different light and temperature environmental conditions, the function of the cpRNPs in growth responses and greening was evaluated. To elucidate the molecular basis of their contribution to photosynthesis and greening responses, the transcript abundances of photosynthesis-associated genes were examined.

The specific aims of this research are:

- 1) To identify the contribution of the cpRNPs to the phytochrome R-light signalling cascades controlling greening, biomass production and photosynthesis.
- 2) To address if the cpRNPs are part of the mechanisms involved in adjusting chloroplasts, not only to light quality, but to changing light environments including high-intensity light and photoperiods.
- 3) To address if the cpRNPs' capacity to integrate environmental signals involves the integration the coordination of light and temperature responses.

2.2 Materials and Methods.

2.2.1 Plant material and genotypes tested.

To evaluate the impact of different environmental inputs on cpRNP transcript abundance and contribution to physiological responses, *Arabidopsis thaliana* wild-type (Col-0), *phyB-9* (Col-0) and *hy5-215* (Col-0) mutants were used. The stock of *phyB-9* mutant used was confirmed to be a true *phyB-9* mutant after sequencing and did not contain a second-site mutation in the *VENOSA4* gene (Yoshida et al., 2018). The following *cprnp* mutants were used: *cp29b_2* (SALK_043415 (S), N543415), *cpsebf_1* (SALK_008984C, N681974), and *cp31a_2* (SALK_109613C, N664816), sourced from the Nottingham Arabidopsis Stock Centre.

2.2.2. Genotyping mutant plants.

Mutant *cprnp* lines (*cp29b_2*, *cpsebf_1*, and *cp31a_2*) were genotyped to confirm the homozygous presence of the T-DNA insert (position shown in Supplementary Figure 2.1). Genomic DNA (gDNA) was extracted by grinding a tissue sample with a pestle and mortar in a 1.5ml Eppendorf tube and adding Thompson Buffer (65% v/v MilliQ H₂O, 20% 1M Tris pH7.5 v/v, 5% 5M NaCl v/v, 5% 0.5M EDTA v/v, 5% SDS (10%) v/v, vortexing, centrifuging (14,000 x g) to separate supernatant, and then removing 300µl to a new tube and adding an equal volume of 2-propanol. Samples were incubated at room temperature and centrifuged (14,000 x g) again to precipitate gDNA on the outer edge of the tube; supernatant was removed and gDNA was resuspended in T.E. Buffer overnight. gDNA was then analysed via PCR using genotyping primers shown in Table 2.1 below. PCR used Redtaq DNA Polymerase Biomix (Bioline, BIO-25043), primers (3µM), and water, according to manufacturers recommended guidelines and scaled to a 10µl reaction volume. An Eppendorf Mastercycler personal PCR machine was used with the following thermal cycling program: 95°C for 1 min, followed by 30x cycles of a denaturation step of 95°C for 15 sec, annealing step of 60°C for 15 sec, and 72°C extension step for 10 sec. Finally, samples were subject to a final 72°C extension for 5 min and cooled at 4°C until collected. This product was then run through a 1.2% (w/v) agarose gel to detect correct band sizes.

Following genotyping, *cpRNP* transcript abundance was measured in the respective mutants using qPCR primers shown in Table 2.1 and methods described in 2.2.7. The *cp29b_2* mutant was identified as showing a -80% expression reduction compared to WT; the *cpsebf_1* mutant was identified as a knock-down showing a -50% expression reduction compared to WT; and the *cp31a_2* mutant is a null mutant showing a -100% expression reduction compared to WT. Primers were targeted to the 3' end of target cpRNP cDNA, overlapping with the 3' untranslated region.

Table 2.1. Genotyping primers (supplied by Eurofins) used in Chapter 2 to identify homozygous T-DNA insertions in mutant plants.

<i>Arabidopsis thaliana</i> Primers		
Genotyping Primers	<i>cp31A_gDNA_F</i>	TGATGGGATATTGCTCCTTTG
	<i>cp31A_gDNA_R</i>	AGAAGCCTTTCATTCTCAGCC
	<i>cp29B_gDNA_F</i>	GTTCTGCTTTGGAGACGACAC
	<i>cp29B_gDNA_R</i>	TACAGATGTGAGGACCCCAAG
	<i>cpSEBF_gDNA_F</i>	ACTCACAAATTGGGGAAAACC
	<i>cpSEBF_gDNA_R</i>	GAAGGACGCGTTTGTATGATC
	<i>LBb1.3</i>	ATTTTGCCGATTTTCGGAAC

2.2.3. Seed Sterilisation and Sowing.

Arabidopsis thaliana seed were sterilised via treatment with a 15% (v/v) bleach solution for 10 min, and dilution and washing with sterilised distilled water. Seeds were plated using a Pasteur pipette.

2.2.4 Plant Growth Conditions.

Plants were grown on 0.5 MS agar (Murashige and Skoog, 1962) with 0% sucrose. Plants were grown in Snidjer Clima Red/Blue Light Monochromatic Light Cabinets, model EB2-N-PB. Plants were germinated with a 3hr white light treatment followed by 21hr darkness at 22°C before being moved to experimental conditions.

Greening-dependence during de-etiolation and gene expression assays. Plants were grown in de-etiolating conditions- after germination plants were kept in darkness for 3 days to promote skotomorphogenesis followed by a treatment of 24hr Red Continuous ($80 \mu\text{mol m}^{-2}\text{s}^{-1}$) at either 17°C, 22°C, or 27°C.

Light Intensity experiments. Plants were grown for 10 days in alternating 1hr High Light (HL) intensity (Red light $150 \mu\text{mol m}^{-2}\text{s}^{-1}$) and 1hr Low Light (LL) (Red light $50 \mu\text{mol m}^{-2}\text{s}^{-1}$), or for 2hr HL and 6hr LL.

Photoperiodic phenotyping experiments. Plants were grown for 10 days in $80 \mu\text{mol m}^{-2}\text{s}^{-1}$ Red light in Long Day (LD) conditions (16hr Light, 22°C/ 8hr Dark, 17°C) or Short Day (SD) conditions (8hr Light, 22°C/16hr Dark, 17°C).

Temperature phenotyping experiments. Plants were grown for 10 days in Red Continuous (RC) light at $80 \mu\text{mol m}^{-2}\text{s}^{-1}$ at either 17°C, 22°C, or 27°C prior to harvest.

2.2.5 Plant Harvesting

Phenotyping Experiments. When ready for harvest, plants were photographed for representative records of growth and weighed for fresh weight (FW). 6 plants were measured for each of the three minimum biological replicates, and then plants were frozen in liquid Nitrogen ($N_{2(l)}$) for chlorophyll extraction. Chlorophyll quantification was performed using frozen plant tissues ground using pestles and mortars and mixed with volumes of ice-cold 80% (v/v) acetone and centrifuged at 10,000 rpm for 15 min until pellets were white. Samples were then measured in a 96-well microplate reader (SpectroStarNano, BMG Labtec, Aylesbury, UK) and chlorophyll concentration calculated as described in Lichtenthaler & Buschmann (2001).

Gene Expression Analysis. Plants were harvested in a dark room with green light ambient illumination to prevent light contamination. Plants were harvested into liquid Nitrogen ($N_{2(l)}$) immediately to prevent degradation.

2.2.6 RNA Extraction and cDNA Synthesis.

RNA extraction was performed using a Sigma Aldrich Spectrum™ Plant Total RNA Kit and cleaned with Qiagen RNase Free DNase Set. RNA was quantified with a Nanodrop and 1µg of RNA was used. To validate its quality, 500ng of RNA was stained with ThermoFisher 6x DNA Loading Dye and run through a 0.5% (w/v) agarose gel. To synthesise cDNA, a Thermo Scientific™ RevertAid First Strand cDNA Synthesis Kit was used according to manufacturer's instructions. For experiments analysing plastid gene expression, Random Hexamer Primers were used in the cDNA synthesis (Schuster et al., 1999), and for experiments analysing nuclear gene expression Oligo dTs were used.

2.2.7 Quantitative RT-PCR Analysis.

RT-qPCR analysis was performed using 5µl PrimerDesign PrecisionPLUS qPCR Master Mix premixed with SYBR Green, 1µl of 3µM Forward and Reverse primer, 1µl of sample cDNA, and 2µl of sterilised water in a 10µl reaction volume. The reaction was performed using a Stratagene Mx qPCR Machine with the following thermal cycling program: 95°C for 10 min, followed by 40x cycles of 95°C for 10 sec, 60°C for 10 sec, and 72°C for 15 sec followed by melting curve from 65°C to 95°C to ensure primer targeting specificity. At least two technical replicates of each biological replicate were performed, and the mean values were used for further calculations. Results were analysed using Stratagene Mx PRO software and Microsoft Excel. Results were normalised to *PP2A* reference gene (Klie and Debener, 2011) for its light-stable properties compared to classical reference genes *ACT2*

or *SAND*, and relative gene expression was calculated as described in Pfaffl's methods for analysing LightCycler PCR data (Pfaffl, 2001). A full list of primers is presented below in Table 2.2.

Table 2.2 qPCR Primers used in Chapter 2. Reference genes were used to identify a stable transcript accumulation to compare experimental gene expression against; *cpRNP* gene primers were used to identify the red light- and phyB-dependency of *cpRNPs*; and plastid-encoded gene primers were used to quantify a contribution of *cpRNPs* to photosynthesis-associated plastid-encoded gene expression.

<i>Arabidopsis thaliana</i> qPCR Primers		
Reference Genes	<i>ACT7_F</i>	CAGTGTCTGGATCGGAGGAT
	<i>ACT7_R</i>	TGAACAATCGATGGACCTGA
	<i>PP2A_F</i>	TATCGGATGACGATTCTTCGTGCAG
	<i>PP2A_R</i>	GCTTGGTCGACTATCGGAATGAGAG
<i>cpRNP</i> Genes	<i>cp28A_F</i>	CTCGATGGAAGTCTGATCTTGG
	<i>cp28A_R</i>	TGGATACAGAGGTTCTTTGTTAGG
	<i>cp29A_F</i>	GCAGCTCAACAGTTCAATGG
	<i>cp29A_R</i>	GCCTTCAAATTCAAGTCCACAC
	<i>cp29B_F</i>	CAATGGAACACAATATGAAGGTCG
	<i>cp29B_R</i>	AAAGCAGAACAGTTGGTTTACG
	<i>cpSEBF_F</i>	TTGGATGGTGCTGATTTGGA
	<i>cpSEBF_R</i>	ATAGGAAGTCATAGATTGGTGCTC
	<i>cp29C_F</i>	ACCTGGAACTTCCAAATCCAC
	<i>cp29C_R</i>	CTTCCAGCAACGAATTGTTAAGAG
	<i>cp31A_F</i>	CGATGGACAGAACTTGGAGG
	<i>cp31A_R</i>	TCTCAGCTTTAATATCCACGCC
	<i>cp31B_F</i>	CAATGAGTACAGTTGAAGAAGCAG
	<i>cp31B_R</i>	TCTGTTTACTGTCAAACGCCT
	<i>cp33A_F</i>	CTGCTTTGGCTACAATGAATGG
	<i>cp33A_R</i>	TACGGAAGGAGGAGACACAG
	<i>cp33B_F</i>	AACTCAATGGGAAGGAGATAATGG
	<i>cp33B_R</i>	TGTTAGCTTCTACACTGTCACC
	<i>cp33C_F</i>	CAGATTGATTGCTCAGAATGTTCC
	<i>cp33C_R</i>	ACATCTCAATGTCGATAAACACTCC
Experimental plastid-encoded genes	<i>atpA_F</i>	AAGCTTCTCCGTGGCTCA
	<i>atpA_R</i>	CTCCTGTATAAGGCGCGAGG
	<i>atpH_F</i>	TTCTGCCTCAGGTTGTCTCG
	<i>atpH_R</i>	TCGGTTATTGCTGCTGGGTT
	<i>atpI_F</i>	ACAATTCCAAGTACGCGCCA
	<i>atpI_R</i>	TTCCACGGTAAAAGGGCTCC
	<i>ndhG_F</i>	GTAGCTGCTGCACAACCTCT
	<i>ndhG_R</i>	CCCCGTACCATGACGTATCG
	<i>petA_F</i>	AGGGGCTTTGAATGTGGGAG
	<i>petA_R</i>	GCAGGGTCTGGAGCAAGAAT

<i>petB_F</i>	TGTTCTCCGCATGTCAACA
<i>petB_R</i>	GCCGACCATCGATGAACTGA
<i>petD_F</i>	CCTGCGGATCCTTTTGCAAC
<i>petD_R</i>	CGCGGTGCCAATCAAAAAGA
<i>petG_F</i>	TTTTTATTTGGAATCGTCTTAGGTCT
<i>petG_R</i>	AAAAGTCCAACCTGATCACCACG
<i>psaB_F</i>	TGGTTGCCTGGCTGGTTAAA
<i>psaB_R</i>	CACAAGTACCACCTCGTCCC
<i>psaJ_F</i>	ACATATCTTTCCGTAGCACCG
<i>psaJ_R</i>	AGGGAAATGTTAATGCATCTGGA
<i>psbA_F</i>	ATTCGGCGGCTCCCTTTTAA
<i>psbA_R</i>	CGGCCAAAATAACCGTGAGC
<i>psbC_F</i>	AGAACGACGTTCCGACAGAAT
<i>psbC_R</i>	CTTCCCGCGTGCCATAAATG
<i>psbD_F</i>	TTTCCCAGGAAATCCGTGCA
<i>psbD_R</i>	TCCACGTGGTAGAACCTCCT
<i>psbF_F</i>	CCTATCCAATTTTTACAGTGCGC
<i>psbF_R</i>	TCGTTGGATGAACTGCATTGC

2.2.8. Statistical Analysis.

Statistical analysis of the data was conducted in Microsoft Excel and R (Team, 2020) using One-Way ANOVA, Two-Way ANOVA, and TUKEY HSD post-hoc where appropriate testing at a significance level of 0.05.

Expression profiles of published datasets were analysed using Microsoft Excel and R (Team, 2020); significant differences in gene expression ratios were analysed with the package GSalightning (Chang and Tian, 2016) and the Mann-Whitney-Wilcoxon test for all genes and were adjusted using the Benjamini-Hochberg False Discovery Rate (FDR) at the significance level of 0.05.

2.2.9. Genomic Datasets Used

Publicly available genome-wide transcriptomic datasets were used to generate Figures 2.1, 2.4, 2.6, 2.11, and 2.12.

The microarray dataset GSE31587 (Hu et al., 2013) was used to generate Figures 2.1 and 2.6; this data was generated using 4-day old WT and *phyABCDE* Arabidopsis seedlings grown in darkness or under continuous red light ($50 \mu\text{mol m}^{-2}\text{s}^{-1}$). Microarray time-course dataset E-MEX-1299 (Michael et al., 2008) was used to generate Figure 2.4 and Figure 2.12, and was used 7-day old WT and *phyB-9* null knock-out mutant plants grown in SD conditions (8hr light ($100 \mu\text{mol m}^{-2}\text{s}^{-1}$) and 16hr dark) at 22°C. Microarray datasets GSE58552 (He et al., 2015), and GSE62119 (Kawashima et al. unpublished

data) were used to generate Figure 2.6; dataset GSE58552 used 4.5-day old WT and *cry1cry2* mutants grown in darkness or continuous blue light ($15 \mu\text{mol m}^{-2} \text{s}^{-1}$), and dataset GSE62119 used 3-day old WT and *hy5* grown under continuous white light (no intensity data provided). The Long Day datasets GSE50438 and data from the DIURNAL Database (Mockler et al., 2007) were used to generate Figure 2.11. Dataset GSE50438 was generated using Col-0 WT plants grown in LD conditions (16hr light ($56 \mu\text{mol m}^{-2} \text{s}^{-1}$) and 8hr dark) at 22 °C for nine to ten days. Microarray DIURNAL database data was generated using Ler WT seedlings grown in LD conditions (16hr light ($100 \mu\text{mol m}^{-2} \text{s}^{-1}$) and 8hr dark) at 22°C for eight days.

Dataset E-MEX-1299 was generated using Random Hexamer Priming technology; all other datasets were generated using oligo-dT based technology.

2.2.10. Selection of gene lists used for chloroplastic genome modulation functional categories.

GO-term categories corresponding to chloroplast regulatory mechanisms (GO:0009507), transcription (GO:0006350), post-transcription (GO:0010608) or translation (GO:0006412) were selected using TAIR website annotation. To identify genes with a function in the chloroplast, genes corresponding to these terms were corroborated with the GO term “chloroplast” (GO:0009507), and the final gene sets were manually curated to remove false positives.

From these gene sets a set of commonly occurring genes with R/B light- or phy/cry-sensitivity that were part of wider families/classes was manually identified. Three families/classes were selected for further examination in each one of the general plastome regulatory categories. Gene lists were manually curated for annotated members of the family that also had a chloroplast function. Where appropriate, the presence of specific functional domains was verified to corroborate classification. Light sensitivity for the genes analysed was established using WT data and an absolute log₂ ratio >0.5 difference compared to dark datasets. After establishing light-sensitivity, subsequent photoreceptor-dependency of these targets was calculated based on an absolute log₂ ratio >0.5. For each category, only a log₂ ratio >0.5 validated by multiple comparisons Wilcoxon test followed with FDR at 0.05 were considered as significant. A Chi² test was used to evaluate the significance of enrichment of differentially modulated genes in each category and differentiate enrichment from random observations. Statistical differences were defined as those with a P-value of <0.05.

2.3 Results: Characterization of cpRNPs in red-light responses.

2.3.1. phyB regulates post-transcriptional mechanisms of plastome gene expression.

Plastome gene expression involves transcription by nuclear- and plastid- encoded RNA polymerases (NEP, PEP) supported by transcriptional co-regulators known as sigma factors (Berry et al., 2013), in addition to extensive post-transcriptional RNA processing (Ruwe et al., 2011), and translational control (Chotewutmontri and Barkan, 2016). However, the plastid mRNAs' organization in polycistronic operons requires extensive processing, stabilization, editing, and splicing, therefore making post-transcriptional control a dominant process in plastid gene regulation (Stern et al., 2010; Barkan, 2011).

Before this work, the global contribution of phys to the light-dependent regulation of nuclear-encoded genes involved in plastid gene expression had not been widely explored. To further evaluate the potential extent of phys' contribution to plastome regulatory mechanisms, a GO-term biological function analysis using the GO-term categories "transcription" (GO:0006350), "post-transcription" (GO:0010608), and "translation" (GO:0006412) were overlapped with the GO-term "chloroplast" (GO:0009507) (see section 2.2. Material and Methods) to generate a shortlist of potential targets in datasets comparing dark vs illumination in different genetic backgrounds. The genes' R-light dependent up-regulation was defined by a log₂ ratio >0.5 vs darkness in the WT in response to R-light dataset (GSE31587) and the contribution of phys to the R-light response was evaluated by comparison between WT and phyABCDE, shown in Figure 2.1. The statistical significance of each factor was established using an FDR-adjusted multiple comparison Mann-Whitney-Wilcoxon at P<0.05 (see 2.2 Materials and Methods).

This investigation revealed that 9% (13 genes out of 141) in the transcription category, 26% (11 genes out of 43) in post-transcription, and 8% (21 genes out of 265) from the translation category were R-phys dependent (Figure 2.1). In addition, R-phys' modulation of genes defined by the GO-term biological function as part of the transcriptional, post-transcriptional, and translational chloroplastic processes showed enrichment in specific gene families/classes with an already described role in plastid gene expression regulation.

This chapter focuses on the role of phys in post-transcriptional processes in the chloroplast. Within the post-transcriptional category, the Pentatricopeptide Repeat-containing domain (PPR) family, the RNA Recognition Motif-containing family (RRM) (including *cp28A* of the cpRNP family), and the Tetratricopeptide Repeat-containing domain protein (TPR) families involved in chloroplastic RNA processing, editing, cleavage, splicing and protection against degradation (Lamb et al., 1995;

Ruwe et al., 2011) were identified. Based on the initial study, a second analysis was conducted to evaluate light responsiveness and photoreceptor dependency for all TAIR-annotated members of these specific gene classes that overlapped with the GO-term chloroplast. Red light was again identified by a log₂ ratio >0.5 difference compared to darkness, and phy-dependency was identified by a log₂ ratio >0.5 in WT vs *phyABCDE*. Statistical support was defined with a multiple comparison Mann-Whitney-Wilcoxon adjusted with FDR test at P<0.05 (See 2.2 Materials and Methods), and a Chi² test was used to evaluate the significance of enrichment in light up-regulated genes from random observations in each category at P<0.05.

Within the post-transcriptional regulation category, the PPR and TPR categories were identified as significant and R-phys-modulated (Figure 2.1). A full evaluation of the role of phys and crys photoreceptors in the modulation of plastome gene expression mechanisms is described in the published paper attached to this thesis (Griffin et al., 2020).

The results therefore show a clear contribution of R-phys in the broader category of post-transcriptional modulation. Phytochromes' involvement in the post-transcriptional regulatory mechanisms of organellar gene expression has not previously been addressed, and given the particular relevance of these mechanisms to plastome mRNAs' maturation, a further exploration of the role of chloroplastic RNA binding proteins by photoreceptor signalling is of interest.

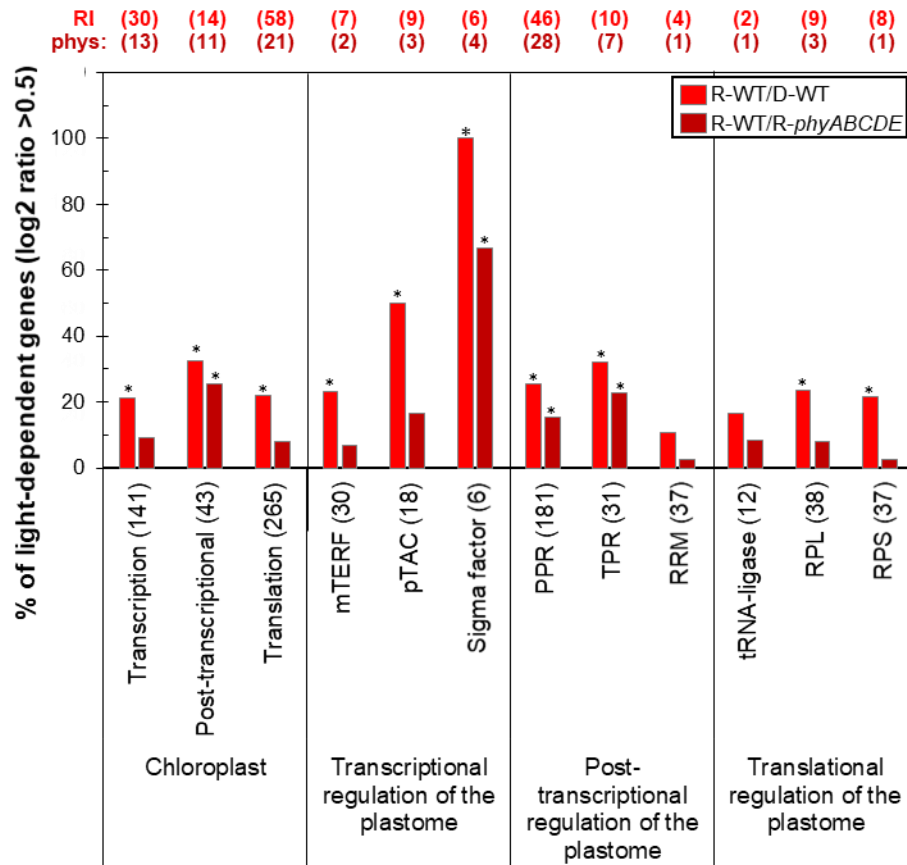


Figure 2.1. Phytochromes modulate the red-light induction of genes with functions in multiple aspects of plastome gene expression. Percentage of genes involved in plastome regulatory processes and R-light up-regulated (red bars) or R-up-regulated in a phytochrome-dependent manner (dark red). Light modulation was calculated comparing to the dark response using a log₂ ratio >0.5 difference. Phytochrome contribution was estimated by comparing WT to the *phyABCDE* response from the GSE31587 dataset. Significant differences on gene expression ratios were conducted by FDR-adjusted multiple comparison Mann-Whitney-Wilcoxon test at the significance level of 0.05. Statistical significance for enrichment was conducted with a Chi² test at $P < 0.05$ (see Materials and methods). Numbers in brackets indicates total number of genes analyzed in each category. Numbers at the top of the graphs indicate the number of genes light modulated and the number dependent on the Phys. Statistical significance is indicated with an asterisk. Figure was adapted and re-produced from Griffin et al (2020).

2.3.2. cpRNPs are downstream signalling components of phytochrome B.

Informed by the role of red light and phytochromes in the mechanisms of post-transcriptional regulation of the plastome, the Chloroplast RNA-binding protein (cpRNP) gene family members in the RRM category were selected for characterisation. The selection of this family for a focussed study was further supported by the identification of four cpRNPs' transcripts as phyB-dependent genes (Tepperman et al., 2006), as well as the converging roles of phyB and cpRNPs in the modulation of the plastome (Franklin and Quail, 2010; Kupsch et al., 2012; Griffin et al., 2020).

The first tests to establish cpRNPs as being involved in the R-phys-dependent photomorphogenic responses were conducted during de-etiolation (selected as a well-characterised model to dissect phy light responses), including examination of greening responses and over the associated assembly of photosynthetic machinery. The initial analysis of *cpRNP* transcript abundance during de-etiolation was conducted by Dr. Karine Prado in the Halliday lab (personal communication); these tests compared *cpRNP* accumulation in WT and *phyB* plants grown in darkness for 3 days and then treated with red continuous $80 \mu\text{mol m}^{-2}\text{s}^{-1}$ light or darkness for a further 24hr. Presented in Figure 2.2, the results showed a strong red-light induction of all *cpRNPs* transcripts compared to darkness, and between a 40-70% reduction in expression in the *phyB* mutant compared to WT. Based on these preliminary results, *cp29B*, *cpSEBF*, and *cp31A* were selected as candidates for characterisation based on their strong phyB-dependency and high red-light induction.

2.3.3. cpRNPs integrate red light signalling to promote greening during de-etiolation.

To characterise the role of cpRNPs as downstream phyB signalling components, *cprnp* mutants were obtained from the Arabidopsis NASC seed collections. Homozygous mutants for *cp29b_2*, *cpsebf_1*, and *cp31a_2* were isolated and the effects of T-DNA insertions on transcript abundance was evaluated via qPCR analysis in collaboration with Dr. Karine Prado, University of Edinburgh. This revealed that *cp29b_2* and *cp31a_2* mutants were null mutant knockouts, and that *cpsebf_1* was a partial knockdown mutant, summarised in Table 2.3, and location of the T-DNA insertion is described in Supplementary Figure 2.1. Preliminary experiments by Toledo-Ortiz et al (personal communication), shown in Figure 1.3 as representative photos, indicated that mutations in *cpRNP* genes induced greening defects during de-etiolation at 17°C. This reduced greening was supported by data from Kupsch et al (2012) in experiments conducted for *cp29a* and *cp31a* mutant plants moved to 8°C after 3 weeks growth at 23°C.

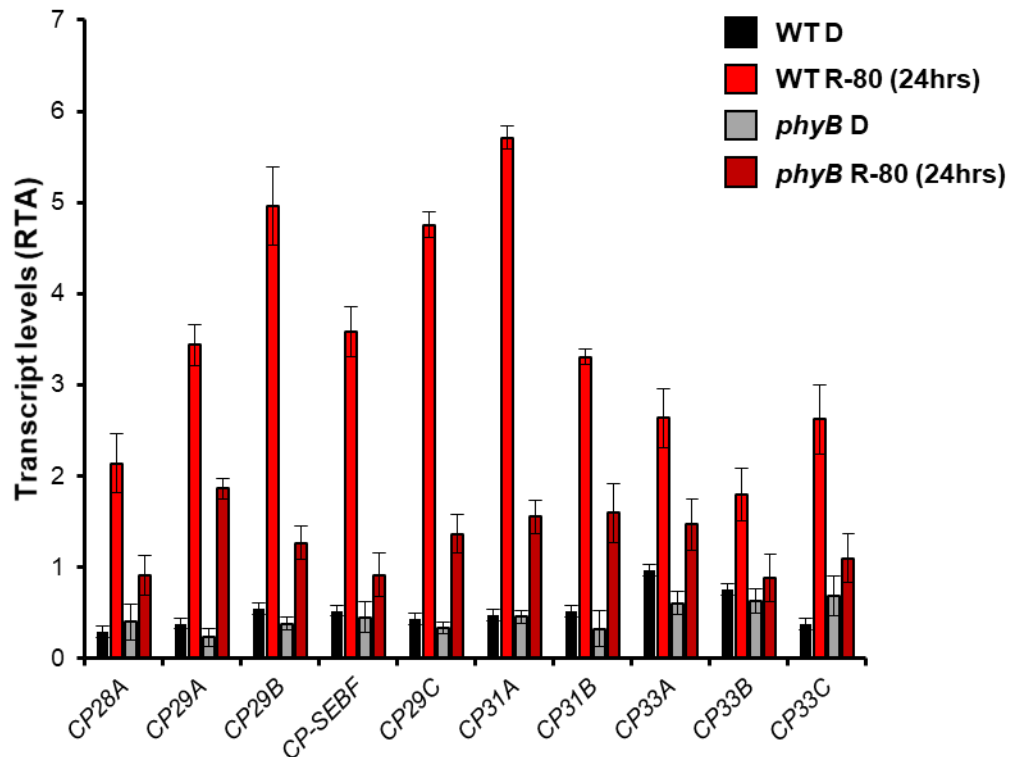


Figure 2.2. Transcript levels for *cpRNPs* in red light is phyB-dependent. Relative transcript abundance of *cpRNPs* in WT and *phyB* mutants grown for 3 days in darkness and treated with 24hrs of red light ($80 \mu\text{mol m}^{-2}\text{s}^{-1}$) or darkness. Relative transcript abundance (RTA) was calculated by comparing experimental gene expression to *PP2A* as a reference gene. Data was provided by Karine Prado, Karen Halliday, and Gabriela Toledo-Ortiz (personal communication).

Table 2.3. Mutant information for *cpRNP* mutants used in this thesis. The table shows the *cp29b* and *cp31a* mutant alleles are knockout mutants, but *cpsebf* mutant is a partial knockdown.

Mutated Gene	Accession	Mutant Allele	Name	NASC Stock	% Expression reduction
<i>cp29B</i>	AT1G01080	<i>cp29b_2</i>	SALK_043415 (S)	N543415	-100
<i>cpSEBF</i>	AT2G37220	<i>cpsebf_1</i>	SALK_008984C	N681974	-50
<i>cp31A</i>	AT4G24770	<i>cp31a_2</i>	SALK_109613C	N664816	-100

To quantify cpRNPs' importance for light-dependent greening during seedling establishment, the greening responses for 3-day old etiolated seedlings was evaluated for mutants *cp29b*, *cpsebf*, and *cp31a* grown at 22°C (the physiological temperature for *Arabidopsis thaliana*) in response to a 24hr red light treatment ($80 \mu\text{mol s}^{-1}\text{m}^{-2}$).

These results are shown in Figure 2.3. While no effect on greening was observed for the *cp29b* mutant, a significant reduction (One-way ANOVA ($p < 0.05$)) in chlorophyll *a* and chlorophyll *b* was observed in *cpsebf* and *cp31a* mutants. These results highlight the importance of cpRNPs for greening responses under red light.

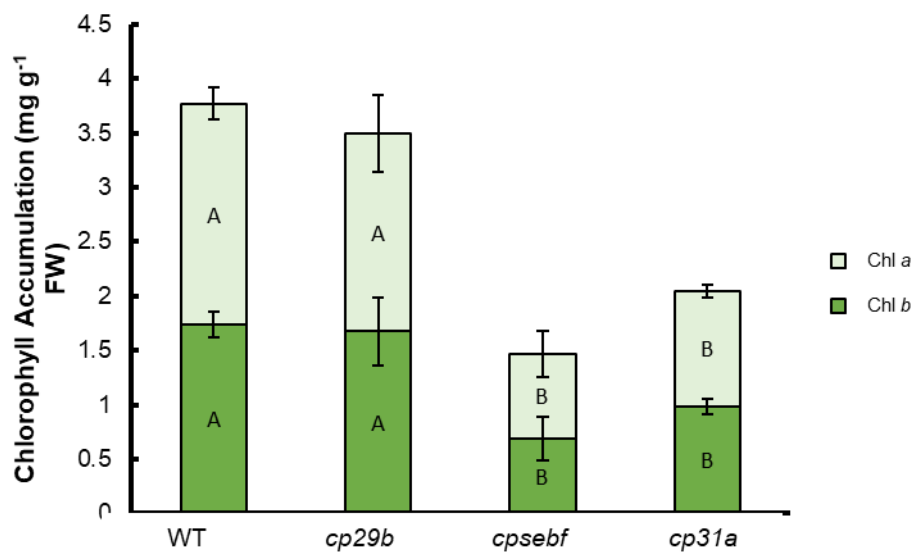


Figure 2.3. *cpsebf* and *cp31a* mutants accumulate less chlorophyll than WT plants. Graph shows chlorophyll *a* (pale green) and chlorophyll *b* (dark green) accumulation per genotype. Plants were grown for 3 days in darkness and treated with 24hrs of red light ($80 \mu\text{mol m}^{-2}\text{s}^{-1}$) at 22°C. Chlorophyll content was calculated from FW measurements using formulae published in Lichtenthaler and Buschmann (2001). Data represent the average of 3 biological replicates and error bars represent the 95% confidence interval. Statistical significance of chlorophyll abundance in each genotype was calculated using One-Way ANOVA with Tukey post hoc testing ($p < 0.05$). Data that do not share a letter are statistically significant.

2.3.4. Investigating the cpRNPs' role in delivering phytochrome-red light signals to plastid encoded genes.

The plastome contains between 120 and 130 genes, including photosynthesis-associated genes and the core components of the plastids' transcription and translational machineries (Sato et al., 1999). In most photosynthetic organisms the plastome is tightly packed inside nucleoids; in green plants, these nucleoids are distributed around the stroma (Kobayashi et al., 2002; Morley et al., 2019). Inside, the plastid DNA is circular and organised into operons- a cluster of genes bound to a single promoter that are transcribed together, and then subject to post-transcriptional processing and editing for specificity (McFadden, 2014).

The plastome contains around 80 genes for proteins involved in plastidial gene expression machinery (including the Large Ribosomal Proteins (*rpl*), Small Ribosomal Proteins (*rps*), and RNA polymerase (*rpo*); photosynthetic apparatus and the electron transport chain (including the Photosystem I (*psa*), Photosystem II (*psb*), NADH Dehydrogenase (*ndh*), Cytochrome b₆f (*pet*), and Rubisco Large Subunit (*rbcL*), ATP Synthase (*atp*)); and hypothetical and uncharacterised proteins (*ycf*) (Dobrogojski et al., 2020). The remaining c.40 genes of the plastome encode for tRNAs and are not protein-coding (Harris et al., 1994). This is summarised in Table 2.4 below.

Table 2.4: List of protein-encoding genes in the plastome by gene name and product in the chloroplast. This table was adapted from Dobrogojski et al (2020).

Gene Name	Gene Product
<i>accD</i>	acetyl-CoA carboxylase, carboxyl transferase subunit beta
<i>atpA</i>	ATP synthase CF1 subunit alpha
<i>atpB</i>	ATP synthase CF1 subunit beta
<i>atpE</i>	ATP synthase CF1 subunit epsilon
<i>atpF</i>	ATP synthase CF0 subunit I
<i>atpH</i>	ATP synthase CF0 subunit III
<i>atpI</i>	ATP synthase CF0 subunit IV
<i>clpP</i>	CLP protease ATP binding subunit
<i>matK</i>	intron maturase K
<i>ndhA</i>	NADH-plastoquinone oxidoreductase subunit 1
<i>ndhB</i>	NADH-plastoquinone oxidoreductase subunit 2
<i>ndhC</i>	NADH-plastoquinone oxidoreductase subunit 3
<i>ndhD</i>	NADH-plastoquinone oxidoreductase subunit 4
<i>ndhE</i>	NADH-plastoquinone oxidoreductase subunit 4L
<i>ndhF</i>	NADH-plastoquinone oxidoreductase subunit 5
<i>ndhG</i>	NADH-plastoquinone oxidoreductase subunit 6
<i>ndhH</i>	NADH-plastoquinone oxidoreductase subunit 7

<i>ndhI</i>	NADH-plastoquinone oxidoreductase subunit I
<i>ndhJ</i>	NADH-plastoquinone oxidoreductase subunit J
<i>ndhK or psbG</i>	NADH-plastoquinone oxidoreductase subunit K
<i>orf77 or ycf15</i>	Uncharacterized protein YCF15
<i>orf77 or ycf15</i>	Uncharacterized protein CYF15
<i>petA</i>	Cytochrome f
<i>petB</i>	Cytochrome b6
<i>petD</i>	Cytochrome b6/f complex subunit 4
<i>petG</i>	Cytochrome b6/f complex subunit 5
<i>petL</i>	Cytochrome b6/f complex subunit 6
<i>petN</i>	Cytochrome b6/f complex subunit 8
<i>psaA</i>	Photosystem I P700 apoprotein A1
<i>psaB</i>	Photosystem I P700 apoprotein A2
<i>psaC</i>	Photosystem I subunit VII (iron-sulfur center)
<i>psaI</i>	Photosystem I reaction center subunit VIII
<i>psaJ</i>	Photosystem I reaction center subunit IX
<i>psbA</i>	Photosystem II reaction center protein D1
<i>psbB</i>	Photosystem II CP47 chlorophyll apoprotein
<i>psbC</i>	Photosystem II CP43 chlorophyll apoprotein
<i>psbD</i>	Photosystem II reaction center protein D2
<i>psbE</i>	Photosystem II cytochrome b559 alpha subunit
<i>psbF</i>	Photosystem II cytochrome b559 beta subunit
<i>psbH</i>	Photosystem II 10 kDa phosphoprotein
<i>psbI</i>	Photosystem II protein I
<i>psbJ</i>	Photosystem II protein J
<i>psbK</i>	Photosystem II protein K
<i>psbL</i>	Photosystem II protein L
<i>psbM</i>	Photosystem II protein M
<i>psbN</i>	Photosystem II protein N
<i>psbT</i>	Photosystem II protein T
<i>psbZ</i>	Photosystem II subunit PsbZ
<i>rbcL</i>	RuBisCo large subunit
<i>rpl14</i>	Ribosomal protein L14
<i>rpl16</i>	Ribosomal protein L16
<i>rpl2</i>	Ribosomal protein L2
<i>rpl2</i>	Ribosomal protein L2
<i>rpl20</i>	Ribosomal protein L20
<i>rpl22</i>	Ribosomal protein L22
<i>rpl23</i>	Ribosomal protein L23
<i>rpl23</i>	Ribosomal protein L23
<i>rpl32</i>	Ribosomal protein L32
<i>rpl33</i>	Ribosomal protein L33
<i>rpl36</i>	Ribosomal protein L36
<i>rpoA</i>	RNA polymerase α subunit (PEP)

<i>rpoB</i>	RNA polymerase β subunit
<i>rpoC2</i>	RNA polymerase β'' -subunit
<i>rpoC1</i>	RNA polymerase β' -subunit
<i>rps11</i>	Ribosomal protein S11
<i>rps12</i>	Ribosomal protein S12
<i>rps12</i>	Ribosomal protein S12
<i>rps14</i>	Ribosomal protein S14
<i>rps15</i>	Ribosomal protein S15
<i>rps16</i>	Ribosomal protein S16
<i>rps18</i>	Ribosomal protein S18
<i>rps19</i>	Ribosomal protein S19
<i>rps2</i>	Ribosomal protein S2
<i>rps3</i>	Ribosomal protein S3
<i>rps4</i>	Ribosomal protein S4
<i>rps7</i>	Ribosomal protein S7
<i>rps7</i>	Ribosomal protein S7
<i>rps8</i>	Ribosomal protein S8
<i>ycf1</i>	Hypothetical protein ArthCp087
<i>ycf1</i>	Hypothetical protein ArthCp070
<i>ycf10 or cemA</i>	Envelope membrane protein
<i>ycf2</i>	Conserved hypothetical chloroplast protein YCF2
<i>ycf2</i>	Conserved hypothetical chloroplast protein YCF2
<i>ycf3</i>	photosystem I assembly protein YCF3
<i>ycf4</i>	photosystem I assembly protein YCF4
<i>ycf5 or ccsA</i>	Cytochrome c biogenesis protein CCSA

2.3.5. Photoreceptors in the modulation of plastid gene expression.

Phytochromes are essential to chloroplast biogenesis, regulating greening, assembly, and maintenance of photosynthetic apparatus, and production of photosynthetic pigments (Franklin and Quail, 2010) in response to light quality and quantity (Oh et al., 2013).

However, the global impact of phys on the plastome had not yet been fully addressed. The role of the R-light receptor *phyB* on the global modulation of the plastome was bioinformatically evaluated bioinformatically for this thesis (see also Griffin et al (2020) (Figure 2.4). The genomic dataset analysed the effect of *phyB* over the plastome in Short Days (SD) (E-MEX-1299) (Michael et al., 2008), and was selected from multiple phy transcriptomic studies published due to the random hexamer priming method used to generate plastid cDNAs, which is required due to the association of poly-A tails in chloroplast mRNAs to degradation pathways (Schuster et al., 1999).

The analysis revealed that *phyB* is required for the modulation of 55 out of the 80 plastome genes evaluated during at least one timepoint of the experiment. Plastome transcript abundances were examined in the *phyB* mutant compared to WT during the light (ZT4-ZT8) and dark (ZT12-ZT0) periods of the time-course experiment and identified using a log₂ ratio >0.5 differences between WT and *phyB*. This shows a strong effect of *phyB* over plastome expression, with *phyB*-dependent modulation of photosynthesis-associated genes from the *psb* family (Photosystem II), *psa* family (Photosystem I), *ndh* family (NADH dehydrogenase complex) and *pet* genes (Cytochrome b₆f complex) (Griffin et al, 2020) (Figure 2.4).

■ log₂ ratio >0.5 ■ log₂ ratio <-0.5

	ZT0	ZT4	ZT8	ZT12	ZT16	ZT20
<i>accD</i>	-0.4658	-0.2881	0.6304	-0.2651	-0.4508	-0.3005
<i>aptA</i>	-0.3354	-0.1628	0.2353	-0.2799	-0.1712	-0.0311
<i>atpB</i>	-0.3643	-0.2212	0.0288	-0.2102	-0.1789	-0.1977
<i>atpE</i>	-0.2710	-0.2183	-0.2180	-0.2052	-0.0630	-0.2990
<i>atpF</i>	-1.0746	-0.7300	-0.0035	-0.3383	-0.1202	-0.5813
<i>atpH</i>	-0.4531	-0.3456	0.1252	-0.3306	-0.1218	-0.5950
<i>atpI</i>	-1.4104	-0.9687	-0.5167	-0.6912	-0.4495	-0.4647
<i>clpP</i>	-0.0688	-0.1301	0.1665	-0.1054	-0.2648	-0.0955
<i>matK</i>	-0.4178	-0.5383	0.0265	-0.0508	-0.1213	-0.2904
<i>ndhA</i>	-0.5170	-0.2886	-0.0495	-0.6142	-0.3202	-0.1070
<i>ndhB.1</i>	0.0860	-0.5613	-0.3888	-0.3163	-0.2131	0.2090
<i>ndhC</i>	-0.2271	-0.1800	-0.1348	-0.2492	-0.0853	-0.0858
<i>ndhD</i>	-0.1732	-0.0763	0.2250	-0.2887	-0.1740	0.0675
<i>ndhE</i>	-0.9910	-0.8126	-0.2103	-0.4567	-0.2234	-0.4021
<i>ndhF</i>	-0.3287	-0.6384	0.0931	-0.6021	0.3352	-0.0520
<i>ndhG</i>	-1.4790	-0.6893	-0.4201	-0.1200	-0.1943	-0.5594
<i>ndhH</i>	-1.4834	-1.3589	0.1050	-1.2915	-0.7468	-0.1033
<i>ndhI</i>	-0.2064	-0.3002	0.0245	-0.3099	-0.1517	-0.0479
<i>ndhJ</i>	-0.7516	-0.9284	0.0326	-0.8819	-0.7300	-0.4606
<i>orf31</i>	-0.8521	-0.5257	-0.6184	-0.3480	-0.3493	-0.5909
<i>orf77.1</i>	0.0289	0.4213	-0.8988	-0.0243	-0.6922	-0.3254
<i>petA</i>	-0.2269	-0.1229	-0.2698	-0.1574	-0.3131	0.0545
<i>petB</i>	-0.1618	-0.0442	-0.0318	-0.1437	-0.3125	0.0124
<i>petD</i>	-0.4739	-0.2697	-0.1727	0.2203	-0.2641	0.0202
<i>petG</i>	-1.4275	-0.0065	-0.5505	-0.0635	-0.1674	-0.2574
<i>psaA</i>	-1.3827	-0.7811	-0.0812	-0.9737	-0.3515	-0.4650
<i>psaB</i>	-0.1118	-0.2005	0.0870	-0.2648	-0.1984	-0.0696
<i>psaC</i>	-0.8946	-0.5119	0.0286	-0.6296	0.2184	-0.1758
<i>psal</i>	-0.2042	-0.2732	0.2778	-0.4129	-0.5703	0.0083
<i>psal</i>	-0.3707	-0.0577	0.0927	-0.2446	-0.3086	-0.3436
<i>psbA</i>	-0.6610	-0.4373	-0.1102	-0.7481	-0.5464	-0.4895
<i>psbB</i>	-2.5526	-0.6708	-0.5928	-1.1163	-0.6616	-0.4619
<i>psbC</i>	-1.6107	-0.2945	-0.1361	-0.8273	-0.5891	-0.6428
<i>psbD</i>	-2.8982	0.1671	-0.9897	-1.7628	-0.5418	-0.6767
<i>psbE</i>	-0.4960	-0.3050	-0.2371	-0.2859	-0.3389	-0.1118
<i>psbF</i>	-0.1093	-0.1928	-0.2876	-0.3209	-0.1536	-0.2738
<i>psbG</i>	-0.9806	-1.0235	0.8401	-1.6759	-0.5066	-0.5426
<i>psbH</i>	-0.9778	-0.3072	-0.2805	-0.3647	-0.0441	-0.3420
<i>psbI</i>	-0.3043	-0.2362	-0.2414	-0.3419	-0.1344	-0.2586
<i>psbJ</i>	-0.5166	-0.3591	-0.6037	-0.3784	-0.0481	-0.3827
<i>psbK</i>	-0.4127	-0.4494	-0.0419	-0.3433	0.0377	-0.4534
<i>psbL</i>	-0.4385	-0.1272	-0.7986	-0.6730	-0.1895	-0.3173
<i>psbM</i>	0.0986	0.1430	-0.1198	-0.2746	-0.3575	0.1478
<i>psbN</i>	-1.0716	-0.7385	0.0719	-0.3066	-0.0053	-0.6231
<i>psbT</i>	-0.5247	-0.4221	-0.8918	-1.2665	-0.4422	-0.5017
<i>rbcl</i>	-0.4747	-0.1021	0.8724	-0.0420	-0.0127	0.0617
<i>rpl1</i>	-0.1775	-0.2202	-0.1763	-0.0655	0.0373	-0.0989
<i>rpl14</i>	-1.0126	-0.8887	-0.3433	-0.4596	0.4206	0.0754
<i>rpl16</i>	-1.0368	-0.6139	-0.0792	-0.4878	-0.3133	-0.2012
<i>rpl20</i>	-0.6376	-0.6199	-0.0735	-1.5666	-0.0601	-0.3795
<i>rpl22</i>	-0.9134	-0.6285	0.0049	0.0480	-0.3675	-0.3406
<i>rpl23.1</i>	-0.4644	-0.2776	-0.3592	-0.2611	-0.2955	0.0046
<i>rpl32</i>	-0.4666	-0.2962	-0.2210	-0.2888	0.0177	-0.4168
<i>rpl33</i>	-0.7583	-0.2493	-0.0926	-0.0529	-0.1401	-0.2309
<i>rpl36</i>	-0.5813	-0.2140	-0.2282	-0.3979	-0.1136	-0.1039
<i>rpoA</i>	-0.2052	-0.0666	-0.2743	-0.6083	-0.0061	0.0391
<i>rpoB</i>	-0.6473	-0.2489	0.5375	0.0865	-0.2327	0.2540
<i>rpoC1</i>	-0.1789	-0.2814	0.1755	0.0559	-0.1846	0.0589
<i>rpoC2</i>	-0.4412	-1.0406	-0.1054	-0.1662	-0.6218	-0.0641
<i>rps2</i>	-0.3203	-0.9234	-0.0843	-0.2570	-0.4321	-0.1400
<i>rps3</i>	-0.5454	-0.3363	-0.3199	-0.0398	-0.0442	-0.2745
<i>rps4</i>	-0.3804	-0.3972	0.2212	-0.1514	-0.8599	-0.1317
<i>rps7.1</i>	-0.4758	-0.2179	0.3725	-0.6061	-0.3403	-0.2494
<i>rps8</i>	-0.9116	-0.7844	-0.4604	-0.3903	0.1117	0.2072
<i>rps11</i>	-0.2857	-0.3944	0.0788	-0.1424	-0.1753	0.1018
<i>rps12.1</i>	-1.3306	-0.6933	-0.4662	-0.2764	-0.3597	-1.2080
<i>rps12.2</i>	-1.0911	-0.4957	-0.1228	-0.3682	-0.1236	-0.6652
<i>rps14</i>	0.1602	0.0184	0.1201	0.1513	-0.3578	0.0522
<i>rps15</i>	-0.4730	-1.0641	-0.1274	0.3349	-0.1282	-0.4537
<i>rps16</i>	-0.4401	-0.6340	0.2799	0.2823	-1.5885	-0.1388
<i>rps18</i>	-0.6691	-0.5501	-0.2410	0.0346	-0.1713	-0.2286
<i>rps19</i>	-0.6267	-0.8439	-0.2254	-0.2254	-0.2880	-0.1687
<i>ycf1.1</i>	-0.3494	-0.0556	-0.0387	-0.0092	-0.6153	-0.3569
<i>ycf2.1</i>	-0.2374	-0.1054	-0.7099	-0.1030	-0.1669	0.0773
<i>ycf3</i>	-0.3712	-0.3150	0.3598	-0.2344	-0.2689	-0.7213
<i>ycf4</i>	-0.7817	-0.3913	-0.3024	-0.3774	-0.5051	-0.0579
<i>ycf5_ccsA</i>	-0.1948	-0.1318	-0.1826	-0.1340	-0.3855	-0.3039
<i>ycf6_petN</i>	-0.9691	-0.2896	-0.3974	0.8479	0.6722	-0.1439
<i>ycf9_psbZ</i>	-0.6254	-0.0962	-0.3044	-0.4253	-0.5524	-0.3601
<i>ycf10_cemA</i>	-0.5845	-0.4743	-0.2933	-0.4754	-0.5321	-0.1094

Figure 2.4. *phyB* has a broad impact in chloroplast genome expression in Short-Days (SD). Table representation of the plastome transcripts' differential accumulation in *phyB* compared to WT. Numbers indicate the *phyB*/WT transcript ratio during a SD dark/light cycle. Color code illustrates gene downregulation in blue (log₂ *phyB*/WT <-0.5) and up-regulation in red (log₂ *phyB*/WT >0.5). Plastome gene expression information was obtained from the dataset E-MEX-1299 to calculate the ratios. Chloroplast genome genes are organized by functional category: *atp* (ATP Synthase); *ndh* (NADH dehydrogenase); *pet* (Cytochrome b6f complex); *psa* (Photosystem I); *psb* (Photosystem II); *rpl* (50S ribosomal proteins large subunits); *rpo* (RNA Polymerase); *rps* (30S ribosomal proteins small subunits) and *ycf* (hypothetical/unknown chloroplast ORFs). The light period (ZT4-8) of the diurnal cycle is indicated with a white rectangle and dark period (ZT12-0) in a grey rectangle. Figure was adapted and re-produced from Griffin et al (2020).

2.3.6. cpRNPs are global regulators of plastid gene expression.

Published literature has linked cpRNPs to the global regulation of plastid-encoded, photosynthesis-associated genes (Nakamura et al., 2004; Kupsch et al., 2012). A strong binding capacity for *psbA*, *rbcL*, and *petD* in tobacco by cpRNPs indicated a potential affinity for PSII-related processes in particular (Nakamura et al., 2004). Transcript abundance of the NADH-dehydrogenase gene *ndhF* is also reduced in a *cp31a* null mutant, accompanied by a subsequent disruption of the electron transport chain and impaired photosynthesis (Tillich et al., 2009).

A further study of the *in-vivo* RNA-binding capacity of cp29A and cp31A on cold-treated 3-week old plants indicated a strong enrichment for *psbB*, *psbD*, *psaA*, *psaB*, *atpB*, and *ndhB*, as well as an intermediate enrichment for almost all other chloroplast mRNAs, confirmed by a dot blot assay (Kupsch et al., 2012). This suggests a near-global binding capacity for the plastome by members of the cpRNP family. An overlap in binding affinities was observed between cp29A and cp31A, also indicating some level of redundancy between family members, although cp31A coprecipitated with a greater number of RNAs than cp29A (Kupsch et al., 2012). An analysis of *cp33a* null mutant identified a strong albino phenotype in plants grown in Long Day (LD) conditions at 23°C, and RIP-chip analysis showed an association for cp33A with most chloroplast mRNAs in the stroma with particular binding to the *psbD/C* operon, *atpA* operon, *ndhA* operon, and *psbE* operon in *Arabidopsis* (Teubner et al., 2017). Additional studies of cp33B showed a binding preference for *psbA*, but also showed binding peaks to *atpH*, *psbD*, *ndhJ*, and *petB* (Teubner et al., 2020). In conjuncture, these experiments revealed a potentially wide-ranging gene targeting affinity for the cpRNPs, and potential candidate genes with clear modulation in the Photosystem I (*psa*), Photosystem II (*psb*), ATP Synthase (*atp*), Cytochrome b6f (*pet*), and NADH dehydrogenase (*ndh*).

2.3.7. Identifying plastome target genes sensitive to R-light and dependent on cpRNP action during de-etiolation.

To evaluate the molecular mechanism behind the effects of *cprnp* mutations on greening reported during de-etiolation (Figure 2.3), the effect of mutations on *cpRNP* genes on the transcript abundance of plastome-encoded genes during de-etiolation was investigated.

De-etiolation is a crucial stage of plant development, during which chloroplast gene expression is critical for the construction of PSI and PSII photosynthetic apparatus (Armarego-Marriott et al., 2020). De-etiolation represents the first time in a seedling's development in which these light-induced genes will be expressed, including nuclear- and plastome-encoded genes, making

it an optimal point in light-induced plant development to quantify the impact of cpRNPs on light-induced plastome gene expression (Armarego-Marriott et al., 2020). As light-sensitive components with a global binding capacity for plastome encoded photosynthesis-associated transcripts, cpRNPs may be actively involved in organellar responses to light cues including the processing and accumulation of transcripts for protein production.

Candidate genes to examine were selected from preliminary red-light induced plastid encoded transcript accumulation experiments conducted by Dr. Prado University of Edinburgh (personal communication). Selected candidates were corroborated to be direct targets of cpRNP activity using the published RIP-chip datasets cp29A and cp31A (Kupsch et al., 2012).

Experimental material was gathered from etiolated plants grown for three days in darkness and treated with 24hr red light ($80 \mu\text{mol m}^{-2}\text{s}^{-1}$) to induce de-etiolation. Transcript accumulation was evaluated for WT, *phyB* and *cprnp* mutants *cp29b*, *cpsebf*, and *cp31a*.

The results of the transcript abundance analysis are shown in Figure 2.5. Panel A shows the transcript abundance of three genes in the ATP Synthase family (*atp*), for which *atpH* was identified as *phyB*- and cpRNP-dependent. *atpH* abundance was statistically significantly reduced in *phyB* mutants, and accumulation was also reduced in all tested *cprnp* mutants, indicating that cpRNPs could act downstream of the phytochromes to modulate this gene. No statistically significant differences in transcript abundance were detected for *atpA* or *atpI*, although trends indicated a lower average transcript abundance in *phyB* and *cprnp* mutants compared to WT.

Panel B showed that *ndhG*, of the NADH-dehydrogenase family, may be *phyB*-dependent but transcript abundance was only reported to be cp31A-dependent. No significant differences were observed between WT and *phyB*, although analysis showed an average fold difference of 1.8x between the genotypes.

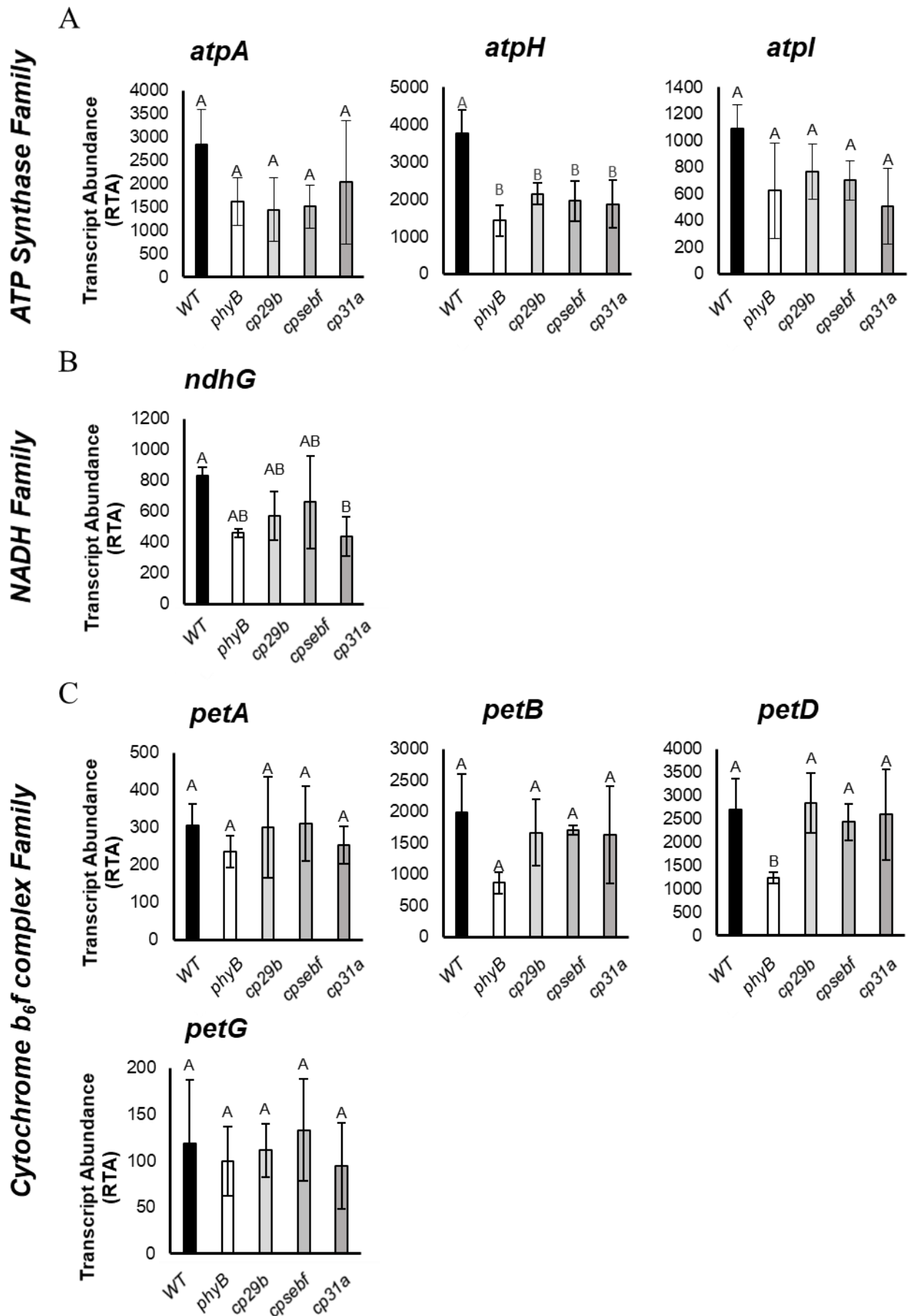
The examination of the Cytochrome b₆f (*pet*) family in panel C showed that *petD* accumulation was *phyB*-dependent. However, neither *petA*, *petB*, or *petG* transcript abundances were affected by *phyB* mutation and no remaining *pet* gene transcript abundances were detected as cpRNP-dependent.

Evaluation of Photosystem I (*psa*) gene transcripts in Panel D showed that *psaJ* transcript accumulation is *phyB*-dependent and *psaB* accumulation shows a trend that indicates a contribution of *phyB* to its accumulation. Analysis showed a significant 2.1-fold reduction in average *psaJ* transcript abundance between *phyB* and WT, indicating that *phyB* is necessary for light up-regulation of this gene. Regarding cpRNPs' contribution to the transcript accumulation, analysis of *cp29b*

mutant compared to WT indicated a significant 1.8-fold reduction, indicating that *cp29B* contributes to *psaJ* accumulation; but for this gene no significant effect of *cpsebf* or *cp31a* mutation was observed. For *psaB* transcript abundance, *phyB* and *cpsebf* mutants showed an average fold reduction of 2.5x and 2.4x, despite no but no statistically significant differences.

Finally, the investigation of Photosystem II (*psb*) transcript abundance is shown in Panel E and identified that *psbA*, *psbC*, *psbD*, and *psbF* are all phyB- and cpRNP-dependent. The analysis of *phyB* mutants compared to WT showed significant reductions in *psbA*, *psbC*, *psbD*, and *psbF* transcript accumulation. Further examination of these genes in *cprnp* mutants identified a statistically significant reduction *psbA* in *cp31a* mutants; of *psbC* abundance in *cp29b* and *cpsebf*; of *psbD* in all tested *cprnp* mutants; and of *psbF* in *cp29b* and *cpsebf*.

Therefore, the overall analysis of plastome transcripts identified a clear phyB-dependency of transcripts from the ATP Synthase, Cytochrome *b₆f*, Photosystem I, and Photosystem II families, representing entry points of light signals for the modulation of photosynthesis-associated processes during de-etiolation. As suggested in Griffin et al (2020), these results show that phyB is a key signal transducer for the global expression of the plastome. This investigation further showed a clear cpRNP-dependency for *atpH*, *ndhG*, *psaB*, *psbA*, *psbC*, *psbD*, and *psbF*, highlighting an important role for cpRNPs in the molecular mechanisms downstream of phyB involved in greening. These findings bring a new understanding of how phyB can co-ordinate photosynthetic responses by acting on a group of proteins that perform essential post-transcriptional processing of plastome-encoded genes involved in photosynthetic metabolism.



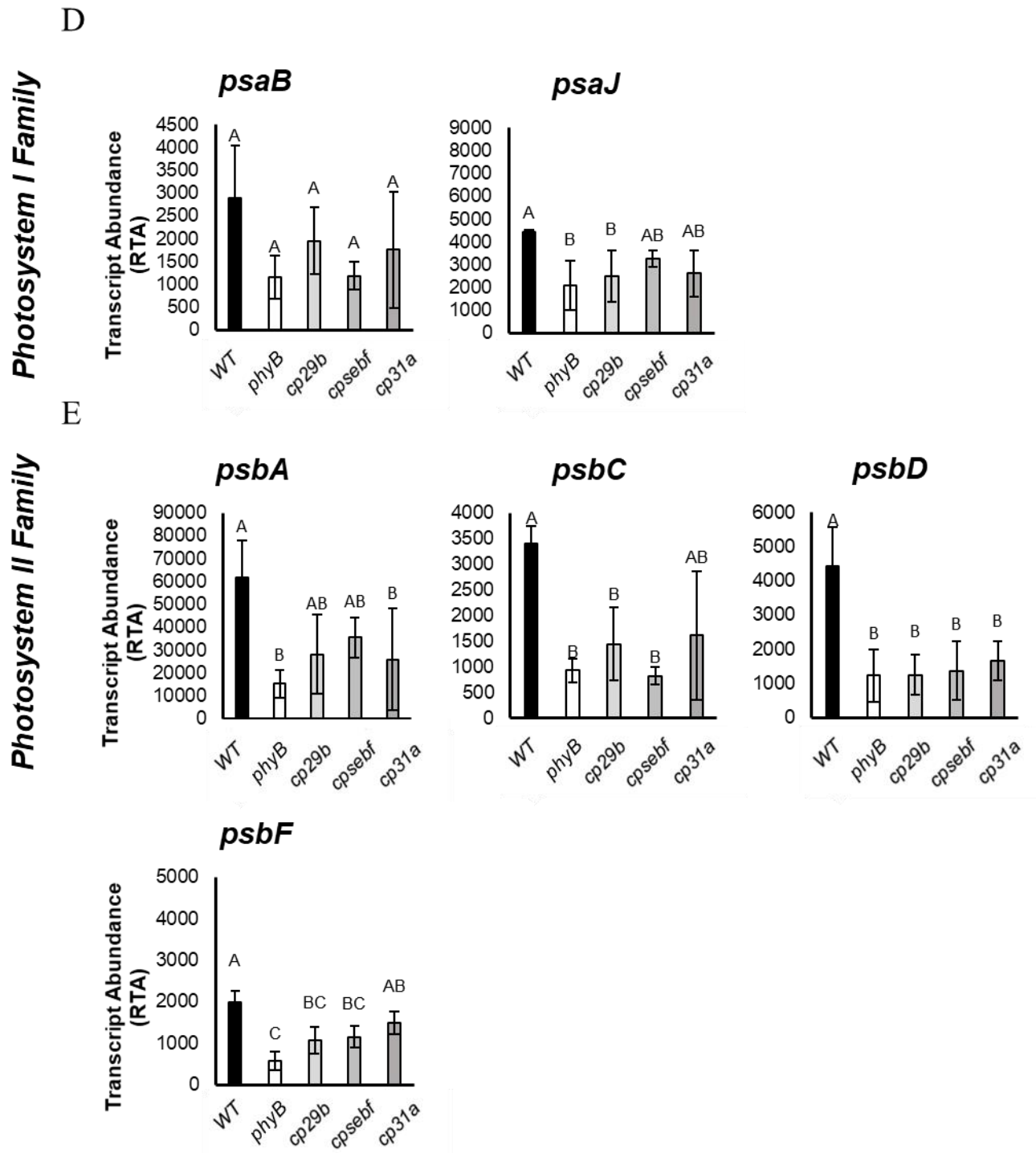


Figure 2.5. *cprnp* mutation reduces transcript accumulation of key ATP Synthase, Photosystem I, and Photosystem II plastome-encoded subunits. Graphs show relative transcript abundance (RTA) of A) ATP Synthase family, B) NADH family, C) Cytochrome *b6f* complex family, D) Photosystem I family, and E) Photosystem II family plastome-encoded subunits in WT, *phyB*, and *cprnp* mutants grown for three days in darkness and treated with 24hrs red light ($80 \mu\text{mol m}^{-2}\text{s}^{-1}$). Relative transcript abundance was calculated by comparing experimental gene expression to *PP2A* as a reference gene. Data represent the average of three biological replicates and error bars represent the 95% confidence interval. Statistical significance of transcript abundance between WT (black bars), *phyB* (white bars), and *cprnp* mutants *cp29b_2*, *cpsebf_1*, *cp31a_2* (shown over a light-to-dark gradient grey bars) was calculated using One-way ANOVA with Tukey post hoc testing ($p < 0.05$). Data that do not share a letter are statistically significant.

2.3.8. HY5 links phy activation to cpRNPs modulation in response to red light.

Phytochrome B enables a vast signalling network to co-ordinate multiple light-dependent responses (Franklin and Quail, 2010). One of the key transcriptional regulators of these pathways is Elongated Hypocotyl 5 (HY5), a bZIP transcription factor that inhibits hypocotyl growth and lateral root development, and promotes photosynthetic gene expression and photopigment accumulation in a light- and temperature-dependent manner (Toledo-Ortiz et al., 2014; Gangappa and Botto, 2016). HY5 can integrate not only red-light signals through phyB, but also blue-light signals through the cryptochrome (cry) photoreceptors (Osterlund et al., 2000; Wang et al., 2017).

Based on its clear impact on greening responses (Toledo-Ortiz et al., 2014), a global evaluation of HY5's impact in the regulation of genes encoding proteins with a regulatory effect on the plastome was conducted to assess its involvement in the modulation of the plastome (Griffin et al., 2020). A genome-level bioinformatics study was conducted to test whether HY5 could act as a signaling component involved in delivering light cues to the plastome by controlling the expression of nuclear genes potentially involved in chloroplast genetic machinery control. The genomic dataset GSE62119, using 3-day old *hy5* and WT seedlings grown under continuous white light (Kawashima et al. unpublished data), was used to examine the contribution of HY5 to the light induction of the genes classified in the general functional categories of chloroplast transcription, post-transcription, and translation (Figure 2.6) as well as for the specific gene families singled within each one.

Figure 2.6 shows that HY5 significantly contributed to around 25% of the light modulation of the genes included in the post-transcriptional regulation category of the plastome, affecting 12 genes. HY5 also contributed to between 10-20% of genes in the chloroplast transcription and translation categories. Within the specific gene families evaluated, HY5 was found to be involved the up-regulation of the 3 mTERFs, 5 pTACs, and 5 sigma factor family members with potential to participate in transcription of the plastome. Despite a lack of statistical enrichment, HY5 contributions were identified to the light-dependent transcript accumulation of 25 PPRs, 4 TPRs, and 3 RRM in the post-transcriptional category and in the translation category 2 tRNA ligase genes and 3 RPSs.

These results highlighted that HY5 could be an important contributor to the nuclear signaling cascades that connect environmental signals by photoreceptors to control of nuclear-encoded genes with proteins that function in the plastome regulation. In particular, HY5's contribution to the light-modulation of RNA binding products indicates a previously underestimated capacity to act in the post-transcriptional pathways.

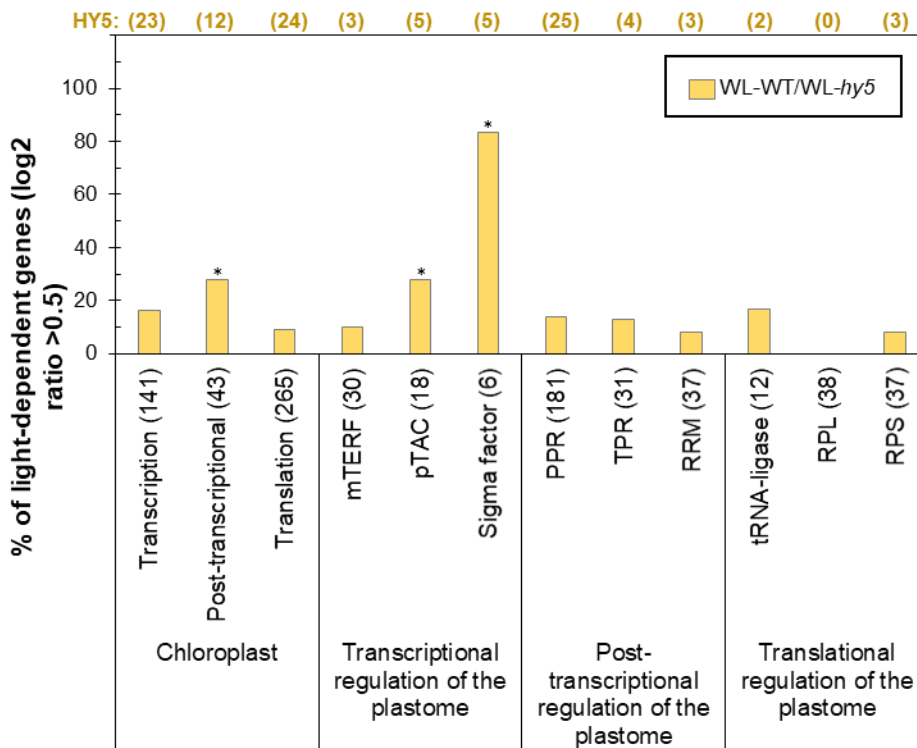


Figure 2.6. HY5 modulates the light induction of genes with potential functions in multiple aspects of plastome gene expression. Percentage of light-induced genes involved in plastome regulatory processes and B or R-light up-regulated and light up-regulated and dependent on HY5 (yellow). Modulation was calculated comparing light- and dark-responses from GSE31587 and GSE58552 using a log₂ ratio >0.5 difference. HY5 dependence was calculated relative to the WT response used the *hy5* data from GSE62119. Significant differences on gene expression ratios were conducted by FDR-adjusted multiple comparison Mann-Whitney-Wilcoxon test at the significance level of 0.05. Statistical significance for enrichment was conducted with a Chi² test at $P < 0.05$ (see Materials and methods). Numbers in brackets indicates total number of genes analyzed in each category. Numbers at the top of the graph is indicate the number of genes light modulated and the number dependent on HY5. Statistical significance is indicated with an asterisk. Figure was adapted and re-produced from Griffin et al (2020).

As phyB-R light signalling components, cpRNPs may also be a part of the HY5-regulated involved in the greening responses; through cpRNPs, HY5 could be involved in previously unaddressed cascades to exert a global influence over the plastome in response to environmental cues. To explore this hypothesis, an analysis of the promoters of *cp31A*, *cp29B*, and *cpSEBF* was conducted to identify known if HY5 binding sites were present. Results are presented in Figure 2.7.

The upstream promoter regions of each of these cpRNPs were examined. The region 1500 nucleotide base pairs upstream from the ATG start codon was examined for each gene, to identify HY5-recognition motifs using the Patterns Locator online bioinformatics tool (Mrázek and Xie, 2006).

A) *cp29B*

G-box: CACGTG	E-box: CANNTG	CA Hybrid-box: GACGTA
ACE-box: ACGT	C-box: GTCANN	CG Hybrid-box: GACGTG

↓ 1500bp before start codon

GAGAGCCACTTCTGACCCCGAGATTTGGAAGAAAGGTCCTG**CATTG**GGATGCCTGGTGTTCATGTTGACGGTATGGATGCTTGAAG**GTCAGG**
 GAAGTCGCTAAAGAAGCT**GTCAGT**AGAGCTAGAAGAGGAGAAGGTCCAACCTTGGTTGAATGTGAGACTTATAGATTAGAGGACACTCCTTGGC
 TGATCCCAGTACGCTCCGTGATGCTGGTAAATATCGACTTCTTCTGCTTCTTATGCTTGTACTGATTATCTAAGGGTTGAAACAACCTTCTCTTTA
 ATTTGAATTTTTTTT**CAGCTG**AGAAAGCCAAATACGCGGCTAGAGACCCAATCGCAGCATTGAAGAAGTATTTGATAGAGAACAAGCTTGCAAA
 GGAAGCAGAGCTAAA**GTCAAAT**AGAGAAAAGATAGACGAGTTGGTGGAGGAAGCGGTTGAGTTTGCAGACGCTAGTCCACAGCCGGTGCAG**G**
T**CAGT****TG**CTAGAGAATGTGTTGCTGATCCAAAAGATTTGGAATTGGACCTGATGGACGGTA**CAGATG**TGAGGACCCCAAGTTTACCGAAGGC
 ACAGCTCAAGTCTGAGAAGCAAGTTTAAACATAAGCTGTCTACTGTCTCTTCGATGTTTCTATATATCTTATTAAAGTTAAATGCTACAGAGAATCAGT
 TTGAAT**CATTG**CACTTTTTGTCTTTTGTGGTGTACTAACTATCACAAGGTTCTTCTGTAGTTCGTTGGGTTTTATTGGTTACCACCTACCAG
 AGAATTTGATTTTTTTTTTAAAGATAATTTTTGCAACCTCGGGTATTACACTCTAAACAAGATGGCTCTGCAACAGGAGCCAGTACCACCAATT
 ACACACAATCTCGTATAAGAACAATACATGCCAATACAGCTTCCACAGCACAGAAAACCTTTTCTCTTGTCTCATCTCTGCATAGCTTGTCTATAA
 TATAGCTTTAAACCTCAAGATTTGCAGACTTCTCATAGTAAAGTCAAAGAGACAGTGTGTGGTTTGCATAACGAT**CATTG****G****GTCAAA**TATATAG
 CTTCAAACCTCTGAGGAGTTCAAACATAGCAGATTTCTACTACCACCTCCCTCAGAGCCAAGGAGTTGTAGATGTAGT**GTCAGA**ATGAAGA
 TTGAGGATGAATGGGCCATTAGACAAGATTGCACGTGTTCTAATTTTCTGGCTCCTACTTTCTTTGTAATAAAGTGTGGTAAAGGGAATAAGAGA
 CTTGAAGAAATGAAATGTTTGAATAATTTTTATTTTTGATTTATAACTTTGGGCTTTTGTATTTCATGAAAACAAAACCTGCTACGCGAAAGA
 GAGTGCT**CATCT****G****ACGT****A**GCGAATACCGAGCAGGATTGTAACGGGTTAAATGACCCGACCCGATTTGTCTATTAATTTCTATTTCTTTT
 TTTTTAATCATTCTCTCAATAATTTACTTTCTGGTCTTCGAT**AATG**

↑ 1bp before start codon

B) *cpSEBF*

↓ 1500bp before start codon

AGGAAGGAAACCCAGACTCTAGTTACGAGATTCTGAAGATAATGTGAGGAGAGGTTGCCCTAGAGAATCAAACG**CATATG**AGCTGCTCATCAAG
 AGTACATGAGCAAAGGTGAGCCTGGAGACGCGAAAACCCGACTGGACAGCATGGTCGAAGACGGCATGTCAGACTCATCGCTTTTCAG**GT**
CAGTGTATTGAGAGTTTGTTCGAGGATGGTAGGGTGCAGACAGCAAAGCCGTGTGATGATGATCATGATAGATAAAA**ACGT**TGGTATCGAAGACAA
 CATGGATTTGATTGCCAAGATCTTGAAGCCCTCTTAATGAGAGGAC**ACGT**AGAAGAAGCCCTGGGGCTATAGATCTTCTGAACCAAACCGGAC
 ACA**CAGCTG**ATCTGGACAGCCTCTTATCTGTCTTAAGCGAGAAAGGGAAGCAGATTGCAGCATTGAAGCTGTAGATTTCCGGTTGGAGAGAGAT
 CTCAGCTTAGAGTTTTTCGAGCTACGACAAAAGTGTGGATGCGCTTTTAGGAGCTGGGAAGACTCTGAATGCGTACTCAGTCTTTTGAAGATCATG
 GAGAAAGGAAGTTCAACAGATTGGAAGAGCTCTGATGAAGTATCAAAGCTTGAACCAAGAAGGGAACACAAGCAAGCTGATGTTCTTTCTAGA
 ATGATCAAGAAGGGACAAGGAATCAAGAAAACAAAACAAATGTTTCTATAGAAGCTGACAAAGTATTCTTTCTTAAAGTATTCTCCTTTTATTGTTG
 GTTCAA**GTCAA****G****GTCAA**AACTTCAAGTATCTTCTCAAATAAATCTTTTTGAAACTGTTTTGAAGGACGCGTTTTGATGATCATCTGTGTTTT
 TTTTTGGTAGGAATTTGATCGTCTGATTTAGTTTCTAACCTCTTGAAG**ACGT**TAAT**ACGT**AAAAGATTTTTTTCGAGATTTGTGTTGGAACA
 AGAGTTGCATCTCCATTGGCTGTTAGTAAAATATCTTATCTTCTCATAGATTTTAGCTTCAGCATGA**G****ACGT****G**CCATCTCCACTGTCATCCAAA
 ATTCGACGGTCCAGATCTCATCTCATCATCACACTTCATATTATGACAAGTAGTTAGTAGACTGTCCAATAAAAACACAACCAACACAACACTAA
 TTTAAGTGAGAAAAGCACATAACTTTATCACAAAAAATATTTAGAAAAGTAAATACAATAAGCATACTAAAATGCAAAACGAAAACAAATTTGGCAGATGT
 ATTAATTTTTTGTATATTACTACTAAACAAGCGAAAATAAATAAATCCTATCATTTATGTGGAACAAAATAGTTGCAAAAGAAAATAAAAATCTTACA
 AAAAAACAGAAATCAGAATATTGAGCCTAAAAAATAGTTTGAAGTAAAATACAAAATAAATAAGTTTGAAGATATTTGTGCAAAAGAACTTAATATATT
 TATT**CATTG**CCCCATAAATACCAAAGACACTGCATCTTATCTCCACTCTCAAATCATCTTCTTACCCAAAAACCCCTAAAAGCCTTATCCCTTCT
 CTTCC**AATG**

↑ 1bp before start codon

C) *cp31A*

↓ 1500bp before start codon

AGAAGGTTAAAGTGGCCATGTTATGAGTTGTGTGCG**GT****C****ACGT****G**ACTG**GTCAGT**TAATTTAGTTGTAACAATCGATTATATTTGTTCTATTATT
 CTTTATATTTTCAAGTATGCTTAAACAGTAAGAAATATAGTTAACTGAAACCAACAAAAGATTGAGAAATCTAGTGTGTTATCAATATGGAATTTAA
 GTAAATCTTAAACTTTAGATTTGTTTTCTGATTTGCTTTAAGAAATGTTTGTATGAATTTCAAATCTGCAATATATCTTGGATTTGATTTCTA
 ATGATTTACTCATGAAACTCAAAGAGGTTTTCATTTCAAATCAATTAATATACAAAGATTTTACAAGACTTTTAGTTTTGAACAACATTGGATTTAATG
 AAATATTTAAATCTTAATTTGAATTAACACCAAACCTTTAAATCTATTAAGCATGATTTACAAATATGAGTTCCAATAACACTAGATTTAAAGCTGGATTT
 AGAATCATTAGTTGAATAACATTGGATTAGTGTGGATTTCAATCTATTAATAATTCATTAAACGAATAACACCCCTTAAAGTTAACTCTTTCAAACCG
 ATCATAACGCACACAAGCCTCCACCGAAATGTTGACACCATAATATTTTACTACCGAGTTCGCAAGGCTAATATGATTTCTTTTGAATTTTTCTC
 TTTATTCGATTCGAGAATAAGTGGATTGTTCTCCGAAAGTTAGATAGATCATTATGAGTTGTTCTTAGAGAGCTAGAAAACCTCAAACAAGTTTAT
 CAAGTCGATCAACTCTTTGATAAATCAACAATAGTTATCATTGCTCATTATAAGATTGAAAATGAGACTTTGATTTGGGAAAATAAATGCTTACC
 T**CAAGT**AAATTTAAAGTTTATGCTATGATGTTTGTGATTTTCGCAATTAATGATTTAATGATTTAAATAATCAAATAAATAAATCAATTAATAAT
 CA**CATATG**GTTTAAATAGGTTAAATGAGTTTATAG**GTCAAA**ATAATTTGATGGTTCTAAATGGGCTTCAAATTAAGTGGTTTATATTACAT
 GAGTGTGTGTTTACATGTAGAGGGGCTTACCCAAATTAACATCCAAATTAACATAGAGTAATTTCCAAAATGAAGTAAAGTAAACATTCAAATTTGT
 GACTAGAACTTTGAATTTGAGTTATAGACTTTGTGATTTTTTTATAATATAAATTCGTTTTGATAAGTTTATAAACCCTGTTTTCGTAAGAGA
 TTGTGAAATTTCTTTGCAGAGGGACATGGTTATTTTTGTCTTTGGTCTTGTAAATGAGATTTAACTATGTTAAATCTAAGAGCC**CATTG**JAAGAT
 GATGCTCGGCCCTCTTATCCTTATCTCGCCACCCTTCTAAAACCTTCCCTTCTCTTTCTTCTCTTCCACTTCCACTTCTCTATCTC
 TCACAATTCAGCA**AATG**

↑ 1bp before start codon

Figure 2.7. Upstream promoter sequences of *cp31A*, *cp29B*, and *cpSEBF* contain multiple HY5 binding motifs. A sequence of 1500bp was examined for each gene's ATG start side using Patterns Locator (Mrázek and Xie, 2006). Motifs were identified through a comprehensive literature analysis. Motifs identified within stream promoters are highlighted in the Legend: G-box (olive), E-box (yellow), CA Hybrid-box (blue), ACE-box (purple), C-box (green), and CG-hybrid box (red).

Motifs investigated included the G-Box (Chattopadhyay et al., 1998), C-Box motifs, CG-Hybrid Box, and CA-Hybrid Box (Song et al., 2008), E-Box and T/G-Box (Abbas et al., 2014), GATA-Box (Shi et al., 2011), ACE-Box (Shin et al., 2013), and Z-Box (Andronis et al., 2008). This revealed the presence of seven E-box motifs, and six C-boxes, a CA Hybrid-box, and an ACE-box in *cp29B*; three E-Box motifs, three C-Boxes, five ACE-boxes, and a CG Hybrid-box in *cpSEBF*; and three C-boxes, three E-boxes, a G-box, and an ACE-box in *cp31A* (Figure 2.7).

The presence of common HY5 binding motifs in these cpRNPs suggests that HY5 may be involved in their regulation. To test the involvement of HY5 in the regulation of the transcript accumulation of cpRNPs in response to red light, transcript levels for *cp31A*, *cp29B*, and *cpSEBF* were measured for WT and *hy5* mutant plants grown for 3 days in darkness and treated with 24hr of R-80 (Figure 2.8). This revealed a 77% reduction of *cp29B* transcript accumulation in *hy5* compared to WT; a 73% reduction for SEBF transcripts; and a 93% reduction for *cp31A* mRNA accumulation. These differences were statistically validated using a Student's *t*-Test. This suggests that HY5 may be a vital regulator of these cpRNPs. This regulation is also supported by a Chromatin Immunoprecipitation assay that detected the binding of HY5 to the *cpSEBF* (Lee et al., 2007).

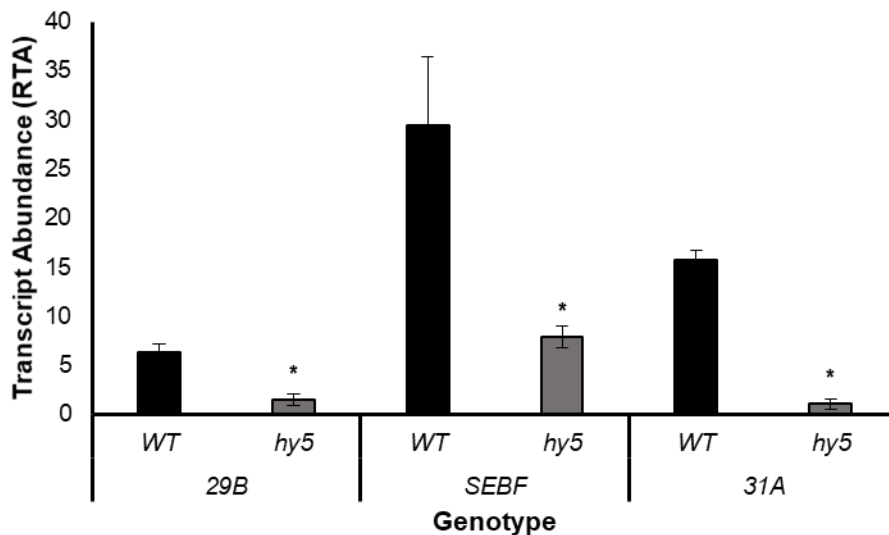


Figure 2.8. Transcript abundance of *cp29B*, *cpSEBF*, and *cp31A* is HY5-dependent. Graph shows relative transcript abundance (RTA) of *cpRNPs* in WT and *hy5* mutants grown for 3 days in darkness and treated with 24hrs of red light ($80 \mu\text{mol m}^{-2}\text{s}^{-1}$). Relative transcript abundance was calculated by comparing experimental gene expression to *PP2A* as a reference gene. Data represent the average of three biological replicates and error bars represent the 95% confidence interval. Statistical significance of transcript abundance in *hy5* (dark grey bars) compared to WT (black bars) was calculated independently for each gene using a Student's *t*-Test ($p < 0.05$). Significance is indicated using asterisks ($p < 0.05 = *$, $p < 0.01 = **$, $p < 0.001 = ***$).

A HY5-dependent modulation of *cpRNP* transcripts accumulation indicates a novel role for HY5 in the cascades leading to the post-transcriptional regulation of the plastome. To further test if HY5 could be involved in the red-light cascades for activation of the plastome, the effect of *hy5* mutation on transcript abundance of previously-examined plastome-encoded genes during de-etiolation was investigated, shown in Figure 2.9.

This experiment revealed HY5-dependent, light-dependent transcript accumulation of genes encoding subunits of the ATP Synthase (*atp*), Photosystem I (*psa*), and Photosystem II (*psb*), but no effect of *hy5* mutation was observed for the Cytochrome *b₆f* (*pet*) or NADH Dehydrogenase (*ndh*) plastid-encoded mRNAs accumulation. Notably, significant reductions in *atpA*, *atpH*, and *atpI* were observed in *hy5* compared to WT, as evaluated using a Student's *t*-Test, as well as for *psaJ*, *psbA*, *psbC*, *psbD*, and *psbF* subunits for Photosystem I and Photosystem II. This hints at a specificity behind HY5-transduced light signals for specific components of the photosynthetic machinery in red light. Interestingly, results for *atpH*, *psaJ*, *psbA*, *psbC*, *psbD*, and *psbF* accumulation in *hy5* correlate with results from *phyB* and *cprnp* mutants.

Altogether, the data show that HY5 is a key transcriptional regulator of *cp31A*, *cp29B*, and *cpSEBF*. The modulation of these cpRNPs by R-phy signals make their inclusion in a phyB-HY5-cpRNPs-plastome regulatory pathway plausible. Figure 2.10 presents a working model for the new regulatory pathway proposed, based on the photoreceptors, nuclear light signalling components in control of cpRNPs, and the potential of cpRNPs to deliver perceived environmental light signals to the plastome.

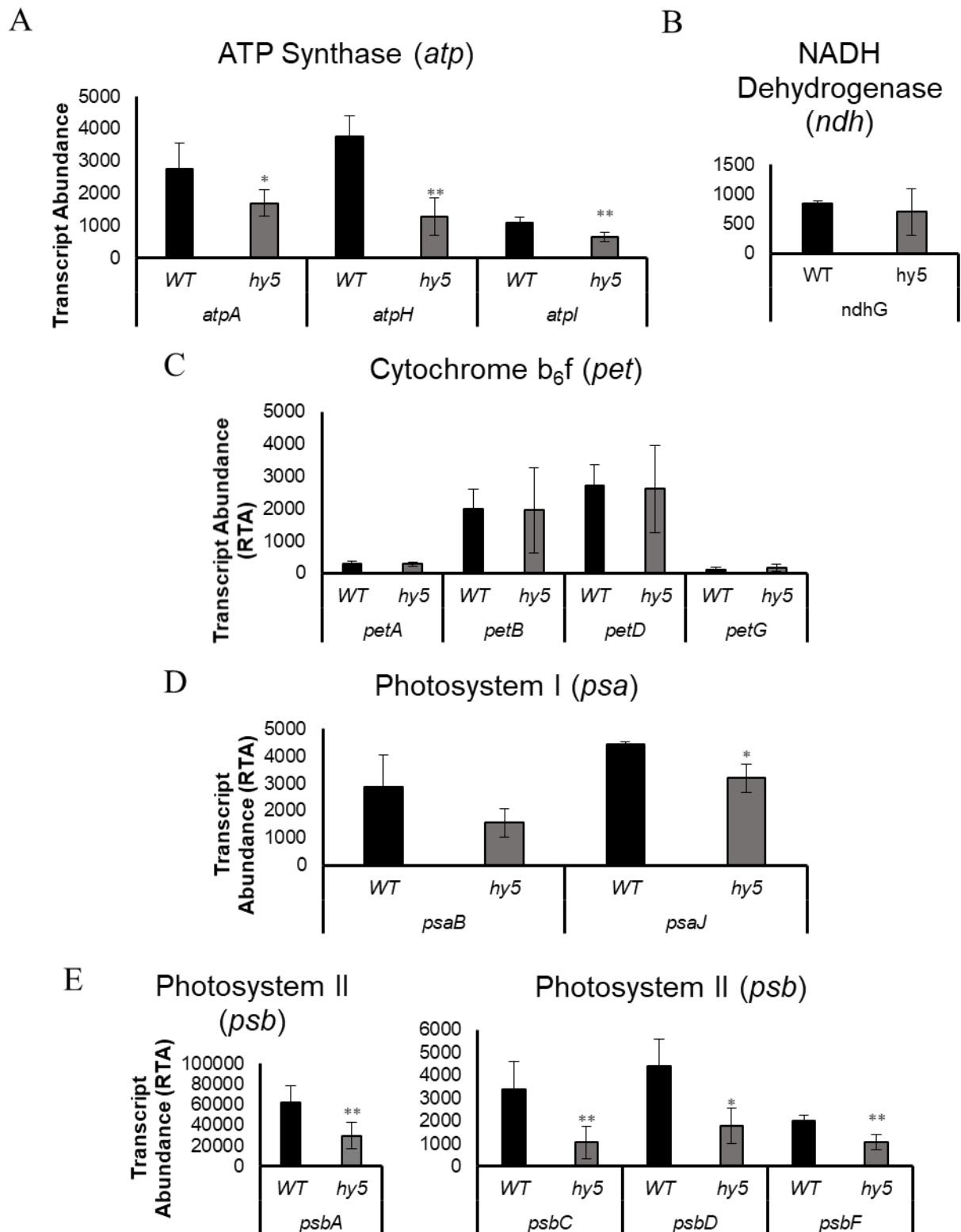


Figure 2.9. Transcript abundance of key ATP Synthase, Photosystem I, and Photosystem II plastome-encoded subunits is HY5-dependent in red light. Graphs show relative transcript abundance (RTA) of A) ATP Synthase family, B) NADH family, C) Cytochrome b_6f complex family, D) Photosystem I family, and E) Photosystem II family plastome-encoded subunits in WT, and *hy5* mutants grown for three days in darkness and treated with 24hrs red light ($80 \mu\text{mol m}^{-2}\text{s}^{-1}$). Relative transcript abundance was calculated by comparing experimental gene transcript accumulation to *PP2A* as a reference gene. Data represent the average of three biological replicates and error bars represent the 95% confidence interval. Statistical significance of transcript abundance between WT (black bars), and *hy5* (dark grey bars). Statistical significance of transcript abundance in *hy5* (dark grey bars) compared to WT (black bars) was calculated independently for each gene using a Student's *t*-Test ($p < 0.05$). Significance is indicated using asterisks ($p < 0.05 = *$, $p < 0.01 = **$, $p < 0.001 = ***$).

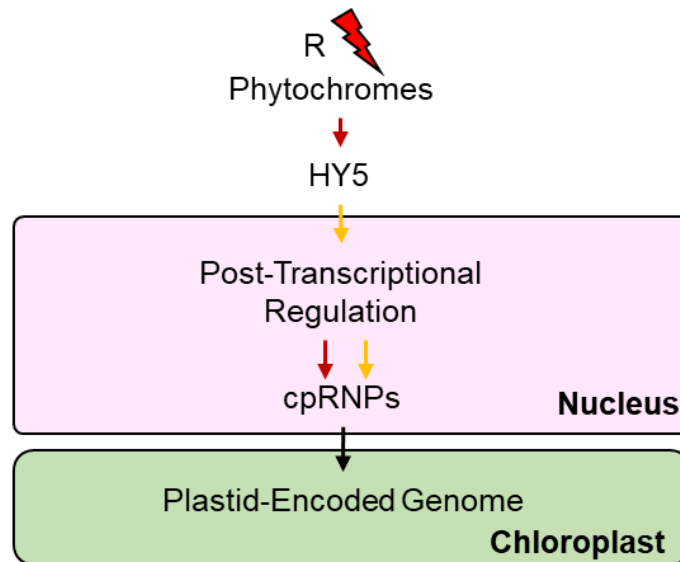


Figure 2.10. Working model for a red-light mediated phytochrome and HY5 involvement in the regulation of the plastome via the cpRNP family. An R-phys- and R-HY5 effect over the cpRNPs and downstream effect over the plastome is statistically demonstrated and represented with a full line.

2.4. Results: Are cpRNPs involved in the photosynthetic stress responses induced by high light and fluctuating light intensities?

In a natural environment plants are subject to a range of light intensities including rapid changes over short periods, that can have a large impact on photosynthesis and photosynthetic apparatus (Way and Pearcy, 2012; Hou et al., 2015). In low light conditions photosynthetic rate is light-limited, but in high light the photosynthetic rate is light-saturated and excessive light absorption can lead to oversaturation and damage caused by reactive oxygen species (ROS) (Kanervo et al., 2005).

Fluctuations in light intensity from low to high light can therefore induce stress in the photosynthetic apparatus by overloading reaction centres, inflicting photoinhibition and lowering photosynthetic efficiency (Aro et al., 1993; Kanervo et al., 2005; Ruban et al., 2012). Plants must therefore maintain an optimum balance of absorption of sunlight and protection of the photosynthetic apparatus and chlorophyll content (Aro et al., 1993).

Photoreceptors play a key role in responding to light fluctuations. Although cryptochromes (crys) have been linked to fluctuations in light intensity (Lin et al., 1998), phytochromes such as phyB have also been linked to the response (Sellaro et al., 2019). The active conformer of phyB is the Pfr-Pfr homodimer, D₂ (Klose et al., 2015): D₂ states respond to light intensity fluctuations in Photosynthetically Active Radiation (PAR), and can rapidly and accurately follow changes from base to over 400 $\mu\text{mol m}^{-2}\text{s}^{-1}$ PAR (Sellaro et al., 2019). Phys also induce photoprotective mechanisms by regulating water-use efficiency (Boccalandro et al.; Kreslavski et al., 2020), maintaining chlorophyll concentration and photosynthetic rates in response to short-term high light stresses (Kreslavski et al., 2020).

2.4.1. Photosynthetic apparatus in chloroplasts are vulnerable to fluctuations in light intensity and high light stress.

As sessile organisms, plants have therefore developed a range of acclimation mechanisms to deal with fluctuations in light intensities (Violet-Chabrand et al., 2017). This can involve modifying thylakoid proteins and photosynthetic machinery through state transitions (Kanervo et al., 2005; Walters, 2005), modulating antenna protein concentration and the contents of the electron transport chain (Anderson et al., 1995), as well as turnover of components such as D1 protein, which is vital to PSII function (Andersson and Aro, 2001).

The acclimation to light intensity responses can be short- and longer-term. Rapid responses to light fluctuations can involve state transitions of LHCII associating reversibly with either Photosystem (Walters, 2005): in high light, overload of PSII increases the pool of reduced plastoquinone and leads to the activation of protein kinase STN7 and phosphorylation of LHCII and its migration between PSII and PSI states (Bellafiore et al., 2005; Allen and Staehelin, 1992). Likewise, oxidation of the plastoquinone pool prompts the opposite, with dephosphorylation of LHCII and a return to PSII (Pribil et al., 2010; Rochaix et al., 2012). Other short-term high light acclimatory mechanisms include rearrangement of chloroplast components or by triggering of non-photochemical quenching (Ruban and Murchie, 2012; Bielczynski et al., 2016; Schumann et al., 2017).

These short-term responses involve modulation of the transcriptome. A rapid high-light response in *Arabidopsis* induced differential expression of over 700 transcripts, including many associated to the plastome gene expression such as sigma factor SIG1 (Suzuki et al., 2015).

Longer-term acclimation occurs over hours or weeks and involves the replacement synthesis and degradation of chloroplast components after damage to Photosystem reaction centres (Tian et al., 2017; Li et al., 2018). Regarded as one of the important protective systems of the thylakoid membrane at high light intensities (Kanervo et al., 2005), repair and replacement of the D1, D2, and additional subunits such as *PsbH* are vital components of the PSII complex and targets of photo-damage in strong irradiance (Komenda and Masojídek, 1995; Rokka et al., 2005). These components are also positioned as potential quenchers of excitation energy themselves that act to protect neighbouring PSII subunits (Lee et al., 2001; Matsubara and Chow, 2004).

Both light-fluctuation acclimation responses imply a further need for proper tuning on the photosynthetic machinery, including the setup of regulatory cascades including transcriptional and post-transcriptional control points for the adjusted expression of the plastome. cpRNPs, as proteins involved in greening responses and as phyB- modulated genes with a post-transcriptional modulatory capacity, may be candidates to investigate in the context of an acclimation pathway. Their modulation of the photosynthetic apparatus, including of cytochrome b_6f plastid-encoded subunits (Kupsch et al., 2012), D1 reaction centre protein-encoding gene *psbA* (Teubner et al., 2020), and of ATP Synthase subunits and both Photosystems I and II (Figure 2.5) could orchestrate a broad responsiveness. Furthermore, HY5, an upstream signalling component involved in cpRNP transcript accumulation, was found to be induced following a 1hr high light stress treatment (Rossel et al., 2002).

2.4.2. Investigating the phenotypic response of *cprnp* mutants to high light stress (HL).

Based on the identified R-light modulated targets of cpRNP targets including the *psbA-D1* (Nakamura et al., 2001) and other PSII components (Figure 2.5), a potential role of for cpRNPs in tolerating high-light stress conditions was investigated.

The effect of fluctuating high-light phenotypes of *cprnp* mutants was evaluated using two modified versions of a method described in Hou et al (2015), designed to constantly stress PSII in plants from day 0. *cprnp* mutants *cp29b*, *cpsebf*, and *cp31a* were grown in regimes of 1hr LL treatment ($50 \mu\text{mol m}^{-2}\text{s}^{-1}$)/1hr HL ($150 \mu\text{mol m}^{-2}\text{s}^{-1}$) treatment and 6hr LL ($50 \mu\text{mol m}^{-2}\text{s}^{-1}$)/2hr HL ($150 \mu\text{mol m}^{-2}\text{s}^{-1}$) treatment. Results were compared to plants grown in non-fluctuating continuous red light ($80 \mu\text{mol m}^{-2}\text{s}^{-1}$) as a control. *cprnp* mutants' responses were evaluated through their capacity to green under constant acclimation stress and accumulate biomass as indicators of photosynthetic efficiency. Experiments were conducted in Red Continuous grown 10-days old plants.

Fresh Weight Analysis. Results are shown in Figure 2.11. The 1hr LL/1hr HL condition (Panel A), shows a statistically significant FW reduction in *phyB* as well as reductions in *cpsebf* and *cp31a*. No statistically significant changes were detected in *cp29b* mutants. This result was compared to plants grown in control red-continuous light conditions, shown in Panel C, in which only a significant reduction in *phyB* FW was reported.

A Two-Way ANOVA analysis reported a significant interaction effect between light regime and genotype on FW accumulation in mutant plants ($P < 0.001$). A post-hoc Tukey HSD test identified there was significant interaction effect on the relationship between FW in WT and *phyB* ($P < 0.001$). The Two-Way ANOVA also revealed a significant effect of light condition in both datasets ($P < 0.001$), showing that the fluctuating light caused a global reduction in FW. An analysis of the interaction effects between light condition (fluctuating light condition vs control) and genotypes also indicated that WT is more greatly inhibited in fluctuating light, compared to *phyB* and *cpsebf*.

An analysis of FW accumulation for the 6hr LL/2hr HL condition (shown in Figure 2.11 Panel B) showed significantly reduced *phyB* FW accumulation compared to WT, but *cprnp* mutants were unaffected. A Two-Way ANOVA analysis comparison of continuous light to fluctuating light (6hr LL/2hr HL) reported a significant interaction effect of light condition and genotype on FW accumulation ($P < 0.001$). A Tukey HSD post-hoc test identified the interaction affected the relationship of WT to *phyB* on FW, with *phyB* plants being more inhibited in control conditions. The

Two-Way ANOVA also reported a significant effect of the fluctuating light treatment on global plant growth ($P < 0.001$).

Unshown repeats of these experiments in older plants (14 days) also showed no effect of fluctuating light regimes on *cprnp* mutant plants. Overall, this indicates only a limited role for cpRNPs in responses to fluctuating light conditions.

Chlorophyll accumulation analysis. For the 1hr HL/1hr LL condition shown in Figure 2.11 panel A, no statistical differences were observed in chlorophyll *a* or *b* accumulation between WT and *cprnp* mutants, but reductions in both Chl *a* and Chl *b* were detected in *phyB* mutant. When compared to control plants grown in red-continuous light conditions, shown in Panel C, in which only a significant reduction in *phyB* FW was reported, a Two-Way ANOVA analysis reported a significant interaction effect between light regime and genotype for Chl *b* ($P < 0.001$), affecting the relationship between WT and *phyB* ($P < 0.01$).

Additionally, for the 2hr HL/6hr LL condition (Figure 2.11, panel B), no significant differences were reported between WT and *cprnp* mutants in the accumulation of chlorophyll *a* or *b*. However, as for the other tested condition, significant reductions in both chlorophylls was observed in *phyB*. When compared to control plants grown in red-continuous light conditions, (panel C), Two-Way ANOVA analysis reported a significant interaction effect between light regime and genotype for both Chl *a* ($P < 0.001$) and Chl *b* ($P < 0.001$), affecting the relationship between WT and *phyB* in both instance ($P < 0.001$, $P < 0.01$ respectively).

Overall, these FW and chlorophyll results indicates only a limited role for cpRNPs in responses to fluctuating light conditions but do identify that *phyB*-dependent accumulation of chlorophyll *b* is affected by fluctuating light regime.

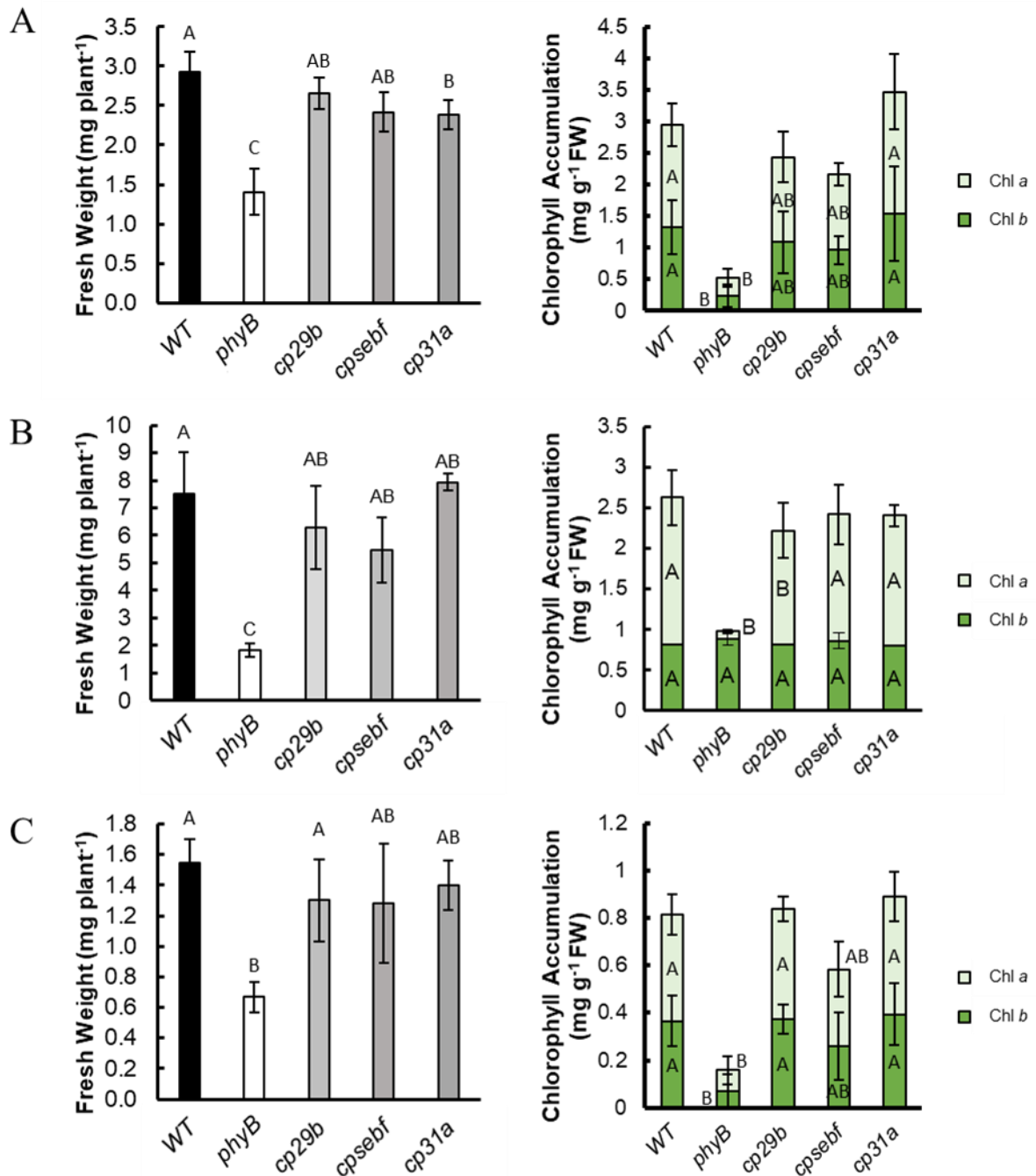


Figure 2.11. Short-term fluctuating light stress reduced Fresh Weight (FW) accumulation in *cprnp* mutants. Graphs show FW and chlorophyll a and b accumulation per plant of WT, *phyB*, and *cprnp* mutants treated with A) an alternating cycle of 1hr high light (HL) ($150 \mu\text{mol m}^{-2}\text{s}^{-1}$) and 1hr low light (LL) ($25 \mu\text{mol m}^{-2}\text{s}^{-1}$) for 10 days, B) in continuous light ($80 \mu\text{mol m}^{-2}\text{s}^{-1}$), or C) an alternating cycle of 2hrs HL and 6hrs LL. Data represent the average of at least 3 biological replicates and error bars show the 95% confidence interval. Statistical significance of FW measurements in each genotype was calculated using One-Way ANOVA with Tukey post hoc testing ($p < 0.05$). Data that do not share a letter are statistically significant.

2.5. Results: Investigating the cpRNPs sensitivity to photoperiodicity.

2.5.1. phyB is a key integrator of photoperiodicity.

Photoperiodicity is a key factor that affect almost all aspects of Arabidopsis growth and development (Adams and Langton, 2005), including a range of photosynthesis-associated processes such as glucose and sucrose distribution (Ceunen and Geuns, 2013), and chlorophyll content (Adams and Langton, 2005). Plants adjust to day-length cycles to optimise growth in response to dark-light cycles depending on latitude and seasonal growth (Graf and Smith, 2011; Baerenfaller et al., 2015).

Long Day (LD; 16hr light, 8hr dark) and Short Day (SD; 8hr light, 16hr dark) photoperiods dramatically affect plant morphology and associated photosynthetic rates (Carpenter et al., 1983). Experiments on *P. tomentosa* showed that LD-grown plants accumulated a greater biomass through larger leaf area, root and stem length, and total dry weight, but SD-grown plants exhibited a higher net photosynthetic rate (Carpenter et al., 1983).

Arabidopsis is a facultative long-day plant, and SD conditions decrease final leaf area and rates of leaf expansion compared to LD (Cookson et al., 2007), as well as affecting leaf shape (Willmann and Poethig, 2011). Plants were also observed to accumulate starch rapidly in light and its degradation in dark was slower in SD compared to LD plants, which instead exhibited the higher growth rates (Sulpice et al., 2014). These changes were represented in the cell by LD-grown leaves having a higher chlorophyll content per area due to an increased leaf thickness (Lepistö and Rintamäki, 2012). At a transcriptomic level, significant differences were found in the Arabidopsis transcriptome between LD and SD (Baerenfaller et al., 2015). Genes involved in RNA processing mechanisms, Photosystem I, and Photosystem II were overrepresented in SD conditions, speculated to be related to the increased rate of photosynthesis to use the limited light most efficiently (Baerenfaller et al., 2015).

The dark-light cycles that define photoperiodicity are in part detected through phytochromes. Phys are sensors of photoperiods with phyB playing a role in the photoperiod-photoperiodic-dependent flowering (Blázquez and Weigel, 1999; Kippes et al., 2020) and CO₂ uptake and loss (Mousseau, 1981). The phyB-photoperiodic flowering pathway relies modulation of *FLOWERING LOCUS T (FT)* (Kaiserli and Chory, 2016) as well as adjustments in transcription factors activity, growth regulators and chromatin remodelling factors (Loudet et al., 2008), suggesting a wide photoperiod-regulated signalling cascade. As such, phyB is both capable of detecting and transducing photoperiodic signals to regulate gene expression.

phyB is therefore a key integrator of both light and photoperiod, and may deliver photoperiodic environmental signals to organelles, including the signals for the modulation of plastid gene expression. An effect of *phyB* mutation has previously been observed on plastome transcript accumulation in data derived from SD plants (Figure 2.4) (Michael et al., 2008).

An evaluation of available photoperiodic databases was conducted to identify whether cpRNP genes could exhibit photoperiod modulation and be part of the signalling cascades.

2.5.2 Bioinformatic examination of cpRNPs' response to different photoperiods.

cpRNPs' transcript accumulation response to Long Day conditions. To investigate whether cpRNPs follow a photoperiod-sensitive transcript accumulation, Long Day (LD; 16hr Light, 8hr Dark, 22°C) microarray timeseries expression datasets were examined. Dataset GSE50438, and data from the DIURNAL dataset (Mockler et al., 2007) were analysed in Figure 2.12 in panels A and B respectively. These datasets indicated a LD-photoperiodic expression pattern for *cp29B* and *cp31A*.

Figure 2.12 panel A, based on data from GSE50438, shows expression of *cp29B* peaking at the very end of the night period and just at dawn with expression dropping to low levels within 8hours/by midday. The pattern for *cp31A* appears to show a peak in expression in the early day and a trough before the dark period with expression slowly rising up to the morning period again. Data show that *cpSEBF* does not have a clear photoperiodic dependent modulation with only minor peaks about 8 hours into each day, and potentially a mild night-time peak. Figure 2.12 panel B, analysing data from the DIURNAL dataset, shows a similar expression pattern for *cp29B* with high accumulation at the end of night/early morning but in a phase just earlier than in panel A, and shows an additional smaller peak just before the night phase. *cpSEBF* shows a less oscillating pattern, with even less variation in its cycling; and results for *cp31A* appear to show a peak in expression before the night period.

The dataset GSE50438 analysed in Figure 2.12 panel A was generated using agar with 0.5% (w/v) sucrose and Col-0, and the data presented in Figure 2.12 panel B from the DIURNAL dataset was generated using agar with 3% (w/v) sucrose and Ler WT seedlings (Mockler et al., 2007). While the datasets are not strictly comparable, and the inclusion of sucrose in media is known to affect phyB signalling pathways (Nemhauser and Chory, 2002), the preliminary evidence points at the possibility of a Long Day expression pattern for *cp29B* transcripts peaking at the end of the night/dawn, and peaks for *cp31A* in the middle of the day. Although some minor oscillations were

observed, *cpSEBF* did not show a strong photoperiodic dependent transcript accumulation, so only *cp29b* and *cp31a* were chosen for phenotypic analysis in Long Day conditions.

***cpRNPs'* transcript accumulation pattern response to Short Day conditions.** To identify whether cpRNPs have a photoperiod sensitive transcript accumulation in Short Days (SD) (8hr Light, 16hr Dark), genomic dataset E-MEX-1299 from the DIURNAL project (Mockler et al., 2007) was examined, using 8-10 days old plants grown in SD conditions (see section 2.2 Materials and Methods).

E-MEX-1299 compared WT and *phyB-9* mutants, allowing examination of how phyB affects SD photoperiodism. This data is shown in Figure 2.13 and shows clear oscillating patterns for *cp29B* and *cp31A* with transcript abundance spiking at the end of the light period and decreasing throughout the night and early light period. A similar pattern was observed for *cpSEBF*, but peak amplitude was much reduced. However, for *cp29B* and *cpSEBF* the only observable differences between *phyB* and WT was a moderate reduction in peak amplitude. No observable differences were detected for *cp31A* expression between *phyB* and WT.

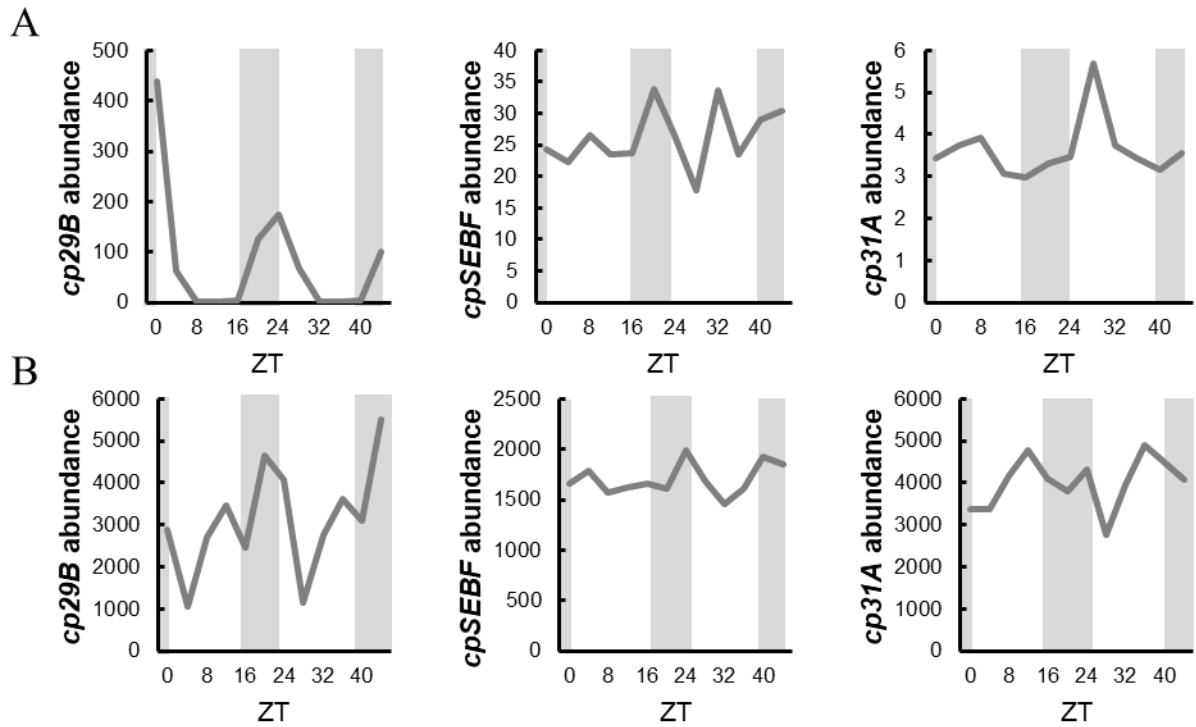


Figure 2.12 *cp29B* and *cp31A* expression cycles in Long Day (LD) photoperiod conditions. Gene expression data was obtained and reproduced from A) Dataset GSE50438 using Col-0 WT plants grown in LD conditions (16hrs light ($56 \mu\text{mol m}^{-2} \text{s}^{-1}$) and 8hrs dark) at 22 °C for nine to ten days and B) data by Mockler et al (2007) using Ler WT seedlings grown in LD conditions (16hrs light ($100 \mu\text{mol m}^{-2} \text{s}^{-1}$) and 8hrs dark) at 22°C for eight days.

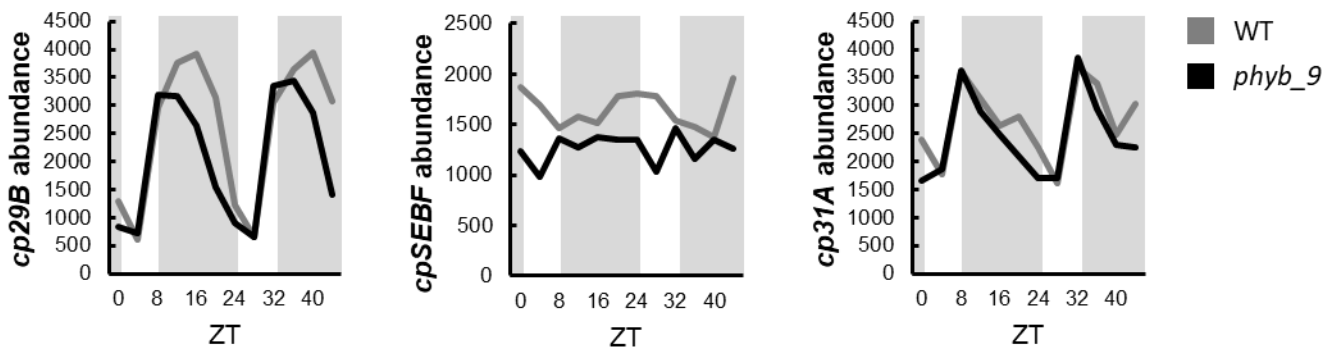


Figure 2.13 *cp29b* and *cp31a* expression cycles in Short Day (SD) photoperiod conditions. Gene expression data was obtained from dataset E-MEX-1299, using Col-0 WT and *phyB* plants grown in SD conditions (8hrs light ($100 \mu\text{mol m}^{-2} \text{s}^{-1}$) and 16hrs dark) at 22°C for eight days.

2.5.3 Phenotypic characterisation of cpRNPs' response to different photoperiods.

Based on the results obtained by bioinformatics studies, the photoperiodic phenotypes of *cprnp* mutants were evaluated. *cprnp* mutants *cp29b* and *cp31a* were grown in Long or Short-Day photoperiodic conditions to evaluate day length effects on their growth, including capacity to green (measured via chlorophyll accumulation) and biomass accumulation (Fresh Weight). The experiments were conducted in 10-day old plants grown under the specified photoperiodic condition in red light ($80 \mu\text{mol m}^{-2} \text{s}^{-1}$).

Phenotypic evaluation of *cprnp* mutants' response to Long Day photoperiodic conditions. Informed by potentially LD-cycling expression patterns, *phyB*, *cp29b* and *cp31a* mutants were examined for effects of LD-cycling on growth and greening phenotypes. Plants were grown in Long Day conditions ($80 \mu\text{mol m}^{-2} \text{s}^{-1}$ /16hr/22°C, darkness/8hr/17°C) for 14 days (Figure 2.14). Phenotypic evaluation illustrated in representative photos from this experiment (panel A) indicated no notable physiological differences between *cp29b* or *cp31a* and WT, and no significant differences to WT were detected for *cp29b* or *cp31a* for FW or chlorophyll *a* or chlorophyll *b* accumulation (panel B). However, significant reductions in biomass accumulation and chlorophyll *a* were observed in the *phyB* mutant compared to WT.

However, while *cp31a* mutants were clearly no different from WT plants, noticeably lower chlorophyll content averages were recorded for *cp29b*. To clarify the possibility of *cp29B* having a photoperiodic role, an experimental repeat was conducted (Supplementary Figure 2.2), which indicated that *cp29b* plants exhibited a statistically lower FW, but no differences in chlorophyll *a* or *b* accumulation. These results may point at *cp29b* plants showing defects in biomass accumulation in Long Day compared to WT, thinly hinting at a role in the modulation of photoperiodic responses associated to growth and greening.

Phenotypic evaluation of *cprnp* mutants' response to Short Day photoperiodic conditions. Equally informed by potentially SD-cycling expression patterns, *phyB*, *cp29b* and *cp31a* mutants were examined for effects of SD-cycling on growth and greening phenotypes. Plants were grown in Short Day conditions ($80 \mu\text{mol m}^{-2} \text{s}^{-1}$ /8hr/22°C, Darkness/16hr/17°C) for 14 days. The results for this analysis are presented in Figure 2.15. Representative photos, biomass accumulation, and chlorophyll accumulation results are shown in panels A, B, and C. These results show no significant reductions in biomass accumulation or chlorophyll accumulation between WT and *cprnp* mutants, but significant reductions were reported in *phyB* mutants for each factor tested.

In summary, data from the described publicly available microarrays show clear LD and SD expression patterns for *cp29B* and *cp31A*. However, experiments with *cprnp* mutants only demonstrated the possibility of a modest phenotype for *cp29b* in LD conditions, and no effect from *cp31A*.

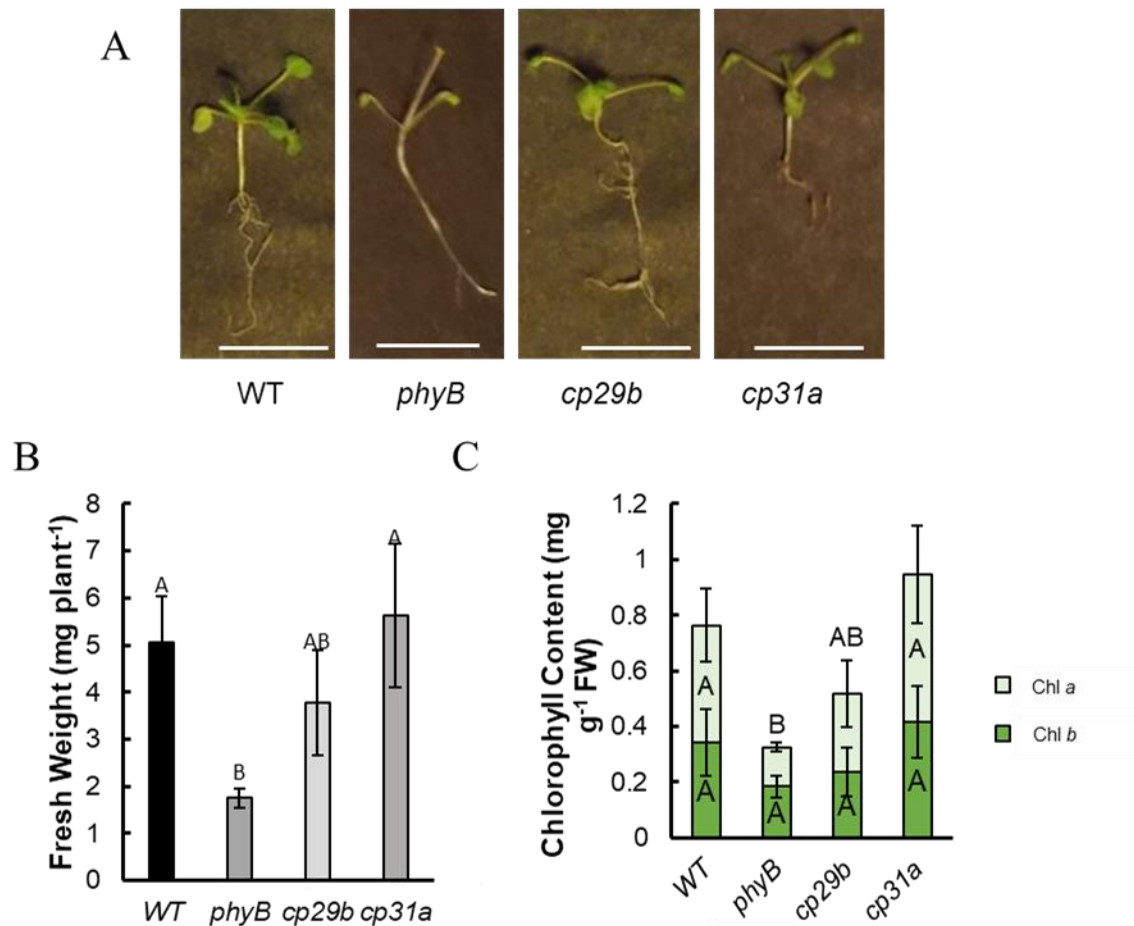


Figure 2.14. *cp29b* and *cp31a* mutants did not express a Long Day-sensitive phenotype. WT, *phyB*, *cp29b_2*, and *cp31a_2* plants were grown in LD conditions (16hrs light (80 $\mu\text{mol m}^{-2}\text{s}^{-1}$ red light) at 22°C and 8hrs dark at 17°C) for 14 days. A) Representative photos of plants with scale bar equal to 1cm. B) Graph shows Fresh Weight (FW) per plant. C) Chlorophyll *a* and chlorophyll *b* content was calculated from FW measurements using formulae published in Lichtenthaler and Buschmann (2001). Data represent the average of 3 biological replicates of c.6 plants each and error bars show the 95% confidence interval. Statistical significance of FW and chlorophyll abundance in each genotype was calculated using One-Way ANOVA with Tukey post hoc testing ($p < 0.05$). Data that do not share a letter are statistically significant.

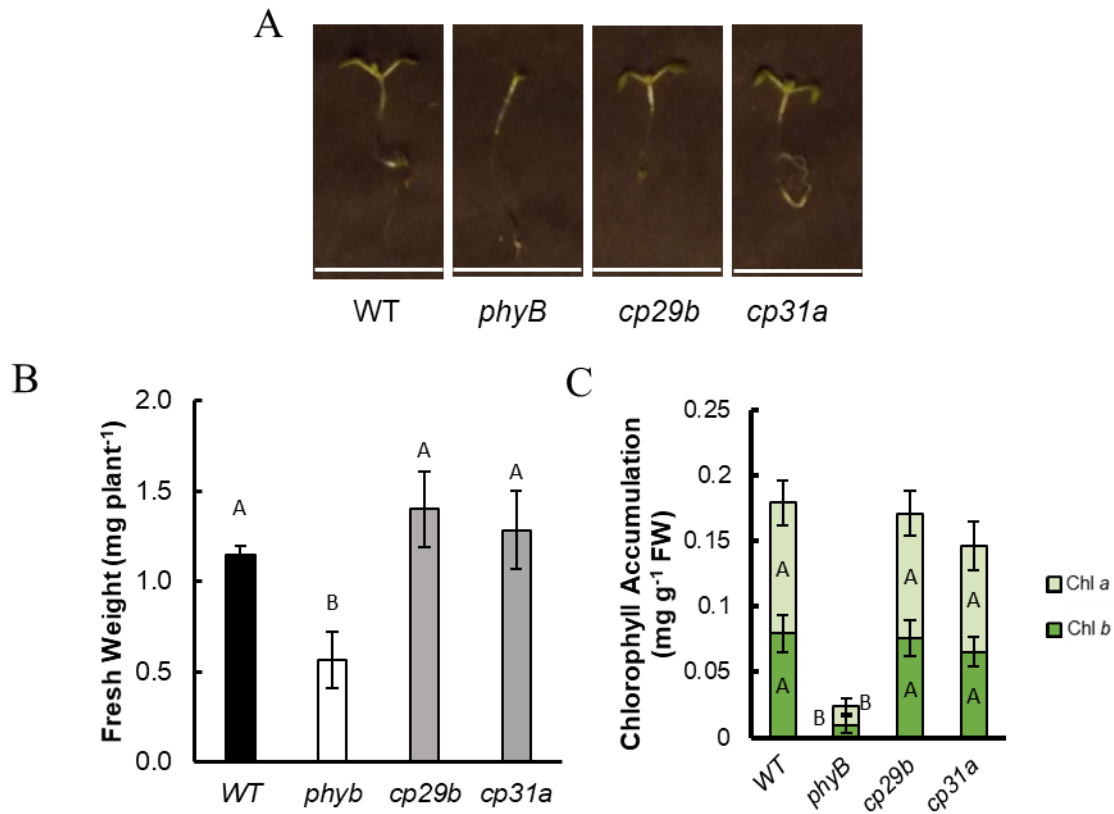


Figure 2.15. *cprnp* mutants did not express a Short Day-sensitive phenotype. WT, *cp29b_2*, and *cp31a_2* plants were grown in SD conditions (8hrs light (80 $\mu\text{mol m}^{-2}\text{s}^{-1}$ red light) at 22°C and 16hrs dark at 17°C) for 14 days. A) Representative photos of plants with scale bar equal to 1cm. B) Graph shows Fresh Weight (FW) per plant. C) Chlorophyll *a* and chlorophyll *b* content was calculated from FW measurements using formulae published in Lichtenthaler and Buschmann (2001). Data represent the average of at least 3 biological replicates of c. 6 plants each and error bars show the 95% confidence interval. Statistical significance of FW and chlorophyll abundance in each genotype was calculated using One-Way ANOVA with Tukey post hoc testing ($p < 0.05$). Data that do not share a letter are statistically significant.

2.6. Results: Beyond light: the cpRNPs and photoreceptor-dependent temperature sensing.

2.6.1. Ambient Temperature responses.

The variation in ambient growth temperatures can have important impacts on a plant phenotype, affecting development, physiology, flowering, and morphology, and therefore an understanding of how plants sense and response will be increasingly important with the ongoing global climate changes (Wigge, 2013; McClung et al., 2016). Physiological and morphological effects vary dependent upon temperature: higher temperatures (27-30°C) induce changes in plant architecture, such as elongation of stems and accelerated flowering (Capovilla et al., 2015), and even mild reductions in temperatures (eg 18°C) induce stunted growth and photobleaching (Samach and Wigge, 2005). cpRNPs have been linked to cold-temperature tolerance (Kupsch et al., 2012), as has their upstream signalling component HY5 (Toledo-Ortiz et al., 2014). This section will examine how cpRNPs may integrate temperature signals to regulate the plastome.

2.6.2. phyB and HY5 are a key integrators of ambient temperature responses, linking temperature sensitivity to cpRNPs' regulation.

phyB is a thermosensor capable of regulating temperature-sensitive genes and affecting transcript accumulation between 17-30°C, indicating a role in ambient-temperature sensing (Jung et al., 2016; Legris et al., 2016).

HY5 is also an ambient temperature sensor (Toledo-Ortiz et al., 2014). In particular, at 17°C HY5 transcripts accumulated more abundantly than at 27°C, with a clear role of HY5 in the accumulation of photopigments in particular at 17°C (Toledo-Ortiz et al., 2014). HY5 also participates in anthocyanin accumulation in chilling conditions (4°C) (Zhang et al., 2011; Catalá et al., 2011), with *hy5* mutants showing lower freezing tolerance than WT. HY5's involvement in heat shock responses include stabilised HY5 protein levels due to reduced COP1 accumulation, suggesting that HY5 may be required for a synergism for heat and light signals (Karayekov et al., 2013).

As downstream components of both phyB and HY5, and in addition to their described involvement in cold responses (Ruwe et al., 2011; Kupsch et al., 2012), cpRNPs are good candidates to investigate as temperature-sensitive signal transducers to the plastome. cpRNPs cp29, cp31, and cp33 highly expressed in cold conditions in wheat and were within the 50 most highly expressed proteins upregulated after two weeks' cold stress (Sarhadi et al., 2010). This may equate to higher levels of protein, as indicated by evidence from *B. thellungiella*, where the CP29-related protein was elevated after a 24-day 4°C chilling treatment (Gao et al., 2009).

2.6.3. *cpRNP* transcript accumulation is ambient temperature-dependent.

In *Arabidopsis*, *cp29B* gene showed induction after 1 week cold-shock treatment at 6°C (Amme et al., 2006). Temperature-sensitive accumulation for *cp29A* and *cp31A* was observed in plantlets transferred to 8°C for 18 days, where *cp29a* and *cp31a* mutants showed bleaching of newly emerged leaves and pale primary leaf development for plants germinated at 8°C (Kupsch et al., 2012). This pale phenotype was proposed to be due to failures in setting up photosynthetic apparatus, based on an analysis of the bleached, newly-emerged tissues which showed a 50% or greater reduction of plastid-encoded transcripts *psaA*, *psbD*, *psbF*, *psbB*, *petB*, *rbcL*, and *ndhF* at 8°C but not at 23°C (Kupsch et al., 2012). An analysis of *cp31a* mutant also showed a cold (8°C)-dependent binding of four *ndh* transcripts (*ndhF*, *ndhK*, *ndhB*, and *ndhD*), further indicating a temperature-dependent effect of *cp31A* protein in cold (Okuzaki et al., 2019).

Results presented in this chapter support the investigation of the role of *cpRNPs* in light- and temperature- integrating pathways under phy control; while most of the current published experimental data had been gathered under chilling or cold stress conditions (0-15°C), the *cpRNPs* position downstream of the ambient-temperature sensing *phyB* may indicate a role at ambient temperature sensing too (Jung et al., 2016). This research therefore examined the role of *phy*, *HY5*, and *cpRNPs* in ambient temperature sensing pathways (17-27°C).

Considering that the *cpRNPs* regulate plastome-encoded transcripts involved in the photosynthetic apparatus (Figure 2.5) and the photosynthetic apparatus is particularly sensitive to changes in temperature (Strand et al., 1997; Samach and Wigge, 2005) it was hypothesized that *cpRNPs* could play a role in integrating ambient temperature signalling. To investigate this possibility, the transcript accumulation of *cpRNPs* was tested at 17°C, 22°C and 27°C in de-etiolating plants was examined first (Figure 2.16).

This analysis revealed a temperature-dependent transcript accumulation of *cp29B*, *cpSEBF*, and *cp31A*. Results showed transcript accumulation for these genes was lowest in 17°C, and highest at 22°C in control conditions, with intermediate expression at 27°C for *cp29B* and *cp31A*. *cpSEBF* accumulation, however, was equally high in 22°C and 27°C.

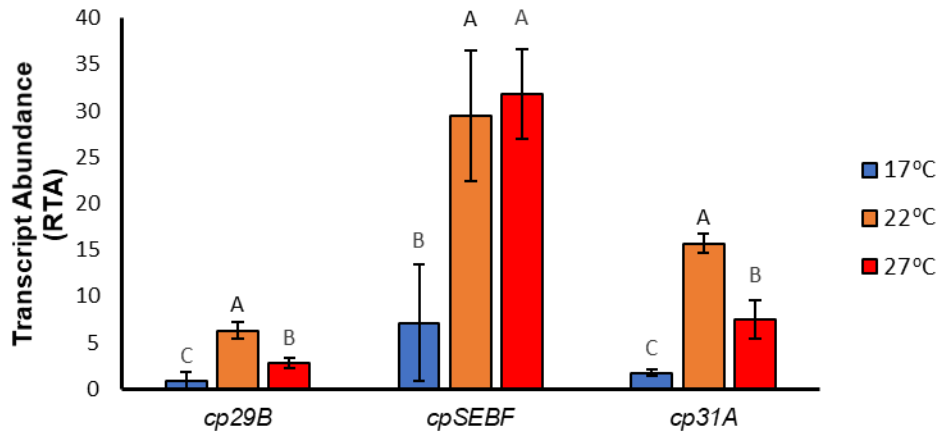


Figure 2.16. Transcript abundance of *cp29B*, *cpSEBF*, and *cp31A* is temperature-dependent. Graph shows relative transcript abundance (RTA) of *cpRNPs* in WT grown for 3 days in darkness in 17°C, 22°C, or 27°C and treated with 24hrs of red light ($80 \mu\text{mol m}^{-2}\text{s}^{-1}$). Relative transcript abundance was calculated by comparing experimental gene transcript accumulation to *PP2A* as a reference gene. Data represent the average of three biological replicates and error bars represent the 95% confidence interval. Statistical significance of transcript abundance in 17°C (blue bars), 22°C (orange bars), or 27°C (red bars) were compared independently for each gene using a One-Way ANOVA with Tukey post hoc testing ($p < 0.05$). Data that do not share a letter are statistically significant.

2.6.4 Biomass and chlorophyll accumulation in *cprnp* mutants are sensitive to warm and cold temperatures.

The role of *cpRNPs* in plantlet development was evaluated through the impact of *cprnp* mutations on greening (measured by chlorophyll accumulation) and biomass accumulation (measured via FW) responses at 17°C, 22°C and 27°C. WT (Col-0), *phyB*, *hy5*, *cp29b*, *cpsebf*, and *cp31a* plants were grown for 10 days in Red Continuous illumination ($80 \mu\text{mol m}^{-2} \text{s}^{-1}$) in the three temperature conditions. Results are shown in Figure 2.17.

Representative photos of results (panel A) pointed at clearly observable, temperature-dependent phenotypes in *cprnp* mutants, and corroborated Arabidopsis WT morphological differences at the 3 temperatures tested. Hypocotyl length in the WT increased proportionally with temperature, as did petiole growth. Furthermore, the leaf area appeared to be greatest at 22°C and reduced at the non-optimal temperatures.

At 22°C, *cprnp* mutants *cp29b* and *cpsebf* show smaller cotyledons and leaves compared to WT. At 17°C, a lower leaf size and slower true leaf emergence can be seen in *cprnp* mutants compared to WT, showing an intermediate phenotype between WT and the effects of *hy5* and *phyB*. At 27°C plants show much smaller leaf sizes and reduced petiole elongation in *cprnp* mutants compared to WT. At this temperature *phyB* and *hy5* mutants show clear morphological changes

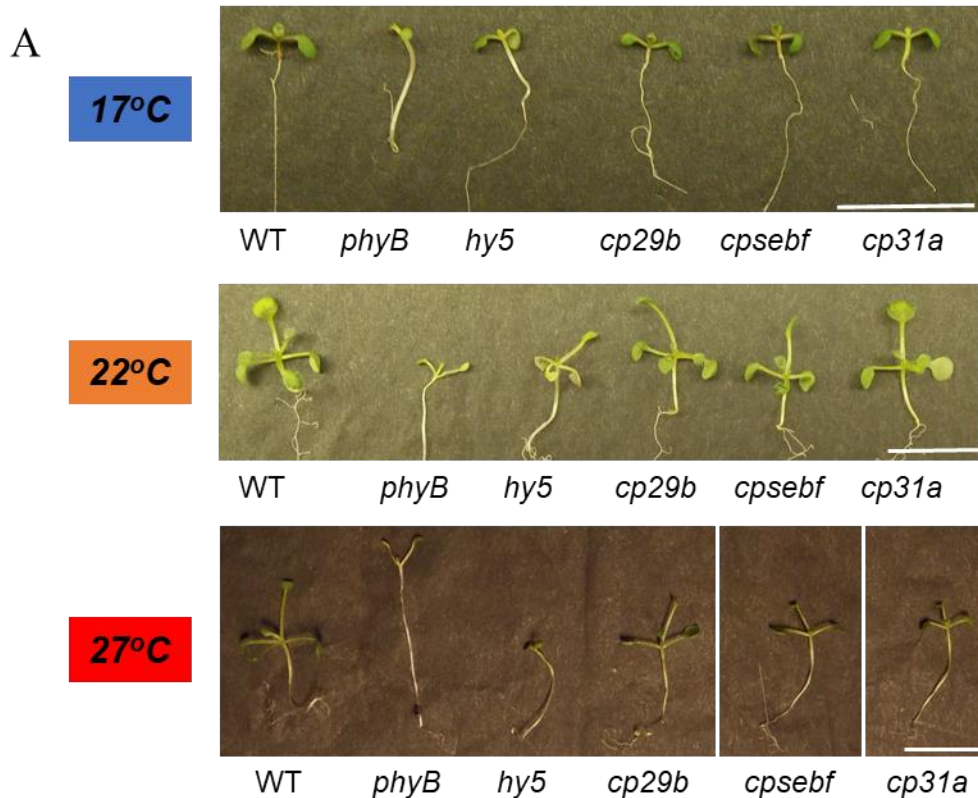


Figure 2.17. *cprnp* mutants express cold- and warm- temperature-sensitive phenotypes. WT, *phyb*, *hy5*, *cp29b_2*, *cpsebf_1*, and *cp31a_2* plants were grown in continuous red light ($80 \mu\text{mol m}^{-2}\text{s}^{-1}$) at for 10 days at 17°C, 22°C, or 27°C. A) Representative photos of plants with scale bar equal to 1cm. B) Graph shows Fresh Weight (FW) per plant. C) Chlorophyll A and chlorophyll B content was calculated from FW measurements using formulae published in Lichtenthaler and Buschmann (2001). Data represent the average of 3 biological replicates and error bars show the 95% confidence interval. Statistical significance of FW and chlorophyll abundance between each genotype was calculated using One-way ANOVA with Tukey post hoc testing ($p < 0.05$). Data that do not share a letter are statistically significant.

including exceedingly long hypocotyls and miniscule cotyledons. Overall, this indicated a role for *phyB*, *HY5*, and *cpRNP* proteins in temperature-dependent growth.

Fresh weight response. Analysis of the plantlets' Fresh Weight (FW) was conducted as a proxy parameter for biomass accumulation, and is shown in Figure 2.17 panel B. This analysis showed a temperature-dependent phenotype of *phyB* and *hy5* at 17°C and 27°C with a pronounced reduction in biomass accumulation. All *cprnp* mutants were more sensitive to a cold ambient temperature compared to WT, and *cpsebf* was also sensitive at the higher ambient temperature. Statistical comparison to control plants grown at 22°C revealed this response was subject to interaction effects between temperature and genotype, implicating *cpRNPs* in a temperature-dependent response.

At 22°C, no *cprnp* mutants were statistically different from the WT control. However, in the 17°C treatment *cprnp* mutants accumulated a lower biomass compared to WT, validated through a One-Way ANOVA statistical analysis by One-Way and Tukey HSD post-hoc testing ($P < 0.001$). Of these mutants, *cpsebf* and *cp31a* showed the greatest sensitivity to cold with strongest effect on fresh weight reductions. At 27°C, *cprnp* mutants were less sensitive to the increased temperature; despite a lower average fresh weight for *cp29b* and *cp31a* mutants, the difference was not statistically significant. However, *cpsebf* did exhibit a significant c.1.5-fold lower fresh weight accumulation. These results indicate that cpRNPs cp29B, cpSEBF, and cp31A are involved in an ambient temperature-response to modulate biomass accumulation.

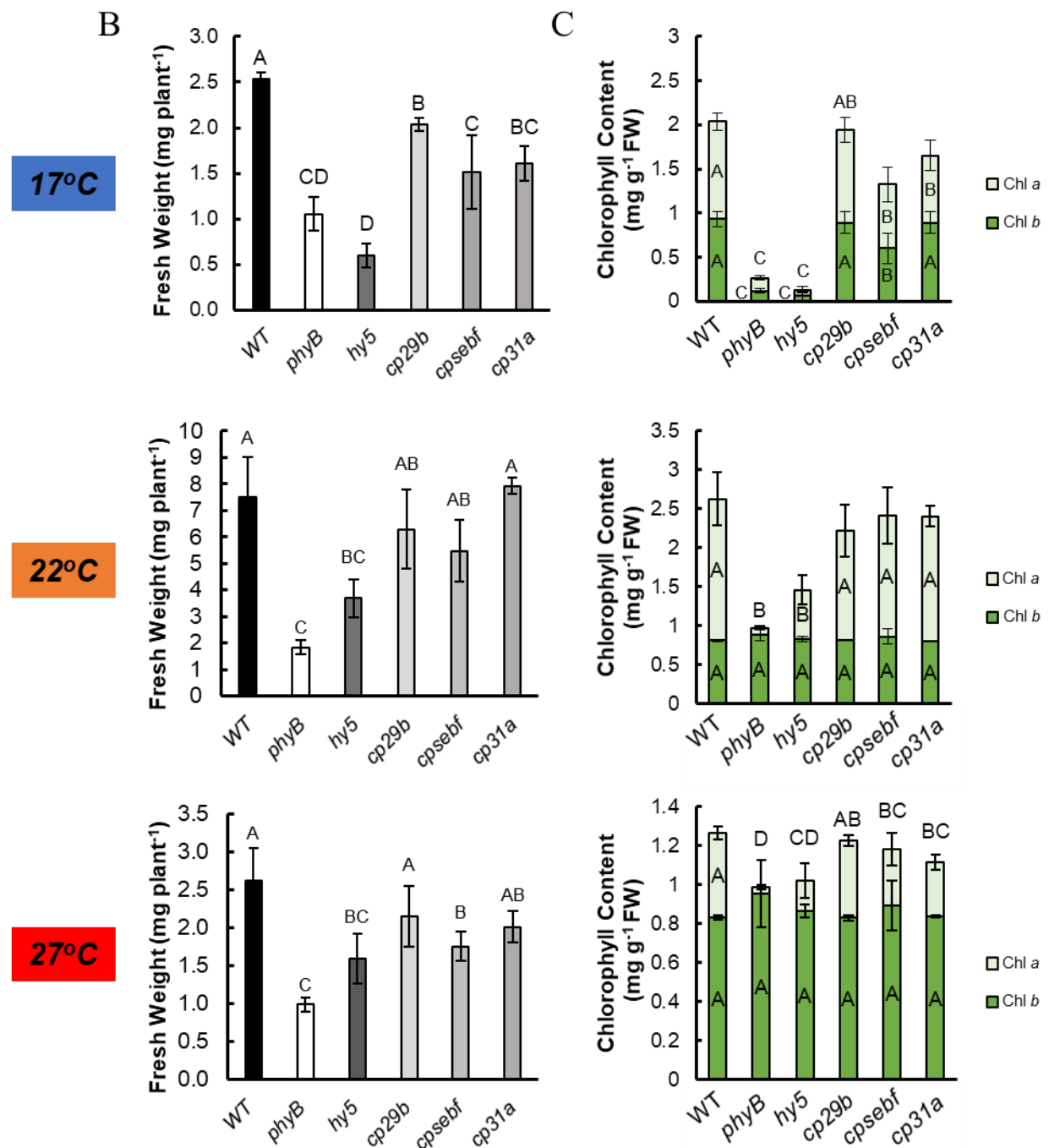
A Two-Way ANOVA analysis of these results revealed a significant interaction effect between genotype and temperature on Fresh Weight ($p < 0.001$). A Tukey HSD post-hoc test identified that the interaction effect significantly affected the relationship between WT and *phyB*, *hy5*, and *cpsebf* ($p < 0.001$), WT and *cp29b* ($p < 0.01$), and WT and *cp31a* ($p < 0.05$). Therefore, the FW of *cprnp* mutants, *phyB*, and *hy5* was dependent on the temperature condition, suggesting that cpRNPs do integrate temperature signals to modulate in the cold and the warm biomass accumulation.

Chlorophyll accumulation response. As shown in Figure 2.17 panel C, Chl *a* accumulation is phyB-dependent in all temperature conditions, and Chl *b* accumulation is phyB-dependent only at 17°C, suggesting a unique temperature-dependent pathway for phyB in cold conditions. Interestingly, accumulation of Chl *a* in *phyB* was less inhibited at 17°C and 27°C compared to WT than at 22°C. Similarly, Chl *a* production is also HY5-dependent at 17°C, 22°C and 27°C.

In the evaluation of contributions of cpRNPs to the Chl *a* accumulation response, Chl *a* content is reduced in *cpsebf* and *cp31a* compared to WT plants in cold (17°C) and warm (27°C) temperature conditions, but not at a standard (22°C) temperature in Arabidopsis plantlets, showing Chl *a* accumulation is affected by temperature-dependent activity of cpSEBF and cp31A. Chl *b* accumulation is additionally shown to be cpSEBF-dependent at 17°C. At 22°C, no notable changes were observed in *cprnp* mutants compared to WT, consistent with biomass accumulation results.

A Two-Way ANOVA statistical analysis reported a significant interaction effect of genotype and temperature on Chl *a* ($P < 0.001$) and Chl *b* ($P < 0.001$) accumulation, showing that both chlorophylls' accumulation was temperature- and genotype-dependent. A post-hoc Tukey HSD test for Chl *a* accumulation identified there was significant interaction effect on the relationship between Chl *a* in WT and *phyB* ($P < 0.001$), WT and *hy5* ($P < 0.001$), WT and *cpsebf* ($P < 0.05$), and for WT and *cp31a* ($P < 0.05$). A post-hoc Tukey HSD test for Chl *b* also reported significant interaction effects on the relationship between Chl *b* in WT and *hy5* ($P < 0.001$).

This indicates that cpSEBF and cp31A may be involved in an ambient temperature-dependent greening and growth response. This expands cpRNPs' known temperature range from their known cold and chilling tolerance response (Kupsch et al., 2012) to perception of ambient temperatures. To further examine the effect of the observed changes temperature changes on functions dependent on the cpRNPs, the effects of *cpnrp* mutation in the temperature-dependent adjustment of the plastome gene transcript accumulation was investigated next.



2.6.5. The plastome response to ambient temperature changes is mediated by cpRNPs.

Analyses of *cprnp* mutant phenotypes in 17°C and 27°C temperature conditions showed significant effects on biomass accumulation and greening (Section 2.6.4). Considering the molecular function of the cpRNPs in modulating the accumulation of plastid encoded genes, an investigation of temperature sensitivity on the cpRNP plastome targets previously identified as light- and phyB-modulated in *cprnp* mutants was conducted. These candidates included *atpH* of the ATP Synthase complex, *psaI* of Photosystem I, and *psbC* and *psbF* of Photosystem II.

The effects of *cprnp* mutations on plastid gene expression were examined compared to *phyB* and *hy5*. This analysis was conducted at both 17°C and 27°C and compared to results obtained at 22°C, using de-etiolation as a model to evaluate cpRNPs' role in light-induced transcript accumulation (Armarego-Marriott et al., 2020).

ATPase complex. As previously described in Figure 2.5, *atpH* transcript abundance was significantly reduced at 22°C in *phyB*, *hy5*, and *cprnp* mutants, indicating a potential cascade to modulate this transcript. Shown in Figure 2.18, at 17°C, the average transcript accumulation of *atpH* was lower than at 22°C, with *phyB* and *hy5* plants showing a significant reduction. However, whilst *cp29b* and *cp31a* mutants accrued a statistically significantly lower *atpH* transcript levels than WT, contribution of *cpsebf* was not supported by the data. At 27°C, *phyB* mutants accumulated lower levels of *atpH* than WT, but in *hy5* mutants the difference was not statistically different, perhaps indicating alternate pathways at higher temperatures to modulate plastid genes. No differences were detected for *cp29b* or *cpsebf* either, but a significant reduction was found for *cp31a*.

A Two-Way ANOVA analysis comparing the effect of genotype and temperature on transcript abundance across all three conditions reported no significant interaction effect between genotype and temperature over transcript abundance ($P=0.74$). However, a significant effect of temperature ($P<0.001$) and a significant effect of genotype ($P<0.001$), was reported. This indicates that temperature is an important factor in *atpH* expression, and that the phyB-signalling pathway is involved in *atpH* accumulation may occur through other signalling components.

Photosystem I. The plastid gene *psaI* was selected as a light-sensitive gene from the Photosystem I (*psa*) family. The temperature-dependent accumulation analysis (Figure 2.18) indicted that at 22°C *psaI* accumulation was phyB- and cp29B-dependent. At 17°C, *psaI* accumulation was reported to be significantly reduced in *phyB* mutants but not *cprnp* mutants or *hy5*. However, at 27°C, overall

transcript abundance of *psaJ* was increased compared for all genotypes compared to 22°C, except in the *phyB* mutant; but compared to WT at 27°C *psaJ* transcript accumulation was significantly reduced in *phyB*, *hy5*, and all tested *cprnp* mutants. A Two-Way ANOVA test reported a significant interaction effect of genotype and temperature on *psaJ* abundance ($P < 0.01$). A Tukey HSD post-hoc analysis revealed that the interaction effect affected the relationship between WT and *phyB* ($P < 0.01$), and for WT and *cp31a* ($P < 0.05$).

Photosystem II. The transcript abundance of two key PSB family members *psbC* and *psbF* was shown to be both in the phyB-HY5 signalling cascade, as well as cp29B- and cpSEBF- dependent at 22°C in section 2.3. Analysis of these transcripts across 17°C and 27°C showed that cpRNP-regulation of *psbC* is temperature-dependent for cp29B, cpSEBF, and cp31A, but regulation of *psbF* is only temperature-dependent for phyB and HY5 (Figure 2.18).

Average WT accumulation of *psbC* was similar at all tested temperatures. Previous results identified that *psbC* is phyB- and HY5- dependent at 22°C. At 17°C significant reductions in transcript abundance were detected between WT and *phyB*, but not for *hy5*. In *cprnp* mutants, significant reductions were observed for *cp29b* and *cp31a* mutants, but not for *cpsebf*- contrasting observations at 22°C. At 27°C, *psbC* accumulation is also significantly reduced in *phyB* but not *hy5*; and in *cprnp* mutants, significant reductions were observed in *cpsebf* and *cp31a* but not for *cp29b*. This may indicate an alternate phyB-cpRNP pathway that does not involve HY5 activity at lower and higher temperatures is involved in the regulation of these genes, as well as a non-redundant role in the control of cpRNPs by temperature responsiveness.

These results suggest that the *psbC* reduction only occurs in the *cp29b* mutant at 22°C and its expression is not dependent upon cp29B at higher or lower temperatures. A further specificity for cpSEBF was observed, in which a reduction *psbC* in *cpsebf* was apparent at 27°C and 22°C but not in 17°C. Results for *cp31a* indicate that cp31A equally specific, and only necessary for *psbC* abundance at 17°C and 27°C but not at 22°C. However, in all conditions, *psbC* expression was observed to be dependent on phyB. A Two-Way ANOVA analysis of these results confirmed a significant interaction of genotype and temperature on *psbC* abundance ($P < 0.01$), with a Tukey HSD post-hoc test reporting the interaction effect was significant for all WT-mutant relationships ($P < 0.001$). This revealed a complex web of temperature-dependent effects that implies a unique role for each tested cpRNP.

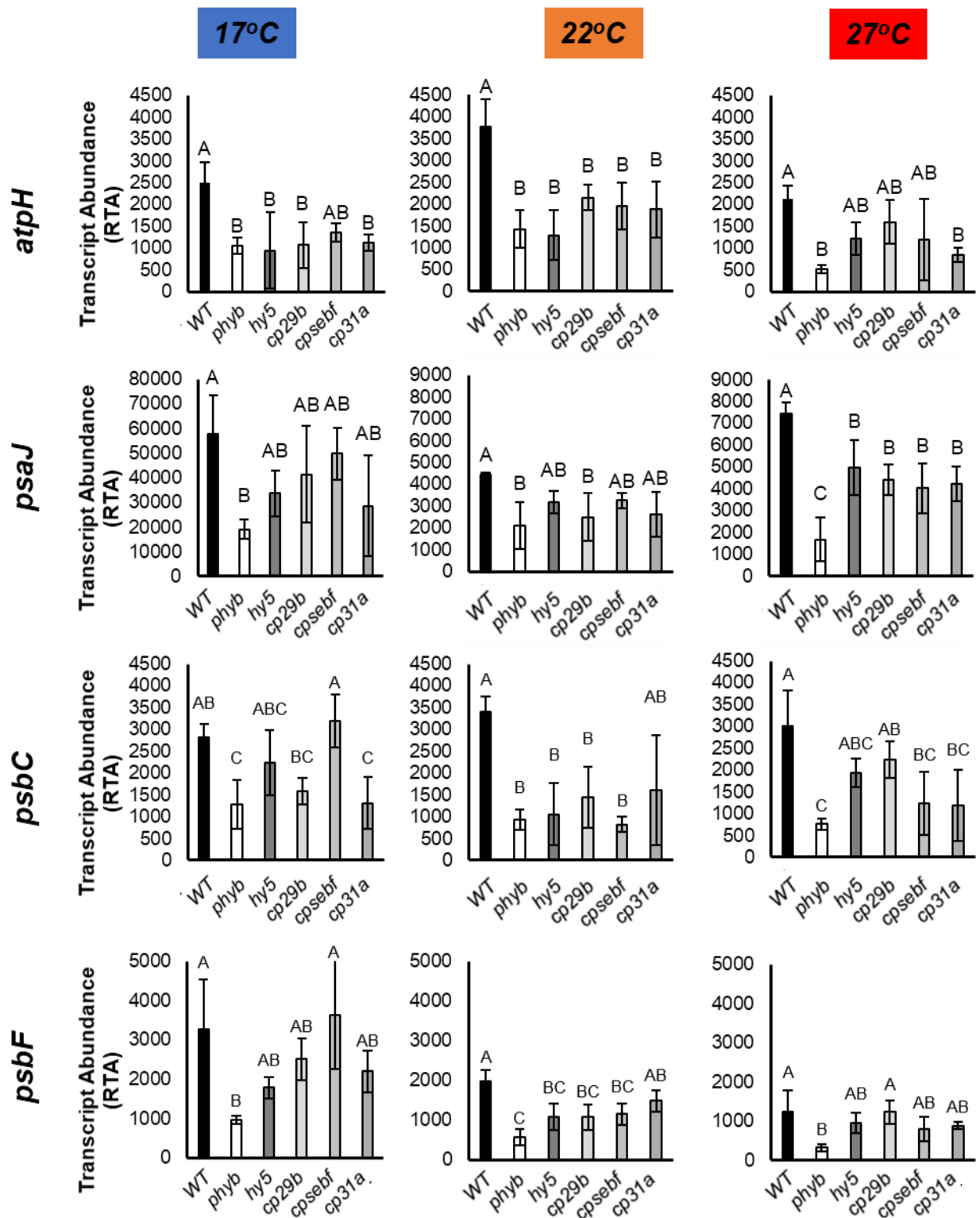


Figure 2.18. *cpmp* mutation affects temperature-dependent regulation of key plastome-encoded subunits. Graphs show relative transcript abundance of *atpH*, *psaJ*, *psbC*, and *psbD* plastome-encoded subunits in WT, *phyb*, *hy5*, *cp29b_2*, *cpsebf_1*, and *cp31a_2* plants grown for three days in darkness and treated with 24hrs red light (80 $\mu\text{mol m}^{-2}\text{s}^{-1}$). Relative transcript abundance was calculated by comparing experimental gene expression to the reference gene *PP2A*. Data represent the average of three biological replicates and error bars show the 95% confidence interval. Statistical significance of expression between WT (black bars), *phyb* (white bars), *hy5* (darkest grey bars), and *cpmp* mutants *cp29b_2*, *cpsebf_1*, *cp31a_2* (shown over a light-to-dark gradient grey bars) was calculated using One-way ANOVA with Tukey post hoc testing ($p < 0.05$). Data that do not share a letter are statistically significant.

At 22°C, abundance of *psbF* was significantly reduced in *phyB* and *hy5*, as well as in *cp29b* and *cpsebf*. At 17°C and 27°C, only *phyB* plants exhibited a significant reduction in *psbF* accumulation; neither *hy5* plants nor *cprnp* mutants showed any significant differences. A Two-Way ANOVA analysis determined that there was a significant interaction effect of genotype and temperature on *psbF* accumulation ($P < 0.05$). A Tukey HSD post-hoc test reported that the interaction effect was significant for the relationship between WT and *phyB* ($p < 0.001$) and *hy5* ($p < 0.001$). This indicates that cpRNP-dependence of *psbF* is not temperature-dependent, although *psbF* expression in all tested temperature is in a temperature-dependent phyB signalling cascade.

Overall, results presented in Figure 2.18 show a significant interaction effect of light and temperature responsiveness for *psaJ* and *psbC* in all *cprnp* mutants, and that *psbF* accumulation is phyB- temperature-dependent. Interestingly, no interaction effect of phyB, HY5, or cpRNPs and temperature was detected for transcript accumulation of *atpH*. Although this experiment only tested selected plastome genes corresponding to 3 complexes, it did reveal that cpRNPs' regulation of the plastome is temperature-dependent and provides insight into the potential of cpRNPs to integrate light and temperature sensing to modulate greening and biomass accumulation as well as the existence of selected subunits in the photosystems that are more prone to temperature and light regulation. This analysis also reaffirms the importance of phyB and HY5 as thermo-sensitive regulators with extended effects over genes encoded in the plastome.

2.7. Discussion

2.7.1. cpRNPs integrate Red-Light phyB- and HY5- signals to regulate greening in Arabidopsis.

This chapter provided evidence that the cpRNPs are involved in a phyB- and likely HY5- directed pathway that integrates both light and temperature signalling to modulate plant development, in particular greening and growth responses. Due to their functional role as post-transcriptional modulators of the plastome gene expression, the phyB-HY5-cpRNP cascade has the potential to deliver signals perceived by the light receptors to the plastome for the modulation of photosynthesis and the functions encoded by the plastome.

Mechanistic insights showed that *cpRNP* transcript accumulation is phyB-dependent in response to red light during de-etiolation and during seedling establishment. Reverse genetics studies in this chapter revealed greening and biomass accumulation defects in knockout mutants *cp29b* and *cp31a* and knockdown mutant *cpsebf* in an array of light conditions; these included red light-mediated de-etiolation in 4-day old seedlings, fluctuating high light intensity stress, and Long Day- photoperiodic grown 10-day old plantlets. Moreover, experimental results support a role of these proteins in the photoreceptor orchestrated cascades for sensing temperature and in the delivery of these signals to plastid genome.

These key findings are summarised and presented in Figure 2.19.

Phytochrome is involved in R-light induced post-transcriptional regulation of the plastome through cpRNPs.

Phytochrome exerts an important influence over chloroplast biogenesis, in part through the assembly and maintenance of the photosynthetic apparatus (Franklin and Quail, 2010), but the extent of its contribution and the detailed mechanisms involved remain under-investigated. Most of the research to date has focused on the effects of the photoreceptors on the modulation of nuclear encoded photosynthetic genes (Tepperman et al., 2006; Franklin and Quail, 2010). In addition, recent genomic evidence supports a role for phyB and cry2 in the global modulation of the plastome (Facella et al., 2017; Griffin et al., 2020). Yet, at present only transcriptional mechanisms- mostly operating through the effects of light on sigma factors and the HEMERA (HMR) complex- have been described (Oh and Montgomery, 2014; Yoo et al., 2019). However, beyond transcription, plastid gene expression is subject to intense regulation by post-transcriptional and translational contributions, and the role of the photoreceptors to such regulatory mechanisms remains highly unexplored (Deng et al., 1989; Griffin et al., 2020).

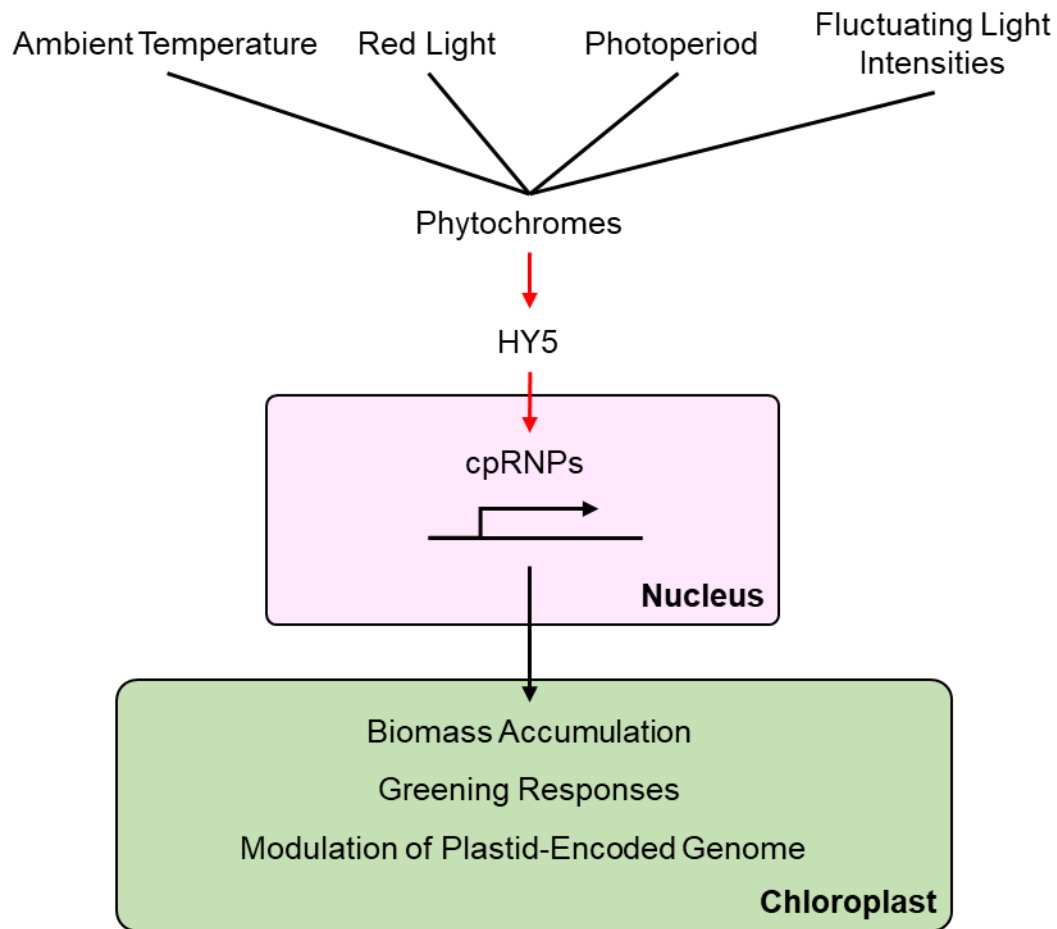


Figure 2.19. A working model for a phyB-HY5-cpRNP pathway that integrates a range of environmental signals including warm and cold ambient temperature (17-27°C), red-light mediated de-etiolation, and fluctuating light intensities to modulate biomass accumulation, greening, and the abundance of plastome encoded transcripts.

In this chapter, bioinformatic genomic evidence demonstrated a significant role for phyB in the regulation of potential post-transcriptional modulators of plastid gene expression. This analysis indicated that modulation could be directed through the phyB-dependent transcriptional control of nuclear-encoded but chloroplast acting RNA binding proteins, including members of the Pentatricopeptide domain-containing (PPR) and Tetratricopeptide domain-containing (TPR) protein families and RRM families (Griffin et al., 2020) (Figure 2.1).

While PPRs and TPRs have a highly specific target range (Lurin et al., 2004; Schmitz-Linneweber et al., 2005), the RRM-containing chloroplast RNA binding protein family (cpRNPs) is involved in the global regulation of the plastome. Members of this family were previously reported to be light-activated (Li and Sugiura, 1990; Kupsch et al., 2012), yet the mechanisms of activation remained undefined. Four members of the cpRNP family were identified among the red light phyB-

regulated genes in microarray genomic analyses (Tepperman et al., 2006), and *cp29A* has been implicated as phy-dependent (Franklin and Quail, 2010).

To corroborate and further investigate this link of red light phyB-cpRNPs, cpRNPs' transcript accumulation during red light-induced de-etiolation was measured (Figure 2.2). Transcript accumulation of *cpRNPs* was reduced in *phyB* mutants compared to WT seedlings, with expression of *cp31A*, *cp29B*, *cp29C*, and *cpSEBF* showing red-light induction and phyB-dependence. These results provide evidence that all the 10 cpRNPs in Arabidopsis are phyB-dependent and are induced by red light during de-etiolation. A light control of the expression of genes involved in post-transcriptional plastid gene expression therefore points at a novel function for phyB in the modulation of the plastome.

cpRNPs modulate greening and plastid transcript accumulation in red-light induced de-etiolation.

Previous studies have shown that cpRNPs are involved in the greening response during cold stress (Kupsch et al., 2012), but no examination had been made of cpRNPs' involvement during de-etiolation, a critical stage of seedling establishment (Armarego-Marriott et al., 2020). Using a reverse genetics approach, experimental evidence in this chapter showed that the cpRNPs *cpSEBF* and *cp31A* were involved in the greening process and affected accumulation of both Chl *a* and Chl *b* (Figure 2.3). No reductions in chlorophyll were observed in *cp29b* mutant, but this may be due to redundancy in the cpRNP family and suggests *cp29B*'s loss may be compensated by other cpRNPs (Kupsch et al., 2012).

Greening and chlorophyll biosynthesis correlates to photosystems structure and function (Smith, 1954), and assembly of photosynthetic apparatus is critical to greening (Kobayashi et al., 2012). Disruption of chloroplast development often results in a pale-greening phenotypes and reduced greening (Pogson and Albrecht, 2011). In addition, inhibition of plastid gene expression pathways also inhibits greening (Huang et al., 2013). Considering their function, the results therefore suggested that the impact of *cpRNP* mutations could be linked to altered plastome transcript accumulation.

While phyB is a major regulator of plastid biogenesis and greening responses (Franklin and Quail, 2010), results included in this chapter revealed that phyB has a near-global impact on the plastome (Griffin et al., 2020). Specifically, evidence provided here showed that phyB is required for the accumulation of 69% of plastid-encoded, protein-coding genes in 7-days old Short-Day grown plants, including members of the Photosystem II (*psb*), Photosystem I (*psa*), NADH Dehydrogenase

(*ndh*), and Cytochrome *b₆f* (*pet*) families (Figure 2.4). Prior data have shown that, mechanistically, phyB has a role in regulating plastid transcription via light modulation of components such as the sigma factors (Oh and Montgomery, 2014), but other mechanisms beyond transcription had not been explored.

To investigate the involvement of phyB in red-light de-etiolating seedlings on plastid gene accumulation, genes corresponding to components of the ATP Synthase (*atp*), Photosystem II (*psb*), Photosystem I (*psa*), NADH Dehydrogenase (*ndh*), and Cytochrome *b₆f* (*pet*) families were examined for R-light phyB dependent modulation. This showed that genes such as *atpH*, *petD*, *psaJ*, *psbA*, *psbC*, *psbD*, and *psbF* were clearly sensitive to R-light inputs in a phyB-dependent modulation (Figure 2.5). The overlap of these genes with those identified in cpRNPs RIP-chip studies (Tillich et al., 2009; Kupsch et al., 2012; Teubner et al., 2017) identified them as potential targets to elucidate the molecular role of the phyB-induced cpRNPs post-transcriptional cascades during greening.

Prior research has indicated a global binding capacity for cpRNPs on the plastid genome (Kupsch et al., 2012), and an examination of impact of *cprnp* mutations revealed statistically significant reductions in *atp*, *ndh*, *psa*, and *psb* gene family transcript accumulations. Specifically, the analysis showed roles for cp29B, cpSEBF, and cp31A on ATP Synthase (*atp*), a unique role for cp31A in NADH Dehydrogenase (*ndh*) and cp29B in Photosystem I (*psa*), and roles for cp29B, cpSEBF, and cp31A in Photosystem II (*psb*) during de-etiolation (Figure 2.5). The modulation of *ndh* transcripts by cp31A is supported by observations from published research (Tillich et al., 2009; Okuzaki et al., 2019). While no effect was observed by cpRNPs on transcripts encoding components of the electron transport chain (*pet*) during de-etiolation, binding by cpRNPs to *pet* genes has previously been documented by RIP-chip analyses (Kupsch et al., 2012; Teubner et al., 2017).

Although not statistically significant, trends in average transcript abundance indicated that the tested cpRNPs may be connected to the expression the identified subunits, and this could be verified in future experiments including the full plastome. Yet, current results hint at specialised roles for cpRNPs in regulating photosynthetic processes during de-etiolation and of an impact on photosynthetic efficiency during later plantlet development. The observed target specificity hints at a complex signalling network regulating cpRNP activity in different environmental conditions (Kupsch et al., 2012; Okuzaki et al., 2019).

The results therefore reinforce and highlight that phyB is critical for the assembly of the photosynthetic apparatus including the modulation of plastid encoded transcripts in response to R-light during de-etiolation. The experimental results provided here further identify that this regulation can be transduced through phyB-dependent components such as the cpRNPs, which show

an important contribution to plastid transcript accumulation in a R-light dependent manner. Physiological studies of the greening response highlight that the cpRNPs' play a critical role during early seedling development, in accordance with the essential role of the photoreceptors in the assembly of photosynthesis.

HY5 links expression of *cpRNPs* to phyB signalling cascade.

HY5 is a master bZIP transcription factor that integrates red-light phyB signals (Osterlund et al., 2000) and blue-light CRY signals (Wang et al., 2017) to promote light dependent-responses such as hypocotyl growth, root development, photosynthetic gene expression, and pigment accumulation (Toledo-Ortiz et al., 2014; Gangappa and Botto, 2016). To begin understanding how phyB-transduced red-light signals could lead to the control of nuclear-encoded genes with a regulatory function in the chloroplast and plastid gene expression, this chapter examined the role of HY5 in such mechanisms.

Analyses of *hy5* mutant genomic datasets identified a significant contribution of HY5 to post-transcriptional pathways-associated to chloroplast-encoded genes (Figure 2.6) (Griffin et al., 2020). This analysis expanded the previously described role of HY5 from plastome transcriptional control through sigma factors (Mellenthin et al., 2014), to the post-transcriptional cascades.

Based on the R-phyB-dependence of cpRNPs and the presence of HY5 binding sites in the promoters of *cp29B*, *cpSEBF*, and *cp31A*, HY5s may bring in phy-R light signals to the regulation of post-transcriptional modulators of the plastome by controlling the light dependent transcription of *cpRNPs*. (Figure 2.7). Promoter studies also indicated that the HY5 binding sites may include different motifs including E-Box, C-Box, ACE-Box, and CG-Hybrid Box (Song et al., 2008; Shi et al., 2011; Shin et al., 2013; Abbas et al., 2014); different binding motifs may be associated with induction strength, or co-regulation of cpRNPs alongside other light signalling components.

Evidence of the relevance of HY5 for *cpRNP* transcript accumulation was obtained from the experiments on the *hy5* mutants during red-light induced de-etiolating conditions (Figure 2.8). This revealed a 73-93% reduction of *cp29B*, *cpSEBF*, and *cp31A* transcript accumulation in a HY5-dependent manner. This data is supported by the genomic chromatin immunoprecipitation (chip) assays that identified global HY5 binding sites to *cpRNPs* promoters for *cpSEBF* (Lee et al., 2007), and microarray analysis that showed a HY5-dependence of *cp31A* (Ma et al., 2005). This genetic and molecular evidence places cpRNPs on a red-light signalling cascade dependent on phyB and HY5.

Further examination of the impact of the *hy5* mutation on plastome encoded transcripts abundance revealed significant reductions in components of the ATP Synthase (*atp*), Photosystem I (*psa*), and Photosystem II (*psb*) (Figure 2.9). This is the first time that a link between HY5 and the modulation of plastome transcripts abundance during de-etiolation has been drawn. Although only a narrow range of transcripts was examined, results hint at a targeted modulation of specific components. The findings correlate with observed effects of *phyB* and the overlap of HY5 and *cpRNPs* targets on the transcript accumulation for specific subunits of multiple complexes including *atpH*, *psaJ*, *psbA*, *psbC*, *psbD*, and *psbF*.

These studies pave a pathway through which HY5 can participate in the integration of R-phys signals and transmit them to the plastome. HY5 modulation of the *cpRNPs* will ensure a general effect over a wide range of plastome encoded genes. The significance of HY5 as a transcriptional regulator of *cpRNPs* can also be part of the wider *cpRNPs*' capacity to integrate multiple environmental signals. Being part of the *phyB*-HY5 signal transduction cascade, *cpRNPs* could integrate *phyB*'s sensing of multiple environmental stimuli including light, temperature, and photoperiodicity (Franklin and Quail, 2010; Baerenfaller et al., 2015; Jung et al., 2016), and through HY5 multiple light and temperature signals (Catalá et al., 2011; Toledo-Ortiz et al., 2014). HY5 transcriptional control over *cpRNPs* could ensure responsiveness to multiple light inputs beyond *phys*, such as other light qualities including blue light and *crys*, (Wang et al., 2017) and circadian inputs (Andronis et al., 2008). Analysis from Griffin et al (2020) indicated an important contribution of *crys* to regulating plastid gene expression. While the relative contribution of *phys* and *crys* remain to be addressed, modulation of components such as the *cpRNPs* could represent convergent points for a global control of the plastome in response to changing light environments and should be examined in the future.

2.7.2. Examining *cpRNPs* functions beyond light quality inputs.

Beyond light quality, photoreceptors are also involved in the perception of light intensity, light fluctuations, and photoperiodicity. All these light inputs are likely interpreted by the plastome for a proper adjustment of chloroplast metabolism to the prevailing environments. Plants must be able to respond to light intensity fluctuations that could inflict photoinhibition and damage to the photosystems (Kanervo et al., 2005), and photoperiods inform plants growth, affecting photosynthesis-associated processes including sugar distribution, chlorophyll content, and photosynthetic rates (Carpenter et al., 1983; Adams and Langton, 2005). *phyB* can integrate all these light environmental signals, but the mechanisms used remain poorly understood (Mousseau, 1981;

Kaiserli and Chory, 2016; Sellaro et al., 2019; Kreslavski et al., 2020). Genome-wide analyses support plastid-encoded gene expression and plastome regulatory processes are modulated in the plant in response to fluctuating light and photoperiod to synchronise photosynthetic rates and repair mechanisms (Rokka et al., 2005; Mockler et al., 2007; Baerenfaller et al., 2015; Suzuki et al., 2015). In this respect, cpRNPs could be part of the phyB-dependent signalling cascades for the integration and delivery of multiple light inputs to the plastome in order to optimise chloroplast metabolism. Yet, analysis of the selected *cprnp* mutants showed a limited role for cpRNPs in modulating plant response to fluctuating light intensity. While previous research indicated that cpRNPs could be involved in the repair of D1 protein (*psbA*) from PSII, one of the most vulnerable targets of photoinhibition in fluctuating light and high light intensity (Komenda and Masojídek, 1995; Rokka et al., 2005), the negative results may be explained by functional redundancy, in particular with cp33A (Teubner et al., 2017).

While no clear role for the tested cpRNPs was detected in conditions that mimic natural light intensity fluctuations, the data supported a moderate role for *phyB* (Figure 2.11) in greening and biomass accumulation during low light acclimation and high light stress periods. In this respect, the role of crys and blue light in the stress responsiveness would be interesting to address, as crys are also photoreceptors involved in the HL and low fluence-dependent photomorphogenic responses (Lin et al., 1998). The limited effect of phyB and cpRNPs in fluctuating light intensities compared to standard growing conditions is consistent with reports that photoinhibited plants don't feature slower growth rates and that mature *cprnp* plants under high light and low light stress (Kupsch et al., 2012; Adams and Langton, 2005) don't show growth phenotypes.

This may point at the relevance of investigating the role of B-light and CRYs in fluctuating environments. A new examination of *cprnp* and *hy5* mutants in fluctuating blue light intensities may reveal different responses from the ones evaluated in R-light.

cpRNP expression cycles with photoperiod, but no phenotypes were detected in mutant backgrounds.

Photoperiodicity regulates plant growth and development, providing vital cues for sugar distribution and chlorophyll production, and optimisation of photosynthesis (Adams and Langton, 2005; Graf and Smith, 2011). *phyB* is involved in photoperiodic responses (Mousseau, 1981; Blázquez and Weigel, 1999; Kaiserli and Chory, 2016), and transcriptomic comparisons between

photoperiods have identified differential expression of plastome regulating mechanisms (Baerenfaller et al., 2015).

The investigation of the role of cpRNPs as potential effectors of photoperiodic signals revealed strong photoperiod cycling for *cp29B* and *cp31A* in dawn/early light phases in Long Days, and in the dusk phase during Short Days (Figure 2.11, 2.12). *cpSEBF* was not observed to show marked cycling behaviour in either conditions. However, phenotypic characterization of *cp29b* and *cp31a* did not show statistically significant growth alterations in either condition, although trends indicated a lower average Fresh Weight in *cp29b* (Figure 2.13). This evidence may point at a redundant role of cpRNPs in integrating photoperiod signals, and would require double- or multiple mutant analyses to further elucidate if the observed changes in transcript accumulation for specific cpRNPs were tied to a phenotype or function, as well as performing an exploration into whether plastid gene expression may change in *cp29b* mutant plants in photoperiodic time course experiment. While phyB is a major contributor to Short Day-dependent plastome gene expression, at present the signalling components involved remain to be dissected. Photoperiod sensing is also a factor of the blue-light crys signalling pathway (Yang et al., 2017); as photoperiod cycling of *cpRNPs* was reported in white light (Mockler et al., 2007), it may be the case that cpRNPs' sensitivity photoperiod signals are not transduced in red light.

No examination of circadian cycling in entrained conditions was conducted yet, but promoter analyses indicated that *cp29B*, *cp29C*, *cp31A*, and *cp33B* contain CCA1-binding sites, and HY5 has been observed to integrate blue-light induced circadian stimuli (Hajdu et al., 2018). Therefore, combined effects of photoperiodism and/or circadian regulation may be a blue-light-induced effect that would require experimental testing.

2.7.3. Beyond Light: cpRNPs in the delivery of temperature signals to regulate the plastome.

Based on phyB and HY5's recently described ambient temperature sensitivities and involvement in temperature dependent greening responses (Toledo-Ortiz et al., 2014; Jung et al., 2016; Legris et al., 2016), evidence gathered here showed that *cp29B*, *cpSEBF*, and *cp31A* transcript accumulation is also temperature-sensitive in cold (17°C) and warm (27°C) conditions. Young *cp29b*, *cpsebf*, and *cp31a* mutant plantlets further revealed temperature-sensitive phenotypes affecting greening and biomass accumulation. These phenotypes correlated with temperature-dependent alterations in plastid gene transcripts' during de-etiolating *cpRNP* mutants.

A role for cpRNPs in temperature-sensing is also supported by reported increases in cpRNP protein abundance in wheat, Brassica, and Arabidopsis during cold treatments (Amme et al., 2006; Gao et al., 2009; Sarhadi et al., 2010), as well as differential accumulation of photosynthesis-associated plastid-encoded genes in chilling conditions (Kupsch et al., 2012; Okuzaki et al., 2019).

cpRNP transcript abundance during de-etiolation at 17°C, 22°C, and 27°C revealed that abundance was temperature-dependent (Figure 2.15). Yet, differential responses of *cp29A*, *cp31A* and *SEBF* in the range of 17-27°C, hint at perception differences between cpRNPs. Overall, *cpSEBF* showed a greater predominance at higher temperatures compared to *cp29B* and *cp31A*, but transcript abundance is not necessarily indicative of changes in protein abundance. This hints that non-transcriptional modulation may be behind the previously reported observations of increments in wheat cpRNPs cp29, cp31, and cp33 protein abundance in cold conditions (Amme et al., 2006; Gao et al., 2009; Sarhadi et al., 2010). An examination of cpRNP protein accumulation in altered temperature conditions in protein blots would be necessary to evaluate responses under ambient temperature regimes and correlations with transcript accumulation. However, the initial observations of altered *cpRNP* transcript accumulation under ambient temperatures support a further investigation of their role as transducers of temperature signals to the plastome.

While the exact mechanism of cpRNPs differential temperature responsiveness has not been dissected yet, phenotypic and physiological experiments place them as part of the temperature signalling cascades. Cold temperatures have previously shown to induce a cold-stress phenotype in *cp29a* and *cp31a* mutants, including bleaching and pale leaves in mature plants moved to cold conditions (Kupsch et al., 2012). The studies conducted here provided evidence that *phyB*, *hy5*, and *cprnp* mutations affected growth and development, revealing reductions in biomass accumulation (measured through Fresh Weight) and chlorophyll accumulation (Chl *a* and Chl *b*) in moderate warm (27°C) and cold (17°C) conditions (Figure 2.16).

phyB's role as an integrator of temperature signals includes reductions on FW and chlorophyll accumulation (Figure 2.16 panels A and B). In particular, interesting effects of temperature were observed on the *phyB* mutant accumulation of chlorophyll *a*. In *phyB*, Chl *a* content was significantly lowered at all temperatures tested but Chl *b* content was only affected at 17°C. This suggested that Chl *b* accumulation at 17°C is strongly *phyB*-dependent, but less impacted at other temperatures; this may be due to a redundant effect of the other members of the *phy* family (Heschel et al., 2007; Halliday and Whitelam, 2003) or the effect of *phy* over the PSI and PSII ratios. Recently, research has shown that mutations in plastid-encoded genes encoding PSI subunits, such as *psaA* and *psaB*, led to a non-functional PSI and triggered a feedback loop that reduced

chlorophyll expression and caused greening defects (Schaffner et al., 1995; Leelavathi et al., 2011; Azarin et al., 2020). Results also corroborated a clear role for HY5 in the modulation of greening responses at 17°C as previously reported (Catalá et al., 2011; Toledo-Ortiz et al., 2014; Jung et al., 2016).

Under these ambient temperature changes (17°C-27°C), the analysis also revealed limited redundancy of cpRNPs in the transduction of different temperature environmental signals. Results pointed at a differential role of cpRNPs in biomass and chlorophyll accumulation, and a Two-Way ANOVA analysis reported an interaction effect of respective *cprnps'* mutation and temperature on both biomass accumulation and Chl *a* and Chl *b* content as significant compared to WT. These results therefore highlight the temperature-sensitivity for cp29B, cpSEBF, and cp31A in cold temperatures and their effects on biomass accumulation and greening, but also hints at roles for cpSEBF and cp31A in warm temperatures. As a family, the cpRNPs may have a combinatorial role where multiple cpRNPs contribute to vital processes in stable conditions, but each may have an important specialised role.

Interestingly, the observed temperature effects extend to the modulation by phyB, HY5 and cpRNPs of plastid gene expression during de-etiolation. This chapter demonstrates a temperature-dependent modulation of components of the Photosystem I (*psa*) and Photosystem II (*psb*) plastid-encoded subunits *psaJ*, *psbC*, and *psbF* (Figure 2.17) by phyB and HY5 in addition to effects by cpRNPs, showing for the first time that phyB and HY5 integrate temperature signals for differential plastome transcript accumulation. This builds on phyB and HY5's roles in integrating temperature signals to control nuclear-encoded genes (Toledo-Ortiz et al., 2014; Jung et al., 2016; Legris et al., 2016) and extends control of genes encoded in a different organelle. Results showed that HY5-dependent regulation *psbC* and *psbF* occurs only 22°C, and a temperature-specific role is consistent with HY5 activity relying on a variety of potentially temperature sensitive co-factors (Catalá et al., 2011), and further indicates that HY5's role in temperature-dependent modulation of the plastome is likely to be complex and involve as-yet unidentified components.

Furthermore, complex relationship between cp29B, cpSEBF, and cp31A and temperature-dependent transcript accumulation of *psaJ* and *psbC* (Figure 2.17) suggests a further specificity of the cpRNP pathways: an influence of cp31A over *psaJ* accumulation occurred only at 27°C; an effect of cp29B was evident over *psbC* accumulation at 22°C but cp31A-dependent regulation occurred in warm or cold conditions, and a cpSEBF-dependent effect over *psbC* occurred in control or warm conditions. This indicates that the cpRNP family has a combinatorial role, with a broad impact of cpRNPs in standard conditions, but specialised roles for individual members in conditions that

require it. This further supports a combinatorial and partially redundant functional role for the cpRNP family as had previously been described for cp31A and cp31B (Tillich et al., 2009).

Beyond the transcriptional effects addressed here, cp31A and other cpRNPs' cold-temperature sensing may involve post-translational modifications including protein phosphorylation (Loza-Tavera et al., 2006; Kupsch et al., 2012; Okuzaki et al., 2019). This mechanism is under-examined but represents an interesting avenue to explore for other cpRNPs such as cp29B and cpSEBF, and their temperature-specific modulation of the plastome.

Ultimately, the experimental results gathered provide support for a phy-directed cpRNP modulation of Photosystem I and Photosystem II plastid-encoded subunits in a temperature-dependent manner. The results expand the cpRNPs' operational beyond the previously described cold temperature roles to include warm conditions. Overall, the phyB-HY5-cpRNPs signalling module provide multiple avenues for the appropriate delivery of light and temperature signals across organelles, with a particular focus on plastome-encoded genes for the modulation of greening and photosynthesis.

Chapter 3: Beyond the chloroplast: plastid-nuclear communication to acclimate photosynthesis to environmental change

3.1. Introduction.

As described in Chapter 1, photoreceptors such as the phytochromes are major regulators of nuclear photosynthetic gene expression (Franklin and Quail, 2010). Recent research has highlighted that photoreceptor control extends beyond the nucleus to the regulation of plastid-encoded genes (Facella et al., 2017; Griffin et al., 2020) (Figure 2.1). For chloroplast function and metabolism, including photosynthesis, plastid-encoded photosynthetic gene expression must be synchronised to nuclear-encoded gene expression, as the photosynthetic apparatus requires subunits encoded in both organelles (Soll and Schleiff, 2004). This co-ordination involves the activity of anterograde and retrograde signalling pathways, relaying information from the nucleus to the plastid and vice versa (Berry et al., 2013). While some of the pathways co-ordinating the plastid and nuclear genomes have been investigated, the mechanisms linking the two are not fully understood (Shimizu et al., 2019).

Bioinformatic studies have shown that phytochromes and cryptochromes can exert control over nuclear-encoded genes that encode for chloroplast-localised proteins involved in the transcriptional, post-transcriptional, and translational modulation of plastome gene expression (Griffin et al., 2020). Experimental evidence from Chapter 2 shows that one pathway involved is through the activation of chloroplast RNA binding proteins (cpRNPs), a family of light-induced post-transcriptional regulators of the plastome (Li and Sugiura, 1990). Among the cpRNPs, three members of this family were shown to be phyB- and HY5-dependent modulators of plastid-encoded genes with the potential to integrate both light and temperature signals.

Interestingly, early studies of cpRNPs reported potential nuclear functions (Kwon and Chung, 2004; Ruwe et al., 2011). These early studies reported that truncated versions of cp31A localised to the nucleus and displayed DNA-binding capacity (Kwon and Chung, 2004), and identified a homologue of cpSEBF in potato that was also reported to have a dual nuclear-chloroplast localisation (Boyle and Brisson, 2001). While a possible nuclear localisation of cpRNPs had not been linked to the activity of photoreceptors, the recent discovery of the phytochromes as global modulators of transcriptional start sites, leading to alternative protein isoforms with differential subcellular distributions, suggests a potential mechanism by which this may occur (Ushijima et al., 2017). For cpRNPs *cp29A*, *cp31a*, *cp29C*, and *cpSEBF* genes, which were reported as targets of this novel phytochrome mechanism to diversify the proteome, this presented a new avenue to research (Ushijima et al., 2017). This chapter examines the hypothesis that cpRNPs have a role beyond the

chloroplast and may regulate nuclear-encoded transcripts by participating in plastid-to-nucleus communication.

The aims of this chapter are:

- 1) To conduct a bioinformatics study to investigate potential alternative localisation for the cpRNPs.
- 2) To conduct *in planta* cell biological studies of subcellular localisation of GFP- tagged cpRNPs with differential N-terminal ends, product of alternative transcriptional start sites.
- 3) To investigate whether nuclear gene transcript accumulation is altered in *cprnp* mutants.
- 4) To determine if environmental inputs can modulate cpRNPs nuclear function as they modulate chloroplastic functions.
- 5) To determine if cpRNPs are targets of retrograde signalling pathways.

3.2. Material and Methods.

3.2.1. Plant material and genotypes tested.

To evaluate the impact of *cprnp* mutation on nuclear-encoded transcript accumulation, *Arabidopsis thaliana* wild-type (Col-0), *phyB-9* (Col-0), *hy5-215* (Col-0), and the following *cprnp* mutants were used: *cp29b_2* (SALK_043415 (S), N543415), *cpsebf_1* (SALK_008984C, N681974), and *cp31a_2* (SALK_109613C, N664816), sourced from the Nottingham Arabidopsis Stock Centre (See Materials and Methods Chapter 2 for further information on mutant lines). The stock of *phyB-9* mutant used was confirmed to be a true *phyBi9* mutant after sequencing and did not contain a second-site mutation in the *VENOSA4* gene (Yoshida et al., 2018). A summary of these mutants and methods for their genotyping is provided in Chapter 2 and are shown in Table 2.1 and Table 2.3.

To evaluate a sub-cellular localisation for cp31A and cpSEBF in response to phytochrome-mediated alternative promoter selection, T2 transgenic lines were provided by Professor Matsuhita's laboratory from Kyushu University. These lines were generated using alternatively transcribed cpRNP sequences with altered N-terminals and were selected for using Basta resistance in both *E. coli* and *A. tumefaciens*-transformed plants. These transgenic lines were screened to T3 stage using a 3:1 segregation ratio and for fluorescence signal detected via epifluorescence. The list of the lines is provided below in Table 3.1.

To evaluate the effect of temperature and the retrograde signal-activating agent Lincomycin on cpRNP protein localisation, T2 transgenic lines were provided by Dr. Karine Prado from Edinburgh University. These lines were generated using a pDONR207 and pGWB4 Gateway Cloning method with resistance to spectinomycin in *E. coli* and kanamycin in *A. tumefaciens*-transformed plants. The constructs included cpRNP coding sequences with a 720kb C-terminus GFP tag and a 2kb N-terminal native promoter respective to each cpRNP. These transgenic lines were screened to T3 for a 3:1 segregation ratio and protein fluorescence as detected via epifluorescence microscopy. A list of transgenic lines is provided below, also in Table 3.1.

Table 3.1. Transgenic Lines used for cell biological analysis using confocal microscopy.

cpRNP	Vector	Promoter	cpRNP form	Background
cp31A	pBIN30	35S	31A (TSS_A, Long)	Col-0
cp31A	pBIN30	35S	31A (TSS_B, Short)	Col-0
cp31A	pGWB4	Native Promoter	31A (Full length CDS)	<i>31a_1</i>
cpSEBF	pBIN30	35S	SEBF (TSS_A, Long)	Col-0
cpSEBF	pBIN30	35S	SEBF (TSS_B, Short)	Col-0
cpSEBF	pGWB4	Native Promoter	SEBF (Full length CDS)	<i>sebf_1</i>

3.2.2. Seed Sterilisation and Sowing.

Arabidopsis thaliana seed were sterilised via treatment with a 15% (v/v) bleach solution for 10 min, and dilution and washed with sterilised distilled water until bleach was undetectable. Seeds were plated using a Pasteur pipette.

3.2.3. Plant Growth Conditions.

Plants were grown on 0.5 MS agar (Murashige and Skoog, 1962) with 0% (w/v) sucrose. Plants were grown in Snidjer Clima Red/Blue Light Monochromatic Cabinets, model EB2-N-PB. Plants were germinated with a 3hr white light treatment followed by 21hr darkness at 22°C before being moved to experimental conditions.

Confocal microscopy and gene expression assays. Plants were grown in de-etiolating conditions, after germination plants were kept in darkness for 3 days to promote skotomorphogenesis followed by a treatment of 24hr Red Continuous ($80 \mu\text{mol m}^{-2}\text{s}^{-1}$) at either 17°C, 22°C, or 27°C. For analysis of retrograde signal inducer Lincomycin on cpRNP localisation, 0.5mM Lincomycin was added to MS media.

Gene expression assays using retrograde signal activators Lincomycin and Norflurazon. Plants were grown in low white light ($10 \mu\text{mol m}^{-2}\text{s}^{-1}$) at 22°C for 6 days in media modified with 0.5mM Lincomycin or 5 μM Norflurazon. These agents act to inhibit plastid translation or carotenoid biosynthesis respectively, leading to photobleaching and repression of Photosynthesis Associated Nuclear Gene (PhANG) expression.

3.2.4. Plant Harvesting.

Gene Expression Analysis. Plants were harvested in a dark room with green light ambient illumination to prevent light contamination. Plants were harvested into liquid Nitrogen ($\text{N}_{2(l)}$) immediately to prevent degradation.

3.2.5. RNA Extraction and cDNA Synthesis.

RNA extraction was performed using a Sigma Aldrich Spectrum™ Plant Total RNA Kit and cleaned with Qiagen RNase Free DNase Set. RNA was quantified with a Nanodrop and 1 μg of RNA was used. To validate its quality, 500ng of RNA was stained with blue Thermo Fisher Scientific™ 6x DNA Loading Dye and run through a 0.5% (w/v) agarose gel. To synthesise cDNA, a Thermo Fisher

Scientific™ RevertAid First Strand cDNA Synthesis Kit was used according to manufacturer's instructions. For experiments analysing plastid gene expression, Random Hexamer Primers were used in the cDNA synthesis (Schuster et al., 1999), and for experiments analysing nuclear gene expression oligo dTs were used.

3.2.6. Quantitative RT-PCR Analysis.

RT-qPCR analysis was performed using 5µl PrimerDesign PrecisionPLUS qPCR Master Mix premixed with SYBR Green, 1µl of 3µM Forward and Reverse primer, 1µl of sample cDNA, and 2µl of sterilised water in a 10µl reaction volume. The reaction was performed using a Stratagene Mx qPCR Machine with the following thermal cycling program: 95°C for 10 min, followed by 40x cycles of 95°C for 10 sec, 60°C for 10 sec, and 72°C for 15 sec followed by melting curve from 65°C to 95°C to ensure primer targeting specificity. Results were analysed using Stratagene Mx PRO software and Microsoft Excel. Results were normalised to the light-stable PP2A reference gene (Klie and Debener, 2011) and relative gene expression was calculated as described in Chapter 2 (Pfaffl, 2001). A full list of primers is presented below in Table 3.2.

Table 3.2. qPCR Primers used in this chapter for the examination of *cpRNP* and candidate nuclear-encoded gene transcript accumulation.

<i>Arabidopsis thaliana</i> Primers		
Reference Genes	<i>PP2A_F</i>	TATCGGATGACGATTCTTCGTGCAG
	<i>PP2A_R</i>	GCTTGGTCGACTATCGGAATGAGAG
cpRNP Genes	<i>cp29B_F</i>	CAATGGAACACAATATGAAGGTCCG
	<i>cp29B_R</i>	AAAGCAGAACAGTTGGTTTACG
	<i>cpSEBF_F</i>	TTGGATGGTGCTGATTTGGA
	<i>cpSEBF_R</i>	ATAGGAAGTCATAGATTGGTGCTC
	<i>cp29C_F</i>	ACCTGGAACTTCCAAATCCAC
	<i>cp29C_R</i>	CTTCCAGCAACGAATTGTTAAGAG
	<i>cp31A_F</i>	CGATGGACAGAACTTGGAGG
	<i>cp31A_R</i>	TCTCAGCTTTAATATCCACGCC
Marker Genes	<i>IAA19_F</i>	TGGCCTTGAAAGATGGTGAC
	<i>IAA19_R</i>	TTGCATGACTCTAGAAACATCCC
Experimental nuclear-encoded genes	<i>LHCB2.3_F</i>	CGGAGGATCCAGAAGCGTT
	<i>LHCB2.3_R</i>	TAGCCACAGGGTCTGCAATG
	<i>LHCB4.2_F</i>	CCCGTTAGGACTAGCGTCTG
	<i>LHCB4.2_R</i>	TGAGTCGCCCAGTTGTTGAG
	<i>PSBO1_F</i>	GTGACTAAGAGCAAGCCGGA
	<i>PSBO1_R</i>	TAGCACCCAAGTCAGTGTCC

<i>PSBO2_F</i>	GCAAACCGGAGACAGGTGAA
<i>PSBO2_R</i>	GCACCCAAGTCAGTATCCGA
<i>PSBQ2_F</i>	CTCACCGCAAAGCTTTTCAA
<i>PSBQ2_R</i>	ACTCTTTGATCTCGCCGCAT
<i>PSBQI2_F</i>	ATGATTACGTTTCAGGCGGCA
<i>PSBQI2_R</i>	GTACACCTTTGGCGTCCGTA
<i>LHCA2.1_F</i>	CGATGCTTGCTTTCCTTGGG
<i>LHCA2.1_R</i>	TGATGTAAATGCCGAAAAGACG
<i>PSAD-2_F</i>	TTGGCTTTAGGTACGAGGTTGA
<i>PSAD-2_R</i>	GAACCTCTCCGTTAGGGAACA
<i>PSAN_F</i>	GAAGCTGCAAGTTCCTGAG
<i>PSAN_R</i>	TGTCCTTGCCTTCGCATTCC
<i>PSY_F</i>	GACACCCGAAAGGCGAAAGG
<i>PSY_R</i>	CAGCGAGAGCAGCATCAAGC
<i>PSB27_F</i>	TACTCGGCGTTGAATGCTGTT
<i>PSB27_R</i>	GAATCCTCGCCTTCCTCTTCG
<i>DEG1_F</i>	CACGTCGGTGAACGGTACAA
<i>DEG1_R</i>	GTCCGGCTTTGGTTCGAGA
<i>NPQ1_F</i>	ACATGTGGTCCTGAACCTGC
<i>NPQ1_R</i>	AGGTCATCTCAGTCCTACCGA
<i>NPQ4_F</i>	TGCCCTCGGTCTCAAAGAAC
<i>NPQ4_R</i>	GCTAATGCTCCTTTCCCGGT
<i>CA_F</i>	GAAGGACTTGTGAAGGGAACA
<i>CA_R</i>	TTTAACAGAGCTAGTTTCGGAGAG

3.2.7. Statistical Analysis

Statistical analysis of the data was conducted in Microsoft Excel and R (Team, 2020) using One-Way ANOVA, Two-Way ANOVA, and TUKEY HSD post-hoc where appropriate testing at a significance level of 0.05.

3.2.8. Genomic Datasets Used

A publicly available genome wide transcriptomic data set (GSE31587) (Hu et al., 2013) was used to identify genes with R-phys dependency. This dataset was generated using 4-day old WT and *phyABCDE* Arabidopsis seedlings grown in darkness or under continuous Red light ($50 \mu\text{mol m}^{-2} \text{s}^{-1}$) using oligo-dT based technology. Genes in this dataset were evaluated for red light induction between WT-Rc and WT-D and *phyABCDE* dependency between WT-Rc and *phyABCDE*-D for genes with a greater than two-fold expression difference. This list was then manually curated using

available literature to identify key representative candidates involved in photoprotective mechanisms and photorepair.

Publicly available genome-wide transcriptomic datasets GSE24517 (Ruckle et al., 2012), GSE110125 (Zhao et al., 2019), and GSE12887 (Koussevitzky et al., 2007) were used to generate Figures 3.17 and 3.18. The microarray dataset GSE24517 used WT plants grown with (L+) or without (L-) Lincomycin (0.5mM), grown in low light ($0.5 \mu\text{mol m}^{-2} \text{s}^{-1}$ blue plus red (BR) light) for 6 days. After 6 days, plants were transferred to $60 \mu\text{mol m}^{-2} \text{s}^{-1}$ blue plus red (BR) light. Plants were harvested immediately before the light treatment, and then at 4hr and 24hr. The microarray dataset GSE110125 examined 5-day old seedlings with Col6-3 (WT) plants grown under 24hr light condition with $100 \mu\text{mol m}^{-2} \text{s}^{-1}$ at 22°C with or without a treatment of 5 μM Norflurazon; and dataset GSE12887 examined WT plants grown in 21°C under continuous light ($100 \mu\text{mol m}^{-2} \text{s}^{-1}$) in the presence of 5 μM Norflurazon.

3.2.9. Confocal Microscopy

All confocal microscopy was conducted using a ZESSIS LSM 880 confocal microscope. Data was gathered and analysed using Zen Black and Zen Blue software.

Whole seedlings were treated with 100 $\mu\text{g/ml}$ 4',6-diamidino-2-phenylindole (DAPI) and incubated in darkness for 10 min. Plants were then washed with sterilised distilled water to remove excess DAPI and mounted using a coverslip for observation.

All confocal images were acquired with a Zeiss LSM 880 microscope. Excitation lasers for the confocal microscope were switched on and fully warmed up for at least 30 min prior to imaging. Fluorescent signals were visualised using the following settings: GFP excitation= 488 nm, emission= 493–573 nm; chlorophyll auto-fluorescence excitation= 633 nm, emission= 639–747 nm; DAPI excitation= 405, emission= 415-508 nm.

No GFP control was tested in this thesis. However, previously published literature has shown that GFP does not 'leak' into subcellular organelles, and so any subcellular localisation observed is likely to be an accurate visualisation of the cpRNP-GFP localisation (Grebenok et al., 1997; Köhler, 1998).

3.3. Results: Investigating a potential dual subcellular localization (chloroplastic-nuclear) for cpRNPs.

3.3.1. cpRNP structure, function, and published literature imply a role for cpRNPs in nuclear-encoded gene expression.

Although commonly described to regulate plastid-encoded mRNAs (Kupsch et al., 2012), *in vivo* evidence has shown the RNA Recognition Motifs (Chapter 1, Figure 1.1) of an *S. tuberosum* cpRNP orthologue of Arabidopsis cp29A binding single-stranded DNA probes, later confirmed through chromatin immunoprecipitation (chip) studies (Boyle and Brisson, 2001; González-Lamothe et al., 2008). Arabidopsis CP29A protein has also been detected in nuclei lysates from Arabidopsis (Gosai et al., 2015), indicating that a nuclear function may be conserved between Arabidopsis and potato. Evidence supports a nuclear role for other cpRNP members too: a cpRNP-telomeric DNA binding was also reported for STEP1, a truncated form of cp31A in Arabidopsis identified using gel shift assays (Kwon and Chung, 2004). Furthermore, a role for cp31A in the nucleus is supported by it sharing an identical partial amino acid sequence with the nuclear Arabidopsis nucleolin-like ribonucleoprotein FMV3bp (Ohta et al., 1995).

3.3.2. Bioinformatics predict cpRNPs localise to the nucleus.

To further investigate potential alternative localisation in organelles for cpRNPs, the ePlant database, a part of the Bio-Analytic Resource for Plant Biology (BAR) (Waese et al., 2017), was used. Results from this database shown in Figure 3.1 panel A suggest that in addition to the chloroplast, cp29B is strongly predicted to localise to the nucleus, and cp31A, cp29A, and cp33C are weakly predicted to have a nuclear localisation. However, the remaining members cp28A, cp29C, cp31B, cp33A, cp33B, and cpSEBF were not predicted to localise to the nucleus (presented in Supplementary Figure 3.1).

A second analysis was conducted using the plant protein subcellular localisation prediction program Localizer (<http://localizer.csiro.au/>). This program includes a database of known nuclear localisation signals (NLSs) against which queries are compared (Sperschneider et al., 2017). This program predicted a chloroplast localization for all cpRNPs, as well as a nuclear localisation for cp29B, cp33B, and cp33C (Figure 3.1, panel B). Nuclear localisation was predicted by the presence of 'KKPR', 'KRKL', and 'RRLKVDYAKTKKKKTY' and 'RRSSGYGFVSFKTKKQ' amino acid sequences respectively (Figure 3.1). Interestingly, predictions for a cp31A mitochondrial localisation, and for a cp33C triple-localisation to nucleus, chloroplast, and mitochondria were also obtained.

While the data from these two sources indicate that cp29B and cp33C may have nuclear localisations and that cp31A may have non-plastid localisations, they differ on their predictions for cp29A and cp33B. However, this initial study supports the investigation of a potential dual nuclear-chloroplast localization in red-light for the cpRNPs.

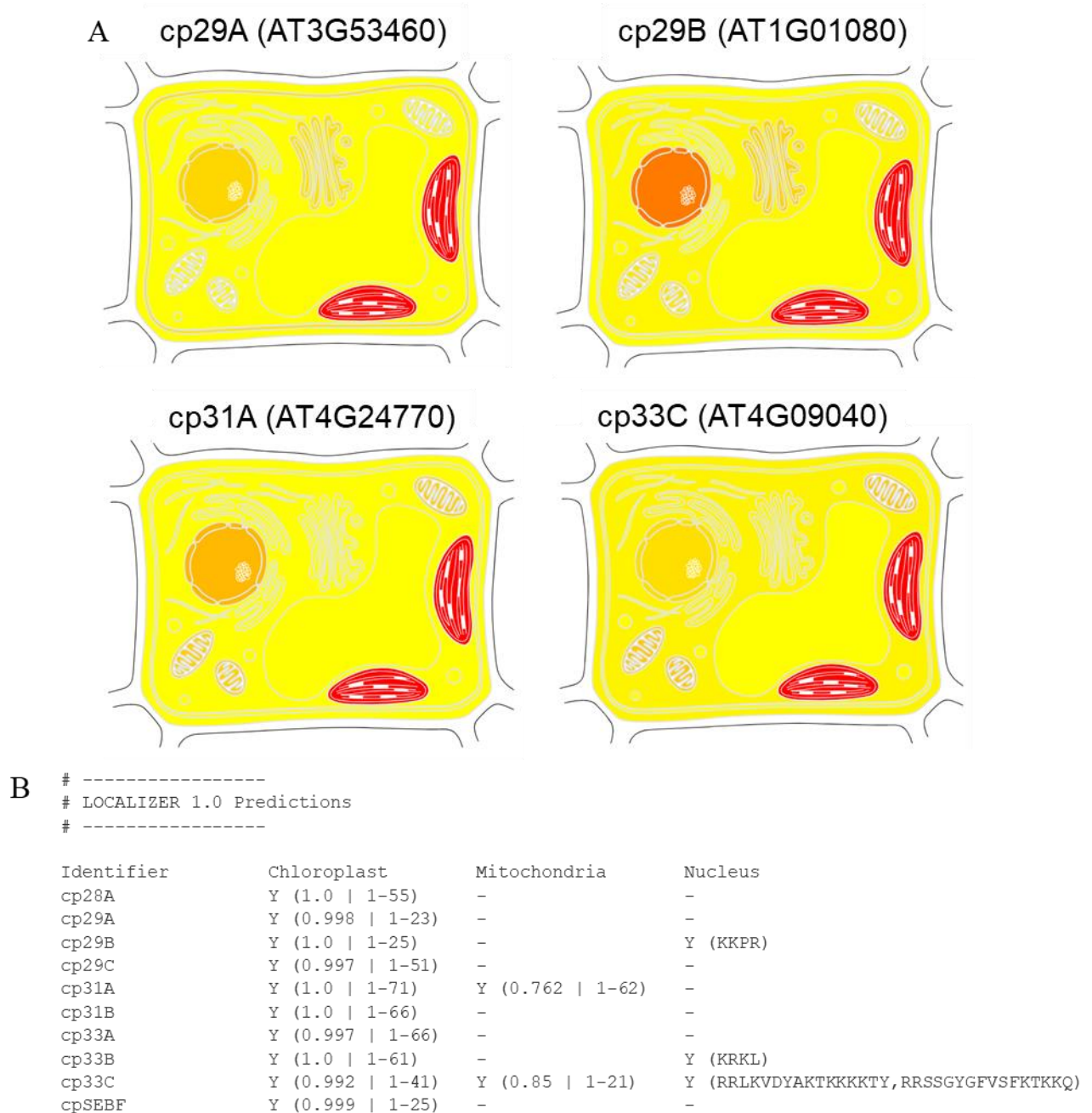


Figure 3.1. Bioinformatic tools predict that cp29A, cp29B, cp31A, cp33B, and cp33C localise to the nucleus. A) Data was obtained and reproduced from ePlant database (Waese et al, 2017). Colours indicate a linear expression intensity of protein to the subcellular compartment on a scale of lowest (yellow) to highest (red) probability. B) Sequence predictions were performed using Localiser, a subcellular localisation prediction program of plant and effector proteins in plant cells (Sperschneider et al, 2017).

3.3.3. Phytochrome-mediated alternative promoter selection for cpRNPs induces non-plastid localisations.

Alternative promoter selection can generate multiple variations of a protein from the same gene, increasing protein diversity from alternative transcriptional start sites (TSSs) (Landry et al., 2003; Davuluri et al., 2008). Recent research provided evidence that R-phytochromes play an important role in regulating alternative promoter selection in *Arabidopsis* to induce alternative subcellular localisations in response to light via expression of isoforms with altered N-terminals (Ushijima et al., 2017; Shikata et al., 2014).

Among the 2104 gene targets identified in Ushijima et al's research, an enrichment was reported in chloroplastic proteins likely to be involved in photosynthesis (Ushijima et al., 2017); these included *cp29A*, *cp29C*, *cp31A*, and *cpSEBF* members of the cpRNPs protein family. Figure 3.2 summarizes the data published by Ushijima et al (2017) on the effects of alternative transcriptional start site (TSS) selection for cpRNPs. Using mRNA-seq, the study showed three alternative transcription start site (TSS) derived forms for *cp29A*, two forms for *cp29C* and *cp31A*, and four forms for *cpSEBF*. Sequence analysis showed that the longest form for each (TSS_A) contained a full chloroplast transit peptide, and shorter forms (TSS_B et al) lacked one. Ushijima et al (2017) predicted that the shorter forms would localise to the nucleus using the ngLOC (v4) software (King and Guda, 2007).

An analysis of 5' RACE transcript abundance reported by Ushijima et al (2017) at 0hr, 1hr, and 3hr in WT and *phyA phyB* double mutant vs WT revealed light-dependent differences in the accumulation of the detected TSS-isoforms.

cp29A. For *cp29A*, the predicted *cp29A* TSS_A corresponds to the *cp29A* protein sequence with chloroplastic localization and produces the full 363 amino acids (aa) long protein (Figure 3.2). *cp29A* TSS_B begins after the chloroplast transit peptide (as shown in Chapter 1, Figure 1.1) and encodes a 217aa long protein. The shortest sequence is produced from TSS_C is only 72aa long, starting approximately 16aa into the second RNA recognition motif (RRM).

TSS-seq reads published in Ushijima et al (2017) indicates that *cp29A* TSS_B was detected at higher rates than *cp29A* TSS_B at 1hr and 3hr in red light compared to 0hr (Table 3.2). Data also indicate that *cp29A* TSS_C was more abundantly accumulated at 3hr, showing the alternative forms are both accumulated under light conditions. A comparison of abundance in WT compared to *phyB* also showed *cp29A* TSS_B and TSS_C levels were proportionally higher compared to TSS_A, showing *phyB* is required for the generation of the alternative transcripts.

A cpSEBF (TSS_A) cpSEBF (TSS_B)

▼
 MAASASSLALSSFNPKSLPFGVSRPASVSLLSPLSLFKLNSDSVSFSIAAKWNSPASRFARNVAITSEFEVEEDGFADVAPPKEQSFSAADLKLFGVGNLFFNVDSAQLAQLFESAGNVEMV
 -----MV

cpSEBF (TSS_C)

cpSEBF (TSS_D)

▼
 EVIYDKITGRSRGFGFVTMSSVSEVEAAAQQFNGYELDGRPLRVNAGPPPKREDGFSRGRSSFGSSGSGYGGGGSGAGSGNRVYVGNLSWGVDDMALESLSFEQGVVEARVIYDRD
 EVIYDKITGRSRGFGFVTMSSVSEVEAAAQQFNGYELDGRPLRVNAGPPPKREDGFSRGRSSFGSSGSGYGGGGSGAGSGNRVYVGNLSWGVDDMALESLSFEQGVVEARVIYDRD
 -----MSSVSEVEAAAQQFNGYELDGRPLRVNAGPPPKREDGFSRGRSSFGSSGSGYGGGGSGAGSGNRVYVGNLSWGVDDMALESLSFEQGVVEARVIYDRD
 -----MALESLSFEQGVVEARVIYDRD

SGRSKGFVYDSSQEVQNAIKSLDGADLDGRQIRVSEAEARPPRRQY
 SGRSKGFVYDSSQEVQNAIKSLDGADLDGRQIRVSEAEARPPRRQY
 SGRSKGFVYDSSQEVQNAIKSLDGADLDGRQIRVSEAEARPPRRQY
 SGRSKGFVYDSSQEVQNAIKSLDGADLDGRQIRVSEAEARPPRRQY

B cp31A (TSS_A)

▼
 MASSIVTSSLKPLAMADSSSTIFSHPSISSTISSRIRSSVSLLTGRINLPLFSRVLSLTKTKHLKSPFVSVFAQTSWAEEGGEGSVAVEETENSLESQDVSEGDSEGDASEG

cp31A (TSS_B)

▼
 DVSEGDSEGDVSEGAVERAEFPEPSEEAKLFGVGNLAYDVNSQALAMLFEQAGTVEIAEVIYNRETQDSRGGFGFVTMSSVDEAETAVEKFNRYDLNGRLLTVNKAAPRGRPERAPRVY
 -----MLFEQAGTVEIAEVIYNRETQDSRGGFGFVTMSSVDEAETAVEKFNRYDLNGRLLTVNKAAPRGRPERAPRVY

EPAFRVYVGNLPWDVNDNGLRLEQLFSEHGKVVVEARVYDRETGRSRGFGFVTMSDVELNEAISALDGGQLEGRAIRVNVAEERPPRRGY
 EPAFRVYVGNLPWDVNDNGLRLEQLFSEHGKVVVEARVYDRETGRSRGFGFVTMSDVELNEAISALDGGQLEGRAIRVNVAEERPPRRGY

C cp29A (TSS_A)

▼
 MSASASSLSAFNPKSLPLCVSRPASVSVLPPSLFKLHSDHLVIFASSALKCSSPAEYPSRFVNRVAVSSDFEVEEDDMFADGDDSAVERNSFSPDLKLVGNLFFNVDSAQLAQLFE

cp29A (TSS_B)

▼
 SAGNVEMVEIYDKVTGRSRGFGFVTMSTAAEVEAAAQQFNGYVSRYLCSLLCLYLLIRVLCGLEFEGRPLRVNAGPPPKREESFSRGRSSGGYGSERGGYGSERGGYGSERGGYGS
 -----MSTAAEVEAAAQQFNGYVSRYLCSLLCLYLLIRVLCGLEFEGRPLRVNAGPPPKREESFSRGRSSGGYGSERGGYGSERGGYGSERGGYGSERGGYGS

cp29A (TSS_C)

▼
 SERGGYGSQRSGGYGGYQRSYSGSGSGSGSGSGNRLYVGNLSWGVDDMALENLFNEQGVVEARVIYDRDSGRSKGFGFVTLSSSQEVQKAINSLNGADLDGRQIRVSEAEARPPR
 SERGGYGSQRSGGYGGYQRSYSGSGSGSGSGSGNRLYVGNLSWGVDDMALENLFNEQGVVEARVIYDRDSGRSKGFGFVTLSSSQEVQKAINSLNGADLDGRQIRVSEAEARPPR
 -----MALENLFNEQGVVEARVIYDRDSGRSKGFGFVTLSSSQEVQKAINSLNGADLDGRQIRVSEAEARPPR

GQF
 GQF
 GQF

D cp29C (TSS_A)

▼
 MATFLTNVWSIKPTIFSQSESFTPLHTRVNVFSSKPPFSLAGTFSRSSRTRFIPYAVTEMATFLTNVWSIKPTIFSQSESFTPLHTRVNVFSSKPPFSLAGTFSRSSRTRFIPYAVTE

cp29C (TSS_B)

▼
 TEEKPAALDPSSEARRVYIGNIPRTVTNEQLTKLVEEHGAVEKVQMYDKYSGRSRRFGFATMKSVEDANAVVEKLNNTVEGREIKVNIITEKPIASSPDLVLSQSEDSAFVDSPYKVY
 -----MKSVEDANAVVEKLNNTVEGREIKVNIITEKPIASSPDLVLSQSEDSAFVDSPYKVY

VGNLAKTVTKEMLENLFSEKGVVSAKVSVPVPTSGTGFVTFSSSEEDVEAAIVALNNSLLEGGQKIRVNKA
 VGNLAKTVTKEMLENLFSEKGVVSAKVSVPVPTSGTGFVTFSSSEEDVEAAIVALNNSLLEGGQKIRVNKA

Figure 3.2. *phyB*-mediated alternative transcription of cpRNPs produces different length isoforms, some of which do not contain the chloroplast transit peptide. Within each protein sequence, the beginning of the isoform is indicated with a label and arrow. Protein domains are indicated by a coloured bar for the chloroplast transit peptide (green), acidic domain (orange), two RNA Recognition Motifs (RRM) (red), and a linker domain (blue). Protein sequences were identified by Ushijima et al (2017) and aligned using ClustalW (Madeira et al., 2019).

cp29C. For *cp29C*, two alternative transcriptional start sites were identified (Figure 3.2). *cp29C* TSS_A encodes a 253aa long full-length protein and TSS_B encodes a 130aa long protein beginning halfway through the first RRM. *cp29C* TSS_B was shown to be proportionally more highly accumulated than TSS_A in WT between 3hr and 0hr of R-illumination (Table 3.3).

cp31A. Two alternative TSSs were identified for *cp31A*: TSS_A, encoding the full-length 329aa long protein, and TSS_B, which encodes a protein 162 aa long (Figure 3.2). The *cp31A* TSS_B-derived protein begins c. 18aa into the sequence of the first RRM. TSS_B was observed to be up-regulated in comparison to TSS_A in red light treated WT plants and upregulated in WT compared to *phyA phyB* (Table 3.3).

cpSEBF. For *cpSEBF*, four TSS forms were identified (TSS_A- TSS_D) (Figure 3.2) The longest form, *cpSEBF* TSS_A, encodes the classical long sequence at 289aa long. The TSS_B protein is 171aa and begins within the second RRM after the chloroplast transit peptide ends; the TSS_C variant is 151aa long and begins 20aa downstream from TSS_B, halfway through the same RRM. Finally, the fourth form TSS_D is only 72aa long and starts c.13 aa into the second RRM motif.

Of these alternatively transcribed *cpSEBF* forms, the longest and shortest TSS_A and TSS_D were found to be more highly reported in TSS-seqs in WT at 1hr compared to WT at 0hr and *phyA phyB* compared to TSS_B and TSS C, but the intermediate length TSS_B, TSS_C, and TSS_D were reported to be more highly expressed than TSS_A at 3hr in WT compared to 0hr. This may suggest that the full length TSS_A may have an important earlier role, but that priority may switch to the non-plastid TSS_B and TSS_C forms at 3hr, suggesting that time, as well as light, may affect their expression.

To explore this further, a collaboration with Professor Matsushita from Kyushu University (now in Kyoto University) and the principal investigator of Ushijima et al (2017) was established. Professor Matsushita's laboratory group generated constructs for the long (TSS_A) and short (TSS_B) form for each *cpSEBF*, *cp29C*, *cp29A*, and *cp31A* with a C-terminal GFP tag under a 35S:: promoter. Expression of these constructs was initially verified in onion cells, in comparison with a tagRFP as maker of plastids and nuclei, and the cytoplasm and nuclei. The results of this experiment are

presented in Figure 3.3. These results demonstrate a transient *in vivo* localisation of the longer cpRNP forms to the chloroplast and in contrast, the shorter forms localisation to the nucleus and cytoplasm. To further validate these findings *in planta*, Arabidopsis plants were transformed with the construct 35S::cpRNP-GFP constructs. Single insertion T3 plants were selected at Lancaster University for further cell biological studies using confocal microscopy.

Table 3.3. Alternative transcriptional start site (TSS) transcribed cpRNPs are differentially expressed in R-light compared to full length counterparts, and are *phyA phyB*-dependent. Data was obtained and reproduced from Ushijima et al, 2017.

Gene	TSS_up	TSS_down	Red light (1h/3h)	Fold Difference (TSS_up/TSS_down) in WT (1h or 3h) / (TSS_up/TSS_down) in WT (0h)	P value: WT (0h) vs WT (1h or 3h)	Fold Difference (TSS_up/TSS_down) in WT (1h or 3h) / (TSS_up/TSS_down) in <i>phyA phyB</i> (1h or 3h)	P value: WT (1hr or 3hr) vs <i>phyA phyB</i> (1h or 3hr)
<i>cp29A</i>	TSS_B	TSS_A	R1H	2.36	1.21E-03	2.18	1.69E-03
	TSS_C	TSS_A	R3H	97.95	0.00E+00	16.88	1.13E-47
	TSS_B	TSS_A	R3H	207.36	0.00E+00	88.23	1.40E-74
<i>cp31A</i>	TSS_B	TSS_A	R3H	49.15	0.00E+00	48.31	0.00E+00
<i>cpSEBF</i>	TSS_A	TSS_B	R1H	7.40	5.19E-08	3.23	7.43E-03
	TSS_D	TSS_B	R1H	11.86	1.09E-07	6.86	2.40E-04
	TSS_A	TSS_C	R1H	12.79	1.65E-09	8.00	6.54E-06
	TSS_D	TSS_C	R1H	20.50	4.58E-11	17.00	2.99E-09
	TSS_D	TSS_A	R3H	275.33	0.00E+00	69.68	7.74E-51
	TSS_B	TSS_A	R3H	68.90	0.00E+00	180.89	6.50E-65
	TSS_C	TSS_A	R3H	519.53	0.00E+00	1347.67	0.00E+00
<i>cp29C</i>	TSS_B	TSS_A	R3H	18.06	1.03E-08	6.27	3.92E-03

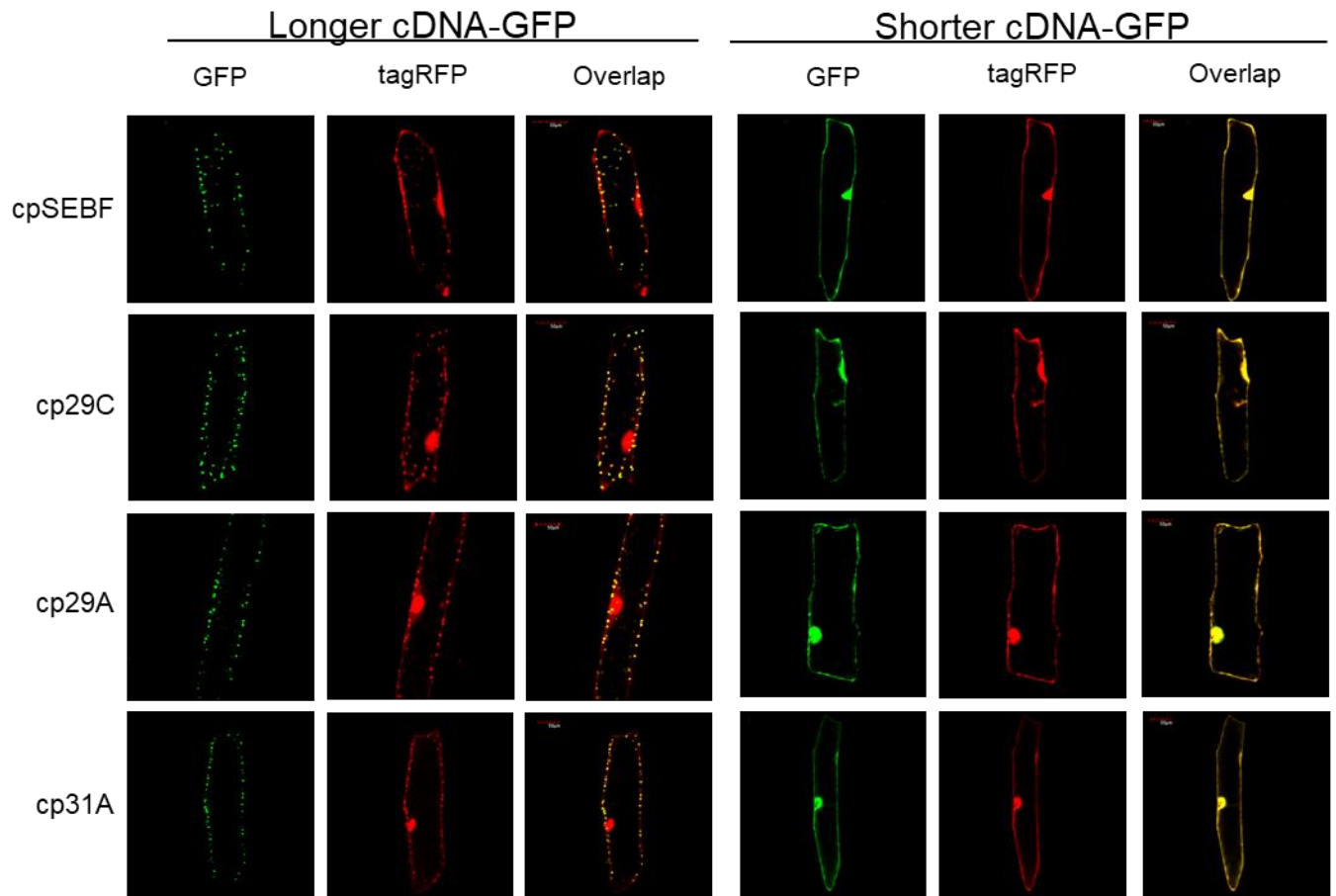


Figure 3.3. Confocal microscopy shows longer cpRNP forms localise to the plastid and shorter cpRNP forms localise to the nucleus when expressed in transformed onion cells. cpRNP forms express GFP (green), and chloroplast and nuclei are tagged with RFP (red). Figure and data were generated by Sara Akune, Matsushita lab, Kyushu University (personal communication).

3.3.4. *In planta* examination of Alternatively Transcribed cpRNP Isoforms reveals nuclear localisation in Arabidopsis.

Seeking to confirm a dual and/or dynamic localisation of the alternatively transcribed cpRNPs *in planta*, an analysis of Arabidopsis transgenic lines was conducted using confocal microscopy. A list of the examined lines is described in Table 3.1. The hypothesis driving the experiments is that alternatively transcribed *cpRNP* isoforms can lead to differential protein subcellular localization. Based on the bioinformatic predictions, longer isoforms would include a longer N-terminal including a chloroplast transit peptide to localise in the plastids, while shorter isoforms without the transit peptide would localise to the cytoplasm and/or the nucleus.

The transgenic lines for analysis were provided by Ms. Sera Akune from the Matsushita lab in Kyushu University. Cp31A- and cpSEBF-GFP tagged isoforms were analysed using confocal microscopy. Transgenic plants were grown for 3 days in darkness and treated with 24hr R-80. For each cpRNP, a transgenic line containing a construct expressing the longer form produced by TSS_A, and a transgenic line containing a construct expressing a shorter form from TSS_B were selected to analyse. To determine a nuclear localisation, a 4',6-diamidino-2-phenylindole (DAPI) stain that binds to adenine-thymine-rich DNA regions was used (DAPI preferentially binds to the condensed nuclear DNA), and chlorophyll auto-fluorescence was used to determine a chloroplast localisation. A WT plant with no GFP was used as control for chlorophyll auto-fluorescence, shown in Figure 3.6.

Confocal microscopy examination of cp31A (TSS_A)-GFP and cp31A (TSS_B)-GFP. Figure 3.4 shows that cp31A (TSS_A)-GFP has a chloroplast localisation. Panels A and F of Figure 3.4 show overlap between PMT brightfield (panels E, J), chloroplast auto-fluorescence (panels B, G), DAPI staining (panels D, I), and GFP fluorescence (panels C, H). The green GFP signal from the constructs under evaluation overlaps with the red chlorophyll auto-fluorescence, but no co-localization was detected within the nuclear blue DAPI. Panel A shows the GFP signal occurs throughout the chloroplast, and panel F demonstrates represents consistent expression across multiple cells. This would be considered a classical cpRNP localisation.

cp31A (TSS_B)-GFP (Figure 3.5 panel C), however, shows an alternate localisation with overlap with the nuclear DAPI stain (panel D) (circled). As can also be observed in panel B, chlorophyll auto-fluorescence is absent from these spots, shown in the overlap panel A. This was observed in multiple cells throughout the cotyledons examined (panels F-J). Panels C and H also illustrate a cp31A (TSS_B)-GFP cytoplasmic localization. This variant of cp31A was absent from the

chloroplast, as shown by the lack of GFP-signal colocalization with auto-fluorescence overlap between panels B, G and C, H.

The control plant, WT, shows no GFP can be detected in Figure 3.6, panels C, H, but classical DAPI-nuclear staining is demonstrated in panels D and I and healthy chlorophyll auto-fluorescence can be seen in panels B and G.

To further confirm observation of single planes, an integration of Z-stacks was performed to construct 3D representations of whole cells Figure 3.7. Z stacks clustered 21 frames taken 1nm apart. The merging of chlorophyll auto-fluorescence (red), DAPI-staining (blue), and cp31A-GFP (green) signals is shown for cp31A (TSS_A)-GFP in panel 3.7 panel A, and for cp31A (TSS_B)-GFP in panels B-D. Panel A indicated a clear GFP co-localization with the red chlorophyll auto-fluorescence, indicating chloroplasts, and no GFP signal was detected in the larger blue-stained nuclei. Panels B-D show the absence of GFP signal from the chlorophyll auto-fluorescence that identified chloroplasts, and a speckled distribution of GFP within the blue-stained nuclei and cytoplasm (indicated with arrows). This speckling, most clearly observable in panel D (indicated with an arrow), also provide insight into potential subcellular distribution patterns of cp31A (TSS_B) in the nucleus *in planta*.

Confocal microscopy examination of cpSEBF (TSS_A)-GFP and cpSEBF (TSS_B)-GFP. cpSEBF (TSS_A)-GFP shows a chloroplast localization through overlap of the GFP signal with chlorophyll auto-fluorescence (Figure 3.8, panels A-C, F-H). No co-localisation was observed between GFP and blue DAPI-stained nuclei (panels D, I). The same localisation pattern was detected for multiple independent plants from the same line (panels A-E, F-J)

cpSEBF (TSS_B)-GFP's localization is shown in Figure 3.9. Similarly to cp31A (TSS_B)-GFP, cpSEBF (TSS_B)-GFP shows localization to the nucleus (panels A, F) through with co-localization with DAPI (panels D, I) (circled). Interestingly, panel C also appears to show a widespread distribution of cpSEBF (TSS_B)-GFP throughout the cell, indicating an additional cytoplasmic localisation. However, while the chlorophyll auto-fluorescence observed in panels B, G is unclear, the GFP fluorescence detected in panels A, C, F, and H indicate a non-chloroplast localisation.

To further confirm these observations from single plane images, a 3D representation of whole cells was constructed by an integration of Z-stacks for cpSEBF-GFP lines, shown in Figure 3.10. This merging of chlorophyll auto-fluorescence (red), DAPI-staining (blue), and cpSEBF-GFP (green), shows cpSEBF (TSS_A)-GFP in panel A, and cpSEBF (TSS_B)-GFP in panel B. Panel A shows the co-localisation of cpSEBF (TSS_A)-GFP signal with the red chlorophyll auto-fluorescence and an no

presence of GFP signal in the blue DAPI-stained nuclei. On the other hand, panel B shows co-localisation of cpSEBF (TSS_B)-GFP to blue-stained nuclei.

In summary, this study provided the first *in planta* evidence for Arabidopsis plants that alternatively-transcribed cpRNPs localise to the nucleus and the chloroplast, and that these localisations are specific to their respective isoforms and transcriptional start sites. The longer forms cp31A (TSS_A)-GFP and cpSEBF (TSS_A)-GFP localised to the chloroplast, and the shorter forms cp31A (TSS_B)-GFP and cpSEBF (TSS_B)-GFP localised to the nucleus.

A nuclear localisation of cp31A and cpSEBF *in planta* during de-etiolation opens the possibility of a function in the regulation of nuclear-encoded transcripts. Beyond the role of R-light-phyB in generating the isoforms, the role of these isoforms in the nucleus and the range of phyB-light-dependent signals that could control localization are underexplored.

cp31A TSSA- Long Sequence

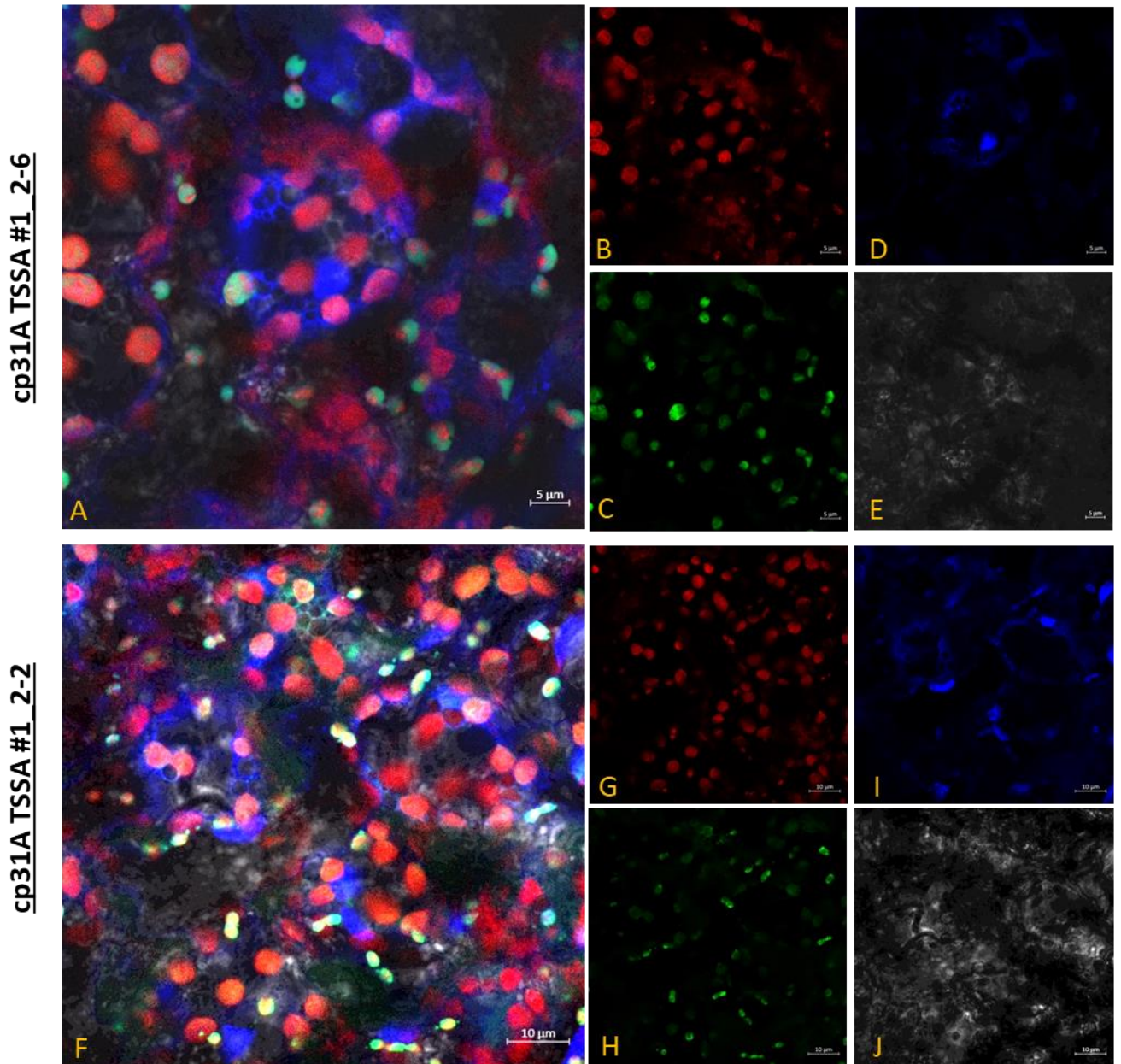


Figure 3.4. Confocal microscopy shows cp31A (TSS_A) localises to the chloroplast. Plants were grown for three days in darkness and treated with 24hrs red light ($80 \mu\text{mol m}^{-2}\text{s}^{-1}$) at 22°C . Images were enhanced in post-image processing software Zen Blue and show: A, F) Overlap of all images; B, G) chloroplasts are identified by chlorophyll auto-fluorescence (red); C, H) cp31A (TSS_A) expressing GFP (green); D, I) nuclei stained with 4',6-diamidino-2-phenylindole (DAPI) (blue); E, J) brightfield image of the plant. Scale bars are present in the lower right-hand corner of each photo. Each set of images are from an independent plant.

cp31A TSSB- Short Sequence

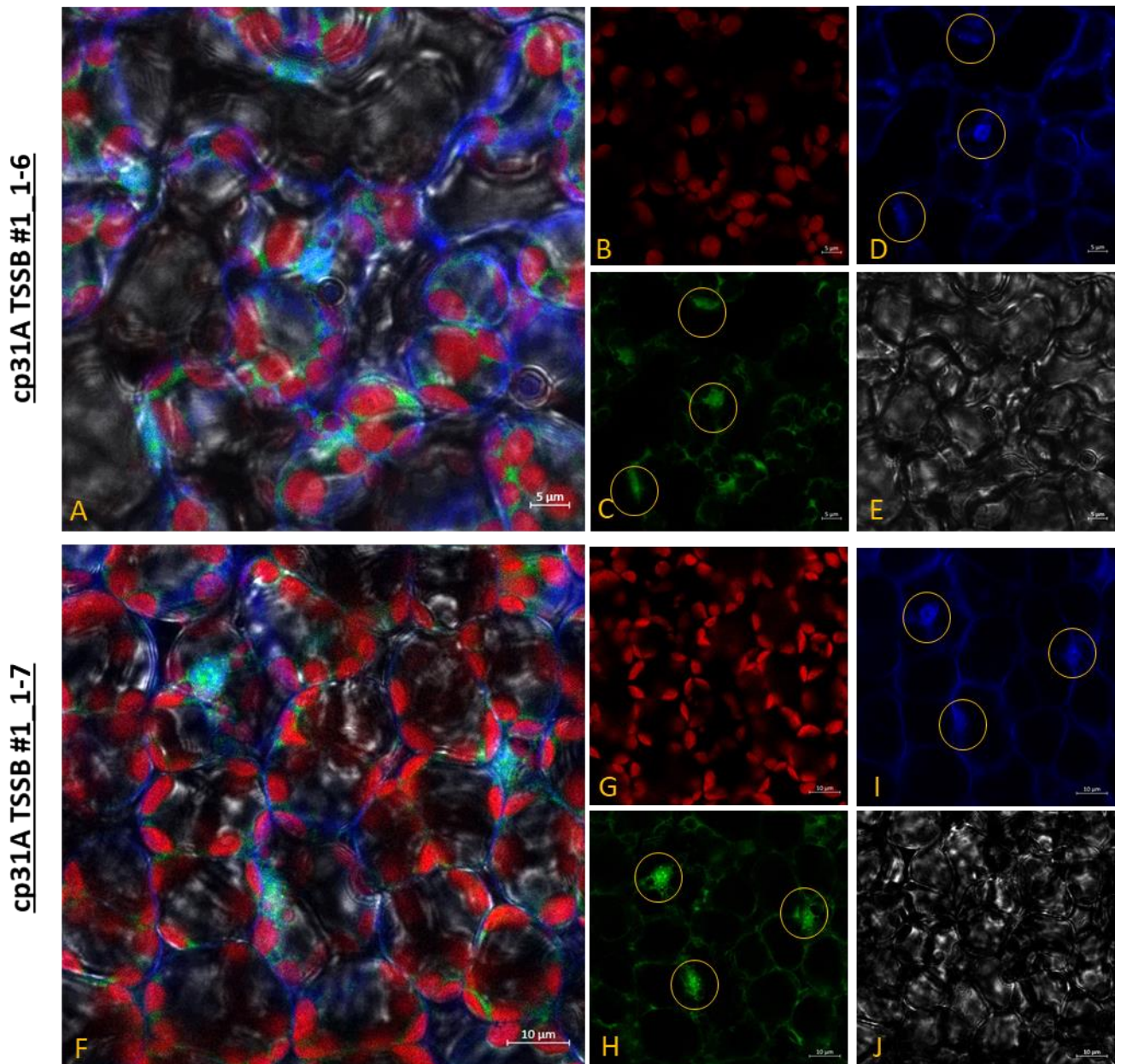


Figure 3.5. Confocal microscopy shows cp31A (TSS_B) localises to the nucleus. Plants were grown for three days in darkness and treated with 24hrs red light ($80 \mu\text{mol m}^{-2}\text{s}^{-1}$) at 22°C . Images were enhanced in post-image processing software Zen Blue and show: A, F) Overlap of all images; B, G) chloroplasts are identified by chlorophyll auto-fluorescence (red); C, H) cp31A (TSS_B) expressing GFP (green); D, I) nuclei stained with 4',6-diamidino-2-phenylindole (DAPI) (blue); E, J) brightfield image of the plant. Scale bars are present in the lower right-hand corner of each photo. Images have been highlighted with golden circles to indicate DAPI and GFP overlap, indicating cpRNP co-localization with the nucleus. Each set of images are from an independent plant.

WT

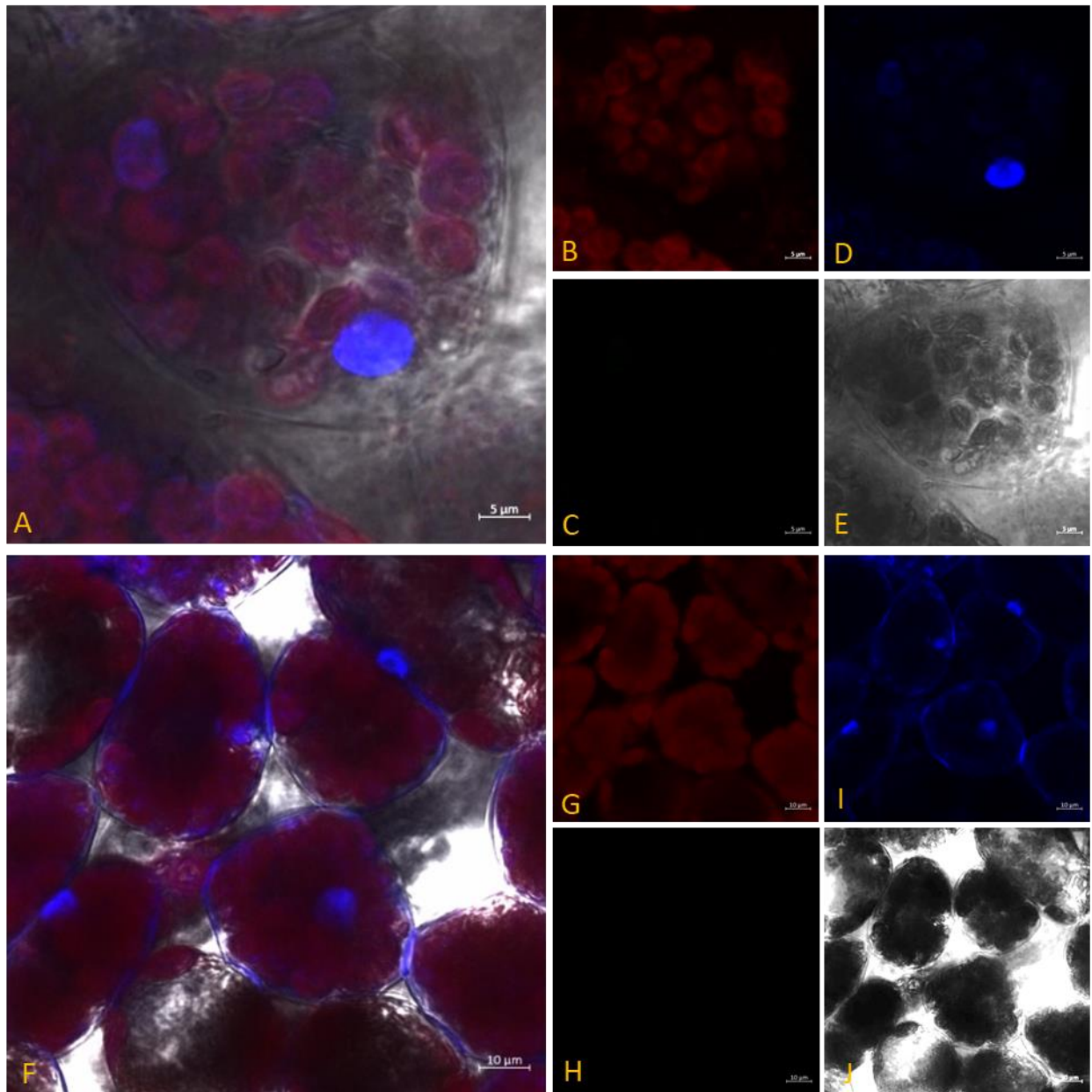


Figure 3.6. Confocal microscopy shows WT control. Plants were grown for three days in darkness and treated with 24hrs red light ($80 \mu\text{mol m}^{-2}\text{s}^{-1}$) at 22°C . Images were enhanced in post-image processing software Zen Blue and show: A, F) Overlap of all images; B, G) chloroplasts are identified by chlorophyll auto-fluorescence (red); C, H) No constructs are present in WT, so field is blank- GFP would be shown in green; D, I) nuclei stained with 4',6-diamidino-2-phenylindole (DAPI) (blue); E, J) brightfield image of the plant. Scale bars are present in the lower right-hand corner of each photo.

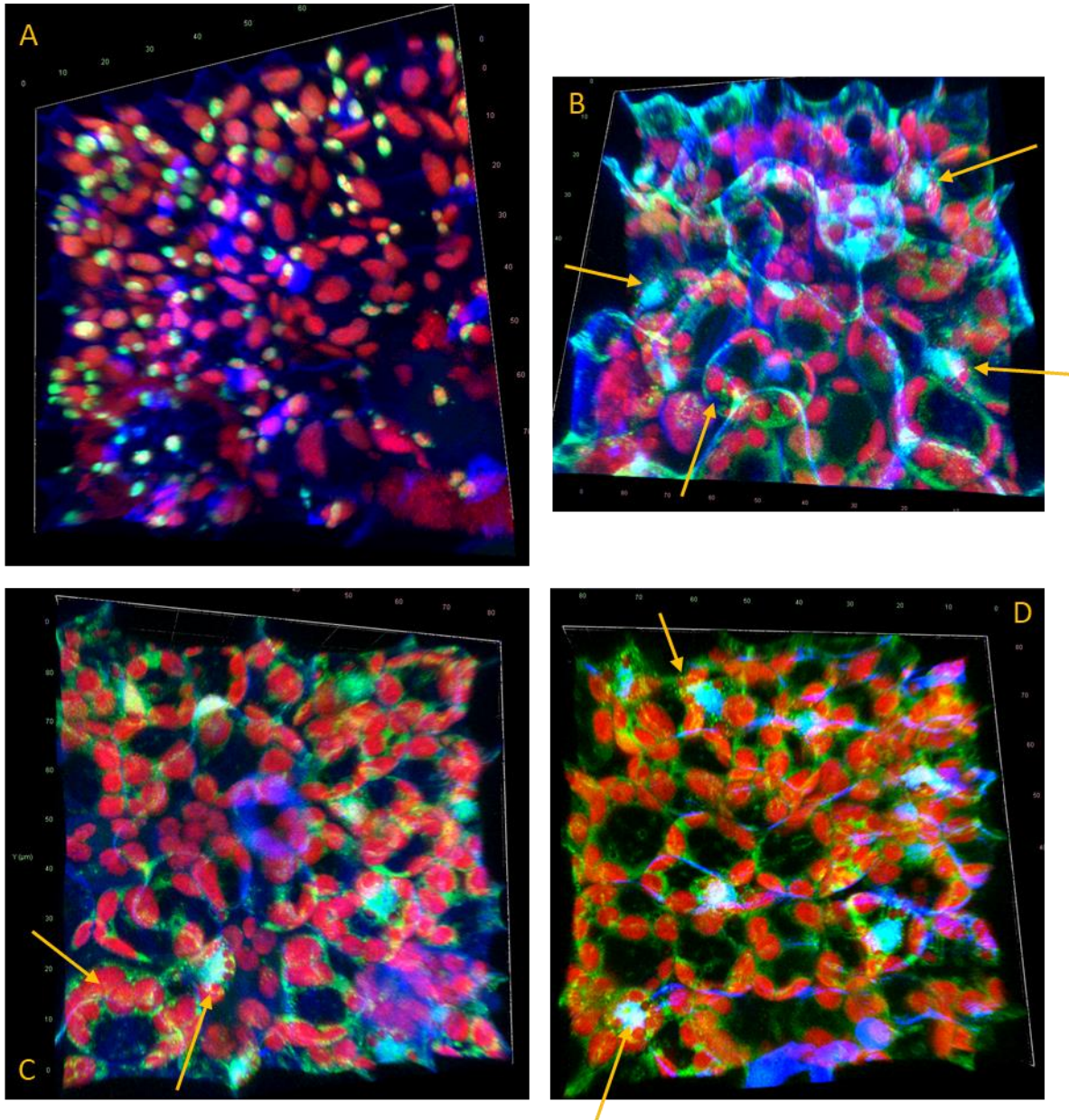


Figure 3.7. Confocal microscopy shows 3-D representations of cp31A (TSS_A) and cp31A (TSS_B) show alternate chloroplast and nuclear localisations. Plants were grown for three days in darkness and treated with 24hrs red light ($80 \mu\text{mol m}^{-2}\text{s}^{-1}$) at 22°C . 3-D representations were collected as a range of Z-stacks and were enhanced in post-image processing software Zen Blue, combining respective cp31A forms with GFP tag (green), chlorophyll auto-fluorescence (red), and nuclear 4',6-diamidino-2-phenylindole (DAPI) staining (blue). The figure depicts: A) Overlap of cp31A (TSS_A) images; B-D) Overlap of cp31A (TSS_B) images. Scale bars are shown at the axis beside each photo. Each set of images are from an independent plant. The PMT brightfield is not represented in these Z-stacks to allow for better 3D-visualisation of fluorescence. Arrows indicate notable observations.

cpSEBF TSSA- Long Sequence

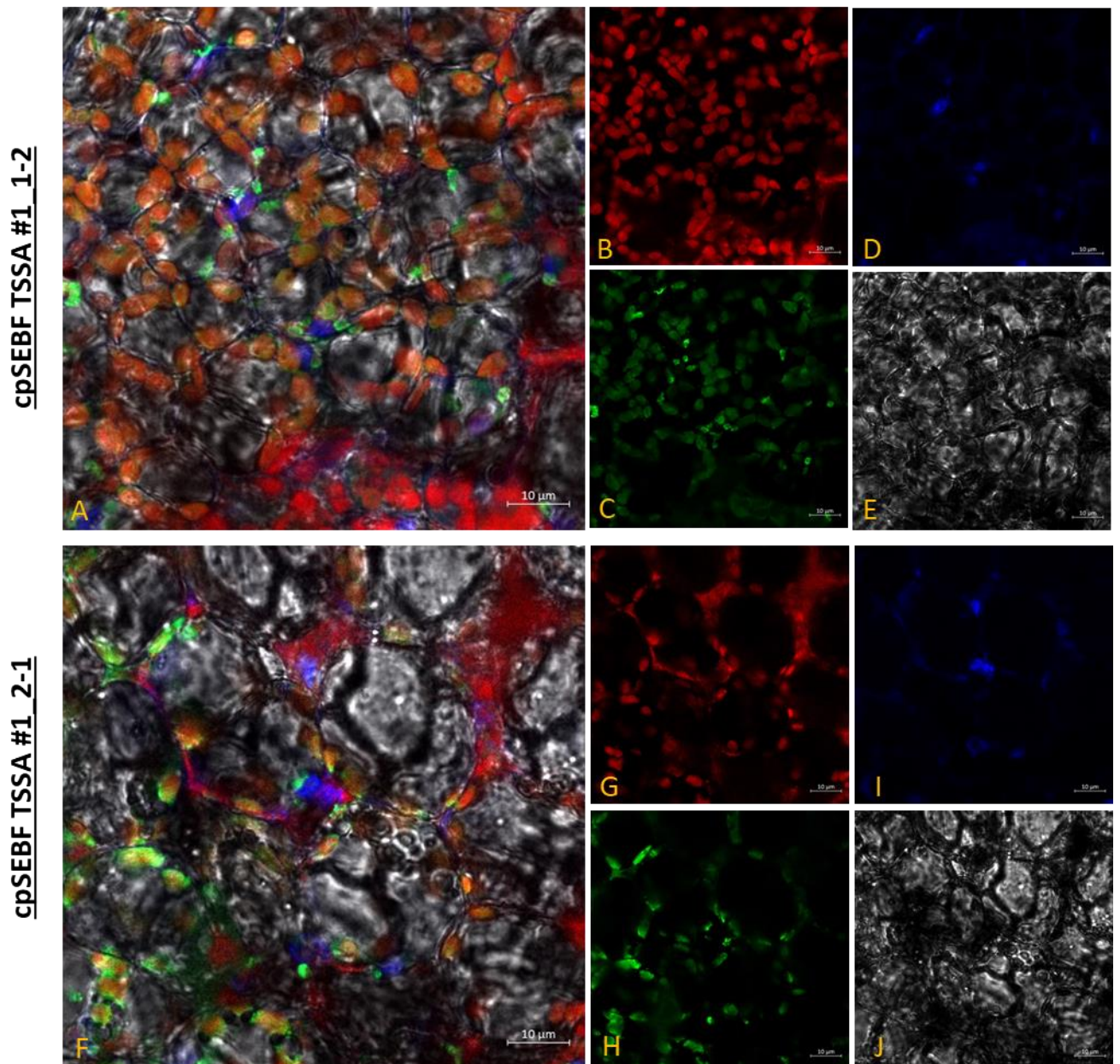


Figure 3.8. Confocal microscopy shows cpSEBF (TSS_A) localises to the chloroplast. Plants were grown for three days in darkness and treated with 24hrs red light ($80 \mu\text{mol m}^{-2}\text{s}^{-1}$) at 22°C . Images were enhanced in post-image processing software Zen Blue and show: A, F) Overlap of all images; B, G) chloroplasts are identified by chlorophyll autofluorescence (red); C, H) cpSEBF (TSS_A) expressing GFP (green); D, I) nuclei stained with 4',6-diamidino-2-phenylindole (DAPI) (blue); E, J) brightfield image of the plant. Scale bars are present in the lower right-hand corner of each photo. Each set of images are from an independent plant.

cpSEBF TSSB- Short Sequence

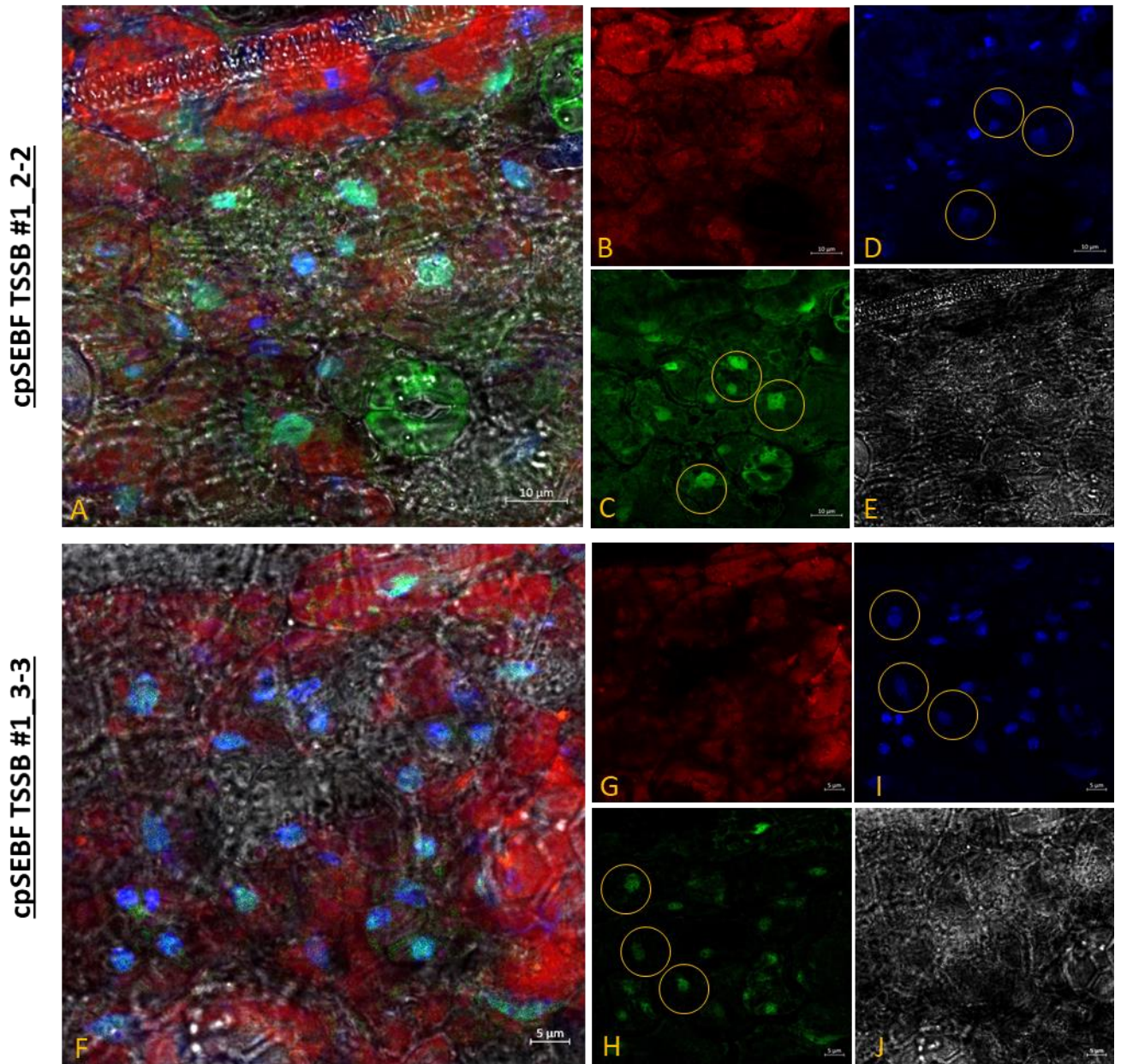


Figure 3.9. Confocal microscopy shows cpSEBF (TSS_B) localises to the nucleus. Plants were grown for three days in darkness and treated with 24hrs red light ($80 \mu\text{mol m}^{-2}\text{s}^{-1}$) at 22°C . Images were enhanced in post-image processing software Zen Blue and show: A, F) Overlap of all images; B, G) chloroplasts are identified by chlorophyll auto-fluorescence (red); C, H) cpSEBF (TSS_B) expressing GFP (green); D, I) nuclei stained with 4',6-diamidino-2-phenylindole (DAPI) (blue); E, J) brightfield image of the plant. Scale bars are present in the lower right-hand corner of each photo. Each set of images are from an independent plant. Overlap between GFP and DAPI-staining is noted with a circle.

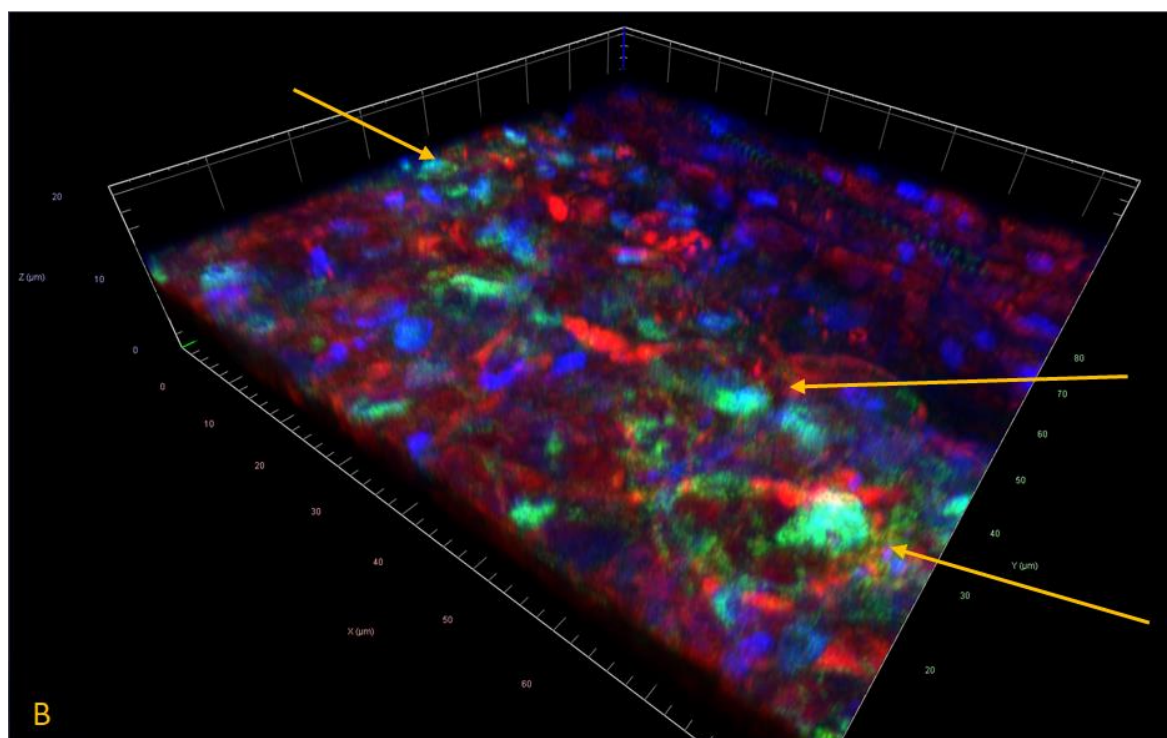
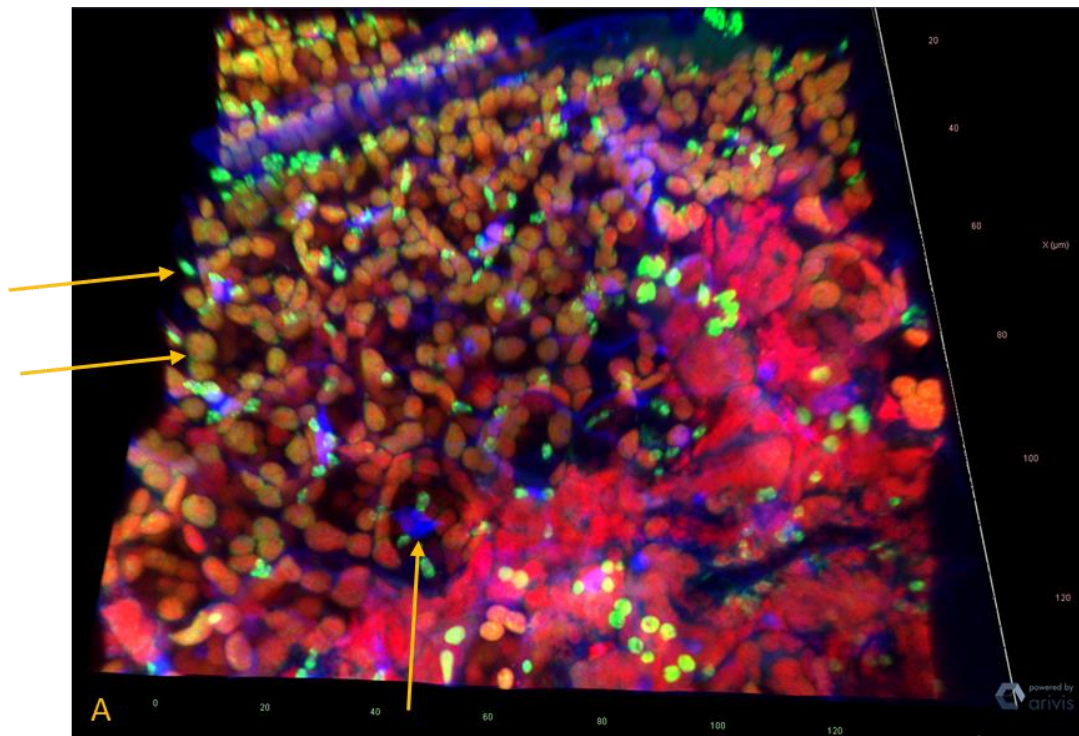


Figure 3.10. Confocal microscopy shows 3-D representations of cpSEBF (TSS_A) and cpSEBF (TSS_B) show alternate chloroplast and nuclear localisations. Plants were grown for three days in darkness and treated with 24hrs red light ($80 \mu\text{mol m}^{-2}\text{s}^{-1}$) at 22°C . 3-D representations were collected as a range of Z-stacks and were enhanced in post-image processing software Zen Blue, combining respective cpSEBF forms with GFP tag (green), chlorophyll autofluorescence (red), and nuclear 4',6-diamidino-2-phenylindole (DAPI) staining (blue). The figure depicts: A) Overlap of cpSEBF (TSS_A) images; B) Overlap of cpSEBF (TSS_B) images. Scale bars are shown at the axis beside each photo. Each set of images are from an independent plant. Notable observations are indicated with an arrow.

3.4. Results: Investigating a potential role for cpRNPs in modulating nuclear-encoded transcript abundance.

3.4.1. Identification of R-phys regulated nuclear-encoded transcript targets.

To examine if the detected nuclear localization of cpRNPs could be linked to mechanisms that modulate nuclear photosynthetic gene expression, a reverse genetics strategy was followed using *cprnp* mutants. Based on the evidence that cpRNPs modulate greening responses (Chapter 2, Figure 2.3) and the transcript accumulation of some of the plastid-encoded subunits from the ATP Synthase, NADH Dehydrogenase, Photosystem I, and Photosystem II photosynthetic complexes (Chapter 2, Figure 2.5), the effect of *cprnp* mutation was evaluated over red-phytochrome modulated nuclear counterparts for these complexes/functions. As previously described in Chapter 2 section 3, analysis of transcript abundance was conducted using 24hr red-light de-etiolated seedlings as a model system to evaluate the impact of *cprnp* mutation on nuclear photosynthetic gene expression, especially for genes linked to the assembly and maintenance of PSI and PSII photosynthetic apparatus (Armarego-Marriott et al., 2020).

The selection of the nuclear-encoded counterparts started with the analyses of transcript accumulation in a R-Phys dependent manner using genomic datasets publicly available for *phyABCDE* (GSE31587) in 4-day old seedlings grown under Rc-50 $\mu\text{mol m}^{-2} \text{s}^{-1}$. This first analysis identified genes that are phy-regulated, and whose dependence on cpRNPs could be investigated. Genes selected showed a statistically significant greater than two-fold difference for red light-*phyABCDE*-dependence vs WT, or were manually selected based on biological relevance in photosynthesis and photoprotection (see 3.2 Materials and Methods for further details). Ultimately, six genes encoding Photosystem II subunits, three genes encoding Photosystem I subunits, and five genes encoding proteins involved in photoprotective mechanisms were selected. These are described in Table 3.4, showing protein function, phyB-dependency, and statistical significance.

The final list of candidate genes included three members from the Light Harvesting Complexes (LHC), involved in harvesting light energy from chlorophylls *a* and *b*, photoprotection, and response to stress (Jansson, 1994; Fristedt and Vener, 2011; Chen et al., 2018). Shown in Table 3.4, transcript accumulation of two members of the LHCI, bound to Photosystem II (Holtzegel, 2016), were identified as R-phys dependent: *LHCB2.3* and *LHCB4.2*. One member of the LHCI, *LHCA2.1*, was also identified as R-phys-dependent. This gene encodes a key protein component of the light harvesting antenna complex for PSI (Otani et al., 2018).

Three genes associated to the oxygen-evolving complex (OEC) of Photosystem II in the thylakoid membrane were identified as R-phys dependent and selected for analysis. The oxygen-evolving complex performs the oxidation of water and is the critical step in the light reactions (Raymond and Blankenship, 2008). These three included *PSBO1* and *PSBO2*, isoforms of the PSBO extrinsic subunit of PSII critical to its assembly and involved in stabilization of the catalytic manganese cluster (Murakami et al., 2002; Bricker et al., 2012), and *PSBQ2*, an extrinsic subunit with a vital role in contributing to the maintenance of the Mn cluster (Kakiuchi et al., 2012).

One nuclear gene from the chloroplast NAD(P)H dehydrogenase complex (NDH). *PSBQ-LIKE 2*, or *PQL2*, was identified as strongly R-phys-dependent. This gene is one of three *PQL* genes required for the NADH complex function (Yabuta et al., 2010) and was selected as a representative of the NADH complex following identification of *ndhF* and *ndhG* as plastome encoded targets of cp31A (Kupsch et al., 2012).

Table 3.4. List of experimental genes delineated for examination in *cprnp* mutants. Genes were identified based on an R-phys dependency or selected for reported biological function. Genome-wide analysis of R-phys activated genes in WT vs *phyABCDE* mutant was conducted using dataset GSE31587, and defined by a $\log_2 >1$ ratio (WT-R/*phyB*-R) and statistical significance of gene expression ratios was estimated with FDR at $P < 0.05$ (see 3.2 Materials and Methods)

Gene Name	Locus	Protein Function	Log2 ratio PhyB-Dependency (WT-R/ <i>phyB</i> -R)	P-value (adj)
<i>LHCB2.3</i>	AT3G27690	Chlorophyll <i>a/b</i> -binding protein in Photosystem II	2.919436609	0.0462
<i>LHCB4.2</i>	AT3G08940	Chlorophyll <i>a/b</i> -binding protein in Photosystem II	2.829665501	0.0049
<i>PSBO1</i>	AT5G66570	Chlorophyll <i>a/b</i> -binding protein in Photosystem II	1.728889218	0.0053
<i>PSBO2</i>	AT3G50820	Chlorophyll <i>a/b</i> -binding protein in Photosystem II	2.564763926	0.0613
<i>PSBQ2</i>	AT4G05180	Chlorophyll <i>a/b</i> -binding protein in Photosystem II	3.063589007	0.0629
<i>PSBQ12</i>	AT1G14150	Chlorophyll <i>a/b</i> -binding protein in Photosystem II	2.261855479	0.0003
<i>LHCA2.1</i>	AT3G61470	Chlorophyll <i>a/b</i> -binding protein in Photosystem II	1.796532822	0.0857
<i>PSAD-2</i>	AT1G03130	Photosystem I reaction centre subunit	2.68768543	0.0397
<i>PSAN</i>	AT5G64040	Photosystem I reaction centre subunit	2.426784457	0.0185
<i>PSY</i>	AT5G17230	Phytoene Synthase	1.80065987	0.0464
<i>PSB27</i>	AT1G03600	Photosystem II repair protein	1.213074807	0.0006
<i>DEG1</i>	AT3G27925	DegP protease	1.619683322	0.0095
<i>NPQ1</i>	AT1G08550	Non-Photochemical Quenching protein	1.318902654	0.0112
<i>NPQ4</i>	AT1G44575	Non-Photochemical Quenching protein	0.66050733	0.0043

From the Photosystem I-associated genes, *LHCA2.1* was selected, encoding a protein that is a key component of the Light Harvesting Complex attached to PSI (LHCI) (Otani et al., 2018). The LHCI complex is involved in binding chlorophylls and state transitions following a light intensity stress response (Benson et al., 2015). Two Photosystem I protein subunit-encoding genes were also identified as R-phys dependent: *PSAD-2* and *PSAN*. *PSAD-2* is a Photosystem I subunit involved electron transport through in forming complexes with ferredoxin and ferredoxin-oxidoreductase to the PSI reaction centre (Ihnatowicz et al., 2004). *PSAN* mediates the binding of antenna complexes and the PSI reaction centre and in linking plastocyanin and the wider PSI complex (Haldrup et al., 1999; Ihalainen et al., 2000).

For genes associated to additional photoprotective and photorepair mechanisms, R-phys dependent *PHYTOENE SYNTHASE (PSY)* was selected. *PSY* is active in the carotenoid biosynthesis pathway and is the first committed step in the carotenoid pathway that leads to lutein, xanthophylls and other carotenoid photoprotectants (Ruiz-Sola and Rodríguez-Concepción, 2012).

To represent photorepair mechanisms, *PHOTOSYSTEM II REPAIR PROTEIN 27 (PSB27)* was identified as R-phys dependent. *PSB27* is closely associated to Photosystem II and involved in adaptation to changes to light intensity; a *psb27* mutant showed lower PSII-efficiency and enhanced ROS production, and represents a gene involved in a longer-term photoprotective mechanism (Hou et al., 2015). A second photorepair-associated gene, a member of the DEGRADATION OF PERIPLASMIC proteins (DEG) Serine Protease family, *DEG1*, was identified as R-Phys dependent. DEGs are active in the thylakoid lumen and are involved in degrading damaged luminal proteins and PSII subunits- in particular, damaged D1 reaction core proteins, a key component of the antenna and target of photo-oxidative damage (Schuhmann and Adamska, 2012).

Finally, two Non-Photochemical Quenching-encoding gene candidates were identified as R-phys dependent: *NPQ1* and *NPQ4*. These genes are involved in short-term non-photochemical quenching responses, with critical roles in maintaining a balance between dissipating and using light energy to protect against photo-oxidative damage (Roach and Krieger-Liszkay, 2012; Ware et al., 2015). Although *NPQ4* was not identified as R-phys dependent (Table 3.4) it was selected for its biological significance after a modest phenotype was detected in *cprnp* mutants grown in fluctuating high light regimes (Chapter 2, Figure 2.11).

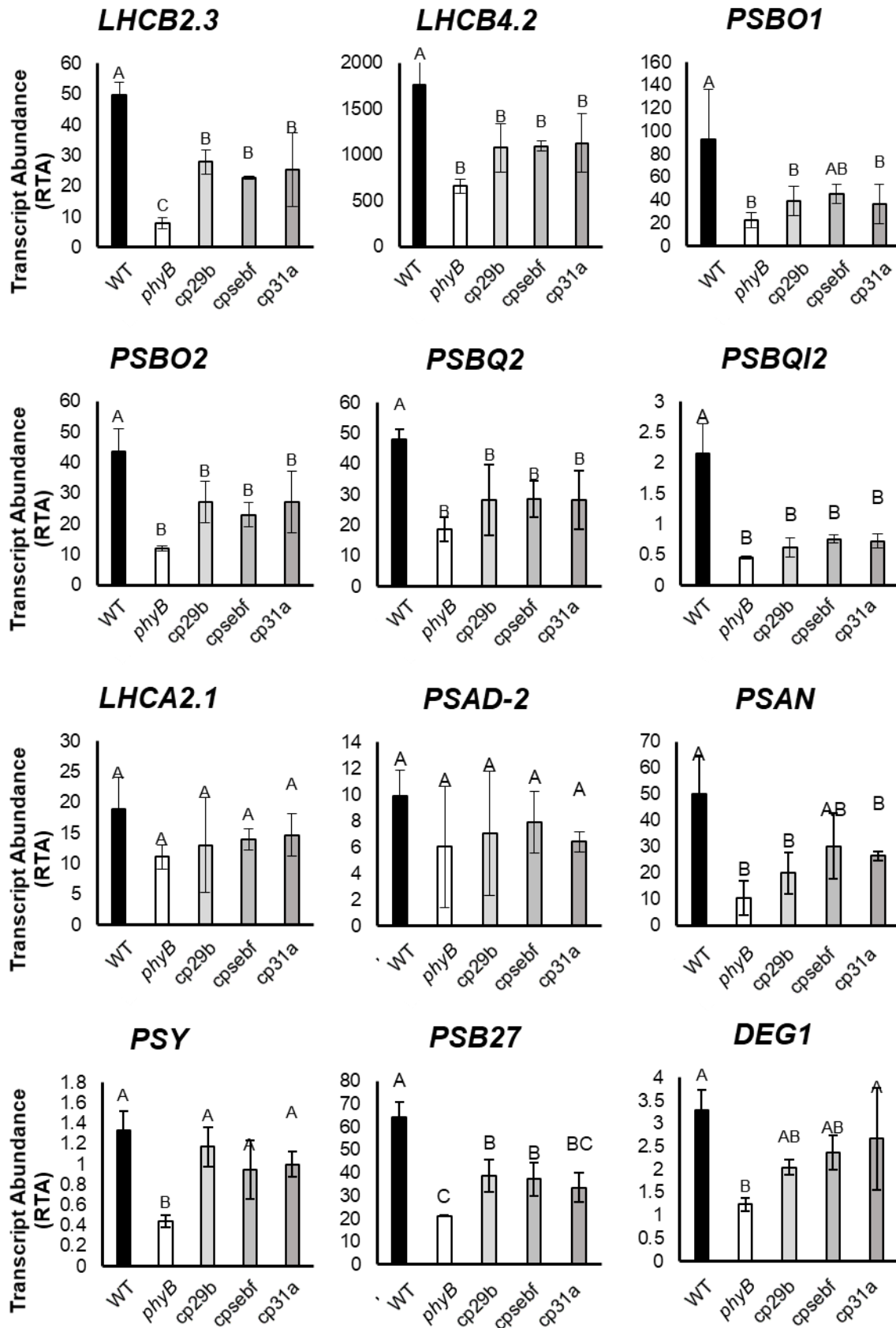
3.4.2. Nuclear-encoded transcript accumulation for selected photosynthesis related genes is lower in *cprnp* mutants.

Analysis of transcript abundance of chloroplast-encoded gene in *cprnp* mutants (Chapter 2, Figure 2.5) demonstrated that cpRNPs were important to the regulation of the plastome. However, photosynthetic metabolisms require co-expression of plastome-encoded genes with nuclear-encoded counterparts. Based on observations that cpRNPs can localise to the nucleus in a Red-phyB-mediated pathway, it was hypothesised that cpRNPs may be involved in co-ordinating the expression of genes encoded in the plastome and nucleus with a photosynthetic function. The impact of *phyB* and *cprnp* mutation on the selected photosynthesis-associated nuclear genes was evaluated during de-etiolation (Figure 3.11). *phyB* was used to confirm the effect of R-phys dependence observed in genomic experiments and analyse the relative contribution of cpRNPs to the light response.

Dependence of Photosystem II-associated nuclear transcripts accumulation on cpRNPs function.

Analysis of the transcript abundance of genes encoding subunits in LHCII, *LHCB2.3* and *LHCB4.2*, showed statistically significant reductions in the *cprnps* and *phyB* mutants compared to WT. The transcript accumulation of *LHCB2.3* in *phyB* mutant was also significantly lower than compared to all three *cprnp* mutants, indicating a greater contribution of phyB. However, accumulation of *LHCB4.2* between *phyB* and *cprnp* mutants was not statistically different, indicating a proportionally greater contribution of cpRNPs to its regulation than for *LHCB2.3*. Transcript accumulation of the three OEC genes *PSBO1*, *PSBO2*, and *PSBQ2* was significantly reduced in *phyB* and all *cprnp* mutants compared to WT, except for abundance of *PSBO1* in *cpsebf* mutants. Together, these results showed that *cprnp* mutation had significant impact upon transcript abundance of Photosystem II genes encoding photosynthetic subunits.

Dependence of NADH Dehydrogenase-associated nuclear transcripts on cpRNP function. Transcript abundance of the NADH Dehydrogenase subunit-encoding *PSBQ12* was significantly reduced in *phyB* and *cpRNP* mutants compared to WT. Statistical analysis reported that the contribution of cpRNPs and phyB to *PSBQ12* accumulation was equal, indicating that cpRNPs are important regulators of the complex.



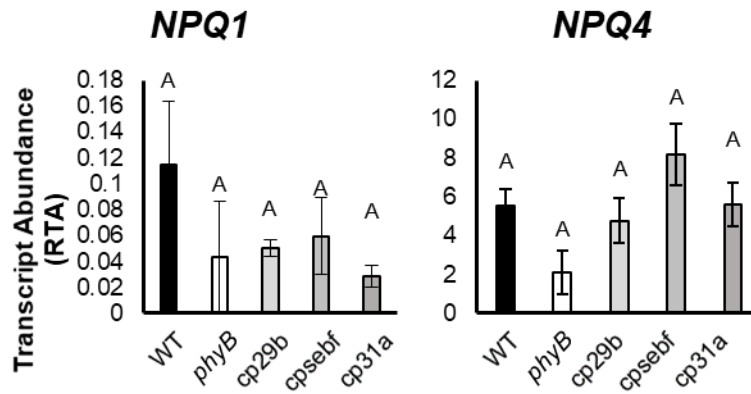


Figure 3.11. *cprnp* mutation affects the transcript abundance of key nuclear-encoded photosynthesis-associated gene expression. Graphs show relative transcript abundance (RTA) of photosynthesis-associated nuclear-encoded genes in WT, *phyB*, *cp29b_2*, *cpsebf_1*, and *cp31a_2* plants grown for three days in darkness and treated with 24hrs red light ($80 \mu\text{mol m}^{-2}\text{s}^{-1}$). Relative transcript abundance was calculated by comparing experimental gene expression to the reference gene *PP2A*. Data represent the average of three biological replicates and error bars show the 95% confidence interval. Statistical significance of expression between WT (black bars), *phyB* (white bars), and *cprnp* mutants *cp29b_2*, *cpsebf_1*, *cp31a_2* (shown over a light-to-dark gradient grey bars) was calculated using One-way ANOVA with Tukey post hoc testing ($p < 0.05$). Data that do not share a letter are statistically significant.

Nuclear Photosystem I-associated genes transcript accumulation dependence on cpRNPs.

Transcript accumulation of selected R-phy dependent genes encoding subunits associated to Photosystem I (PSI) was partially affected by *cprnp* mutation. *LHCA2.1*, of the Light Harvesting Complex I (LHCI), accumulation was not significantly reduced in *phyB* or *cprnp* mutants, despite a lower average trend; neither was transcript accumulation for *PSAD-2* of the PSI reaction centre super complex was reduced in any of the tested mutant genotypes. However, abundance of *PSAN* transcript, involved in linkage of PSI to plastocyanin, was significantly reduced in *phyB*, *cp29b*, and *cp31a*. This indicates a limited but important role of cpRNPs and *phyB* in PSI complex production.

Effect of cpRNP-dependence of photoprotection and photorepair-associated gene transcript accumulation. Analysis of genes associated to photoprotective and photorepair mechanisms showed that *PSY* and *DEG1* transcript accumulation is strongly dependent on *phyB* but was not reduced in *cprnp* mutants. However, abundance of *PSB27* was both *phyB*- and cpRNP-dependent compared to WT. For *NON-PHOTOCHEMICAL QUENCHING* genes' accumulation, *NPQ1* and *NPQ4* revealed no statistically significant effect in *phyB* or *cprnp* mutants, despite the lower average accumulation observed for *NPQ1*.

Overall, RT-qPCR revealed a clear contribution of cpRNPs to the transcript accumulation of nuclear-encoded Photosystem II-associated transcripts, with pronounced reductions in the accumulation of transcripts for genes encoding nuclear subunits of the Light Harvesting Complex II (LHCII), the oxygen-evolving complex (OEC), and NADH Dehydrogenase. However, only one tested gene associated to Photosystem I was found to be cp29B- and cp31A-dependent. Similarly, only one of photoprotection and photorepair involved genes was found to be cpRNP-dependent, *PSB27*. This points at a potential role for cpRNPs in regulating Photosystem II-associated processes, with a more limited effect on Photosystem I-associated nuclear transcript accumulation.

3.5 Results: Investigating the effect of temperature on the modulation of cpRNP subcellular localisation and function.

As previously mentioned, cpRNPs have been linked to the integration of temperature responses in chilling temperatures (4-8°C) (Kupsch et al., 2012), through changes in ambient temperatures (17-27°C) (Chapter 2, section 2.6), and through upstream signalling components phyB and HY5 (Toledo-Ortiz et al., 2014; Jung et al., 2016). Chapter 2 showed that *cpnnp* mutants' defects in greening responses are particularly observable in cold and warm conditions compared to WT and plants grown in control conditions in 22°C. Mutant *cpnnp*s showed temperature-sensitive phenotypes with effects on greening and biomass accumulation in young plantlets, which correlated with altered transcript accumulation responses of plastome-encoded transcripts during de-etiolation, in particular for Photosystem II and Photosystem I subunits protein-encoding genes (Chapter 2 Figures 2.16, 2.17).

As described in Chapter 2, ambient temperatures from 17°C to 27°C can affect plant development and growth, altering greening and morphology (Samach and Wigge, 2005; Lorenzo et al., 2016). Under this temperature range, phytochromes integrate light and temperature-dependent signals to modulate plant growth and development (Jung et al., 2016; Legris et al., 2016). In Chapter 2, transcript accumulation of *cpRNPs* was demonstrated to be temperature-sensitive (Chapter 2, Figure 2.15). In brief, *cp29B*, *cpSEBF*, and *cp31A* transcript accumulation was dramatically reduced at 17°C, highest at 22°C, and for *cp29B* and *cp31A* accumulation at 27°C was intermediate between the two at 17°C and 22°C. However, the effects of temperature at the transcriptional level may not be representative of the final protein abundance, as transcript accumulation alone is not sufficient to determine protein abundance (Liu et al., 2016). To begin investigating whether temperature alters cpRNP protein abundance and distribution, native-promoter driven cpRNPs tagged with C-terminal GFP were examined using confocal microscopy.

3.5.2. Cell Biological studies of Native-Promoter driven GFP fusion of *cp31A* and *cpSEBF* using confocal microscopy.

Evidence presented in Chapter 2 section 2.6 indicated that cpRNPs transcript accumulation and functionality are temperature-sensitive. In addition, in red light phyB induces alternatively-transcribed forms of the cpRNPs with alternate localisations (Ushijima et al., 2017). As phyB is also a key ambient temperature sensor, it was hypothesised that cpRNPs' response to temperature may involve changes in protein subcellular localisation or abundance.

To evaluate temperature-dependent protein accumulation patterns, native-promoter driving C-terminal GFP tagged *cpRNPs* (NP::cpRNP-GFP) were generated for *cp31A* and *cpSEBF* in collaboration with Dr Karine Prado from the University of Edinburgh. Constructs were used to transform *cprnp* mutants *cp31a_1* and *cpsebf_1*, each including a 2kB native promoter region. Single insertion T3 plants were selected and used for cell biological experiments to evaluate the protein distribution and abundance at 17°C, 22°C, and 27°C conditions during 24hr R-80- driven de-etiolation in 3-day old seedlings. Images shown in Figure 3.12, and 3.14 are representative results of the confocal observations conducted, which included at least 3 independent biological samples.

Confocal examination of NP::cp31A-GFP. *In planta* confocal analysis showed that NP::cp31A-GFP fluorescence was low at 22°C and 27°C, but high fluorescence signal was detected at 17°C (Figure 3.12). At 22°C, an examination of subcellular NP::cp31A-GFP protein distribution in mesophyll cells revealed co-localisation of GFP with DAPI-stained nuclei, as well as chlorophyll auto-fluorescence-identified chloroplasts (Figure 3.13 panel F). A similar localisation was also observed at 17°C (Figure 3.12 panel A), but at 27°C GFP fluorescence was only observed to co-localise with chlorophyll auto-fluorescence and not with DAPI (panel K). This indicated that cp31A localises to both chloroplast and nucleus in cold (17°C) and physiological (22°C) temperatures, but not at warm temperatures (27°C), where localisation was mostly chloroplastic.

At 22°C, GFP fluorescence of NP::cp31A-GFP was high throughout the seedling cotyledons (Figure 3.12, panels C-D). Subcellular evaluation of protein distribution (panels F-J), shows that NP::cp31A-GFP (green) colocalises with the DAPI-stained nucleus (blue) (circled), as well as with chloroplast identified by overlap with the chlorophyll auto-fluorescence channel (red). At 17°C, GFP fluorescence signal was brighter than at 22°C in cotyledons (Figure 3.12, panel A). A subcellular examination of GFP distribution in mesophyll cells revealed co-localisation of the NP::cp31A-GFP signal with DAPI fluorescence (circled) and chlorophyll auto-fluorescence (indicated by arrows) (Figure 3.13, panels A-E), showing a dual nuclear and chloroplast localisation. By contrast, NP::cp31A-GFP fluorescence was weaker in 27°C than at 22°C in cotyledons (Figure 3.12, panels E-F), and GFP fluorescence was only observed to co-localise with chlorophyll auto-fluorescence (Figure 3.13, panel M, L), and not to the nuclei stained with DAPI (panels K, N). As GFP fluorescence was very weak at 27°C, an enhanced image is shown in Supplementary Figure 3.2 to show that GFP does not overlap with DAPI fluorescence and only weak GFP-chloroplast signal was detected. All comparisons were conducted using same pinhole and gain confocal microscope settings.

3D representations of whole cells constructed using an integration of Z-stacks was constructed for the NP::cp31A-GF/nucleus co-localization at 17°C and 22°C merging single-plane

images. As shown in Supplementary Figure 3.3. Panel A (17°C) and panel B (22°C) the reconstructions show GFP fluorescence-cpRNP signal (green) overlapping with DAPI fluorescence (blue) (circled), and chlorophyll auto-fluorescence (red), pointing at a dual localization of the cpRNP-GFP construct .

Confocal examination of NP::cpSEBF-GFP. *In planta* confocal analysis revealed NP::cpSEBF-GFP fluorescence signal in seedling cotyledons was stronger at 17°C, intermediate at 22°C, and weakest at 27°C, indicating that temperature may affect cpSEBF abundance (Figure 3.14). A subcellular examination of GFP fluorescence revealed only a co-localisation with chloroplasts, as indicated through chlorophyll auto-fluorescence (red) (Figure 3.15), showing that cpSEBF may not localise to the nucleus in these conditions. However, while pinhole settings used in Figure 3.14 were the same for all temperature conditions, the fluorescence gain setting was set to 650 for plants examined at 22°C, and 690 for the 17°C and 27°C conditions. Despite the difference in settings, fluorescence intensity detected at 27°C is still lower.

A subcellular examination of NP::cpSEBF-GFP fluorescence in mesophylls cells at 22°C showed clear GFP co-localisation with chlorophyll auto-fluorescence (Figure 3.15 panels G, H), but no overlap was detected between GFP and the DAPI-stained nucleus in the merged images (panel F, I). Results observed at 17°C showed identical distributions (panel A, D). This pattern was also observed at 27°C (panels K-O), however at this temperature the GFP fluorescence signal (panel M) was very weakly detected and had to be enhanced in post-image processing to conclude an overlap of GFP with chlorophyll auto-fluorescence signal (red) but not with DAPI (blue) (Supplementary Figure 3.4).

A 3D reconstruction of whole cells integrating the Z-stacks was conducted to confirm the subcellular distribution of NP::cpSEBF-GFP (Supplementary Figure 3.5). This reconstruction clearly shows an overlap of the GFP fluorescence signal (green) and chlorophyll auto-fluorescence (red), but no overlap with the DAPI-stained nuclei (blue), indicating that NP::cpSEBF-GFP is only detected in the chloroplast during de-etiolation at 17°C (panel A), 22°C (panel B), and 27°C (panel C).

In summary, this confocal analysis indicated that cp31A protein accumulation as indicated through GFP fluorescence intensity is greatest in colder conditions and reduced in warm conditions and localises to the nucleus and chloroplast at 17°C and 22°C. Analysis of cpSEBF protein GFP fluorescence intensity indicated a similar increased intensity in cold conditions and reduced intensity in warm conditions but was only detected to localise to the chloroplast in all three temperature conditions.

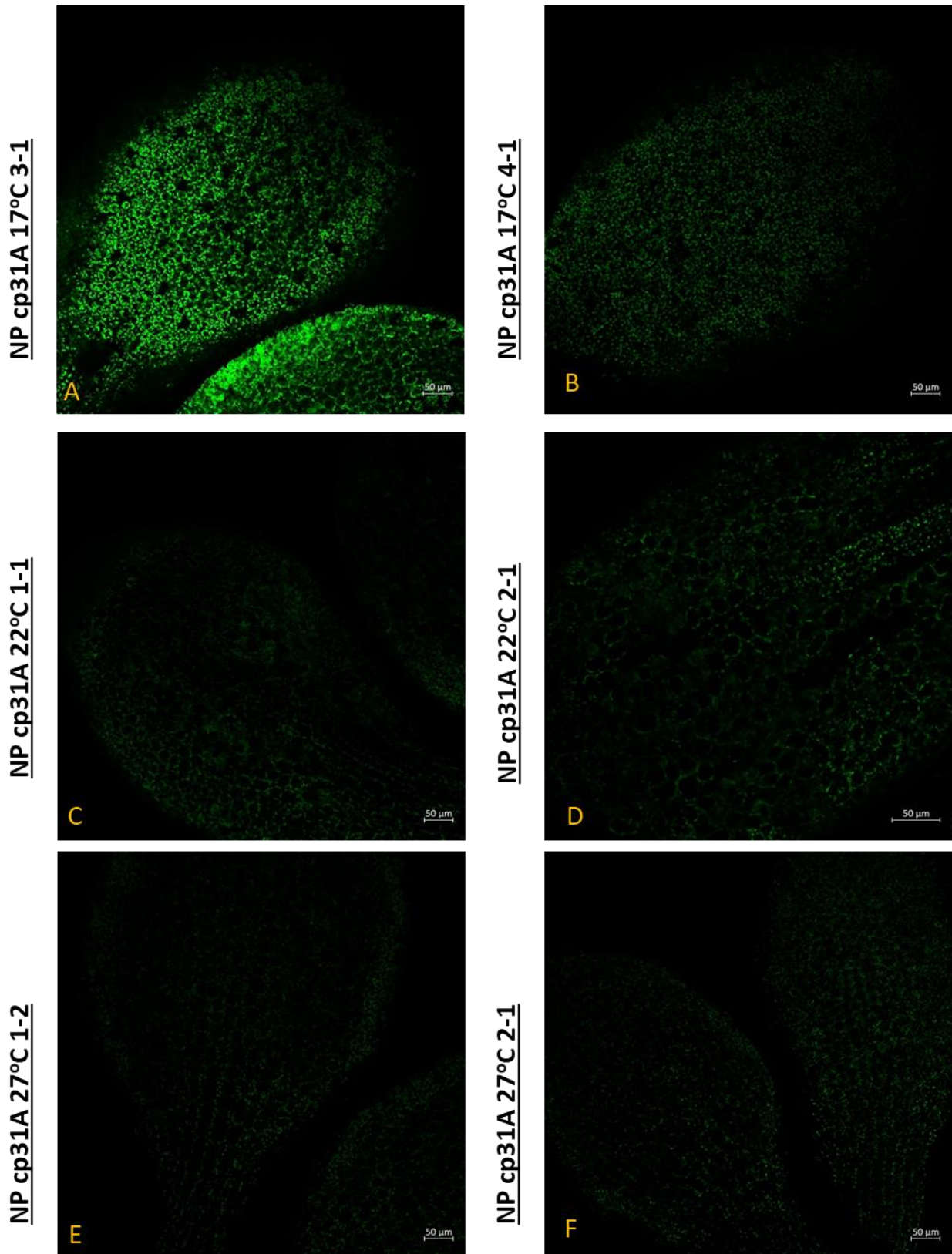
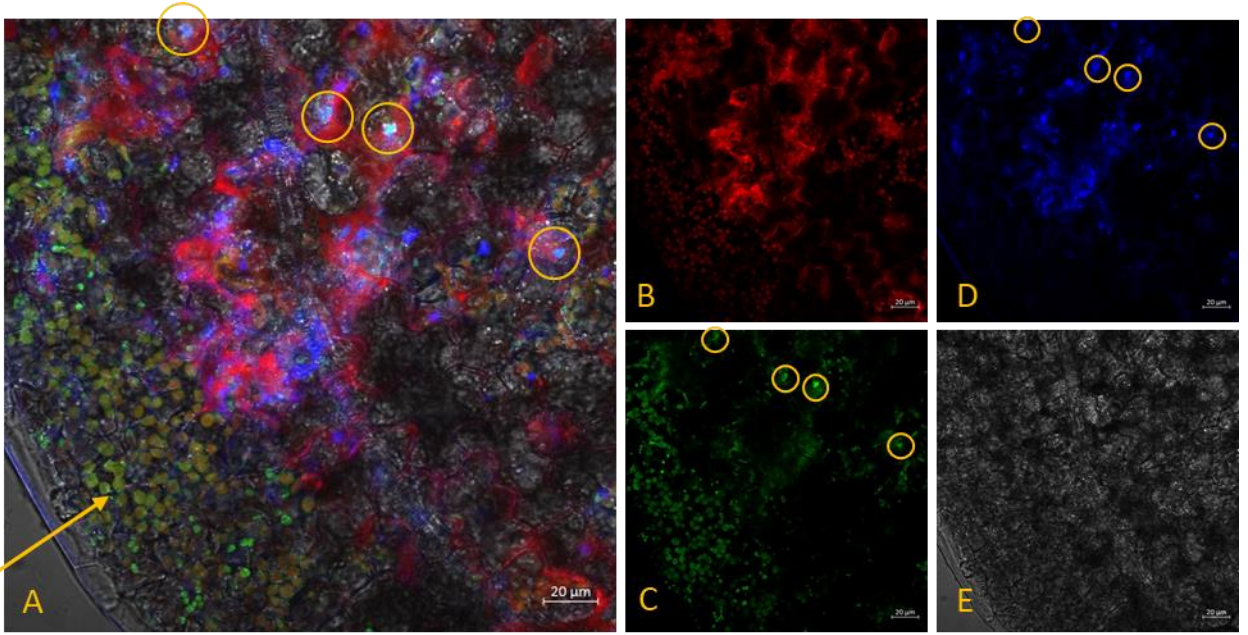
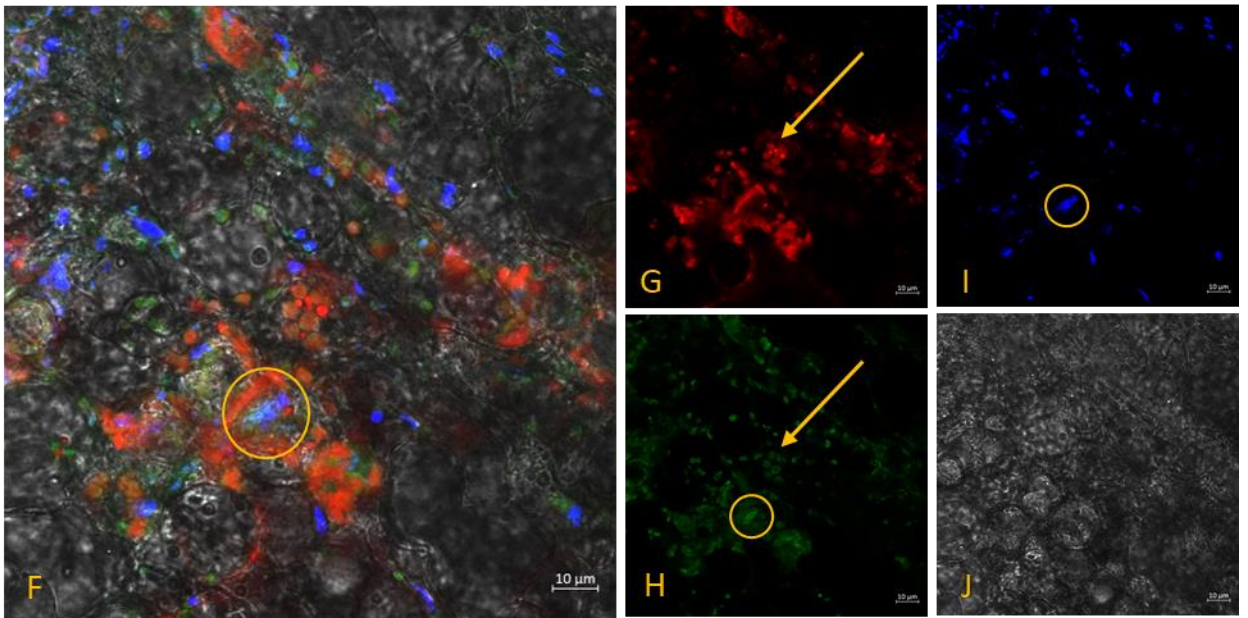


Figure 3.12. Confocal microscopy shows GFP fluorescence intensity in Native Promoter (NP)-expressed cp31A tagged with GFP (*cp31a_1*) appears highest in cold temperatures *in planta*. Images show GFP fluorescence of NP::cp31A-GFP (*cp31a_1*) plants grown for three days in darkness and treated with 24hrs red light ($80 \mu\text{mol m}^{-2}\text{s}^{-1}$) at A-B) 17°C, C-D) 22°C, or E-F) 27°C. All capture criteria were consistent between different conditions (pinhole= 0.73 AU; Gain= 657.8). Each set of images are from an independent plant.

NP cp31A 17°C 2-5



NP cp31A 22°C 1-4



NP cp31A 27°C 1-7

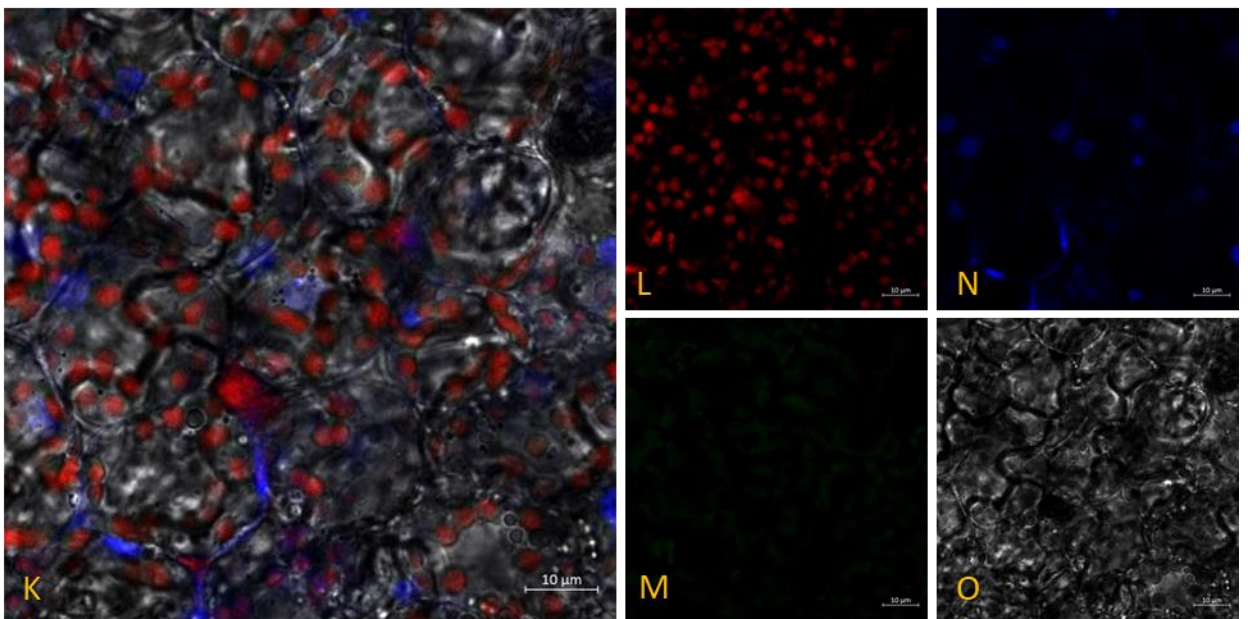


Figure 3.13. Confocal microscopy shows Native Promoter (NP)-expressed cp31A (*cp31a_1*) tagged with GFP localise to chloroplast and nucleus *in planta* at 17°C and 22°C. NP::cp31A-GFP (*cp31a_1*) plants were grown for three days in darkness and treated with 24hrs red light ($80 \mu\text{mol m}^{-2}\text{s}^{-1}$) at 17°C, 22°C, or 27°C. Images show: A, F, K) Overlap of all images; B, G, L) chloroplasts are identified by chlorophyll auto-fluorescence (red); C, H, M) NP::cp31A (*cp31a_1*) expressing GFP (green); D, I, N) nuclei stained with 4',6-diamidino-2-phenylindole (DAPI) (blue); E, J, O) brightfield image of the plant. Scale bars are present in the lower right-hand corner of each photo. Each set of images are from an independent plant. Overlap of GFP and DAPI is indicated by a circle; overlap of GFP and chlorophyll auto-fluorescence is indicated by an arrow.

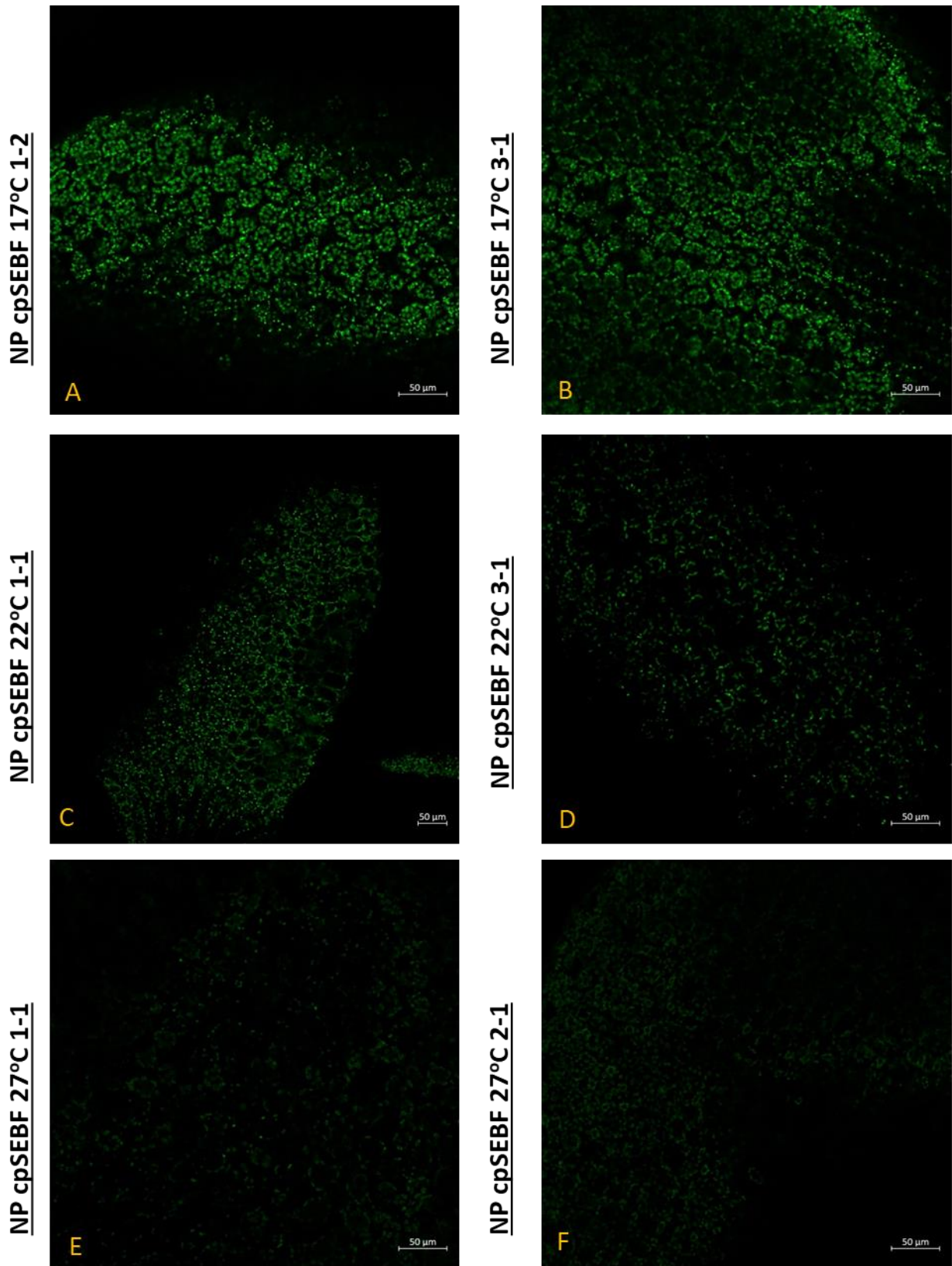
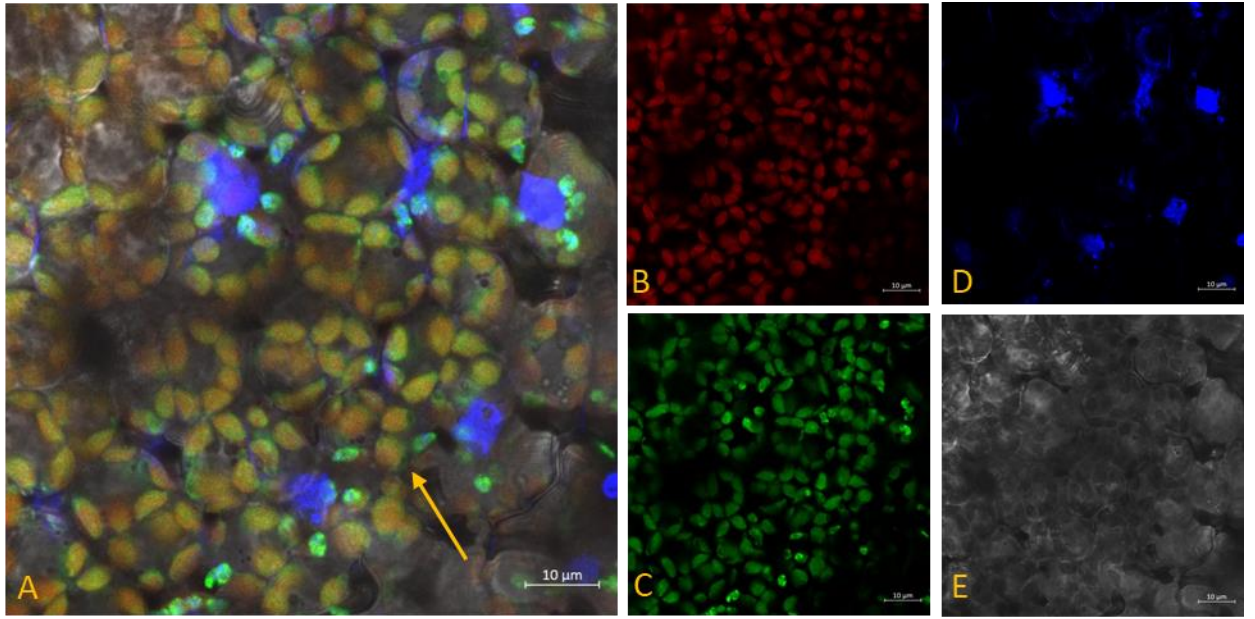
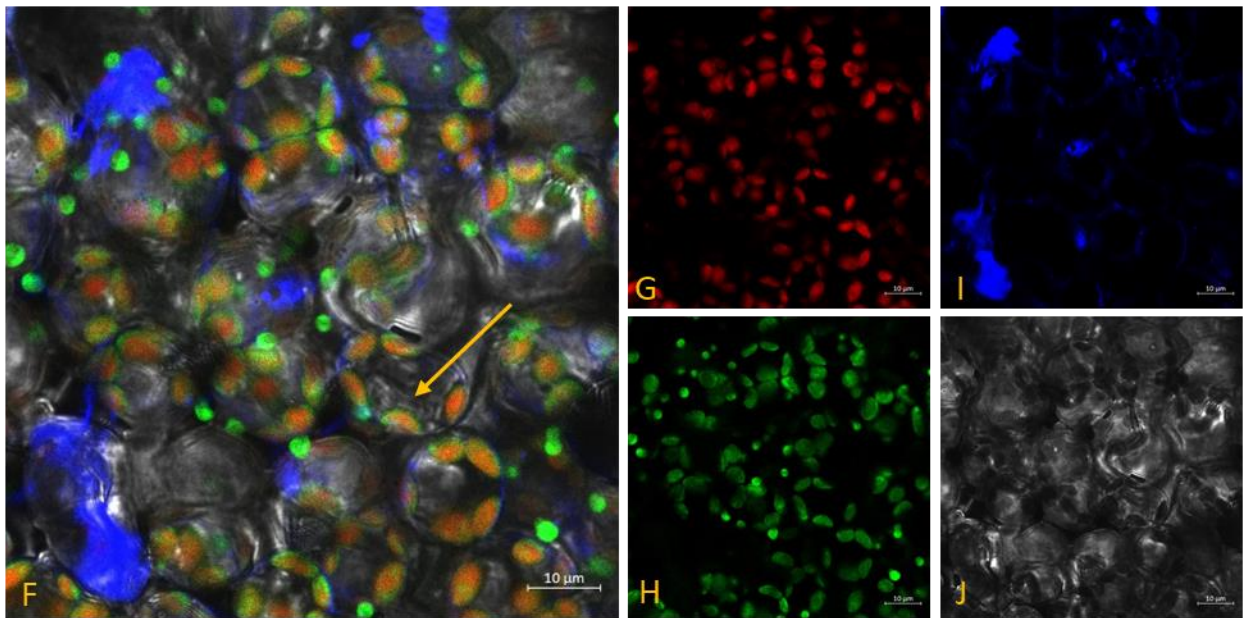


Figure 3.14. Confocal microscopy shows GFP fluorescence intensity in Native Promoter (NP)-expressed cpSEBF tagged with GFP (*cpsebf_1*) appears highest in cold temperatures *in planta*. Images show GFP fluorescence of NP::cpSEBF-GFP (*cpsebf_1*) plants grown for three days in darkness and treated with 24hrs red light ($80 \mu\text{mol m}^{-2}\text{s}^{-1}$) at A-B) 17°C, C-D) 22°C, or E-F) 27°C. All capture criteria were consistent between 17°C and 27°C conditions (pinhole= 0.73 AU; Gain= 690) but Gain was lower for images collected at 22°C (Gain=650). Each set of images are from an independent plant.

NP cpSEBF 17°C 2-2



NP cpSEBF 22°C 3-3



NP cp31A 27°C 3-5

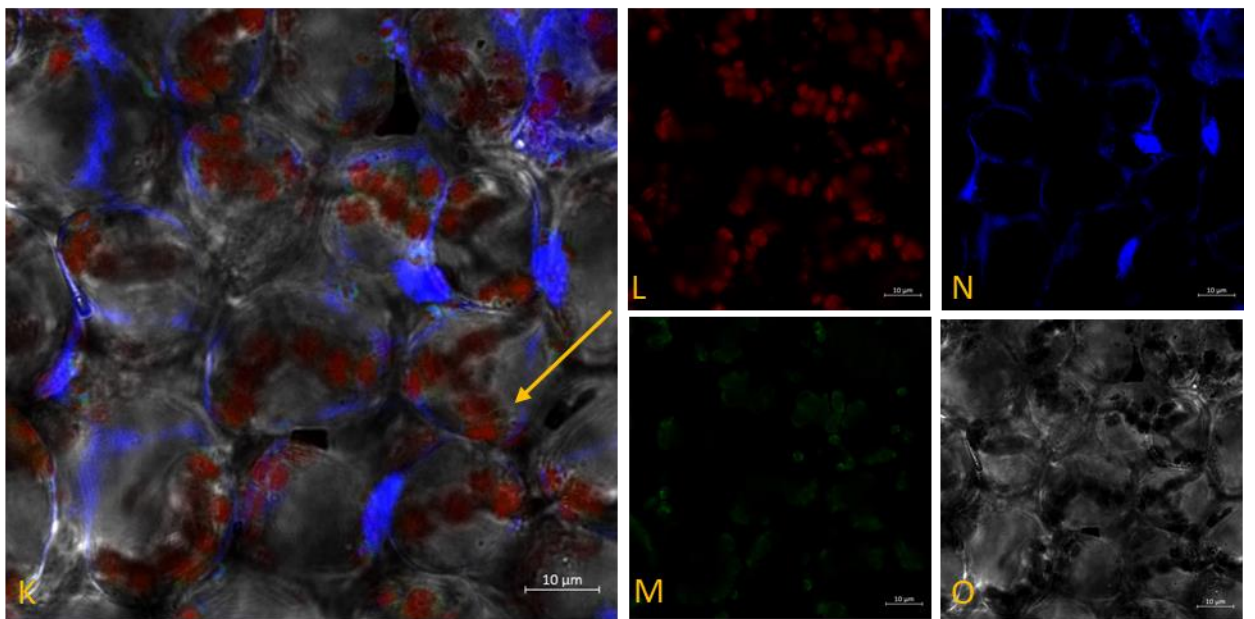


Figure 3.15. Confocal microscopy shows Native Promoter (NP)-expressed cpSEBF (*cpsebf_1*) tagged with GFP localises to chloroplast *in planta* in all temperature conditions. NP::cpSEBF-GFP (*cpsebf_1*) plants were grown for three days in darkness and treated with 24hrs red light ($80 \mu\text{mol m}^{-2}\text{s}^{-1}$) at 17°C, 22°C, or 27°C. Images show: A, F, K) Overlap of all images; B, G, L) chloroplasts are identified by chlorophyll auto-fluorescence (red); C, H, M) NP::cpSEBF (*cpsebf_1*) expressing GFP (green); D, I, N) nuclei stained with 4',6-diamidino-2-phenylindole (DAPI) (blue); E, J, O) brightfield image of the plant. Scale bars are present in the lower right-hand corner of each photo. Each set of images are from an independent plant. Overlap of GFP and chlorophyll auto-fluorescence is indicated by an arrow.

3.5.2. cpRNPs integrate light and temperature signals to modulate nuclear gene expression

Evidence in Figures 3.5 and 3.11 show that *cprnp* mutation reduces nuclear transcript accumulation at 22°C, and that alternatively transcribed forms of cpRNPs can localise to the nucleus, as indicated by subcellular localisation of cpRNPs TSS isoforms fused to GFP. Next, it was investigated whether light- and temperature-integrated signals also affected nuclear-encoded transcript accumulation in *cprnp* mutants, as cpRNPs do for plastid encoded transcripts. The impact of *phyB* and *cprnp* mutation in plants grown for 3 days in darkness and treated with 24hr of red light (80 $\mu\text{mol m}^{-2}\text{s}^{-1}$) at both 17°C and 27°C was evaluated to complement the results obtained at 22°C (Figure 3.11). *phyB* was included to corroborate the R-phys dependence response of the target gene transcript accumulation and compare it to transcript accumulation in *cprnps*.

Effect of temperature on cpRNP-dependence nuclear transcripts associate to Photosystem II-functions. As shown in Figure 3.16, regulation of LHCII-genes *LHC2.3* and *LHCB4.2* was phyB- and temperature-dependent. *phyB* mutation did not affect accumulation in the cold, but was critical to abundance at 22°C and 27°C. The analyses also showed that *LHCB4.2* accumulation is temperature-dependent but a contribution of cpRNPs was only observed at 22°C. While transcript accumulation of *LHCB2.3* and *LHCB4.2* showed significant reductions in *phyB* and *cprnp* mutants at 22°C compared to WT, no reductions were detected at 17°C. At 27°C, reductions were only observed in *phyB* mutant, and not in any of the tested *cprnp* mutants. A Two-Way ANOVA analysis reported significant interaction of temperature and genotype on *LHCB2.3* transcript abundance ($P < 0.001$), and a Tukey HSD post-hoc test reported that this affected the relationship between WT and *phyB* on transcript accumulation. For *LHCB4.2*, an interaction effect was also reported ($P < 0.01$), and post hoc testing identified this affected the relationship between WT and *phyB* ($P < 0.001$), *cp29b* ($P < 0.05$), and for *cpsebf* and *cp31a* ($P < 0.001$).

Transcript accumulation of *PSBO1* and *PSBO2* was observed to be temperature-dependent in *phyB* and *cprnp* mutants- for *PSBO1*, this regulation only occurred at 22°C for cpRNPs but was phyB-dependent at 22°C and 27°C. For *PSBO2*, cpRNP modulation occurred in 17°C and 22°C, and phyB-dependence was more pronounced in cold and warm conditions. In contrast, *PSBQ2* accumulation was only temperature-dependent for cpSEBF at 22°C, and for cp31A at 17°C and 22°C, with phyB-dependence showing a marked temperature sensitivity at 27°C. At 22°C, previous analysis showed that three OEC genes *PSBO1*, *PSBO2*, and *PSBQ2* were phyB- and cpRNP-dependent. At 17°C, no reductions were observed in mutant genotypes for *PSBO1*, but all genotypes showed reductions for *PSBO2*. *PSBQ2* only showed reductions in *cp31a* mutant. At 27°C, reductions for all three genes'

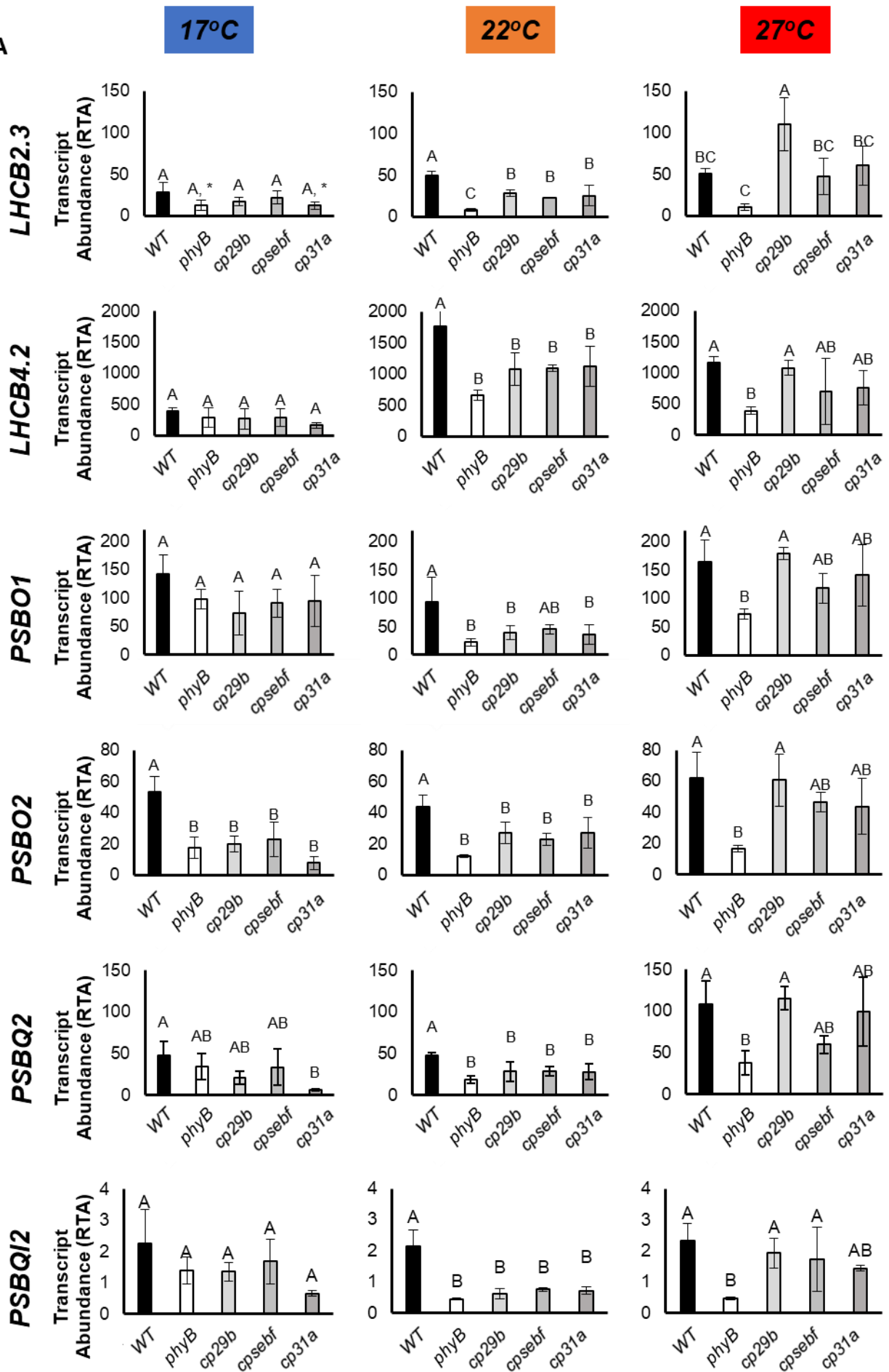
transcript accumulation were only observed in *phyB* mutant. A Two-Way ANOVA analysis revealed significant interaction effects of temperature and genotype for *PSBO1* ($P < 0.05$), *PSBO2* ($P < 0.01$), and *PSBQ2* ($P < 0.001$). Tukey HSD post hoc testing reported that this affected the relationship between WT and *phyB* ($P < 0.001$) and WT and each *cprnp* mutant ($P < 0.05$) for *PSBO1*; between WT and *phyB* ($P < 0.001$) and WT and each *cprnp* mutant ($P < 0.01$) for *PSBO2*; and between WT and *phyB* ($P < 0.001$) and WT to *cpsebf* ($P < 0.001$) and *cp31a* ($P < 0.05$) for *PSBQ2*.

Overall, this demonstrated temperature-dependent regulation of PSII gene-encoding subunits by *phyB* for *LHCB2.3*, *LHCB4.2*, *PSBO1*, *PSBO2* and *PSBQ2* at 22°C and 27°C. Regulation by tested cpRNPs was reported to be temperature-dependent at 22°C for *LHCB4.2* and *PSBO1*, and at both 17°C and 22°C *PSBO2*. A more complex regulation was observed by cpSEBF and cp31A in *PSBQ2*, occurring at 22°C and 17°C respectively.

Effect of temperature- and cpRNP- dependence on nuclear-encoded NADH Dehydrogenase-associated gene transcript accumulation. Analysis of the NADH Dehydrogenase subunit-encoding gene *PSBQ12* revealed its regulation was temperature-dependent by *phyB* at 22°C and 27°C, and that abundance was temperature- and cpRNP-dependent at 22°C. At 22°C, *PSBQ12* transcript accumulation was observed to be reduced in *phyB* and *cprnps*. However, at 17°C and 27°C, no significant reductions were observed in *cprnp* mutants. At 27°C, *PSBQ12* accumulation was also observed to be reduced in *phyB*. A Two Way ANOVA analysis reported a significant interaction effect of temperature and genotype in transcript accumulation ($P < 0.05$), and Tukey HSD post hoc testing reported this affected this relationship between WT and *phyB* ($P < 0.001$) and between WT and all *cprnp* mutants respectively ($P < 0.001$), revealing that *phyB*- and cpRNP-dependence was temperature dependent.

Effect of temperature- and cpRNP- dependence on nuclear-encoded Photosystem I-associated gene transcript accumulation. Analysis of the Light Harvesting Complex I subunit-encoding gene *LHCA2.1* could only be conducted at 17°C (Figure 3.16, panel B). This revealed its accumulation was cp31A-dependent at 17°C, but was unaffected by mutation of *phyB*, *cp29b*, or *cpsebf* in either temperature condition. This interaction effect of temperature and genotype was reported by Two-Way ANOVA analysis ($P < 0.05$) and Tukey HSD post hoc testing reported it significantly affecting the relationship between WT and *cp31a* on transcript abundance ($P < 0.01$).

A



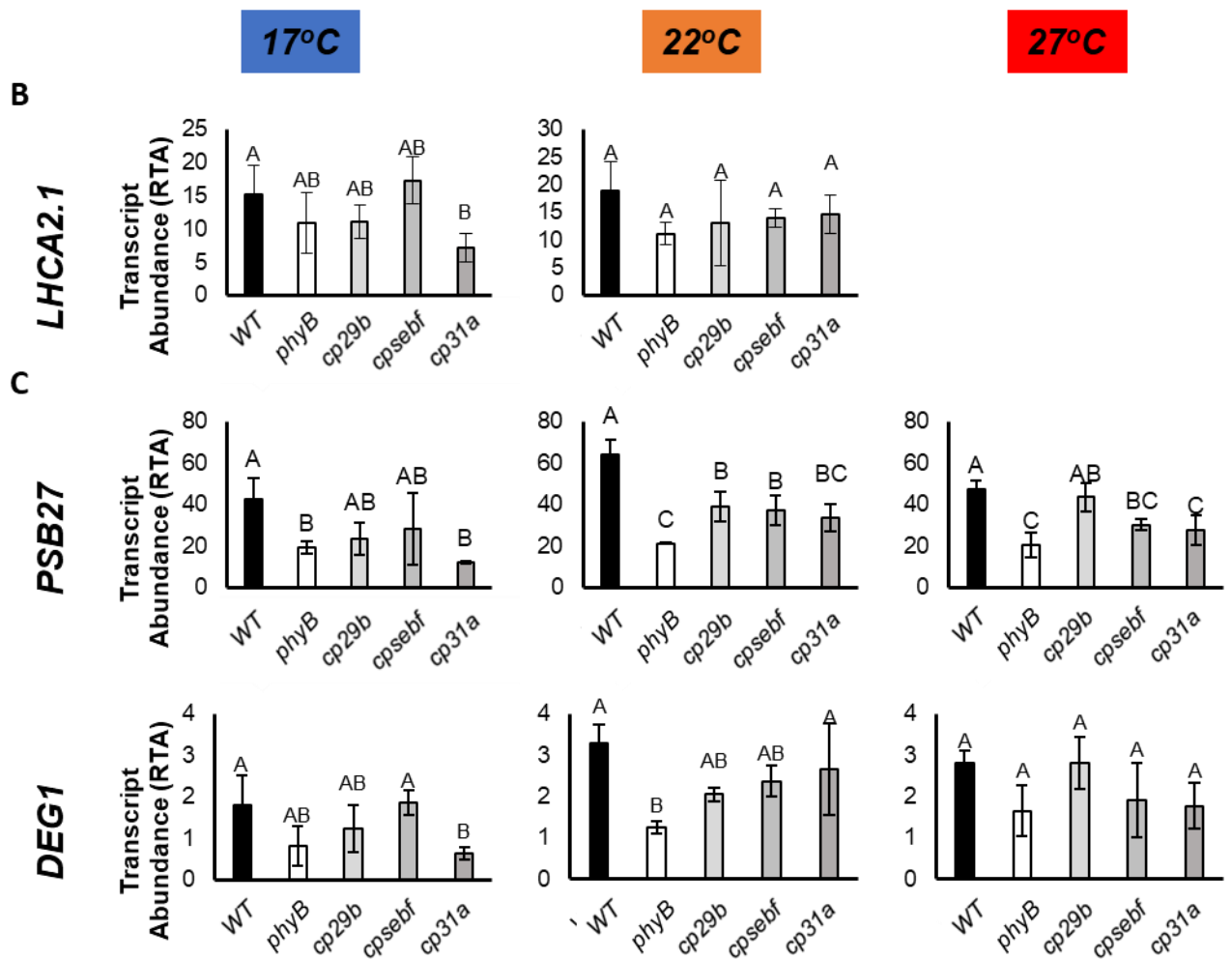


Figure 3.16. *cprnp* mutation affects temperature-dependent regulation of key nuclear-encoded subunits. Graphs show relative transcript abundance (RTA) of A) Photosystem II-associated genes; B) Photosystem I-associated genes; and C) Photoprotection-association genes in WT, *phyB*, *hy5*, *cp29b_2*, *cpsebf_1*, and *cp31a_2* plants grown for three days in darkness and treated with 24hrs red light ($80 \mu\text{mol m}^{-2}\text{s}^{-1}$) at 22°C . Relative transcript abundance was calculated by comparing experimental gene expression to the reference gene *PP2A*. Data represent the average of three biological replicates and error bars show 95% confidence intervals. Statistical significance of expression between WT (black bars), *phyB* (white bars), and *cprnp* mutants *cp29b_2*, *cpsebf_1*, *cp31a_2* (shown over a light-to-dark gradient grey bars) was calculated using One-way ANOVA with Tukey post hoc testing ($p < 0.05$). Data that do not share a letter are statistically significant.

Effect of temperature on photoprotection and photorepair-associated nuclear gene transcript accumulation and contribution of cpRNPs to the response. Analysis of the three photoprotection and photorepair genes is shown in Figure 3.16 panel C. Evaluation of *PSB27*, a gene involved in adapting to changes in light intensity, revealed a temperature-sensitive cpRNP-dependence. This revealed a cp29B-dependence that only occurred at 22°C , and at 22°C and 27°C for cpSEBF. *PSB27* was cp31A-dependent in all three temperature conditions, but dependence was double at 17°C

compared to at 22°C or 27°C. The interaction of temperature and genotype on transcript accumulation for *PSB27* was reported by Two Way ANOVA ($P < 0.05$), and Tukey HSD post hoc testing identified it affected the relationship between WT and *phyB* ($P < 0.001$), and between WT and each tested *cpnrp* mutant ($P < 0.001$).

The final examined gene *DEG1* encodes a gene from the Degradation of Periplasmic proteins (DEG) Serine Protease family involved in turnover of damaged D1 protein, and was observed to be cp31A-dependent at 17°C. Previous examination of *DEG1* accumulation at 22°C showed no cpRNP-dependence, but examination at 17°C identified a reduction in *cp31a*. No reductions were observed in *phyB* or *cpnrp* mutants at 27°C. A Two-Way ANOVA analysis reported a significant interaction effect of temperature and genotype on *DEG1* accumulation ($P < 0.5$), and Tukey HSD post hoc testing reported this affected the relationship between WT and *phyB* ($P < 0.001$) and WT and *cp31a* ($P < 0.01$) on transcript abundance.

Overall, it was therefore observed that cpRNP regulation of Photosystem II subunit-encoding genes was temperature-dependent (Figure 3.16 panel A). This affected transcripts for genes encoding Light Harvesting Complex II (LHCII) subunits *LHCB4.2*, OEC-encoding subunit *PSBO1*, and NADH Dehydrogenase subunit *PSBQI2* at only 22°C. Temperature-dependent regulation by cpRNPs was observed for *PSBO2* at 17°C and 22°C. cpSEBF and cp31A were reported to contribute to temperature-dependent regulation of the OEC transcript *PSBQ2* at 22°C and 17°C respectively in *PSBQ2*. However, cp31A-specific temperature dependence was observed for the LHCI complex-subunit encoding *LHCA2.1* at 17°C (panel B). In the case of photoprotection and photorepair related genes (panel C), a temperature- and cpRNP-dependent accumulation response for *PSB27* unique to each cpRNP was observed. cp29B was involved in the transcript accumulation response only at 22°C; cpSEBF at 22°C and 27°C, and cp31A contributed to all temperatures, but with a strongest effect at 17°C. In addition, cp31A also contributed to the cold-dependent regulation of *DEG1* at 17°C.

In summary, cpRNP modulation of nuclear-encoded transcripts was therefore observed to be temperature-sensitive during R-light mediated de-etiolation. Although exceptions were observed, for cp29B and cpSEBF this modulation mostly occurred only at 22°C and was often insensitive to cold or warm conditions. However, a notable role for cp31A was observed in the cold-dependent regulation of multiple transcripts. This analysis also highlighted the temperature-sensitive role of *phyB* in contributing to Photosystem II-associated transcript abundance in warm conditions.

3.6. Results: Investigating whether a retrograde signalling pathway regulates cpRNP transcript accumulation and localisation.

The operation and biosynthesis of photosynthetic apparatus requires constant communication between the chloroplast and the nucleus (Jarvis and López-Juez, 2013). This communication co-ordinates the expression and import of photosynthetic subunits and proteins from the anterograde nucleus-to-chloroplast signalling required for regulation of the chloroplast. The communication of signals from the chloroplast to the nucleus is retrograde signalling, and is a means for the plastid to regulate nuclear-encoded gene expression in response to developmental cues and stresses (Singh et al., 2015; Chan et al., 2016).

The retrograde signalling pathways can involve a wide range of signals, encompassing tetrapyrrole signalling, phosphoadenosines, carotenoid oxidation products, isoprenoid precursors, carbohydrate metabolites, and chloroplastic or nuclear proteins (Strand et al., 2003; Koussevitzky et al., 2007; Lee et al., 2007; Estavillo et al., 2011; Šimková et al., 2012; Xiao et al., 2012; Ramel et al., 2012; Woodson et al., 2013; Shumbe et al., 2014; Häusler et al., 2014; Vogel et al., 2014). Retrograde signalling is a highly complex regulatory system and its elucidation is still ongoing; the pathways are further reviewed in Chan et al (2016).

One of the retrograde signalling pathways is biogenic signalling, during which photosystem assembly and maintenance and other processes for a fully functioning chloroplast are regulated (Pogson et al., 2008). This kind of signalling occurs from plastid biogenesis during de-etiolation when chloroplasts develop from proplastids or etioplasts, and thylakoids and photosynthetic subunits are rapidly biosynthesised within hours (Jarvis and López-Juez, 2013). Biogenic signalling is known to involve tetrapyrrole signalling (Strand et al., 2003; Woodson et al., 2011), the GUN1-PTM-ABI4 pathway (Koussevitzky et al., 2007; Sun et al., 2011), PRIN2-PEP pathway (Kindgren et al., 2012), and the GLK family (Kakizaki et al., 2009; Waters et al., 2009). A second paradigm for retrograde signal is operational signalling, in which mature chloroplasts respond to a stimulus- often a stress response- and leads to an adjustment of chloroplast homeostasis (Chan et al., 2016). The operational pathway regulates PSII overexcitation via B-cyclocitral (Ramel et al., 2012), and the EX pathway (Lepistö et al., 2012). The experiments described in section 3.4.2, examining alterations of photosynthesis-associated nuclear gene transcript accumulation in *cpRNP* mutants, were conducted in de-etiolation- a stage where biogenic retrograde signalling pathways are active.

Activation of retrograde signalling by chemical agents that inhibit chloroplast development include the use of the herbicide Norflurazon that inhibits carotenoid biosynthesis and induces bleaching, and Lincomycin that inhibits plastid translation and leads to bleaching and repression of

Photosynthesis Associated Nuclear Genes (PhANGs), especially for the Photosystem II-associated Light Harvesting Complex II (LHCB) genes (Ruckle et al., 2012; Martín et al., 2016). Use of these chemicals has previously identified *gun* phenotypes related to the genome uncoupled status, linked to the high expression of various PhANGs in plants with inhibited chloroplast biogenesis (Susek et al., 1993; Larkin, 2014). In section 3.4.2, it was demonstrated that *cpRNP* mutation reduced the accumulation of PhANG transcripts, indicating a role for cpRNPs in PhANG expression. In this section, bioinformatic and experiment evidence is provided to show that *cpRNP* transcript accumulation is repressed by Lincomycin and Norflurazon treatments, and that Lincomycin alters the subcellular distribution of native promoter-expressed cp31A-GFP. Therefore, cpRNPs may be involved in the regulation of PhANGs via retrograde signalling pathway.

3.6.1. Analysis of published Retrograde Signalling datasets and experimental validation.

Results described section 3.4.2 showed an effect of *cpRNP* mutation on nuclear-encoded Photosynthesis associated nuclear genes' (PhANGs) transcript accumulation, including *LHCB2.3*, *LHCB4.2*, *PSBO1*, *PSBO2*, *PSBQ2*, *PSBQI2*, and *PSAN* genes. PhANGs are commonly affected in the biogenic retrograde signalling pathway during de-etiolation, and a recent meta-analysis recently published genome-wide expression studies revealed *LHCB2.3*, *LHCB4.2*, and *PSBQ2* are common targets of the biogenic signalling pathway (Grübler et al., 2021). Using retrograde signal activators Lincomycin and Norflurazon, three publicly available microarrays were examined to evaluate whether cpRNPs' expression is affected by the retrograde signalling pathway. One dataset was generated using Lincomycin as a retrograde signal activator, and two using Norflurazon. The analysis revealed a strong down-regulation of *cpRNP* transcripts in response to both retrograde signal activator treatments. These results were then experimentally verified using RT-qPCR analysis.

Analysis of Lincomycin Datasets. The publicly available dataset GSE24517 (Ruckle et al., 2012) was used to evaluate the effects of Lincomycin (Linc) on *cpRNP* transcript accumulation. Results were analysed for fold-difference in expression, and genes were adjusted using the Benjamini-Hochberg False Discovery Rate (FDR) at the significance level of 0.05.

Shown in Figure 3.17, dataset GSE24517 examined WT plants grown with (Linc+) or without (Linc-) Lincomycin in low light ($0.5 \mu\text{mol m}^{-2} \text{s}^{-1}$ blue plus red (BR) light) for 6 days. After 6 days, plants were transferred to $60 \mu\text{mol m}^{-2} \text{s}^{-1}$ blue plus red (BR) light for 4hr and 24hr. This array showed significant down-regulation of *cpSEBF* and *cp31A* at 0hr in the Linc+ treated plants, and of

cp29C at 4hr. A significant down-regulation of *cp29B* was also observed at 24hr, and although the difference was not statistically significant as reported by FDR analysis, a down-regulation trend was observed for *cp29C*, *cpSEBF*, *cp31A*, and *cp29A* was in Linc+ plants.

Analysis of Norflurazon Datasets. To evaluate the effect of Norflurazon (NF) treatment on *cpRNP* expression, the public datasets GSE110125 (Zhao et al., 2019) and GSE12887 (Koussevitzky et al., 2007) were used (Figure 3.18).

Dataset GSE110125 examined 5-day old WT seedlings grown in 24hr light ($100 \mu\text{mol m}^{-2}\text{s}^{-1}$) at 22°C with or without a treatment of 5 μM Norflurazon. Differentially expressed genes in WT after NF treatment were published in Zhao et al (2019), having been identified with a Log₂-converted fold change ≥ 1 or ≤ -1 by FDR (False Discovery Rate) ≤ 0.05 and representing a two-fold difference. This identified that *cp29B*, *cp29C*, and *cp31A* transcripts are accumulated to higher levels in WT (NF-) compared to WT (NF+) (Figure 3.18 panel A).

Dataset GSE12887 examined plants grown in 21°C under continuous light ($100\mu\text{mol m}^{-2}\text{s}^{-1}$) in the presence of 5 μM Norflurazon. This dataset corroborated the trend observed for *cp29B*, *cp29C*, and *cp31A* and added a similar response for *SEBF*. These *cpRNPs* transcripts accumulated to higher levels in untreated WT (NF-) compared to WT (NF+) at a $1 > \text{Log}_2$ fold change, indicating that these *cpRNPs transcripts* were down-regulated when exposed to the retrograde-signal activator (Figure 3.18, panel B).

Experimental verification of cpRNPs transcript accumulation in response to Lincomycin and Norflurazon. Transcript levels of *cpRNPs cp29B*, *cpSEBF*, *cp29C* and *cp31A* were evaluated after exposure to 0.5mM Lincomycin and 5 μM Norflurazon in plants grown for 6 days under low white light ($10\mu\text{mol m}^{-2}\text{s}^{-1}$). These conditions were selected for their effectiveness in identifying crosstalk between photoreceptors and RS pathways (Martín et al., 2016).

Experimental results are shown in Figure 3.19. *CARBONIC ANHYDRASE (CA)* and *LIGHT HARVESTING COMPLEX B 2.3 (LHCB2.3)* were selected as two positive control genes responsive to the retrograde signal activator treatments. Transcript accumulation for these genes corroborated that both Lincomycin and Norflurazon treatments produced a statistically significant decrease in transcript abundance compared to untreated controls.

Transcript abundances of *cp29B*, *cpSEBF*, *cp31A*, and *cp29C* were significantly reduced in the Lincomycin treatment. However, only *cp29B* showed a significant reduction in the Norflurazon

treatment, and no significant reductions were detected for *cpSEBF*, *cp31A*, or *cp29C*. The experimental data broadly correlate with the genomic datasets analysis for Lincomycin results, showing the tested cpRNPs are subject to regulation by retrograde signals activated by the Lincomycin-induced biogenic signalling pathway. However, it is possible that the responsiveness to Norflurazon-activated signals may be specific for some members of the family.

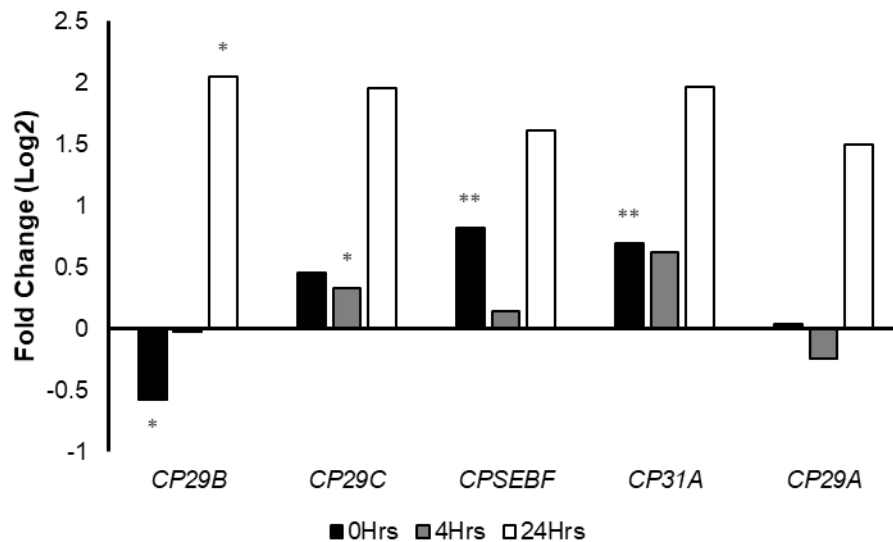


Figure 3.17. *cpRNP* expression in WT is repressed by Lincomycin treatment after 24hrs of light (WT (L-)/WT (L+)). Gene expression data was obtained and reproduced from dataset GSE24517 using WT plants grown with (L+) or without (L-) Lincomycin (200µg/mL), grown in low light (0.5 µmol m⁻² s⁻¹ blue plus red (BR) light) for 6 days. After 6 days, plants were transferred to 60 µmol m⁻² s⁻¹ blue plus red (BR) light. Plants were harvested immediately before the light treatment, and then at 4hrs and 24hrs. Data are expressed as a log₂-fold difference between WT (L-) divided by WT (L+) and significance was determined using a Benjamini & Hochberg False Discovery rate correction at significance level of p<0.05.

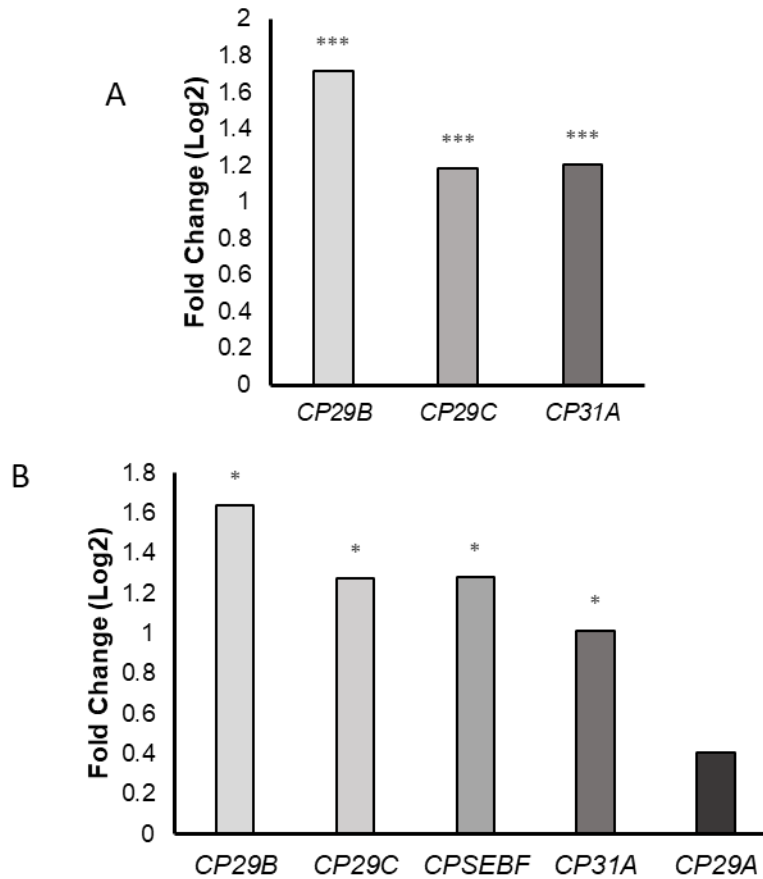


Figure 3.18. *cpRNP* expression is repressed by Norflurazon treatment. Gene expression data was obtained and reproduced from A) Zhao et al (2020) (dataset GSE110125) examined 5-day old seedlings with Col6-3 (wild type) plants grown under 24h light condition with $100 \mu\text{mol m}^{-2}\text{s}^{-1}$ at 22°C with or without a treatment of $5 \mu\text{M}$ Norflurazon; C) dataset GSE12887 examined WT plants grown in 21°C under continuous light ($100 \mu\text{mol m}^{-2}\text{s}^{-1}$) in the presence of $5 \mu\text{M}$ Norflurazon. Data are expressed as a log₂-fold difference and significance was determined using a Benjamini & Hochberg False Discovery rate correction at significance level of $p < 0.05$.

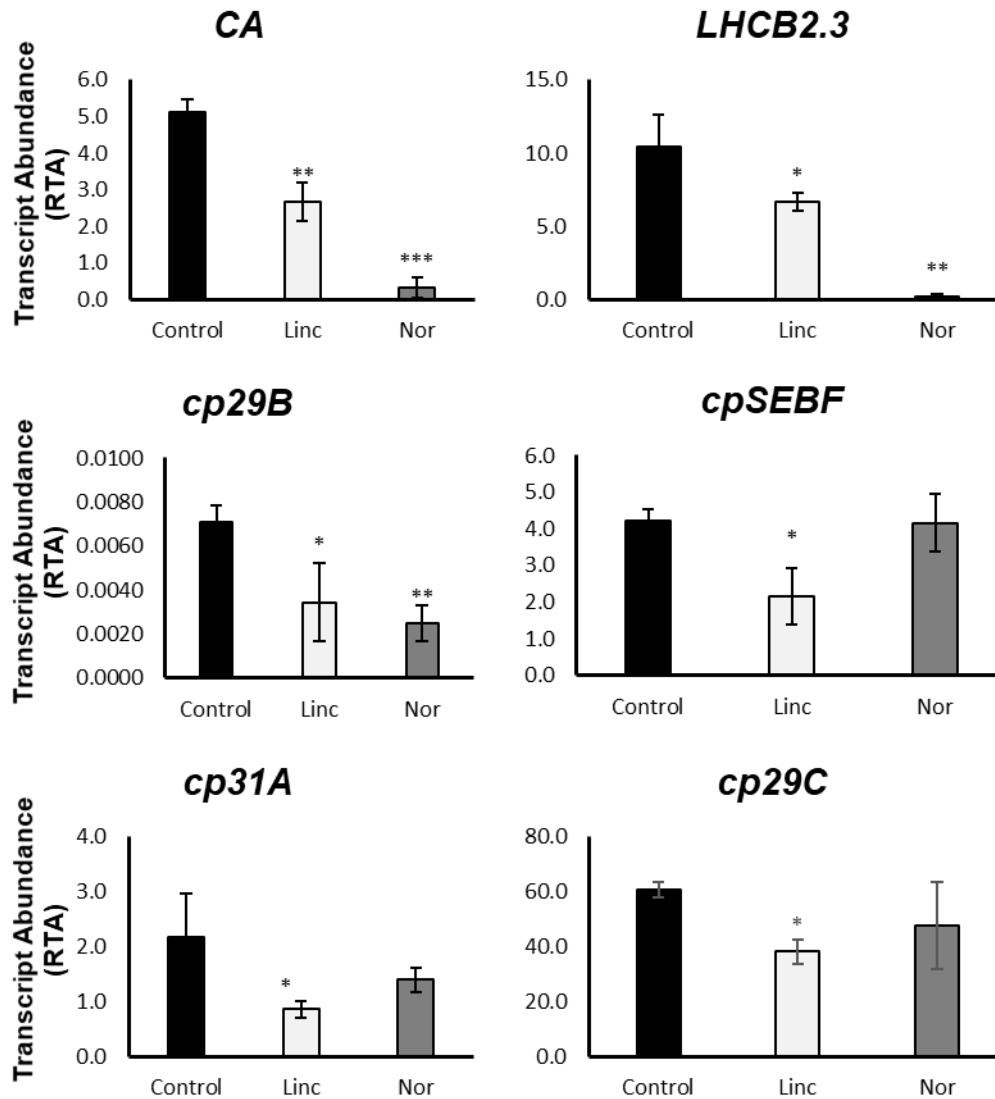


Figure 3.19. All *cpRNPs* and marker gene expression is repressed in lincomycin-treated WT (Linc+), and *cp29B* expression is repressed in norflurazon-treated WT (Nor+). Graph shows relative transcript abundance of *cpRNP* and marker gene expression in WT grown for 6 days in white light ($10 \mu\text{mol m}^{-2}\text{s}^{-1}$) on untreated, lincomycin (0.5mM), or Norflurazon (5 μM) treated media. Relative transcript abundance was calculated by comparing experimental gene expression to the reference gene *PP2A*. Data represent the average of three biological replicates and error bars show the 95% confidence interval. Statistical significance of expression between untreated WT (black bars), Linc+ (pale grey bars), or Nor+ (dark grey bars) WT was calculated using Students *t*-Test ($P < 0.05 = *$, $P < 0.01 = **$, $P < 0.001 = ***$)

3.6.2. Retrograde Signal Activator treatments alter the subcellular localisation of cp31A, but not cpSEBF.

Retrograde signals can alter protein behaviour and subcellular localisation and distribution (Ren et al., 2017). Evidence suggests that cpRNP transcript accumulation is changed when treated with retrograde signal activators (Figure 3.18), and a nuclear localisation has been observed for alternatively transcribed forms of cp31A and cpSEBF (section 3.3.3), indicating the possibility that these cpRNPs' subcellular localisations may be affected by retrograde signals.

To investigate whether retrograde signalling affected cpRNP localisation and distribution in addition to transcript accumulation, transgenic lines cp31A (NP::cp31A-GFP (*cp31a_1*)) and cpSEBF (NP::cpSEBF-GFP (*cpsebf_1*)) using *cpRNP* native promoters and GFP fusions were examined (see Materials and Methods). Seedlings were germinated and grown on control media or media containing 0.5mM Lincomycin. These plants were grown at 22°C for 3 days in darkness and treated with 24hr R-80 to induce de-etiolation, before being treated with DAPI staining and mounted for examination with a confocal microscope.

Comparison of NP::cp31A-GFP treated with and without Lincomycin by confocal examination. *In planta* confocal analysis showed that, without Lincomycin, NP::cp31A-GFP transgenic seedlings showed clear GFP fluorescence in cotyledons (Figure 3.20 panel C). Observations of GFP in mesophyll cells showed a co-localisation of NP::cp31A-GFP with chlorophyll auto-fluorescence (Figure 3.20, panels F, G, H), and a possible co-localisation with DAPI-stained nuclei (blue) (panel I) (red circle). The pattern of expression correlates with the one observed in similar experiments described in section 3.4.2.

When treated with Lincomycin NP::cp31A-GFP fluorescence was observed in the cotyledons (Figure 3.21, panel C). No chlorophyll auto-fluorescence could be detected in Lincomycin-treated plants (panel B, G), consistent with the chloroplast biogenesis arrest by Lincomycin and seedlings did not accumulate chlorophyll, remaining white. In a closer examination of mesophyll cells, GFP was observed to co-localise to multiple few DAPI-stained nuclei (blue) (panels F, I, H) (circled).

3D representations of whole cells were constructed using an integration of Z-stacks for NP::cp31A-GFP fluorescence in seedlings treated with (Supplementary Figure 3.6 panel B) or without Lincomycin (Supplementary Figure 3.6, panel A). These images were enhanced in post-processing. In the 3D reconstructions, the GFP in seedlings without Lincomycin co-localises with red-indicated chlorophyll auto-fluorescence, and with DAPI-staining (circled). Seedlings treated with Lincomycin

did not show chlorophyll auto-fluorescence, and GFP is seen to co-localise with DAPI-stained nuclei. A cytoplasmic distribution was also observed.

Therefore, without Lincomycin, NP::cp31A-GFP shows a dual localisation nucleus-chloroplast distribution and a nucleus/cytoplasmic distribution in Lincomycin-treated plants.

Subcellular localisation of NP::cpSEBF-GFP treated with and without Lincomycin. *In planta*

subcellular distribution of NP::cpSEBF-GFP in seedlings not treated with Lincomycin showed GFP-fluorescence in cotyledons with co-localisation with chlorophyll auto-fluorescence (red), indicating a plastid localisation (Figure 3.22, panels A, B, C, F, G, H). However, GFP signal was not observed to co-localise with DAPI-stained nuclei (panels D, I).

In seedlings treated with Lincomycin, no chlorophyll auto-fluorescence could be observed (Figure 3.23, panel B, G) due to the treatment. NP::cpSEBF-GFP fluorescence was strong (panels C, H), but did not co-localise with DAPI-stained nuclei (blue) (panels A, D, F, I), indicating that retrograde signal activators did not induce a nuclear localisation in NP::cpSEBF-GFP. However, NP::cpSEBF-GFP can be seen fluorescing in structures that may correspond to a proplastid distribution.

Z-stacks were integrated into a 3-D representation to better analyse the NP::cpSEBF-GFP fluorescence distribution in the whole cell without Lincomycin (Supplementary Figure 3.7, panels A, B) and with Lincomycin (panels C, D). The 3-D reconstruction shows an exclusively chloroplast localisation for NP::cpSEBF-GFP in control seedlings, and no co-localisation with DAPI-stained nuclei (blue) in Lincomycin-treated seedlings.

In summary, *in planta* confocal analysis of NP::cp31A-GFP indicated a dual chloroplast and nuclear localisation without Lincomycin, and a nuclear and cytoplasmic localisation in plants treated with Lincomycin. In contrast, NP::cpSEBF-GFP showed a chloroplast localisation in control conditions, and did not show a nuclear localisation in Lincomycin-treated seedlings. This indicates a capability for cp31A to alter localisation dependent upon retrograde signal activator treatment, but indicates that this is not the case for cpSEBF, suggesting both additional function for cp31A and diversification between the two.

cp31A- Native Promoter (Control Conditions)

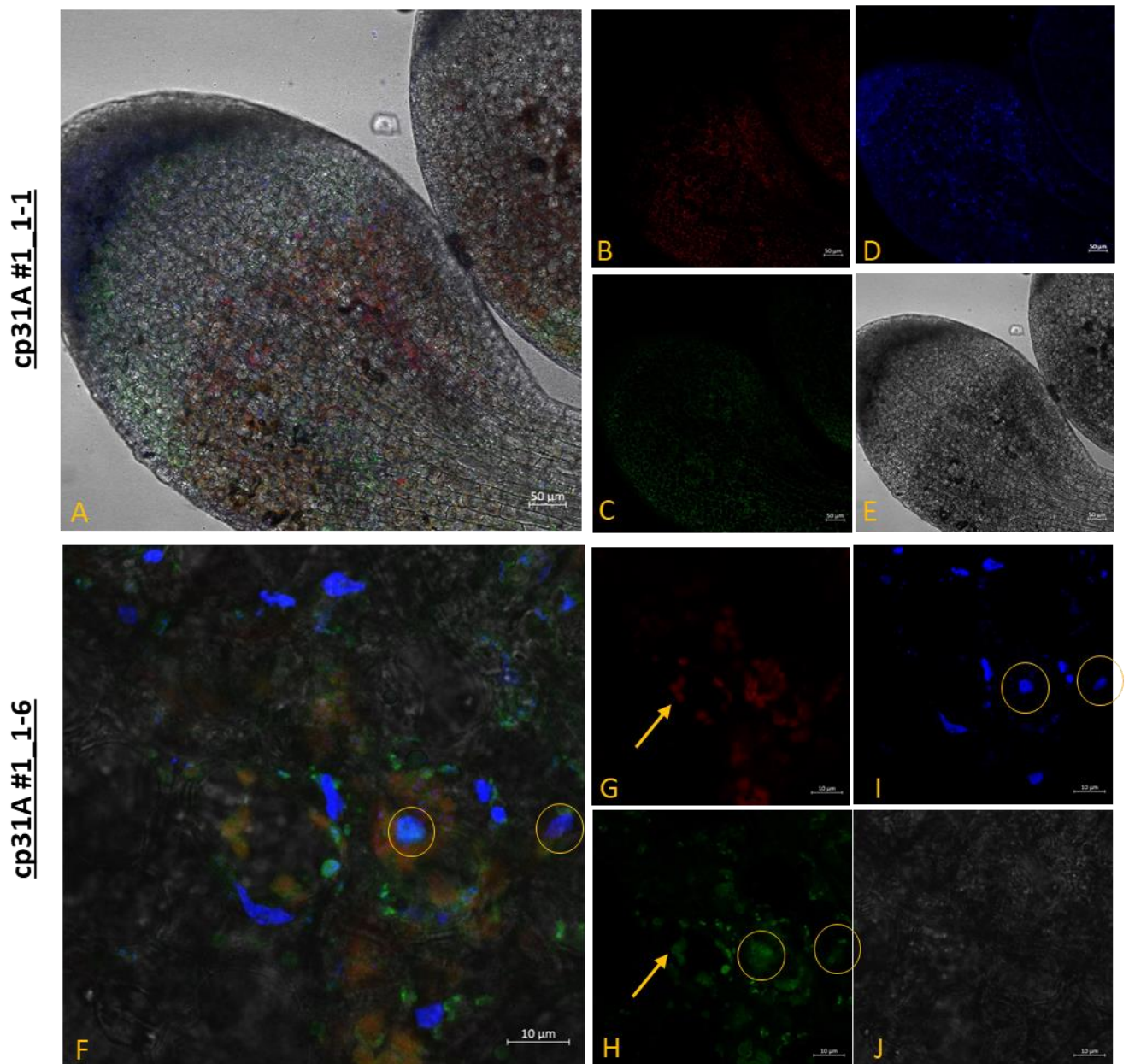


Figure 3.20. Confocal microscopy shows Native Promoter (NP)-expressed cp31A (*cp31a_1*) tagged with GFP localise to chloroplast *in planta* in control conditions. NP::cp31A-GFP (*cp31a_1*) plants were grown for three days in darkness and treated with 24hrs red light ($80 \mu\text{mol m}^{-2}\text{s}^{-1}$) at 22°C . Images show: A, F) Overlap of all images; B, G) chloroplasts are identified by chlorophyll auto-fluorescence (red); C, H) NP::cp31A (*cp31a_1*) expressing GFP (green); D, I) nuclei stained with 4',6-diamidino-2-phenylindole (DAPI) (blue); E, J, O) brightfield image of the plant. Scale bars are present in the lower right-hand corner of each photo. Both sets of images are from the same plant. Overlap between GFP and DAPI is indicated with a circle. Overlap between GFP and chlorophyll auto-fluorescence is indicated with an arrow.

cp31A- Native Promoter (treated with Lincomycin)

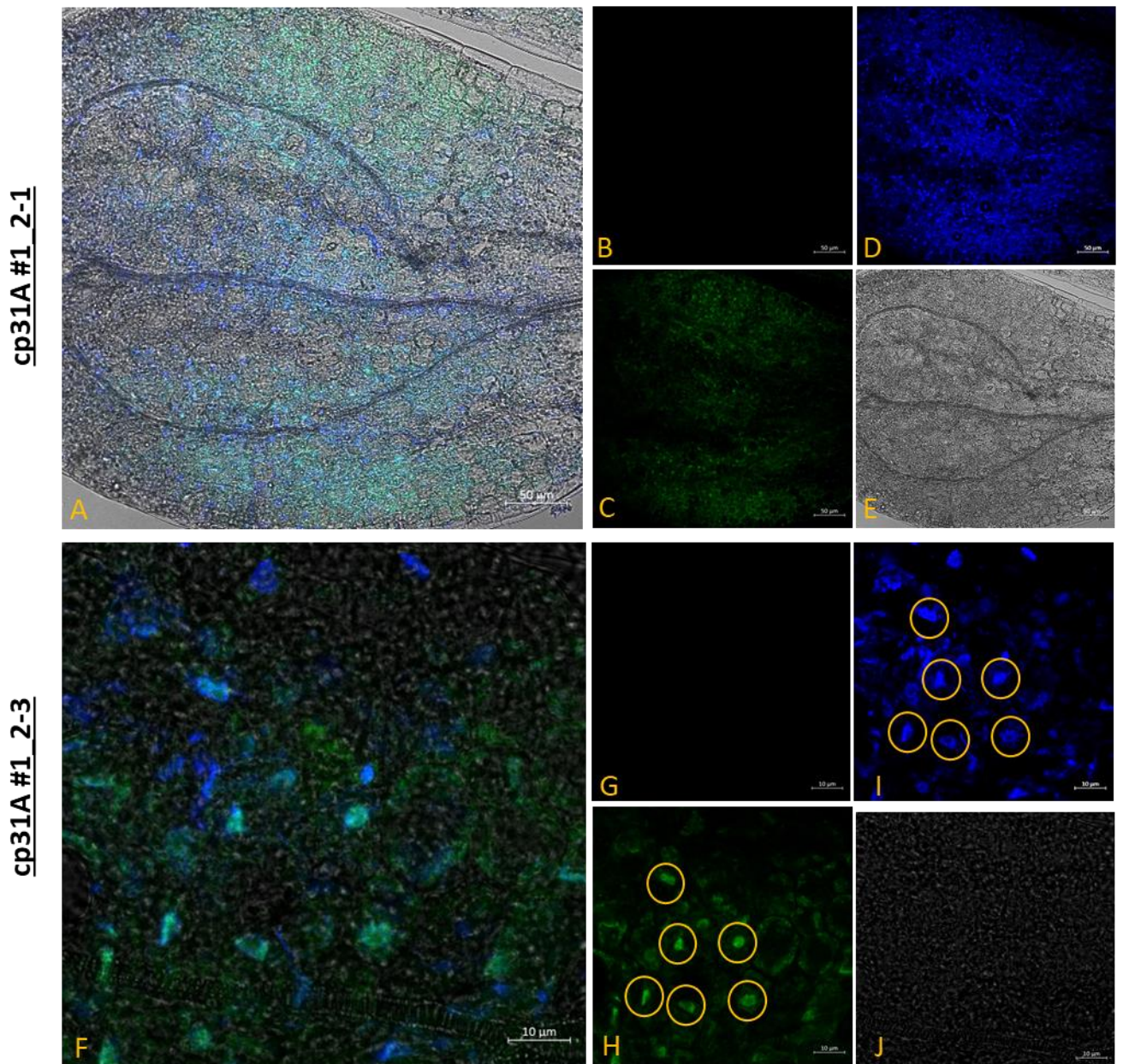


Figure 3.21. Confocal microscopy shows Native Promoter (NP)-expressed cp31A (*cp31a_1*) tagged with GFP localise to the nucleus *in planta* when treated with Lincomycin (Linc+). NP::cp31A-GFP (*cp31a_1*) plants were grown for three days in darkness and treated with 24hrs red light ($80 \mu\text{mol m}^{-2}\text{s}^{-1}$) at 22°C and grown on Lincomycin-containing media (0.5 mM). Images show: A, F) Overlap of all images; B, G) chloroplasts are identified by chlorophyll autofluorescence (red); C, H) NP::cp31A (*cp31a_1*) expressing GFP (green); D, I) nuclei stained with 4',6-diamidino-2-phenylindole (DAPI) (blue); E, J, O) brightfield image of the plant. Scale bars are present in the lower right-hand corner of each photo. Both sets of images are from the same plant. Overlap between GFP and DAPI is indicated with a circle.

cpSEBF- Native Promoter (Control Conditions)

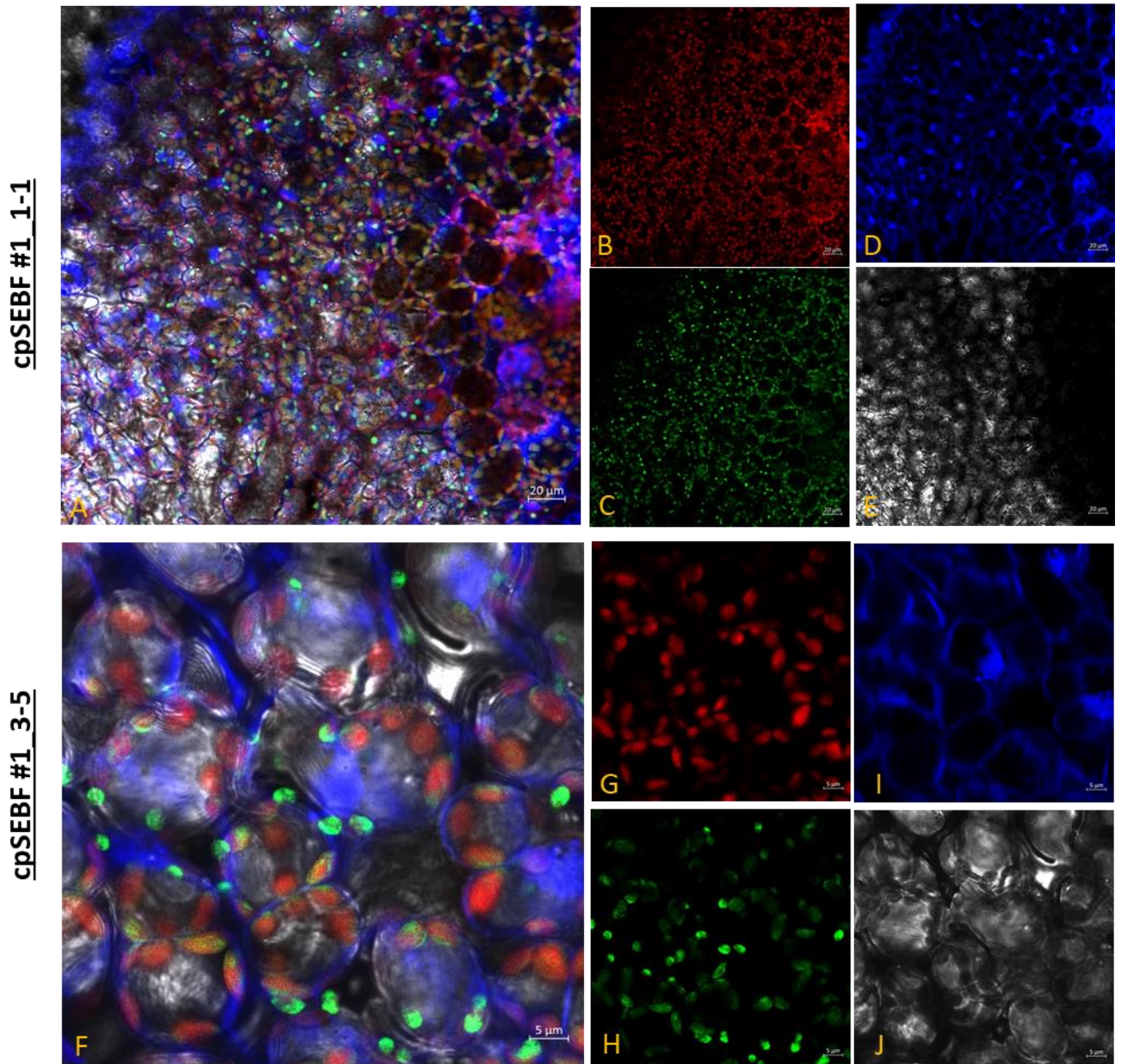


Figure 3.22. Confocal microscopy shows Native Promoter (NP)-expressed cpSEBF (*cpsebf_1*) tagged with GFP localise to chloroplast *in planta* in control conditions. NP::cpSEBF-GFP (*cpsebf_1*) plants were grown for three days in darkness and treated with 24hrs red light ($80 \mu\text{mol m}^{-2}\text{s}^{-1}$) at 22°C . Images show: A, F) Overlap of all images; B, G) chloroplasts are identified by chlorophyll autofluorescence (red); C, H) NP::cpSEBF-GFP (*cpsebf_1*) expressing GFP (green); D, I) nuclei stained with 4',6-diamidino-2-phenylindole (DAPI) (blue); E, J, O) brightfield image of the plant. Scale bars are present in the lower right-hand corner of each photo. Both sets of images are from different plants.

cpSEBF- Native Promoter (treated with Lincomycin)

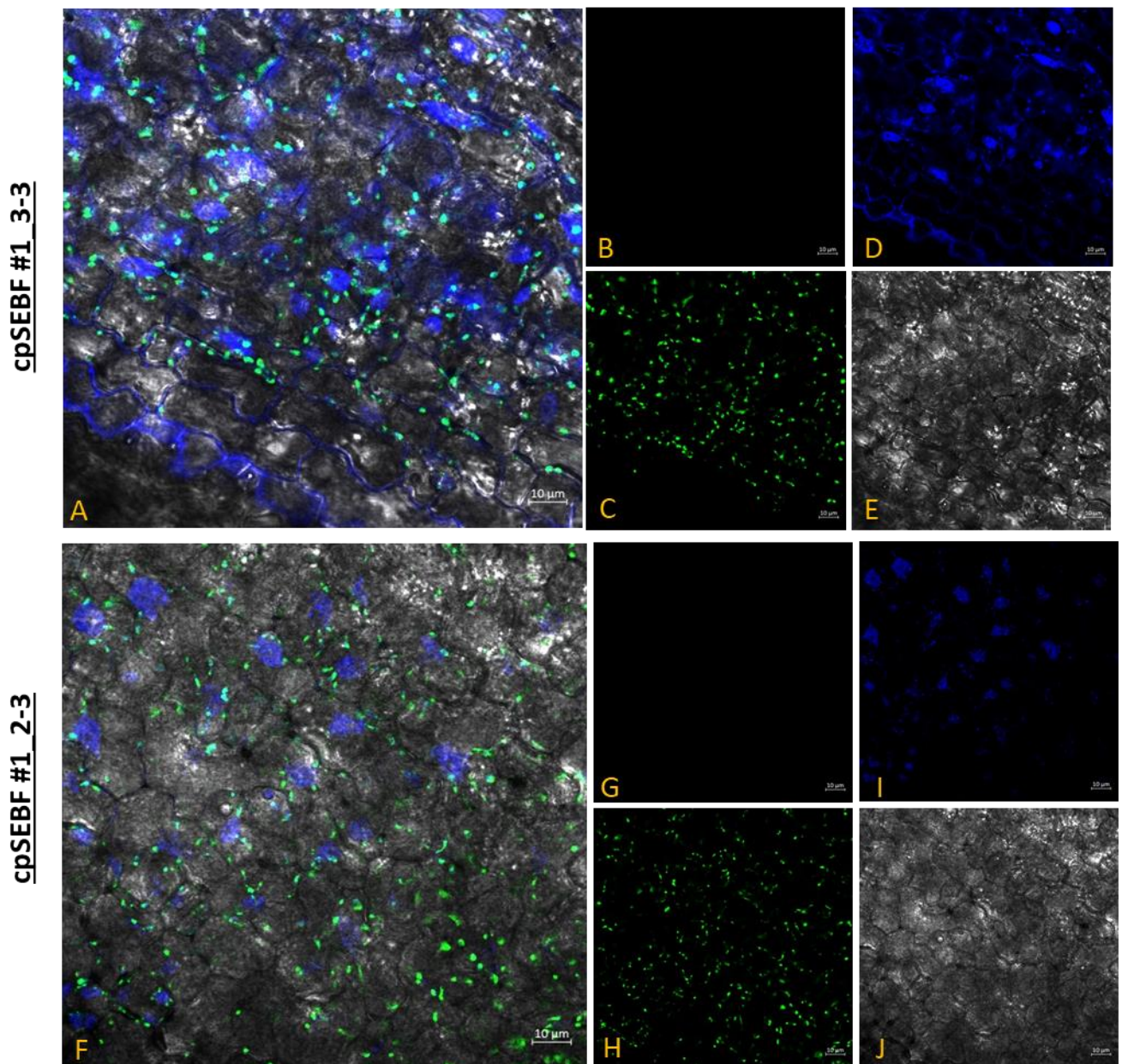


Figure 3.23. Confocal microscopy shows Native Promoter (NP)-expressed NP::cpSEBF-GFP (*cpsebf_1*) tagged with GFP do not appear to localise to the nucleus *in planta* when treated with Lincomycin (Linc+). NP::cpSEBF-GFP (*cpsebf_1*) plants were grown for three days in darkness and treated with 24hrs red light ($80 \mu\text{mol m}^{-2}\text{s}^{-1}$) at 22°C and grown on Lincomycin-containing media (0.5 mM). Images show: A, F) Overlap of all images; B, G) chloroplasts are identified by chlorophyll autofluorescence (red); C, H) NP::cpSEBF-GFP (*cpsebf_1*) expressing GFP (green); D, I) nuclei stained with 4',6-diamidino-2-phenylindole (DAPI) (blue); E, J, O) brightfield image of the plant. Scale bars are present in the lower right-hand corner of each photo. Both sets of images are from different plants.

3.7. Discussion.

This chapter investigated the potential functions of the cpRNPs beyond the chloroplast, with focus on nuclear roles and the involvement of light- and temperature- signals in driving changes in subcellular distribution and accumulation, as well as the potential links in chloroplast-nuclear coordination for photosynthesis.

3.7.1. cpRNPs localise to the nucleus and are critical to photosynthesis-associated nuclear gene transcript accumulation.

Chapter 2, section 2.3.7 reported evidence that plastid mRNAs' transcript abundance is dependent upon cpRNPs' functioning during de-etiolation. However, many of the processes that cpRNPs contribute to (such as the transcript accumulation for genes required for the photosynthetic apparatus) involve not only plastid-encoded subunits, but nuclear-encoded subunits too. The assembly of the photosynthetic complexes requires a tight co-ordination between the plastid and the nuclear genomes, including regulatory mechanisms that link them (Hernández-Verdeja and Strand, 2018), and the cpRNPs are therefore implicated as one of these mechanisms.

While some experimental evidence using *in vitro* gel shift assays on truncated forms of cp31A (Kwon and Chung, 2004) and protein blots from of cp29A on purified nuclei lysates (Gosai et al., 2015), predicted a nuclear subcellular localisation for cpRNPs, no *in planta* evidence of accumulation in the nucleus had been reported. In this chapter, in addition to further bioinformatic evidence presented to support predictions of a nuclear distribution for cp29B, cp33B, cp33C, cp31A, and cp29A, experimental results provide not only evidence an *in vivo* nuclear localisation for alternatively transcribed versions of cpRNPs but also mechanistic insights into how light and photoreceptors may be involved in their expression.

In particular, the mechanism of phy action investigated was the recently described phy-light dependent modulation of alternative transcriptional start sites linked to alternative subcellular localisations (TSS) (Ushijima et al., 2017). Ushijima et al's research described the global role of phy in controlling the light-dependent selection of TSS, and identified cp31A, cpSEBF, cp29A, and cp29C among the potential targets of this mechanism to produce longer and shorter isoforms. The experimental evidence gathered in this chapter showed that, as predicted by Ushijima et al (2017), the longer and shorter TSS isoforms for cpRNPs cp31A and cpSEBF (TSS_A and TSS_B) have a chloroplast and nuclear localisation *in planta* (section 3.3.3). This evidence therefore supports a light-dependent mechanism that alters subcellular localisation of these proteins, and a nuclear

localization indicates a wider role for cpRNPs beyond the previously described effects over plastome regulation (Ruwe et al., 2011; Kupsch et al., 2012). Interestingly, the STEP1 cp31A isoform described by Kwon and Chung (2004) has an identical sequence to cp31A (TSS_B). The STEP1 isoform was previously described to bind single-stranded G-rich plant telomeric DNA, but not double-stranded telomeric DNA; this indicates that the nuclear localisation observed for the shorter cpRNP TSS_B isoforms may function through binding to single-stranded DNA (Kwon and Chung, 2004).

For some of the cpRNPs additional TSS isoforms were also described by Ushijima et al, (2017); in particular multiple shorter isoforms were described for cp29C and cpSEBF. While the localisation and function of these further isoforms was not addressed in this thesis, these alternate forms might localise in multiple alternative localisations, including mitochondrial, and contribute to the inter-organelle communication networks necessary to cellular metabolism to environmental changes.

Revealing a novel function of cpRNPs in the coordination of the photosynthetic gene expression between nuclear and the plastid transcriptomes during de-etiolation.

De-etiolation is a critical phase of seedling establishment (Armarego-Marriott et al., 2020) that requires the co-ordinated expression of photosynthesis-associated nuclear genes to complement plastome gene expression. The *in planta* nuclear localisation of cpRNPs suggested a potential role for cpRNPs in this process, complementing their influence reported in the plastome (Chapter 2 Section 2.3.7). The evidence presented in this chapter supports a novel role for cpRNPs as a part of the mechanism controlling the accumulation of nuclear transcripts in response to phy-transduced signals (Figure 3.11). This expands the role of cpRNPs beyond the modulation of plastid-encoded transcripts (Kupsch et al., 2012; Teubner et al., 2017; Teubner et al., 2020), and therefore points to a much wider biological function for cpRNPs in regulating photosynthesis-associated processes. Furthermore, this discovery hints at a potential of cpRNPs to act in the networks that co-ordinate the nuclear and plastome genomes. Whilst the exact mechanism and function of the cpRNPs localised in the nucleus was not addressed, future studies, potentially including RIP-chip, protein-protein interactions and subnuclear localisation, would be of interest to dissect their exact nuclear role.

The novel function of cpRNPs in modulating nuclear transcripts in this chapter was described over PhANGs that encode complementary genes to plastome-encoded subunits. The data gathered (section 3.4.2) therefore supports that the investigated phy-cpRNP mechanism contributes to the

synchronisation of complementary nuclear-encoded and plastome-encoded subunits. For example, a cpRNP-dependent effect was reported in this chapter for *PSBQ12*, a part of the NADH Dehydrogenase apparatus; and over *PSAN* of Photosystem I; two processes over which cpRNPs have been documented to effect in the plastome (*ndhF*, *ndhK*, *ndhB*, *ndhG*, *psaJ*) (Kupsch et al., 2012; Okuzaki et al., 2019) (Chapter 2, Figure 2.5). In addition to informing a deeper understanding of how photosynthetic apparatus is built and maintained as a complex processes encoded in two compartments, this also provides an entry point from which to investigate further nuclear-encoded transcripts that the cpRNPs may be involved in regulating in a global manner.

Furthermore, a nuclear-localisation for cpRNPs may extend to the modulation of genes that may not have a direct 'counterpart' in the plastome, but are associated to a photosynthetic function. This role was illustrated by cpRNPs' modulation of the nuclear-encoded oxygen evolving complex (OEC) of PSII (Figure 3.11) (Thornton et al., 2004; Bricker et al., 2012), the *LHCB2.3* and *LHCB2.4* nuclear-encoded Light Harvesting Antenna complexes (Holtzegel, 2016), and *PSB27*, involved in the high light intensity response (Hou et al., 2015). The targets may also vary depending on the environmental growth conditions, such as the light and cold temperature effects observed over *DEG1*, involved in D1 protein turnover in PSII (Schuhmann and Adamska, 2012). As such, their nuclear targets indicate that cpRNPs also regulate chloroplast responses to stimuli and stresses linked to photosynthetic function.

In addition, the data gathered indicate that different members of the family, by having a differential environmental responsiveness and target preference, could differentially contribute to the modulation of different photosynthetic complexes. While some targets are common to more than one cpRNP, but others have a preferential regulation by a specific cpRNP under specific environmental conditions. A combinatorial role for cpRNPs was previously described for cp31A and cp31B (Tillich et al., 2009), and results presented in section 3.4.2 indicate this extends to the wider family too.

3.7.2. Temperature is a significant regulator of cpRNP subcellular distribution and nuclear functioning

This chapter showed some evidence that ambient temperature (17-27°C) may be a significant regulator of cpRNPs' protein accumulation. While no direct protein quantifications were carried out, cell biological studies showed that for cpRNP-GFP protein fusions, fluorescence intensity varied with temperature. These results support a higher accumulation of cpRNPs-GFP in the cold in

support of their described participation in cold temperature responsiveness (Amme et al, 2006, Goulas et al, 2006). The data also indicated a lower GFP fluorescence signal for cp31A-GFP and cpSEBF-GFP in warmer temperatures, and may reflect a temperature-dependent protein dynamic correlating with their function (Section 3.5.2). Evidence gathered in Chapter 2, section 2.6.3 showed an additional temperature-dependent transcriptional control of the cpRNP genes; however, no clear-cut links between transcript abundance and protein accumulation were detected at the level of cpRNPs-GFP fluorescent signal. As indicated by the study of GFP-tagged versions of the cpRNPs under native promoter expression, the abundance of cpRNPs varies with temperature, and whether the observed preferential accumulation of cp31A and cpSEBF in the cold is exclusive during de-etiolation remains to be addressed. Yet, during this developmental stage, cpRNPs are essential for plastid development and the construction of a functional chloroplast. Cold sensitivity may vary over development as studies in older plants showed no change in protein abundance in the cold (Kupsch et al., 2012; Waese et al., 2017) .

In addition to temperature-dependent changes in protein abundance, this chapter provides initial evidence of a temperature-dependent impact on subcellular distribution. Cell biological studies of cp31A-GFP showed a dual nucleus-chloroplast localisation at 17°C and 22°C, but an exclusively chloroplast localisation at 27°C (Figure 3.13). Temperature-dependent changes in subcellular localisation may be a key influence over the cold and physiological temperature-specific roles for cpRNPs. The chloroplast- or nuclear-specific localisation observed under different temperature regimes may be a product of temperature-dependent expression of the TSS isoforms of cp31A. For example, this indicates expression of a nuclear-localised cp31A (TSS_B) isoform during 17°C and 22°C, but not at 27°C. This likely linked to the thermosensing capacity of phyB's thermal reversion properties at higher temperatures (Jung et al., 2016; Legris et al., 2016), and its control of cpRNP TSS isoform expression (Ushijima et al., 2017). Interestingly, alternative TSS- and temperature-dependent subcellular localisation may be a specific characteristic of some cpRNPs, as cpSEBF subcellular localisation was not observed to be temperature-dependent. However, the specific molecular connections between TSS-derived cpRNPs isoforms and phyB thermosensing remain to be elucidated.

Overall, results suggest that under natural cold-warm temperature gradients cpRNP protein abundance varies, with promoting accumulation favoured at the cold end of the gradient and reduced at the warm end. The role of temperature also extends to the modulation of cpRNP subcellular localisation and the generation of phy-dependent TSS-derived isoforms. Further dissection of the mechanisms behind the temperature dependent generation of TSS-isoforms will be

of interest towards elucidating the impact and function of cpRNPs in different subcellular compartments.

In accordance with the observed effects of temperature on protein abundance and subcellular localisation, an analysis of nuclear-encoded, photosynthesis-associated transcripts also showed that the modulation of nuclear transcripts by cpRNPs is temperature-dependent, and that the contributions of different cpRNPs can deliver specific temperature-sensitive effects (Figure 3.16).

Experimental evidence in this chapter revealed a role for cp31A in modulating cold-sensitive regulation of multiple nuclear transcripts (Figure 3.11). This parallels the cold-sensitive phenotype and differential RNA-editing activity of cp31A in chloroplasts (Kupsch et al., 2012). Whilst no direct investigation was carried out on the mechanisms surrounding phosphorylation-dependent modulation of cpRNPs, cold- and light-sensitive phosphorylation has previously been reported as a regulator of cpRNP mRNA binding affinity (Lisitsky and Schuster, 1995; Loza-Tavera et al., 2006; Okuzaki et al., 2019). This may point to a post-translational modification as a key regulator of cpRNP functioning: multiple phosphorylation sites have been reported for the cpRNP family, including at multiple phosphorylation sites for cp31A, cp29A, cp29B, cp33B, and cpSEBF (Reiland et al., 2009; Roitinger et al., 2015; Baginsky, 2016). While not yet demonstrated for cpRNPs, protein phosphorylation has also previously been linked to protein accumulation in cold stress (8°C) conditions (Kamal et al., 2020).

This possibility is supported by the effects of *cp31a* mutation on Photosystem I and photorepair processes, which were detected on transcripts at 17°C but not at 22°C. The cold sensitivity of cp31A may also be linked to specific cold responsiveness of transcripts from Photosystem II, Photosystem I, and photorepair-associated processes, for which protein abundance has been shown to increase during cold-acclimation processes (Badger et al., 1982; Strand et al., 1997). Overall, results provided here support a role for cp31A in mechanisms to adapt photosynthesis to lower temperature, extending its previously described role in non-chilling cold temperature (Kupsch et al., 2012), and participating in the adaptation of photosynthetic gene expression to lower temperatures in both the nucleus and the plastome.

However, in contrast to cp31A, regulation of nuclear transcripts by cp29B and cpSEBF occurred predominantly at 22°C and was often insensitive to cold or warm conditions (although exceptions were observed, such as the cold-sensitivity of *PSBO2* and warm-sensitive regulation of *PSB27* by cpSEBF). While an increase in cp29B and cpSEBF protein abundance has been reported in the chloroplast in cold conditions (Amme et al., 2006; Goulas et al., 2006), modulation of nuclear

mRNA accumulation was not correlated and the cold-related roles of cp29B and cpSEBF may be chloroplast-specific. This possibility is supported by observations that cpSEBF was not detected in the nucleus *in planta* in cold conditions. However, only a limited range of targets was investigated, and more extensive analysis such as via RNAseq experiments may be necessary to fully analyse the temperature responsiveness of nuclear mRNAs in a cp29B- and cpSEBF-dependent manner. Therefore, although the mechanisms behind the different cpRNPs' acquisition of temperature sensitivity are still unclear, the evidence provided suggests that these mechanisms affect nuclear targets that are linked to the phys.

For the studied cpRNPs cp29B, cpSEBF, and cp31A, a role in warm-temperature responses seem to be lesser compared to cold conditions; in correlation with trends in cpRNPs-GFP reduced fluorescence signals. Only *PSB27* transcripts for a thylakoid protein with a role in adapting to light intensity changes (Hou et al., 2015) were detected to be cpSEBF- and cp31A- dependent in the warm (Figure 3.16); whether other photoprotection-associated genes have a cpRNP-dependence in the warm awaits further genomic experimental data.

In summary, this section suggests that nuclear-encoded transcript regulation by cpRNPs occurs predominantly in cold (17°C) and at 22°C, and in the warm the function of these proteins can be affected by mechanisms that lead to a lower accumulation. The reduced effect of cpRNPs contrasts with the warm-temperature sensitivity observed by phyB over nuclear-encoded transcripts, which affected all tested Photosystem II- and NADH Dehydrogenase-associated transcripts (Figure 3.16). Whether other cpRNPs not investigated here are exclusively working in the warm and in a phy-dependent manner, remains to be explored, together with the full sensitivity of the plastome and the nuclear transcripts linked to cpRNPs functions.

3.7.3. cpRNPs are regulated by the retrograde signalling pathway.

The operation and assembly of the photosynthetic apparatus is dependent upon anterograde and retrograde signalling pathways between the chloroplast and nucleus. The retrograde signalling pathways are activated when the plastid is stressed or subject to a specific stimulus and alters nuclear processes such as nuclear transcripts accumulation in response (Jarvis and López-Juez, 2013; Szechyńska-Hebda and Karpiński, 2013; Chan et al., 2016). This thesis provides evidence that indicates cpRNPs regulate both plastome- and nuclear-encoded transcripts that contribute to the assembly of photosynthetic apparatus in the chloroplast (Chapter 2, section 2.3.7, Chapter 3 section 3.5.2); cpRNPs functional role in modulating nuclear-encoded genes that are among the targets of

Retrograde signals including PhANGS such as the Light Harvesting Complexes (LHCBs) (Susek et al., 1993; Strand et al., 2003) prompted the exploration of testing whether they are part of the RS pathways.

The data collected suggests cpRNPs respond to treatments that activate retrograde signals (RS) such as Lincomycin (Linc) and Norflurazon (NF), which reduce *cpRNP* transcript abundance in treated plants. This suggests that cpRNP transcript accumulation is retrograde-signal dependent, and that cpRNPs could be functionally involved in integrating signals from the plastid in addition to delivering phyB, nuclear-derived signals in the anterograde pathway. Furthermore, while experimental data indicated a consistent down-regulation of all tested cpRNPs to Lincomycin, a differential sensitivity to Norflurazon was detected between members (Figure 3.18). The regulation of cpRNPs by retrograde signals is under-explored, but published Northern Blot analyses previously revealed the down-regulation of barley *Hvcp31A* in Norflurazon-treated plants; showed no change to *Hvcp31B*; and detected an up-regulation of *Hvcp33A* (Churin et al., 1999). Although transcript accumulation of Arabidopsis orthologues for *Atcp31B* and *Atcp33A* were not examined, evidence supports the observed differential sensitivity of *At-cpRNPs* to Norflurazon-induced retrograde signals with only *cp29B* showing down-regulation among the tested ones (Figure 3.18). Yet, this data contrasts with genomic experiments that show *cp29B*, *cp29C*, *cpSEBF*, and *cp31A* down-regulation in Norflurazon (Figure 3.17). The differences may reflect changes in the light environments used, with experiments presented here conducting in low light ($10 \mu\text{mol white light m}^{-2}\text{s}^{-1}$) versus the higher light conditions used in genomic tests ($100 \mu\text{mol white light m}^{-2}\text{s}^{-1}$). Whether cpRNPs also respond to light intensity signals was not addressed in this thesis, with the exception of fluctuating light environments.

Although overlapping in their signal ranges, light intensity is a key regulator of retrograde signals (Pfannschmidt et al., 2008; Szechyńska-Hebda and Karpiński, 2013). Previous comparisons of Norflurazon-treated plants in low light compared to high light in cucumber revealed higher levels of 33-kDa protein of the Oxygen Evolving Complex, a higher quantum yield of electron transport, and better photochemical quenching capacities (Jung et al., 2000). Interestingly, the 33-kDa protein described is encoded by *PSBO* genes in Arabidopsis, shown to be cpRNP-dependent during de-etiolation (Figure 3.11). This may suggest cpRNP function is also modulated by retrograde signals in different light intensities, therefore allowing a greater specificity for plants to respond to specific stress-inducing signals, and a more finely-tuned and energetically-responsible response.

Retrograde signals are transduced through a plethora of pathways, but recent research has indicated the participation of phyB/PIFs in a GUN1-mediated pathways (Martín et al., 2016; Jiang et

al., 2020). Interestingly, cp28A was identified within the Martin et al (2016) dataset as PIF-repressed, light-induced, RS-downregulated gene. As such, dissection of the role of phys and PIFs in modulating RS modulation of cpRNPs function would be an interesting area for future exploration.

In addition, experiments with Lincomycin showed an alteration in patterns of cpRNP subcellular localisation and distribution. Examination of native-promoter cp31A-GFP transgenic provided with indication that retrograde signals can induced cpRNPs changes in subcellular distribution. In contrast to the dual chloroplast-nucleus localisation observed in control plants, NP::cp31A-GFP was detected only in the nucleus and cytoplasm in Lincomycin-treated plants (Figure 3.19, Figure 3.20). This alteration in localisation suggests that the nuclear-localised cp31A (TSS_B) may be the preferentially expressed isoform, and not the chloroplast-localised cp31A (TSS_A). This hints at a RS-modulation of the phyB-TSS selection mechanisms, and further suggests that differential expression of alternatively transcribed cpRNP isoforms is an important mechanism to diversify the functional roles of cpRNP proteins. Published research shows that Lincomycin represses photomorphogenesis via a GUN1-mediated, phytochrome/PIF-repressed pathway (Gommers et al., 2020). Whether this pathway is involved in the RS-modulation of cpRNPs and links to the phyB-dependent TSS-isoforms remains to be determined, but this possibility is supported by initial bioinformatics identification of cpRNPs as targets of the GUN1/phyB dependent mechanisms, including changes in their transcript accumulation.

A Lincomycin-RS-induced differential expression of nuclear-localised cpRNPs such as cp31A could contribute to specific modulation of nuclear-encoded transcripts in the absence of functioning chloroplasts. The identification of cp31A-dependent nuclear-encoded transcripts with a function in photoprotective mechanisms and responsiveness to light fluctuations that are RS-modulated (such as *PSB27*), points at a potential area to develop new studies on the links between cpRNPs and retrograde signals (Szechyńska-Hebda and Karpiński, 2013; Richter et al., 2020).

The data also point at some cpRNPs having additional alternatively localisations, non-chloroplast and non-nuclear, when treated with Lincomycin. These localisations may be linked to the unexamined cpSEBF isoforms TSS_C and TSS_D. The data shown in Figure 3.21 may reflect a localisation in other plastid forms, such as proplastids, as indicated by previously reported plastid sizes (Sakamoto et al., 2008), appearance (Robertson et al., 1995; Haseloff et al., 1997), and biological function of proplastids as an undifferentiated chloroplast precursor (Mullet, 1988b). In support of the possibility, a proteome analysis of proplastids in *Z. mays* identified multiple ZmcpRNP orthologs present, including an AtcpSEBF orthologue (Majeran et al., 2012), the presence of cpSEBF and cp31A orthologues in rice etioplasts (von Zychlinski et al., 2005), and cp31A in tobacco

proplastids (Baginsky et al., 2004). As Lincomycin arrests plastid translation and cpRNPs have previously been detected in such a wide range of plastids, the cpRNP functional mRNA targets in these plastids would likely change depending on the plastids' developmental status and needs. This may point at an unexplored role for cpRNPs in the control of developmental plastid transitions. However, an important caveat to the investigation for overlap between cpRNP-GFP and chloroplasts treated with Lincomycin is that, while Lincomycin may induce photobleaching and inhibit chlorophyll accumulation, the chloroplast itself still exists. Therefore chlorophyll autofluorescence is absent and cannot be used as a marker for chloroplasts- to circumvent this problem, a dye such as carboxyfluorescein diacetate could be used in future experiments to identify chloroplasts and make a more definitive study of chloroplast co-localisations in this condition.

The central message of this chapter is that the impact of cpRNPs extends beyond exclusively plastid-encoded mRNAs, and identifies that a mechanism likely to be at the heart of cpRNPs' integration of environmental responses is the generation of phy- and TSS-derived isoforms. In turn, phy-directed mechanism hints at an even broader participation of cpRNPs in environmental sensing and inter-organellar (plastid-nuclear and potentially beyond) response co-ordination. Furthermore, results presented in this chapter highlight potential functional differences between members of the cpRNP family, including differing subcellular localisation, differential control of nuclear and plastidic mRNA targets, and differential temperature- and retrograde signal sensitivity. These findings are summarised in a working model for the influence of cpRNPs on photosynthetic processes (Figure 3.23).

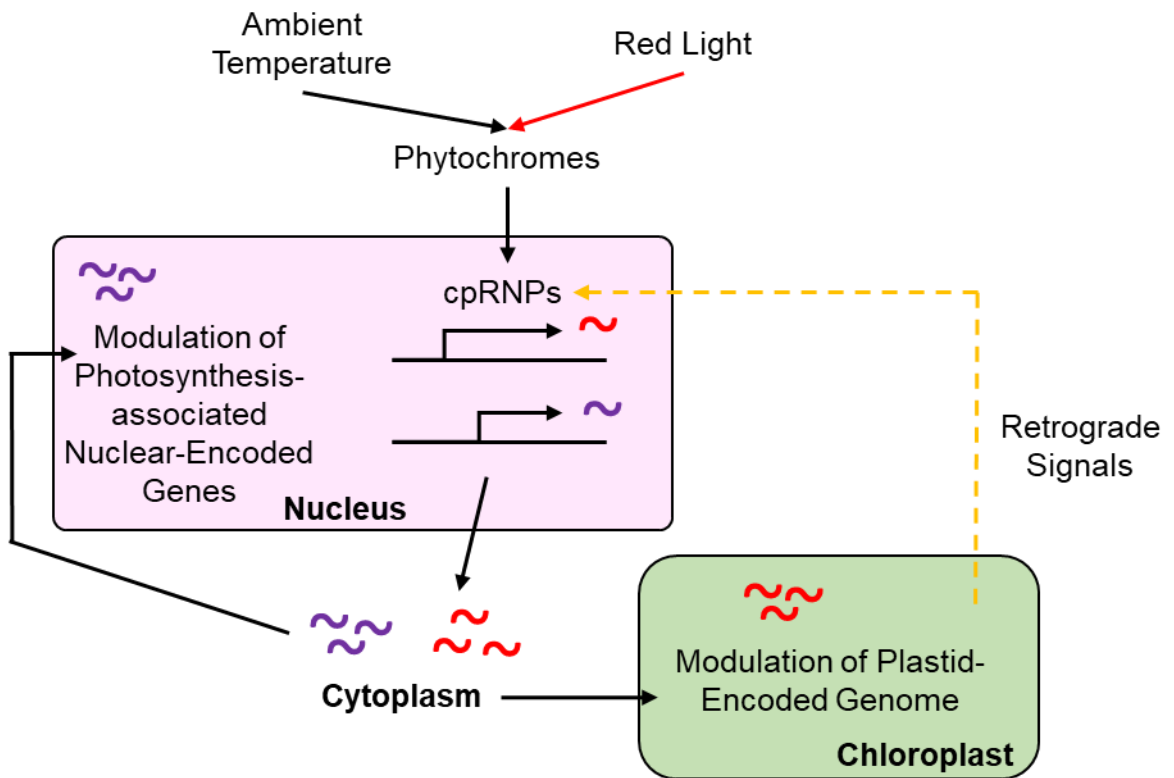


Figure 3.24. A working model showing that red light, temperature, and retrograde signals modulate *cpRNP* expression and subcellular localisation. The model proposes that these environmental signals alter the expression of the long forms (TSS_A, red) and short forms (TSS_B, purple) of cpRNPs that were observed to localise respectively between the chloroplast and the nucleus after translation. The proposed model also suggests that cpRNPs are involved in the modulation of mRNAs from photosynthesis-associated nuclear genes in addition to the plastid-encoded genome.

Chapter 4: Beyond Arabidopsis: Investigation into the functional conservation of cpRNPs between Arabidopsis and tomato.

4.1. Introduction.

This chapter builds on evidence that Chloroplast RNA Binding Proteins (cpRNPs) are highly conserved in a range of crop plants beyond Arabidopsis, including both dicot and monocot species. The chapter also investigates a role for cpRNPs beyond the construction and maintenance of photosynthetic apparatus in the chloroplast to their potential roles in different types of plastids by evaluating their transcript accumulation profiles in different ripening stages of tomato fruits.

Phylogenetic analysis of cpRNPs has previously been conducted using the first RNA Recognition Motif (RRM) featured in the protein sequence (Ohta et al., 1995). This classified the then-identified Arabidopsis proteins Atcp29, Atcp31A, and Atcp33 into three subgroupings defined by sequence similarity. Orthologous cpRNPs had also been identified in the dicot species *N. sylvestris*, *N. plumbaginifolia* and *S. oleracea*, showing that cpRNPs were well conserved amongst dicot plants (Li and Sugiura, 1990; Schuster and Gruissem, 1991; Ye et al., 1991; Mieszczyk et al., 1992; Ohta et al., 1995). cpRNP orthologues were also been identified in the monocot Maize (Cook and Walker, 1992), and later in Barley (Churin et al., 1999). With the sequencing of the Arabidopsis genome further cpRNPs were identified (Tillich et al., 2009) bringing the total to 10 genes (Ruwe et al., 2011). Recently, orthologs of all ten Arabidopsis cpRNPs were described in rice (Wu et al., 2021), indicating that cpRNPs are widespread in crops and likely strongly conserved across higher plants. This chapter generates an updated phylogenetic tree of cpRNPs protein sequences using genomic information from available plants as a starting point to examine how widespread cpRNPs are conserved in context of exploring functions beyond the model plant Arabidopsis.

cpRNPs are induced during de-etiolation (Schuster and Gruissem, 1991) and are critical to greening in this stage (Chapter 2, section 2.3.3), regulating multiple transcripts in the plastome (Tillich et al., 2009; Kupsch et al., 2012; Teubner et al., 2017). During de-etiolation, dark-grown etioplasts transition into photosynthetically active chloroplasts with a consequent increase in cpRNP transcripts and proteins (Smith, 1954; Armarego-Marriott et al., 2020). Yet, RNA processing activities are essential to determine which transcripts are selected for translation and expression as plastid proteins. Within developmental transitions, the proteome will undergo changes as the requirements for plastid functions will vary. Therefore, an investigation was conducted to evaluate whether cpRNPs are involved in the re-organization of the plastome-encoded transcripts necessary for non-photosynthetic plastid transitions; this chapter speculates that cpRNPs have a role in regulating

plastid transition states beyond the regulation of chloroplast-encoded transcripts. Chloroplast-to-chromoplasts transition will include changes in the protein complexes required in the chloroplast, with the disassembly of photosynthetic complexes and accumulation of ATP Synthase required at high levels in non-autotrophic but metabolically active chromoplasts (Piechulla et al., 1987; Livne and Gepstein, 1988).

The tomato (*Solanum lycopersicum*) was selected as an established research model for evaluation of the developmental transition from chloroplast-to-chromoplast (Cheung et al., 1993). This chapter investigated the links between cpRNPs' capacity for a global modulation of the plastome and the required reshuffling of the plastome transcripts accumulation. One of the associated pathways to chromoplast development, the carotenoid biosynthesis pathway, is highly active in chromoplasts for the production of red lycopene (Llorente et al., 2017) and was used as marker to follow the involvement of cpRNPs on chloroplast to chromoplast transition.

The investigation into the cpRNPs' role in the plastome regulation during plastid transitions examined *SlcpRNPs* transcripts abundance during different tomato ripening stages. Micro-Tom was used as model for ripening studies, and *SlcpRNP31* was selected as a model based on bioinformatics studies. A transient silencing Virus Induced Gene Silencing (VIGS) strategy was then used to silence *SlcpRNP31* and evaluate its impact on ripening progression and links to plastome transcripts accumulation.

4.2. Materials and Methods.

4.2.1. Plant material and genotypes tested.

Two cultivars of *Solanum lycopersicum* (tomato) plants were used for experiments: Micro-Tom and Money Maker. Micro-Tom plants were used to examine *SlcpRNPs* transcript accumulation during different fruit ripening stages, and Money Maker was the model selected by the BRACIT Institute in our collaborative project to generate CRISPR-CAS knock out transgenic plants. The BRACIT crop transformation facility has a long history working with the research community to provide crop transformation resources, including RNA-guided Cas9 to produce gene knockouts in wheat, barley, and tomato. For more information, see: (<https://www.jic.ac.uk/research-impact/technology-research-platforms/crop-transformation/>). For transient Virus Induced Gene Silencing experiments a transgenic line *DelilaRosea1* (Del/Ros1) (Orzaez et al., 2009) was used in collaboration with CRAG-Barcelona Rodriguez-Concepcion Lab.

4.2.2. Plant Growth Conditions.

Tomato plants were grown under standard greenhouse conditions (14h light, 27°C /10h dark, 24°C).

4.2.3. Plant Harvesting.

Micro-Tom experiments. Micro-tom fruits were selected from maturing plants grown at the Centre of Research for Agricultural Genomics (CRAG), Barcelona. Plants and fruits were made available by the Dr. Rodriguez-Concepcion Lab and were selected based on visual colour cues. To ensure selected fruits were in the correct ripening stage, RT-qPCR of ripening marker genes was performed (see Table 4.1).

4.2.4. RNA Extraction and cDNA Synthesis.

RNA extraction was performed on lyophilized tissue by an automated system supplied by Promega® Maxwell® 16 LEV Plant RNA Kit according to manufacturer's instructions. RNA was quantified using a NanoDrop 1000 spectrophotometer (Thermo Scientific) and checked for integrity by 1% agarose gel electrophoresis. To synthesise cDNA, a Thermo Scientific™ RevertAid First Strand

cDNA Synthesis Kit was used according to manufacturer's instructions. Oligo dTs were used in the reaction.

4.2.5. Quantitative RT-PCR Analysis.

RT-qPCR was performed using 10µl LightCycler480 SYBR Green I Master Mix (Roche), 0.6µl forward primer (300nM) and 0.6µl reverse primer (300nM), 1µl of 50ng template cDNA, and 7.8µl of water in a 20µl final reaction volume. Reaction was performed in a LightCycler 480 real-time PCR system (Roche), using the following thermal cycling program: 95°C for 10 min, followed by 45x cycles of 95°C for 10 sec, and 60°C for 30 sec. At least two technical replicates of each biological replicate were performed, and the mean values were used for further calculations. Results were analysed using Microsoft Excel. Results were normalised to the tomato ACT (Solyc04g011500) reference gene and relative gene expression was calculated as described in Pfaffl (2001). A full list of primers used is presented below in Table 4.1.

Table 4.1. qPCR Primers used in this chapter for the examination of *SlcpRNPs* in fruit ripening stages and in examination of the impact of *Slcp31* on the process of carotenogenesis.

<i>Solanum lycopersicum</i> qPCR Primers		
Reference Gene	<i>SI</i> ACT_F	CCTTCCACATGCCATTCTCC
	<i>SI</i> ACT_R	CCACGCTCGGTCAGGATCT
Ripening Marker Genes	<i>SIE</i> 8_F	AGCTGCAAGTTGGAGAGACACG
	<i>SIE</i> 8_R	CCGCATGGAGTTGGAAATTC
	<i>SI</i> ACS2_F	CGTTTGAATGTCAAGAGCCAGG
	<i>SI</i> ACS2_R	TCGCGAGCGCAATATCAAC
	<i>SIP</i> G2A_F	ATGGCAATGGACAAGTATGGTG
	<i>SIP</i> G2A_R	TTAAGGCCGTTGGTGCATC
	<i>SIR</i> IN_F	GCTAGGTGAGGATTTGGGACAA
	<i>SIR</i> IN_R	AATTTGCCTCAATGATGAATCCA
Tomato cpRNP Genes	<i>Slcp</i> 28A_F	GGGTACTGTATGATGGTGAGAC
	<i>Slcp</i> 28A_R	CATCCAATTCCACTCCATTGAG
	<i>Slcp</i> 29A_F	CTCACAGGAAGAAGCAGAGG
	<i>Slcp</i> 29A_R	CTCCCGTCGATTTTCATATCCA
	<i>Slcp</i> SEBF_F	TTCTTCTTACCAGGGAGGCA
	<i>Slcp</i> SEBF_R	TTGCTCACTGAACAAGGTCTC
	<i>Slcp</i> 31_F	CTGATAGAAGTCGTGGATTCCGG
	<i>Slcp</i> 31_R	CCTTCCATTGAGATCATAACGG
	<i>Slcp</i> 33A_F	TGATGGATCTCAAGTTGGAGG
	<i>Slcp</i> 33A_R	CACTCATTACTTGCCTTTCACC
	<i>Slcp</i> 33B_F	AGATGGAAAGGAACTGATGGG

	<i>Slcp33B_R</i>	AGTCATCTATGGCTCTTCAGG
	<i>Slcp33C_F</i>	TGACGGAAAGGAATTTATGGGA
	<i>Slcp33C_R</i>	TTCAGATGGTAGTTCTTGGGAC
Carotenoid Biosynthesis Pathway Genes	<i>SIPSY1_F</i>	GCCATTGTTGAAAGAGAGGGTG
	<i>SIPSY1_R</i>	AGGCAAACCAACTTTTCCTCAC
	<i>SIZDS_F</i>	GACCTGATCAGAAGACGCCA
	<i>ZIZDS_R</i>	GCAGAAGCTTGCCTACCTGA
	<i>SILYCE_F</i>	GCCACAAGAACGAAAACGAC
	<i>SILYCE_R</i>	CGCGGAAAAATGACCTTATC
	<i>SICYCB_F</i>	TGGCAAGGGTTCCTTTCTTC
	<i>SICYCB_R</i>	AGTCATGTTTGAGCCATGTCC
	<i>SILYCB_F</i>	TTGTGGCCCATAGAAAGGAG
	<i>SILYCB_R</i>	GGCATCGAAAAACCTTCTTG

4.2.6. Virus Induced Gene Silencing Experiments.

Nucleic Acid Techniques.

PCR for cloning, and colony screening experiments. Protocols were performed using 1µl *GoTaq* Green Master Mix, 1µl MgCl₂ 2.4µL dNTPs, 0.6µl of Forward and Reverse primers, 2.2µl template DNA, and 19.2µl water in a 30µl final reaction volume. Thermal cycling settings were determined by optimal primer melting temperatures and used a 72°C final extension temperature.

Gateway Cloning. *Slcp*RNPs were PCR amplified from a mix of green, ripening and ripened Microtom tomato cDNAs and cloned in the Gateway pDONR207 vector through a BP reaction by Dr. Karine Prado (University of Edinburgh Halliday Lab). The subcloning of these constructs into a pTRV/DR/Gateway vector via the LR reaction was performed by myself at Dr. Rodriguez-Concepcion lab in the Centre of Research for Agricultural Genomics. Reactions were performed using recommendations by Invitrogen for Gateway Cloning.

Bacterial transformation by heat shock. For cloning and plasmid amplifications, competent *E. coli* DH5α cells were used; for plant transformation experiments, *Agrobacterium tumefaciens* GV3101-pMP90 was used. All competent cells were incubated on ice for 20 min after the addition of plasmid DNA.

For *E. coli* transformations a 42°C heatshock treatment was applied to cells for 1 min, and then moved to ice for 5 min. After this 900µL sterile LB was added and cells were incubated for 1hr at 37°C. Bacteria were then plated on a selection medium containing gentamycin.

For *A. tumefaciens* a frost-thaw treatment was applied to cells by incubating cells in liquid nitrogen for 1 min, and then transferring them to ice for 5 mins. After this 900µl sterile YEB was

added and cells were incubated for 1hr at 28°C. Bacteria were then plated on a selection medium containing rifampicin (100 µg/ml) and gentamicin (10 µg/ml).

Plasmidic DNA extraction. The resulting colonies were analysed via colony-PCR and positive colonies were used to inoculate LB medium (5ml) with the respective antibiotic. They were incubated at 37°C and 180rpm and left overnight. Grown cultures were spun at 13,000rpm in a centrifuge for 5 min and pellets collected. Plasmid DNA was extracted using a High Pure Plasmid Isolation kit (Roche®) according to manufacturer’s instructions.

Plant Transformation. Tomato fruit agroinjection for VIGS experiments was performed as described in Orzaez et al (2009) and Fantini et al (2013). Constructs containing VIGS sequences to induce silencing of the Gene of Interest (GOI) and the anthocyanin over-accumulating genes *Rosea 1* and *Delila* at the same time were injected into R/D fruits (Butelli et al., 2008). Successful silencing of *Rosea1* and *Delila* removed the purple colouration caused by anthocyanin overaccumulation and acted as a visual reporter. These areas were marked and extracted for RNA isolation.

4.2.7 CRISPR-CAS9 generation of stable silencing in transgenic tomato.

The CRISPR-Cas9 mediated silencing for *Slcp29A* lines was conducted using two guide RNAs. The generation of the transgenic lines was performed by the BRAC facility (Lawrenson et al., 2015). For further information, see (<https://www.jic.ac.uk/research-impact/technology-research-platforms/crop-transformation/>). To verify that the target sequence in Money Maker tomatoes is the same as the published *Slcp29A* sequence, sequencing primers were designed and used. After the sequence was confirmed, primers were designed for use in screening the guide cut site. For a list of all primers used, see Table 4.2.

Table 4.2. Primers used to sequence *Slcp29A* in Money Maker tomato plants, and screening primers

<i>Solanum lycopersicum Slcp29A</i> CRISPR-Cas9 project primers		
<i>Slcp29A</i> sequencing primers	<i>Slcp29A</i> _Sequencing_F	TGCCACTTTGGCAATAAAGC
	<i>Slcp29A</i> _Sequencing_R	GGGTGTCAATTTCTTTGCCGA
<i>Slcp29A</i> guide target primers	<i>Slcp29A</i> _Guide_Screening_F	AACTCGGCGTCTTAGCAACA
	<i>Slcp29A</i> _Guide_Screening_R	GTGCTGCAAATACTATAACAGGGC

4.2.8 Bioinformatic Analysis of cpRNPs' conservation.

79 cpRNP sequences from *H. vulgare*, *V. vinifera*, *M. truncatolata*, *Z. mayes*, *P. trichocarpum*, *S. tuberosum*, *O. sativa*, *G. max*, *S. lycopersicum*, *N. sylvestris*, *N. plumbaginifolia*, and *S. oleracea* were sourced from putative and confirmed protein sequences listed in the eFP Tomato database (Waese et al., 2017) respective to 10 identified Arabidopsis cpRNP sequences. Sequences were aligned and a nonrooted, bootstrapped tree without distance corrections was conducted in MEGA X (Kumar et al., 2018). The evolutionary relationships of taxa were analysed by neighbour-joining (Saitou and Nei, 1987), and bootstrap consensus was calculated from 1000 replicates (Felsenstein, 1985). The evolutionary distances were computed using the Poisson correction method (Zuckerandl and Pauling, 1965). Tree data was exported and uploaded to Interactive Tree of Life (iTOL) (Letunic and Bork, 2019). Sequences were aligned in CLUSTAL W (<http://www.ebi.ac.uk/clustalw>) (Thompson et al., 1994). All accessions used are provided in Supplementary Table 4.1.

4.2.9. Statistical analysis.

Statistical analysis of the data was conducted in Microsoft Excel and R (Team, 2020) using One-Way ANOVA, Two-Way ANOVA, and TUKEY HSD post-hoc where appropriate testing at a significance level of 0.05.

4.3. Results: Investigating cpRNPs conservation across plant species.

The cpRNPs have been identified in multiple higher plant species, including spinach (Schuster and Gruissem, 1991), maize (Cook and Walker, 1992), barley (Churin et al., 1999), and rice (Wu et al., 2021). Ohta et al (1995) first showed the evolutionary relationships between *N. plumbaginifolia*, *N. sylvestris*, *A. thaliana*, *S. oleracea*, and *Z. mays* for three cpRNPs, demonstrating that the RNA-binding domain sequences for cp31, cp29, and cp33 were strongly conserved in three identified groups Groups-III based on amino acid similarity (Ohta et al., 1995). However, many more plant genomes have now been sequenced and are available for analysis. This chapter provides with an updated phylogenetic analysis and outlines additional subgroupings for the cpRNP family.

4.3.1. cpRNPs are conserved across green plants.

To determine the evolutionary relationships between cpRNPs reported in newly sequences plant genomes, protein sequences were identified for cpRNPs as described on the ePlant database (Waese et al., 2017). A multiple sequence analysis in MEGA X (Kumar et al., 2018) was conducted to verify structural similarities. A neighbour-joining method was then used to generate an unrooted phylogenetic tree, from which evolutionary history could be inferred (See 3.2 Materials and Methods).

The identified sequences included all 10 cpRNP sequences from *Arabidopsis thaliana*, 5 sequences from *Hordeum vulgare*, 8 sequences from *Vitis vinifera*, 7 sequences from *Medicago truncatulata*, 6 sequences from *Zea mays*, 10 sequences from *Poplar trichocarpum*, 4 sequences from *Solanum tuberosum*, 7 sequences from *Oryza sativa*, 15 sequences from *Glycine max*, 7 sequences from *Solanum lycopersicum*, 5 sequences from *Nicotiana sylvestris*, 2 sequences from *Nicotiana plumbaginifolia*, and 2 sequences from *Spinacia oleracea*. This tree, shown in Figure 4.1, indicates a wide conservation of cpRNPs between crop plants.

All cpRNPs are present across monocot and dicot plants. A phylogenetics comparison previously classified cpRNP members into three subgroups (Groups I, II, and III) based on similarity in RNA-binding domain I (Ohta et al., 1995). These subgroups are indicated in red (Group I), blue (Group II), and green (Group III) in Figure 4.1. Within these groups, members from *N. sylvestris* and *Arabidopsis* were found in all three groups. Based on these observations, Ohta et al (1995) predicted that chloroplast RNPs were therefore essential to chloroplast functions in dicot plants.

Now that additional genomes have been identified, as illustrated in Figure 4.1 cpRNPs can be seen to not be exclusive to dicot plants but widely present also in monocots like *O. sativa* (rice), *Z. mays* (maize), and *H. vulgare* (barley). Monocot RNPs have multiple members within two or more of the previously defined subgroups, indicating a strong orthologous evolutionary relationship across cpRNPs. The weakest grouping observed was for Atcp33A, for which bootstrap analysis was 57 when comparing to the other cp33A orthologues. This analysis shows that conservation of cpRNPs across both dicots and monocots may reflect their importance for chloroplast function. The phylogenetic analysis also shows that, as expected, cpRNPs in monocot plants rice, maize, and barley are more closely related to each other compared to dicot members.

Interestingly, no orthologue of Atcp33A was reported in any monocot plants in eFP tomato (Waese et al., 2017). A subsequent BLAST search (data not shown) of the Arabidopsis cp33A protein sequence in *O. sativa*, *Z. mays*, and *H. vulgare* reported close sequence matches, indicating putative proteins as orthologous candidates for Hvc33A, Oscp33A, and Zmcp33A in these organisms. Research has also experimentally confirmed the putative Oscp33A rice orthologue (Wu et al., 2021), Hvc33C (Churin et al., 1999), indicating that cp33A is also strongly conserved in monocot plants.

Subgroups I-III do not accurately describe all cpRNPs. Now that additional cpRNP members have been identified, the groupings described by Ohta et al (1995) using first RNA Recognition Motif no longer definitively describe all cpRNPs- Group I contains predominantly orthologues of AtcpSEBF and Atcp29A; Group II contains mostly 31-kDa molecular weight members and orthologs of Atcp31A; and Group III contains 33-kDa members similar to Atcp33A. Figure 4.1 shows that subgroupings can also be observed for proteins similar to Atcp28A, Atcp29C, Atcp29B, and for Atcp33C and Atcp33B together, supported by bootstrap values >80. The tree presented in Figure 4.1 was generated using whole protein sequences rather than the conserved RRM motif and so the subgroupings shown are only comparable as a guide, but nevertheless show support for the previous subgroupings and reveal additional subgroupings.

Interestingly, cpRNPs identified in *S. tuberosum* were not found to be closely related to other cpRNP subgroupings despite previously being described as an orthologue of AtcpSEBF (Boyle and Brisson, 2001), and similarly unrelated was *S. lycopersicum* cp33B. This implies that cpRNPs in *S. tuberosum* are not as closely conserved and may have varied functionality.

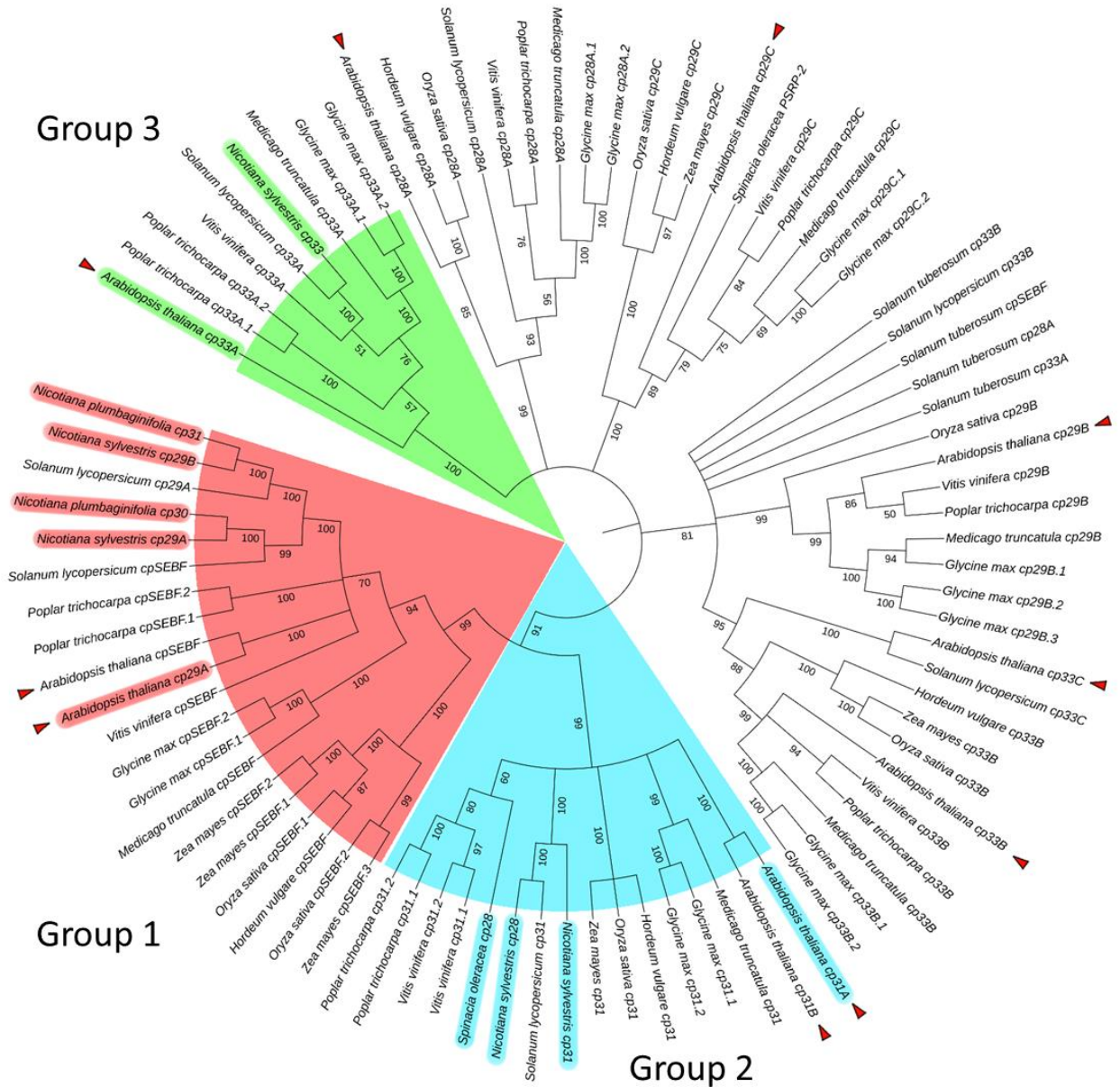


Figure 4.1. Phylogenetic analysis of cpRNP proteins from *Arabidopsis thaliana* and a range of other species. The nonrooted, bootstrapped tree was constructed in MEGA X (Kumar et al, 2018) and presented using Interactive Tree of Life (iTOL) software Letunic and Bork (2019). Evolutionary relationships of taxa were inferred using the Neighbor-Joining method (Saitou and Nei, 1987). The bootstrap consensus tree was inferred from 1000 replicates (Felsenstein, 1985) is taken to represent the evolutionary history of the taxa analyzed. Branches corresponding to partitions reproduced in less than 50% bootstrap replicates are collapsed. The evolutionary distances were computed using the Poisson correction method and are in the units of the number of amino acid substitutions per site (Zuckermandl and Pauling, 1965). This analysis involved 89 amino acid sequences from *A. thaliana*, *H. vulgare*, *V. vinifera*, *M. truncatula*, *Z. mays*, *P. trichocarpum*, *S. tuberosum*, *O. sativa*, *G. max*, *S. lycopersicum*, *N. sylvestris*, *N. plumbaginifolia*, and *S. oleracea*. All ambiguous positions were removed for each sequence pair (pairwise deletion option). There were a total of 1089 positions in the final dataset. cpRNP Groups 1, 2, and 3 are presented as described in Ohta et al (1995) in red, cyan, and green respectively. Arabidopsis cpRNPs are highlighted with red arrows.

4.3.2. Investigating sequence differences between paralogous cpRNPs.

The previously reported phylogenetics analysis (Ohta et al., 1995) and phylogram shown in Figure 4.1, revealed the paralogous gene duplication of multiple cpRNPs, including cp29A and cpSEBF, and for cp31A and cp31B. Similar potential gene duplications can also be observed in multiple crop species, such as for multiple proteins for cpSEBF in *P. trichocarpa* and *G. max*, and *Z. mays*. Functional redundancy within the Arabidopsis cpRNP family was previously described between cp29A and cp31A during mutant phenotype analysis (Kupsch et al., 2012).

To evaluate the differences between AtcpSEBF and Atcp29A and between Atcp31A and Atcp31B and how they may relate to function, a sequence analysis was performed. This was conducted using a pairwise sequence analysis via EMBOSS NEEDLE program (Madeira et al., 2019) on whole protein sequences and comparing results to protein domain function (Figure 4.2). cpRNP protein sequences contain the following domains: a chloroplast transit peptide that localises cpRNPs to the chloroplast; an acidic linker domain; and two RNA-Recognition Motifs that regulate RNA-binding divided by a spacer domain (Ohta et al., 1995; Ruwe et al., 2011). An overall view of Arabidopsis protein sequences and their domains is shown in Figure 1.2 in Chapter 1, Section 1.3.2.

Comparing Atcp29A and AtcpSEBF. Pairwise analysis reported a shared 65.2% amino acid identity between cp29A and cpSEBF, and a 71.2% amino acid similarity. The comparative sequence analysis showed minor differences in the chloroplast transit peptides, but that cp29A features a much longer RNA Recognition Motif 1 than cpSEBF (Figure 4.2), as well as a longer spacer domain.

Comparing Atcp31A and Atcp31B. Pairwise sequence analysis reported a 205/329 (62.3%) identity and a 240/329 (72.9%) similarity between protein sequences between cp31A and cp31B. Differences between the sequences showed that cp31A has a longer chloroplast transit peptide than cp31B, accounting for 7aa. cp31A also contains a longer acidic domain than cp31B (Figure 4.2).

Overall, the phylogenetics analysis presents an updated perspective on the conservation of cpRNPs between dicot and monocot species to show a strong evolutionary conservation that implies a conservation of function. This work builds on the subgroupings identified in Ohta et al (1995) and expands them, showing the need for additional subgroupings to categories all cpRNP proteins. This section also shows that the gene duplication of paralogous cp29 and cp31 variants contain notable sequence differences that will inform function.

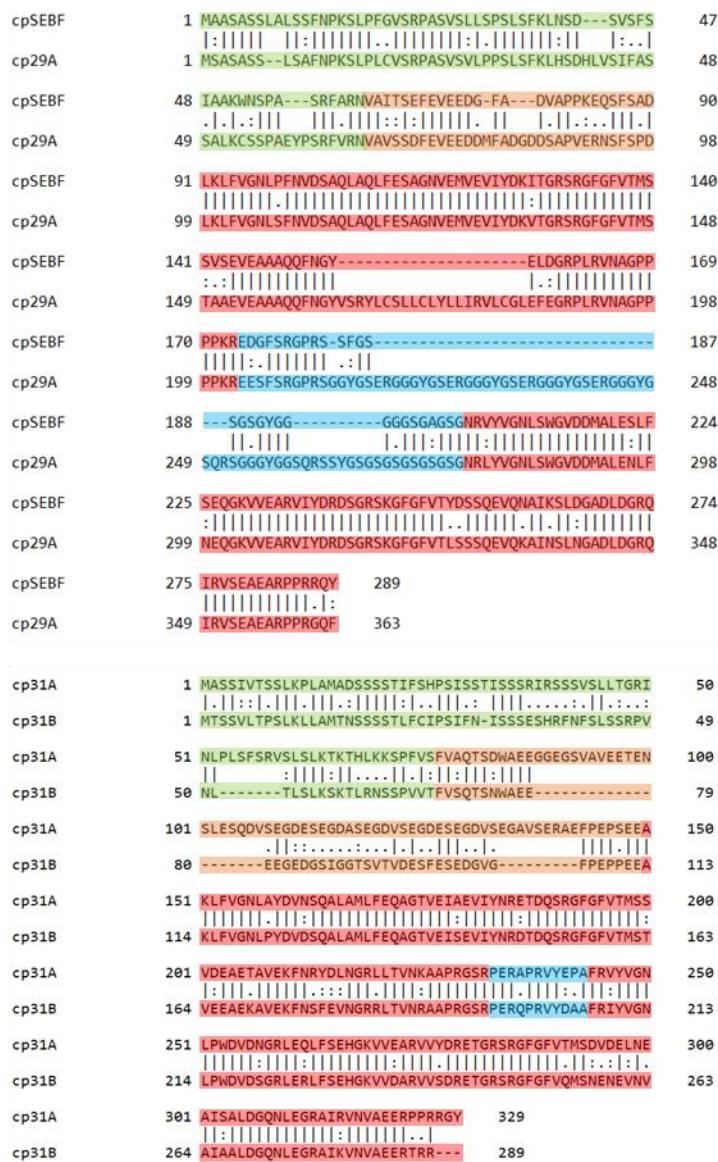


Figure 4.2. A) cp31A and cp31B, and B) cpSEBF and cp29A are likely duplications of each other. Figure shows pairwise sequence alignments of cpRNP protein sequences (Madeira et al, 2019) highlighted to show chloroplast transit peptide (green), acidic domain (orange), RNA Recognition Motif (red) and spacer domain (blue). Identical amino acids are shown with a solid dash between sequences, small positive score hits are shown with ‘,’ and a similarity between amino acids greater than 1 is shown as ‘:’. Alignment was performed using Needle EMBOSS (Thompson et al., 1994).

4.4. Results: Investigating cpRNP functionality in plastid development in *Solanum lycopersicum*

4.4.1. Tomato as a model to crop to investigate cpRNP role in plastid developmental transitions.

cpRNPs are critical to light-induced plastid greening during de-etiolation, as demonstrated in Chapter 2, section 2.3.3. Greening responses involve the activation of multiple plastome transcripts to build the photosynthetic machinery; this process involves remodelling of the plastid from an etioplast to a chloroplast and points at the importance of cpRNPs in modulating processes necessary for, or related to, plastid transitions (Mullet, 1988a). Being global post-transcriptional modulators of the plastome encoded mRNAs (Kupsch et al., 2012; Teubner et al., 2017), cpRNPs may also be involved in subsequent plastid developmental transitions, such chloroplasts to chromoplasts, being well-placed to modulate the changes in processing and stabilization to allow translation of the appropriate transcripts required to promote ATP synthesis and halt the activity of the photosystems (Livne and Gepstein, 1988).

The tomato, *Solanum lycopersicum*, is an ideal model crop to investigate chloroplast-to-chromoplast transitions including the re-organization of the plastome genome (Cheung et al., 1993); additionally, it is a plant in which cpRNPs are strongly conserved (Figure 4.1). In addition, the tomato is one of the world's most important fruit crops and one of the largest fruit horticultural crops with a market worth billions (FAO, 2019). Globally, tomato is also a key dietary source of provitamin A and antioxidants, produced in the plastidic carotenoid biosynthesis pathways (Klee, 2010). Maintaining tomato's agricultural yields and product quality in view of changing climates will be important economically and nutritionally for many cultures due to the high sensitivity of commercial tomato cultivars to environmental changes (FAO, 2019; Van Ploeg and Heuvelink, 2005).

Red light signalling pathways in Tomato are similar to Arabidopsis. Red light is an environmental input for tomato fruit development, and carotenoid accumulation (Schofield and Paliyath, 2005; Azari et al., 2010; Liu et al., 2015). Despite their evolutionary histories diverging c. 100 million years ago (Ku et al., 2000), phytochrome signalling pathways are similar between Tomato and Arabidopsis. Multiple phytochrome genes have been identified in tomato: *phyA*, *phyB1*, *phyB2*, *phyE*, and *phyF* (Hauser et al., 1997). *SphyA*, as in Arabidopsis, is abundant in darkness and degraded in the light, and the *SphyB1*, *SphyB2*, *SphyE*, and *SphyF* are light-stable and abundant in the light (Hauser et al., 1997), contributing to the photomorphogenic development (Weller et al., 2000).

Phytochromes in tomato are also tightly linked to the fruit ripening process (Piringer and Heinze, 1954) including the light-induced accumulation of carotenoids in fruits (Alba et al., 2000).

Notably, SlphyB1 and SlphyB2 are involved in regulating the timing of the fruit ripening transitions and have been linked to anthocyanin accumulation (Husaineid et al., 2007; Ernesto Bianchetti et al., 2018). Other phy-directed mechanisms, such as the role of PHYTOCHROME-INTERACTING FACTORS (PIFs) are also conserved in tomato fruit to modulate fruit carotenoid biosynthesis (Llorente et al., 2016). Fruit maturation is also driven by temperature inputs, in which elevated temperatures inhibit ripening by affecting carotenoid biosynthesis (Yoshida et al., 1984; Biggs et al., 1988), implying a link to phytochrome regulation and phyB activity as a thermosensor (Jung et al., 2016; Legris et al., 2016).

Plastid transitions in tomato. As previously mentioned, the tomato is a classical research model to investigate plastid transitions. During fruit ripening the plastids undergo extensive reorganisation, converting the photosynthetic chloroplasts to carotenoid-storing chromoplasts (Cheung et al., 1993). In addition, the genome of *Solanum lycopersicum* is fully sequenced genome and published (Sato et al., 2012), making it ideal to conduct genomic studies.

Tomato fruits appear green in their immature and pre-breaker fruit stages due to their chlorophyll content; the bright red colouration of mature fruits is achieved through the accumulation of carotenoids (Egea et al., 2010). The accumulation of high levels of carotenoids is associated to extensive modifications in the plastids, including the breakdown of chlorophyll, disruption of the thylakoid membrane from chloroplasts to form new membranes that can accumulate carotenoids in chromoplasts (Rosso, 1968; Harris and Spurr, 1969a; Harris and Spurr, 1969b). The transition also involves a decline in the expression of proteins involved in photosynthetic reactions (Piechulla et al., 1987; Livne and Gepstein, 1988) and adjustments in metabolism towards and energy consuming fruit. By the red ripe stage of fruit ripening, the plastids are almost exclusively chromoplasts (Egea et al., 2010). Real-time analysis of the transition indicated no new plastid generation, with all the chromoplasts deriving from pre-existing chloroplasts (Pyke and Howells, 2002; Waters et al., 2004; Egea et al., 2010). This transition is associated with a decline in photosynthesis-associated gene expression, and increments in the activity of different complexes such as ATPase during ripening (Livne and Gepstein, 1988).

In Arabidopsis, cpRNPs are involved in adjusting plastid gene expression to light- and temperature-environmental stimuli (Chapter 2, sections 2.3.6, 2.6). Therefore, it is reasonable to suggest that cpRNPs' regulation of the plastome may extend to the massive structural changes associated with the chloroplast-chromoplast transition, and the co-ordination with light and temperature cues.

Stages of tomato fruit ripening. Tomato fruit ripening occurs in four principle stages, starting with immature green (IG) fruits, characterised by cell expansion and an increase in weight. The second stage is the mature green (MG), when a fruit increases in size to its final mass, although this can vary enormously between cultivars and environmental influence (Gonzalez et al., 2007; Czerednik et al., 2012). Approximately 2 days after entering the MG stage, the fruit begins an extensive metabolic reorganisation and enters the first of the fruit ripening stage into the Breaker or Orange stage (BR/O) in which chloroplasts begin to transition into chromoplasts and high carotenoid accumulation begins in concert with chlorophyll degradation. The final stage is of Ripening (RR), up to 10 days afterwards and marks the end of the transition and accumulation of chromoplasts (Ho, 1986).

To investigate if cpRNPs in tomato can drive remodelling of the plastome in plastid transition stages, transcript accumulation of tomato cpRNPs was be measured during each fruit ripening stage, using a bioinformatics and experimental approach.

4.4.2 Increasing cpRNP transcript abundance indicates they remain active in chloroplast-chromoplast transitions.

To begin addressing the role of cpRNPs in chloroplast-to-chromoplast transitions in tomato, an evaluation of cpRNPs' transcript accumulation was conducted. This was conducted first using bioinformatics tools and corroborated by *in vivo* analysis of cpRNP transcript abundance during fruit ripening stages in tomato cultivar Micro-Tom (see 4.2 Materials and Methods).

Bioinformatics analysis of *SlcpRNP* transcript abundance. The Tomato eFP database, a tool within the Bio-Analytic Resource for Plant Biology (BAR) (Waese et al., 2017), was used to investigate tomato *cpRNP* accumulation during different fruit ripening stages. This showed that transcript abundance of *Slcp33A* modestly increased during in *S. lycopersicum cv Heinz 2-3cm* fruits (Figure 4.3, panel A). However, no notable transcript accumulation was observed for other *SlcpRNPs* (data not shown). An analysis *SlcpRNP* transcript accumulation from microarray data set GSE108415 (Diretto et al., 2020) of plant fruits harvested in Mature Green, Orange, and Red Ripe (Breaker +10) ripening stages in *Solanum lycopersicum* (cultivar Money Maker) was also conducted (Figure 4.3, panel B). This revealed differential accumulation of *Slcp28A*, *Slcp29A*, *Slcp31*, *Slcp33A*, and *Slcp33C*, often showing reductions in accumulation in the Orange/Breaker, and Red Ripe/Breaker+10 stages compared to the Mature Green stages of the chloroplast-chromoplast transition. However, for *Slcp33B*, an increase was observed, and an increase for *cp31* was observed between O and RR stages. This points at *SlcpRNPs* transcripts being differentially expressed during plastid transition and

may indicate functional specialisation in different plastid types and with potential impact in regulating the abundances of different plastome-encoded subunits of plastidic complexes.

Experimental analysis of *SlcpRNP* transcript abundance in tomato fruits. To verify that Micro-Tom fruits were in the correct ripening stages, transcript abundance of ripening-associated marker genes *E8*, *1-AMINOCYCLOPROPANE-1-CARBOXYLATE SYNTHASE 2 (ACS2)*, and *POLYGALACTURONASE 2 (PG2A)* were tested first (Supplementary Figure 4.2). Transcripts of these genes are expressed very low in the IG stage, modestly higher in the MG stage, and accumulation spikes dramatically in the O stage, followed by intermediate accumulation in the RR stage. All fruit samples used were confirmed for these transcript accumulation patterns.

Transcript abundance of *SlcpRNPs* was examined in Micro-Tom fruits during different ripening stages (Figure 4.4) by RT-qPCR. This analysis showed differential accumulation of multiple *SlcpRNPs* during tomato fruit maturation. *Slcp31*, *Slcp33A*, and *Slcp33B* transcript abundances increased during the Orange (O) stage from the Mature Green (MG) stage, followed by a decrease in accumulation in the Red Ripe stage. For *Slcp29A*, accumulation significantly increased during the O phase, and increased again in the Red Ripe (RR) phase. *Slcp33C* showed reductions in transcript through all four ripening stages, with significant reductions reported from the Immature Green (IG) phase to the RR phase. However, while average transcript abundance showed a reduction from IG to RR stages for *Slcp28A* and *SlcpSEBF*, no significant differences between phases was reported. Overall, this analysis indicates *Slcp29A*, *Slcp31*, *Slcp33A*, and *Slcp33B* accumulation increases significantly during the chloroplast-chromoplast transition phase, pointing at a potential functional role for these cpRNPs in the remodelling of the plastids.

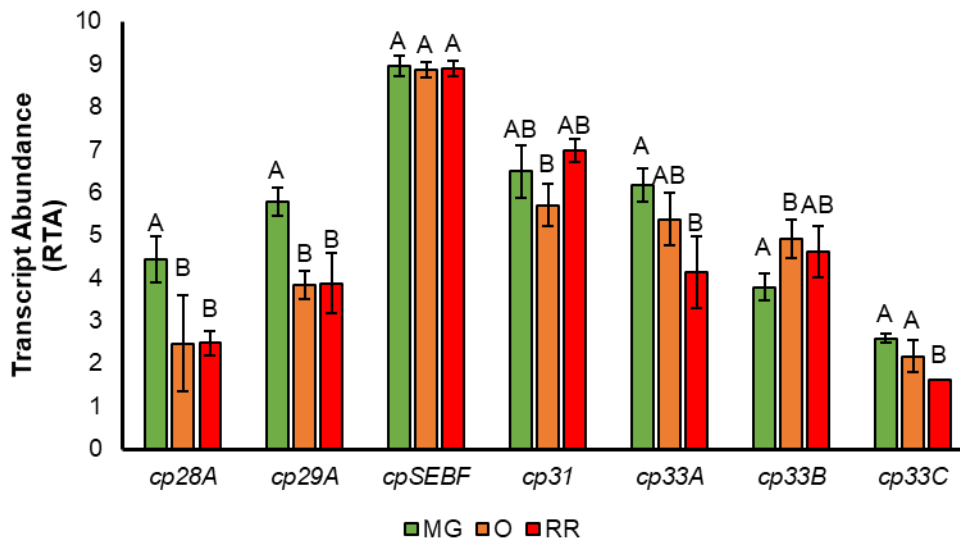
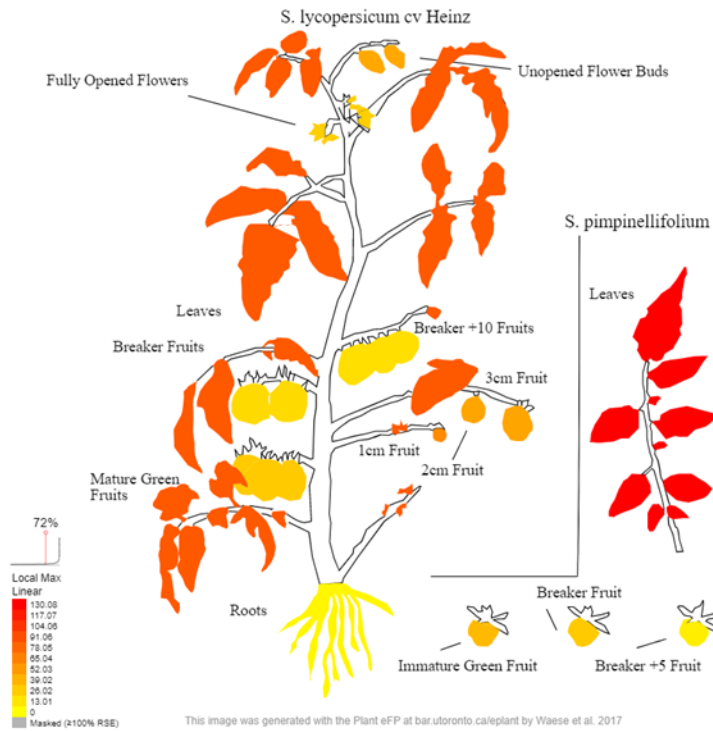


Figure 4.3. *SlcpRNPs* transcripts are differentially accumulated in ripening fruit stages. A) transcript accumulation level of *cp33A* in different tissues over time. Data was obtained and reproduced from ePlant database (Waese et al, 2017). Scale bar indicates a linear expression intensity of protein to the subcellular compartment on a scale of lowest (yellow) to highest (red) probability. B) Relative Transcript abundance (RTA) of *SlcpRNPs* in WT (cv Money Maker MM) harvested in Mature Green (MG, green), Breaker (O, orange), and Breaker+10 (RR, red) stages of fruit ripening. Data represent the average of three biological replicates and error bars represent the 95% confidence interval. Statistical significance was calculated using One-Way ANOVA with Tukey post-hoc testing ($p < 0.05$). Data that do not share a letter are significantly different.

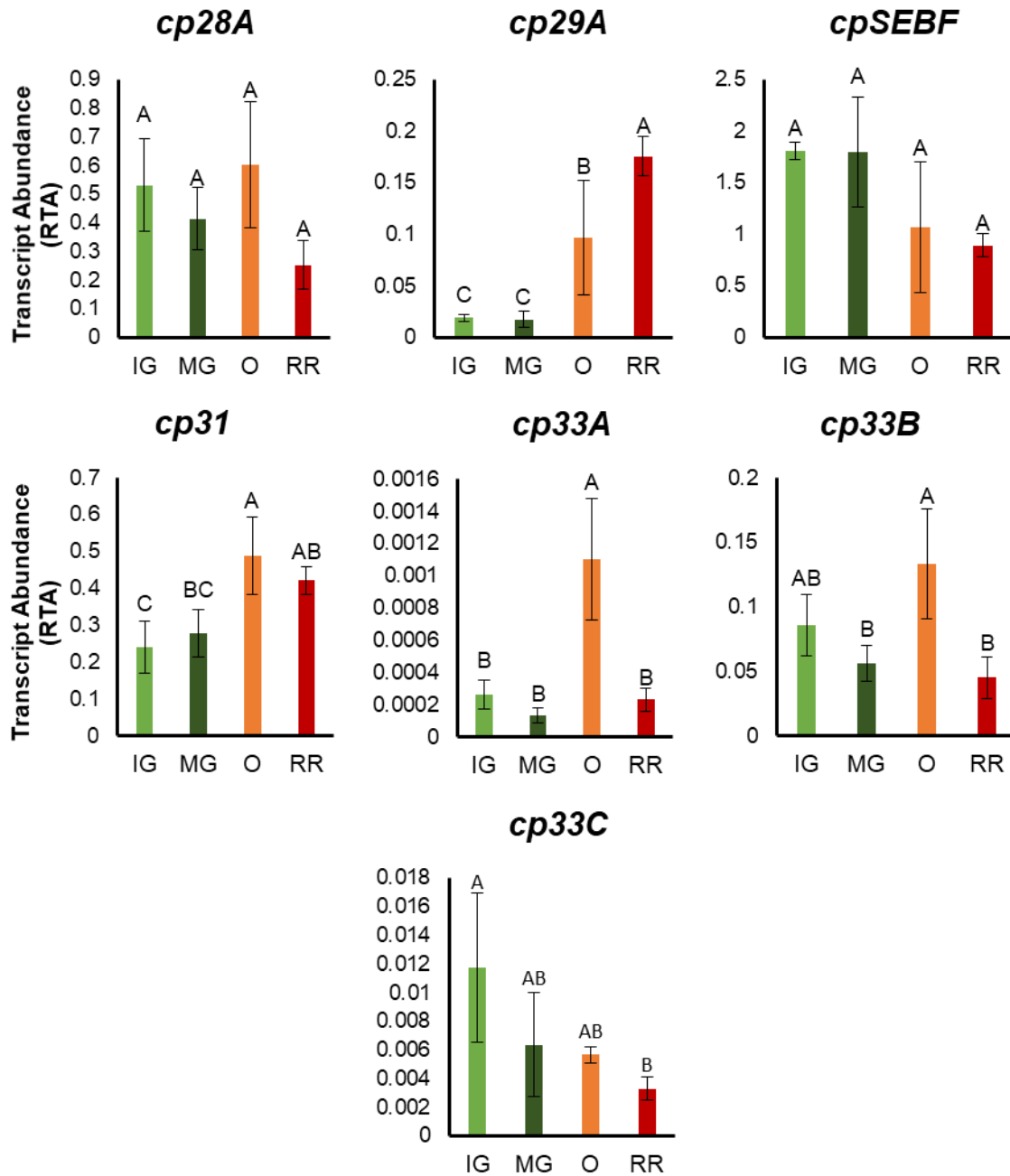


Figure 4.4. *SlcpRNP* accumulation changes with ripening progression in *Solanum lycopersicum* cultiv. MicroTom fruits. MicroTom plants were grown under standard greenhouse conditions (14 h light at $27 \pm 1^\circ\text{C}$ and 10 h dark at $24 \pm 1^\circ\text{C}$) and harvested in the necessary ripening stage. Relative transcript abundance (RTA) was calculated by comparing experimental gene expression to the reference gene *ACT4*. Data represent the average of three biological replicates and error bars show the 95% confidence interval. Statistical significance of expression between Immature Green (IG, light green bars), Mature Green (MG, dark green bars), Orange (O, orange bars), and Red Ripe (RR, red bars) was calculated using One-way ANOVA with Tukey post hoc testing ($p < 0.05$). Data that do not share a letter are statistically significant.

4.5. Results: Carotenogenesis as an indicator pathway of plastid transition in *Solanum lycopersicum*.

Carotenoids are C₄₀ terpenoid isoprenoid compounds that are synthesised by photosynthetic organisms and are essential for photoprotection against excess light. They are the most abundant naturally occurring pigments in a yellow-to-red range in fruits and vegetables like oranges, tomatoes, carrots, and pumpkin (Bramley, 2002).

Carotenoid Biosynthesis pathway. During the transition of chloroplasts-to-chromoplasts, the high accumulation of carotenoids begins. Carotenoid isoprenoids are synthesised in plastids via the methylerythritol phosphate (MEP) pathway, and are all derived from isopentenyl diphosphate (IPP) (Hirschberg., 2011), which is isomerized into dimethylallyl diphosphate (DMAPP), the substrate for GGPP synthase (GGPS) to synthesise geranylgeranyl diphosphate (GGPP), the precursor for phytoene, the first carotenoid in the biosynthetic pathway (Cunningham and Gantt, 1998; Okada et al., 2000).

The condensation of two GGPPs into phytoene is catalysed by phytoene synthase (PSY), a rate-limiting step among most organisms. Tomato contains three phytoene synthase genes, but only *PSY1* is involved in fruit ripening (Fraser et al., 1999; Kachanovsky et al., 2012), demonstrated through mutation in *PSY1* causing a yellow-flesh phenotype and absence of carotenoids in ripe fruits (Bird et al., 1991). Following the synthesis of phytoene, phytoene desaturase (PDS) and ζ-carotene desaturase (ZDS) can convert phytoene into lycopene via ζ-carotene desaturase as an intermediary (Moise et al., 2014). From lycopene, lycopene β-cyclase (LYC-B) can produce β-carotene, and lycopene ε-cyclase (LYC-E) can produce δ-carotene. α-carotene is formed as a by-product from both reactions (Moise et al., 2014).

In the breaker fruit stage of ripening, the fruit begins to turn red with the accumulation of high levels of lycopene as chlorophyll concentration decreases. In this stage, MEP-isoprenoid gene expression increases together with carotenogenic genes such as *PSY1* and *PDS*, demonstrating a transcriptional regulation of carotenogenesis (Pecker et al., 1992; Giuliano et al., 1993; Fraser et al., 1994; Corona et al., 1996; Lois et al., 2000).

Carotenogenesis is therefore a metabolic pathway whose up-regulation is linked to the transition from chloroplasts to chromoplasts. An analysis of the status of carotenogenesis in cpRNPs would be an indirect measurement of the developmental transitions in plastids and the activity of the cpRNPs beyond chloroplasts.

4.5.2 Using Virus Induced Gene Silencing (VIGS) to silence cpRNPs during plastid transitions in tomato fruits.

Section 4.4, Figure 4.4 revealed that *SlcpRNPs* transcript abundance, including *Slcp29A*, *Slcp31*, *Slcp33A*, and *Slcp33B*, is significantly increased during plastid transitions, indicating a potential role in modulating plastid-encoded mRNAs that be involved in the disassembly of the photosynthetic apparatus and the up-regulation of ATP Synthesis in plastids. To address the contribution of cpRNP proteins to plastid transitions during fruit ripening, carotenogenesis was used as an indicator of the ripening and plastids status. An *in planta* Virus Induced Gene Silencing (VIGS) method was used to silence tomato cpRNP *Slcp31* (Au - Velásquez et al., 2009).

Briefly, the RNAi silencing method utilises the bipartite Tobacco Rattle Virus to deliver a recombinant virus that carries a target gene sequence to be silenced. The virus spreads within the localised zone, and endogenous plant RNAi machinery silences all instances of the sequence through siRNAs and the RNA-induced silencing complex (RISC) machinery.

The VIGS method was performed in transgenic tomatoes that overexpress two transcription factors: *Delila* (*Del*), and *Rosea1* (*Ros1*), involved in anthocyanin biosynthesis. Called *Delila-Rosea1* (DR1) tomatoes, these fruits turn purple when ripe due to overaccumulation of anthocyanins that mask the lycopene's red colouration. The VIGS vectors contain both a sequence that silences *Del* and *Ros1* expression and a site to allow cloning of the target sequence to trigger silencing of the candidate gene of interest. Therefore, the silenced areas can be visually followed by the absence of the intense purple colouration otherwise represented by the over-accumulated anthocyanins and can be extracted and examined for co-silencing of the gene of interest.

As a positive control, a construct that silences *PHYTOENE DESATURASE* (*PDS*) was also used. *PDS* encodes the second enzyme of the carotenoid biosynthesis pathway and its silencing results in yellow fruits devoid of carotenoids, and a pale phenotype in the silenced zone (Au - Velásquez et al., 2009) (not shown). A table of the silencing constructs used is provided in the Materials and Methods (Section 4.5.2).

In these tomatoes, the silencing of a gene involved in carotenoid accumulation is seen as a delayed-accumulation phenotype with colour differences in the fruit. If transiently-silenced *SlcpRNPs* impact plastome genes, including those related to photosynthetic functions and those for other complexes necessary in different types of plastids present during tomato fruit ripening therefore altering the fruit maturation process as a consequence, this alteration will be reflected in an altered transcript accumulation for carotenogenetic genes compared to non-silenced material.

VIGS-induced silencing of *Slcp31*. Of the samples treated, only enough tissue was available for RNA extractions of *Slcp31*-silenced fruits. A representative photo of the silenced tomatoes is shown in Figure 4.5 panel A. In the picture a delayed-ripening red-green phenotype in the target zone of silenced fruits can be observed. To verify the effect of silencing on ripening, and therefore on plastid transitioning, an examination of ripening-associated marker genes was performed at a transcriptomic level.

Transcript abundance was determined for *Ripening inhibitor (RIN)*, an essential regulator of fruit ripening that activates genes such as *PSY1* and is induced after the Mature Green stage (Martel et al., 2011; Llorente et al., 2016), and for the gene *E8*, which encodes a dioxygenase enzyme that is induced at the onset of the ripening process in the 'Orange' phase (Lincoln et al., 1987; Penarrubia et al., 1992). Transcript abundance for both of these genes was significantly reduced in the *cp31*-silenced fruits compared to unsilenced control fruits treated with empty vector pTRV (Figure 4.5, panel B), showing that the ripening process had been delayed.

Finally, transcript accumulation of *Slcp31* was examined (Figure 4.5, panel C), showing a significant 50% decrease in transcript accumulation in the silenced region. To evaluate the impact that this would have on plastid transition-associated genes relevant to fruit ripening, genes in the carotenoid biosynthesis pathways were examined.

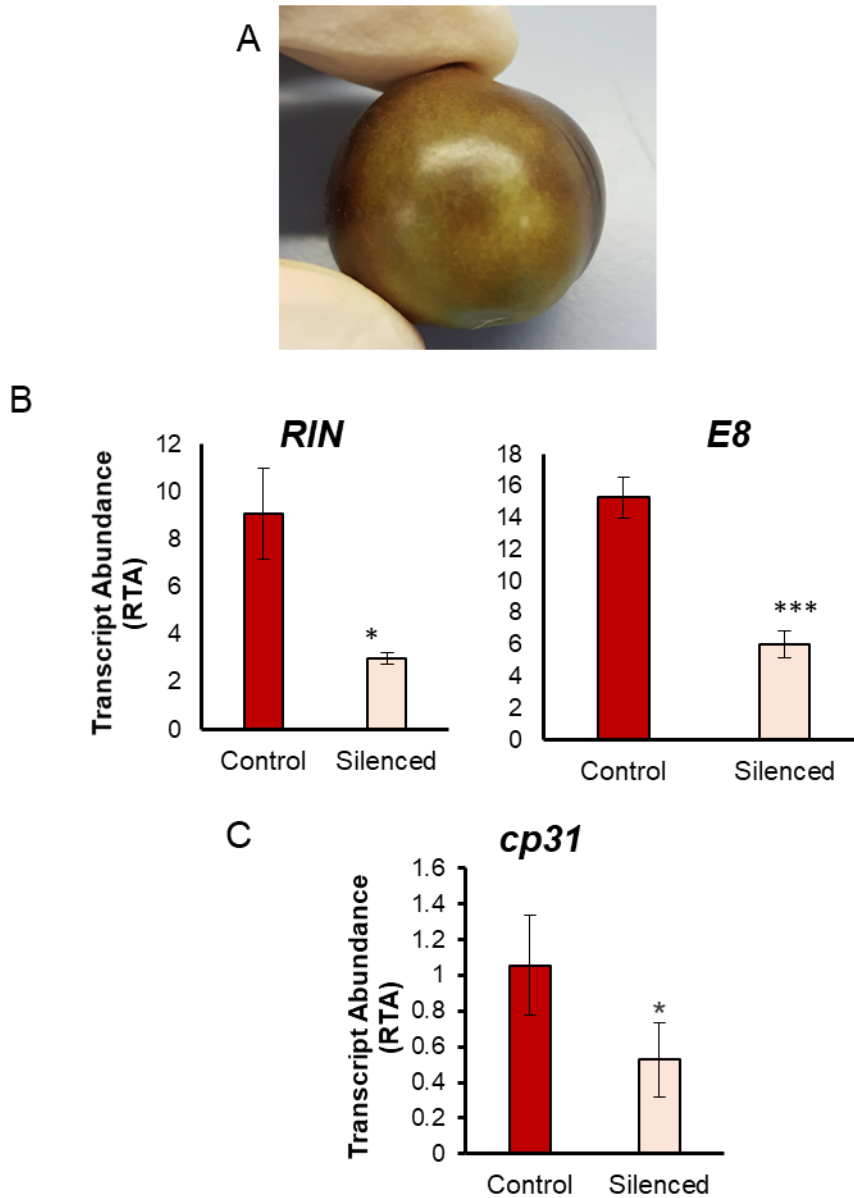


Figure 4.5. Silencing *Slcp31* in transgenic *Delila-Rosea1* fruits delayed ripening progression. A) Representative photos show a red-green phenotype in *Slcp31*-silenced fruits. RNA was extracted from silenced zones at the site of insertion, indicated with a circle by black marker pen. Graphs show reduced transcript abundance (RTA) of B) ripening-associated marker genes *RIN* and *E8* and C) *Slcp31* in *cp31*-silenced tissues (pale red bars) compared to control tissues (red bars). Relative transcript abundance was calculated by comparing experimental gene expression to the reference gene *ACT4*. Data represent the average of three biological replicates and error bars show the 95% confidence interval. Statistical significance of expression in control and silenced tissues was calculated independently for each gene using a Student's *t*-Test ($p < 0.05$). Significance is indicated using asterisks ($p < 0.05 = *$, $p < 0.01 = **$, $p < 0.001 = ***$).

4.5.3. Investigating the effects of silencing *Slcp31* on the Carotenoid Biosynthesis Pathway.

As described in section 4.4.1, the carotenoid biosynthesis pathway is over-activated in chromoplasts compared to chloroplasts. This includes the accumulation of carotenoids with different functions, such as the carotenoids with photosynthetic roles vs the carotenoids with stronger antioxidant and human nutritional roles. A summary of the pathway is shown in Figure 4.6 panel A. The pathway involves the condensation of two GGPP molecules to form 15-cis-phytoene, catalysed by Phytoene Synthase (PSY) (Ruiz-Sola and Rodríguez-Concepción, 2012). Phytoene is then converted to all-trans-lycopene by desaturation and isomerization reactions catalysed by Phytoene Desaturase (PDS) and ζ -carotene Desaturase (ZDS). These reactions are catalysed by ζ -carotene Isomerase (ZISO) and Carotenoid Isomerase (CRTISO) respectively. This produces an all-*trans*-lycopene which can then be transformed into δ -carotene or γ -carotene in a branching step through Lycopene ϵ -cyclase (LCYE) or Lycopene β -cyclase (LYCB or CYCB, wherein CYCB refers to chromoplast-associated isoforms involved in tomato fruit ripening) (Ruiz-Sola and Rodríguez-Concepción, 2012).

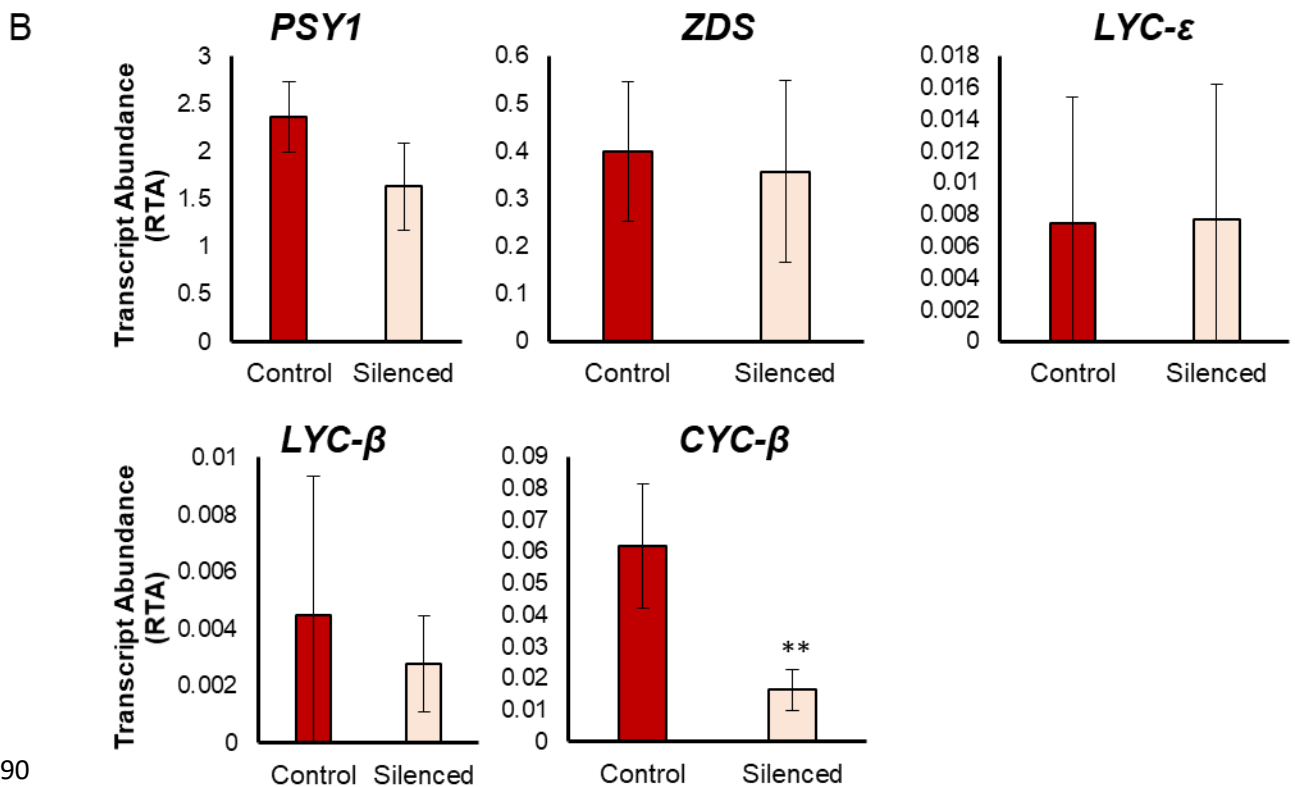
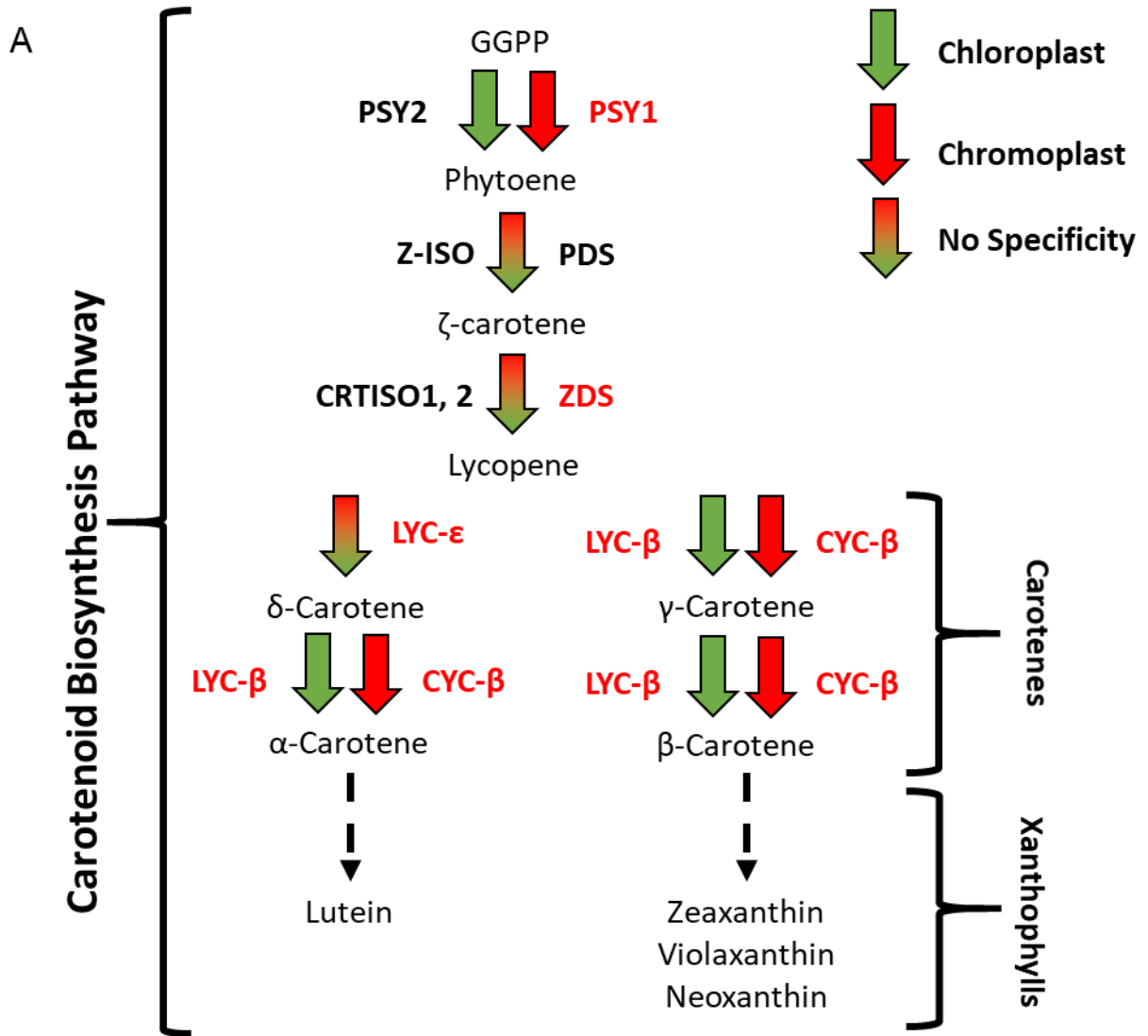
The LYCE branch produces δ -carotene, which can undergo cyclization by LYCB or CYCB into chloroplast- or chromoplast-specific α -carotene. The final product of this is the xanthophyll lutein. The LYCB and CYCB cyclization of all-*trans*-lycopene produces γ -carotene. This product undergoes a subsequent plastid-specific cyclization again by LYCB or CYCB to produce β -Carotene, a precursor for the Xanthophylls Zeaxanthin, Violaxanthin, and Neoxanthin (Ruiz-Sola and Rodríguez-Concepción, 2012).

The carotenoid biosynthesis pathway therefore contains chloroplast- and chromoplast-specific pathways, as well as proteins contributing to both. Genes *PSY1* and *CYC-B* were selected as chromoplast-specific genes; genes *ZDS* and *LYC-E* were selected as genes contributing to both pathways; and *LYC-B* was selected as a chloroplast-specific gene. If *Slcp31* is important for plastid developmental transitions, its silencing may therefore lead to altered expression these genes in different ripening stages associated to different types of plastids.

Silencing of *Slcp31* repressed-prevents the high-upregulation of chromoplast-specific *CYC-B*. This analysis revealed down regulation of *CYC-B* in *Slcp31*-silenced fruits, showing a significant 3-fold reduction in transcript accumulation. Reductions were also observed in average *PSY1* transcript levels, but statistical analysis was not significant. No reductions were observed in *ZDS*, *LYC-E*, or *LYC-B* transcript abundances between control and silenced fruits. This analysis shows that *Slcp31* is

important to the transition between chloroplasts and chromoplasts, with the impaired biosynthesis of lycopene, and a reduced accumulation of chromoplast-associated *CYC-B* transcripts. The data correlates with the green-red phenotype observed in Figure 4.5 panel A and the reduction of ripening marker genes *RIN* and *E8* (Figure 4.5, panel B).

Figure 4.6. Representation of the Carotenoid Biosynthesis pathway and effect silencing *Slcp31* on key genes associated to plastid transitions. A) Figure was reproduced and adapted from D'Andrea (2016), with acronyms for intermediates and enzymes listed in text. Arrow colour indicates which plastid the enzyme isoforms accumulate. B) Graphs show transcript accumulation of selected experimental genes (indicated in red in panel A) in control tissues (red bars) and *Slcp31*-silenced tissues (pale red bars). Relative transcript abundance was calculated by comparing experimental gene expression to the reference gene *ACT4*. Data represent the average of three biological replicates and error bars show the 95% confidence interval. Statistical significance of expression in control and silenced tissues was calculated independently for each gene using a Student's *t*-Test ($p < 0.05$). Significance is indicated using asterisks ($p < 0.05 = *$, $p < 0.01 = **$, $p < 0.001 = ***$).



4.6. Results: CRISPR/Cas9-mediated knockout of *Slcp29A*.

In November 2017, the BRAC T crop transformation facility at the John Innes Centre accepted applications for collaboration to produce CRISPR-CAS9 transgenic tomato lines. Collaboration included the design of guide RNAs selection, construct assembly, transformation, and some initial screening for the CRISPR-CAS9 mutants.

CRISPR-Cas9 is an adaptive immunity system found in prokaryotes, and is composed of a type II clustered, regularly interspaced, short palindromic repeats (CRISPR) interference system. The CRISPR loci encodes the Cas9 endonuclease that forms a complex with two short RNA molecules called CRISPR RNA (crRNA) and transactivating crRNA (tracrRNA) that guide Cas9 to cleave a site. Jinek et al demonstrated that these two short RNAs can be replaced by a chimeric single guide RNA (sgRNA) made from functional sequences of crRNA and tracrRNA to guide the endonuclease into cleaving a directed target (Mali et al., 2013; Cong et al., 2013; Jinek et al., 2012). This method has been used to induce mutations and silencing in multiple crop plants, being used in rice, wheat, barley, and cabbage, and brassica (Shan et al., 2013; Lawrenson et al., 2015).

In section 4.3.2, results show that *SlcpRNPs Slcp29A, Slcp31, Slcp33A, and Slcp33B* were significantly increased during Orange and Red Ripe fruit ripening stages, indicating a potential role for cpRNPs in the chloroplast-to-chromoplast transitions potentially participating in plastid reorganisation and development. Of these candidate cpRNPs, *Slcp29A* was selected in collaboration with BRAC T for its increased accumulation in the latter two stages of fruit ripening (Figure 4.4).

Generation of CRISPR-CAS silenced plants. Two sets of guides, shown in Figure 4.7, were designed with the BRAC T collaborators to target the first exon of *Slcp29A* with no risk of off-target mutations. This would create an easily identifiable large deletion detectable by PCR screening.

A single T-DNA construct was transformed into immature embryos and stable transgenic lines that contain targeted mutations regenerated through tissue culture. These mutations can then be detected in T0 plants that were screened and segregated to T1 and T2 generations to provide lines cis-genic lines that carry the mutation of interest in the target locus.

T0 transformed plants were generated by BRAC T collaborators. These plants included a transgene for kanamycin resistance, allowing for initial screening to confirm that T-DNA is present before any subsequent PCR screening to select mutant plants. Antibiotic-treated plantlets were dispatched to Lancaster University in February of 2020. However, the COVID-19 pandemic only allowed the collection of the seeds for future screening.

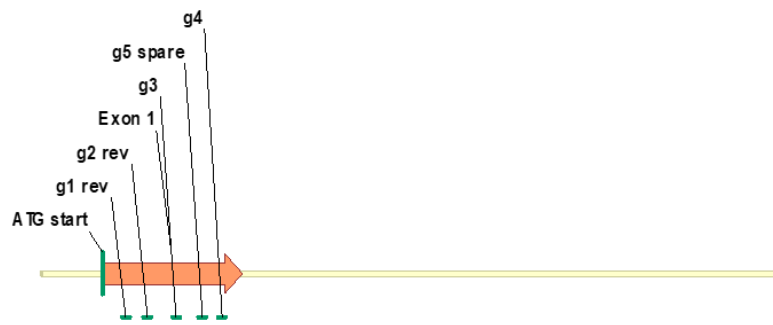


Figure 4.7. Crispr/Cas-9 construct guides and target developed alongside BRAC1 partners, showing targets for in exon 1 of *cp29A.1*.

4.7. Discussion.

4.7.1. Members of the Arabidopsis cpRNPs family are conserved across multiple dicot and monocot crop species.

Prior phylogenetic analysis of cpRNPs showed that cp29, cp31, and cp33 were conserved across dicot species including *A. thaliana* and *N. sylvestris* (Ohta et al., 1995). This analysis also hinted at conservation of cpRNPs in monocot species such as maize (Cook and Walker, 1992); presence of Hvc31A, Hvc31B, and Hvc33A in barley (Churin et al., 1999), and orthologues of all ten Arabidopsis cpRNPs in rice (Wu et al., 2021). Phylogenetic analysis also described three subgroups of cpRNPs (Groups I-III) based on sequence similarity (Ohta et al., 1995); since this initial phylogenetic studies many more sequenced genomes and cpRNPs' amino acid sequences became available.

Using data published on the ePlant database from isolated and published cpRNPs as well as bioinformatically predicted cpRNPs (Waese et al., 2017), this chapter presented a new phylogenetic tree (Figure 4.1) which revealed a strong conservation of cpRNPs across monocots as well as dicots, spanning food crops such as maize, barley, rice, and tomato, to the trees like poplar and grape vines (Figure 4.1). While not a fully comprehensive study, since the ePlant database did not include cp33A orthologues identified in barley (Churin et al., 1999) and rice (Wu et al., 2021), and putative bioinformatically- identified cpRNPs in maize (Schnable et al., 2009), the new extended phylogenetic tree revealed a close evolutionary conservation of cpRNPs in Arabidopsis and multiple monocot and dicot species, indicating that cpRNPs' function is critical to plant growth. Ultimately, cpRNPs' conservation between monocots and dicots may point at a general contribution to the regulation of photosynthesis-related processes and plastid functions across higher plants.

The previous phylogenetic analysis conducted by Ohta et al (1995) described Groups I, II, and III based on amino acid similarity in the highly conserved parts of the first RNA recognition motif in each sequence. This identified Arabidopsis cp29A, *N. sylvestris* cp29A and cp29B, *N. plumbaginifolia* cp30 and cp31 in Group I; Arabidopsis cp31A, *Z. mays* NBP, *N. sylvestris* cp28 and c31, and *S. oleracea* cp28 in Group II; and Arabidopsis cp33A and *N. sylvestris* cp33 in Group III. An updated version of the cladogram included *H. vulgare* cp31A and cp31B in Group II, and cp33A in Group III (Churin et al., 1999). Although the phylogenetic tree in this chapter differs in its constructed, instead using full length protein sequences with the intention of establishing if divergent parts of the protein could change the current groups' classification, the results obtained indicated that the subgroups' classification remained valid, but at the same time classified new cpRNPs within these groups. This included Arabidopsis cpSEBF's addition to Group I, and Arabidopsis cp31B to Group II. Furthermore,

the new tree also revealed that cp28A, cp29C, cp29B, and cp33B/cp33C orthologues form distinct, undefined subgroups, and highlighting the need for additional subgroups beyond the three subgroups identified by the RRM-based subgroupings that could be described as Groups IV, V, VI, and VII.

Most of these subgroups contain only a single *Arabidopsis* cpRNP member, but there are instances of multiple cpRNPs in some subgroups. Atcp29A and Atcp29B are part of Group I, and Atcp31A and Atcp31B in part of Group II. These proteins have previously been identified as paralogous duplicates attributed to gene duplications (Tillich et al., 2009; Ruwe et al., 2011). Additional duplication events may also have occurred in multiple putative cp31 proteins in *G. max*, *V. vinifera*, and *P. trichocarpa*, and barley (Churin et al., 1999). Beyond phylogenetic groupings, a comparative sequence analysis between cpRNPs in *Arabidopsis* provided insights on potential functional differences between members. For example, *Arabidopsis* cp29A, a paralogue of cpSEBF, contains a longer chloroplast transit peptide, a longer RNA Recognition Motif (RRM), and a longer spacer domain between RRMs compared to cp29A (Figure 4.2). These differences in the RRM suggest that binding properties may vary between the two proteins with potential impact in target recognition. While published RIP-chip data for reporting the of cp29A mRNAs targets is available (Tillich et al., 2009), a similar study for SEBF has not been conducted, but could provide with insight into changes in binding specificity, preferential targets and joint/differential regulatory functions.

The spacer domain is proposed to be involved in the prevention of non-specific interactions between discrete protein domains, but glycine-rich linkers are flexible and promote domain-domain interactions (Reddy Chichili et al., 2013). Compared to cpSEBF, the spacer domain in cp29A is rich in glycine and serine residues and bears three tandem repeats of a sequence (GSERGGGY) (Ohta et al., 1995). This may indicate that the RRM domains of cp29A could be interacting with each other in a way that the RRMs of cpSEBF cannot. These interactions could play a role in the differential affinity for RNA and/or the target specificity, or the capacity to respond to specific environmental stimuli.

In addition, post-translational modifications may also be associated to variations in the cpRNPs' structure and function. A phosphorylation site has been previously detected in the linker domain between RRMs of cp29A (Reiland et al., 2009), and phosphorylation sites have been connected to light sensitivity (Kleffmann et al., 2006) and RNA binding specificity (Loza-Tavera et al., 2006; Okuzaki et al., 2019). The linker structural differences between different cpRNPs, such as cpSEBF and cp29A, may be relevant to control responsiveness to light or other environmental stimuli, and lead to non-redundant functions among the family members. Physiological data (Chapter 2) already points at a non fully-functional redundancy among cpRNPs such as cp31A and

SEBF, despite a joint contribution to a global greening response. Similar phenotypes may be associated to the regulation of common, as well as different, plastome transcripts (Chapter 2, Figure 2.5), and further exploration of full genome targets under different environmental conditions will further address specificity and redundancy among family members and evaluate a combinatorial effect.

The pairwise comparison of cp31A and cp31B in Figure 4.2 showed a longer acidic domain present in cp31A located between the chloroplast transit peptide and the first RRM. In this respect, cp31A's longer acidic domain is also the longest of the Arabidopsis cpRNPs, followed by cp33A (Figure 1.1). An analysis of functional redundancy using *cp31a* and *cp31b* single and *cp31a cp31b* double mutants revealed functional redundancy between the two in the editing of plastome mRNA targets. Yet, some editing events depended required the presence of both cpRNPs (Tillich et al., 2009), again pointing at a non fully-functional redundancy. The difference in the acidic linker domain may be involved in regulating cp31A's differential binding specificity; while comparative structure-function experimental studies have not been conducted, phosphorylation of acidic linker domains are also suggested to be involved in modulating cpRNP binding specificity (Lisitsky and Schuster, 1995; Okuzaki et al., 2019). cp31A's acidic domain contains Ser-phosphorylation sites (Reiland et al., 2009), but pairwise alignments (Supplementary Figure 4.1) revealed that these sites are not present in cp31B, and cp31B is not reported as a phosphoprotein. Therefore, the absence of this acidic domain in closely related cpRNPs such as cp31B and cp31A may be related their differential sensitivity to stimulus and the fulfilment of specific functions.

Alternatively, these functions could also involve protein-protein interactions (Li and Sugiura, 1990). cpRNPs associate with a High Molecular Weight Complex (HMWC) that is involved in RNA processing and degradation in spinach (Hayes et al., 1996). HMWCs associated to cpRNPs conduct the 3' processing of chloroplast mRNAs, including both site-specific endoribonucleases and PNPase-like non-specific exoribonucleases. Biochemical evidence indicates that in the absence of cpRNPs, 3'-end maturation of plastid mRNAs is prevented and the mRNAs are instead degraded (Hayes et al., 1996). It is possible that the acidic linker domain is involved in mediating the protein:protein interactions within the cpRNPs and the components of these RNA processing complexes. While this possibility awaits investigation, it may explain the association of cpRNPs with multiple post-transcriptional events including processing, splicing, and editing.

cpRNPs may be specific to green plants and have eukaryotic, not prokaryotic, origins.

Chloroplasts and the photosynthetic apparatus are derived from cyanobacterial endosymbionts. Since cpRNPs are critical to chloroplast functions and greening, they may have evolved alongside photosynthesis in cyanobacteria, algae or in early plants. An investigation of cpRNP orthologues in the bryophyte *Physcomitrella patens* revealed 25 putative chloroplast RRM-domain containing proteins (Uchiyama et al., 2018). Two of these RRM-containing proteins shared a >40% amino acid similarity to Arabidopsis cpRNPs cp28A, cp29B, and cp31B and were identified as the cpRNP-like PpRBP2a and PpRBP2b. Like Arabidopsis, both PpRBPs were cold-inducible at 4°C (Amme et al., 2006; Sarhadi et al., 2010), but a mutant phenotype analysis revealed no effect on mRNA processing or RNA editing. This showed that despite some structural similarity, *P. patens* cpRNPs may be functionally distinct (Uchiyama et al., 2018), and hint at a possible cpRNPs convergent evolution in the function of RRM domains after the appearance of land plants.

Furthermore, a published phylogenetic comparison of cpRNPs with RNPs from cyanobacteria revealed a greater sequence similarity of Arabidopsis cp29A and cp31A, and *N. sylvestris* cpRNPs to the eukaryotic heterogeneous nuclear ribonucleoprotein (hnRNP) family than to older chloroplast ancestor cyanobacteria (Maruyama et al., 1999). hnRNPs are a diverse family of RNA Recognition Motif (RRM) and K homology (KH) domain-containing proteins that post-transcriptionally regulate nuclear RNAs through capping, pre-mRNA splicing, and polyadenylation (Burd and Dreyfuss, 1994). Maruyama et al (1999) therefore suggested that cpRNPs diverged from other eukaryotic RNA-binding proteins to regulate the chloroplast genome and were not derived from a cyanobacterial ancestor, unlike much of the chloroplast proteome (Abdallah et al., 2000; Yagi and Shiina, 2014). This correlates with the multiple functional roles of cpRNPs in the post-transcriptional regulation of the plastome mRNAs, while the regulation of the cyanobacterial plastome is far less complex than the eukaryotic plastome (Yagi and Shiina, 2014). The cpRNPs' divergence from other eukaryotic genes may have been part a mechanism for plants to moderate chloroplasts functional mRNAs in higher green plants.

4.7.2. cpRNPs are active in different plastids.

cpRNPs' functions during de-etiolation are important for greening and are critical for the accumulation of plastome encoded photosynthetic mRNAs and nuclear-encoded photosynthesis-associated mRNAs whose protein products are imported to the chloroplast (Schuster and Gruissem, 1991; Churin et al., 1999). During red light-mediated de-etiolation, etioplasts, which lack chlorophyll,

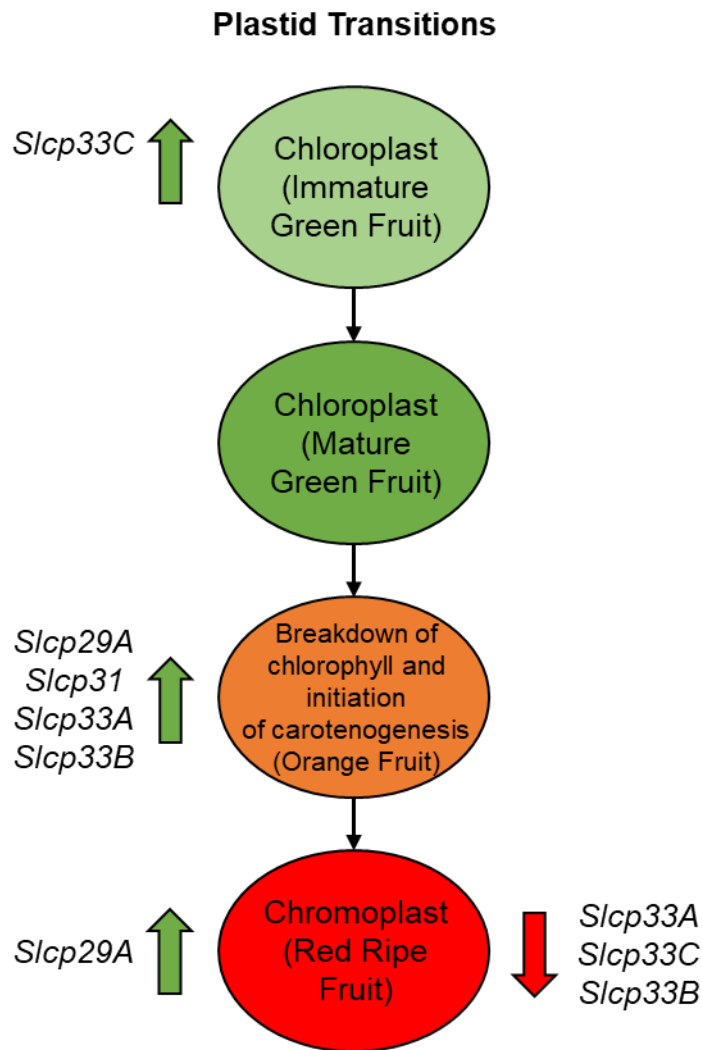


Figure 4.8. A model showing *Solanum lycopersicum* cpRNPs are up- and down-regulated during different plastid transition stages correlating to different tomato fruit ripening stages.

differentiate into chloroplasts in response to light stimuli in a phy-mediated pathway (Mullet, 1988a; Tepperman et al., 2006). Yet, the role for cpRNPs could extend to other plastid transitions, such as the transition of chloroplasts to chromoplasts in fruits. To gather initial evidence for this possibility, closely related cpRNP orthologues of Arabidopsis were selected for preliminary studies in *Solanum lycopersicum*, a model organism for addressing chloroplast-to-chromoplast transition.

During tomato fruit ripening, a change in colour is associated to transitions between different plastids. Green tomatoes accumulate chlorophyll in chloroplasts, while the high accumulation of red lycopene is linked to chromoplasts (Cheung et

al., 1993). 7 cpRNP proteins have been identified in tomato, and they are closely conserved with Arabidopsis cpRNPs (Figure 4.1). During fruit ripening, phy-dependent light- and temperature-sensitive pathways impact fruit ripening (Hauser et al., 1997; Alba et al., 2000; Weller et al., 2000; Llorente et al., 2016). Considering that the chromoplast transition is essential for fruit maturation and the accumulation of nutritious carotenoids in tomato fruits, dissecting the regulatory components involved in adjusting the plastid and nucleus transcriptomes that lead to the disassembly of photosynthetic apparatus and the changes in metabolic activities for chromoplast functions is of relevance.

Bioinformatic and experimental analysis of *SlcpRNP* transcript abundances showed significant increases in *Slcp29A*, *Slcp31A*, *Slcp33A*, *Slcp33B* during the Orange or Red Ripe stages compared to Immature and Mature Green stages, and higher levels of *Slcp33C* and *Slcp28A* in the green stages (Figures 4.3, 4.4) (Diretto et al., 2020). This suggests functional specialization of the cpRNPs during the ripening process, and therefore in plastid transitions. Differential accumulation of cpRNPs in Green stages may indicate a preferential function in chloroplast functions, and accumulation in the Orange stage may suggest a role in the dismantling of thylakoid photosynthetic apparatus to allow transition to chromoplasts. A presence of cpRNPs in the Red stage suggests a role in the regulation of chromoplast-specific processes such as carotenogenesis. Specialised roles for cpRNPs in integrating different environmental signals may allow the co-ordination of specific functions to environmental stimuli and the co-ordination of inter-organellar genome responses to pace the transitions and is worth exploring in future experiments. A summary of these findings is presented in Figure 4.8.

A role for cpRNPs in a potential chromoplast-to-chromoplast transition is also supported by transient silencing experiments of *Slcp31* that showed a delay in ripening with reduction in markers of ripening progression *RIN* and *E8* (Penarrubia et al., 1992; Llorente et al., 2016). In addition, in silenced *Slcp31* fruits, accumulation of *SICYC-B*, a chromoplast associated gene for carotenoid biosynthesis was significantly lower (Figures 4.5, 4.6). This indirectly indicates that presence of *Slcp31* may impact a fruit's capacity to conduct plastid transitions. Based on their functions and identified targets, including PSI, PSII and ATPase plastid-encoded mRNAs, cpRNPs may be linked to the switch between active photosynthetic complexes in chloroplasts and the enhancement of the ATP synthase machinery required to drive the transition and to maintain a high metabolic activity in chromoplasts once the photosynthetic machinery is disassembled (Livne and Gepstein, 1988). In this respect, redirecting the types of messages that are stabilized in different plastids may be a key role for the cpRNPs to permit shifts in the active functions in different plastids.

This chapter highlights novel possibilities and complex roles for cpRNPs in plastid developmental transitions and in different types of plastids, as cpRNPs are now observed to impact both de-etiolation during the etioplast-to-chloroplast transition in photomorphogenesis as well as in the chloroplast-chromoplast transitions during fruit ripening. Future characterisation of their role in modulating the plastome and integrating environmental signals in a developmental context may be of high interest to better understand not only photosynthesis, but also for fruit maturation, fruit nutritional content, and yield.

Chapter 5. General Discussion of Results.

5.1. Novel mechanisms behind the photoreceptors' modulation of greening and photosynthetic responses

The importance of photoreceptors to photosynthetic metabolism has been widely acknowledged for a long time, but beyond the modulation of PhANGS via nuclear transcriptional cascades, the involvement of photoreceptors in other mechanisms for the establishment and environmental adaptation of photosynthesis remains an active field of research. In particular, the role and mechanisms through which light photoreceptors contribute to the co-ordination of photosynthetic responses across multiple organelles is not fully understood.

Notably, photosynthesis requires the co-ordination of genes from two organelles, the nucleus and the chloroplast, for the construction and maintenance of photosynthetic apparatus (Soll and Schleiff, 2004). However, both genomes are subject to different levels and mechanisms of genomic control; the eukaryotic nuclear genome is regulated by a strong transcriptional influence, but the plastid genome, due to its prokaryotic origins, requires an important contribution of post-transcriptional regulation (Deng et al., 1989; Shi et al., 2016).

Light photoreceptors have recently been more tightly linked to the modulation of the plastome: studies on plastid transcripts accumulation have shown a contribution of the phytochrome and cryptochrome photoreceptor families in photoperiodic conditions (Michael et al., 2008; Facella et al., 2017). Notably, Facella et al (2017) demonstrated a strong contribution of CRY2 to the global modulation of the plastome under Long Day photoperiods, but the global role of phy had not been previously investigated. This thesis presents bioinformatic analyses of phyB's role in the modulation of the plastome in Short Days (SD) (Mockler, 2007), showing a wide-spread impact over all plastid-encoded gene families (Griffin et al., 2020) (Chapter 2). This represents a marked extension of the known roles of phy in greening responses (Lifschitz et al., 1990).

Yet, experimental data provided in this thesis shows that phyB is not only a major regulator of the plastome in SD conditions but also during de-etiolation, a stage during photomorphogenesis where the photosynthetic apparatus is assembled for the first time and where a plant has very active mechanisms of environmental adaptation to properly build and modulate photosynthesis (Armarego-Marriott et al., 2020) (Chapter 2, section 2.3). Furthermore, bioinformatics analysis conducted in this thesis showed that beyond the previously described transcriptional modulation of the plastome genes by phy-mediated, light-modulated components such as HEMERA (HMR) and the sigma factors that operate with the RNA polymerases (Oh and Montgomery, 2014; Qiu et al., 2019),

phyB also contributes to the modulation of plastid-encoded mRNAs through post-transcriptional mechanisms (Chapter 2, section 2.3). This discovery expands phyB's contributions to a different level, showing a global role essential for the maturation of chloroplast encoded mRNAs, and vital for the production of photosynthetic proteins in the plastids (Deng et al., 1989; Griffin et al., 2020).

One of the molecular components of the post-transcriptional pathways that phyB regulate is the chloroplast RNA Binding Protein family (cpRNP) (Ye et al., 1991). The cpRNP protein family is capable of global binding to the plastid encoded mRNAs (Kupsch et al., 2012; Teubner et al., 2017), and evidence in Chapter 2, section 2.3.2 indicated that cpRNP expression is phyB-dependent. This thesis also provided with experimental evidence to show that cpRNPs contribute to the regulation of the plastome during de-etiolation, and that the defects in plastome-encoded transcripts accumulation observed in *cpRNP* mutants contribute to the alterations in greening responses detected in mutant phenotypes (Chapter 2, section 2.3.2, section 2.3.7). The placement of post-transcriptionally acting cpRNPs in a phyB-dependent signalling pathway that can deliver environmental signals perceived by the receptors to most of the genes encoded in the plastome represents an expansion in the previously defined mechanisms of phytochrome signalling to the chloroplast.

The thesis also examined which light signalling components may act with photoreceptors to transduce signals for the control of plastome-regulating proteins (Chapter 2, section 2.3.8). Examination of the bZIP transcription factor HY5, a downstream component of R-phyB and B-cry2 cascades to the plastome (Wang et al., 2017), demonstrated that HY5 shares the light dependent modulation of plastome-encoded genes with R-phyB- and/or B-cry2 (Griffin et al., 2020). Experimental data presented corroborated an effect on plastome transcripts by the *hy5* mutation for the first time, as well as an effect of HY5 on the accumulation of *cpRNP* transcripts. The modulation of HY5 on the transcript levels of *cpRNPs* is supported by microarray analysis showing that *cp31A* accumulation is HY5-dependent (Ma et al., 2005); and genome wide chip experiments for HY5 point at a potential direct control by direct promoter binding to *cpRNPs* such *cpSEBF* (Jiao et al., 2007). Data gathered expands our understanding of the influence of HY5 over photosynthesis, extending it to novel components involved in the modulation of greening and which have an effect over the plastome encoded genes necessary to build photosynthesis. Furthermore, the involvement of B-cry2 in the regulation of the plastome and in the regulation of HY5 suggests further new avenues of investigation for the cpRNPs in blue light signalling pathways (Griffin et al., 2020).

The placement of cpRNPs in phyB signalling cascades, opened up the possibility of a wider range of environmental stimuli that are perceived and transduced by these components. In addition

to providing downstream components with a responsiveness to red light signals during de-etiolation (Quail, 2002; Tepperman et al., 2006), phyB is a sensor of photoperiodism and light intensity (Blázquez and Weigel, 1999; Loudet et al., 2008; Kaiserli and Chory, 2016), a temperature-sensor (Jung et al., 2016; Legris et al., 2016), and is involved in the communication between the plastids and the nucleus via anterograde and retrograde signals (Martín et al., 2016; Jiang et al., 2020). This thesis showed that as phyB signalling components, cpRNPs play an important role tuning greening and biomass accumulation responses to environmental conditions, with an important effect over photosynthesis (Chapter 2). Experimental evidence gathered further showed the potential of cpRNPs to co-ordinate photosynthesis across two genomes (Chapter 3). Their responsiveness at the level of transcript and/or protein accumulation to temperature, photoperiodism and activation of retrograde signals, together with their global modulatory capacity of plastid transcripts make them powerful components to deliver information to orchestrate environmental responsiveness of chloroplast metabolism, but also to respond to emitted chloroplastic signals.

5.2. cpRNPs are key regulators of transcripts encoded in the plastome and in the nucleus and could synchronise photosynthesis to the environment.

Previously, cpRNPs have been described as regulators of plastid-encoded functions of photosynthesis (Tillich et al., 2009; Kupsch et al., 2012; Teubner et al., 2017). This thesis supports this model, demonstrating that during red-dependent de-etiolation, cpRNPs contribute to plastid-encoded photosynthesis-associated processes, affecting mRNAs that encode for proteins involved in ATP Synthesis, NADH Dehydrogenase, PSI, and PSII processes (Chapter 2). However, this thesis also introduces multiple additional roles for cpRNPs, expanding our understanding of cpRNPs functionality (Chapter 2, Chapter 3, Chapter 4).

In addition to linking cpRNPs to perception and transduction of multiple environmental conditions, an additional key role of phyB is mediation of cpRNP subcellular localisation by modulating the expression of different cpRNP isoforms via alternative transcriptional start sites (Ushijima et al., 2017). The data presented in this thesis demonstrates that phyB-mediated cpRNP isoforms with differential localisation does occur *in planta*, and localise to the nucleus in addition to the previously described chloroplast localisation. The alternative nuclear localisation extends the cpRNPs function to a role beyond the chloroplast, in this respect the data gathered in Chapter 3 showed that transcript accumulation for Photosynthesis-associated, nuclear-encoded genes (PhANGs) is also altered *cpnp* mutants. Alterations include effects on subunits of the NADH Dehydrogenase (*PSBQI2*), and PSI (*PSAN*) that are counterparts to some of the plastome-encoded

transcripts (*ndhF*, *ndhG*, *psaJ*) for photosynthetic complexes also under cpRNPs regulation (Kupsch et al., 2012; Okuzaki et al., 2019).

However, an effect of cpRNPs was also detected over the Light Harvesting Complexes 2 and 1 (LHCII, LHCI), the Oxygen Evolving Complex (OEC), and photoprotection involved genes such as *PSB27* and *DEG1*, which contribute to the light-intensity adaptations and turnover of PSII antenna protein D1 (Hou et al., 2015; Schuhmann and Adamska, 2012). This suggests that cpRNPs' co-ordination of photosynthesis could be wide-reaching, extending to both, the co-ordination of subunits of the photosystems across two genomes, but also the turnover and tuning of proteins associated to photosynthetic functions without a chloroplast-encoded component.

Although the exact mechanism regarding how cpRNPs may act in the nucleus was not dissected here, the experimental evidence presented in this thesis supports a regulatory capacity for cpRNPs over both organelles that shows they bridge the nucleus-plastid divide, and are involved in inter-organelle communication for the regulation of photosynthetic processes and in a changing environment. The data gathered supports a wider influence of cpRNPs on photosynthesis; while a direct RNA binding has been demonstrated for cpRNPs in the plastome (Tillich et al., 2009; Kupsch et al., 2012; Teubner et al., 2020), it is yet to be determined how they modulate nuclear transcripts. A direct role for cpRNPs in the nucleus is supported by previously published research that identified nuclear STEP1, an alternative isoform of cp31A with an identical amino acid sequence to the phyB-mediated cp31A (TSS_B) isoform (Kwon and Chung, 2004). This isoform was observed to bind to single-stranded G-rich DNA sequences characteristic of telomeres (Dionne and Wellinger, 1996), and provides a precedent of a potential nuclear role for cp31A in preventing the access of nucleases to single-stranded telomeric DNA and modulate telomere replication, protecting cells from apoptosis (Kwon and Chung, 2004). Although not investigated further in this thesis, this role may be related to cpRNP's possible evolutionary similarity to the hnRNPs (Maruyama et al., 1999).

Importantly, the effects over genes encoded in two organelles were not only light quality-dependent, but extended to a temperature responsiveness. When grown in cold or warm ambient temperature conditions, nuclear- and plastome-encoded transcripts were differentially modulated in *cprnp* mutants, with cpRNP contribution changing in strength as well as in target specificity (Chapter 2, section 2.6). Overall, this supports a potentially combinatorial role for multiple cpRNPs, in which they may all contribute to the regulation of photosynthesis, but different family members integrate responsiveness to multiple environmental signals. By each having a specific response and role linked to environmental cues, cpRNPs can effectively and differentially orchestrate proper photosynthetic responses, contributing to a more energy-efficient regulation. While the exact mechanism of how

temperature affects cpRNP function was not addressed in this thesis, some of the specificity may be modulated by post-translational modifications, as phosphorylation is involved in controlling cpRNP function in the cold (Okuzaki et al., 2019) and in the light (Lisitsky and Schuster, 1995), and phosphorylation sites have been identified in cp31A, cp29A, cp29B, cp33B, and cpSEBF (Reiland et al., 2009; Roitinger et al., 2015). However, whether this mechanism affects cpRNPs function in a wider range of environmental conditions and whether phosphorylation is linked to photoreceptors signals remains to be examined.

Interestingly, the subcellular localisation of cpRNPs was also impacted by both temperature and retrograde signals. Therefore, the evidence suggests that by controlling alternative transcriptional start sites of the *cpRNPs*, phyB could deliver a wide range of stimuli to two genomes to properly adjust photosynthesis to external cues (Chapter 3, section 3.5). Although no experimental evidence was gathered to support this possibility, bioinformatic evidence indicates the presence of HY5 binding motifs in the *cpRNP* gene and promoter regions that control transcriptional start sites selection (demonstrated for *cp31A* in Supplementary Figure 5.1). This suggests that, once more, HY5 could be a phy signalling component involved in the generation of the cpRNPs isoforms with alternative subcellular localizations. This possibility awaits to be tested, as well as any potential direct impact of temperature and/or retrograde signals acting over HY5 binding sites to modulate the abundance of the cpRNPs in the chloroplast and the nucleus.

5.3. cpRNPs are conserved across plant species and may have further roles in plastid functions.

A new phylogenetic tree presented in this thesis showed that cpRNPs are present as a family across monocot and dicots (Ohta et al., 1995), suggesting a strongly conserved evolutionary history (Chapter 4, section 3.2.1). The conservation of each cpRNP, including cpRNPs some generated through duplication events, is likely important for functional specialisation and may indicate only partial redundancy. Previous research has shown a complementary role for the paralogous cp31A and cp31B in both RNA binding and RNA editing over combinations of plastid-encode transcripts (Tillich et al., 2009); this thesis further shows that while cp29B, cpSEBF, and cp31A were all identified to contribute similarly to Red light-dependent plastome- and nuclear- transcript accumulation at 22°C (Chapter 2, section 2.3.6, Chapter 3, section 3.4.2), further specialisation of each cpRNPs is illustrated by the cold-responsiveness of the target transcripts for cp31A. Furthermore, a potential role for cpSEBF in regulating greening and transcript accumulation in warm temperatures was described, and cp29B was observed to be RS-sensitive in low light. This suggests that each cpRNP can cover general functions in optimal conditions, but can also have highly specialised roles linked to the

essential requirements of photosynthesis under changing environments. Overall, this understanding can be used in the future to develop new toolkits for crop improvement mechanisms, but before this can be accomplished, further mechanistic insight into which processes are affected in response to which environmental conditions, and how these processes may be regulated by cpRNPs is needed.

Additionally, recent research has suggested that cpRNPs do not have cyanobacterial origins and may instead have descended from eukaryotic hnRNPs (Maruyama et al., 1999; Uchiyama et al., 2018). This hypothesis indicates that cpRNPs' function is not chloroplast- or prokaryotic organelle-specific. Their proposed origin may have additional support by the evidence gathered in this study regarding dependence of photosynthesis-associated nuclear-transcript abundance on cpRNPs and the *in-vivo* evidence of their nuclear localisation. Bioinformatics studies conducted also indicate that cpRNPs may have roles in multiple subcellular compartments, including the cytoplasm (Chapter 3, section 3.3.2). While further exploration of other subcellular compartments functions awaits proper studies, what is clear is that cpRNPs are linked to the inter-organellar control of photosynthetic metabolism and greening responses.

Finally, the evidence gathered also suggests that cpRNPs are regulators of plastid transitions and have a wider role in different types of plastids. Using *Solanum lycopersicum* as a model research crop, this thesis reported potential links between cpRNPs and chloroplast-to-chromoplast transition (Rosso, 1968; Harris and Spurr, 1969a; Harris and Spurr, 1969b) (Chapter 4, section 4.5). This finding provides evidence that cpRNPs activity extends from the etioplast-to-chloroplast transition in de-etiolation when the assembly of the photosynthetic apparatus occurs, to chloroplast-to-chromoplast transition in maturing fruits, which the disassembly of photosynthesis and maintenance of a high ATP metabolism are required (Livne and Gepstein, 1988). cpRNPs have also been detected *in vivo* in proplastids in maize and tobacco, and in rice etioplasts (Baginsky et al., 2004; von Zychlinski et al., 2005; Majeran et al., 2012); this suggests that cpRNPs are rather plastidic proteins and not exclusively chloroplastic, despite their name. Their functions in different types of plastids and their links to the co-ordination of developmental and environmental transitions, for which the communication between the plastome and the nuclear genome remains highly important, awaits future study.

5.4. Conclusions.

This thesis expands our knowledge of the phy signalling cascades involved in the co-ordination of plastid metabolism with the external environment and describes previously uncharacterized post-transcriptional events linked to plastome regulation and interorganellar (nuclear-chloroplastic) communication. The cpRNPs, as global controllers of post-transcriptional events in the chloroplast, have an essential role in greening and in the co-ordination of the plastome and nuclear gene expression for the proper assembly and environmental adjustment of the photosynthetic activities in the chloroplast. As a highly conserved protein family across higher plants, their characterization can deliver new toolkits to address regulation of photosynthesis across different subcellular organelles and to optimise photosynthetic outputs in a changing environment.

Ultimately, the main conclusions of this thesis are:

1. phy photoreceptors are master modulators for the expression of the plastome in response to R-light (Chapter 2).

2. phys control nuclear genes involved in the plastome gene expression machinery, with a particular contribution to the modulation of RNA-binding proteins that act in the chloroplast and that are likely part of the post-transcriptional modulation of plastid mRNAs (Chapter 2).

3. Amongst the families of RNA-binding proteins with a strong R-light modulation are the cpRNPs, which are shown to be essential to R-light mediated greening responses (Chapter 2).

4. A novel role of master photomorphogenic factor HY5 has been identified as a light signalling component that incorporates signals from both R-phys and B-crys to control genes with a regulatory function in the expression of the plastome (Chapter 2).

5. The cpRNPs, which are global post-transcriptional modulators of the plastome genes, are a part of a R-phys-HY5-cpRNP signalling cascade that delivers light signals to chloroplast-encoded genes for proper greening responses (Chapter 2).

6. This R-phys-HY5-cpRNP pathway can not only deliver light quality signals, but a diverse range of environmental cues perceived by the phys to modulate photosynthesis, including light quality, quantity, and temperature (Chapter 2).

7. Experimental evidence is provided to support a role of cpRNPs beyond the chloroplast, with the phyB-modulation of alternative transcriptional start site (TSS) selection as the mechanism

through which cpRNPs isoforms with alternative chloroplast-nucleus subcellular localisations are generated (Chapter 3).

8. Reductions in photosynthesis-associated nuclear-encoded gene transcripts were reported in *cprnp* mutants, making cpRNPs a part of the co-ordination of nuclear- and plastid-encoded genes pathways involved in building and tuning photosynthesis in response to environmental changes (Chapter 3).

9. cpRNPs are also sensitive to retrograde signals from the chloroplast. Retrograde signals affect both cpRNP subcellular localisation and accumulation of *cpRNP* transcripts and have been previously documented to modulate downstream cpRNP targets (Chapter 3).

10. Conservation of cpRNPs across higher plants make them worth characterizing as part of the global efforts to generate new toolkits to maintain photosynthetic rates in crops under changing environments (Chapter 4).

Chapter 6: References used in this thesis.

- Abbas, N., Maurya, J. P., Senapati, D., Gangappa, S. N. & Chattopadhyay, S. (2014) Arabidopsis CAM7 and HY5 physically interact and directly bind to the HY5 promoter to regulate its expression and thereby promote photomorphogenesis. *The Plant Cell*, 26(3), 1036-1052.
- Abdallah, F., Salamini, F. & Leister, D. (2000) A prediction of the size and evolutionary origin of the proteome of chloroplasts of Arabidopsis. *Trends in Plant Science*, 5(4), 141-142.
- Adams, S. R. & Langton, F. A. (2005) Photoperiod and plant growth: a review. *The Journal of Horticultural Science and Biotechnology*, 80(1), 2-10.
- Alba, R., Cordonnier-Pratt, M.-M. & Pratt, L. H. (2000) Fruit-Localized Phytochromes Regulate Lycopene Accumulation Independently of Ethylene Production in Tomato. *Plant Physiology*, 123(1), 363.
- Allen, D. J. & Ort, D. R. (2001) Impacts of chilling temperatures on photosynthesis in warm-climate plants. *Trends in Plant Science*, 6(1), 36-42.
- Allen, K. D. & Staehelin, L. A. (1992) Biochemical characterization of photosystem II antenna polypeptides in grana and stroma membranes of spinach. *Plant physiology*, 100(3), 1517-1526.
- Allison, L. A., Simon, L. D. & Maliga, P. (1996) Deletion of *rpoB* reveals a second distinct transcription system in plastids of higher plants. *Embo Journal*, 15(11), 2802-2809.
- Amme, S., Matros, A., Schlesier, B. & Mock, H.-P. (2006) Proteome analysis of cold stress response in Arabidopsis thaliana using DIGE-technology. *Journal of experimental botany*, 57(7), 1537-1546.
- Anderson, J. M., Chow, W. S. & Park, Y.-I. (1995) The grand design of photosynthesis: acclimation of the photosynthetic apparatus to environmental cues. *Photosynthesis Research*, 46(1), 129-139.
- Andersson, B. & Aro, E.-M. (2001) Photodamage and D1 protein turnover in photosystem II. *Regulation of photosynthesis*. Springer.
- Andronis, C., Barak, S., Knowles, S. M., Sugano, S. & Tobin, E. M. (2008) The clock protein CCA1 and the bZIP transcription factor HY5 physically interact to regulate gene expression in Arabidopsis. *Molecular Plant*, 1(1), 58-67.
- Armarego-Marriott, T., Sandoval-Ibañez, O. & Kowalewska, Ł. (2020) Beyond the darkness: recent lessons from etiolation and de-etiolation studies. *Journal of experimental botany*, 71(4), 1215-1225.
- Aro, E. M., Virgin, I. & Andersson, B. (1993) Photoinhibition of photosystem-2 - inactivation, protein damage and turnover. *biochimica et biophysica acta*, 1143(2), 113-134.
- Asseng, S., Ewert, F., Rosenzweig, C., Jones, J. W., Hatfield, J. L., Ruane, A. C., Boote, K. J., Thorburn, P. J., Rotter, R. P., Cammarano, D., Brisson, N., Basso, B., Martre, P., Aggarwal, P. K., Angulo, C., Bertuzzi, P., Biernath, C., Challinor, A. J., Doltra, J., Gayler, S., Goldberg, R., Grant, R., Heng, L., Hooker, J., Hunt, L. A., Ingwersen, J., Izaurralde, R. C., Kersebaum, K. C., Muller, C., Kumar, S. N., Nendel, C., O'leary, G., Olesen, J. E., Osborne, T. M., Palosuo, T., Priesack, E., Ripoche, D., Semenov, M. A., Shcherbak, I., Steduto, P., Stockle, C., Stratonovitch, P., Streck, T., Supit, I., Tao, F., Travasso, M., Waha, K., Wallach, D., White, J. W., Williams, J. R. & Wolf, J. (2013) Uncertainty in simulating wheat yields under climate change. *Nature Climate Change*, 3(9), 827-832.
- Au - Velásquez, A. C., Au - Chakravarthy, S. & Au - Martin, G. B. (2009) Virus-induced Gene Silencing (VIGS) in Nicotiana benthamiana and Tomato. *JoVE*(28), e1292.
- Azari, R., Tadmor, Y., Meir, A., Reuveni, M., Evenor, D., Nahon, S., Shlomo, H., Chen, L. & Levin, I. (2010) Light signaling genes and their manipulation towards modulation of phytonutrient content in tomato fruits. *Biotechnology Advances*, 28(1), 108-118.
- Azarin, K., Usatov, A., Makarenko, M., Kozel, N., Kovalevich, A., Dremuk, I., Yemelyanova, A., Logacheva, M., Fedorenko, A. & Averina, N. (2020) A point mutation in the photosystem I

- P700 chlorophyll a apoprotein A1 gene confers variegation in *Helianthus annuus* L. *Plant Molecular Biology*, 103(4), 373-389.
- Badger, M. R., Bjorkman, O. & Armond, P. A. (1982) An analysis of photosynthetic response and adaptation to temperature in higher-plants - temperature-acclimation in the desert evergreen nerium-oleander l. *Plant Cell and Environment*, 5(1), 85-99.
- Baerenfaller, K., Massonnet, C., Hennig, L., Russenberger, D., Sulpice, R., Walsh, S., Stitt, M., Granier, C. & Gruissem, W. (2015) A long photoperiod relaxes energy management in Arabidopsis leaf six. *Current Plant Biology*, 2, 34-45.
- Baginsky, S. (2016) Protein phosphorylation in chloroplasts—a survey of phosphorylation targets. *Journal of experimental botany*, 67(13), 3873-3882.
- Baginsky, S., Siddique, A. & Gruissem, W. (2004) Proteome analysis of tobacco bright yellow-2 (BY-2) cell culture plastids as a model for undifferentiated heterotrophic plastids. *Journal of proteome research*, 3(6), 1128-1137.
- Barber, J. (1995) Molecular basis of the vulnerability of photosystem II to damage by light. *Functional Plant Biology*, 22(2), 201-208.
- Barkan, A. (2011) Expression of Plastid Genes: Organelle-Specific Elaborations on a Prokaryotic Scaffold. *Plant Physiology*, 155(4), 1520-1532.
- Barkan, A. & Goldschmidt-Clermont, M. (2000) Participation of nuclear genes in chloroplast gene expression. *Biochimie*, 82(6-7), 559-572.
- Bashir, H., Qureshi, M. I., Ibrahim, M. & Iqbal, M. (2015) Chloroplast and photosystems: Impact of cadmium and iron deficiency. *Photosynthetica*, 53 321-335.
- Bassu, S., Brisson, N., Durand, J. L., Boote, K., Lizaso, J., Jones, J. W., Rosenzweig, C., Ruane, A. C., Adam, M., Baron, C., Basso, B., Biernath, C., Boogaard, H., Conijn, S., Corbeels, M., Deryng, D., De Sanctis, G., Gayler, S., Grassini, P., Hatfield, J., Hoek, S., Izaurralde, C., Jongschaap, R., Kemanian, A. R., Kersebaum, K. C., Kim, S. H., Kumar, N. S., Makowski, D., Muller, C., Nendel, C., Priesack, E., Pravia, M. V., Sau, F., Shcherbak, I., Tao, F., Teixeira, E., Timlin, D. & Waha, K. (2014) How do various maize crop models vary in their responses to climate change factors? *Global Change Biology*, 20(7), 2301-2320.
- Bellaïf, S., Barneche, F., Peltier, G. & Rochaix, J.-D. (2005) State transitions and light adaptation require chloroplast thylakoid protein kinase STN7. *Nature*, 433(7028), 892-895.
- Ben-Shem, A., Frolov, F. & Nelson, N. (2003) Crystal structure of plant photosystem I. *Nature*, 426(6967), 630-635.
- Benson, S. L., Maheswaran, P., Ware, M. A., Hunter, C. N., Horton, P., Jansson, S., Ruban, A. V. & Johnson, M. P. (2015) An intact light harvesting complex I antenna system is required for complete state transitions in Arabidopsis. *Nature plants*, 1(12), 1-9.
- Berry, J. & Bjorkman, O. (1980) Photosynthetic response and adaptation to temperature in higher-plants. *Annual Review of Plant Physiology and Plant Molecular Biology*, 31, 491-543.
- Berry, J. O., Yerramsetty, P., Zielinski, A. M. & Mure, C. M. (2013) Photosynthetic gene expression in higher plants. *Photosynthesis Research*, 117(1-3), 91-120.
- Bielczynski, L. W., Schansker, G. & Croce, R. (2016) Effect of light acclimation on the organization of photosystem II super- and sub-complexes in Arabidopsis thaliana. *Frontiers in plant science*, 7, 105.
- Biggs, M. S., Woodson, W. R. & Handa, A. K. (1988) Biochemical basis of high-temperature inhibition of ethylene biosynthesis in ripening tomato fruits. *Physiologia Plantarum*, 72(3), 572-578.
- Bird, C. R., Ray, J. A., Fletcher, J. D., Boniwell, J. M., Bird, A. S., Teulieres, C., Blain, I., Bramley, P. M. & Schuch, W. (1991) Using Antisense RNA to Study Gene Function: Inhibition of Carotenoid Biosynthesis in Transgenic Tomatoes. *Bio/Technology*, 9(7), 635-639.
- Blázquez, M. A. & Weigel, D. (1999) Independent Regulation of Flowering by Phytochrome B and Gibberellins in Arabidopsis. *Plant Physiology*, 120(4), 1025.

- Boccalandro, H. E., Rugnone, M. L., Moreno, J. E., Ploschuk, E. L., Serna, L., Yanovsky, M. J. & Casal, J. J. Phytochrome B Enhances Photosynthesis at the Expense of Water-Use Efficiency in Arabidopsis. *Plant Physiology*, 150 (2), 1083-92.
- Börner, T., Aleynikova, A. Y., Zubo, Y. O. & Kusnetsov, V. V. (2015) Chloroplast RNA polymerases: Role in chloroplast biogenesis. *Biochimica et Biophysica Acta (BBA)-Bioenergetics*, 1847(9), 761-769.
- Boyle, B. & Brisson, N. (2001) Repression of the defense gene PR-10a by the single-stranded DNA binding protein SEBF. *The Plant Cell*, 13(11), 2525-2537.
- Bramley, P. M. (2002) Regulation of carotenoid formation during tomato fruit ripening and development. *Journal of Experimental Botany*, 53(377), 2107-2113.
- Bricker, T. M., Roose, J. L., Fagerlund, R. D., Frankel, L. K. & Eaton-Rye, J. J. (2012) The extrinsic proteins of Photosystem II. *Biochimica Et Biophysica Acta-Bioenergetics*, 1817(1), 121-142.
- Burd, C. G. & Dreyfuss, G. (1994) Conserved structures and diversity of functions of RNA-binding proteins. *Science*, 265(5172), 615.
- Butelli, E., Titta, L., Giorgio, M., Mock, H.-P., Matros, A., Peterek, S., Schijlen, E. G. W. M., Hall, R. D., Bovy, A. G., Luo, J. & Martin, C. (2008) Enrichment of tomato fruit with health-promoting anthocyanins by expression of select transcription factors. *Nature Biotechnology*, 26(11), 1301-1308.
- Capovilla, G., Schmid, M. & Posé, D. (2015) Control of flowering by ambient temperature. *Journal of Experimental Botany*, 66(1), 59-69.
- Carpenter, S. B., Immel, M. J. & Smith, N. D. (1983) Effect of Photoperiod on the Growth and Photosynthetic Capacity of Paulownia Seedlings. *Castanea*, 48(1), 13-18.
- Casal, J. J. & Questa, J. I. (2018) Light and temperature cues: multitasking receptors and transcriptional integrators. *New Phytologist*, 217(3), 1029-1034.
- Catalá, R., Medina, J. & Salinas, J. (2011) Integration of low temperature and light signaling during cold acclimation response in Arabidopsis. *Proceedings of the National Academy of Sciences*, 108(39), 16475-16480.
- Ceunen, S. & Geuns, J. M. C. (2013) Glucose, sucrose, and steviol glycoside accumulation in Stevia rebaudiana grown under different photoperiods. *Biologia Plantarum*, 57(2), 390-394.
- Challinor, A. J., Watson, J., Lobell, D. B., Howden, S. M., Smith, D. R. & Chhetri, N. (2014) A meta-analysis of crop yield under climate change and adaptation. *Nature Climate Change*, 4(4), 287-291.
- Chan, K. X., Phua, S. Y., Crisp, P., Mcquinn, R. & Pogson, B. J. (2016) Learning the languages of the chloroplast: retrograde signaling and beyond. *Annual review of plant biology*, 67, 25-53.
- Chang, B. H. W. & Tian, W. (2016) GSA-Lightning: ultra-fast permutation-based gene set analysis. *Bioinformatics*, 32(19), 3029-3031.
- Chattopadhyay, S., Ang, L.-H., Puente, P., Deng, X.-W. & Wei, N. (1998) Arabidopsis bZIP protein HY5 directly interacts with light-responsive promoters in mediating light control of gene expression. *The Plant Cell*, 10(5), 673-683.
- Chen, M., Galvao, R. M., Li, M., Burger, B., Bugea, J., Bolado, J. & Chory, J. (2010) Arabidopsis HEMERA/pTAC12 Initiates Photomorphogenesis by Phytochromes. *Cell*, 141(7), 1230-U237.
- Chen, Y.-E., Ma, J., Wu, N., Su, Y.-Q., Zhang, Z.-W., Yuan, M., Zhang, H.-Y., Zeng, X.-Y. & Yuan, S. (2018) The roles of Arabidopsis proteins of Lhcb4, Lhcb5 and Lhcb6 in oxidative stress under natural light conditions. *Plant Physiology and Biochemistry*, 130, 267-276.
- Cheung, A. Y., Mcnellis, T. & Piekos, B. (1993) Maintenance of Chloroplast Components during Chromoplast Differentiation in the Tomato Mutant Green Flesh. *Plant Physiology*, 101(4), 1223.
- Cho, W. K., Geimer, S. & Meurer, J. (2009) Cluster analysis and comparison of various chloroplast transcriptomes and genes in Arabidopsis thaliana. *DNA research*, 16(1), 31-44.
- Chotewutmontri, P. & Barkan, A. (2016) Dynamics of Chloroplast Translation during Chloroplast Differentiation in Maize. *Plos Genetics*, 12(7).

- Christie, J., Jones, M., Sullivan, S. & Thomson, C. (2007) Structure-function analysis of phototropin blue-light receptors. *Comparative Biochemistry and Physiology a-Molecular & Integrative Physiology*, 146(4), S227-S227.
- Churin, Y., Hess, W. R. & Börner, T. (1999) Cloning and characterization of three cDNAs encoding chloroplast RNA-binding proteins from barley (*Hordeum vulgare* L.): differential regulation of expression by light and plastid development. *Current genetics*, 36(3), 173-181.
- Cléry, A., Blatter, M. & Allain, F. H. (2008) RNA recognition motifs: boring? Not quite. *Current opinion in structural biology*, 18(3), 290-298.
- Clough, R. C., Casal, J. J., Jordan, E. T., Christou, P. & Vierstra, R. D. (1995) Expression of functional oat phytochrome a in transgenic rice. *Plant Physiology*, 109(3), 1039-1045.
- Cong, L., Ran, F. A., Cox, D., Lin, S., Barretto, R., Habib, N., Hsu, P. D., Wu, X., Jiang, W., Marraffini, L. A. & Zhang, F. (2013) Multiplex Genome Engineering Using CRISPR/Cas Systems. *Science*, 339(6121), 819.
- Cook, W. B. & Walker, J. C. (1992) Identification of a maize nucleic acid-binding protein (NBP) belonging to a family of nuclear-encoded chloroplast proteins. *Nucleic Acids Research*, 20(2), 359-364.
- Cookson, S. J., Chenu, K. & Granier, C. (2007) Day Length Affects the Dynamics of Leaf Expansion and Cellular Development in *Arabidopsis thaliana* Partially through Floral Transition Timing. *Annals of Botany*, 99(4), 703-711.
- Corona, V., Aracri, B., Kosturkova, G., Bartley, G. E., Pitto, L., Giorgetti, L., Scolnik, P. A. & Giuliano, G. (1996) Regulation of a carotenoid biosynthesis gene promoter during plant development. *The Plant Journal*, 9(4), 505-512.
- Croce, R., Morosinotto, T., Castelletti, S., Breton, J. & Bassi, R. (2002) The Lhca antenna complexes of higher plants photosystem I. *Biochimica Et Biophysica Acta-Bioenergetics*, 1556(1), 29-40.
- Cunningham, F. X. & Gantt, E. (1998) Genes and enzymes of carotenoid biosynthesis in plants. *Annual Review of Plant Physiology and Plant Molecular Biology*, 49(1), 557-583.
- Czerednik, A., Busscher, M., Bielen, B. a. M., Wolters-Arts, M., De Maagd, R. A. & Angenent, G. C. (2012) Regulation of tomato fruit pericarp development by an interplay between CDKB and CDKA1 cell cycle genes. *Journal of Experimental Botany*, 63(7), 2605-2617.
- Davuluri, R. V., Suzuki, Y., Sugano, S., Plass, C. & Huang, T. H. M. (2008) The functional consequences of alternative promoter use in mammalian genomes. *Trends in Genetics*, 24(4), 167-177.
- Deng, X. W., Tonkyn, J. C., Peter, G. F., Thornber, J. P. & Gruissem, W. (1989) Post-transcriptional control of plastid messenger-rna accumulation during adaptation of chloroplasts to different light quality environments. *Plant Cell*, 1(6), 645-654.
- Dionne, I. & Wellinger, R. J. (1996) Cell cycle-regulated generation of single-stranded G-rich DNA in the absence of telomerase. *Proceedings of the National Academy of Sciences*, 93(24), 13902-07.
- Diretto, G., Frusciante, S., Fabbri, C., Schauer, N., Busta, L., Wang, Z., Matas, A. J., Fiore, A., K.C. rose, J., Fernie, A. R., Jetter, R., Mattei, B., Giovannoni, J. & Giuliano, G. (2020) Manipulation of β -carotene levels in tomato fruits results in increased ABA content and extended shelf life. *Plant Biotechnology Journal*, 18(5), 1185-1199.
- Dmitrieva, V. A., Tyutereva, E. V. & Voitsekhovskaja, O. V. (2020) Singlet oxygen in plants: Generation, detection, and signaling roles. *International journal of molecular sciences*, 21(9), 3237.
- Dobrogojski, J., Adamiec, M. & Luciński, R. (2020) The chloroplast genome: a review. *Acta Physiologiae Plantarum*, 42, 1-13.
- Dohmann, E. M., Levesque, M. P., De Veylder, L., Reichardt, I., Jürgens, G., Schmid, M. & Schwechheimer, C. (2008) The *Arabidopsis* COP9 signalosome is essential for G2 phase progression and genomic stability. *Development*, 135(11), 2013-2022.
- Eberhard, S., Finazzi, G. & Wollman, F. A. (2008) The Dynamics of Photosynthesis. *Annual Review of Genetics*, 42, 463-515.

- Egea, I., Barsan, C., Bian, W., Purgatto, E., Latché, A., Chervin, C., Bouzayen, M. & Pech, J.-C. (2010) Chromoplast Differentiation: Current Status and Perspectives. *Plant and Cell Physiology*, 51(10), 1601-1611.
- Ernesto Bianchetti, R., Silvestre Lira, B., Santos Monteiro, S., Demarco, D., Purgatto, E., Rothan, C., Rossi, M. & Freschi, L. (2018) Fruit-localized phytochromes regulate plastid biogenesis, starch synthesis, and carotenoid metabolism in tomato. *Journal of Experimental Botany*, 69(15), 3573-3586.
- Estavillo, G. M., Crisp, P. A., Pornsiriwong, W., Wirtz, M., Collinge, D., Carrie, C., Giraud, E., Whelan, J., David, P. & Javot, H. (2011) Evidence for a SAL1-PAP chloroplast retrograde pathway that functions in drought and high light signaling in Arabidopsis. *The Plant Cell*, 23(11), 3992-4012.
- Facella, P., Carbone, F., Placido, A. & Perrotta, G. (2017) Cryptochrome 2 extensively regulates transcription of the chloroplast genome in tomato. *Febs Open Bio*, 7(4), 456-471.
- Falk, J. & Munne-Bosch, S. (2010) Tocochromanol functions in plants: antioxidation and beyond. *Journal of Experimental Botany*, 61(6), 1549-1566.
- Fao (2019) The State of the World's Biodiversity for Food and Agriculture. *FAO Commission on Genetic Resources for Food and Agriculture Assessments*.
- Farah, J., Rappaport, F., Choquet, Y., Joliot, P. & Rochaix, J. D. (1995) Isolation of a psaf-deficient mutant of *Chlamydomonas reinhardtii* - efficient interaction of plastocyanin with the photosystem-i reaction-center is mediated by the psaf subunit. *Embo Journal*, 14(20), 4976-4984.
- Favory, J. J., Kobayashi, M., Tanaka, K., Peltier, G., Kreis, M., Valay, J. G. & Lerbs-Mache, S. (2005) Specific function of a plastid sigma factor for *ndhF* gene transcription. *Nucleic Acids Research*, 33(18), 5991-5999.
- Felsenstein, J. (1985) Confidence limits on phylogenies: an approach using the bootstrap. *Evolution*, 39(4), 783-791.
- Fischer, N., Boudreau, E., Hippler, M., Drepper, F., Haehnel, W. & Rochaix, J. D. (1999) A large fraction of Psaf is nonfunctional in photosystem I complexes lacking the Psaj subunit. *Biochemistry*, 38(17), 5546-5552.
- Foyer, C. H., Neukermans, J., Queval, G., Noctor, G. & Harbinson, J. (2012) Photosynthetic control of electron transport and the regulation of gene expression. *Journal of Experimental Botany*, 63(4), 1637-1661.
- Franklin, K. A. & Quail, P. H. (2010) Phytochrome functions in Arabidopsis development. *Journal of Experimental Botany*, 61(1), 11-24.
- Fraser, P. D., Kiano, J. W., Truesdale, M. R., Schuch, W. & Bramley, P. M. (1999) Phytoene synthase-2 enzyme activity in tomato does not contribute to carotenoid synthesis in ripening fruit. *Plant Molecular Biology*, 40(4), 687-698.
- Fraser, P. D., Truesdale, M. R., Bird, C. R., Schuch, W. & Bramley, P. M. (1994) Carotenoid Biosynthesis during Tomato Fruit Development (Evidence for Tissue-Specific Gene Expression). *Plant Physiology*, 105(1), 405-13.
- Fristedt, R. & Vener, A. V. (2011) High light induced disassembly of photosystem II supercomplexes in Arabidopsis requires STN7-dependent phosphorylation of CP29. *PLoS one*, 6(9), e24565.
- Fromme, P., Jordan, P. & Krauss, N. (2001) Structure of photosystem I. *Biochimica Et Biophysica Acta-Bioenergetics*, 1507(1-3), 5-31.
- Galmes, J., Aranjuelo, I., Medrano, H. & Flexas, J. (2013) Variation in Rubisco content and activity under variable climatic factors. *Photosynthesis Research*, 117(1-3), 73-90.
- Gangappa, S. N. & Botto, J. F. (2016) The Multifaceted Roles of HY5 in Plant Growth and Development. *Molecular Plant*, 9(10), 1353-1365.
- Gao, F., Zhou, Y., Zhu, W., Li, X., Fan, L. & Zhang, G. (2009) Proteomic analysis of cold stress-responsive proteins in *Thellungiella* rosette leaves. *Planta*, 230(5), 1033-1046.

- Giuliano, G., Bartley, G. E. & Scolnik, P. A. (1993) Regulation of carotenoid biosynthesis during tomato development. *The Plant Cell*, 5(4), 379-87.
- Gommers, C. M. M., Ruiz-Sola, M. Á., Ayats, A., Pereira, L., Pujol, M. & Monte, E. (2020) GUN1-independent retrograde signaling targets the ethylene pathway to repress photomorphogenesis. *bioRxiv*, 2020.09.02.280206.
- González-Lamothe, R., Boyle, P., Dulude, A., Roy, V., Lezin-Doumbou, C., Kaur, G. S., Bouarab, K., Després, C. & Brisson, N. (2008) The transcriptional activator Pti4 is required for the recruitment of a repressosome nucleated by repressor SEBF at the potato PR-10a gene. *The Plant Cell*, 20(11), 3136-3147.
- Gonzalez, N., Gévaudant, F., Hernould, M., Chevalier, C. & Mouras, A. (2007) The cell cycle-associated protein kinase WEE1 regulates cell size in relation to endoreduplication in developing tomato fruit. *The Plant Journal*, 51(4), 642-655.
- Gosai, Sager j., Foley, Shawn w., Wang, D., Silverman, Ian m., Selamoglu, N., Nelson, Andrew d. L., Beilstein, Mark a., Daldal, F., Deal, Roger b. & Gregory, Brian d. (2015) Global Analysis of the RNA-Protein Interaction and RNA Secondary Structure Landscapes of the Arabidopsis Nucleus. *Molecular Cell*, 57(2), 376-388.
- Goulas, E., Schubert, M., Kieselbach, T., Kleczkowski, L. A., Gardeström, P., Schröder, W. & Hurry, V. (2006) The chloroplast lumen and stromal proteomes of Arabidopsis thaliana show differential sensitivity to short-and long-term exposure to low temperature. *The Plant Journal*, 47(5), 720-734.
- Gould, K. S. (2004) Nature's Swiss army knife: The diverse protective roles of anthocyanins in leaves. *Journal of Biomedicine and Biotechnology*(5), 314-320.
- Graf, A. & Smith, A. M. (2011) Starch and the clock: the dark side of plant productivity. *Trends in Plant Science*, 16(3), 169-175.
- Grebenok, R. J., Pierson, E., Lambert, G. M., Gong, F.-C., Afonso, C. L., Haldeman-Cahill, R., Carrington, J. C. & Galbraith, D. W. (1997) Green-fluorescent protein fusions for efficient characterization of nuclear targeting. *The Plant Journal*, 11(3), 573-586.
- Griffin, J. H. C., Prado, K., Sutton, P. & Toledo-Ortiz, G. (2020) Coordinating light responses between the nucleus and the chloroplast, a role for plant cryptochromes and phytochromes. *Physiologia Plantarum*, 169(4), 515-528.
- Grübler, B., Cozzi, C. & Pfannschmidt, T. (2021) A Core Module of Nuclear Genes Regulated by Biogenic Retrograde Signals from Plastids. *Plants*, 10(2), 296.
- Gutteridge, S., Manavski, N., Schmid, L.-M. & Meurer, J. (2018) RNA-stabilization factors in chloroplasts of vascular plants. *Essays in biochemistry*, 62(1), 51-64.
- Hajdu, A., Dobos, O., Domijan, M., Bálint, B., Nagy, I., Nagy, F. & Kozma-Bognár, L. (2018) ELONGATED HYPOCOTYL 5 mediates blue light signalling to the Arabidopsis circadian clock. *The Plant Journal*, 96(6), 1242-1254.
- Hajdukiewicz, P. T. J., Allison, L. A. & Maliga, P. (1997) The two RNA polymerases encoded by the nuclear and the plastid compartments transcribe distinct groups of genes in tobacco plastids. *Embo Journal*, 16(13), 4041-4048.
- Haldrup, A., Naver, H. & Scheller, H. V. (1999) The interaction between plastocyanin and photosystem I is inefficient in transgenic Arabidopsis plants lacking the PSI-N subunit of photosystem I. *Plant Journal*, 17(6), 689-698.
- Haldrup, A., Simpson, D. J. & Scheller, H. V. (2000) Down-regulation of the PSI-F subunit of photosystem I (PSI) in Arabidopsis thaliana - The PSI-F subunit is essential for photoautotrophic growth and contributes to antenna function. *Journal of Biological Chemistry*, 275(40), 31211-31218.
- Halliday, K. J. & Whitelam, G. C. (2003) Changes in photoperiod or temperature alter the functional relationships between phytochromes and reveal roles for phyD and phyE. *Plant physiology*, 131(4), 1913-1920.

- Hansson, A., Amann, K., Zygadlo, A., Meurer, J., Scheller, H. V. & Jensen, P. E. (2007) Knock-out of the chloroplast-encoded PSI-J subunit of photosystem I in *Nicotiana tabacum* - PSI-J is required for efficient electron transfer and stable accumulation of photosystem I. *Febs Journal*, 274(7), 1734-1746.
- Harris, E. H., Boynton, J. E. & Gillham, N. W. (1994) Chloroplast ribosomes and protein synthesis. *Microbiological Reviews*, 58(4), 700-754.
- Harris, W. M. & Spurr, A. R. (1969a) Chromoplasts of tomato fruits. i. ultrastructure of low-pigment and high-beta mutants. carotene analyses. *American Journal of Botany*, 56(4), 369-379.
- Harris, W. M. & Spurr, A. R. (1969b) Chromoplasts of tomato fruits. ii. the red tomato. *American Journal of Botany*, 56(4), 380-389.
- Haseloff, J., Siemering, K. R., Prasher, D. C. & Hodge, S. (1997) Removal of a cryptic intron and subcellular localization of green fluorescent protein are required to mark transgenic *Arabidopsis* plants brightly. *Proceedings of the National Academy of Sciences*, 94(6), 2122-27.
- Hashimoto, M., Endo, T., Peltier, G., Tasaka, M. & Shikanai, T. (2003) A nucleus-encoded factor, CRR2, is essential for the expression of chloroplast *ndhB* in *Arabidopsis*. *Plant Journal*, 36(4), 541-549.
- Hauser, B. A., Pratt, L. H. & Cordonnier-Pratt, M.-M. (1997) Absolute quantification of five phytochrome transcripts in seedlings and mature plants of tomato (*Solanum lycopersicum* L.). *Planta*, 201(3), 379-387.
- Häusler, R. E., Heinrichs, L., Schmitz, J. & Flügge, U.-I. (2014) How sugars might coordinate chloroplast and nuclear gene expression during acclimation to high light intensities. *Molecular Plant*, 7(7), 1121-1137.
- Havaux, M. & Gruszecki, W. I. (1993) Heat-induced and light-induced chlorophyll-a fluorescence changes in potato leaves containing high or low-levels of the carotenoid zeaxanthin - indications of a regulatory effect of zeaxanthin on thylakoid membrane fluidity. *Photochemistry and Photobiology*, 58(4), 607-614.
- Hayes, R., Kudla, J., Schuster, G., Gabay, L., Maliga, P. & Grissem, W. (1996) Chloroplast mRNA 3'-end processing by a high molecular weight protein complex is regulated by nuclear encoded RNA binding proteins. *The EMBO journal*, 15(5), 1132-1141.
- He, S.-B., Wang, W.-X., Zhang, J.-Y., Xu, F., Lian, H.-L., Li, L. & Yang, H.-Q. (2015) The CNT1 Domain of *Arabidopsis* CRY1 Alone Is Sufficient to Mediate Blue Light Inhibition of Hypocotyl Elongation. *Molecular Plant*, 8(5), 822-825.
- Hernández-Verdeja, T. & Strand, Å. (2018) Retrograde Signals Navigate the Path to Chloroplast Development. *Plant Physiology*, 176(2), 967-76.
- Heschel, M. S., Selby, J., Butler, C., Whitelam, G. C., Sharrock, R. A. & Donohue, K. (2007) A new role for phytochromes in temperature-dependent germination. *New Phytologist*, 174(4), 735-741.
- Hikosaka, K., Ishikawa, K., Borjigidai, A., Muller, O. & Onoda, Y. (2006) Temperature acclimation of photosynthesis: mechanisms involved in the changes in temperature dependence of photosynthetic rate. *Journal of Experimental Botany*, 57(2), 291-302.
- Hikosaka, K., Murakami, A. & Hirose, T. (1999) Balancing carboxylation and regeneration of ribulose-1,5-bisphosphate in leaf photosynthesis: temperature acclimation of an evergreen tree, *Quercus myrsinaefolia*. *Plant Cell and Environment*, 22(7), 841-849.
- Hirose, T. & Sugiura, M. (2001) Involvement of a site-specific trans-acting factor and a common RNA-binding protein in the editing of chloroplast mRNAs: development of a chloroplast in vitro RNA editing system. *The EMBO journal*, 20(5), 1144-1152.
- Ho, L. C. H., J.D. (1986) Fruit development. . In: Atherton J.G., R. J. (ed.) *The Tomato Crop*. . Dordrecht: Springer.
- Holtzegel, U. (2016) The Lhc family of *Arabidopsis thaliana*. *Endocytobiosis and Cell Research*, 27(2), 71-89.

- Hou, L. Y., Liu, Y., Du, J. C., Wang, M. Y., Wang, H. & Mao, P. S. (2016a) Grazing effects on ecosystem CO₂ fluxes differ among temperate steppe types in Eurasia. *Scientific Reports*, 6, 29028.
- Hou, W., Sun, A., Chen, H., Yang, F., Pan, J. & Guan, M. (2016b) Effects of chilling and high temperatures on photosynthesis and chlorophyll fluorescence in leaves of watermelon seedlings. *Biologia plantarum*, 60(1), 148-154.
- Hou, X., Fu, A., Garcia, V. J., Buchanan, B. B. & Luan, S. (2015) PSB27: a thylakoid protein enabling Arabidopsis to adapt to changing light intensity. *Proceedings of the National Academy of Sciences*, 112(5), 1613-1618.
- Hu, W., Franklin, K. A., Sharrock, R. A., Jones, M. A., Harmer, S. L. & Lagarias, J. C. (2013) Unanticipated regulatory roles for Arabidopsis phytochromes revealed by null mutant analysis. *Proceedings of the National Academy of Sciences of the United States of America*, 110(4), 1542-1547.
- Huang, C., Yu, Q.-B., Lv, R.-H., Yin, Q.-Q., Chen, G.-Y. & Xu, L. (2013) The Reduced Plastid-Encoded Polymerase-Dependent Plastid Gene Expression Leads to the Delayed Greening of the Arabidopsis fln2 Mutant. *PLoS ONE*, 8(9), e73092.
- Huang, Z., Shen, L., Wang, W., Mao, Z., Yi, X., Kuang, T., Shen, J.-R., Zhang, X. & Han, G. (2021) Structure of photosystem I-LHCI-LHCII from the green alga *Chlamydomonas reinhardtii* in State 2. *Nature Communications*, 12(1), 1100.
- Husainid, S. S. H., Kok, R. A., Schreuder, M. E. L., Hanumappa, M., Cordonnier-Pratt, M.-M., Pratt, L. H., Van Der Plas, L. H. W. & Van Der Krol, A. R. (2007) Overexpression of homologous phytochrome genes in tomato: exploring the limits in photoperception. *Journal of Experimental Botany*, 58(3), 615-626.
- Ihalainen, J. A., Gobets, B., Sznee, K., Brazzoli, M., Croce, R., Bassi, R., Van Grondelle, R., Korppi-Tommola, J. E. I. & Dekker, J. P. (2000) Evidence for two spectroscopically different dimers of light-harvesting complex I from green plants. *Biochemistry*, 39(29), 8625-8631.
- Ihnatowicz, A., Pesaresi, P., Varotto, C., Richly, E., Schneider, A., Jahns, P., Salamini, F. & Leister, D. (2004) Mutants for photosystem I subunit D of Arabidopsis thaliana: effects on photosynthesis, photosystem I stability and expression of nuclear genes for chloroplast functions. *Plant Journal*, 37(6), 839-852.
- Ishige, F., Takaichi, M., Foster, R., Chua, N. H. & Oeda, K. (1999) AG-box motif (GCCACGTGCC) tetramer confers high-level constitutive expression in dicot and monocot plants. *The Plant Journal*, 18(4), 443-448.
- Ishizaki, Y., Tsunoyama, Y., Hatano, K., Ando, K., Kato, K., Shinmyo, A., Kobori, M., Takeba, G., Nakahira, Y. & Shiina, T. (2005) A nuclear-encoded sigma factor, Arabidopsis SIG6, recognizes sigma-70 type chloroplast promoters and regulates early chloroplast development in cotyledons. *Plant Journal*, 42(2), 133-144.
- Jansson, S. (1994) The light-harvesting chlorophyll ab-binding proteins. *Biochimica et Biophysica Acta (BBA)-Bioenergetics*, 1184(1), 1-19.
- Jarvi, S., Suorsa, M. & Aro, E. M. (2015) Photosystem II repair in plant chloroplasts - Regulation, assisting proteins and shared components with photosystem II biogenesis. *Biochimica Et Biophysica Acta-Bioenergetics*, 1847(9), 900-909.
- Jarvis, P. & López-Juez, E. (2013) Biogenesis and homeostasis of chloroplasts and other plastids. *Nature Reviews Molecular Cell Biology*, 14(12), 787-802.
- Jensen, P., Amann, K., Zygadlo, A., Hansson, A., Meurer, J. & Scheller, H. (2007) The chloroplast encoded PSI-J subunit is required for formation of the plastocyanin binding domain of photosystem I. *Photosynthesis Research*, 91(2-3), 154-155.
- Jensen, P. E., Haldrup, A., Zhang, S. P. & Scheller, H. V. (2004) The PSI-O subunit of plant photosystem I is involved in balancing the excitation pressure between the two photosystems. *Journal of Biological Chemistry*, 279(23), 24212-24217.
- Jiao, Y. L., Lau, O. S. & Deng, X. W. (2007) Light-regulated transcriptional networks in higher plants. *Nature Reviews Genetics*, 8(3), 217-230.

- Jinek, M., Chylinski, K., Fonfara, I., Hauer, M., Doudna, J. A. & Charpentier, E. (2012) A Programmable Dual-RNA–Guided DNA Endonuclease in Adaptive Bacterial Immunity. *Science*, 337(6096), 816.
- Jung, J. H., Domijan, M., Klose, C., Biswas, S., Ezer, D., Gao, M. J., Khattak, A. K., Box, M. S., Charoensawan, V., Cortijo, S., Kumar, M., Grant, A., Locke, J. C. W., Schafer, E., Jaeger, K. E. & Wigge, P. A. (2016) Phytochromes function as thermosensors in Arabidopsis. *Science*, 354(6314), 886-889.
- Jung, S., Kim, J. S., Cho, K. Y., Tae, G. S. & Kang, B. G. (2000) Antioxidant responses of cucumber (*Cucumis sativus*) to photoinhibition and oxidative stress induced by norflurazon under high and low PPFs. *Plant Science*, 153(2), 145-154.
- Kachanovsky, D. E., Filler, S., Isaacson, T. & Hirschberg, J. (2012) Epistasis in tomato color mutations involves regulation of phytoene synthase; expression by carotenoids. *Proceedings of the National Academy of Sciences*, 109(46), 19021-19026.
- Kaiserli, E. & Chory, J. (2016) The Role of Phytochromes in Triggering Plant Developmental Transitions. *eLS*, 1-11.
- Kakiuchi, S., Uno, C., Ido, K., Nishimura, T., Noguchi, T., Ifuku, K. & Sato, F. (2012) The PsbQ protein stabilizes the functional binding of the PsbP protein to photosystem II in higher plants. *Biochimica et Biophysica Acta (BBA)-Bioenergetics*, 1817(8), 1346-1351.
- Kakizaki, T., Matsumura, H., Nakayama, K., Che, F.-S., Terauchi, R. & Inaba, T. (2009) Coordination of plastid protein import and nuclear gene expression by plastid-to-nucleus retrograde signaling. *Plant physiology*, 151(3), 1339-1353.
- Kamal, M. M., Ishikawa, S., Takahashi, F., Suzuki, K., Kamo, M., Umezawa, T., Shinozaki, K., Kawamura, Y. & Uemura, M. (2020) Large-Scale Phosphoproteomic Study of Arabidopsis Membrane Proteins Reveals Early Signaling Events in Response to Cold. *Int J Mol Sci* 16, 21(22): 8631.
- Kanervo, E., Suorsa, M. & Aro, E.-M. (2005) Functional flexibility and acclimation of the thylakoid membrane. *Photochemical & Photobiological Sciences*, 4(12), 1072-1080.
- Karayekov, E., Sellaro, R., Legris, M., Yanovsky, M. J. & Casal, J. J. (2013) Heat shock–induced fluctuations in clock and light signaling enhance phytochrome B–mediated arabidopsis deetiolation. *The Plant Cell*, 25(8), 2892-2906.
- Khrouchtchova, A., Hansson, M., Paakkanen, V., Vainonen, J. P., Zhang, S. P., Jensen, P. E., Scheller, H. V., Vener, A. V., Aro, E. M. & Haldrup, A. (2005) A previously found thylakoid membrane protein of 14 kDa (TMP14) is a novel subunit of plant photosystem I and is designated PSI-P. *Febs Letters*, 579(21), 4808-4812.
- Kindgren, P., Kremnev, D., Blanco, N. E., De Dios Barajas López, J., Fernández, A. P., Tellgren-Roth, C., Small, I. & Strand, Å. (2012) The plastid redox insensitive 2 mutant of Arabidopsis is impaired in PEP activity and high light-dependent plastid redox signalling to the nucleus. *The Plant Journal*, 70(2), 279-291.
- King, B. R. & Guda, C. (2007) ngLOC: an n-gram-based Bayesian method for estimating the subcellular proteomes of eukaryotes. *Genome Biology*, 8(5), R68.
- Kippes, N., Vangessel, C., Hamilton, J., Akpınar, A., Budak, H., Dubcovsky, J. & Pearce, S. (2020) - Effect of phyB and phyC loss-of-function mutations on the wheat transcriptome under short and long day photoperiods. *BMC Plant Biol.* 20, 297.
- Klee, H. J. (2010) Improving the flavor of fresh fruits: genomics, biochemistry, and biotechnology. *New Phytologist*, 187(1), 44-56.
- Kleffmann, T., Von Zychlinski, A., Russenberger, D., Hirsch-Hoffmann, M., Gehrig, P., Gruißem, W. & Baginsky, S. (2006) Proteome Dynamics during Plastid Differentiation in Rice. *Plant Physiology*, 143(2), 912-923.
- Klie, M. & Debener, T. (2011) Identification of superior reference genes for data normalisation of expression studies via quantitative PCR in hybrid roses (*Rosa hybrida*). *BMC Research Notes*, 4(1), 1-9.

- Klose, C., Viczián, A., Kircher, S., Schäfer, E. & Nagy, F. (2015) Molecular mechanisms for mediating light-dependent nucleo/cytoplasmic partitioning of phytochrome photoreceptors. *New Phytologist*, 206(3), 965-971.
- Kobayashi, K., Baba, S., Obayashi, T., Sato, M., Toyooka, K., Keranen, M., Aro, E. M., Fukaki, H., Ohta, H., Sugimoto, K. & Masuda, T. (2012) Regulation of Root Greening by Light and Auxin/Cytokinin Signaling in Arabidopsis. *Plant Cell*, 24(3), 1081-1095.
- Kobayashi, T., Takahara, M., Miyagishima, S.-Y., Kuroiwa, H., Sasaki, N., Ohta, N., Matsuzaki, M. & Kuroiwa, T. (2002) Detection and localization of a chloroplast-encoded HU-like protein that organizes chloroplast nucleoids. *The Plant Cell*, 14(7), 1579-1589.
- Köhler, R. H. (1998) GFP for in vivo imaging of subcellular structures in plant cells. *Trends in Plant Science*, 3(8), 317-320.
- Komenda, J. & Masojídek, J. (1995) Functional and Structural Changes of the Photosystem II Complex Induced by High Irradiance in Cyanobacterial Cells. *European Journal of Biochemistry*, 233(2), 677-682.
- Kouril, R., Dekker, J. P. & Boekema, E. J. (2012) Supramolecular organization of photosystem II in green plants. *Biochimica Et Biophysica Acta-Bioenergetics*, 1817(1), 2-12.
- Koussevitzky, S., Nott, A., Mockler, T. C., Hong, F., Sachetto-Martins, G., Surpin, M., Lim, J., Mittler, R. & Chory, J. (2007) Signals from Chloroplasts Converge to Regulate Nuclear Gene Expression. *Science*, 316(5825), 715-719.
- Krapp, A. & Stitt, M. (1995) An evaluation of direct and indirect mechanisms for the sink-regulation of photosynthesis in spinach - changes in gas-exchange, carbohydrates, metabolites, enzyme-activities and steady-state transcript levels after cold-girdling source leaves. *Planta*, 195(3), 313-323.
- Krause, K., Oetke, S. & Krupinska, K. (2012) Dual targeting and retrograde translocation: regulators of plant nuclear gene expression can be sequestered by plastids. *International journal of molecular sciences*, 13(9), 11085-11101.
- Kreps, J. A. & Simon, A. E. (1997) Environmental and genetic effects on circadian clock-regulated gene expression in Arabidopsis. *Plant Cell*, 9(3), 297-304.
- Kreslavski, V. D., Huang, X., Semenova, G., Khudyakova, A., Shirshikova, G., Hummatov, N., Zharmukhamedov, S. K., Li, X., Allakhverdiev, S. I. & Nie, C. (2020) Linking sensitivity of photosystem II to UV-B with chloroplast ultrastructure and UV-B absorbing pigments contents in *A. thaliana* L. phyAphyB double mutants. *Plant Growth Regulation*, 91, 13-21.
- Ksas, B., Becuwe, N., Chevalier, A. & Havaux, M. (2015) Plant tolerance to excess light energy and photooxidative damage relies on plastoquinone biosynthesis. *Scientific Reports*, 5, 10919.
- Ku, H.-M., Vision, T., Liu, J. & Tanksley, S. D. (2000) Comparing sequenced segments of the tomato and *Arabidopsis* genomes: Large-scale duplication followed by selective gene loss creates a network of synteny. *Proceedings of the National Academy of Sciences*, 97(16), 9121-9126.
- Kumar, S., Stecher, G., Li, M., Niyaz, C. & Tamura, K. (2018) MEGA X: Molecular Evolutionary Genetics Analysis across Computing Platforms. *Molecular Biology and Evolution*, 35(6), 1547-1549.
- Kupsch, C., Ruwe, H., Gusewski, S., Tillich, M., Small, I. & Schmitz-Linneweber, C. (2012) Arabidopsis chloroplast RNA binding proteins CP31A and CP29A associate with large transcript pools and confer cold stress tolerance by influencing multiple chloroplast RNA processing steps. *The Plant Cell*, 24(10), 4266-4280.
- Kwon, C. & Chung, I. K. (2004) Interaction of an Arabidopsis RNA-binding protein with plant single-stranded telomeric DNA modulates telomerase activity. *Journal of Biological Chemistry*, 279(13), 12812-12818.
- Lamb, J. R., Tugendreich, S. & Hieter, P. (1995) Tetratricopeptide repeat interactions - to tpr or not to tpr. *Trends in Biochemical Sciences*, 20(7), 257-259.

- Landry, J.-R., Mager, D. L. & Wilhelm, B. T. (2003) Complex controls: the role of alternative promoters in mammalian genomes. *Trends in Genetics*, 19(11), 640-648.
- Larkin, R. M. (2014) Influence of plastids on light signalling and development. *Philosophical Transactions of the Royal Society B: Biological Sciences*, 369(1640), 20130232.
- Lawrenson, T., Shorinola, O., Stacey, N., Li, C., Østergaard, L., Patron, N., Uauy, C. & Harwood, W. (2015) Induction of targeted, heritable mutations in barley and Brassica oleracea using RNA-guided Cas9 nuclease. *Genome Biology*, 16(1), 258.
- Lee, H. Y., Hong, Y. N. & Chow, W. S. (2001) Photoinactivation of photosystem II complexes and photoprotection by non-functional neighbours in Capsicum annuum L. leaves. *Planta*, 212(3), 332-342.
- Lee, J., He, K., Stolc, V., Lee, H., Figueroa, P., Gao, Y., Tongprasit, W., Zhao, H., Lee, I. & Deng, X. W. (2007) Analysis of transcription factor HY5 genomic binding sites revealed its hierarchical role in light regulation of development. *The Plant Cell*, 19(3), 731-749.
- Leelavathi, S., Bhardwaj, A., Kumar, S., Dass, A., Pathak, R., Pandey, S. S., Tripathy, B. C., Padmalatha, K. V., Dhandapani, G., Kanakachari, M., Kumar, P. A., Cella, R. & Siva Reddy, V. (2011) Genome-wide transcriptome and proteome analyses of tobacco psaA and psbA deletion mutants. *Plant Molecular Biology*, 76(3), 407-423.
- Legris, M., Klose, C., Burgie, E. S., Rojas, C. C., Neme, M., Hiltbrunner, A., Wigge, P. A., Schafer, E., Vierstra, R. D. & Casal, J. J. (2016) Phytochrome B integrates light and temperature signals in Arabidopsis. *Science*, 354(6314), 897-900.
- Leivar, P., Tepperman, J. M., Cohn, M. M., Monte, E., Al-Sady, B., Erickson, E. & Quail, P. H. (2012) Dynamic antagonism between phytochromes and PIF family basic helix-loop-helix factors induces selective reciprocal responses to light and shade in a rapidly responsive transcriptional network in Arabidopsis. *The Plant Cell*, 24(4), 1398-1419.
- Lepistö, A. & Rintamäki, E. (2012) Coordination of Plastid and Light Signaling Pathways upon Development of Arabidopsis Leaves under Various Photoperiods. *Molecular Plant*, 5(4), 799-816.
- Lepistö, A., Toivola, J., Nikkanen, L. & Rintamäki, E. (2012) Retrograde signaling from functionally heterogeneous plastids. *Frontiers in plant science*, 3, 286.
- Lerbs-Mache, S. (2011) Function of plastid sigma factors in higher plants: regulation of gene expression or just preservation of constitutive transcription? *Plant molecular biology*, 76(3-5), 235-249.
- Letunic, I. & Bork, P. (2019) Interactive Tree Of Life (iTOL) v4: recent updates and new developments. *Nucleic Acids Research*, 47(W1), W256-W259.
- Li, G., Siddiqui, H., Teng, Y. B., Lin, R. C., Wan, X. Y., Li, J. G., Lau, O. S., Ouyang, X. H., Dai, M. Q., Wan, J. M., Devlin, P. F., Deng, X. W. & Wang, H. Y. (2011a) Coordinated transcriptional regulation underlying the circadian clock in Arabidopsis. *Nature Cell Biology*, 13(5), 616-U275.
- Li, J., Li, G., Wang, H. & Deng, X. W. (2011b) Phytochrome signaling mechanisms. *The Arabidopsis Book/American Society of Plant Biologists*, 9.
- Li, L., Aro, E.-M. & Millar, A. H. (2018) Mechanisms of Photodamage and Protein Turnover in Photoinhibition. *Trends in Plant Science*, 23(8), 667-676.
- Li, Y. & Sugiura, M. (1990) Three distinct ribonucleoproteins from tobacco chloroplasts: each contains a unique amino terminal acidic domain and two ribonucleoprotein consensus motifs. *The EMBO journal*, 9(10), 3059-3066.
- Lifschitz, S., Gepstein, S. & Horwitz, B. A. (1990) Phytochrome regulation of greening in wild-type and long-hypocotyl mutants of *Arabidopsis thaliana*. *Planta*, 181(2), 234-238.
- Lin, C., Yang, H., Guo, H., Mockler, T., Chen, J. & Cashmore, A. R. (1998) Enhancement of blue-light sensitivity of Arabidopsis seedlings by a blue light receptor cryptochrome 2. *Proceedings of the National Academy of Sciences*, 95(5), 2686-2690.

- Lincoln, J. E., Cordes, S., Read, E. & Fischer, R. L. (1987) Regulation of gene expression by ethylene during *Lycopersicon esculentum* (tomato) fruit development. *Proceedings of the National Academy of Sciences*, 84(9), 2793-2797.
- Lipova, L., Krchnak, P., Komenda, J. & Ilik, P. (2010) Heat-induced disassembly and degradation of chlorophyll-containing protein complexes in vivo. *Biochimica Et Biophysica Acta-Bioenergetics*, 1797(1), 63-70.
- Lisitsky, I. & Schuster, G. (1995) Phosphorylation of a chloroplast rna-binding protein-changes its affinity to RNA. *Nucleic Acids Research*, 23(13), 2506-2511.
- Liu, L., Shao, Z., Zhang, M. & Wang, Q. (2015) Regulation of Carotenoid Metabolism in Tomato. *Molecular Plant*, 8(1), 28-39.
- Liu, Y., Beyer, A. & Aebersold, R. (2016) On the dependency of cellular protein levels on mRNA abundance. *Cell*, 165(3), 535-550.
- Liu, Z. F., Yan, H. C., Wang, K. B., Kuang, T. Y., Zhang, J. P., Gui, L. L., An, X. M. & Chang, W. R. (2004) Crystal structure of spinach major light-harvesting complex at 2.72 angstrom resolution. *Nature*, 428(6980), 287-292.
- Livne, A. & Gepstein, S. (1988) Abundance of the Major Chloroplast Polypeptides during Development and Ripening of Tomato Fruits. *Plant Physiology*, 87(1), 239-243
- Llorente, B., D'andrea, L., Ruiz-Sola, M. A., Botterweg, E., Pulido, P., Andilla, J., Loza-Alvarez, P. & Rodriguez-Concepcion, M. (2016) Tomato fruit carotenoid biosynthesis is adjusted to actual ripening progression by a light-dependent mechanism. *The Plant Journal*, 85(1), 107-119.
- Llorente, B., Martinez-Garcia, J. F., Stange, C. & Rodriguez-Concepcion, M. (2017) Illuminating colors: regulation of carotenoid biosynthesis and accumulation by light. *Current Opinion in Plant Biology*, 37, 49-55.
- Lobell, D. B. & Gourjji, S. M. (2012) The Influence of Climate Change on Global Crop Productivity. *Plant Physiology*, 160(4), 1686-1697.
- Lois, L. M., Rodríguez-Concepción, M., Gallego, F., Campos, N. & Boronat, A. (2000) Carotenoid biosynthesis during tomato fruit development: regulatory role of 1-deoxy-D-xylulose 5-phosphate synthase. *The Plant Journal*, 22(6), 503-513.
- Long, S. P., Zhu, X. G., Naidu, S. L. & Ort, D. R. (2006) Can improvement in photosynthesis increase crop yields? *Plant Cell and Environment*, 29(3), 315-330.
- Lorenzo, C. D., Sanchez-Lamas, M., Antonietti, M. S. & Cerdán, P. D. (2016) Emerging hubs in plant light and temperature signaling. *Photochemistry and photobiology*, 92(1), 3-13.
- Lorković, Z. J. & Barta, A. (2002) Genome analysis: RNA recognition motif (RRM) and K homology (KH) domain RNA-binding proteins from the flowering plant *Arabidopsis thaliana*. *Nucleic acids research*, 30(3), 623-635.
- Loschelder, H., Schweer, J., Link, B. & Link, G. (2006) Dual temporal role of plastid sigma factor 6 in *Arabidopsis* development. *Plant physiology*, 142(2), 642-650.
- Loudet, O., Michael, T. P., Burger, B. T., Le Metté, C., Mockler, T. C., Weigel, D. & Chory, J. (2008) A zinc knuckle protein that negatively controls morning-specific growth in *Arabidopsis thaliana*. *Proceedings of the National Academy of Sciences*, 105(44), 17193.
- Loza-Tavera, H., Vargas-Suarez, M., Diaz-Mireles, E., Torres-Marquez, M., De La Vara, L. G., Moreno-Sanchez, R. & Grussem, W. (2006) Phosphorylation of the spinach chloroplast 24 kDa RNA-binding protein (24RNP) increases its binding to petD and psbA 3' untranslated regions. *Biochimie*, 88(9), 1217-1228.
- Lu, Y. (2016) Identification and Roles of Photosystem II Assembly, Stability, and Repair Factors in *Arabidopsis*. *Frontiers in Plant Science*, 7 (168) 1-17.
- Lurin, C., Andres, C., Aubourg, S., Bellaoui, M., Bitton, F., Bruyere, C., Caboche, M., Debast, C., Gualberto, J., Hoffmann, B., Lecharny, A., Le Ret, M., Martin-Magniette, M. L., Mireau, H., Peeters, N., Renou, J. P., Szurek, B., Taconnat, L. & Small, I. (2004) Genome-wide analysis of

- Arabidopsis pentatricopeptide repeat proteins reveals their essential role in organelle biogenesis. *Plant Cell*, 16(8), 2089-2103.
- Ma, L., Sun, N., Liu, X., Jiao, Y., Zhao, H. & Deng, X. W. (2005) Organ-Specific Expression of Arabidopsis Genome during Development. *Plant Physiology*, 138(1), 80.
- Madeira, F., Park, Y. M., Lee, J., Buso, N., Gur, T., Madhusoodanan, N., Basutkar, P., Tivey, A. R. N., Potter, S. C., Finn, R. D. & Lopez, R. (2019) The EMBL-EBI search and sequence analysis tools APIs in 2019. *Nucleic acids research*, 47(W1), W636-W641.
- Majeran, W., Friso, G., Asakura, Y., Qu, X., Huang, M., Ponnala, L., Watkins, K. P., Barkan, A. & Van Wijk, K. J. (2012) Nucleoid-enriched proteomes in developing plastids and chloroplasts from maize leaves: a new conceptual framework for nucleoid functions. *Plant physiology*, 158(1), 156-189.
- Mali, P., Yang, L., Esvelt, K. M., Aach, J., Guell, M., Dicarlo, J. E., Norville, J. E. & Church, G. M. (2013) RNA-Guided Human Genome Engineering via Cas9. *Science*, 339(6121), 823.
- Malnoe, A., Wang, F., Girard-Bascou, J., Wollman, F. A. & De Vitry, C. (2014) Thylakoid FtsH Protease Contributes to Photosystem II and Cytochrome b(6)f Remodeling in *Chlamydomonas reinhardtii* under Stress Conditions. *Plant Cell*, 26(1), 373-390.
- Maris, C., Dominguez, C. & Allain, F. H. T. (2005) The RNA recognition motif, a plastic RNA-binding platform to regulate post-transcriptional gene expression. *The FEBS journal*, 272(9), 2118-2131.
- Martel, C., Vrebalov, J., Tafelmeyer, P. & Giovannoni, J. J. (2011) The Tomato MADS-Box Transcription Factor RIPENING INHIBITOR Interacts with Promoters Involved in Numerous Ripening Processes in a COLORLESS NONRIPENING-Dependent Manner. *Plant Physiology*, 157(3), 1568.
- Martín, G., Leivar, P., Ludevid, D., Tepperman, J. M., Quail, P. H. & Monte, E. (2016) Phytochrome and retrograde signalling pathways converge to antagonistically regulate a light-induced transcriptional network. *Nature communications*, 7(1), 1-10.
- Martin, W. & Kowallik, K. V. (1999) Annotated English translation of Mereschkowsky's 1905 paper 'Über Natur und Ursprung der Chromatophoren im Pflanzenreiche. *European Journal of Phycology*, 34(3), 287-295.
- Martino-Catt, S. & Ort, D. R., (1992) Low temperature interrupts circadian regulation of transcriptional activity in chilling-sensitive plants. *Proceedings of the National Academy of Sciences*, 89 (9), 3731-3735.
- Maruyama, K., Sato, N. & Ohta, N. (1999) Conservation of structure and cold-regulation of RNA-binding proteins in cyanobacteria: Probable convergent evolution with eukaryotic glycine-rich RNA-binding proteins. *Nucleic Acids Research*, 27(9), 2029-2036.
- Mathur, S. & Jajoo, A. (2014) Alterations in photochemical efficiency of photosystem II in wheat plant on hot summer day. *Physiology and Molecular Biology of Plants*, 20(4), 527-531.
- Matsubara, S. & Chow, W. S. (2004) Populations of photoinactivated photosystem II reaction centers characterized by chlorophyll auto-fluorescence lifetime. *Proceedings of the National Academy of Sciences*, 101(52), 18234.
- Matthews, H. D., Eby, M., Weaver, A. J. & Hawkins, B. J. (2005) Primary productivity control of simulated carbon cycle-climate feedbacks. *Geophysical Research Letters*, 32(14).
- Mcclung, C., Lou, P., Hermand, V. & Kim, J. A. (2016) The importance of ambient temperature to growth and the induction of flowering. *Frontiers in Plant Science*, 7, 1266.
- Mcfadden, G. I. (2014) Origin and evolution of plastids and photosynthesis in eukaryotes. *Cold Spring Harbor perspectives in biology*, 6(4), a016105.
- Mellenthin, M., Ellersiek, U., Boerger, A. & Baier, M. (2014) Expression of the Arabidopsis Sigma Factor SIG5 Is Photoreceptor and Photosynthesis Controlled. *Plants-Basel*, 3(3), 359-391.
- Melonek, J., Oetke, S. & Krupinska, K. (2016) Multifunctionality of plastid nucleoids as revealed by proteome analyses. *Biochimica et Biophysica Acta (BBA)-Proteins and Proteomics*, 1864(8), 1016-1038.

- Mène-Saffrané, L. & Dellapenna, D. (2010), Biosynthesis, regulation and functions of tocochromanols in plants. *Plant Physiology and Biochemistry*, 48 (5), 301-309.
- Mentzen, W. I. & Wurtele, E. S. (2008) Regulon organization of Arabidopsis. *BMC plant biology*, 8(1), 1-22.
- Michael, T. P., Breton, G., Hazen, S. P., Priest, H., Mockler, T. C., Kay, S. A. & Chory, J. (2008) A morning-specific phytohormone gene expression program underlying rhythmic plant growth. *Plos Biology*, 6(9), 1887-1898.
- Mieszczak, M., Klahre, U., Levy, J. H., Goodall, G. J. & Filipowicz, W. (1992) Multiple plant RNA binding proteins identified by PCR: expression of cDNAs encoding RNA binding proteins targeted to chloroplasts in *Nicotiana plumbaginifolia*. *Molecular and General Genetics MGG*, 234(3), 390-400.
- Minagawa, J. & Takahashi, Y. (2004) Structure, function and assembly of Photosystem II and its light-harvesting proteins. *Photosynthesis research*, 82(3), 241-263.
- Mockler, T., Michael, T., Priest, H., Shen, R., Sullivan, C., Givan, S., Mcentee, C., Kay, S. & Chory, J. *The DIURNAL project: DIURNAL and circadian expression profiling, model-based pattern matching, and promoter analysis*. Cold Spring Harbor symposia on quantitative biology. 2007. Cold Spring Harbor Laboratory Press, 353-363.
- Moise, A. R., Al-Babili, S. & Wurtzel, E. T. (2014) Mechanistic Aspects of Carotenoid Biosynthesis. *Chemical Reviews*, 114(1), 164-193.
- Moore, F. C. & Lobell, D. B. (2014) Adaptation potential of European agriculture in response to climate change. *Nature Climate Change*, 4(7), 610-614.
- Morley, S. A., Ahmad, N. & Nielsen, B. L. (2019) Plant organelle genome replication. *Plants*, 8(10), 358.
- Mousseau, M. (1981) Effect of a change in photoperiod on subsequent CO₂ exchange. *Photosynthesis Research*, 2(2), 85-94.
- Mrázek, J. & Xie, S. (2006) Pattern locator: a new tool for finding local sequence patterns in genomic DNA sequences. *Bioinformatics*, 22(24), 3099-3100.
- Mullet, J. E. (1988a) Chloroplast development and gene-expression. *Annual Review of Plant Physiology and Plant Molecular Biology*, 39, 475-502.
- Mullet, J. E. (1988b) Chloroplast development and gene expression. *Annu Rev Plant Physiol Plant Mol Biol*, 39, 475-502.
- Mullet, J. E. & Arntzen, C. J. (1980) Simulation of grana stacking in a model membrane system - mediation by a purified light-harvesting pigment-protein complex from chloroplasts. *Biochimica Et Biophysica Acta*, 589(1), 100-117.
- Murakami, R., Ifuku, K., Takabayashi, A., Shikanai, T., Endo, T. & Sato, F. (2002) Characterization of an Arabidopsis thaliana mutant with impaired psbO, one of two genes encoding extrinsic 33-kDa proteins in photosystem II. *FEBS letters*, 523(1-3), 138-142.
- Murashige, T. & Skoog, F. (1962) A revised medium for rapid growth and bio assays with tobacco tissue cultures. *Physiologia plantarum*, 15(3), 473-497.
- Nagashima, A., Hanaoka, M., Fujiwara, M., Shikanai, T., Kanamaru, K., Takahashi, H. & Tanaka, K. (2004a) Analysis of the chloroplast RNA polymerase sigma factor, SIG5, in Arabidopsis thaliana: Roles in the stress-responsive chloroplast transcription. *Plant and Cell Physiology*, 45, S33-S33.
- Nagashima, A., Hanaoka, M., Motohashi, R., Seki, M., Shinozaki, K., Kanamaru, K., Takahashi, H. & Tanaka, K. (2004b) DNA microarray analysis of plastid gene expression in an Arabidopsis mutant deficient in a plastid transcription factor sigma, SIG2. *Bioscience Biotechnology and Biochemistry*, 68(3), 694-704.
- Nagashima, A., Hanaoka, M., Shikanai, T., Fujiwara, M., Kanamaru, K., Takahashi, H. & Tanaka, K. (2004c) The multiple-stress responsive plastid sigma factor, SIG5, directs activation of the psbD blue light-responsive promoter (BLRP) in Arabidopsis thaliana. *Plant and Cell Physiology*, 45(4), 357-368.

- Nakamura, T., Ohta, M., Sugiura, M. & Sugita, M. (2001) Chloroplast ribonucleoproteins function as a stabilizing factor of ribosome-free mRNAs in the stroma. *Journal of Biological Chemistry*, 276(1), 147-152.
- Nakamura, T., Schuster, G., Sugiura, M. & Sugita, M. (2004) Chloroplast RNA-binding and pentatricopeptide repeat proteins. Portland Press Ltd.
- Nelson, N. & Ben-Shem, A. (2004) The complex architecture of oxygenic photosynthesis. *Nature Reviews Molecular Cell Biology*, 5(12), 971-982.
- Nemhauser, J. & Chory, J. (2002) Photomorphogenesis. *The arabidopsis book*, 1, e0054-e0054.
- Nickelsen, J. & Rengstl, B. (2013) Photosystem II Assembly: From Cyanobacteria to Plants. In: Merchant, S. S. (ed.) *Annual Review of Plant Biology*, Vol 64.
- Niu, Y. & Xiang, Y. (2018) An Overview of Biomembrane Functions in Plant Responses to High-Temperature Stress. *Frontiers in Plant Science*. 9: 915.
- Oh, S. & Montgomery, B. L. (2013) Phytochrome-induced SIG2 expression contributes to photoregulation of phytochrome signalling and photomorphogenesis in *Arabidopsis thaliana*. *Journal of Experimental Botany*, 64(18), 5457-5472.
- Oh, S. & Montgomery, B. L. (2014) Phytochrome-dependent coordinate control of distinct aspects of nuclear and plastid gene expression during anterograde signaling and photomorphogenesis. *Frontiers in Plant Science*, 5 (171), 1-8.
- Oh, S., Warnasooriya, S. N. & Montgomery, B. L. (2013) Downstream effectors of light- and phytochrome-dependent regulation of hypocotyl elongation in *Arabidopsis thaliana*. *Plant Molecular Biology*, 81(6), 627-640.
- Ohgishi, M., Saji, K., Okada, K. & Sakai, T. (2004) Functional analysis of each blue light receptor, cry1, cry2, phot1, and phot2, by using combinatorial multiple mutants in *Arabidopsis*. *Proceedings of the National Academy of Sciences of the United States of America*, 101(8), 2223-2228.
- Ohta, M., Sugita, M. & Sugiura, M. (1995) Three types of nuclear genes encoding chloroplast RNA-binding proteins (cp29, cp31 and cp33) are present in *Arabidopsis thaliana*: presence of cp31 in chloroplasts and its homologue in nuclei/cytoplasms. *Plant molecular biology*, 27(3), 529-539.
- Okada, K., Saito, T., Nakagawa, T., Kawamukai, M. & Kamiya, Y. (2000) Five Geranylgeranyl Diphosphate Synthases Expressed in Different Organs Are Localized into Three Subcellular Compartments in *Arabidopsis*. *Plant Physiology*, 122(4), 1045.
- Okuda, K., Myouga, F., Motohashi, R., Shinozaki, K. & Shikanai, T. (2007) Conserved domain structure of pentatricopeptide repeat proteins involved in chloroplast RNA editing. *Proceedings of the National Academy of Sciences of the United States of America*, 104(19), 8178-8183.
- Okuzaki, A., Lehniger, M.-K., Muino, J. M., Lenzen, B., R uhe, T., Leister, D., Ohler, U. & Schmitz-Linneweber, C. (2019) The Chloroplast RNA binding protein CP31A shows cold-dependent RNA association and mediates cold-resistance via its acidic domain. *bioRxiv*, 832337.
- Orzaez, D., Medina, A., Torre, S., Fern andez-Moreno, J. P., Rambla, J. L., Fern andez-Del-Carmen, A., Butelli, E., Martin, C. & Granell, A. (2009) A Visual Reporter System for Virus-Induced Gene Silencing in Tomato Fruit Based on Anthocyanin Accumulation. *Plant Physiology*, 150(3), 1122.
- Osterlund, M. T., Hardtke, C. S., Wei, N. & Deng, X. W. (2000) Targeted destabilization of HY5 during light-regulated development of *Arabidopsis*. *Nature*, 405(6785), 462-466.
- Otani, T., Kato, Y. & Shikanai, T. (2018) Specific substitutions of light-harvesting complex I proteins associated with photosystem I are required for supercomplex formation with chloroplast NADH dehydrogenase-like complex. *The Plant Journal*, 94(1), 122-130.
- Pakrasi, H. B., Deciechi, P. & Whitmarsh, J. (1991) Site directed mutagenesis of the heme axial ligands of cytochrome-b559 affects the stability of the photosystem-ii complex. *Embo Journal*, 10(7), 1619-1627.

- Pecker, I., Chamovitz, D., Linden, H., Sandmann, G. & Hirschberg, J. (1992) A single polypeptide catalyzing the conversion of phytoene to zeta-carotene is transcriptionally regulated during tomato fruit ripening. *Proceedings of the National Academy of Sciences*, 89(11), 4962.
- Penarrubia, L., Aguilar, M., Margossian, L. & Fischer, R. L. (1992) An Antisense Gene Stimulates Ethylene Hormone Production during Tomato Fruit Ripening. *The Plant Cell*, 4(6), 681.
- Pfaffl, M. W. (2001) A new mathematical model for relative quantification in real-time RT-PCR. *Nucleic acids research*, 29(9), e45-e45.
- Pfalz, J., Liere, K., Kandlbinder, A., Dietz, K. J. & Oelmüller, R. (2006) PTAC2, -6, and -12 are components of the transcriptionally active plastid chromosome that are required for plastid gene expression. *Plant Cell*, 18(1), 176-197.
- Pfannschmidt, T., Bräutigam, K., Wagner, R., Dietzel, L., Schröter, Y., Steiner, S. & Nykytenko, A. (2008) Potential regulation of gene expression in photosynthetic cells by redox and energy state: approaches towards better understanding. *Annals of Botany*, 103(4), 599-607.
- Piechulla, B., Glick, R. E., Bahl, H., Melis, A. & Grisse, W. (1987) Changes in Photosynthetic Capacity and Photosynthetic Protein Pattern during Tomato Fruit Ripening. *Plant Physiology*, 84(3), 911.
- Piringer, A. A. & Heinze, P. H. (1954) Effect of Light on the Formation of a Pigment in the Tomato Fruit Cuticle. *Plant physiology*, 29(5), 467-472.
- Pogson, B. J. & Albrecht, V. (2011) Genetic Dissection of Chloroplast Biogenesis and Development: An Overview. *Plant Physiology*, 155(4), 1545.
- Pogson, B. J., Woo, N. S., Förster, B. & Small, I. D. (2008) Plastid signalling to the nucleus and beyond. *Trends in plant science*, 13(11), 602-609.
- Pribil, M., Pesaresi, P., Hertle, A., Barbato, R. & Leister, D. (2010) Role of plastid protein phosphatase TAP38 in LHClI dephosphorylation and thylakoid electron flow. *PLoS Biol*, 8(1), e1000288.
- Privat, I., Hakimi, M. A., Buhot, L., Favory, J. J. & Lerbs-Mache, S. (2003) Characterization of Arabidopsis plastid sigma-like transcription factors SIG1, SIG2 and SIG3. *Plant Molecular Biology*, 51(3), 385-399.
- Pyke, K. A. & Howells, C. A. (2002) Plastid and Stromule Morphogenesis in Tomato. *Annals of Botany*, 90(5), 559-566.
- Qiu, Y., Li, M., Kim, R. J.-A., Moore, C. M. & Chen, M. (2019) - Daytime temperature is sensed by phytochrome B in Arabidopsis through a transcriptional activator HEMERA. - 10(- 1).
- Quail, P. H. (2002) Photosensory perception and signalling in plant cells: new paradigms? *Current Opinion in Cell Biology*, 14(2), 180-188.
- Ramel, F., Birtic, S., Ginies, C., Soubigou-Taconnat, L., Triantaphylidès, C. & Havaux, M. (2012) Carotenoid oxidation products are stress signals that mediate gene responses to singlet oxygen in plants. *Proceedings of the National Academy of Sciences*, 109(14), 5535-5540.
- Raven, J. A. & Allen, J. F. (2003) Genomics and chloroplast evolution: what did cyanobacteria do for plants? *Genome Biology*, 4(3).
- Raymond, J. & Blankenship, R. E. (2008) The origin of the oxygen-evolving complex. *Coordination chemistry reviews*, 252(3-4), 377-383.
- Reddy Chichili, V. P., Kumar, V. & Sivaraman, J. (2013) Linkers in the structural biology of protein-protein interactions. *Protein Science*, 22(2), 153-167.
- Reed, J. W., Nagpal, P., Poole, D. S., Furuya, M. & Chory, J. (1993) Mutations in the gene for the red far-red light receptor phytochrome-b alter cell elongation and physiological-responses throughout arabidopsis development. *Plant Cell*, 5(2), 147-157.
- Reiland, S., Messerli, G., Baerenfaller, K., Gerrits, B., Endler, A., Grossmann, J., Grisse, W. & Baginsky, S. (2009) Large-scale Arabidopsis phosphoproteome profiling reveals novel chloroplast kinase substrates and phosphorylation networks. *Plant physiology*, 150(2), 889-903.
- Ren, Y., Li, Y., Jiang, Y., Wu, B. & Miao, Y. (2017) Phosphorylation of WHIRLY1 by CIPK14 shifts its localization and dual functions in Arabidopsis. *Molecular Plant*, 10(5), 749-763.

- Renger, G. & Kuhn, P. (2007) Reaction pattern and mechanism of light induced oxidative water splitting in photosynthesis. *Biochimica Et Biophysica Acta-Bioenergetics*, 1767(6), 458-471.
- Richter, A. S., Tohge, T., Fernie, A. R. & Grimm, B. (2020) The genomes uncoupled-dependent signalling pathway coordinates plastid biogenesis with the synthesis of anthocyanins. *Philosophical Transactions of the Royal Society B: Biological Sciences*, 375(1801), 20190403.
- Roach, T. & Krieger-Liszkay, A. (2012) The role of the PsbS protein in the protection of photosystems I and II against high light in *Arabidopsis thaliana*. *Biochimica et Biophysica Acta (BBA)-Bioenergetics*, 1817(12), 2158-2165.
- Robertson, E. J., Pyke, K. A. & Leech, R. M. (1995) *arc6*, an extreme chloroplast division mutant of *Arabidopsis* also alters proplastid proliferation and morphology in shoot and root apices. *Journal of Cell Science*, 108(9), 2937.
- Rochaix, J.-D., Lemeille, S., Shapiguzov, A., Samol, I., Fucile, G., Willig, A. & Goldschmidt-Clermont, M. (2012) Protein kinases and phosphatases involved in the acclimation of the photosynthetic apparatus to a changing light environment. *Philosophical Transactions of the Royal Society B: Biological Sciences*, 367(1608), 3466-3474.
- Rochaix, J. D. (2011) Assembly of the Photosynthetic Apparatus. *Plant Physiology*, 155(4), 1493-1500.
- Roitinger, E., Hofer, M., Köcher, T., Pichler, P., Novatchkova, M., Yang, J., Schlögelhofer, P. & Mechtler, K. (2015) Quantitative phosphoproteomics of the ataxia telangiectasia-mutated (ATM) and ataxia telangiectasia-mutated and rad3-related (ATR) dependent DNA damage response in *Arabidopsis thaliana*. *Molecular & Cellular Proteomics*, 14(3), 556-571.
- Rokka, A., Suorsa, M., Saleem, A., Battchikova, N. & Aro, E.-M. (2005) Synthesis and assembly of thylakoid protein complexes: multiple assembly steps of photosystem II. *Biochemical Journal*, 388(1), 159-168.
- Rossel, J. B., Wilson, I. W. & Pogson, B. J. (2002) Global Changes in Gene Expression in Response to High Light in *Arabidopsis*. *Plant Physiology*, 130(3), 1109.
- Rosso, S. W. (1968) The ultrastructure of chromoplast development in red tomatoes. *Journal of Ultrastructure Research*, 25(3), 307-322.
- Ruban, A. V., Johnson, M. P. & Duffy, C. D. P. (2012) The photoprotective molecular switch in the photosystem II antenna. *Biochimica Et Biophysica Acta-Bioenergetics*, 1817(1), 167-181.
- Ruban, A. V. & Murchie, E. H. (2012) Assessing the photoprotective effectiveness of non-photochemical chlorophyll fluorescence quenching: A new approach. *Biochimica Et Biophysica Acta-Bioenergetics*, 1817(7), 977-982.
- Ruckle, M. E., Burgoon, L. D., Lawrence, L. A., Sinkler, C. A. & Larkin, R. M. (2012) Plastids Are Major Regulators of Light Signaling in *Arabidopsis*. *Plant Physiology*, 159(1), 366.
- Ruiz-Sola, M. Á. & Rodríguez-Concepción, M. (2012) Carotenoid biosynthesis in *Arabidopsis*: a colorful pathway. *The Arabidopsis book/American Society of Plant Biologists*, 10.
- Ruwe, H., Kupsch, C., Teubner, M. & Schmitz-Linneweber, C. (2011) The RNA-recognition motif in chloroplasts. *Journal of Plant Physiology*, 168(12), 1361-1371.
- Saitou, N. & Nei, M. (1987) The neighbor-joining method: a new method for reconstructing phylogenetic trees. *Molecular Biology and Evolution*, 4(4), 406-425.
- Sakamoto, K. & Nagatani, A. (1996) Nuclear localization activity of phytochrome B. *Plant Journal*, 10(5), 859-868.
- Sakamoto, W., Miyagishima, S.-Y. & Jarvis, P. (2008) Chloroplast biogenesis: control of plastid development, protein import, division and inheritance. *The arabidopsis book*, 6, e0110-e0110.
- Samach, A. & Wigge, P. A. (2005) Ambient temperature perception in plants. *Current Opinion in Plant Biology*, 8(5), 483-486.
- Sarhadi, E., Mahfoozi, S., Hosseini, S. A. & Salekdeh, G. H. (2010) Cold acclimation proteome analysis reveals close link between the up-regulation of low-temperature associated proteins and vernalization fulfillment. *Journal of proteome research*, 9(11), 5658-5667.

- Sato, S., Nakamura, Y., Kaneko, T., Asamizu, E. & Tabata, S. (1999) Complete structure of the chloroplast genome of *Arabidopsis thaliana*. *DNA research : an international journal for rapid publication of reports on genes and genomes*, 6(5), 283-90.
- Sato, S., Tabata, S., Hirakawa, H., Asamizu, E., Shirasawa, K., Isobe, S., Kaneko, T., Nakamura, Y., Shibata, D., Aoki, K., Egholm, M., Knight, J., Bogden, R., Li, C., Shuang, Y., Xu, X., Pan, S., Cheng, S., Liu, X., Ren, Y., Wang, J., Albiero, A., Dal Pero, F., Todesco, S., Van Eck, J., Buels, R. M., Bombarely, A., Gosselin, J. R., Huang, M., Leto, J. A., Menda, N., Strickler, S., Mao, L., Gao, S., Teclé, I. Y., York, T., Zheng, Y., Vrebalov, J. T., Lee, J., Zhong, S., Mueller, L. A., Stiekema, W. J., Ribeca, P., Alioto, T., Yang, W., Huang, S., Du, Y., Zhang, Z., Gao, J., Guo, Y., Wang, X., Li, Y., He, J., Li, C., Cheng, Z., Zuo, J., Ren, J., Zhao, J., Yan, L., Jiang, H., Wang, B., Li, H., Li, Z., Fu, F., Chen, B., Han, B., Feng, Q., Fan, D., Wang, Y., Ling, H., Xue, Y., Ware, D., Richard McCombie, W., Lippman, Z. B., Chia, J.-M., Jiang, K., Pasternak, S., Gelley, L., Kramer, M., Anderson, L. K., Chang, S.-B., Royer, S. M., Shearer, L. A., Stack, S. M., Rose, J. K. C., Xu, Y., Eannetta, N., Matas, A. J., McQuinn, R., Tanksley, S. D., Camara, F., Guigó, R., Rombauts, S., Fawcett, J., Van De Peer, Y., Zamir, D., Liang, C., Spannagl, M., Gundlach, H., Bruggmann, R., et al. (2012) The tomato genome sequence provides insights into fleshy fruit evolution. *Nature*, 485(7400), 635-641.
- Schaffner, C., Laasch, H. & Hagemann, R. (1995) Detection of point mutations in chloroplast genes of *Antirrhinum majus* L. I. Identification of a point mutation in the *psaB* gene of a photosystem I plastome mutant. *Molecular and General Genetics MGG*, 249(5), 533-544.
- Scheller, H. V., Jensen, P. E., Haldrup, A., Lunde, C. & Knoetzel, J. (2001) Role of subunits in eukaryotic Photosystem I. *Biochimica et Biophysica Acta (BBA) - Bioenergetics*, 1507(1), 41-60.
- Schmitz-Linneweber, C., Williams-Carrier, R. & Barkan, A. (2005) RNA immunoprecipitation and microarray analysis show a chloroplast pentatricopeptide repeat protein to be associated with the 5' region of mRNAs whose translation it activates. *Plant Cell*, 17(10), 2791-2804.
- Schnable, P. S., Ware, D., Fulton, R. S., Stein, J. C., Wei, F., Pasternak, S., Liang, C., Zhang, J., Fulton, L., Graves, T. A., Minx, P., Reily, A. D., Courtney, L., Kruchowski, S. S., Tomlinson, C., Strong, C., Delehaunty, K., Fronick, C., Courtney, B., Rock, S. M., Belter, E., Du, F., Kim, K., Abbott, R. M., Cotton, M., Levy, A., Marchetto, P., Ochoa, K., Jackson, S. M., Gillam, B., Chen, W., Yan, L., Higginbotham, J., Cardenas, M., Waligorski, J., Applebaum, E., Phelps, L., Falcone, J., Kanchi, K., Thane, T., Scimone, A., Thane, N., Henke, J., Wang, T., Ruppert, J., Shah, N., Rotter, K., Hodges, J., Ingenthron, E., Cordes, M., Kohlberg, S., Sgro, J., Delgado, B., Mead, K., Chinwalla, A., Leonard, S., Crouse, K., Collura, K., Kudrna, D., Currie, J., He, R., Angelova, A., Rajasekar, S., Mueller, T., Lomeli, R., Scara, G., Ko, A., Delaney, K., Wissotski, M., Lopez, G., Campos, D., Braidotti, M., Ashley, E., Golser, W., Kim, H., Lee, S., Lin, J., Dujmic, Z., Kim, W., Talag, J., Zuccolo, A., Fan, C., Sebastian, A., Kramer, M., Spiegel, L., Nascimento, L., Zutavern, T., Miller, B., Ambroise, C., Muller, S., Spooner, W., Narechania, A., Ren, L., Wei, S., Kumari, S., Faga, B., Levy, M. J., McMahan, L., Van Buren, P., Vaughn, M. W., et al. (2009) The B73 Maize Genome: Complexity, Diversity, and Dynamics. *Science*, 326(5956), 1112.
- Schofield, A. & Paliyath, G. (2005) Modulation of carotenoid biosynthesis during tomato fruit ripening through phytochrome regulation of phytoene synthase activity. *Plant Physiology and Biochemistry*, 43(12), 1052-1060.
- Schönberg, A. & Baginsky, S. (2012) Signal integration by chloroplast phosphorylation networks: an update. *Frontiers in plant science*, 3, 256.
- Schuhmann, H. & Adamska, I. (2012) Deg proteases and their role in protein quality control and processing in different subcellular compartments of the plant cell. *Physiologia Plantarum*, 145(1), 224-234.
- Schumann, T., Paul, S., Melzer, M., Dörmann, P. & Jahns, P. (2017) Plant growth under natural light conditions provides highly flexible short-term acclimation properties toward high light stress. *Frontiers in plant science*, 8, 681.

- Schuster, G. & Gruissem, W. (1991) Chloroplast mRNA 3' end processing requires a nuclear-encoded RNA-binding protein. *The EMBO journal*, 10(6), 1493-1502.
- Schuster, G., Lisitsky, I. & Klaff, P. (1999) Polyadenylation and degradation of mRNA in the chloroplast. *Plant Physiology*, 120(4), 937-944.
- Seaton, D. D., Ebenhöh, O., Millar, A. J. & Pokhilko, A. (2014) Regulatory principles and experimental approaches to the circadian control of starch turnover. *Journal of the Royal Society Interface*, 11(91), 20130979.
- Sellaro, R., Smith, R. W., Legris, M., Fleck, C. & Casal, J. J. (2019) Phytochrome B dynamics departs from photoequilibrium in the field. *Plant, cell & environment*, 42(2), 606-617.
- Shan, Q., Wang, Y., Li, J., Zhang, Y., Chen, K., Liang, Z., Zhang, K., Liu, J., Xi, J. J., Qiu, J.-L. & Gao, C. (2013) Targeted genome modification of crop plants using a CRISPR-Cas system. *Nature Biotechnology*, 31(8), 686-688.
- Sharma, A., Kumar, V., Shahzad, B., Ramakrishnan, M., Sidhu, G. P. S., Bali, A. S., Handa, N., Kapoor, D., Yadav, P., Khanna, K., Bakshi, P., Rehman, A., Kohli, S. K., Khan, E. A., Parihar, R. D., Yuan, H., Thukral, A. K., Bhardwaj, R. & Zheng, B. S. (2020) Photosynthetic Response of Plants Under Different Abiotic Stresses: A Review. *Journal of Plant Growth Regulation*, 39(2), 509-531.
- Sharrock, R. A. & Clack, T. (2002) Patterns of expression and normalized levels of the five Arabidopsis phytochromes. *Plant Physiology*, 130(1), 442-456.
- Shen, Y., Khanna, R., Carle, C. M. & Quail, P. H. (2007) Phytochrome induces rapid PIF5 phosphorylation and degradation in response to red-light activation. *Plant Physiology*, 145(3), 1043-1051.
- Shi, C., Wang, S., Xia, E.-H., Jiang, J.-J., Zeng, F.-C. & Gao, L.-Z. (2016) Full transcription of the chloroplast genome in photosynthetic eukaryotes. *Scientific Reports*, 6(1), 30135.
- Shi, L. X. & Schroder, W. P. (2004) The low molecular mass subunits of the photosynthetic supracomplex, photosystem II. *Biochimica Et Biophysica Acta-Bioenergetics*, 1608(2-3), 75-96.
- Shi, Q.-M., Yang, X., Song, L. & Xue, H.-W. (2011) Arabidopsis MSBP1 is activated by HY5 and HYH and is involved in photomorphogenesis and brassinosteroid sensitivity regulation. *Molecular plant*, 4(6), 1092-1104.
- Shikata, H., Hanada, K., Ushijima, T., Nakashima, M., Suzuki, Y. & Matsushita, T. (2014) Phytochrome controls alternative splicing to mediate light responses in Arabidopsis. *Proceedings of the National Academy of Sciences*, 111(52), 18781-18786.
- Shimizu, T., Kacprzak, S. M., Mochizuki, N., Nagatani, A., Watanabe, S., Shimada, T., Tanaka, K., Hayashi, Y., Arai, M., Leister, D., Okamoto, H., Terry, M. J. & Masuda, T. (2019) The retrograde signaling protein GUN1 regulates tetrapyrrole biosynthesis. *Proceedings of the National Academy of Sciences*, 116(49), 24900-24906.
- Shin, D. H., Choi, M., Kim, K., Bang, G., Cho, M., Choi, S.-B., Choi, G. & Park, Y.-I. (2013) HY5 regulates anthocyanin biosynthesis by inducing the transcriptional activation of the MYB75/PAP1 transcription factor in Arabidopsis. *FEBS letters*, 587(10), 1543-1547.
- Shumbe, L., Bott, R. & Havaux, M. (2014) Dihydroactinidiolide, a high light-induced β -carotene derivative that can regulate gene expression and photoacclimation in Arabidopsis. *Molecular Plant*, 7(7), 1248-1251.
- Šimková, K., Moreau, F., Pawlak, P., Vriet, C., Baruah, A., Alexandre, C., Hennig, L., Apel, K. & Laloi, C. (2012) Integration of stress-related and reactive oxygen species-mediated signals by Topoisomerase VI in Arabidopsis thaliana. *Proceedings of the National Academy of Sciences*, 109(40), 16360-16365.
- Singh, R., Singh, S., Parihar, P., Singh, V. P. & Prasad, S. M. (2015) Retrograde signaling between plastid and nucleus: A review. *Journal of Plant Physiology*, 181, 55-66.
- Smith, J. H. (1954) The Development of Chlorophyll and Oxygen-evolving Power in Etiolated Barley Leaves When Illuminated. *Plant physiology*, 29(2), 143-148.

- Soll, J. & Schleiff, E. (2004) Protein import into chloroplasts. *Nature Reviews Molecular Cell Biology*, 5(3), 198-208.
- Song, Y. H., Yoo, C. M., Hong, A. P., Kim, S. H., Jeong, H. J., Shin, S. Y., Kim, H. J., Yun, D.-J., Lim, C. O. & Bahk, J. D. (2008) DNA-binding study identifies C-box and hybrid C/G-box or C/A-box motifs as high-affinity binding sites for STF1 and LONG HYPOCOTYL5 proteins. *Plant physiology*, 146(4), 1862-1877.
- Sperschneider, J., Catanzariti, A.-M., Deboer, K., Petre, B., Gardiner, D. M., Singh, K. B., Dodds, P. N. & Taylor, J. M. (2017) LOCALIZER: subcellular localization prediction of both plant and effector proteins in the plant cell. *Scientific Reports*, 7(1), 44598.
- Stern, D. B., Goldschmidt-Clermont, M. & Hanson, M. R. (2010) Chloroplast RNA Metabolism. In: Merchant, S., Briggs, W. R. & Ort, D. (eds.) *Annual Review of Plant Biology*, Vol 61.
- Strand, Å., Asami, T., Alonso, J., Ecker, J. R. & Chory, J. (2003) Chloroplast to nucleus communication triggered by accumulation of Mg-protoporphyrinIX. *Nature*, 421(6918), 79-83.
- Strand, A., Hurry, V., Gustafsson, P. & Gardestrom, P. (1997) Development of Arabidopsis thaliana leaves at low temperatures releases the suppression of photosynthesis and photosynthetic gene expression despite the accumulation of soluble carbohydrates. *Plant Journal*, 12(3), 605-614.
- Strand, A., Hurry, V., Henkes, S., Huner, N., Gustafsson, P., Gardestrom, P. & Stitt, M. (1999) Acclimation of Arabidopsis leaves developing at low temperatures. Increasing cytoplasmic volume accompanies increased activities of enzymes in the Calvin cycle and in the sucrose-biosynthesis pathway. *Plant Physiology*, 119(4), 1387-1397.
- Sugita, M. & Sugiura, M. (1996) Regulation of gene expression in chloroplasts of higher plants. *Plant Molecular Biology*, 32(1-2), 315-326.
- Sugita, M., Uchiyama, H. & Ichinose, M. (2016) RRM and PPR proteins network as a global regulator for plastid RNA metabolism. *Endocytobiosis Cell Res.*, 27, 41-44.
- Sugiura, M. (1992) THE CHLOROPLAST GENOME. *Plant Molecular Biology*, 19(1), 149-168.
- Sulpice, R., Flis, A., Ivakov, A. A., Apelt, F., Krohn, N., Encke, B., Abel, C., Feil, R., Lunn, J. E. & Stitt, M. (2014) Arabidopsis Coordinates the Diurnal Regulation of Carbon Allocation and Growth across a Wide Range of Photoperiods. *Molecular Plant*, 7(1), 137-155.
- Sun, X., Feng, P., Xu, X., Guo, H., Ma, J., Chi, W., Lin, R., Lu, C. & Zhang, L. (2011) A chloroplast envelope-bound PHD transcription factor mediates chloroplast signals to the nucleus. *Nature communications*, 2(1), 1-10.
- Susek, R. E., Ausubel, F. M. & Chory, J. (1993) Signal transduction mutants of Arabidopsis uncouple nuclear CAB and RBCS gene expression from chloroplast development. *Cell*, 74(5), 787-799.
- Suzuki, N., Devireddy, A. R., Inupakutika, M. A., Baxter, A., Miller, G., Song, L., Shulaev, E., Azad, R. K., Shulaev, V. & Mittler, R. (2015) Ultra-fast alterations in mRNA levels uncover multiple players in light stress acclimation in plants. *The Plant Journal*, 84(4), 760-772.
- Swiatek, M., Regel, R. E., Meurer, J., Wanner, G., Pakrasi, H. B., Ohad, I. & Herrmann, R. G. (2003) Effects of selective inactivation of individual genes for low-molecular-mass subunits on the assembly of photosystem II, as revealed by chloroplast transformation: the psbEFLJ operon in Nicotiana tabacum. *Molecular Genetics and Genomics*, 268(6), 699-710.
- Szechyńska-Hebda, M. & Karpiński, S. (2013) Light intensity-dependent retrograde signalling in higher plants. *Journal of Plant Physiology*, 170(17), 1501-1516.
- Team, R. C. (2020) R: the R project for statistical computing. 2019. URL: <https://www.r-project.org/>[accessed 2020-03-30].
- Tepperman, J. M., Hwang, Y. S. & Quail, P. H. (2006) phyA dominates in transduction of red-light signals to rapidly responding genes at the initiation of Arabidopsis seedling de-etiolation. *Plant Journal*, 48(5), 728-742.
- Teubner, M., Fuß, J., Kühn, K., Krause, K. & Schmitz-Linneweber, C. (2017) The RNA recognition motif protein CP 33A is a global ligand of chloroplast mRNA s and is essential for plastid biogenesis and plant development. *The Plant Journal*, 89(3), 472-485.

- Teubner, M., Lenzen, B., Espenberger, L. B., Fuss, J., Nickelsen, J., Krause, K., Ruwe, H. & Schmitz-Linneweber, C. (2020) The chloroplast ribonucleoprotein CP33B quantitatively binds the psbA mRNA. *Plants*, 9(3), 367.
- Thompson, J. D., Higgins, D. G. & Gibson, T. J. (1994) CLUSTAL W: improving the sensitivity of progressive multiple sequence alignment through sequence weighting, position-specific gap penalties and weight matrix choice. *Nucleic Acids Research*, 22(22), 4673-4680.
- Thornton, L. E., Ohkawa, H., Roose, J. L., Kashino, Y., Keren, N. & Pakrasi, H. B. (2004) Homologs of plant PsbP and PsbQ proteins are necessary for regulation of photosystem II activity in the cyanobacterium *Synechocystis* 6803. *Plant Cell*, 16(8), 2164-2175.
- Tian, Y., Sacharz, J., Ware, M. A., Zhang, H. & Ruban, A. V. (2017) Effects of periodic photoinhibitory light exposure on physiology and productivity of *Arabidopsis* plants grown under low light. *Journal of experimental botany*, 68(15), 4249-4262.
- Tillich, M., Hardel, S. L., Kupsch, C., Armbruster, U., Delannoy, E., Gualberto, J. M., Lehwark, P., Leister, D., Small, I. D. & Schmitz-Linneweber, C. (2009) Chloroplast ribonucleoprotein CP31A is required for editing and stability of specific chloroplast mRNAs. *Proceedings of the National Academy of Sciences*, 106(14), 6002-6007.
- Toledo-Ortiz, G., Johansson, H., Lee, K. P., Bou-Torrent, J., Stewart, K., Steel, G., Rodriguez-Concepcion, M. & Halliday, K. J. (2014) The HY5-PIF Regulatory Module Coordinates Light and Temperature Control of Photosynthetic Gene Transcription. *Plos Genetics*, 10(6).
- Uchiyama, H., Ichinose, M. & Sugita, M. (2018) Chloroplast ribonucleoprotein-like proteins of the moss *Physcomitrella patens* are not involved in RNA stability and RNA editing. *Photosynthetica*, 56(1), 62-66.
- Ushijima, T., Hanada, K., Gotoh, E., Yamori, W., Kodama, Y., Tanaka, H., Kusano, M., Fukushima, A., Tokizawa, M., Yamamoto, Y. Y., Tada, Y., Suzuki, Y. & Matsushita, T. (2017) Light Controls Protein Localization through Phytochrome-Mediated Alternative Promoter Selection. *Cell*, 171(6), 1316-1325.e12.
- Van Ploeg, D. & Heuvelink, E. (2005) Influence of sub-optimal temperature on tomato growth and yield: a review. *The Journal of Horticultural Science and Biotechnology*, 80(6), 652-659.
- Varela-Ortega, C., Blanco-Gutierrez, I., Esteve, P., Bharwani, S., Fronzek, S. & Downing, T. E. (2016) How can irrigated agriculture adapt to climate change? Insights from the Guadiana Basin in Spain. *Regional Environmental Change*, 16(1), 59-70.
- Vargas-Suárez, M., Castro-Sánchez, A., Toledo-Ortiz, G., De La Vara, L. E. G., García, E. & Loza-Tavera, H. (2013) Protein phosphorylation regulates in vitro spinach chloroplast petD mRNA 3'-untranslated region stability, processing, and degradation. *Biochimie*, 95(2), 400-409.
- Varotto, C., Pesaresi, P., Jahns, P., Lessnick, A., Tizzano, M., Schiavon, F., Salamini, F. & Leister, D. (2002) Single and double knockouts of the genes for photosystem I subunits G, K, and H of *Arabidopsis*. Effects on photosystem I composition, photosynthetic electron flow, and state transitions. *Plant Physiology*, 129(2), 616-624.
- Varotto, C., Pesaresi, P., Meurer, J., Oelmüller, R., Steiner-Lange, S., Salamini, F. & Leister, D. (2000) Disruption of the *Arabidopsis* photosystem I gene *psaE1* affects photosynthesis and impairs growth. *Plant Journal*, 22(2), 115-124.
- Velitchkova, M., Popova, A. V., Faik, A., Gerganova, M. & Ivanov, A. G. (2020) Low temperature and high light dependent dynamic photoprotective strategies in *Arabidopsis thaliana*. *Physiologia plantarum*, 170(1), 93-108.
- Violet-Chabrand, S., Matthews, J. S., Simkin, A. J., Raines, C. A. & Lawson, T. (2017) Importance of fluctuations in light on plant photosynthetic acclimation. *Plant Physiology*, 173(4), 2163-2179.
- Vogel, M. O., Moore, M., König, K., Pecher, P., Alsharafa, K., Lee, J. & Dietz, K.-J. (2014) Fast retrograde signaling in response to high light involves metabolite export, MITOGEN-ACTIVATED PROTEIN KINASE6, and AP2/ERF transcription factors in *Arabidopsis*. *The Plant Cell*, 26(3), 1151-1165.

- Von Zychlinski, A., Kleffmann, T., Krishnamurthy, N., Sjölander, K., Baginsky, S. & Gruissem, W. (2005) Proteome analysis of the rice etioplast: metabolic and regulatory networks and novel protein functions. *Molecular & Cellular Proteomics*, 4(8), 1072-1084.
- Waese, J., Fan, J., Pasha, A., Yu, H., Fucile, G., Shi, R., Cumming, M., Kelley, L. A., Sternberg, M. J. & Krishnakumar, V. (2017) ePlant: visualizing and exploring multiple levels of data for hypothesis generation in plant biology. *The Plant Cell*, 29(8), 1806-1821.
- Wallace, J. M. (2014) Global warming and winter weather (vol 343, pg 729, 2014). *Science*, 343(6174), 969-969.
- Walters, R. G. (2005) Towards an understanding of photosynthetic acclimation. *Journal of experimental botany*, 56(411), 435-447.
- Wang, B. C., Wang, H. X., Feng, J. X., Meng, D. Z., Qu, L. J. & Zhu, Y. X. (2006) Post-translational modifications, but not transcriptional regulation, of major chloroplast RNA-binding proteins are related to Arabidopsis seedling development. *Proteomics*, 6(8), 2555-2563.
- Wang, P., Hendron, R.-W. & Kelly, S. (2017) Transcriptional control of photosynthetic capacity: conservation and divergence from Arabidopsis to rice. *New Phytologist*, 216(1), 32-45.
- Wang, S., Bai, G., Wang, S., Yang, L., Yang, F., Wang, Y., Zhu, J.-K. & Hua, J. (2016) Chloroplast RNA-binding protein RBD1 promotes chilling tolerance through 23S rRNA processing in Arabidopsis. *PLoS genetics*, 12(5), e1006027.
- Ware, M. A., Belgio, E. & Ruban, A. V. (2015) Comparison of the protective effectiveness of NPQ in Arabidopsis plants deficient in PsbS protein and zeaxanthin. *Journal of Experimental Botany*, 66(5), 1259-1270.
- Waters, M. T., Fray, R. G. & Pyke, K. A. (2004) Stromule formation is dependent upon plastid size, plastid differentiation status and the density of plastids within the cell. *The Plant Journal*, 39(4), 655-667.
- Waters, M. T., Wang, P., Korkaric, M., Capper, R. G., Saunders, N. J. & Langdale, J. A. (2009) GLK Transcription Factors Coordinate Expression of the Photosynthetic Apparatus in Arabidopsis. *Plant Cell*, 21(4), 1109-1128.
- Way, D. A. & Pearcy, R. W. (2012) Sunflecks in trees and forests: from photosynthetic physiology to global change biology. *Tree Physiology*, 32(9), 1066-1081.
- Weller, J. L., Schreuder, M. E. L., Smith, H., Koornneef, M. & Kendrick, R. E. (2000) Physiological interactions of phytochromes A, B1 and B2 in the control of development in tomato. *The Plant Journal*, 24(3), 345-356.
- Wigge, P. A. (2013) Ambient temperature signalling in plants. *Current opinion in plant biology*, 16(5), 661-666.
- Willmann, M. R. & Poethig, R. S. (2011) The effect of the floral repressor FLC on the timing and progression of vegetative phase change in Arabidopsis. *Development*, 138(4), 677.
- Wise, R. R., Olson, A. J., Schrader, S. M. & Sharkey, T. D. (2004) Electron transport is the functional limitation of photosynthesis in field-grown Pima cotton plants at high temperature. *Plant Cell and Environment*, 27(6), 717-724.
- Woodson, J. D., Perez-Ruiz, J. M. & Chory, J. (2011) Heme synthesis by plastid ferrochelatase I regulates nuclear gene expression in plants. *Current Biology*, 21(10), 897-903.
- Woodson, J. D., Perez-Ruiz, J. M., Schmitz, R. J., Ecker, J. R. & Chory, J. (2013) Sigma factor-mediated plastid retrograde signals control nuclear gene expression. *The Plant Journal*, 73(1), 1-13.
- Wu, J., Liu, H., Lu, S., Hua, J. & Zou, B. (2021) Identification and expression analysis of chloroplast ribonucleoproteins (cpRNPs) in Arabidopsis and rice. *Genome*, 99(999), 1-10.
- Xiao, Y., Savchenko, T., Baidoo, E. E., Chehab, W. E., Hayden, D. M., Tolstikov, V., Corwin, J. A., Kliebenstein, D. J., Keasling, J. D. & Dehesh, K. (2012) Retrograde signaling by the plastidial metabolite MEcPP regulates expression of nuclear stress-response genes. *Cell*, 149(7), 1525-1535.

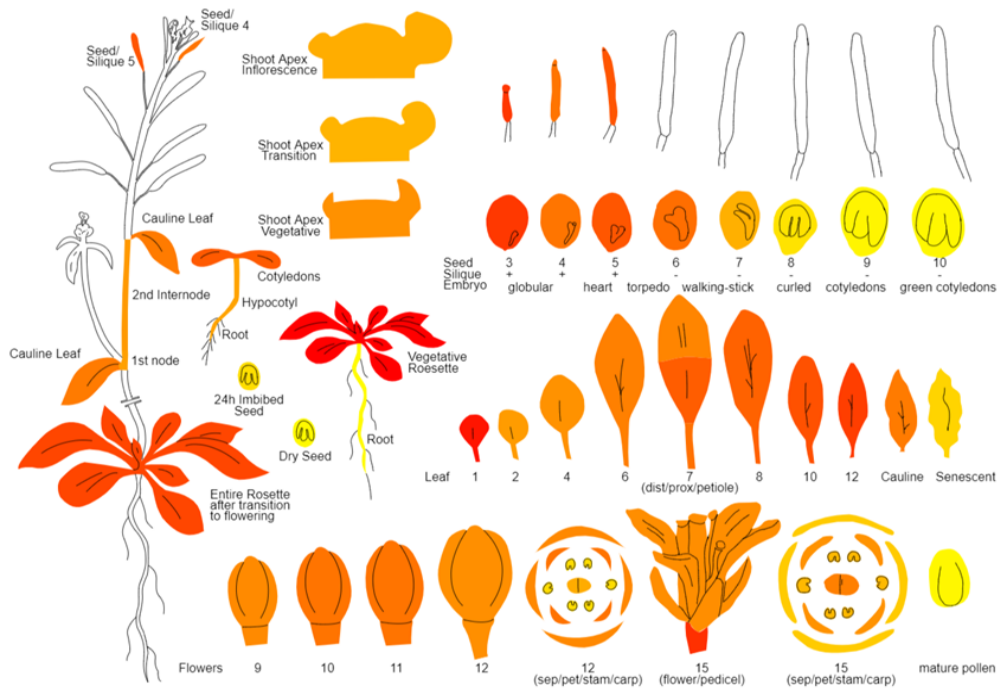
- Yabuta, S., Ifuku, K., Takabayashi, A., Ishihara, S., Ido, K., Ishikawa, N., Endo, T. & Sato, F. (2010) Three PsbQ-Like Proteins are Required for the Function of the Chloroplast NAD(P)H Dehydrogenase Complex in Arabidopsis. *Plant and Cell Physiology*, 51(6), 866-876.
- Yagi, Y. & Shiina, T. (2014) Recent advances in the study of chloroplast gene expression and its evolution. *Frontiers in Plant Science*, 5, 61.
- Yamori, W., Asakura, Y., Nakai, M., Noguchi, K. & Terashima, I. (2005a) Analyses of mechanisms of photosynthetic temperature acclimation: Temperature acclimation of Rubisco characteristics in spinach leaves. *Plant and Cell Physiology*, 46, S185-S185.
- Yamori, W., Noguchi, K. & Terashima, I. (2005b) Temperature acclimation of photosynthesis in spinach leaves: analyses of photosynthetic components and temperature dependencies of photosynthetic partial reactions. *Plant Cell and Environment*, 28(4), 536-547.
- Yang, Z., Liu, B., Su, J., Liao, J., Lin, C. & Oka, Y. (2017) Cryptochromes orchestrate transcription regulation of diverse blue light responses in plants. *Photochemistry and photobiology*, 93(1), 112-127.
- Ye, L., Li, Y., Fukami-Kobayashi, K., Go, M., Konishi, T., Watanabe, A. & Sugiura, M. (1991) Diversity of a ribonucleoprotein family in tobacco chloroplasts: two new chloroplast ribonucleoproteins and a phylogenetic tree of ten chloroplast RNA-binding domains. *Nucleic Acids Research*, 19(23), 6485-6490.
- Yoo, C. Y., Pasoreck, E. K., Wang, H., Cao, J., Blaha, G. M., Weigel, D. & Chen, M. (2019) Phytochrome activates the plastid-encoded RNA polymerase for chloroplast biogenesis via nucleus-to-plastid signaling. *Nature Communications*, 10.
- Yoshida, O., Nakagawa, H., Ogura, N. & Sato, T. (1984) Effect of Heat Treatment on the Development of Polygalacturonase Activity in Tomato Fruit during Ripening. *Plant and Cell Physiology*, 25(3), 505-509.
- Yoshida, Y., Sarmiento-Mañús, R., Yamori, W., Ponce, M. R., Micol, J. L. & Tsukaya, H. (2018) The Arabidopsis phyB-9 mutant has a second-site mutation in the VENOSA4 gene that alters chloroplast size, photosynthetic traits, and leaf growth. *Plant physiology*, 178(1), 3-6.
- Yoshioka, M., Uchida, S., Mori, H., Komayama, K., Ohira, S., Morita, N., Nakanishi, T. & Yamamoto, Y. (2006) Quality control of photosystem II - Cleavage of reaction center D1 protein in spinach thylakoids by FtsH protease under moderate heat stress. *Journal of Biological Chemistry*, 281(31), 21660-21669.
- Zghidi-Abouzid, O., Merendino, L., Buhr, F., Ghulam, M. M. & Lerbs-Mache, S. (2011) Characterization of plastid psbT sense and antisense RNAs. *Nucleic Acids Research*, 39(13), 5379-5387.
- Zhang, S. P. & Scheller, H. V. (2004) Photoinhibition of photosystem I at chilling temperature and subsequent recovery in Arabidopsis thaliana. *Plant and Cell Physiology*, 45(11), 1595-1602.
- Zhang, Y., Zheng, S., Liu, Z., Wang, L. & Bi, Y. (2011) Both HY5 and HYH are necessary regulators for low temperature-induced anthocyanin accumulation in Arabidopsis seedlings. *Journal of plant physiology*, 168(4), 367-374.
- Zhao, X., Huang, J. & Chory, J. (2019) GUN1 interacts with MORF2 to regulate plastid RNA editing during retrograde signaling. *Proceedings of the National Academy of Sciences*, 116(20), 10162.
- Zimmermann, P., Hennig, L. & Grussem, W. (2005) Gene-expression analysis and network discovery using Genevestigator. *Trends in plant science*, 10(9), 407-409.
- Zoschke, R. & Bock, R. (2018) Chloroplast Translation: Structural and Functional Organization, Operational Control, and Regulation. *Plant Cell*, 30(4), 745-770.
- Zuckerkandl, E. & Pauling, L. (1965) Evolutionary Divergence and Convergence in Proteins. In: Bryson, V. & Vogel, H. J. (eds.) *Evolving Genes and Proteins*. Academic Press.

Statement for Submission with a Thesis Impacted by the COVID-19 Pandemic for PGR Students

The purpose of this form is to capture the impact of the pandemic on your research. We recommend you submit this form with your thesis to be sent to your examiners for consideration.			
Student Name	Jonathan Griffin	ID No.	31938681
Department	Lancaster Environment Center	Faculty	
Research type eg Laboratory, field, desk	Laboratory	FT/PT	Full Time
1. Stage of study when pandemic began (March 2020) e.g. were you planning your project, in the middle of data collection, writing up			
During March 2020, I was in the critical and final stages of data collection and had begun the writing up process.			
2. In what way did the pandemic affect your work? This might be both personal including additional caring responsibilities or your own health and wellbeing, or practical that you were unable to continue data collection, unable to access labs or office for essential reasons etc			
I was unable to continue the final experiments for data collection. Notably, I was unable to access labs and the confocal microscopy facility run by Dr. Elisabeth Shaw in BLS; or to conduct the remaining RT-qPCR experiments I had planned. The experiments affected included different analyses of gene expression under varying temperature conditions, under treatments with retrograde signal-activator chemicals, and the analysis of the full plastome under selected conditions. Data was gathered but some of datasets either did not include multiple experimental replicas or were rather kept to the minimal number of genes. Also, the CRISPR-CAS9 tomato mutants from Chapter 4 could not be subject to any analysis since they arrived in Lancaster just before the lockdown. While initial phenotype-genotype characterization would have been feasible, the closing of the labs made it impossible and only the seeds were gathered for future testing.			
3. How did you try to address the impact of the pandemic on your thesis? You may have had to access alternative data, change aims and objectives, collected less data etc			
I prioritized other avenues of work including bioinformatics for the publication of the paper attached to this thesis (Griffin et al, 2020), and continued the collating and writing up the available results. When laboratories re-opened in September-December 2020 I was granted access by the department safety officers and was able to gather the minimum data from the confocal microscopy experiments that were planned. However, due to the requisitioning of department RT-qPCR machines and the breakage of the remaining machine, I was unable to finish the remaining RT-qPCR experiments. While a new qPCR machine arrived in the department in early 2021 and I have since received training on it, I did not have the time to complete additional experiments that would have benefitted from replication towards publication.			
4. Are there any other comments you would like to make?			
Student Signature	Jonathan Griffin	Date	29/03/2021
Primary supervisor signature	 Gabriela Toledo-Ortiz	Date	29/03/2021

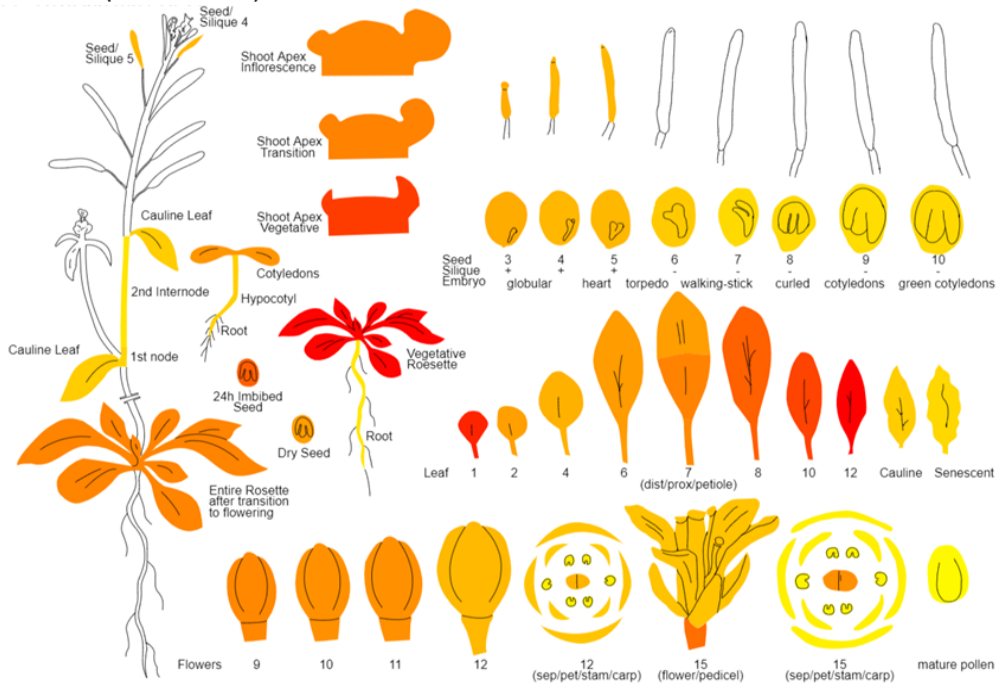
Chapter 7: Appendix

CP28A (AT1G60000)



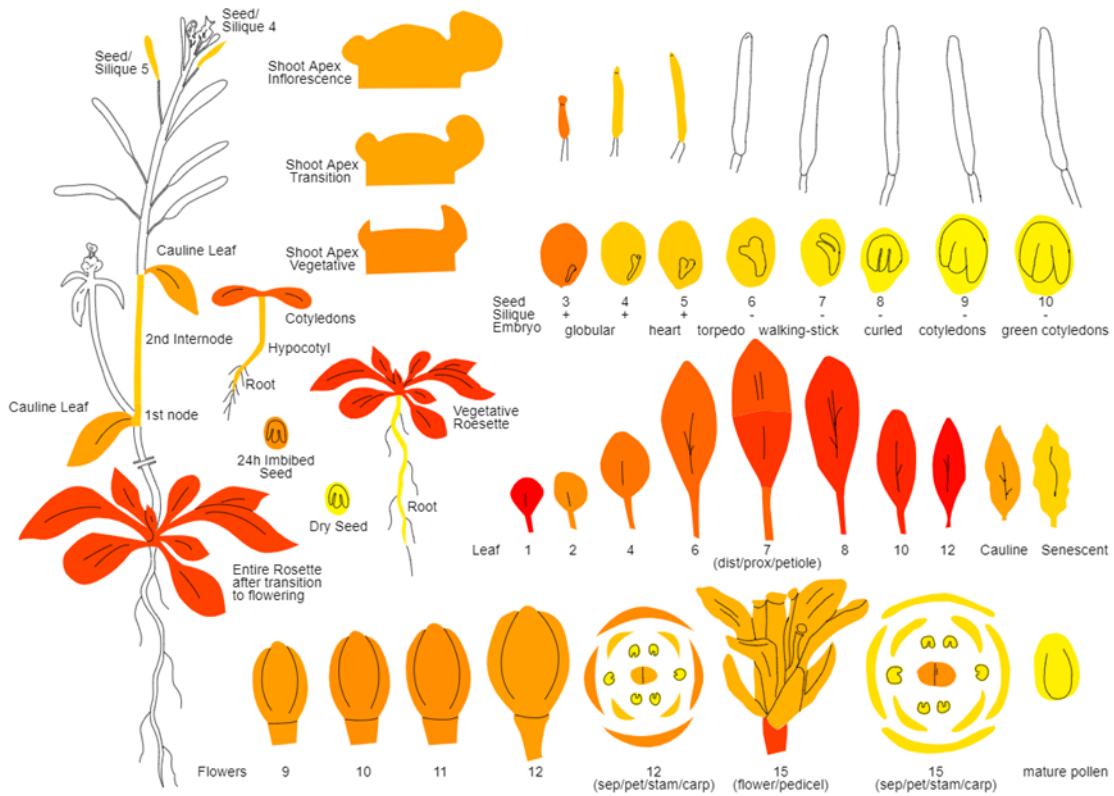
This image was generated with the AIGenExpress eFP at bar.utoronto.ca/epfplant by Waese et al. 2017

CP29A (AT3G53460)



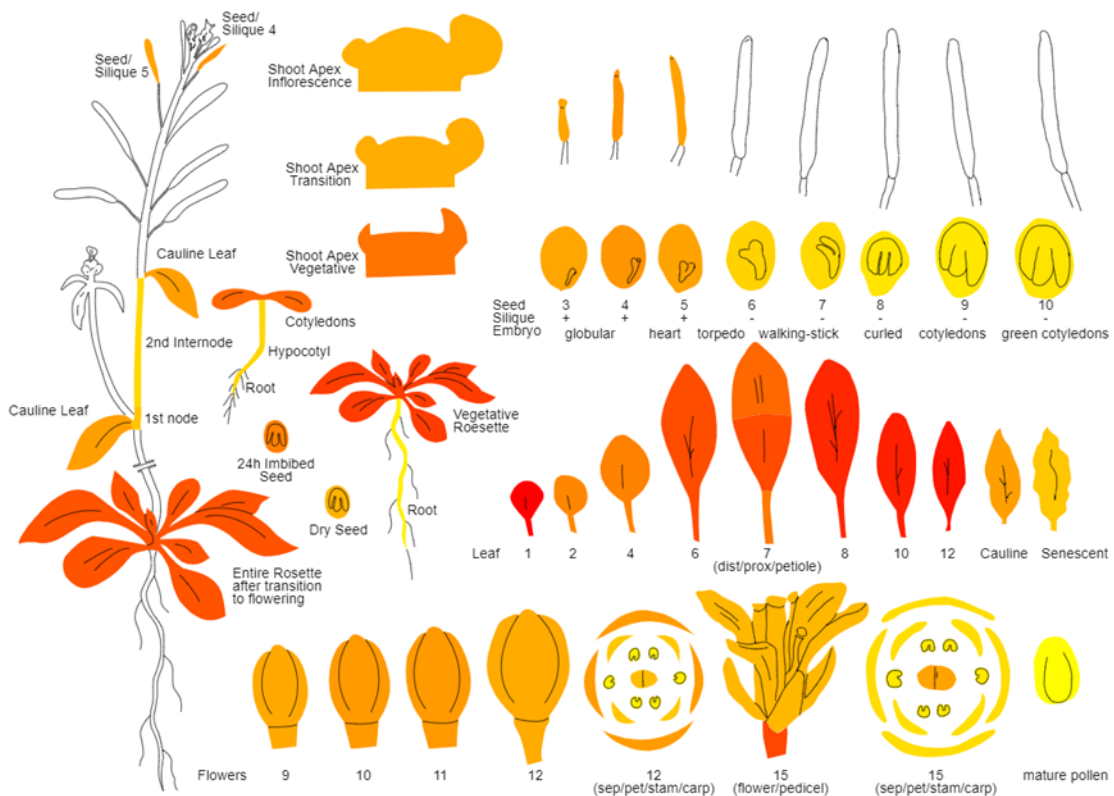
This image was generated with the AIGenExpress eFP at bar.utoronto.ca/epfplant by Waese et al. 2017

CP29B (AT1G01080)



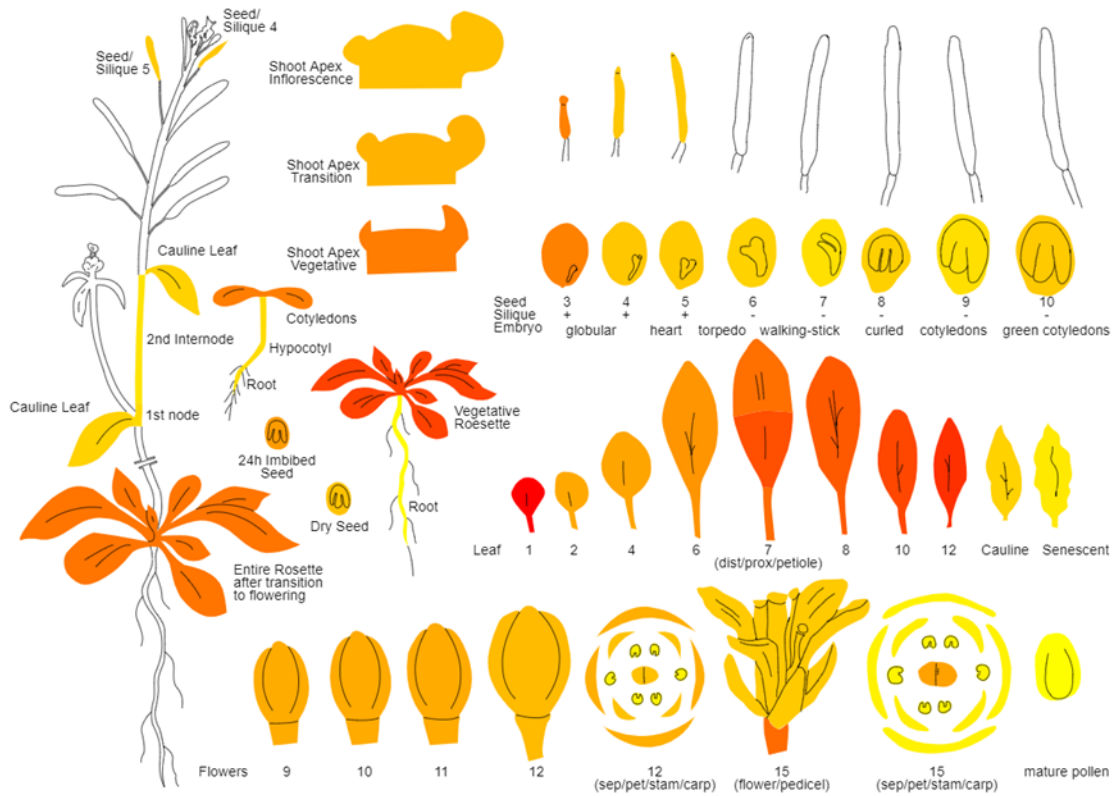
This image was generated with the AtGenExpress eFP at bar.utoronto.ca/epant by Waese et al. 2017

CPSEBF (AT2G37220)



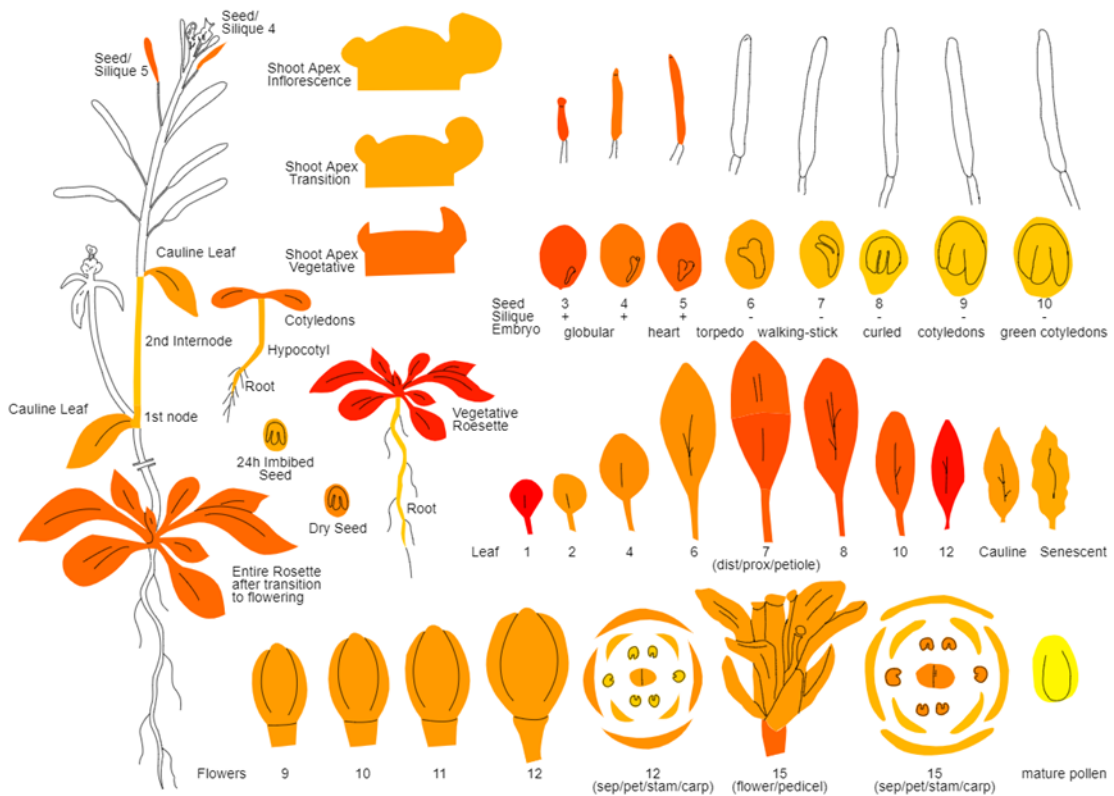
This image was generated with the AtGenExpress eFP at bar.utoronto.ca/epant by Waese et al. 2017

CP29C (AT3G52150)



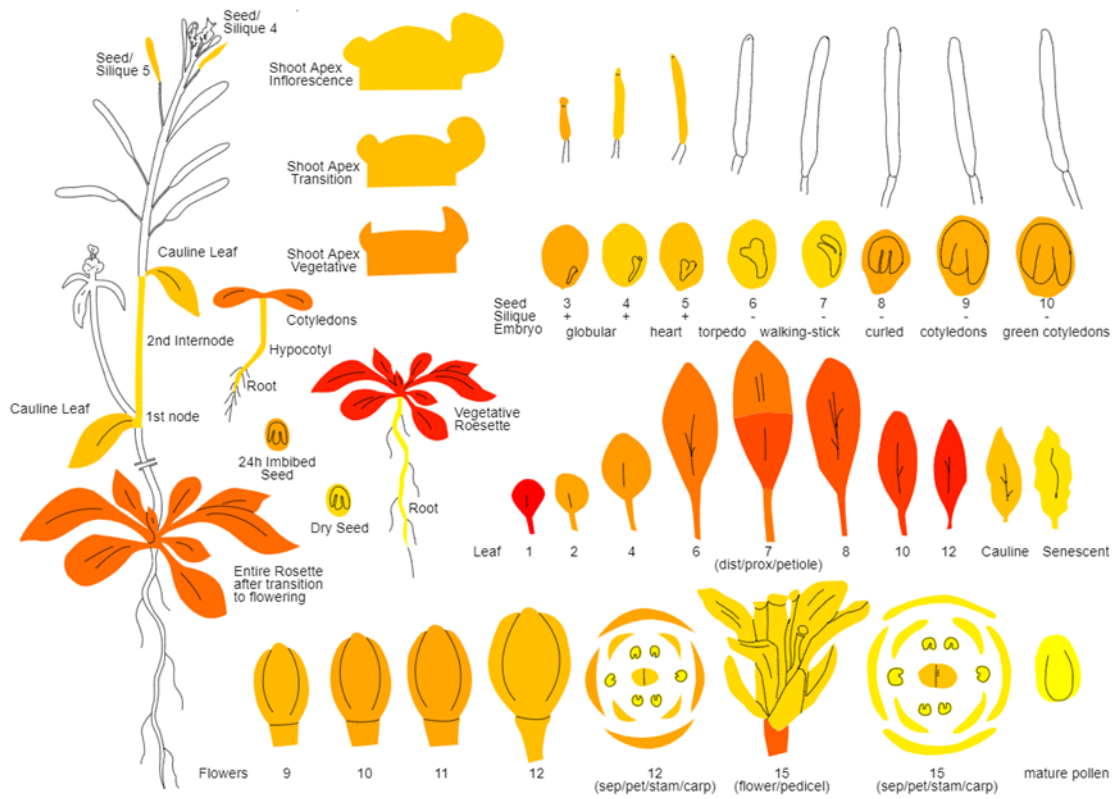
This image was generated with the ATGenExpress eFP at bar.utoronto.ca/eplant by Waese et al. 2017

CP31B (AT5G50250)



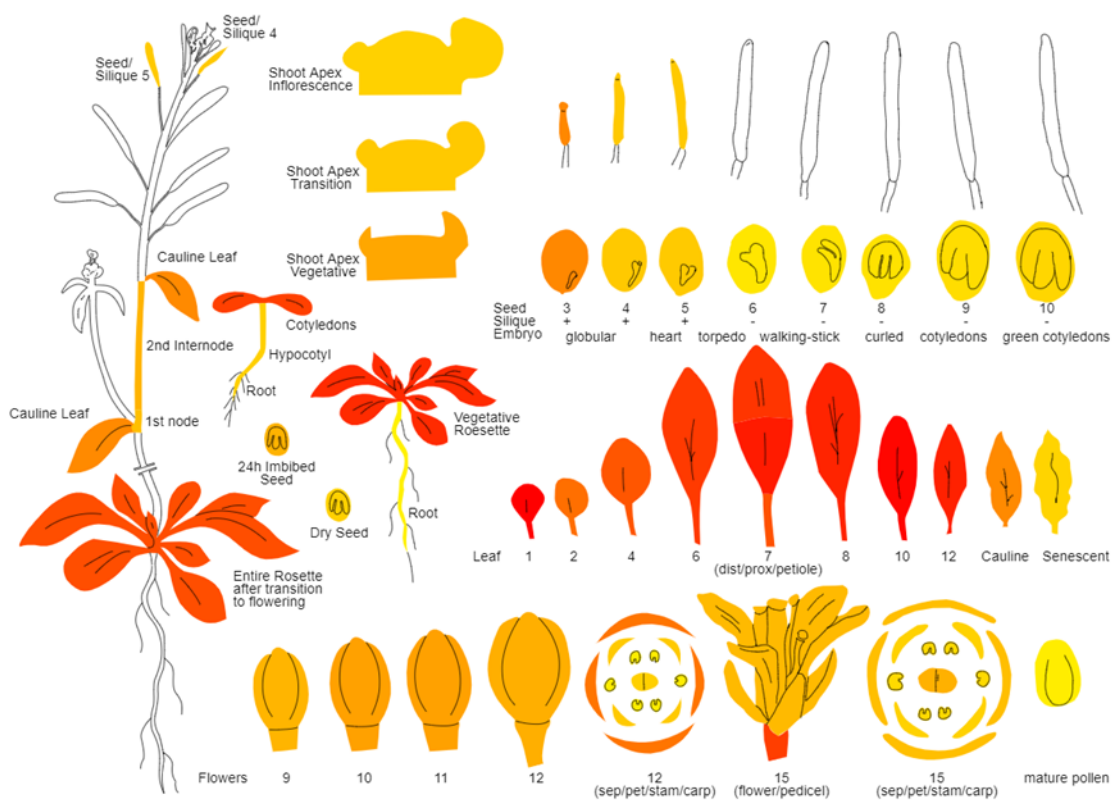
This image was generated with the ATGenExpress eFP at bar.utoronto.ca/eplant by Waese et al. 2017

CP33A (AT3G52380)



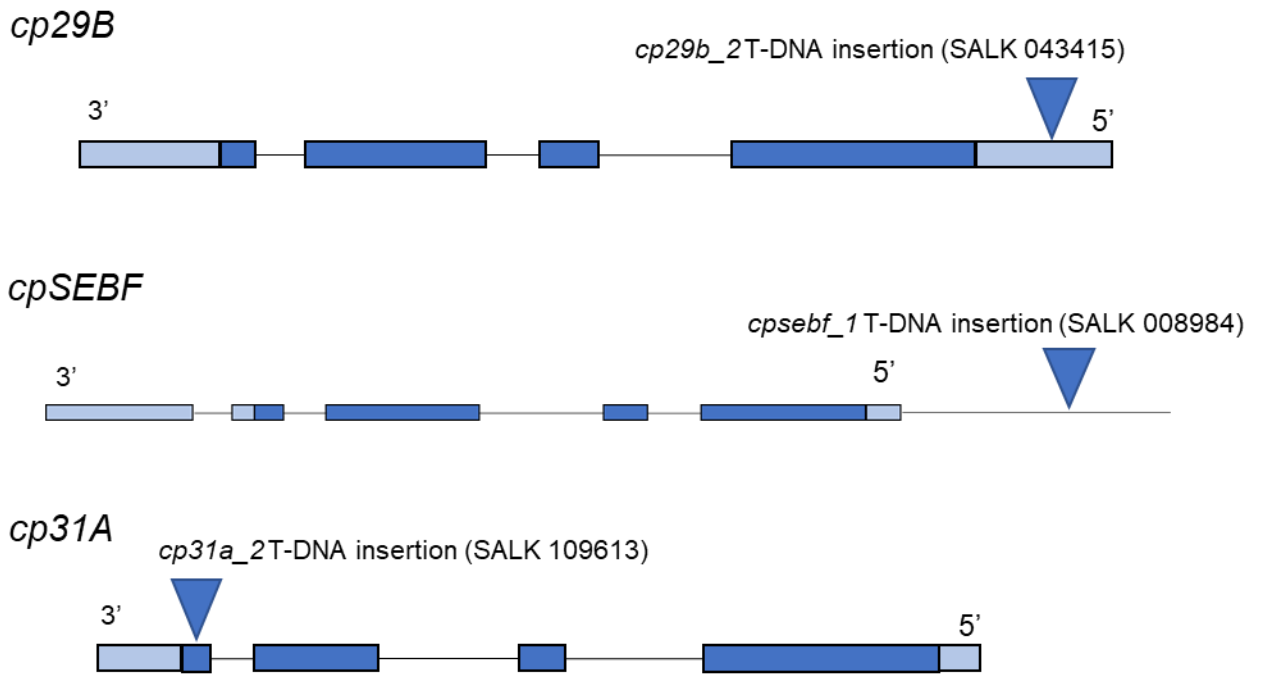
This image was generated with the AIGenExpress eFP at bar.utoronto.ca/epant by Waese et al. 2017

CP33B (AT2G35410)

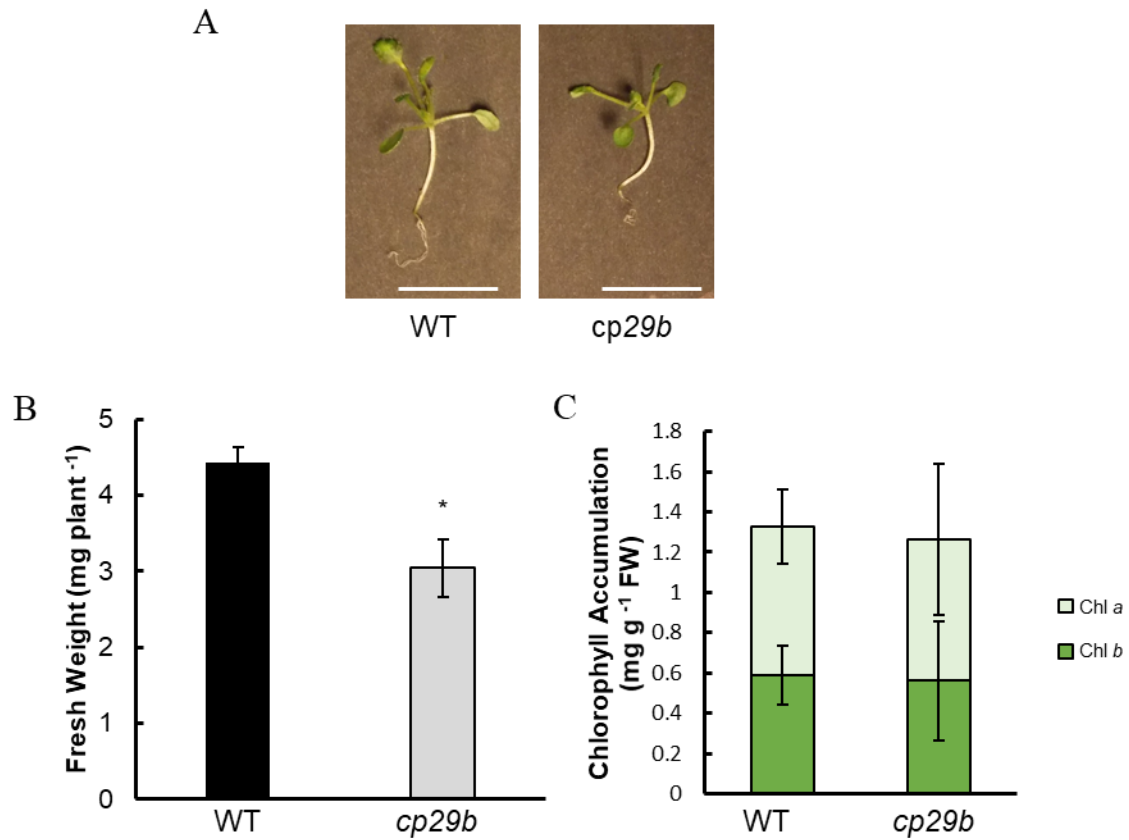


This image was generated with the AIGenExpress eFP at bar.utoronto.ca/epant by Waese et al. 2017

Supplementary Figure 1.1. *cpRNPs* *cp28a*, *cp29A*, *cp29B*, *cpSEBF*, *cp31B*, *cp33A*, and *cp33B* accumulate strongly in aerial leaf tissues in *Arabidopsis thaliana*, and notably during early leaf developmental stages. Data was obtained and reproduced from ePlant database (Waese et al, 2017). No data was published for *cp33C*. Scale bar indicates a linear expression intensity of protein to the subcellular compartment on a scale of lowest (yellow) to highest (red) probability.



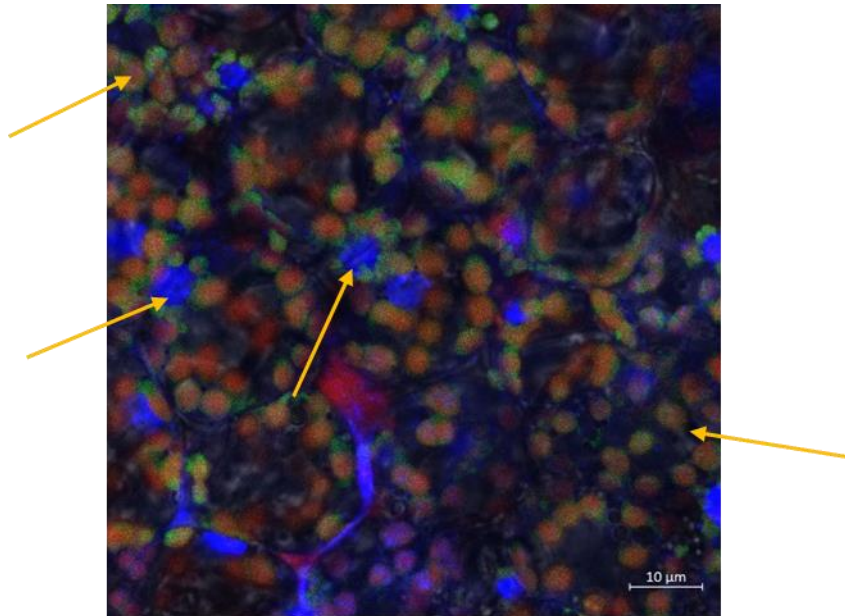
Supplementary Figure 2.1. *cpRNP* single mutants *cp29b_2*, *cpsebf_1*, and *cp31a_2* were obtained from Nottingham Arabidopsis Research Centre and screened for homozygous T-DNA inserts. Mutant lines were then examined for transcript accumulation to determine % reduction in transcript abundance.



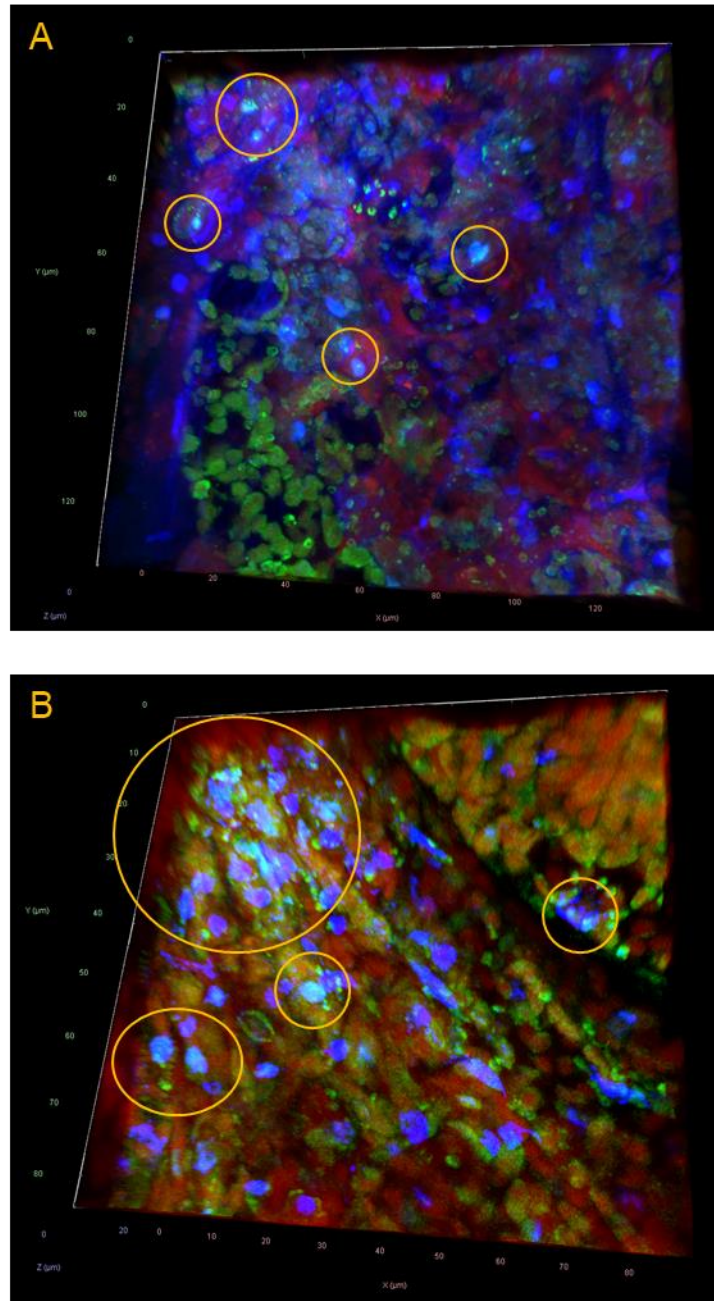
Supplementary Figure 2.2. *cp29b* expressed a Long Day (LD)-sensitive phenotype. Plants were grown in LD conditions (16hrs light ($80 \mu\text{mol m}^{-2}\text{s}^{-1}$ red light) at 22°C and 8hrs dark at 17°C) for 14 days. A) Representative photos of WT and *cp29b_2* mutants. Scale bar is equal to 1cm. B) Graph shows Fresh Weight (FW) per plant of WT and *cp29b_2* mutants. C) Chlorophyll *a* and chlorophyll *b* content was calculated from FW measurements using formulae published in Lichtenthaler and Buschmann (2001). Data represent the average of 3 biological replicates and errors bars represent the 95% confidence interval. Statistical significance of FW was calculated using a Student's *t*-Test ($p < 0.05$). Significance is indicated using asterisks ($p < 0.05 = *$, $p < 0.01 = **$, $p < 0.001 = ***$).



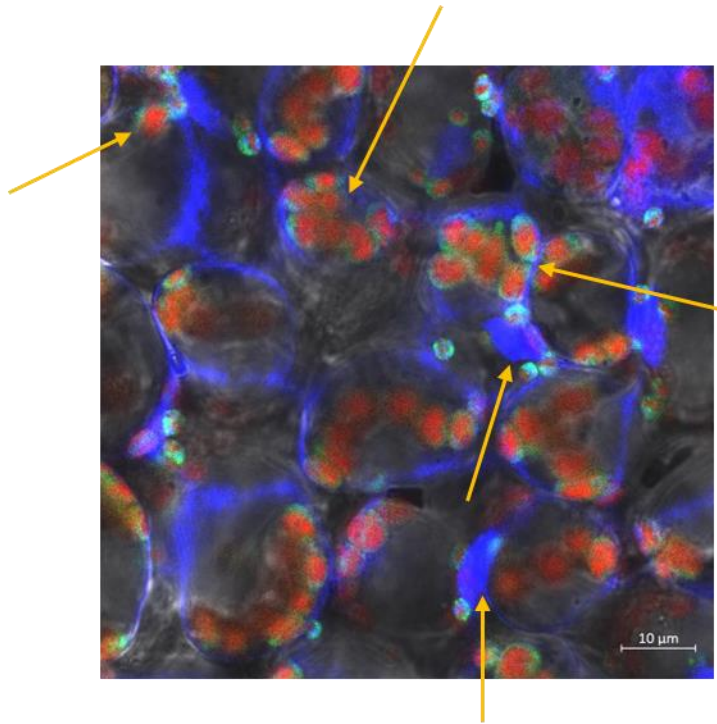
Supplementary Figure 3.1. The ePlant database predicts that cp28A, cpSEBF, cp29C, cp31B, cp33A, and cp33B do not localise to the nucleus. Data was obtained and reproduced from ePlant database (Waese et al., 2017). Colours indicate a linear expression intensity of protein to the subcellular compartment on a scale of lowest (yellow) to highest (red) probability.



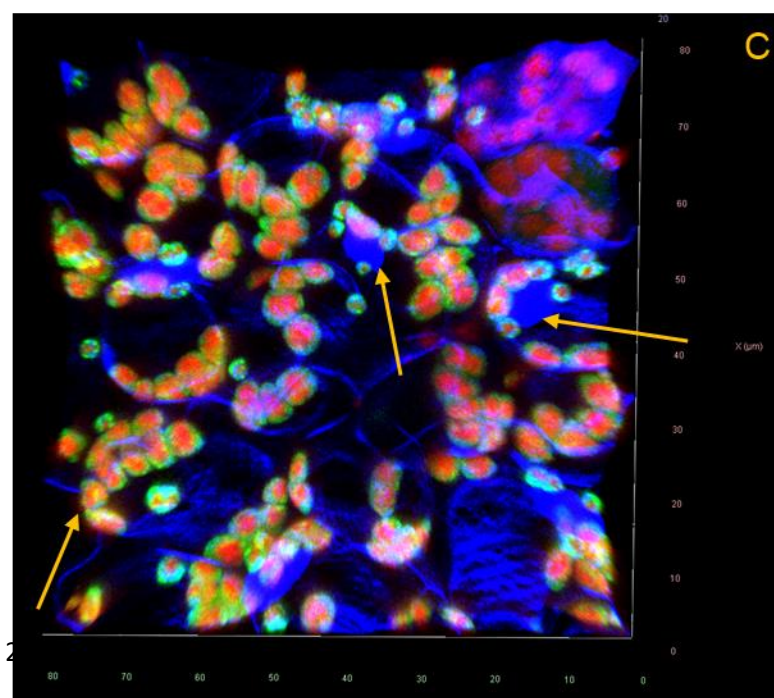
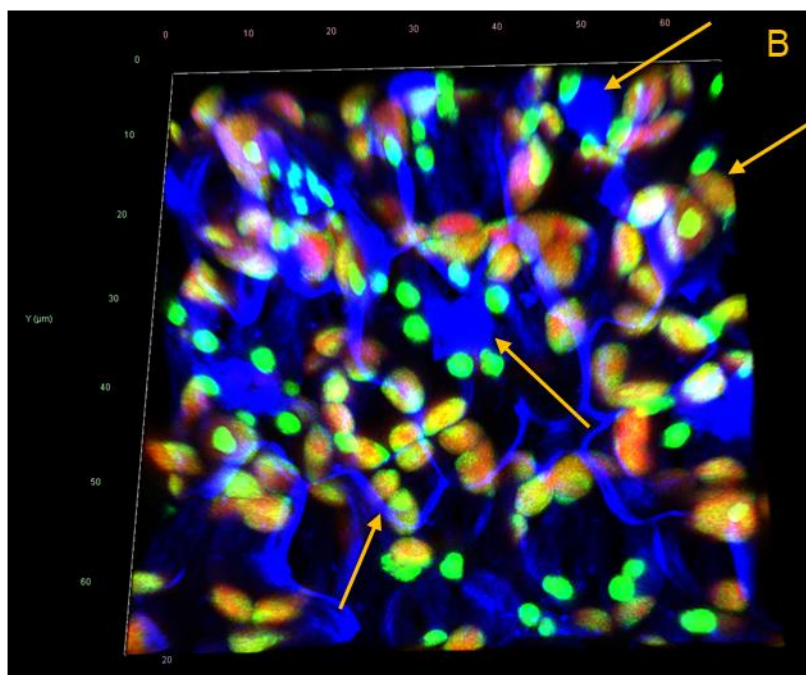
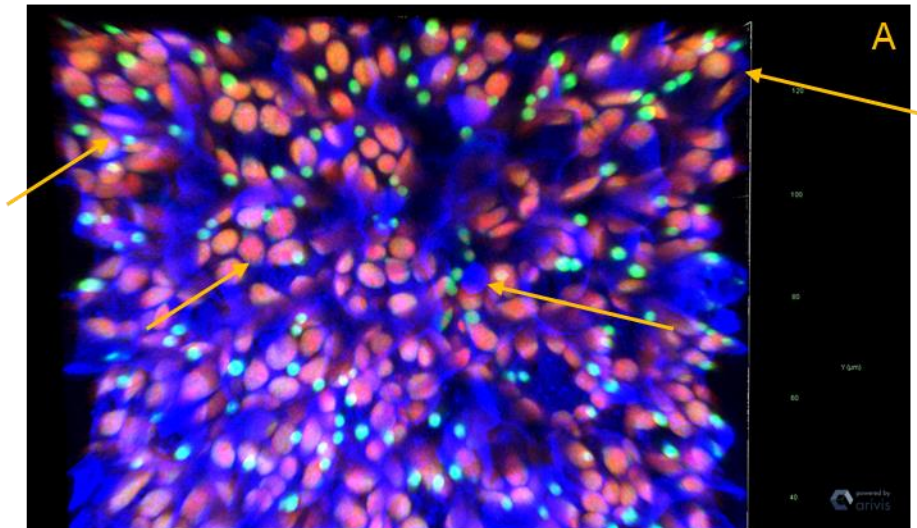
Supplementary Figure 3.2. Confocal microscopy shows Native Promoter (NP)-expressed cp31A (*cp31a_1*) tagged with GFP localises to the chloroplast and not the nucleus at 27°C. This image was enhanced in Zen Blue image-processing software to highlight GFP (green) co-localisation with chlorophyll auto-fluorescence (red) and not nuclei stained with 4',6-diamidino-2-phenylindole (DAPI) (blue). Scale bar is present in the lower right-hand corner of the photo. Arrows indicate that GFP overlaps only with chlorophyll auto-fluorescence and not with DAPI.



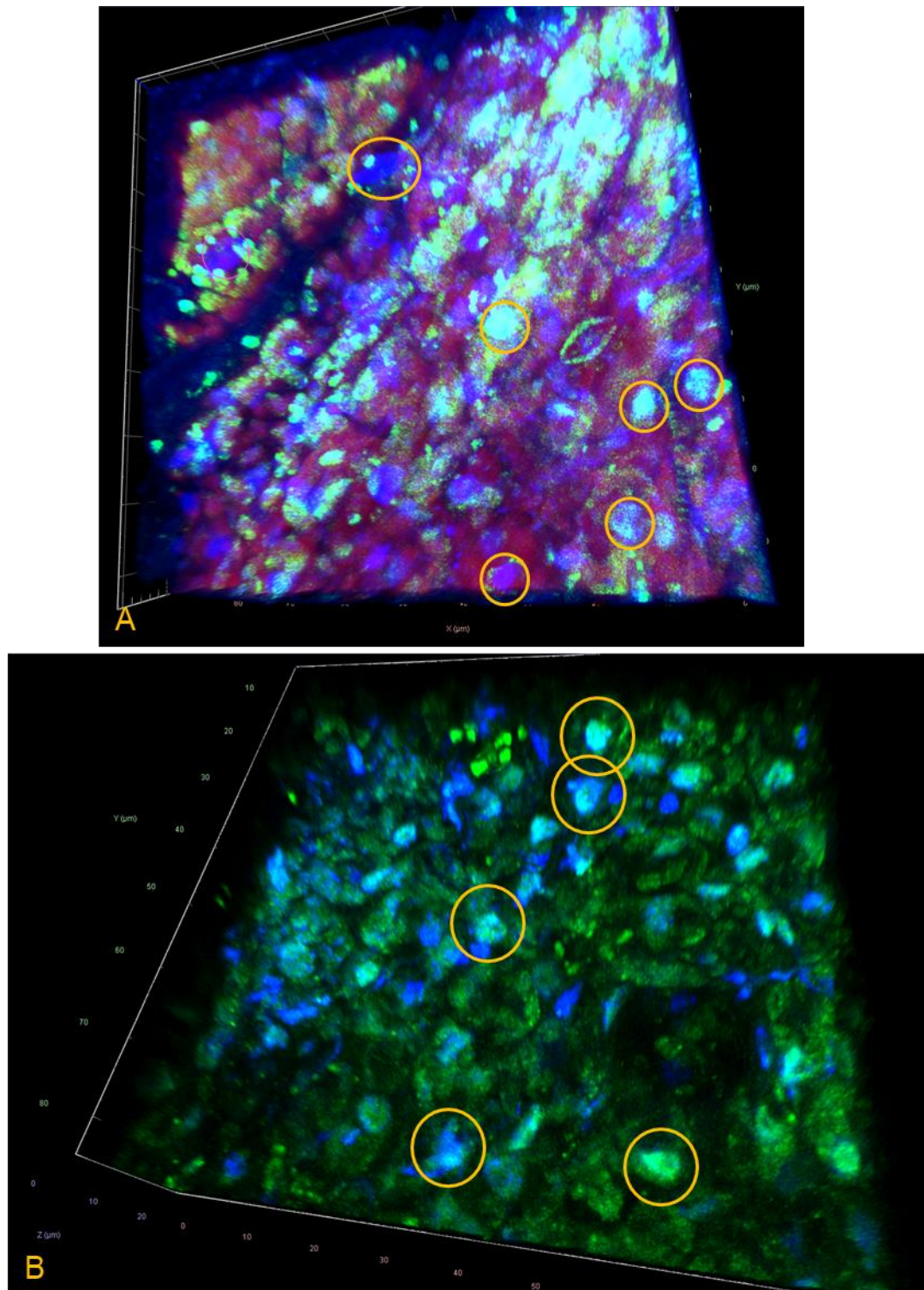
Supplementary Figure 3.3. Confocal microscopy shows 3-D representations of Native Promoter (NP)-expressed *cp31A* (*cp31a_1*) tagged with GFP co-localising with nuclei and chloroplasts at 17°C and 22°C. Plants were grown for three days in darkness and treated with 24hrs red light ($80 \mu\text{mol m}^{-2}\text{s}^{-1}$) at A) 17°C or B) 22°C. 3-D representations were collected as a range of Z-stacks were enhanced in post-image processing software Zen Blue, combining GFP fluorescence (green), chlorophyll auto-fluorescence (red), and nuclear 4',6-diamidino-2-phenylindole (DAPI) staining (blue). Scale bars are shown at the axis beside each photo. Co-localisation between GFP and DAPI fluorescence is highlighted with golden circles. PMT brightfield was not included in the images for clarity.



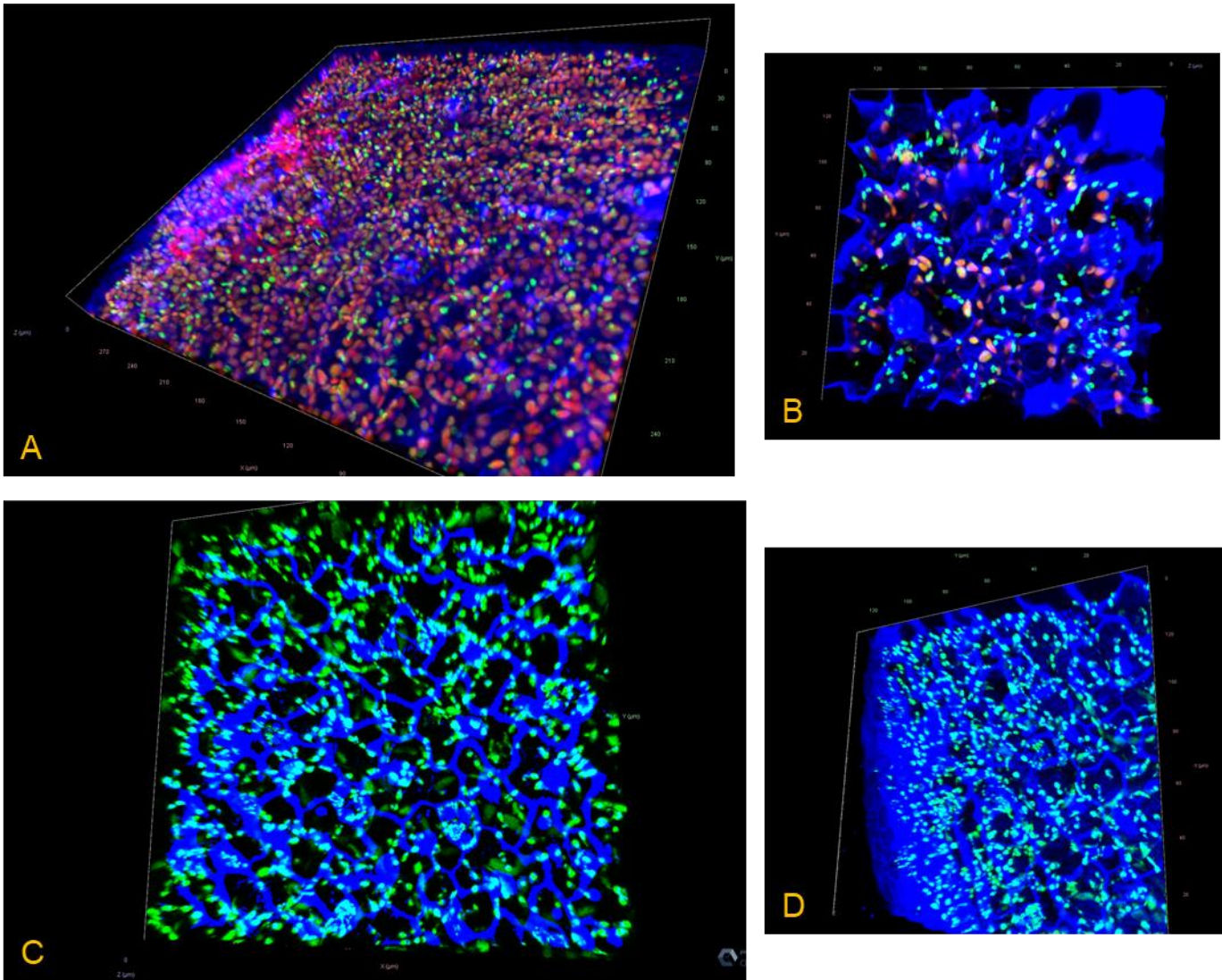
Supplementary Figure 3.4. Confocal microscopy shows Native Promoter (NP)-expressed cpSEBF (*cpsebf_1*) tagged with GFP localises to the chloroplast and not the nucleus at 27°C. This image was enhanced in Zen Blue image-processing software to highlight GFP (green) co-localisation with chlorophyll autofluorescence (red) and not nuclei stained with 4',6-diamidino-2-phenylindole (DAPI) (blue). Scale bar is present in the lower right-hand corner of the photo. Arrows indicate the GFP overlap to chlorophyll auto-fluorescence and not DAPI.



Supplementary Figure 3.5. Confocal microscopy shows 3-D representations of Native Promoter (NP)-expressed cpSEBF (*cpsebf_1*) tagged with GFP co-localises with chloroplasts at all temperature conditions. Plants were grown for three days in darkness and treated with 24hrs red light ($80 \mu\text{mol m}^{-2}\text{s}^{-1}$) at A) 17°C or B) 22°C or C) 27°C . 3-D representations were collected as a range of Z-stacks and were enhanced in post-image processing software Zen Blue, combining GFP fluorescence (green), chlorophyll auto-fluorescence (red), and nuclear 4',6-diamidino-2-phenylindole (DAPI) staining (blue). Scale bars are shown at the axis beside each photo. Arrows indicate that GFP does only overlaps with chlorophyll auto-fluorescence. PMT brightfield was not included in the images for clarity.



Supplementary Figure 3.6. Confocal microscopy shows 3-D representations of Native Promoter (NP)-expressed *cp31A* (*cp31a_1*) tagged with GFP co-localises with nuclei and chloroplasts in untreated conditions, but principally to nuclei when treated with Lincomycin (Linc+). Plants were grown for three days in darkness and treated with 24hrs red light ($80 \mu\text{mol m}^{-2}\text{s}^{-1}$) without (A) or with (B) Lincomycin (0.5 mM). 3-D representations were collected as a range of Z-stacks and were enhanced in post-image processing software Zen Blue, combining GFP fluorescence (green), chlorophyll auto-fluorescence (red), and nuclear 4',6-diamidino-2-phenylindole (DAPI) staining (blue). Scale bars are shown at the axis beside each photo. Circles show notable overlap between GFP and DAPI. PMT brightfield was not included in the images for clarity.



Supplementary Figure 3.7. Confocal microscopy shows 3-D representations of Native Promoter (NP)-expressed NP::cpSEBF-GFP (*cpsebf_1*) tagged with GFP co-localises with nuclei and chloroplasts in untreated conditions, but principally to nuclei when treated with Lincomycin (Linc+). Plants were grown for three days in darkness and treated with 24hrs red light ($80 \mu\text{mol m}^{-2}\text{s}^{-1}$) without (A-B) or with (C-D) Lincomycin (0.5 mM). 3-D representations were collected as a range of Z-stacks and were enhanced in post-image processing software Zen Blue, combining GFP fluorescence (green), chlorophyll autofluorescence (red), and nuclear 4',6-diamidino-2-phenylindole (DAPI) staining (blue). Scale bars are shown at the axis beside each photo. Both sets of images are from different plants. Co-localisation between GFP and DAPI fluorescence is highlighted with golden circles in Panel A. PMT brightfield was not included in the images for clarity.

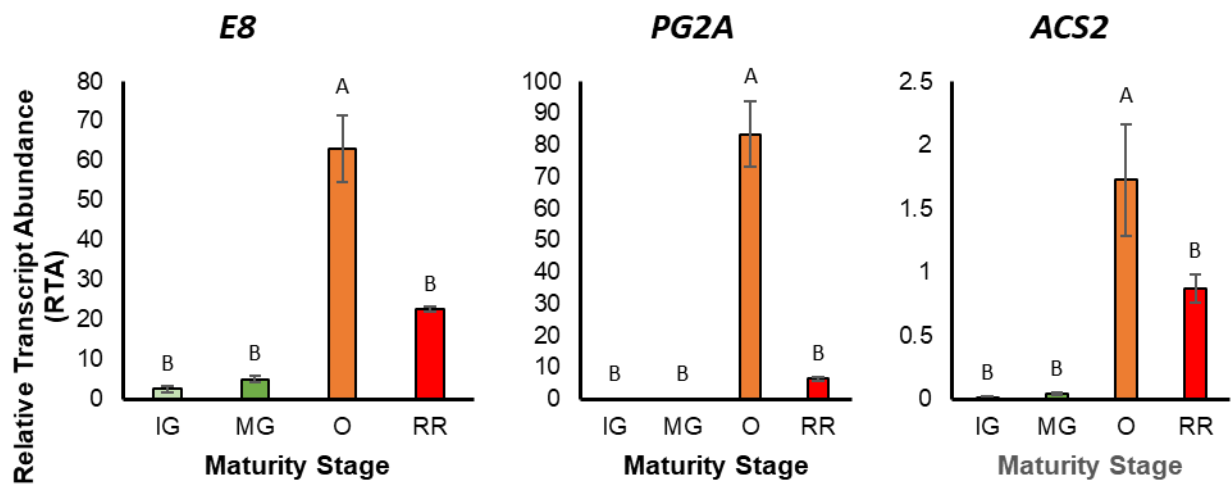
Supplementary Table 4.1. List of accession numbers used to generate the phylogenetic tree presented in Figure 4.1. All accessions were retrieved from the ePlant database (Waese et al., 2017).

cpRNP	Organism	Locus
cp28A	<i>Arabidopsis (A. thaliana)</i>	AT1G60000
cp29A	<i>Arabidopsis (A. thaliana)</i>	AT3G53460
cp29B	<i>Arabidopsis (A. thaliana)</i>	AT1G01080
cp29C	<i>Arabidopsis (A. thaliana)</i>	AT3G52150
cp31A	<i>Arabidopsis (A. thaliana)</i>	AT4G24770
cp31B	<i>Arabidopsis (A. thaliana)</i>	AT5G50250
cp33A	<i>Arabidopsis (A. thaliana)</i>	AT3G52380
cp33B	<i>Arabidopsis (A. thaliana)</i>	AT2G35410
cp33C	<i>Arabidopsis (A. thaliana)</i>	AT4G09040
cpSEBF	<i>Arabidopsis (A. thaliana)</i>	AT2G37220
cp28A	Barley (<i>H. vulgare</i>) (Predicted Protein)	AK357470
cp29C	Barley (<i>H. vulgare</i>) (Predicted Protein)	AK361812
cp31	Barley (<i>H. vulgare</i>) (Predicted Protein)	AK354155
cp33B	Barley (<i>H. vulgare</i>) (Predicted Protein)	AK367276
cpSEBF	Barley (<i>H. vulgare</i>) (Predicted Protein)	AK356209
cp28A	Barrelclover (<i>M. truncatula</i>)	MTR_1g045510
cp29B	Barrelclover (<i>M. truncatula</i>)	MTR_7G118230
cp29C	Barrelclover (<i>M. truncatula</i>)	MTR_3G027140
cp31	Barrelclover (<i>M. truncatula</i>)	MTR_3G075500
cp33A	Barrelclover (<i>M. truncatula</i>)	MTR_7G106440
cp33B	Barrelclover (<i>M. truncatula</i>)	MTR_5G030020
cpSEBF	Barrelclover (<i>M. truncatula</i>)	MTR_1G064230
cp28A	Grape (<i>V. vinifera</i>) (Uncharacterised Protein)	VIT_05S0049G01930
cp29B	Grape (<i>V. vinifera</i>) (Uncharacterised Protein)	VIT_15S0048G02560
cp29C	Grape (<i>V. vinifera</i>) (Uncharacterised Protein)	VIT_13S0064G01430
cp31	Grape (<i>V. vinifera</i>) (Uncharacterised Protein)	VIT_14S0066G00140
cp31	Grape (<i>V. vinifera</i>) (Uncharacterised Protein)	VIT_17S0000G09680
cp33A	Grape (<i>V. vinifera</i>) (Uncharacterised Protein)	VIT_08S0032G01180
cp33B	Grape (<i>V. vinifera</i>) (Uncharacterised Protein)	VIT_02S0012G01420
cpSEBF	Grape (<i>V. vinifera</i>) (Uncharacterised Protein)	VIT_08S0040G01760
cp29C	Maize (<i>Z. mays</i>)	GRMZM2G143870_P02
cp31	Maize (<i>Z. mays</i>)	GRMZM2G011129_P01
cp33B	Maize (<i>Z. mays</i>)	GRMZM2G090271_P01
cpSEBF	Maize (<i>Z. mays</i>)	GRMZM2G158835_P01
cpSEBF	Maize (<i>Z. mays</i>)	GRMZM2G068715_P01
cpSEBF	Maize (<i>Z. mays</i>)	GRMZM2G042683_P01
cp29B	Poplar (<i>P. trichocarpa</i>)	POPTR_014G105800
cp29C	Poplar (<i>P. trichocarpa</i>)	POPTR_009G065900
cp31	Poplar (<i>P. trichocarpa</i>)	POPTR_012G090200
cp31	Poplar (<i>P. trichocarpa</i>)	POPTR_015G086500
cp33A	Poplar (<i>P. trichocarpa</i>)	POPTR_006G202000
cp33B	Poplar (<i>P. trichocarpa</i>)	POPTR_016G068300
cp33C	Poplar (<i>P. trichocarpa</i>)	POPTR_001G141300
cpSEBF	Poplar (<i>P. trichocarpa</i>)	POPTR_016G090700
cpSEBF	Poplar (<i>P. trichocarpa</i>)	POPTR_006G127200
cp28A	Poplar (<i>P. trichocarpa</i>) (uncharacterised protein)	POPTR_008G172100
cp28A	Potato (<i>S. tuberosum</i>)	PGSC0003DMg400002694
cp33A	Potato (<i>S. tuberosum</i>)	PGSC0003DMg400037033
cp33B	Potato (<i>S. tuberosum</i>)	PGSC0003DMg400030598
cpSEBF	Potato (<i>S. tuberosum</i>)	m29041

cp29B	Rice (<i>O. sativa</i>)	LOC_OS08G02390
cp29C	Rice (<i>O. sativa</i>)	LOC_OS09G10760
cp31	Rice (<i>O. sativa</i>)	LOC_OS09G39180
cp33A	Rice (<i>O. sativa</i>)	LOC_OS02G57010
cp33B	Rice (<i>O. sativa</i>)	LOC_OS04G50110
cpSEBF	Rice (<i>O. sativa</i>)	LOC_OS07G43810
cpSEBF	Rice (<i>O. sativa</i>)	LOC_OS03G25960
cp28A	Soybean (<i>G. max</i>)	GLYMA.10G134100
cp28A	Soybean (<i>G. max</i>)	GLYMA.20G082800
cp29B	Soybean (<i>G. max</i>)	GLYMA.16G018200
cp29B	Soybean (<i>G. max</i>) (Uncharacterised)	GLYMA.19G260200
cp29B	Soybean (<i>G. max</i>) (Uncharacterised)	GLYMA.07G049500
cp29C	Soybean (<i>G. max</i>) (Uncharacterised)	GLYMA.15G271200
cp29C	Soybean (<i>G. max</i>) (Uncharacterised)	GLYMA.08G151700
cp31	Soybean (<i>G. max</i>) (Uncharacterised)	GLYMA.04G190100
cp31	Soybean (<i>G. max</i>) (Uncharacterised)	GLYMA.06G175400
cp33A	Soybean (<i>G. max</i>) (Uncharacterised)	GLYMA.03G202900
cp33A	Soybean (<i>G. max</i>) (Uncharacterised)	GLYMA.19G200700
cp33B	Soybean (<i>G. max</i>) (Uncharacterised)	GLYMA.01G017400
cp33B	Soybean (<i>G. max</i>) (Uncharacterised)	GLYMA.09G205500
cpSEBF	Soybean (<i>G. max</i>) (Uncharacterised)	GLYMA.10g058500
cpSEBF	Soybean (<i>G. max</i>) (Uncharacterised)	GLYMA.13G145200
cp28	Spinach (<i>S. oleracea</i>)	P28644
PSRP-2	Spinach (<i>S. oleracea</i>)	P82277
cp30	Tex-Mex Tobacco (<i>N. plumbaginifolia</i>)	P49313
cp31	Tex-Mex Tobacco (<i>N. plumbaginifolia</i>)	P49314
cp28	Tobacco (<i>N. sylvestris</i>)	LOC104242583
cp29A	Tobacco (<i>N. sylvestris</i>)	Q08935
cp29B	Tobacco (<i>N. sylvestris</i>)	LOC104230517
cp31	Tobacco (<i>N. sylvestris</i>)	LOC104227036
cp33	Tobacco (<i>N. sylvestris</i>)	P19684
cp28A	Tomato (<i>S. lycopersicum</i>)	SOLYC09G090960
cp29A.1	Tomato (<i>S. lycopersicum</i>)	SOLYC10G086150
cp31	Tomato (<i>S. lycopersicum</i>)	SOLYC03G111840
cp33A	Tomato (<i>S. lycopersicum</i>)	SOLYC01G006940
cp33B	Tomato (<i>S. lycopersicum</i>)	SOLYC08G076840
cp33C	Tomato (<i>S. lycopersicum</i>)	Solyc04g074750
cpSEBF	Tomato (<i>S. lycopersicum</i>)	SOLYC09G007850

cp31B	MTSSVLTPLSKLLAMTNSSSSTLFCIPSI FNISSES HR-FNFSLSSR-----PVNLT	52
cp31A	MASSIVTSSLKPLAMADSSSSTIFSHPSISSTISSSRIRSSSVLLTGRINLPLSFSRVS	60
PsiteA	-----	0
PsiteB	-----	0
PsiteC	-----	0
PsiteD	-----	0
cp31B	LSLKS KTLRNSSPVVTFVVSQTSNWAE EEEGEDGSIGGTSVTV-----	94
cp31A	LSLKT KTHLKKSPFVSFVAQTS DWAE EGGEGSVAVEETENSLESQDVSEGDSEGDASEG	120
PsiteA	-----	0
PsiteB	-----	0
PsiteC	-----	0
PsiteD	-----VpS-----	3
cp31B	--DE-----SFESE DG VGFPEPPEEAKLFVGNLPYDVDSQALAM LFEQAGTVEISE	143
cp31A	DVSEGDSEGDVSEGA VSERA EFPPEPSEAKLFVGNL AYDVNSQALAM LFEQAGTVEIAE	180
PsiteA	---DEpSEGDVSEGA VSER-----	16
PsiteB	----EpSEGDVSEGA VSER-----	15
PsiteC	---GDEpSEGDVSEGA VSER-----	17
PsiteD	--EGDEpSEGDVSEGA VSER-----	21
	. . .	
cp31B	VIYNRDTDQSRGFGFVTMSTV EEAKEKAVEKFN SFVNGRRLTVNRAAPRGS RPERQPRVY	203
cp31A	VIYNRET DQSRGFGFVTMSSVDEAETA VEKFNRYDLN GRLLTVNKAAPRGS RPERAPRVY	240
PsiteA	-----	16
PsiteB	-----	15
PsiteC	-----	17
PsiteD	-----	21
cp31B	DAAFR IYVGNLPWDVDSGR LERL FSEHGKVVDARV VSDRETGRSRGFGFVQMSNENEVNV	263
cp31A	EPAFRVYVGNLPWDV DNGRLEQLFSEHGKVVEARV VYDRETGRSRGFGFVTMSDVDELNE	300
PsiteA	-----	16
PsiteB	-----	15
PsiteC	-----	17
PsiteD	-----	21
cp31B	AIAALDQGNLEGRAIKVNVAEERTRR---	289
cp31A	AISALDQGNLEGRAIRVNVAEERPPRRGY	329
PsiteA	-----	16
PsiteB	-----	15
PsiteC	-----	17
PsiteD	-----	21

Supplementary Figure 4.1. Pairwise alignment of *cp31A*, *cp31B*, and *cp31A* acidic domain Ser-phosphorylation sites (Reiland et al., 2009). Phosphorylation sites are underlined in red. Alignment was conducted using Clustal W (Thompson et al., 1994).



Supplementary Figure 4.2. Transcript accumulation of fruit ripening marker genes *E8*, *PG2A*, and *ACS2* were used to confirm fruit ripening stages in *Solanum lycopersicum* cultiv. MicroTom fruits. MicroTom plants were grown under standard greenhouse conditions (14 h light at $27 \pm 1^\circ\text{C}$ and 10 h dark at $24 \pm 1^\circ\text{C}$) and harvested in the necessary ripening stage. Relative transcript abundance (RTA) was calculated by comparing experimental gene expression to the reference gene *ACT4*. Data represent the average of three biological replicates and error bars show the 95% confidence interval. Statistical significance of expression between Immature Green (IG, light green bars), Mature Green (MG, dark green bars), Orange (O, orange bars), and Red Ripe (RR, red bars) was calculated using One-way ANOVA with Tukey post hoc testing ($p < 0.05$). Data that do not share a letter are statistically significant.

cp31A genomic sequence

C-box: **GTCANN**

...CTTATCTCGCCCACCGTTCTAAAACCCCTCCCTTCTTCTTTCTTCTCCTTCCACTTCCACTTCTTCTATCTCTCACAATT
CAGCA

cp31A (TSS_A)

▼
ATGGCTTCTTCTATAGTTACCTCTAGCTTGAAGCCTTTAGCCATGGCCGATTCTTCTTCTACCATTTCTCCCATC
CTTCCATCTCCTCTACCATCTTCTCCTCCAGAATTCGCAGCTCCAGTGTTCCTCCTTACCGGACGCATTAACCTGCCCTCTC
TTTCTCTCGCGTCTCTCTATCTTAAAACCAAACCCACCTTAAAAAATCCCCCTTGTCTCCTTCGTTGCCAGACTTCGGAT
TGGGCTGAAGAAGGTGGAGAAGGAAGCGTCGCTGTTGAGGAGACCGAGAACAGTTT**GTCACA** AGATGTGAGCGAAG
GAGATGAGAGCGAAGGAGATGCGAGCGAAGGAGATGTGAGCGAAGGAGATGAGAGCGAAGGAGATGTGAGCGAAGGAG
CTGTGAGCGAAAGAGCTGAGTCCCGGAGCCATCGGAAGAAGCCAAGCTTTTCGTCGGAAATTTGGCTTATGATGTTAATAG
CCAAGCTTTGGCT

cp31A (TSS_B)

▼
ATG CTCTTTGAGCAAGCCGGTACTGTTGAAATCGCCGAGGTGAATTTAGCTGCTTTCTTCTTGCTCATATG GTC
GTCTTGATGCGTTTATATGTTGTTCAATTATGCATTGCTTAAGGTTATTTATGTGTGTTTTGTGCATTGCAATTTGCATCAACTAT
GAGTCTAATGGATGAGAAAAGTAGAATTCTTTGGCCTGATGACTGTGTTTGGAGCATCTCTGCTTTGAGAGTTAGAATTCGCT
GGATTGAATTCATATCTGTTGACATTATACTTTGGTTCTCTTTTTTATTTAGTTC AAGAGATAATGTTGTTAGTCTGACTT
GTTCTTTGAATCTTGTGG...

Supplementary Figure 5.1. A C-box HY5 binding site (Song et al., 2008) is present upstream of the cp31A (TSS_B) transcriptional start site, but downstream of the cp31A (TSS_A) transcriptional start site. Upstream sequences for each alternative TSS of cp31A starting from the respective ATG start side were examined using Patterns Locator (Mrázek and Xie, 2006). C-box motifs is identified in green. Start codons are indicated in red text and shown with an arrow.

Chapter 8: Publication.

“Coordinating light responses between the nucleus and the chloroplast, a role for plant cryptochromes and phytochromes”.

Jonathan Henry Charles Griffin^{a, †}, Karine Prado^{b, †}, Phoebe Sutton^a and Gabriela Toledo-Ortiz^{a,*}

[†] Co-lead authors

^aLancaster Environment Centre, Lancaster University, United Kingdom

^bDepartment of Plant Biology, Carnegie Institution for Science, Stanford, California 94305, USA

This paper is published in *Physiologia Plantarum* (2020) and is reproduced here in alignment with its distribution under the Creative Commons CC BY license, as described in Wiley’s Open Access Terms and Conditions.

Special Issue Article

Coordinating light responses between the nucleus and the chloroplast, a role for plant cryptochromes and phytochromesJonathan Henry Charles Griffin^{a,†}, Karine Prado^{b,†}, Phoebe Sutton^a and Gabriela Toledo-Ortiz^{a,*} ^aLancaster Environment Centre, Lancaster University, Lancaster, UK^bDepartment of Plant Biology, Carnegie Institution for Science, Stanford, California, 94305, USA**Correspondence***Corresponding author,
e-mail: g.toledo-ortiz@lancaster.ac.ukReceived 23 January 2020;
revised 4 June 2020

doi:10.1111/ppl.13148

To promote photomorphogenesis, including plastid development and metabolism, the phytochrome (phy) and the cryptochrome (cry) photoreceptors orchestrate genome-wide changes in gene expression in response to Red (R)- and Blue (B)-light cues. While phys and crys have a clear role in modulating photosynthesis, their role in the coordination of the nuclear genome and the plastome, essential for functional chloroplasts, remains underexplored. Using publicly available genome datasets for WT and *phyABCDE* or *cry1cry2* Arabidopsis seedlings, grown, respectively, under R- or B-light, we bioinformatically analyzed the influence of light inputs and photoreceptors in the control of nuclear genes with a function in the chloroplast, and evaluated the role of phyB in the modulation of plastome-encoded genes. We show gene co-induction by R-phys and B-crys for genes with a chloroplastic function, and also apparent photoreceptor-driven preferential responses. Evidence from phyB in Arabidopsis together with published evidence from CRY2 in tomato also supports the participation of both photoreceptor families in the global modulation of the plastome genes. To begin addressing how these light-sensors orchestrate changes in an organellar genome, we evaluated their effect over genes with potential functions in plastid gene-expression regulation based on their TAIR annotation. Results indicate that both crys and phys modulate 'plastome-regulatory genes' with enrichment in the contribution of crys to all processes and of phys to post-transcription and transcription. Furthermore, we identified a new role for HY5 as a relevant light-signaling component in photoreceptor-based anterograde signaling leading to plastome gene regulation.

Introduction

Light is a vital environmental signal for plant development and function. Both Red (R) and Blue (B) light, perceived by the phytochromes (phys) and cryptochromes

(crys) photoreceptors, respectively, are essential wavelengths for photomorphogenesis including photosynthesis and plastid development. As part of the greening responses both photoreceptor families modulate chloroplast biogenesis, the assembly and maintenance of the

Abbreviations – *accD*, acetyl-CoA carboxylase; *ATAB2*, Arabidopsis translation of *psaB 2*; *BPG2*, Brz-insensitive pale green 2; cDNA, complementary DNAs; Crys, cryptochromes; FDR, false discovery rate; GO, gene ontology; HY5, elongated hypocotyl 5; LFZ1, light regulated zing finger 1; mTERF, mitochondrial transcription termination factor; NCP, nuclear control of PEP; *ndh*, NADH dehydrogenase; NEP, nuclear-encoded polymerase; PEP, plastid-encoded polymerase; PhANG, photosynthesis associated nuclear genes (s); Phys, phytochromes; PPR, pentatricopeptide repeat; PRDA1, PEP-related development arrested 1; PSII, photosystem I/photosystem II; PSRPs, plastid specific ribosomal proteins; pTAC, plastid transcriptionally active chromosome; *rbcl*, rubisco large subunit; Rpl, large ribosomal protein; Rpo, RNA polymerase; Rps, small ribosomal protein; RRM, RNA recognition motif; SD, short days; TPR, tetratricopeptide repeat; TPRS, tetratricopeptide domain-containing family.

[†]These authors equally contributed to this work.

photosynthetic apparatus components, and the production of photosynthetic pigments (Franklin and Quail 2010).

Control of similar developmental pathways in response to different light quality inputs is accomplished via shared and independent signaling pathways (Wang et al. 2017). Their co-action involves multiple mechanisms including the use of common signaling intermediates and signal convergence downstream of the receptor (Wang et al. 2017). Examples of such synergisms and interactions include phytochrome and cryptochrome co-regulation of master light-development promoting transcription factors (Franklin and Quail 2010, Su et al. 2017). Such signaling cascades fine-tune the activity and gene expression of photosynthesis associated nuclear genes (PhANGs), including subunits for photosystem I (PSI), photosystem II (PSII), the carbon fixation reactions of the Calvin–Benson cycle, the photosynthetic reduction/oxidation balance and energy production (ATPase) in response to light quality and quantity inputs (Thum et al. 2000, Oh et al. 2013).

However, the onset of functional chloroplasts requires not only the activation of nuclear-encoded genes, but also the regulation of the plastid genome (Berry et al. 2013). As semi-autonomous organelles of prokaryotic origin, chloroplasts maintain their own genome and gene expression mechanisms. The chloroplast genome, known as the plastome, encodes for approximately 120–130 genes including photosynthesis-related genes and core components of the plastids' transcription and translational machineries (Sato et al. 1999). Yet, during evolution, the majority of the genes encoding for proteins with a function in the chloroplast were transferred to the nucleus (Martin et al. 1998). Modern chloroplasts are therefore organelles that require the expression and coordination of two genomes for proper functioning and require the import of over 95% of their proteins that are nuclear-encoded (Soll and Schleiff 2004). To ensure coordinated responses across organelles, the plant cell utilizes anterograde and retrograde signals to tune the expression of the genetic information encoded in these two organelles, thereby ensuring the correct assembly and stoichiometry of multiple chloroplast protein complexes (mostly involved in photosynthesis), and the accurate sensing and interpretation of light and developmental inputs (Singh et al. 2015).

Despite photoreceptor mutants affecting chloroplast development, their individual and comparative contributions to the plastome gene expression have not been fully addressed. Arabidopsis studies on mesophyll-expressed phytochromes have shown they regulate the expression

of the sigma factors that modulate plastid transcription (Oh and Montgomery 2014). On the other hand, in tomato, overexpression of CRY2 leads to a wide modulation of the entire plastome, including light induction of subunits of PSI, PSII and cytochrome b6f, and the down-regulation of ribosomal protein transcripts (Facella et al. 2017).

Control of plastome gene expression is complex, including regulatory processes similar to both prokaryotic and eukaryotic organisms (Barkan 2011). Plastome transcription involves the activity of a nuclear-encoded RNA polymerase (NEP) and a plastid-encoded RNA polymerase (PEP) (Del Campo 2009). Photoreceptor links to the modulation of transcriptional processes in the chloroplast are illustrated by the NEP activity repression by CRY2 (Facella et al. 2017), and the modulation by phy and cry of several components required for PEP activity, including the transcriptional co-factors sigma factors and proteins, such as nuclear control of PEP (NCP), PEP-related development arrested 1 (PRDA1) (Ohgishi et al. 2004, Qiao et al. 2013, Oh and Montgomery 2014, Yang et al. 2019, Yoo et al. 2019), and HEMERA (HMR)/plastid transcriptionally active chromosome complex 12 (pTAC12) (Pfalz et al. 2006, Chen et al. 2010). Yet, plastid-encoded genes are generally organized into polycistronic operons, and chloroplast transcription rates and steady-state mRNA levels tend not to be comparable, pointing at a broad impact of post-transcriptional regulation in modulating the plastome gene expression (Deng et al. 1989). Plastid mRNAs require extensive processing, stabilization, editing and intron splicing before translation (Deng et al. 1989, Del Campo 2009), carried out by nuclear-encoded (but chloroplast-localized) RNA-binding proteins including the pentatricopeptide repeat proteins (PPRs) and the tetratricopeptide domain-containing family (TPRs) (Lamb et al. 1995, Ruwe et al. 2011). While the involvement of the photoreceptors in the modulation of the activity of these RNA-binding proteins has not been fully investigated, what is known is that these RNA-dependent regulatory pathways are active during chloroplast development and respond to light quality inputs (Deng et al. 1989).

Chloroplast translation also has an important role in rapidly shaping the plastid proteome in response to environmental cues (Zoschke and Bock 2018). While the plastome encodes for plastid rRNA and tRNA genes, additional nuclear-encoded enzymes are involved in translation-related processing and modifications, including the aminoacyl-tRNA synthetases and 60% of the plastid ribosomal proteins (RPs) (Yamaguchi and Subramanian 2000). There is also evidence that dark/light transitions reshape the plastids protein synthesis rates, including the translation of plastid-encoded

transcripts for photosynthetic subunits (Kim and Mullet 2003). In addition, some plastid-specific ribosomal proteins (PSRPs) have been identified as light-sensitive (Yamaguchi and Subramanian 2003) and the phys have been reported to regulate ribosomal RNA processing and the induction of rRNA accumulation during de-etiolation (Kim et al. 2012). CRY2, on the other hand, modulates genes such as *Arabidopsis* translation of *psaB2* (*ATAB2*) involved in translation of the plastome encoded PSI and PSII mRNAs (Barneche et al. 2006).

Overall, the available evidence points at a potential global role of the cryptochromes and the phytochromes in coordinating the nuclear and the plastome gene expression by targeting components, involved in the plastome regulatory processes. In this paper, we bioinformatically investigated whether similarly to CRY2, phyB is also involved in delivering light signals for a broad modulation of the plastome gene expression. In addition, we addressed the role of both photoreceptor families and long hypocotyl 5 (HY5) in the light-induction of nuclear-encoded genes with an annotated function in the regulation of the plastome expression.

Materials and methods

Genomic datasets used

Publicly available genome-wide transcriptomic data sets were used to generate all main figures. Datasets analyzed include microarrays GSE31587 (Hu et al. 2013), GSE62119 (Kawashima et al. unpublished data), GSE58552 (He et al. 2015), and E-MEX-1299 (Michael et al. 2008) for *Arabidopsis* seedlings at comparable developmental stages. The GSE31587 dataset was generated using 4-day old WT and *phyABCDE* *Arabidopsis* seedlings grown in darkness or under continuous Red light ($50 \mu\text{mol m}^{-2} \text{s}^{-1}$). The GSE62119 dataset was generated with 3-day old WT and *hy5* grown under continuous white light (no intensity data provided). The GSE58552 dataset included 4.5 day-old WT and *cry1-cry2* grown in darkness or in continuous Blue light ($15 \mu\text{mol m}^{-2} \text{s}^{-1}$). The E-MEX-1299 dataset was generated using 7-day Col and *phyB-9* null knock-out mutant grown under short day (SD) conditions (8 h light 100 uE/16 h dark at 22°C-SD). Datasets GSE31587, GSE62119 and GSE58552 generated cDNAs using oligo-dT based technology, while the *phyB* dataset E-MEX-1299 used random hexamer primers.

Statistical analysis of gene expression

Expression profiles were analyzed using Microsoft Excel and R (R Core Team 2020). Significant differences on gene expression ratios were analyzed with the package

GSALighning (Chang and Tian 2015, Chang 2020) and the Mann–Whitney–Wilcoxon test for all genes, and were adjusted using the Benjamini–Hochberg false discovery rate (FDR) at the significance level of 0.05.

Gene ontology enrichment

Gene ontology (GO) enrichment information for GO terms ‘biological processes’ and ‘cellular component’ against light modulated genes expressed in each dataset were searched using Cytoscape version 3.8.0 (<http://www.cytoscape.org/>) along with its plugin Bingo version 3.0.3 (Maere et al. 2005). Annotations and ontologies were those released in April 2020. Hypergeometric test was used with a Benjamini and Hochberg FDR correction at the significance level of 0.05 to determine the categories overrepresented. Only the 15 top categories significantly overrepresented were considered in Fig. 1. A cut off of $\log_2 > 0.5$ for differential expression was chosen to take into account moderate responses. Lists of genes were compared by using Venny2.1 (Oliveros 2007–2015). Only significant ratios by Mann–Whitney–Wilcoxon adjusted with FDR were considered for GO enrichment analysis.

Heatmap

The heatmap display in Fig. S1B was created with pheatmap R package (R Core Team 2019, Kolde 2019). Results were clustered according to Z-score.

Selection of genes lists used for chloroplastic genome modulation functional categories

GO-term categories corresponding to chloroplast genome regulatory mechanisms (GO:0009507), transcription (GO:0006350), post-transcription (GO:0010608) or translation (GO:0006412) were selected using TAIR website annotation. To ensure function in the chloroplast, overlap with the GO term ‘chloroplast’ (GO:0009507) was verified and the final gene sets were manually curated to remove false positives. From these gene sets, we manually identified commonly occurring genes with R/B light- or phy/cry-sensitivity that were part of wider families/classes. Three families/classes were selected for further examination in each one of the general plastome regulatory categories. Gene lists were manually curated for annotated members of the family that also had a chloroplast function. Where appropriate, the presence of specific functional domains was verified to corroborate classification. Light sensitivity for the genes analyzed was established using WT data and an absolute \log_2 ratio > 0.5 difference compared to dark datasets. This cut off was selected aiming to pick strong and moderate light responsiveness. After establishing light-sensitivity, subsequent photoreceptor-dependency of these targets was

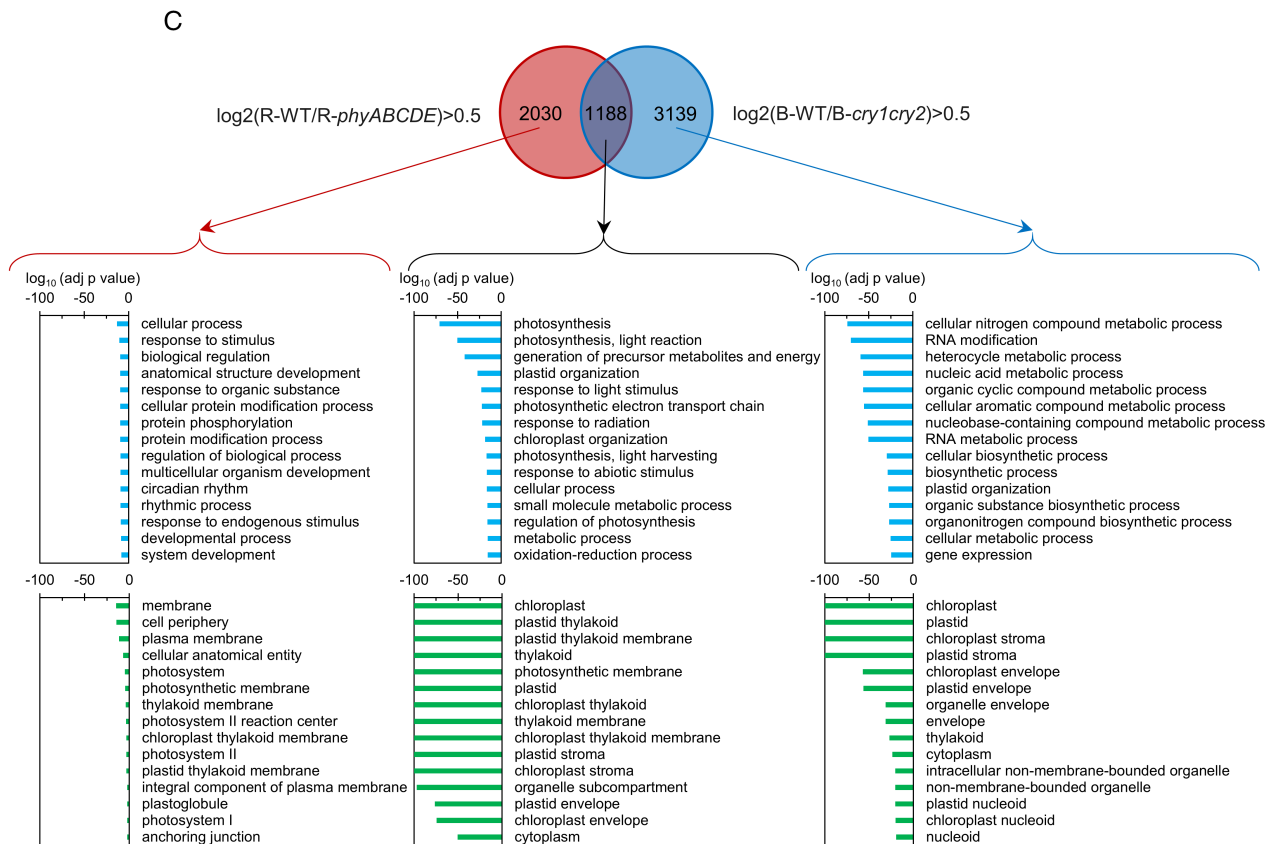
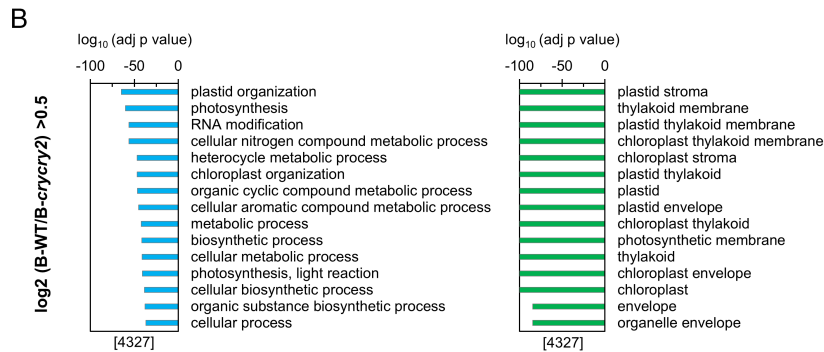
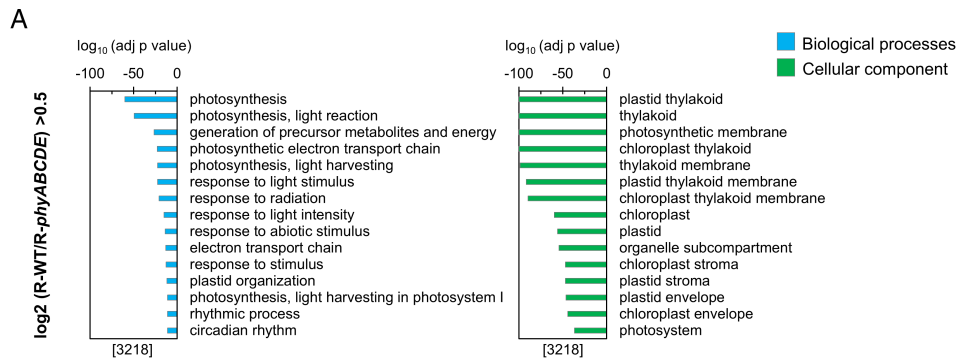


(Figure legend continues on next page.)

calculated based on an absolute log₂ ratio > 0.5. For each category, only a log₂ ratio > 0.5 validated by multiple comparisons Wilcoxon test followed with FDR at 0.05 were considered as significant. A χ^2 test was used to evaluate the significance of enrichment of mis-regulated genes in each category and differentiate enrichment from random observations. Statistical differences were defined as those with a *P*-value of <0.05.

Results

Phytochromes and cryptochromes regulate chloroplastic and photosynthesis-associated biological processes at a genomic level in *Arabidopsis*

In accordance with the extensive reprogramming of the nuclear genome by the phytochrome and cryptochrome photoreceptors during photomorphogenesis (Chen and Chory 2011), multiple R/B light-responsive genes with a functional role in chloroplast biogenesis and photosynthetic metabolism have been identified in parallel with the greening defects observable in the *phy* and *cry* mutants (Ohgishi et al. 2004, Franklin and Quail 2010). Nonetheless, no formal chloroplast function-focused genome-wide study of the contribution of *crys* in Blue light and *phys* in Red light has been conducted. The availability of full genome data for young *Arabidopsis* seedlings in comparable stages of development (~4 day-old) grown under 15 $\mu\text{mol m}^{-2} \text{s}^{-1}$ blue light (B) (dataset GSE58552) (He et al. 2015) or 50 $\mu\text{mol m}^{-2} \text{s}^{-1}$ red light (R) (dataset GSE31587) (Hu et al. 2013) and defective in *cry1cry2* or the five phytochromes (*phyABCDE*), allowed us to explore their respective global contribution to chloroplast functions. Within the limitations of datasets obtained with different methodologies, raw data curation parameters and different level of variation among biological replicas, we surveyed the role of the cryptochromes and phytochromes in chloroplast metabolism and functions. We selected genes with a log₂ ratio > 0.5 gene expression difference and validated with an FDR-adjusted multiple comparison

Mann–Whitney–Wilcoxon test at *P* < 0.05 between the WT and R-*phyABCDE* (3,218 genes out of 22,810 genes evaluated, Fig. 1A) or B-*cry1cry2* (4,327 genes out of 27,417 genes evaluated, Fig. 1B). GO-term biological processes and cellular component analyses singled out notable enrichment in chloroplastic and photosynthetic functions for both receptors (Fig. 1A,B). The high number of genes identified points at a broad role of both photoreceptor families in photosynthesis, the tuning of chloroplast metabolism and plastid organization. In addition, the photoreceptors impact all the chloroplasts sub-compartments, as indicated by the cellular component data (Fig. 1A,B). We singled out 1,188 genes common to both datasets, likely representing genes co-regulated by R-*phys* and B-*crys* (Fig. 1C). This gene subset is enriched in functions including photosynthesis, light reactions, plastid organization, light harvesting, electron transport and regulation of photosynthesis, and likely illustrates the adaptation of photosynthesis in higher plants to natural environments enriched in both wavelengths. However, the data also points at potential bifurcation of signals that could derive in differential sensitivity of specific processes. Among the non-overlapping gene sets for R-*phy* (2,030 genes) and B-*cry* (3,139 genes), we still observe the presence of broad functional categories potentially related to chloroplast functions such as anatomical structure development and circadian and rhythmic processes in the R-*phy* set and RNA modification, plastid organization and biosynthetic processes in the B-*cry* set (Fig. 1B). It is also apparent that there is a subset of photosynthetic genes that are B-*cry* modulated, which in the datasets analyzed did not overlap with the R-regulation.

In summary, our study further emphasizes a genome-wide role of *phys* and *crys* in the modulation of the chloroplast and its metabolism, including genes whose products act in the chloroplast for the onset of photosynthesis, plastid development and for the production of plastidic essential metabolites. Both an imposed co-sensitivity to R- and B-light mode of action and a light quality-dependent bifurcation of functionalities are potential

(Figure legend continued from previous page.)

Fig. 1. GO-term analysis of biological processes and cellular component for *phyABCDE* in red (R) light (A) and *cry1cry2* in blue (B) light shows significant enrichment in the contribution of these receptors to photosynthesis and chloroplastic processes. GO-term genome-wide analysis of R-light activated genes in WT vs the *phyABCDE* mutant (A) and B-light activated genes in WT vs *cry1cry2* mutant (B) was conducted using the publicly available datasets GSE31587 and GSE58552, respectively. (C) GO-term biological processes and cellular component categories evaluating *phy* and *cry* photoreceptors co-targeting and individual contribution to light-up-regulated genes indicate an enrichment in photosynthesis and chloroplast functions. In all panels, light up-regulated genes were defined by a log₂ ratio > 0.5 difference with WT and statistical significance of gene expression ratios was estimated with FDR adjusted multiple comparison Mann–Whitney–Wilcoxon at *P* < 0.05 (for details see Section 2). Hypergeometric test was used with an FDR correction at the significance level of 0.05 to determine the categories overrepresented. Only the 15 top categories significantly overrepresented were considered. The bar diagrams represent significant log₁₀ of adjusted *P*-values and the number of genes evaluated to estimate enrichment is indicated in brackets.

mechanisms used by the photoreceptors in the building of a functional chloroplast.

Beyond the nucleus: photoreceptors role in the global regulation of the plastome gene expression

While the interpretation of light signals from both the nuclear genome and the plastome is essential for chloroplast development, function and the onset of photosynthesis, our understanding of the role of the light photoreceptors in the global regulation of the plastome gene expression mechanisms remains fragmented. The plastome encodes for ~80 genes for proteins involved in: (1) the organellar gene expression machinery, such as the large ribosomal proteins (*rpl*), the plastidic RNA polymerase (*rpo*) and small ribosomal proteins (*rps*); (2) photosynthesis and the electron transport chain including subunits of the ATP synthase (*atp*), NADH dehydrogenase (*ndh*), Cytochrome b6f complex (*pet*), photosystem I (*psa*), photosystem II (*psb*) and rubisco large subunit (*rbcL*); (3) hypothetical and uncharacterized proteins (*ycf*). Recently, a key role for CRY2 in the modulation of 58% of the genes encoded in the plastome was described for tomato (Facella et al. 2017). In this study, based on CRY2 over-expressing plants, authors reported the CRY2-dependent positive modulation of 88% of the plastome encoded subunits of PSII and PSI and the down-regulation of most of the genes participating in translation (Facella et al. 2017). No full investigation of the global impact of the phys on the plastome-encoded gene expression has been conducted to date. We addressed this question by analyzing the effect of phyB in short days (SD) (E-MEX-1299) (Michael et al. 2008). For transcriptomic studies, the synthesis of complementary DNAs (cDNAs) by reverse transcription from mRNA templates is achieved by the use of oligo-dT complementary to the poly-A tails of mature mRNAs or by random hexamer priming technology. While both methodologies are efficient for the quantification of nuclear mRNAs, in the case of plastome-encoded mRNAs the links between poly-A tails in chloroplast mRNAs and the degradation pathways (Schuster et al. 1999) make the use of random hexamer priming technology necessary. The genomic dataset E-MEX-1299 for phyB was the only one among the multiple published phy transcriptomic studies for which we could verify this requirement.

We checked GO-term cellular component analyses for the E-MEX-1299 dataset that phyB in SD shows enrichment in plastid functions including PSII, PSII reaction centers, photosynthetic membranes, and thylakoids (Fig. S1A). We then evaluated the impact of *phyB*-SD over 80 plastome transcripts abundances during the course of the light (ZT4-ZT8) and dark (ZT12-ZT0)

periods using a log₂ ratio > 0.5 difference between WT and *phyB*. Further statistical validation for each timepoint was not possible, as only average results for each time point were provided for the dataset E-MEX-1299 (Michael et al. 2008) (Fig. 2). This analysis revealed that phyB is required for the modulation of 55 out of the 80 genes evaluated (69%) in at least one time point during the dark–light cycle. The analysis supports a wide impact of phyB on the plastome expression that extends to the accumulation of 24 out of the 40 plastome-encoded photosynthesis functioning genes, including the *psb* family (Photosystem II), the *psa* family (Photosystem I), the *ndh* family (NADH dehydrogenase complex) and the *pet* genes (cytochrome b6f complex), as well as modulation of genes involved in the plastome gene expression functions such as *rpl* and *rps* encoding for the large and small ribosomal protein gene families and *rpo* coding for the plastid RNA polymerase subunits (Figs 2 and S1B).

In 53 out of the 55 genes with phyB contribution to their transcript accumulation, phyB has a positive role. We only identified two genes, *accD* (acetyl-CoA carboxylase) and *rbcL* (rubisco large subunit), where phyB had apparently exclusively negative modulatory activity under the conditions tested. In the case of *psbG* (PSII), *rpoB* (RNA polymerase), *ycf6* (unknown) and *petN* (cytochrome b6f), a mixed role for phyB between up- and down-regulation was observed depending on the time point analyzed (Figs 2 and S1B).

Interestingly, the effect of *phyB* is observed not only during the illumination period, but extends broadly into the dark cycle with 49 plastome genes (61.25% of the set analyzed) dependent on phyB at least one time point in the dark, including effects at dawn for 37 of the 80 genes studied (46.25%). An equal number of genes (37) showed phyB-dependent modulation during the illumination period (ZT4–ZT12), including an effect at the earliest time point measured (ZT4) in 27 of them (Figs 2 and S1B). Closer inspection indicates that in SD, phyB does not alter the timings of expression over the dark/light cycle but has an effect on the relative transcript abundance (Fig. S1B).

These preliminary observations point at a broad effect of phyB in the expression of the Arabidopsis plastome in the light and in the dark, similar in magnitude to the effect described for CRY2 in tomato.

Phytochrome and cryptochromes are involved in setting up the regulatory machinery for the expression of plastome genes

Plastome gene expression involves processes that are similar to both prokaryotic and eukaryotic organisms. These mechanisms include transcription by a nuclear-

■ log2 ratio > 0.5 ■ log2 ratio < -0.5

	ZT0	ZT4	ZT8	ZT12	ZT16	ZT20
-0.4658	-0.2881	0.6304	-0.2651	-0.4508	-0.3005	
-0.3354	-0.1628	0.2353	-0.2799	-0.1712	-0.0311	
-0.3643	-0.2212	0.0288	-0.2102	-0.1789	-0.1977	
-0.2710	-0.2183	-0.2180	-0.2052	-0.0630	-0.2990	
-1.0746	-0.7300	-0.0035	-0.3383	-0.1202	-0.5813	
-0.4531	-0.3456	0.1252	-0.3306	-0.1218	-0.5950	
-1.4104	-0.9887	-0.5167	-0.6812	-0.4495	-0.4647	
-0.0688	-0.1301	0.1665	-0.1054	-0.2648	-0.0955	
-0.4178	-0.5383	0.0265	-0.0508	-0.1213	-0.2904	
-0.5170	-0.2886	-0.0495	-0.6142	-0.3202	-0.1070	
0.0860	-0.5613	-0.3888	-0.3163	-0.2131	0.2090	
-0.2271	-0.1800	-0.1348	-0.2492	-0.0853	-0.0858	
-0.1732	-0.0763	0.2250	-0.2887	-0.1740	0.0675	
-0.9910	-0.8126	-0.2103	-0.4557	-0.2234	-0.4021	
-0.3287	-0.6384	0.0931	-0.5021	0.3352	-0.0520	
-1.4790	-0.6893	-0.4201	-0.1200	-0.1943	-0.5594	
-1.4834	-1.3589	0.1050	-1.2915	-0.7468	-0.1033	
-0.2064	-0.3002	0.0245	-0.3099	-0.1517	-0.0479	
-0.7516	-0.9284	0.0326	-0.8819	-0.7300	-0.4606	
-0.8521	-0.5257	-0.6184	-0.3480	-0.3493	-0.5909	
0.0269	0.4213	-0.8988	-0.0243	-0.6922	-0.3254	
-0.2269	-0.1229	-0.2698	-0.1574	-0.3131	0.0545	
-0.1618	-0.0442	-0.0318	-0.1437	-0.3125	0.0124	
-0.4739	-0.2697	-0.1727	0.2203	-0.2641	0.0202	
-1.4275	-0.0065	-0.5605	-0.0635	-0.1674	-0.2574	
-1.3827	-0.7811	-0.0812	-0.9737	-0.3515	-0.4650	
-0.1118	-0.2005	0.0870	-0.2648	-0.1984	-0.0696	
-0.8946	-0.5119	0.0286	-0.6296	0.2184	-0.1758	
-0.2042	-0.2732	0.2778	-0.4129	-0.5703	0.0063	
-0.3707	-0.0577	0.0927	-0.2446	-0.3086	-0.3436	
-0.6610	-0.4373	-0.1102	-0.7481	-0.5464	-0.4895	
-2.5526	-0.6708	-0.5928	-1.1163	-0.6616	-0.4619	
-1.6107	-0.2945	-0.1361	-0.8273	-0.5891	-0.6428	
-2.6982	0.1671	-0.9897	-1.7628	-0.5418	-0.6767	
-0.4960	-0.3050	-0.2371	-0.2859	-0.3389	-0.1118	
-0.1093	-0.1928	-0.2876	-0.3209	-0.1536	-0.2738	
-0.9806	-1.0235	0.8401	-1.6759	-0.5066	-0.5426	
-0.9778	-0.3072	-0.2805	-0.3647	-0.0441	-0.3420	
-0.3043	-0.2362	-0.2414	-0.3419	-0.1344	-0.2586	
-0.5166	-0.3591	-0.5037	-0.3784	-0.0481	-0.3827	
-0.4127	-0.4494	-0.0419	-0.3433	0.0377	-0.4534	
-0.4385	-0.1272	-0.7886	-0.6730	-0.1895	-0.3173	
0.0966	0.1430	-0.1198	-0.2746	-0.3575	0.1478	
-1.0716	-0.7365	0.0719	-0.3066	-0.0053	-0.6231	
-0.5247	-0.4221	-0.8918	-1.2665	-0.4422	-0.5017	
-0.4747	-0.1021	0.8724	-0.0420	-0.0127	0.0617	
-0.1775	-0.2202	-0.1763	-0.0655	0.0373	-0.0989	
-1.0126	-0.8887	-0.3433	-0.4596	0.4206	0.0754	
-1.0368	-0.6139	-0.0792	-0.4878	-0.3133	-0.2012	
-0.5376	-0.6199	-0.0735	-1.5666	-0.0601	-0.3795	
-0.9134	-0.6295	0.0049	0.0480	-0.3675	-0.3406	
-0.4644	-0.2776	-0.3592	-0.2611	-0.2955	0.0046	
-0.4666	-0.2962	-0.2210	-0.2888	0.0177	-0.4168	
-0.7583	-0.2493	-0.0926	-0.0529	-0.1401	-0.2309	
-0.5813	-0.2140	-0.2282	-0.3979	-0.1136	-0.1039	
-0.2052	-0.0666	-0.2743	-0.6083	-0.0061	0.0391	
-0.6473	-0.2489	0.5375	0.0865	-0.2327	0.2540	
-0.1789	-0.2814	0.1755	0.0559	-0.1846	0.0589	
-0.4412	-1.0406	-0.1054	-0.1662	-0.5218	-0.0641	
-0.3203	-0.9234	-0.0843	-0.2570	-0.4321	-0.1400	
-0.5454	-0.3363	-0.3199	-0.0398	-0.0442	-0.2745	
-0.3804	-0.3972	0.2212	-0.1514	-0.8599	-0.1317	
-0.4758	-0.2179	0.3725	-0.5051	-0.3403	-0.2494	
-0.9116	-0.7844	-0.4604	-0.3903	0.1117	0.2072	
-0.2857	-0.3944	0.0788	-0.1424	-0.1753	0.1018	
-1.3306	-0.6933	-0.4662	-0.2764	-0.3597	-1.2080	
-1.0911	-0.4957	-0.1228	-0.3682	-0.1236	-0.6652	
0.1602	0.0184	0.1201	0.1513	-0.3578	0.0522	
-0.4730	-1.0641	-0.1274	0.3349	-0.1282	-0.4537	
-0.4401	-0.6340	0.2799	0.2823	-1.5885	-0.1388	
-0.6691	-0.5501	-0.2410	0.0346	-0.1713	-0.2286	
-0.6267	-0.8439	-0.2254	-0.2254	-0.2880	-0.1687	
-0.3494	-0.0556	-0.0387	-0.0092	-0.5153	-0.3569	
-0.2374	-0.1054	-0.7099	-0.1030	-0.1669	0.0773	
-0.3712	-0.3150	0.3598	-0.2344	-0.2689	-0.7213	
-0.7817	-0.3913	-0.3024	-0.3774	-0.5051	-0.0579	
-0.1948	-0.1318	-0.1826	-0.1340	-0.3855	-0.3039	
-0.9691	-0.2896	-0.3974	0.8479	0.6722	-0.1439	
-0.6254	-0.0962	-0.3044	-0.4253	-0.5524	-0.3601	
-0.5845	-0.4743	-0.2933	-0.4754	-0.5321	-0.1094	

log2(phyB/WT)

encoded RNA polymerase (NEP) and a plastid-encoded (PEP) RNA polymerase supported by transcriptional co-regulators known as sigma factors (Berry et al. 2013), in addition to extensive RNA processing (Ruwe et al. 2011) and translational control (Chotewutmontri and Barkan 2016). All of these regulatory processes depend on nuclear-encoded proteins imported by the plastids (Del Campo 2009, Berry et al. 2013). However, plastid mRNAs' organization in polycistronic operons requires extensive processing, stabilization, editing and splicing, making post-transcriptional control a dominant process in plastid gene regulation (Stern et al. 2010, Barkan 2011).

The contribution of phys and crys to the light-dependent modulation of the nuclear-encoded genes with regulatory activity over plastome gene expression is illustrated by their control of genes encoding for subunits of the plastid RNA polymerase (PEP), HEMERA (HMR)/plastid transcriptionally active chromosome 12 (pTAC12) (Chen et al. 2010, Yoo et al. 2019), the transcriptional cofactors sigma factors that direct the PEP, and plastid-translational factors such as Brz-insensitive pale green 2 (BPG2) and ATAB2 (Barneche et al. 2006, Kim et al. 2012, Oh and Montgomery 2014).

However, the full extent of the regulatory networks and functions orchestrated by the photoreceptors to deliver environmental signals to the plastome has not been fully explored. To begin addressing whether phys and crys exert a broad control over plastome gene expression by modulating the accumulation of transcripts for nuclear-encoded genes, whose proteins act in the control of the plastome gene expression, we conducted a GO-term biological function analysis based on the GO-term categories 'transcription' (GO:0006350), 'post-transcription' (GO:0010608), and 'translation' (GO:0006412) overlapped with the GO-term 'chloroplast' (GO:0009507) (for more details see Material and methods). From these subsets, those genes up-regulated (log2 ratio > 0.5) in

Fig. 2. phyB has a broad impact in chloroplast genome expression in short-days (SD). Table representation of the plastome transcripts' differential accumulation in *phyB* compared to WT. Numbers indicate the *phyB*/WT transcript ratio during a SD dark/light cycle. Color code illustrates gene downregulation in blue (log2 *phyB*/WT < -0.5) and up-regulation in red (log2 *phyB*/WT > 0.5). Plastome gene expression information was obtained from the dataset *E-MEX-1299* to calculate the ratios. Chloroplast genome genes are organized by functional category: *atp* (ATP synthase); *ndh* (NADH dehydrogenase); *pet* (cytochrome b6f complex); *psa* (photosystem I); *psb* (photosystem II); *rpl* (50S ribosomal proteins large subunits); *rpo* (RNA polymerase); *rps* (30S ribosomal proteins small subunits) and *ycf* (hypothetical/unknown chloroplast ORFs). The light period (ZT4-8) of the diurnal cycle is indicated with a white rectangle and dark period (ZT12-0) in a gray rectangle.

the WT in response to R-light dataset (GSE31587) or B-light (dataset GSE58552) compared to darkness were selected, and the contribution of phys and crys to the R- and B-light response was evaluated by comparison between WT and *phyABCDE* (Fig. 3A) or *cry1cry2* (Fig. 3B). Statistical significance of the differential with WT was established using an FDR-adjusted multiple comparison Mann–Whitney–Wilcoxon at $P < 0.05$ (see Section 2). Results show that 9% (13 genes out of 141) in the transcription category, 26% (11 genes out of 43) in post-transcription, and 8% (21 genes out of 265) from the translational category were R-phy dependent (Fig. 3A). On the other hand, B-crys contributed to the modulation of 30% (43 genes out of 141) in the transcription category; 47% (20 genes out of 43) in the post-transcription and 38% (101 genes out of 265) in the translational category (Fig. 3B).

A closer inspection of the genes dependent on R-phys' and B-crys' modulation represented in each of the general transcription, post-transcription and translation GO-term biological function categories, showed enrichment in specific gene families/classes with an already described role in plastid gene expression regulation. In the transcriptional category, we identified members of the mitochondrial transcription termination factor (mTERF) family, involved in transcriptional initiation and termination (Kleine 2012); the plastid transcription active chromosome (pTAC) class of proteins involved in PEP activity (Pfalz et al. 2006, Chen et al. 2010); and the sigma factors required for PEP promoter recognition (Borner et al. 2015). In the post-transcriptional category, we focused on the pentatricopeptide repeat-containing domain (PPR) family, the RNA recognition motif (RRM), and the tetratricopeptide repeat-containing domain proteins (TPR) involved in chloroplastic RNA processing, editing, cleavage, splicing and protection against degradation (Lamb et al. 1995, Ruwe et al. 2011). In the translational subgroup, we singled out the t-RNA ligases, the large ribosomal proteins (RPL), and the small ribosomal proteins (RPS) gene families (Yamaguchi and Subramanian 2000, Yamaguchi and Subramanian 2003, Berg et al. 2005) (Fig. 3).

For all the TAIR-annotated members of these specific gene classes with a GO-term chloroplast overlap, we evaluated the light responsiveness and photoreceptor dependency. These were defined based on a log₂ ratio > 0.5 difference with darkness and statistical support defined with multiple comparison Mann–Whitney–Wilcoxon adjusted with FDR test at $P < 0.05$ (see Section 2). A χ^2 test was used to evaluate the significance of enrichment in light up-regulated genes from random observations in each category at $P < 0.05$.

Within the transcription category, we identified 2 genes as R-phys dependent and 11 genes as B-crys

dependent out of the 30 analyzed mTERFs; of the 18 pTAC class genes evaluated, 3 were R-phys dependent and all of them were modulated by B-crys. Of the 6 sigma factors, 4 were R-phys dependent and 5 of them B-crys induced. (Fig. 3A,B). Statistical analysis of enrichment within the light modulated genes in the transcriptional category showed significance for the R-phy regulation of the sigma factors and for the three gene families/classes (sigma factors, mTERFs and pTAC) for B-crys.

Among the post-transcriptional regulation category, out of the 181 members of the PPR category 28 genes were R-phys modulated and 100 were B-crys dependent. In the TPR domain-containing category of 31 members, 7 were R-phys dependent and 11 were B-crys controlled. Within the 37 RRM, 1 member was R-phys modulated and 17 were B-crys up-regulated (Fig. 3A,B). Statistical enrichment of light responsiveness was observed within all families for the B-cry modulation and for R-phys in the PPRs' and TPRs' cases.

In the translational activity category, out of the 12 tRNA ligases 1 R-phys dependent gene was detected vs 7 B-crys modulated genes. For the RPL, out of the 38 members, 3 were R-phys dependent and 20 were B-crys dependent. For the 37RPS, 1 was found to be R-phys dependent and 10 were B-crys modulated (Fig. 3A,B). Statistical enrichment showed significance for the B-crys modulation of the tRNA-ligase and RPL families (Fig. 3).

Globally, the results show a clear contribution of B-crys to the modulation of a large number of genes with potential function in different levels of the plastome expression. This result highlights the crys potential to orchestrate a whole range of plastome regulatory mechanisms based on the control of the light-sensitivity of multiple members of the regulatory gene families singled out in this study.

In the case of phys, while more moderate modulatory effects were detected, we identified statistically significant enrichment in the global category of post-transcription. And, at the level of the specific gene families analyzed, we detected enrichment in their contribution to the R-induction of the sigma factors (transcription), and PPRs and TPRs genes (post-transcription).

Anterograde signaling: HY5, a light signaling component linking the photoreceptors to the regulation of the plastome

The cry and phy photoreceptors share some signal transduction mechanisms including the control of nuclear-localized 'master' transcription factors that stimulate large-scale changes in gene expression. The b-ZIP HY5 transcriptional modulator HY5 is one of such key B- and R-light signaling components, with functions in

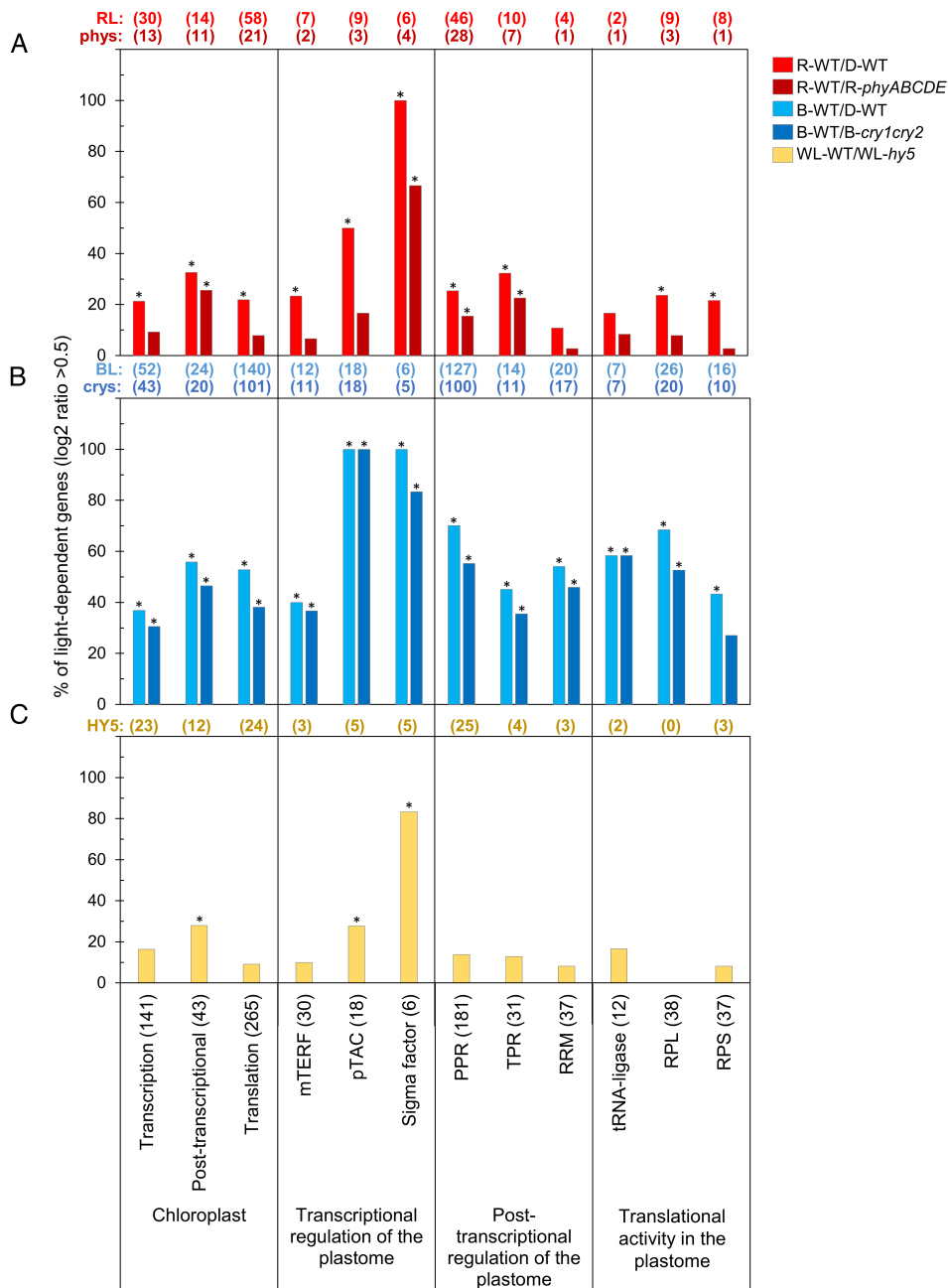


Fig. 3. Phytochromes, cryptochromes and HY5 modulate the light induction of genes with potential functions in multiple aspects of plastome gene expression. (A) Percentage of genes involved in plastome regulatory processes and R-light up-regulated (red bars) or R-up-regulated in a phytochrome-dependent manner (dark red). Light modulation was calculated comparing to the dark response using a log₂ ratio > 0.5 difference. Phytochrome contribution was estimated by comparing WT to the *phyABCDE* response. Significant differences on gene expression ratios were conducted by FDR-adjusted multiple comparison Mann–Whitney–Wilcoxon test at the significance level of 0.05. Statistical significance for enrichment was conducted with a χ^2 test at $P < 0.05$ (see Section 2). Transcript information was obtained from the GSE31587 dataset. (B) Percentage of light-induced genes involved in plastome regulatory processes and B-light up-regulated (blue bars) or B-up-regulated in a phytochrome dependent manner (dark blue bars). Light modulation was estimated as described in (A) and cryptochrome contribution calculated using the dataset for *cry1cry2* (GSE58552). Statistical significances for differences on gene expression ratios and enrichment were conducted as described in (A). (C) Percentage of light-induced genes involved in plastome regulatory processes and B or R-light up-regulated and light up-regulated and dependent on HY5. Light up-regulation was calculated as described in panel (A). HY5 dependence was calculated relative to the WT response used the *hy5* data from GSE62119. Statistical significances for differences on gene expression ratios and enrichment were conducted as described in (A). For all panels numbers in (Figure legend continues on next page.)

chloroplast development, plastid metabolism and the transcriptional control of light-responsive genes that act in the chloroplast (Osterlund et al. 2000, Wang et al. 2017), roles further corroborated by our GO-term biological function analysis for *hy5* (Fig. S2). Previous studies have also provided with evidence to support the involvement of HY5 in the regulation of the plastome gene expression. Specifically, HY5 participates in the light modulation of the plastid transcriptional co-regulator SIG5 (Mellenthin et al. 2014, Belbin et al. 2017) and the light-regulated zinc finger 1 (LFZ1) with functions in early chloroplast development and in the coordination of the light-regulated translational activation of chloroplast mRNAs (Chang et al. 2008). However, no global evaluation of the involvement of HY5 in the regulation of genes whose protein products could impact the expression of the plastome has been conducted to date.

We investigated at a genome level whether HY5 could act as a relevant anterograde signaling component involved in delivering light cues to the plastome by controlling the expression of nuclear genes (identified previously) potentially involved in chloroplast genetic machinery control. For the study, we used the genomic dataset GSE62119 generated for 3-day old *hy5* and WT seedlings grown under continuous white light (Kawashima et al., unpublished data) to examine the contribution of HY5 to the light induction of the genes previously classified in the general functional categories of chloroplast transcription, post-transcription and translation as well as for the specific gene families singled within each one (Fig. 3). Light modulation was established by a log2 ratio > 0.5 compared to darkness, and statistical differences between WT and *hy5* evaluated by FDR-adjusted multiple comparison Mann–Whitney–Wilcoxon at $P < 0.05$.

HY5 showed a contribution ranging from ~10 to 30% of the light modulation of the genes included in the general categories with 23 genes in chloroplast transcription category, 12 in post-transcription and 24 in the translational category (Fig. 3C). Within the specific gene families evaluated, HY5 participated in the light up-regulation of the transcripts of 3 mTERFs, 5 pTACs and 5 sigma factors with potential to participate in transcription of the plastome. Statistical analysis showed HY5 significant enrichment in the modulation of the pTAC and sigma factors. The possibility of a HY5 contribution to the light-dependent transcript accumulation of 25 PPRs, 4 TPRs and 3 RRM in the post-transcriptional category

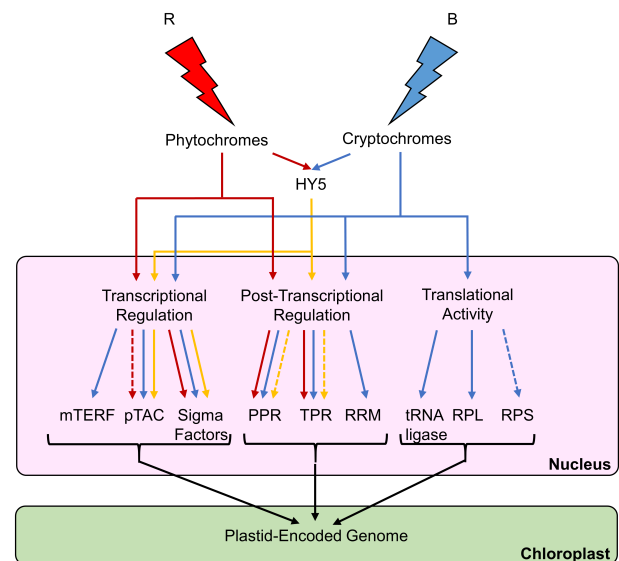


Fig. 4. Working model for the phytochrome and cryptochrome photoreceptors and HY5 involvement in the regulation of the plastome. Schematic representation of the activity of the phys, crys and HY5 in modulating the expression of the plastome. Photoreceptors target-specific subsets of nuclear encoded genes whose protein products have a functional role in the chloroplast transcriptional, post-transcriptional, and translational processes. HY5 may play a central role as a photoreceptor signaling component with capacity to integrate light information for the modulation of genes that act in the transcriptional and post-transcriptional modulation of the plastome. Full lines represent statistically significant enrichment in the links between the photoreceptors or HY5 and the modulation of light-dependent genes in the indicated processes or specific gene families (see Section 2). Dotted lines represent based on a noticeable number of genes, the possibility of a contribution of HY5 or photoreceptor to the light-dependent induction that deserves further study.

(Fig. 3C) and in the translation category 2, tRNA ligase genes and 3 RPSs deserves further study.

These results illustrate that HY5 could be part of the nuclear transcriptional cascades connecting the environmental signals perceived by the light photoreceptors to the control of nuclear-encoded genes whose protein products act over the plastome (Fig. 4). Notably, the identification of HY5 light-modulation of RNA binding proteins (Fig. S2) with function in the chloroplast illustrates a previously underestimated capacity to act in the post-transcriptional control of plastome gene expression. The future characterization of these HY5-dependent genes would be of interest in relation to their biological function in plastid gene expression and light-signaling cascades.

(Figure legend continued from previous page.)

brackets indicate total number of genes analyzed in each category. Numbers at the top of the graphs indicate the number of genes light modulated and the number dependent on the photoreceptors (A, B) or HY5 (C). Statistical significance for enrichment by χ^2 test at $P < 0.05$ is indicated with an asterisk.

Discussion

The phy and cry photoreceptors exert an important role in chloroplast biogenesis and plastid metabolic gene expression. Yet, their contribution towards building a functional chloroplast by coordinating the nuclear genome and the plastome remains underexplored.

In this work, we conducted genome-wide GO-term biological processes and cellular component analyses to show that in *Arabidopsis thaliana*, both phys and crys share a global role in the regulation of genes whose protein products act in the chloroplast to build a functional organelle and orchestrate photosynthesis (Ohgishi et al. 2004, Hu et al. 2013). Our focused analysis provides evidence that although R-phys and B-crys co-regulate 1,188 genes in chloroplastic processes, independently they target an even larger number of genes (2,030 R-phys; 3,139 B-crys) whose functions remain enriched in chloroplast processes (Fig. 1).

While in our studies the apparent contribution of B-crys is larger than the R-phys, we need to acknowledge limitations for a fully comparative analysis, derived from datasets obtained under different experimental conditions and the potential under-estimation of the number of R-sensitive and R-phy-dependent genes. However, our study is in agreement with previous studies on the importance of both photoreceptor families for photosynthesis (Ohgishi et al. 2004, Hu et al. 2013), and shows that crys and phys share an important global role in the regulation of genes whose protein products act in the chloroplast to build a functional organelle. In addition, we provide evidence of a cooperative gene co-targeting mode of action as well as bifurcation of functionalities in a light quality dependent manner for the regulation of chloroplastic processes (Figs. 1 and 4). It would be of interest to further investigate light-specific responses such as the R-phys role in circadian and rhythmic processes and the B-crys involvement in RNA metabolism and plastid organization.

The involvement of both photoreceptor families in building a functional chloroplast is observed not only at the level of nuclear genes with a chloroplastic related function, but on the global modulation of the plastome. Previous studies on tomatoes overexpressing CRY2 had established that 58% of the plastome ORFs are controlled by this photoreceptor in a light-dependent manner in long days (Facella et al. 2017). While multiple transcriptomic datasets had been generated for phys, the requirement of using random hexamer priming to measure the abundance of plastome-encoded genes was only met by a study of *phyB* in SD. Oligo-dT-based technologies suffer from the limitation derived from polyA-tails in plastid transcripts association to degradation pathways

(Schuster et al. 1999). Despite the specific photoperiodic environment used to evaluate the *phyB* effects over the plastome, the results show that its contribution is global, and comparable in magnitude to the impact of CRY2 in long days. Out of the 80 plastome genes analyzed, 55 showed a phy-dependent modulation in at least one time point of the cycle (Fig. 2). Interestingly, the role of *phyB* was not restricted to photosynthetic genes or to the light period. This contrasts to the effect of CRY2 on plastome-encoded photosynthesis-associated genes in long days, with only the exception of *psbN* and *petD*. This broad effect of *phyB* over the dark/light cycle extends to the genes from the chloroplast genetic machinery, affecting expression of RPL and RPS and subunits of the plastid-encoded polymerase. Only a few genes provided some indication of a potential *phyB* role as a negative modulator of plastid gene expression, including *accD* (acetyl CoA carboxylase) and *rbcL* (rubisco large subunit). Another interesting observation is that no alterations in timings of transcript accumulation were detected in *phyB* compared to WT, consistent with observations of the effect of *phyB* over the regulation of nuclear genes. Withal, our analysis highlights a broad role of *phyB* in delivering light signals to the plastome that was not previously described. In future experiments, it would be of interest to contrast the effects of crys and phys under comparable monochromatic and photoperiodic conditions, to dissect their relative contributions and whether preferential light quality responses of the plastome are necessary to build a functional chloroplast.

This co-regulation of crys and phys of chloroplastic processes is also observed in the modulation of nuclear genes whose protein products act in the chloroplast, including those with an annotated function in GO-term biological processes in transcriptional, post-transcriptional, and translational control of the plastome (Fig. 4). Our analysis of the B-crys showed a statistically significant enrichment in the light-modulation of genes across all the three general functional categories (Fig. 3). This statistical significance was also maintained for the B-crys contribution to the light modulation of the singled-out gene families/classes derived from these general categories and with clear links to the plastome genetic machinery control.

Thus, our results reinforce the view of crys as master modulators of the plastome gene expression and suggest a mechanistic basis for the wide regulatory capacity observed for CRY2 (Facella et al. 2017). Future studies should address the mode of action of the members of the gene families identified here, whose specific contributions would extend the CRY2 involvement beyond the transcriptional control of the plastome (Tsunoyama et al. 2004, Pfalz et al. 2006, Chen et al. 2010).

Despite the limitations of the phy datasets analyzed, we also identified R-phys modulation of genes with potential function in the different levels of plastome regulation. Due to the presence of only duplicate replicates for R-WT samples with a potential wider biological variation, we acknowledge the possibility of an underestimation of the R-light responsiveness and the contribution of phys to the response. Nonetheless, we identified R-light sensitive genes across all the chloroplast genome regulatory processes and within the specific gene families studied. In particular, R-phys sensitive genes were part of the transcriptional and post-transcriptional categories, pointing also at an extended regulatory capacity of the receptor. Statistical enrichment for the pTAC class of transcriptional regulators and the contribution to the up-regulation in R- of the sigma factors, further emphasizes the importance of phys in plastome transcriptional control. Yet, the statistical enrichment detected for the GO-term post-transcriptional category together with the identification of 36 R-controlled genes encoding for chloroplastic RNA binding proteins (PPRs and TPRs) indicate that one of the regulatory mechanisms orchestrated by R-phys may be the post-transcriptional modulation of chloroplast gene expression, an area unexamined in the light-signaling field. Post-transcriptional regulation is widely accepted as a mechanism with deep impact in the plastome expression (Ruwe et al. 2011). RNA-binding proteins may therefore be key signaling components in delivering environmental information perceived by the photoreceptors to the plastome-encoded proteome. This is broadly supported from studies in spinach where despite the transcriptional activity of chloroplasts being similar in red, yellow and white light-adapted plants, expression of PSI and PSII proteins differed in red light, hinting at an important role for post-transcriptional activity in light quality responsiveness (Deng et al. 1989).

The environmental input of the photoreceptors to translation of the plastome has been much less explored, beyond the phys and crys modulation of *BPG2* (Kim et al. 2012) and of *ATAB2* (Barneche et al. 2006). We have identified a clear link between the crys and the regulation of chloroplastic ribosomal proteins genes, whose future evaluation would be of interest.

To begin understanding how the phys and crys set up their signaling cascades to coordinate nucleo-chloroplastic light responses, we investigated whether HY5, a transcription factor controlling photosynthetic gene expression (Fig. S2), had an effect on the light-modulation of nuclear genes whose protein products could act at the level of the plastome gene expression. We observed regulation of 59 genes by HY5 across the chloroplast transcription, post-transcription and translational categories. Our study extends the already described contribution of

HY5 to the plastome transcriptional control by sigma factors (Mellenthin et al. 2014) to the light modulation of pTAC protein genes.

Although not statistically significant, we observed a contribution of HY5 to the light up-regulation of 29 RNA binding proteins (25 PPRs, 4 TPRs). This suggests that HY5 could be an important signaling component linking the crys and phys to the post-transcriptional modulation of the plastome (Fig. 4). HY5 links to translational activity were also observed with 24 light-HY5 dependent genes potentially linked to this process including a small number of tRNA ligases Small Ribosomal Protein genes.

Thus, our bioinformatics studies indicate that HY5 is an important photoreceptor signaling component with capacity to integrate the phys' and crys' perceived light cues and transmit them to the chloroplast genome (Fig. 4). Through HY5, the phys and crys could orchestrate from the nucleus a wide set of plastome controlling mechanisms for the coordination of nucleo-chloroplastic light responses. Further characterization of HY5 functions will corroborate this possibility.

Author contributions

J.H.C.G, K.P. and G.T.O conceived the original research plan. J.H.C.G and K.P conducted the bioinformatic analyses. J.H.C.G, K.P, and P.S. generated the figures. J.H.C.G. and G.T.O wrote the article with contributions from all authors.

Acknowledgements – This work was supported by a Royal Society Grant RG150711 to G.T.O. and a Lancaster University Studentship to J.H.C.G. We thank our reviewers for their time and their comments to our manuscript.

Data availability statement

The data sets used in this study are openly available in the Gene Expression Omnibus at <https://www.ncbi.nlm.nih.gov/geo/> using reference numbers GSE31587, GSE62119, GSE58552 and the dataset E-MEX-1299 is accessible through the DIURNAL project (<https://www.ncbi.nlm.nih.gov/pubmed/18419293>).

References

- Barkan A (2011) Expression of plastid genes: organelle-specific elaborations on a prokaryotic scaffold. *Plant Physiol* 155: 1520–1532
- Barneche F, Winter V, Crececoeur M, Rochaix J (2006) *ATAB2* is a novel factor in the signaling pathway of light-controlled synthesis of photosystem proteins. *EMBO J* 25: 5907–5918

- Belbin FE, Noordally ZB, Wetherill SJ, Atkins KA, Franklin KA, Dodd AN (2017) Integration of light and circadian signals that regulate chloroplast transcription by a nuclear-encoded sigma factor. *New Phytol* 213: 727–738
- Berg M, Rogers R, Muralla R, Meinke D (2005) Requirement of aminoacyl-tRNA synthetases for gametogenesis and embryo development in *Arabidopsis*. *Plant J* 44: 866–878
- Berry JO, Yerramsetty P, Zielinski AM, Mure CM (2013) Photosynthetic gene expression in higher plants. *Photosynth Res* 117: 91–120
- Chang BHW and Tian W (2015). GSA-Lightning: Ultra Fast Permutation-based Gene Set Analysis. *Bioinformatics*. <https://doi.org/10.1093/bioinformatics/btw349>
- Chang BHW (2020). GSA Lightning: Fast Permutation-based Gene Set Analysis. R package version 1.16.0. <https://github.com/billyhw/GSALightning>
- Borner T, Aleynikova AY, Zubo YO, Kusnetsov V (2015) Chloroplast RNA polymerases: role in chloroplast biogenesis. *Biochimica et Biophysica Acta (BBA) Bioenergetics* 1847: 761–769
- Chang CJ, Li Y, Chen L (2008) LFZ1, a HY5-regulated transcriptional factor, functions in *Arabidopsis* de-etiolation. *Plant J* 54: 205–219
- Chen M, Chory J (2011) Phytochrome signaling mechanisms and the control of plant development. *Trends Cell Biol* 21: 664–671
- Chen M, Galvao RM, Li M, Burger B, Bugea J, Bolado J, Chory J (2010) HEMERA/pTAC12 initiates photomorphogenesis by phytochromes. *Cell* 141: 1230–1240
- Chotewutmontri P, Barkan A (2016) Dynamics of chloroplast translation during chloroplast differentiation in maize. *PLoS Genet* 12: e1006106
- Del Campo EM (2009) Post-transcriptional control of chloroplast gene expression. *Gene Regul Syst Biol* 3: 31–47
- Deng XW, Tonkyn J, Peter G, Thornber J, Gruissem W (1989) Post-transcriptional control of plastid mRNA accumulation during adaptation of chloroplasts to different light quality environments. *Plant Cell* 1: 645–654
- Facella P, Carbone F, Placido A, Perrotta G (2017) Cryptochrome 2 extensively regulates transcription of chloroplast genome in tomato. *FEBS Open Bio* 7: 456–471
- Franklin KA, Quail PH (2010) Phytochrome functions in *Arabidopsis* development. *J Exp Bot* 61: 11–24
- He SB, Wang WX, Zhang JY, Xu F, Lian HL, Li L, Yang HQ (2015) The CNT1 domain of *Arabidopsis* CRY1 alone is sufficient to mediate blue light inhibition of hypocotyl elongation. *Mol Plant* 8: 822–825
- Hu W, Franklin KA, Sharrock RA, Jones MA, Harmer SL, Lagarias JC (2013) Unanticipated regulatory roles for *Arabidopsis* phytochromes revealed by null mutant analysis. *Proc Nat Acad Sci USA* 110: 1542–1547
- Kim BH, Malec P, Waloszek A, von Arnim AG (2012) *Arabidopsis* BPG2: a phytochrome-regulated gene whose protein product binds to plastid ribosomal RNAs. *Planta* 236: 677–690
- Kim J, Mullet JE (2003) A mechanism for light-induced translation of the *rbcL* mRNA encoding the large subunit of Ribulose-1,5-bisphosphate carboxylase in barley chloroplasts. *Plant Cell Physiol* 44: 194–499
- Kleine T (2012) *Arabidopsis thaliana* mTERF proteins: evolution and functional classification. *Front Plant Sci* 3: 1–15
- Kolde R (2019) pheatmap: Pretty Heatmaps. R package version 1.0.12. <https://CRAN.R-project.org/package=pheatmap>
- Lamb JR, Tugendreich S, Heiter P (1995) Tetratricopeptide repeat interactions: to TPR or not to TPR? *Trends Biochem Sci* 20: 257–259
- Maere S, Heymans K, Kuiper M (2005) BiNGO: a Cytoscape plugin to assess overrepresentation of gene ontology categories in biological networks. *Bioinformatics* 21: 3448–3449
- Martin W, Stoebe B, Goremykin V, Hansmann S, Hasegawa M, Kowallik KV (1998) Gene transfer to the nucleus and evolution of the chloroplasts. *Nature* 393: 162–165
- Mellenthin M, Ellersiek U, Borger A, Baier M (2014) Expression of the *Arabidopsis thaliana* sigma factor SIG5 is photoreceptor and photosynthesis controlled. *Plan Theory* 3: 359–391
- Michael TP, Breton G, Hazen SP, Priest H, Mockler TC, Kay SA, Chory J (2008) A morning-specific Phytohormone gene expression program underlying rhythmic plant growth. *PLoS Biol* 6: 1887–1898
- Oh S, Montgomery BL (2014) Phytochrome-dependent coordinate control of distinct aspects of nuclear and plastid gene expression during anterograde signaling and photomorphogenesis. *Front Plant Sci* 5: 1–8
- Oh S, Warnasooriya SN, Montgomery BL (2013) Downstream effectors of light- and phytochrome-dependent regulation of hypocotyl elongation in *Arabidopsis thaliana*. *Plant Mol Biol* 81: 627–640
- Ohgishi M, Saji K, Okada K, Sakai T (2004) Functional analysis of each blue light receptor *cry1*, *cry2*, *phot1*, and *phot2*, by using combinatorial multiple mutants in *Arabidopsis*. *Proc Nat Acad Sci USA* 101: 2223–2228
- Oliveros J.C. (2007–2015) Venny. An interactive tool for comparing lists with Venn's diagrams. <https://bioinfogp.cnb.csic.es/tools/venny/index.html>
- Osterlund MT, Hardtke CS, Wei N, Deng XW (2000) Target destabilization of HY5 during light-regulated development of *Arabidopsis*. *Nature* 405: 462–466
- Pfalz J, Liere K, Kandlbinder A, Dietz KJ, Oelmüller R (2006) pTAC2, –6, and –12 are components of the transcriptionally active plastid chromosome that are required for plastid gene expression. *Plant Cell* 18: 176–197

- Qiao J, Li J, Chu W, Luo M (2013) PRDA1, a novel chloroplast nucleoid protein, is required for early chloroplast development and is involved in the regulation of plastid gene expression in *Arabidopsis*. *Plant Cell Physiol* 54: 2071–2084
- R Core Team (2019) R: A language and environment for statistical computing. R Foundation for Statistical Computing, Vienna, Austria. <https://www.R-project.org/>
- R Core Team (2020). R: A language and environment for statistical computing. R Foundation for Statistical Computing, Vienna, Austria. <https://www.R-project.org/>.
- Ruwe H, Kupsch C, Teubner M, Schmitz-Linneweber C (2011) The RNA-recognition motif in chloroplasts. *J Plant Physiol* 168: 1361–1371
- Sato S, Nakamura Y, Kaneko T, Asamizu E, Tabata S (1999) Complete structure of the chloroplast genome of *Arabidopsis thaliana*. *DNA Res* 6: 283–290
- Schuster G, Lisitsky I, Klaff P (1999) Polyadenylation and degradation of mRNA in the chloroplast. *Plant Physiol* 120: 937–944
- Singh R, Singh S, Parihar P, Singh VP, Prasad SM (2015) Retrograde signaling between plastid and nucleus: a review. *J Plant Physiol* 181: 55–66
- Soll J, Schleiff E (2004) Protein import into chloroplasts. *Nat Rev Molec Cell Biol* 5: 198–208
- Stern DB, Goldschmidt-Clermont M, Hanson MR (2010) Chloroplast RNA metabolism. *Annu Rev Plant Biol* 61: 125–155
- Su J, Liu B, Liao J, Yang Z, Lin C, Oka Y (2017) Coordination of Cryptochrome and Phytochrome signals in the regulation of plant light responses. *Agronomy* 7: 1–22
- Thum KE, Kim M, Christopher DA, Mullet JE (2000) Cryptochrome 1, Cryptochrome 2, and Phytochrome a co-activate the chloroplast *psbD* blue light-responsive promoter. *Plant Cell* 13: 2747–2760
- Tsunoyama Y, Ishizaki Y, Morikawa K, Kobori M, Nakahira Y, Takeba G, Toyoshima Y, Shiina T (2004) Blue light-induced transcription of plastid-encoded *psbD* gene is mediated by a nuclear-encoded transcription initiation factor, AtSIG5. *Proc Natl Acad Sci USA* 101: 3304–3309
- Wang P, Hendron R, Kelly S (2017) Transcriptional control of photosynthetic capacity: conservation and divergence from *Arabidopsis* to rice. *New Phytol* 216: 32–45
- Yamaguchi K, Subramanian AR (2000) The plastid ribosomal proteins: identification of all the proteins in the 50S subunit of an organelle ribosome (chloroplast). *J Biol Chem* 275: 28466–28482
- Yamaguchi K, Subramanian AR (2003) Proteomic identification of all plastid-specific ribosomal proteins in higher plant chloroplast 30S ribosomal subunit. *Eur J Biochem* 270: 190–205
- Yang EJ, Yoo CY, Liu J, Wang H, Cao J, Li FW, Pryer KM, Sun TP, Weigel D, Zhou P, Chen M (2019) NCP activates chloroplast transcription by controlling phytochrome-dependent dual nuclear and plastidial switches. *Nat Commun* 10: 2630
- Yoo CY, Pasoreck EK, Wang H, Cao J, Blaha GM, Weigel D, Chen M (2019) Phytochrome activates the plastid-encoded RNA polymerase for chloroplast biogenesis via nucleus-to-plastid signaling. *Nat Commun* 10: 2629
- Zoschke R, Bock B (2018) Chloroplast translation: structural and functional organization, operational control, and regulation. *Plant Cell* 30: 745–770

Supporting information

Additional supporting information may be found online in the Supporting Information section at the end of the article.

Fig. S1. PhyB has a broad impact on chloroplastic processes and plastome gene expression under short days (SD).

Fig. S2. GO-term analysis of biological process and cellular component for *hy5* in white light (WL) shows significant enrichment in the contribution of HY5 to chloroplastic processes and ribosomal and ribonucleo-protein complexes.